

University of Nebraska - Lincoln

DigitalCommons@University of Nebraska - Lincoln

---

Student Research Projects, Dissertations, and  
Theses - Chemistry Department

Chemistry, Department of

---

4-2010

## Functionalization of Aromatic Organic Molecules by Anhydrous Flourides and by Reductive Elimination of Iodine(III)

Bijia Wang

University of Nebraska - Lincoln, wangbijia@gmail.com

Follow this and additional works at: <https://digitalcommons.unl.edu/chemistrydiss>

 Part of the [Organic Chemistry Commons](#)

---

Wang, Bijia, "Functionalization of Aromatic Organic Molecules by Anhydrous Flourides and by Reductive Elimination of Iodine(III)" (2010). *Student Research Projects, Dissertations, and Theses - Chemistry Department*. 4.

<https://digitalcommons.unl.edu/chemistrydiss/4>

This Article is brought to you for free and open access by the Chemistry, Department of at DigitalCommons@University of Nebraska - Lincoln. It has been accepted for inclusion in Student Research Projects, Dissertations, and Theses - Chemistry Department by an authorized administrator of DigitalCommons@University of Nebraska - Lincoln.

FUNCTIONALIZATION OF AROMATIC ORGANIC MOLECULES WITH  
ANHYDROUS FLUORIDES AND BY REDUCTIVE ELIMINATION FROM  
IODINE(III)

by

Bijia Wang

A DISSERTATION

Presented to the Faculty of

The Graduate College at the University of Nebraska

In Partial Fulfillment of Requirements

For the Degree of Doctor of Philosophy

Major: Chemistry

Under the Supervision of Professor Stephen G. DiMagno

Lincoln, Nebraska

May, 2010



FUNCTIONALIZATION OF AROMATIC ORGANIC MOLECULES WITH  
ANHYDROUS FLUORIDES AND BY REDUCTIVE ELIMINATION FROM  
IODINE(III)

Bijia Wang, Ph.D.

University of Nebraska, 2010

Adviser: Stephen G. DiMagno

Solution phase reactivity of nucleophilic fluoride reagents is attenuated by ion-pairing interactions.  $^1\text{H}$ - $^{19}\text{F}$  HOESY competition experiments permit generation of a fluoride ion affinity scale in the weak-binding regime. Direct DFT calculations of ion pair interaction energies as well as calculated cation electrostatic potential maps can be used to predict solution phase ion pairing tendencies for closely related ammonium cations. It was found by studying the decomposition of tetra-substituted ammonium cations by fluoride that: 1) rates of E2 decomposition is faster than the  $\text{S}_{\text{N}}2$  pathway; 2) aryl substituents destabilize the cations; 3) steric strain tends to promote decomposition. This led us to prepare anhydrous trineopentylmethylammonium fluoride as a fluorinating reagent with superior thermal stability.

We show that the reagent combination of  $\text{PhIF}_2/\text{TBAF}^*$  is a convenient and effective dehydrating agent for anhydrous fluoride salts. In conjunction with  $^{19}\text{F}$  NMR

spectroscopy, this reagent combination can be used as a rapid, convenient, general, and exquisitely sensitive aquametry method.

Fluorination via reductive elimination of diaryliodonium salts is investigated. Use of non-polar solvents suppresses disproportionation and leads to significant improvements in total fluorination yields. Fluoride promotes aryl ligand exchange processes of diaryliodonium species, which lowers the apparent regioselectivity of aryl fluoride extrusion from diaryliodonium fluorides under stoichiometric conditions, but this problem disappears at low fluoride ion concentration. A computational study shows that the regioselectivity is determined by transition state stability. We also show that  $^{18}\text{F}$ -DOPA can be synthesized in good yield with our improved procedures.

Diaryliodonium(III) species can also be used to functionalize arenes with a variety of nucleophiles. Aryl azide formation is found to be a robust reaction that is insensitive to change of solvent, and which offers fast access to various azido aromatic compounds. Lastly, we show that an increase in steric demand above the plane of the aromatic ring leads to a high degree of regioselectivity in reductive elimination reactions of  $\text{Ar}_2\text{I(III)}$  salts. This effect is sufficiently large to provide stereoelectronic control of unidirectional reductive elimination (*SECURE*).

## ACKNOWLEDGEMENTS

I would like to thank my advisor Professor Stephen DiMagno for his many years of instruction, support, and patience. Without his guidance I could not have completed this work and achieved this goal. I would like to thank the members of my supervisory committee; in particular, the dissertation readers Professors Jim Takacs and Professor David Berkowitz for their helpful suggestions. I would like to thank the late Professor Adrian George, who was on my committee, for selflessly trying his best to give me support and encouragement. I would like to thank Professor Joseph Dumais and Ms. Sara Basiaga for helping me with using the many useful facilities the department has to offer. I would also like to thank the many staff members of University of Nebraska's department of chemistry for all they do.

I am thankful to the current and previous members of the DiMagno group: Dr. Haoran Sun, Dr. Justin Biffinger, Dr. Valeriy Smirnov, Harsha Uppaluri, Linlin Qin, Jason Kempinger, Kiel Neumann, Sara Hitchcock, Joseph Graskemper, Sara Kruse, Mark Craddock, Partha Jana and Daniel Moore. I have learned a great deal about chemistry and life from you all and each of you has played a significant role in helping me complete this work. I wish you all the very best.

To my parents, a simple thank you is not sufficient to express my gratefulness for the years of love, encouragement and support. Thank you for always believing in me and helped me to become who I am.

Lastly I am forever grateful to my husband Jiaqing. I will always thank you for the sacrifices that you have made these last few years. I would not have completed this work without you by my side. Thank you for being my constant source of reassurance and my best friend.

## TABLE OF CONTENTS

ABSTRACT.....	ii
ACKNOWLEDGEMENTS.....	iv
TABLE OF CONTENTS.....	vi
LIST OF FIGURES .....	ix
LIST OF TABLES.....	xv
LIST OF SCHEMES .....	xvii
NOMENCLATURE AND ABBREVIATIONS.....	xx
CHAPTER 1 DEVELOPING WEAKLY COORDINATED NUCLEOPHILIC FLUORINATING AGENTS .....	22
1.1 Introduction.....	22
1.2 Developing a scale for characterizing ion pairing of “weakly coordinated” fluoride salts.....	30
1.3 Stability of tetrasubstituted ammonium cations.....	41
1.4 Synthesis of anhydrous trineopentylmethylammonium fluoride as a stable nucleophilic fluorinating reagent compatible with high temperature applications.....	47
1.5 Experimental.....	53
CHAPTER 2 REMOVAL OF SMALL AMOUNT OF WATER AND ALTERNATIVE AQUAMETRY BASED ON I(III) CHEMISTRY .....	71
2.1 Introduction.....	71
2.2 Water sensitivity of $\text{PhIF}_2$ .....	74

2.3	Alternative aquametry to Karl Fisher titration.....	79
2.4	Experimental.....	85
CHAPTER 3 FLUORINATION OF ELECTRON-RICH AROMATICS VIA		
REDUCTIVE ELIMINATION OF DIARYL IODONIUM SALTS AND THE		
APPLICATION OF DIARYLIODONIUM SALTS IN RADIOTRACER SYNTHESIS		
3.1	Introduction.....	89
3.2	Decomposition of diaryliodonium salts by fluoride .....	99
3.3	Fluoride promoted aryl-swapping of the diaryliodonium cations.....	106
3.4	Computational approach to address the regioselectivity of reductive elimination on diaryliodonium salts: an explanation for the “ortho effect” .....	123
3.5	Application in PET chemistry: Synthesis of [ $^{18}\text{F}$ ]-DOPA .....	132
3.6	Experimental.....	140
CHAPTER 4 METAL FREE ARYLATION OF HETEROATOM NUCLEOPHILES		
VIA DIARYLIODONIUM SALTS .....		
4.1	Background.....	186
4.2	Decomposition of bis(4-methoxyphenyl)iodonium salts in benzene: reactivity of various nucleophiles.....	193
4.3	Formation of azidoarenes.....	200
4.4	Stereoelectronic control of unidirectional reductive elimination (SECURE) of I(III) species .....	206
4.5	Experimental.....	218
APPENDIX A List of Nuclear Magnetic Resonance Spectra .....		234

APPENDIX B List of Chromatograms.....	322
REFERENCES.....	339

## LIST OF FIGURES

Figure 1-1 Fluorine effects in organofluorine compounds. ....	23
Figure 1-2 Examples of fluorine containing pharmaceuticals and agrochemicals. ....	24
Figure 1-3 Commercially available N-F electrophilic fluorinating agents. ....	25
Figure 1-4 Examples of cations used for the preparation of anhydrous fluoride salts. ....	28
Figure 1-5 $^1\text{H}$ - $^{19}\text{F}$ HOESY spectra of TBAF* (left) and TBAF* + 4-methyl- trimethylanilinium triflate (right) in $\text{d}_6$ -DMSO. ....	32
Figure 1-6 Plot of integrated cross-peak volumes in HOESY one-dimensional projection vs. TBA-fluoride concentration. ....	34
Figure 1-7 Competitive fluoride ion pairing between 4-dimethylamino- and 4-methyl- substituted trimethylanilinium cations. ....	36
Figure 1-8 Calculated (B3LYP/6-311G++(d,p), BSSE and ZPE corrected) ion pair of trimethylanilinium fluoride in end-on and side-on binding modes. ....	37
Figure 1-9 $^{19}\text{F}$ - $^1\text{H}$ HOESY spectrum for competitive fluoride binding by cation 1-4 and 1- 5 in $\text{d}_6$ -DMSO. ....	38
Figure 1-10 Structures and corresponding calculated electrostatic potential maps (B3LYP/6-311G+(d)) for selected tetrasubstituted ammonium cations. ....	40
Figure 1-11 Calculated electrostatic potential maps (B3LYP/6-311G+(d)) for selected tetrasubstituted ammonium cations. ....	42
Figure 1-12 List of cations made and/or used in the stability study. ....	43



Figure 1-13 Decomposition of tetrasubstituted ammonium salts by fluoride via demethylation pathway.....	44
Figure 1-14 Decomposition of tetrasubstituted ammonium cations by fluoride via Hofmann elimination pathway.....	45
Figure 1-15 Half lives for the decomposition of tetrasubstituted cations by fluoride in $d_6$ -DMSO.....	46
Figure 1-16 Calculated (B3LYP/6-311G++(d,p))structures of TNPMA-fluoride ion pair. ....	49
Figure 1-17 Competitive fluoride binding indicated by $^1\text{H}$ - $^{19}\text{F}$ HOESY spectra of 1:1 mixture of TNPMAOTf and TBAF* in $d_6$ -DMSO.....	50
Figure 1-18 Decomposition of TNPMAF* @ 80 °C monitored by $^1\text{H}$ NMR. ....	51
Figure 2-1 Changes in the $^1\text{H}$ NMR spectra obtained during the water titration of a 0.5 ml $\text{PhIF}_2$ (0.2 M) and TBAF* (0.2 M) acetonitrile- $d_3$ solution. Successive spectra (bottom to top) were taken at approximately 10 minute intervals. This interval was the time required to remove the sample from the magnet, inject the appropriate amount of water, replace the sample, and gather the $^1\text{H}$ and $^{19}\text{F}$ NMR (Figure 2-2) spectra. From bottom to top, the spectra correspond to the addition of 0, 100, 200, 400, 700, 1000, 1300, 1500, and 1800 micrograms of water. ....	77
Figure 2-2 Successive $^{19}\text{F}$ NMR spectra obtained during the addition of water to a 0.5 ml $\text{PhIF}_2$ (0.2 M) and TBAF* (0.2 M) acetonitrile- $d_3$ solution; this is the identical experiment to that shown in Figure 2-1. Note that there is no evidence for $\text{DF}_2^-$ in these spectra, as is discussed in the text. ....	78

Figure 2-3 Graphical representation of the water determination experiment. From left to right: 1) TBAF/PhI(OAc) <sub>2</sub> /TBABF <sub>4</sub> mixture in a reaction tube; 2) assay mixture in CD <sub>3</sub> CN; 3) side (bottom) and top (top) views of a customized 5 mm NMR tube featuring a fused crimp cap vial septum seal; 4) tube containing solid reagents (TBAF, TBABF <sub>4</sub> , PhI(OAc) <sub>2</sub> ), CD <sub>3</sub> CN and sample after the addition of the solvent being tested. The process arrows indicate a) addition of CD <sub>3</sub> CN, b) installation of the cap, c) collection of the background <sup>19</sup> F NMR spectrum, d) injection of the solvent being tested, e) collection of the final <sup>19</sup> F NMR spectrum. ....	80
Figure 2-4 Results from the titration of a PhIF <sub>2</sub> /CD <sub>3</sub> CN solution with standardized aqueous acetonitrile. ....	81
Figure 2-5 Single injection water determination by <sup>19</sup> F NMR: bottom, background spectrum before the addition of “dry” CH <sub>3</sub> CN; top, spectrum collected after the injection of a CH <sub>3</sub> CN sample containing 49 µg of H <sub>2</sub> O. ....	82
Figure 3-1 Illustration of Positron Emission Tomography (PET). ....	89
Figure 3-2 Structures of <sup>18</sup> F-labeled radiopharmaceuticals for clinical use or under preclinical studies. ....	91
Figure 3-3 Multistep synthesis of n.c.a. [ <sup>18</sup> F]FTyr, [ <sup>18</sup> F]FDOPA and 4-[ <sup>18</sup> F]FmTyr. <sup>67</sup> ...	94
Figure 3-4 List of diaryliodonium fluorides made and studied. ....	101
Figure 3-5 <sup>1</sup> H and <sup>19</sup> F NMR spectra of 3-1 decomposition mixture in benzene. ....	103
Figure 3-6 GC spectrum: reaction mixture of 3-1 decomposition in dry benzene. ....	104
Figure 3-7 Proposed exchange in 5-aryl-3,7-dimethyl-5H-dibenziodoles. <sup>93</sup> ....	108

Figure 3-8 Diaryliodonium salts discussed in this section. Throughout the text, the particular counterion of interest ( $X = \text{PF}_6, \text{OTf}, \text{F}$ ) is denoted in parentheses following the compound number (i.e. 3-1( $\text{PF}_6$ )).	109
Figure 3-9 $^1\text{H}$ NMR spectra in $\text{CD}_3\text{CN}$ of a) 3-1( $\text{F}$ ), b) 3-11( $\text{F}$ ), c) 3-6( $\text{PF}_6$ ), and d) 3-6( $\text{PF}_6$ ) after it was treated with TMAF in $\text{CH}_3\text{CN}$ , desalted with benzene, and dissolved in $\text{CD}_3\text{CN}$ . Only the aromatic regions are displayed for clarity.	110
Figure 3-10 ES-MS spectrum of 3-6( $\text{OTf}$ ) that had previously converted to the fluoride salt and exchanged back to the triflate.	112
Figure 3-11 $^{19}\text{F}$ NMR spectra of 1( $\text{F}$ ), 3( $\text{F}$ ) and 4( $\text{F}$ ) in $d_8$ -toluene at various temperatures.	114
Figure 3-12 Stacked $^1\text{H}$ NMR spectra (detail showing the <i>p</i> -methoxy region) of 3-6( $\text{PF}_6$ ) and 0.89 equiv of TMAF. Elapsed time = 160 min.	115
Figure 3-13 Plot of $\ln[\text{Ar}_1\text{-I-Ar}_2]/[\text{Ar}_1\text{-I-Ar}_2]_{\text{eq}}$ vs. time for aryl-swapping of 1( $\text{PF}_6$ ) with 0.89 equiv added fluoride.	116
Figure 3-14 Plot of $\ln[\text{Ar}_1\text{-I-Ar}_2]/[\text{Ar}_1\text{-I-Ar}_2]_{\text{eq}}$ vs. time for aryl-swapping of 1( $\text{PF}_6$ ) with 0.81 equiv added fluoride.	117
Figure 3-15 Calculated geometries of ground state and transition state of monomeric diphenyliodonium fluoride with (above) and without (bottom) mapped surface potentials.	127
Figure 3-16 Calculated ground state of $\text{Ph}_2\text{IF}$ dimer (B3LYP/Midix).	128
Figure 3-17 Transition state leads to 2,6-dimethylfluorobenzene formation is lower in energy for compound 3-17 due to two $\text{C-H}\cdots\text{F}$ stabilization.	131

Figure 3-18 Synthesis of benzyl-Boc protected iodonium fluoride precursor of 6-fluoro-DOPA.....	135
Figure 3-19 $^1\text{H}$ NMR showing the decomposition of benzyl-Boc DOPA iodonium fluoride.....	137
Figure 3-20 $^1\text{H}$ and $^{19}\text{F}$ NMR spectra of isolated benzyl-Boc protected FDOPA. ....	138
Figure 3-21 Chiral HPLC chromatograms of benzyl-Boc protected FDOPA.....	139
Figure 4-1 Two different mechanisms of decomposition of diaryliodonium(III) by nucleophiles. <sup>106</sup> .....	187
Figure 4-2 Decomposition of aryl( <i>p</i> -tolyl)-iodonium bromide at molten phase and in DMF solution. ....	189
Figure 4-3 Observed rate constants for thermo decomposition of diaryliodonium bromide in DMF. <sup>196</sup> .....	190
Figure 4-4 Two possible mechanistic pathway for ligand exchange of diaryl- $\lambda^3$ -iodanes. ....	192
Figure 4-5 $^1\text{H}$ NMR spectra of bis(4-methoxyphenyl)-halo- $\lambda^3$ -iodane decomposition mixtures in $\text{d}_6$ -benzene (only aromatic regions are displayed).....	195
Figure 4-6 $^1\text{H}$ NMR spectra of the reaction mixture of bis(4-methoxyphenyl)-thiocyanato- $\lambda^3$ -iodane decomposition in $\text{d}_6$ -benzene.....	197
Figure 4-7 Decomposition of bis(4-methoxyphenyl)-azido- $\lambda^3$ -iodane to form 4-azidoanisole and its coupling with phenyl acetylene to form the corresponding triazole. ....	198

Figure 4-8 $^1\text{H}$ NMR spectra of the reaction mixture of bis(4-methoxyphenyl)-cyano- $\lambda^3$ -iodane decomposition in $\text{d}_6$ -benzene. ....	199
Figure 4-9 Calculated TS structures and activation barriers for xylyl and cyclophanyl I(III) species. ....	210

## LIST OF TABLES

Table 1-1 Fluorination of various substrates using TBAF*, CoCp <sub>2</sub> F, TBAT or vacuum-dried “anhydrous” TBAF.....	29
Table 1-2 Calculated (B3LYP/6-311G++(d,p), BSSE and ZPE corrected) gas phase ion pair energy for substituted trimethylanilinium fluorides in end-on and side-on binding modes. ....	37
Table 1-3 Helix reactions of selective unactivated chloroaromatic compounds by TBAF*. <sup>22</sup> .....	47
Table 3-1 Nuclear properties of commonly used positron emitters. (Data taken from Browne and Firestone 1986 and from Brookhaven National Laboratory internet data base, BNL 2003.) .....	90
Table 3-2 Production routes to [ <sup>18</sup> F]fluoride and [ <sup>18</sup> F]fluorine. <sup>60</sup> .....	92
Table 3-3 Observed yields of ArF from the decomposition of 3-1 through 3-8.....	102
Table 3-4 <sup>a</sup> Equilibrium populations of symmetrically and unsymmetrically substituted diaryliodonium fluorides.....	121
Table 3-5 Energies (hartree), activation barriers (kcal/mol), and transition normal mode for Ph <sub>2</sub> IF (ZPE corrected). ....	126
Table 3-6 Energies and activation barriers (kcal/mol) for ArPhIF (calculated at B3LYP/Midix level, ZPE corrected). ....	130
Table 4-1 Arylations of nucleophilic species by diaryliodonium salts.....	188
Table 4-2 Decomposition of bis(4-methoxyphenyl)-λ <sup>3</sup> -iodanes in benzene. ....	194

Table 4-3 Yields and reaction time of reductive elimination of aryl-(4-methoxyphenyl)- azido- $\lambda^3$ -iodanes and aryl-(4-methoxyphenyl)-fluoro- $\lambda^3$ -iodanes in benzene and acetonitrile.....	204
Table 4-4 Results for the reductive elimination of salt 4-11, 4-12, and 4-13 with various nucleophiles in acetonitrile. ....	213

## LIST OF SCHEMES

Scheme 1-1 Examples of methods used to enhance reactivity of simple metal fluorides. <sup>11-</sup>	
13 .....	26
Scheme 1-2 Generation of truly anhydrous TBAF (TBAF*) from low-temperature S <sub>N</sub> Ar reaction of hexafluorobenzene and TBACN.....	30
Scheme 1-3 Experiment design to generate a linked ion pair scale of fluoride affinity... 33	
Scheme 1-4 Structure of tetrasubstituted ammonium cations used for the HOESY study. .....	35
Scheme 2-1 <i>In situ</i> removal of water by hexacyanobenzene in the presence of fluoride. 72	
Scheme 2-2 Generation of anhydrous TBAF via F-relay and cyanide-free method with thiophenoxide as the nucleophile.....	72
Scheme 2-3 Preparation of PhIF <sub>2</sub> by ion exchange under anhydrous basic conditions....	73
Scheme 2-4 Reaction of PhIF <sub>2</sub> with water in the presence of excess fluoride. ....	74
Scheme 2-5 Simplified scheme for hydroxide catalyzed deuterium exchange. ....	75
Scheme 3-1 Pd-catalyzed aromatic fluorination utilizing tBuBrettPhos as the ligand. <sup>69</sup> . 95	
Scheme 3-2 One-step methods to n.c.a. 1-bromo-4-[ <sup>18</sup> F]fluorobenzene. <sup>72</sup> .....	96
Scheme 3-3 More stable complex formed by diaryliodonium cation and the nucleophile with the sterically demanding aryl group occupying the equatorial position (left); Structure proposed by Lancer to explain the observed “ortho effect” for decomposition of (2-methylphenyl)phenyliodonium by nucleophiles (right).....	98



Scheme 3-4 Observed regioselectivity for 3-6(PF <sub>6</sub> ) (featuring the relatively electron-poor phenyl substituent) is worse than that of 3-2(PF <sub>6</sub> ) (featuring relatively electron-rich 3,4-dimethoxyphenyl group.) a. TMAF/CH <sub>3</sub> CN, evaporation of solvent, addition of d <sub>6</sub> -benzene, filtration; b. 140 °C, 15 minutes.....	107
Scheme 3-5 Possible origins of the additional complexity observed in the <sup>1</sup> H NMR spectrum of 3-6(PF <sub>6</sub> ) after addition of fluoride. ....	111
Scheme 3-6 Fluoride-catalyzed aryl exchange of diaryliodonium salts. ....	113
Scheme 3-7 Mechanism for the generation of iodobenzene during the thermal decomposition of 3-6(F). ....	119
Scheme 3-8 Proposed utilization of aryl-swapping in bis-drug iodonium salts synthesis. ....	122
Scheme 3-9 Fluxional geometry of T-shaped fluoro(diaryl)-λ <sup>3</sup> -iodanes. <sup>120</sup> .....	123
Scheme 3-10 Reaction pathways for monomeric dialkynyliodonium species. ....	125
Scheme 3-11 Interconversion of the two different T-shaped monomers through I-F stretching in dimer. ....	128
Scheme 3-12 Reaction pathways for monomeric diaryliodonium fluorides. ....	129
Scheme 3-13 Racemization of L-FDOPA derivative using sodium hexamethyldisilazide. ....	139
Scheme 4-1 Benzyne formation from diaryliodonium acetate as a competing side reaction for its thermo decomposition. <sup>198</sup> .....	191
Scheme 4-2 Preparation of bis(4-methoxyphenyl)-λ <sup>3</sup> -iodanes and their decomposition in benzene. ....	193

Scheme 4-3 Reductive elimination of aryl-(4-methoxyphenyl)-azido- $\lambda^3$ -iodanes in benzene and acetonitrile.....	203
Scheme 4-4 Examples of regioselectivities obtained in thermal decomposition reactions of unsymmetrical diaryliodonium salts. <sup>76, 78, 103, 176, 231, 232</sup> .....	207
Scheme 4-5 Regiochemically controlled reductive elimination of an electron-rich, cyclophane-derived diaryliodonium salt .....	209
Scheme 4-6 Reductive elimination of compounds 4-11, 4-12, and 4-13 by various nucleophiles in acetonitrile. ....	212
Scheme 4-7 Synthesis of (7-methoxy-[2.2]paracyclophan-4-yl)(4'-methoxyphenyl)-iodonium hexafluorophosphate. (a. 1. <i>t</i> -BuLi, Et <sub>2</sub> O, -78 °C, 2. B(OMe) <sub>3</sub> , 3. H <sub>2</sub> O <sub>2</sub> , NaOH, H <sub>2</sub> O; b. ....	216
Scheme 4-8 Anisole functionalization by thermal decomposition of salt 4-14 in CD <sub>3</sub> CN. ....	217

## NOMENCLATURE AND ABBREVIATIONS

AADC	Amino acid decarboxylase
BAI	[Bis(acyloxy)iodo]arenes in general
BDE	Bond dissociation energy
S-Boc-BMI	(S)-1-Boc-2- <i>tert</i> -butyl-3-methyl-4-imidazolidinone
DCM	Dichloromethane, methylene chloride
DFT	Density function theory
DMAP	Dimethylaminopyridine
DMF	Dimethylformamide
DMSO	Dimethylsulfoxide
DOPA	Dihydroxyphenylalanine
[ <sup>18</sup> F]FDG	2-[ <sup>18</sup> F]Fluoro-2-deoxy-D-glucose
[ <sup>18</sup> F]FDOPA	6-[ <sup>18</sup> F]Fluoro-L-DOPA
4-[ <sup>18</sup> F]FmTyr	4-[ <sup>18</sup> F]Fluoro- <i>meta</i> -L-tyrosine
[ <sup>18</sup> F]FTyr	2-[ <sup>18</sup> F]Fluoro-L-tyrosine
HF	Hydrogen fluoride
HPLC	High performance liquid chromatography

IP	Ionization potential
IRC	Intrinsic reaction coordinate
NET	Neuroendocrine tumor
OAc	Acetate
OTf	Trifluoromethanesulfonate
OTs	4-Toluenesulfonate
PET	Positron emission tomography
RCY	Radiochemical yield
SECURE	Stereoelectronic control of unidirectional reductive elimination
SW	Sweep width (NMR)
TBAF	Tetrabutylammonium fluoride
TBAF*	Anhydrous tetrabutylammonium fluoride
TFA	Trifluoroacetic acid
THF	Tetrahydrofuran
TLC	Thin layer chromatography
TMAF	Tetramethylammonium fluoride
TMS	Trimethylsilyl
TNPMF	Trineopentylmethylammonium fluoride

## CHAPTER 1

### DEVELOPING WEAKLY COORDINATED NUCLEOPHILIC FLUORINATING AGENTS

#### 1.1 Introduction

Fluorine has played key roles in organic chemistry since the middle of the 20<sup>th</sup> century. The use of fluorine substitution expanded dramatically with the development in synthetic methods for organofluorine compounds.<sup>1</sup> Fluorine is most electronegative element and has the third largest ionization potential (IP) after helium and neon. Fluorine forms the shortest single bond to carbon after hydrogen (C-H BDE = 98 Kcal/mol) but the C-F bond is much stronger (BDE = 117 Kcal/mol). The carbon of a C-F bond is polarized and bears a partial positive charge in contrast to the carbon of a C-H bond. Thus, the replacement of hydrogen in an organic compound by fluorine causes a change in polarization with very little change in total bulk. Therefore, organofluorine compounds demonstrate a variety of unique properties. Despite the fact that naturally occurring organofluorine compounds are rare, they have demonstrated utility in pharmaceutical, agrochemical, and material chemistry.

Figure 1-1 demonstrates the so-called “Fluorine effects” in terms of chemical, physical and biological properties of organofluorine compounds. In the pharmaceutical industry, fluorine substitution is a powerful tool to improve a drug’s bioavailability and enhance its metabolism properties. To be more specific, the incorporation of fluorine into a drug can alter its metabolism or enzyme recognition; the hydrophobic nature of

fluorinated compounds is known to improve their lipophilicity, and their transport across the blood brain barrier.

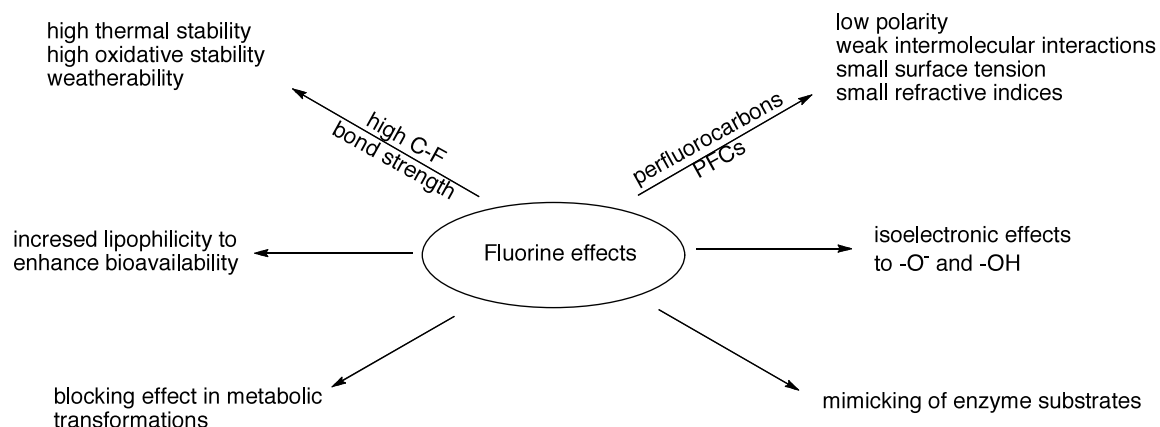


**Figure 1-1 Fluorine effects in organofluorine compounds.**

The chemical inertness and relatively small size of fluorine have made C-F substitution attractive for replacement of oxidizable C-H bonds. Due to the similarity of fluorine and oxygen in terms of electronegativity and van der Waals radii, fluoroalkanes and fluoroalkenes are considered to be isosteres of alkanols and carbonyl compounds. Such isosteric effect has been successfully applied to the design of pharmaceuticals and agrochemicals (Figure 1-2). Since organofluorine compounds are extremely rare in nature, they can only be accessed synthetically. The incorporation of fluorine into the carbon backbone can be achieved by using either a nucleophilic (*e.g.*, HF, KF, CsF, TMAF) or an electrophilic (*e.g.*, F<sub>2</sub>, FClO<sub>3</sub>, Selectfluor®) fluorinating reagent. An alternative approach is to incorporate a group featuring the required number of fluorine atoms (*e.g.* CF<sub>3</sub>). An expansive set of nucleophilic and electrophilic reagents has been developed to replace various C-X groups with C-F.

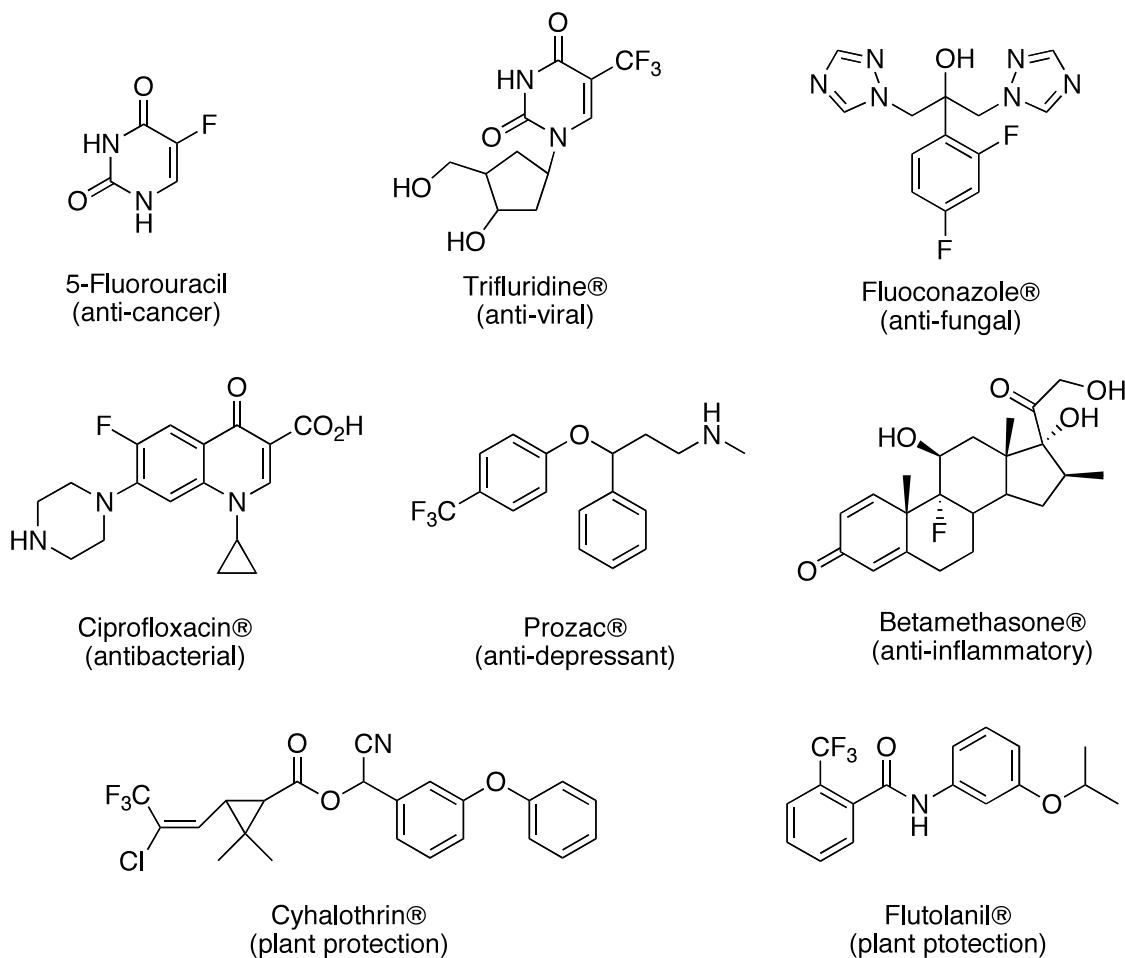


**Figure 1-2 Examples of fluorine containing pharmaceuticals and agrochemicals.**

The development of electrophilic fluorinating agents requires attenuating the oxidizing power of  $F_2$  to engineer “ $F^+$ ” donors. Xenon difluoride ( $Xe-F$ ), perchloryl fluoride ( $O-F$ ), and perfluoroalkyl and perfluoroacyl hypofluorites ( $O-F$ ) are examples of tamed electrophilic fluorine, although they are still strongly oxidizing reagents that must be handled with caution. A newer generation of “ $F^+$ ” reagents features  $N-F$  bonds (Figure 1-3). These compounds tend to be stable crystalline solids that are convenient to handle. Because the decreased electronegativity of nitrogen and the increased  $N-F$  bond energy ( $58.5 \text{ kcal/mol}$  in  $NF_3$ )<sup>2</sup> compared to  $O-F$  ( $39.1 \text{ kcal/mol}$  in  $F_2O$ )<sup>3</sup> or  $F-F$  ( $38.4 \text{ kcal/mol}$ ),<sup>4</sup>

the electrophilic nature of these reagents is attenuated significantly. Such reagents are capable of fluorinating organometallic compounds, enolates and electron rich aromatic rings, among other nucleophiles.

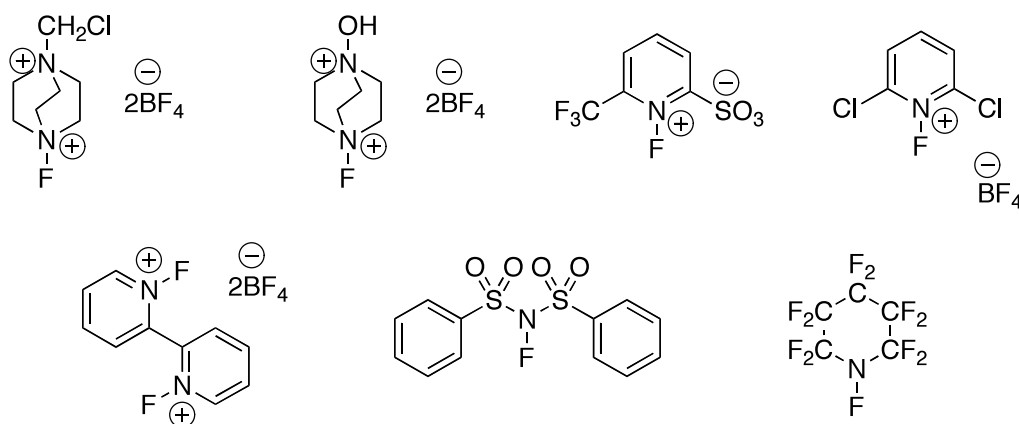


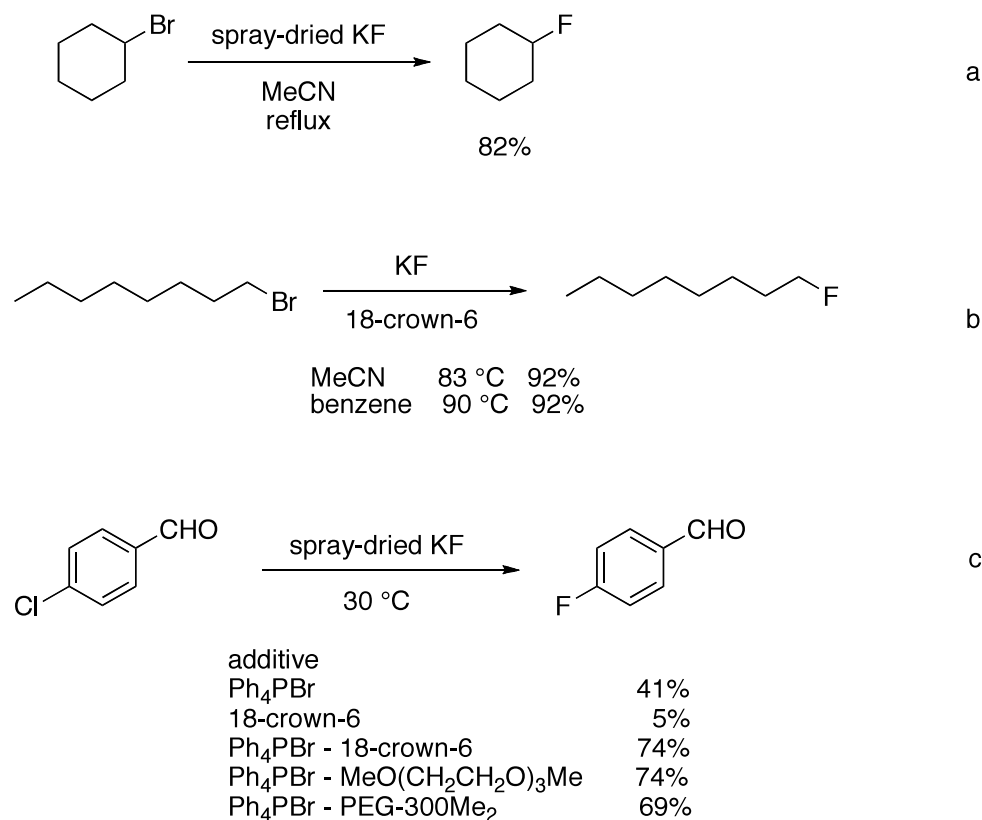
**Figure 1-3 Commercially available N-F electrophilic fluorinating agents.**

Direct transition metal catalyzed fluorination of aromatic and heteroaromatic compounds is uncommon. Usually, a two-step strategy involving metalation (metal = Li, Sn) of the aromatic compound followed by treatment with an electrophilic fluorinating agent (demetalation) is employed.<sup>5-9</sup> The advantage of this approach is that regioselective fluorination is possible by exploitation of directing group abilities in the metalation step. Substituted benzenes,<sup>7</sup> naphthalenes,<sup>8</sup> indoles,<sup>5</sup> thiophenes,<sup>6</sup> pyrroles,<sup>6</sup> and purines<sup>9</sup> have been successfully fluorinated in this manner. Sanford and coworkers recently showed that directed oxidative addition of palladium into a C-H bond, followed by treatment with an electrophilic fluorinating agent, is a useful direct route into fluorinated phenyl pyridines.<sup>10</sup>

For the development of nucleophilic fluorinating agents, fluoride reagents are desirable targets because they are inexpensive, stable, and easy to handle when compared



to the toxic, corrosive, and/or pricy liquids or gases such as HF, sulfur tetrafluoride and their derivatives. Direct substitution of halogen or sulfonate groups by fluoride salts in aromatic and aliphatic substrates has long been known. These reactions are simple in principle, and they make up the bulk of our synthetic capability.



**Scheme 1-1 Examples of methods used to enhance reactivity of simple metal fluorides.**<sup>11-13</sup>

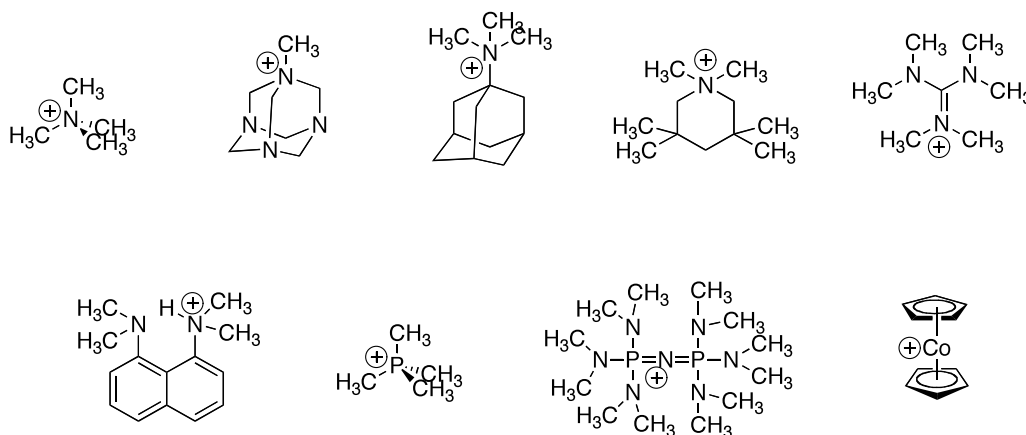
In contrast to electrophilic fluorination, the main challenge in nucleophilic fluorination is to enhance the solution phase reactivity of fluoride reagents. Gas phase fluoride ion is a potent nucleophile. However, it is strongly solvated in water ( $\Delta G^0_{\text{(solv)}} = -104.3 \text{ kcal/mol}$ )<sup>14</sup> and other protic solvents, so that it is considered a poor nucleophile in solution. In anhydrous aprotic solvents, it forms tight ion pairs with most cations; these

ion-pairing interactions must be overcome if fluoride is to participate in nucleophilic reactions.

Simple metal fluorides (KF, CsF, and AgF) are highly hygroscopic; they have high lattice energies and low solubility in organic solvents. Therefore, much effort has been dedicated to developing soluble and anhydrous fluoride sources. Spray-dried KF (Scheme 1-1 a)<sup>11</sup> is less hygroscopic and has much larger surface area than conventional KF and is thus much more reactive. The use of a crown ether (Scheme 1-1 b)<sup>12</sup> or a phase-transfer catalyst (Scheme 1-1 c)<sup>13</sup> is an effective way to make KF more soluble in organic solvents and enhance fluoride nucleophilicity.

Fluoride salts of organic cations have much better solubility in organic solvents. Such salts featuring shielded, sterically demanding, or simply large cations are ideal for use as nucleophilic fluorinating agents. The idea here is to delocalize the positive charge over a larger surface area and hence reduce the extent of ion pairing. Examples of commonly used “weakly coordinated” fluoride salts are tetramethylammonium fluoride (TMAF), tetrabutylammonium fluoride (TBAF), 1-methylhexamethylenetetramine fluoride (MHAF), and tetramethylphosphonium fluoride. These tetraalkylammonium or phosphonium fluorides are usually prepared in a hydrated state by ion exchange followed by subsequent dehydration under dynamic vacuum or by azeotropic distillation. However, the conditions needed to remove water are often incompatible with a variety of desirable cations. For example, tetrabutylammonium fluoride (TBAF)<sup>15</sup> is extremely hygroscopic, and the water content of the “anhydrous” reagent may be significant. Exposure of the salt to a combination of reduced pressure and even very modest heating (> 40 °C) lead to

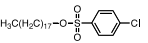
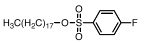
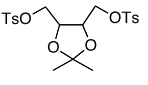
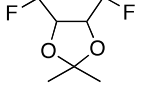
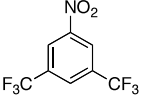
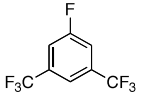
decomposition by Hofmann elimination to yield tributylamine, 1-butene and  $\text{HF}_2^-$ .<sup>16</sup> These considerations had led to the belief that “ it is very unlikely that pure, anhydrous tetraalkylammonium fluoride salts have ever, in fact, been produced in the case of ammonium ions susceptible to E2 eliminations”.<sup>16</sup>



**Figure 1-4** Examples of cations used for the preparation of anhydrous fluoride salts.

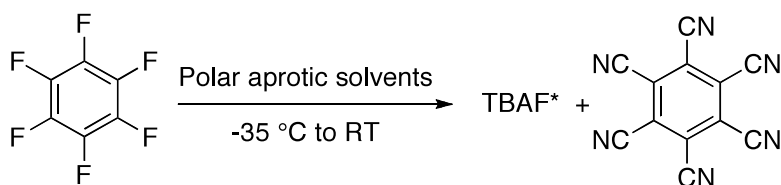
In practice, anhydrous organic fluoride salts that have been isolated always have cations featuring one of the following: methyl groups, quaternary  $\beta$ -carbon atoms, non carbon atoms at  $\beta$ -positions, or bicyclic systems that would give rise to a Bredt's rule<sup>17</sup> violation upon E2 elimination. Examples of these cations are shown in Figure 1-4. The methyl C-H bonds on these cations are exposed, bear substantial positive charge and tend to form tight electrostatic contacts with fluoride ion. These ion pairing interactions result in poorly soluble, less nucleophilic fluoride sources. Therefore, the reliance on methyl blocking groups severely limits the diversity of anhydrous tetrasubstituted ammonium fluorides. It is desirable to develop synthetic methods to generate directly anhydrous fluorides and circumvent the rather harsh dehydration procedures that give rise to cation decomposition.

**Table 1-1 Fluorination of various substrates using TBAF\*, CoCp<sub>2</sub>F, TBAT or vacuum-dried “anhydrous” TBAF.**

Run	Substrate	Reagent	Solvent	Conditions	Product	Yield <sup>a</sup> (%)	Comments	Ref.
1	PhCH <sub>2</sub> Br	1.3 ~ 1.5 equiv TBAF*	CD <sub>3</sub> CN	- 35 °C, < 5 min	PhCH <sub>2</sub> F	100		18
2	PhCH <sub>2</sub> Br	2 equiv TBAF “anhydrous”	THF	RT, 8 h	PhCH <sub>2</sub> F	> 90	PhCH <sub>2</sub> OH (5 %)	19
3	CH <sub>3</sub> I	1.5 equiv TBAF*	CD <sub>3</sub> CN	- 40 °C, < 5 min	CH <sub>3</sub> F	100		18
4	CH <sub>3</sub> I	CoCp <sub>2</sub> F	THF	RT, 6 h	CH <sub>3</sub> F	100		20
5	CH <sub>3</sub> (CH <sub>2</sub> ) <sub>7</sub> Br	TBAF*	THF	RT, < 5 min	CH <sub>3</sub> (CH <sub>2</sub> ) <sub>7</sub> F	40 ~ 50	remainder alkene	18
6	CH <sub>3</sub> (CH <sub>2</sub> ) <sub>7</sub> Br	6 equiv TBAT	CH <sub>3</sub> CN	Reflux 24 h	CH <sub>3</sub> (CH <sub>2</sub> ) <sub>7</sub> F	85		21
7	CH <sub>3</sub> (CH <sub>2</sub> ) <sub>7</sub> Br	4 equiv TBAF “anhydrous”	THF	RT, 1 h	CH <sub>3</sub> (CH <sub>2</sub> ) <sub>7</sub> F	48	40 % octanol	19
8		TBAF*	THF	RT, < 5 min		100		18
9		4 equiv TBAF*	THF or CD <sub>3</sub> CN	RT, < 5 min		>90		18
10		1.3 equiv TBAF*	THF or CD <sub>3</sub> CN	RT, < 2 min		>95		18
11	PhCOCl	1 equiv TBAF*	THF	RT, < 2 min	PhCOF	100		18
12	Tosyl-Cl	1 equiv TBAF*	THF	RT, < 2 min	Tosyl-F	100		18

<sup>a</sup> Yields were calculated by integration of starting material and product signals in the <sup>1</sup>H and/or <sup>19</sup>F spectra.

The DiMagno group has developed a useful synthesis of “truly anhydrous TBAF” (TBAF\*) via a low-temperature, nucleophilic aromatic substitution ( $S_NAr$ ) reaction.<sup>18, 22</sup> Treatment of hexafluorobenzene with tetrabutylammonium cyanide (TBACN) in the polar aprotic solvents THF, acetonitrile or DMSO at or below room temperature gave excellent yields of anhydrous TBAF (>95 % measured by  $^{19}\text{F}$  NMR in solution). In head-to-head comparisons, anhydrous TBAF thus generated shows dramatically enhanced rates of fluorination compared to dynamic vacuum-dried “anhydrous” TBAF,  $\text{CoCp}_2\text{F}$ , or TBAT (Table 1-1) Typically, neither heating nor a gross excess of TBAF is needed to effect fluorination. The high nucleophilicity and basicity of TBAF\* can be explained by the low ability of TBA cation to coordinate the “naked fluoride”.



**Scheme 1-2 Generation of truly anhydrous TBAF (TBAF\*) from low-temperature  $S_NAr$  reaction of hexafluorobenzene and TBACN.**

## 1.2 Developing a scale for characterizing ion pairing of “weakly coordinated” fluoride salts

The term “naked fluoride” has been used extensively in the literature to describe weakly coordinated, soluble, fluoride donor salts or coordination compounds. The extent of solution ion pairing of fluoride with organic or inorganic cations in these complexes has been inferred from manifested differences in reactivity or by extrapolating the results

of gas phase or solid state computational studies to solution. The coordination state of fluoride ion is important, because ion pairing and solvation are the principal factors that attenuate its potent gas phase nucleophilicity.

Although TBAF\* shows the hallmarks of weakly-coordinated fluoride ion, namely high solubility and enhanced nucleophilicity in aprotic media, it is hard to characterize precisely how weakly-coordinated this particular salt is, compared to other fluoride donor complexes. Comparisons have been made based on determination of the rates of substitution reactions of TBAF\* and other commonly employed nucleophilic fluorinating agents. Relative rate arguments rely on benchmark reactions, and thus are a function of the precise experimental parameters used in different laboratories. In order to study the influence of counterion on the ion-pairing interactions, we sought to develop a straightforward method to rank fluoride ion affinities unambiguously in the weak binding regime.

NMR techniques have often been applied to the problem of understanding ion pair structures and dynamics; the interionic nuclear Overhauser effects (NOEs) in a contact ion pair has been shown to provide a description of time-average structures of the ion pair. The relaxation controlled NOEs fall off dramatically as a function of distance ( $r^{-6}$ ), hence they are only important if the nuclei are in proximity ( $<5\text{\AA}$ ). Pregosin and coworkers<sup>23</sup> have used  $^1\text{H}$ - $^{19}\text{F}$  NOE studies to gain insight into the nature of ion pairing between organic and organometallic cations and fluorinated anions. For a tight ion pair between an organic cation and a fluorinated anion,  $^1\text{H}$ - $^{19}\text{F}$  heteronuclear Overhauser effect

spectroscopy (HOESY) data can provide structural information to pinpoint the site(s) of the strongest interactions.

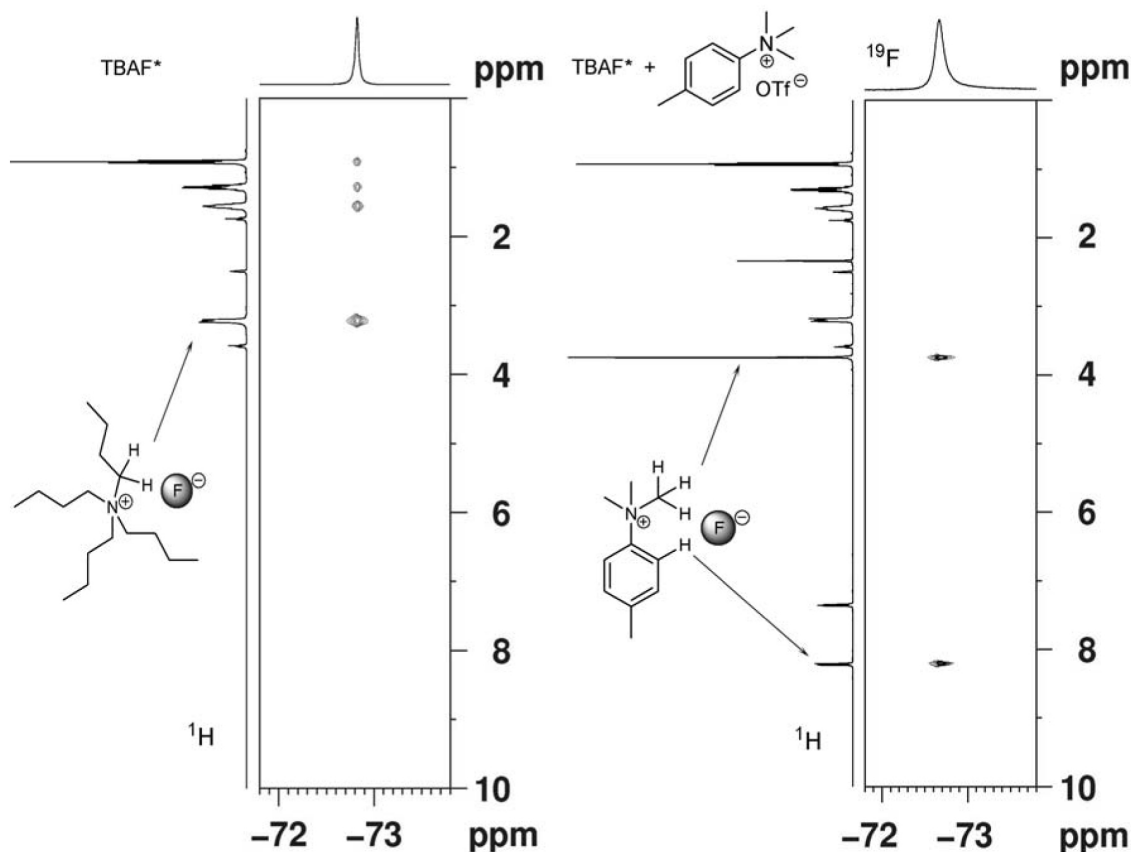


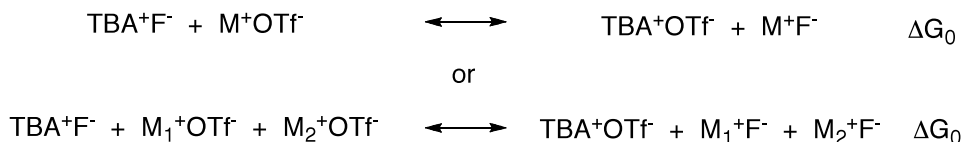
**Figure 1-5**  $^1\text{H}$ - $^{19}\text{F}$  HOESY spectra of  $\text{TBAF}^*$  (left) and  $\text{TBAF}^* + 4\text{-methyltrimethylanilinium triflate}$  (right) in  $\text{d}_6\text{-DMSO}$ .

While Pregosin and coworkers have focused mainly on studies featuring complex fluorinated anions ( $\text{BF}_4$ ,  $\text{PF}_6$ , etc.), we have demonstrated that high quality  $^1\text{H}$ - $^{19}\text{F}$  HOESY data can be obtained for fluoride salts as well. In the  $^1\text{H}$ - $^{19}\text{F}$  HOESY spectrum of  $\text{TBAF}^*$  in  $\text{d}_6\text{-DMSO}$  shown on the left in Figure 1-5, it is clear that the ion pairing between TBA and fluoride is significant; cross-peaks observed for all four types of hydrogen atoms in the butyl chains. The strongest interaction site is at the  $\alpha\text{-CH}_2\text{s}$

adjacent to the positively charged nitrogen atom. As the smallest monoanion, fluoride forms very tight ion-pairs, which makes it well suited to form the basis of an ion pairing scale featuring relatively weakly coordinating cations.

Upon addition of TBAF\*, the  $^1\text{H}$  NMR spectrum of 4-methyl-trimethylanilinium triflate in  $\text{d}_6$ -DMSO showed significant larger separations in the chemical shifts of the *ortho* and *meta* proton signals, indicative of the ion exchange. The attribution of ion exchange was supported by  $^1\text{H}$ - $^{19}\text{F}$  HOESY spectra (Figure 1-5, right) of the mixed solution, which showed disappearance of the cross-peaks from protons on TBA and fluoride and the emergence of cross-peaks from protons on anilinium cation and fluoride. This demonstrates that fluoride is transferred from tetrabutylammonium cation to the trimethylanilinium cation; and within the detection limits of this experiment, the ion exchange appears quantitative.

I performed experiments designed to evaluate the fluoride ion pairing equilibria using HOESY spectroscopy. To develop a linked fluoride ion pairing scale, we chose an approach analogous to that developed by Streitwieser for measuring ion pair carbon acidities.<sup>24</sup> The approach requires a series of indicator compounds with closely spaced fluoride affinities so that pairwise measurement may be conducted (Scheme 1-3).



**Scheme 1-3 Experiment design to generate a linked ion pair scale of fluoride affinity.**



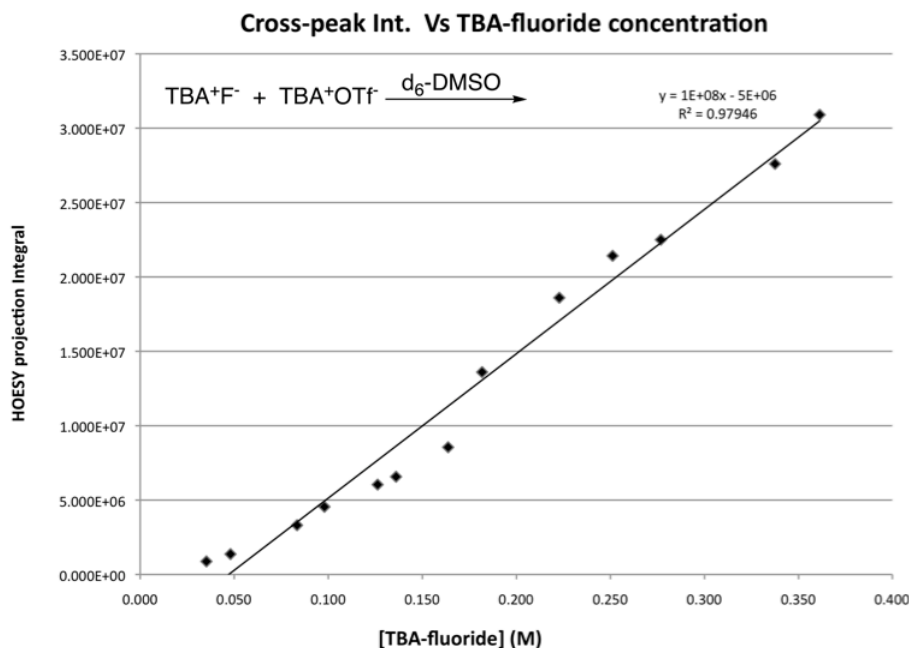
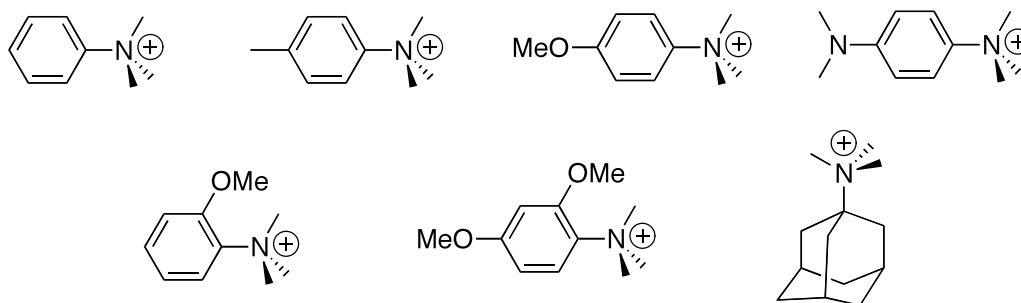


**Figure 1-6 Plot of integrated cross-peak volumes in HOESY one-dimensional projection vs. TBA-fluoride concentration.**

Triflate salts were chosen for the study because triflate anion is thought to have relatively poor ion pairing ability, thereby giving relatively sensitive measure of the fluoride ion affinities of the various cations. To test the hypothesis that integrated cross-peak volumes in HOESY one-dimensional projection represents the concentration of cation-fluoride ion pair, we did a HOESY titration of the TBA-fluoride ion pair in  $\text{d}_6$ -DMSO. The total TBA concentration was kept constant at 0.4 M, while the fluoride concentration was attenuated by mixing TBAF\* with TBAOTf. The integrated cross-peak volumes show a linear correlation to the change of TBA-fluoride concentration (Figure 1-6), which suggests that ion pair equilibrium constants can be estimated by measuring the integrated cross-peak volumes in  $^1\text{H}$ - $^{19}\text{F}$  HOESY plots.

We went on to compare the ion pairing abilities of a selection of tetrasubstituted ammonium cations in a pairwise fashion via HOESY. In a typical experiment, two tetrasubstituted ammonium triflates (structures of salts used in the pairwise HOESY study are shown in Scheme 1-4) were dissolved in  $d_6$ -DMSO and treated with a sub-stoichiometric amount of TBAF. Total salt concentration was kept at 0.4 M in  $d_6$ -DMSO for all experiments. Competition for the fluoride ion between the ammonium cations was evaluated by measuring the integrated cross-peak volumes from the  $^1\text{H}$ - $^{19}\text{F}$  HOESY spectra. An example of the  $^1\text{H}$ - $^{19}\text{F}$  HOESY spectra is shown in Figure 1-7. Mixing times (0.1 s, 0.5 s, 1.0 s) were assayed to control for differences in NOE build up. It was found that only alkyl-alkyl and aryl-aryl comparisons were valid.



**Scheme 1-4 Structure of tetrasubstituted ammonium cations used for the HOESY study.**

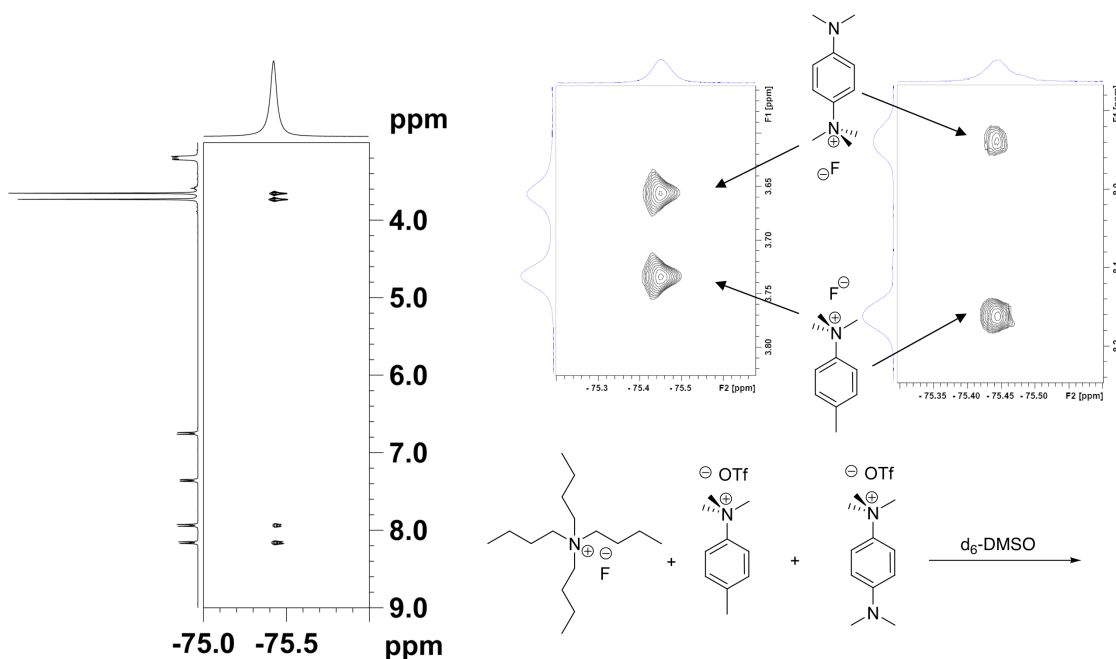


**Figure 1-7 Competitive fluoride ion pairing between 4-dimethylamino- and 4-methyl-substituted trimethylanilinium cations.**

Previous computational work has shown the importance of three strong  $\text{C-H}\cdots\text{F}^-$  interactions from independent carbon atoms to fluoride ion pairing in tetraalkylammonium salts.<sup>25</sup> In contrast to symmetrical cations like tetramethylammonium, trimethylanilinium cations can adopt two distinct anion-binding modes, namely end-on and side-on. Each of these anion binding modes permits three  $\text{C-H}\cdots\text{F}^-$  contacts to three different carbon atoms (Figure 1-8).<sup>25</sup> Density function theory (DFT) calculations (B3LYP/6-311G++(d,p), BSSE and ZPE corrected) indicate that the two binding modes are nearly equal in energy in most cases (Table 1-2). The side-on binding mode is apparent in solution, as is shown by the observation of a strong  $^1\text{H}$ - $^{19}\text{F}$

HOESY cross peak arising from the *ortho*-aryl C-H $\cdots$ F<sup>-</sup> interaction (Figure 1-7, expanded aromatic region on the right).

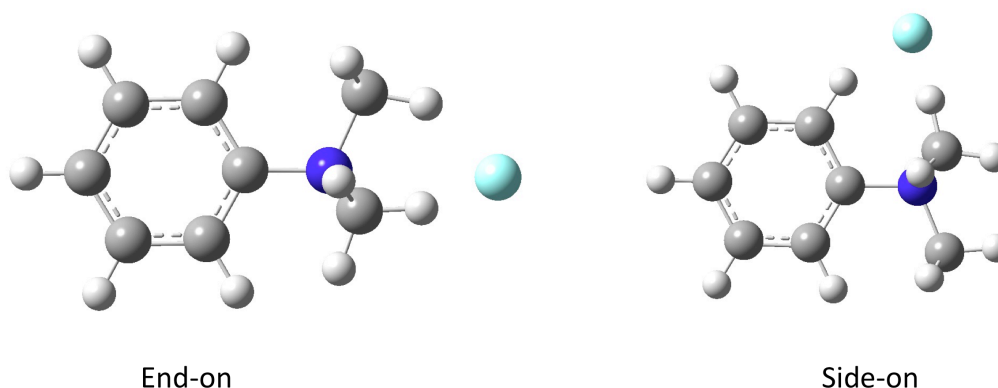


**Figure 1-8** Calculated (B3LYP/6-311G++(d,p), BSSE and ZPE corrected) ion pair of trimethylanilinium fluoride in end-on and side-on binding modes.

It is perhaps unexpected that the *ortho*-aryl C-H bonds compete effectively for fluoride with the alkyl  $\alpha$ -C-H bonds of the methyl groups, given that the former are one additional bond removed from the electropositive nitrogen atom. However, the electrophilic nature of the sp<sup>2</sup>-hybridized carbon and arene polarization are sufficient to overcome the attenuation of electron-withdrawing effect through the additional C-C bond.

**Table 1-2** Calculated (B3LYP/6-311G++(d,p), BSSE and ZPE corrected) gas phase ion pair energy for substituted trimethylanilinium fluorides in end-on and side-on binding modes.

Cation #	Substituent(s)	End-on $\Delta G_{ip}$ (kcal/mol)	Side-on $\Delta G_{ip}$ (kcal/mol)
1-1	4-H	-102.917	-102.449
1-2	4-Me	-101.529	-101.561
1-3	4-OMe	-100.645	-100.832
1-4	4-N(Me) <sub>2</sub>	-97.345	-96.102
1-5	2-OMe	-98.206	-95.412
1-6	2,4-OMe	-97.983	-95.857

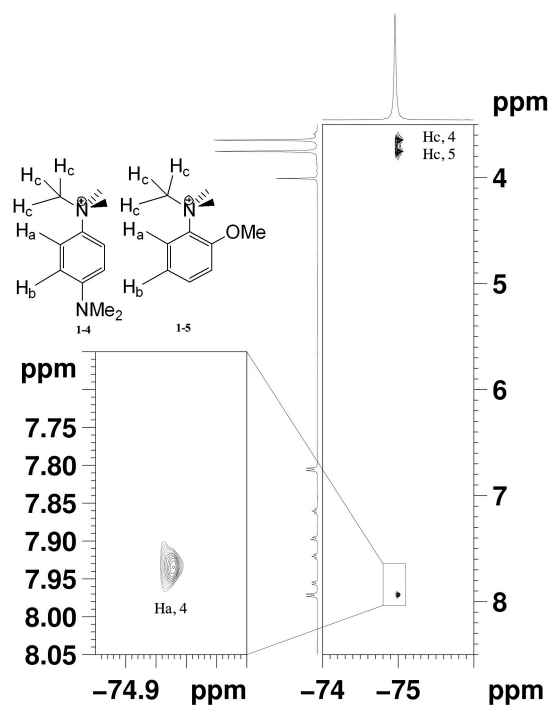
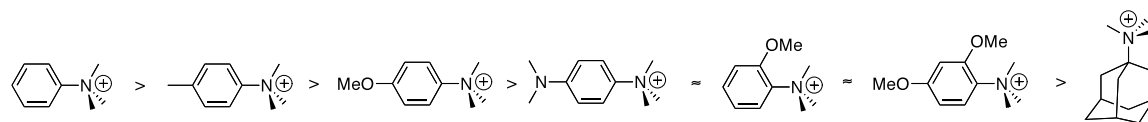


**Figure 1-9**  $^{19}\text{F}$ - $^1\text{H}$  HOESY spectrum for competitive fluoride binding by cation **1-4** and **1-5** in  $\text{d}_6$ -DMSO.

The relative affinities of *para*-substituted cations (Table 1-2, cation **1-2**, **1-3**, and **1-4**) follow the trend expected based upon the relative electron donating abilities of the substituents ( $\sigma_{\text{p}}$ : Me, -0.14; OMe, -0.27;  $\text{NMe}_2$ , -0.32). In contrast, cations **1-5** and **1-6** bind fluoride unexpectedly weakly, and the HOESY spectra show no cross peak arising from side-on binding of the fluoride ion (Figure 1-9). These observations can be understood as arising from the steric consequences of the *ortho*-methoxy substituent. The “three C-H bond” criterion requires that in side-on binding mode, the two participating methyl groups be positioned above and below the plane to the hydrogen atom at the 6-position. Such a geometry introduces significant allylic strain between the non-coordinating methyl group and the substituent at the 2-position, and strongly destabilizes

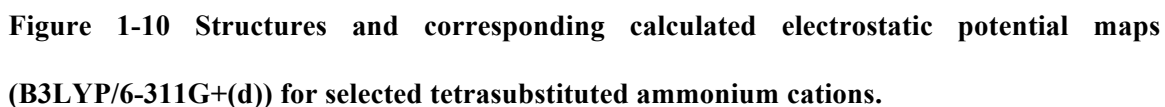
the side-on fluoride binding geometry. This allylic strain phenomenon is expected to be general and will result in decreased fluoride ion affinities for all 2-substituted trimethylanilinium cations with respect to the corresponding 4-substituted analogues. The destabilization effect is also indicated in the DFT study, which shows that side-on ion pairing energies for cation 5 and 6 are significantly higher (Table 1-2).

A comprehensive comparison of pairwise experiments permitted the cations to be ranked easily in terms of their fluoride ion affinities:



The result is in good agreement with the DFT calculated gas phase ion pair energy data shown in Table 1-2, indicating that the DFT method used accurately predicts the experimental trends. This might be surprising considering that DFT is not thought useful for modeling intermolecular interactions. However, here the interactions are actually so strong ( $\approx 90$  Kcal/mol) that they fall in the range typical for bonds.

Direct calculation of ion pair interaction energies involves significant computational effort, thus we sought an inexpensive method that would provide a reliable ranking of fluoride ion affinities. Shown in Figure 1-10 are calculated electrostatic potential maps for a selection of tetrasubstituted ammonium cations. For ease of visual comparison, a common scale indicating the variance of electrostatic potential (+0.08 a.u. (red) to +0.16 a.u. (blue)) was used for all cations. The degree of localization of positive charge indicated by the blue color in the figure is easily correlated with fluoride ion affinity except for the case of cation **1-5** and **1-6**, where steric effects are implicated in



In conclusion,  $^1\text{H}$ - $^{19}\text{F}$  HOESY experiments provide a straightforward means to rank fluoride ion affinities in the weak-binding regime. The observation of significant  $^1\text{H}$ - $^{19}\text{F}$  NOE signals for all cations studied, including the most weakly bonded TBA, indicate

that fluoride ion pairing is significant even in DMSO, a high dielectric aprotic solvent. Claims that anhydrous fluoride sources of this type are “naked” must be regarded with some skepticism. Competition experiments permit generation of a fluoride ion affinity scale and provide detailed structural information concerning the site of fluoride ion binding. The importance of three strong C-H $\cdots$ F $^-$  interactions to fluoride ion recognition in these compounds is demonstrated conclusively by the  $^1\text{H}$ - $^{19}\text{F}$  HOESY spectra and the reduced fluoride affinity of cation 5 and 6. Direct DFT calculations of ion pair interaction energies as well as calculated cation electrostatic potential maps may be used to predict solution phase ion pairing tendencies for closely related ammonium cations.

### 1.3 Stability of tetrasubstituted ammonium cations

With the methods for predicting and characterizing the fluoride affinity developed, we set out to explore fluoride ion pairing in diverse anhydrous tetrasubstituted ammonium fluorides. Our aim was to synthesis a more weakly coordinating, stable ammonium cation. Calculated electrostatic potential maps of a series of tetrasubstituted ammonium cations (Figure 1-11), showed that: 1) extending the size of alkyl substituent enhance the “blocking ability”, and weakens fluoride affinity (series TMA to TPA); 2) branched alkyl substituents are more effective in shielding the positive charge; and 3) aryl substituents appear to be more effective in delocalizing the positive charge on the central nitrogen atom. Taking into account the steric effects of *ortho* aryl substituent on disturbing fluoride binding, structures like tetrakis(2-methoxyphenyl)ammonium would be predicted to have a remarkably low fluoride affinity. However, such cations are not



synthetically accessible. Therefore, we opted to make triarylmethyl- and diaryldimethyl substituted ammonium salts instead.

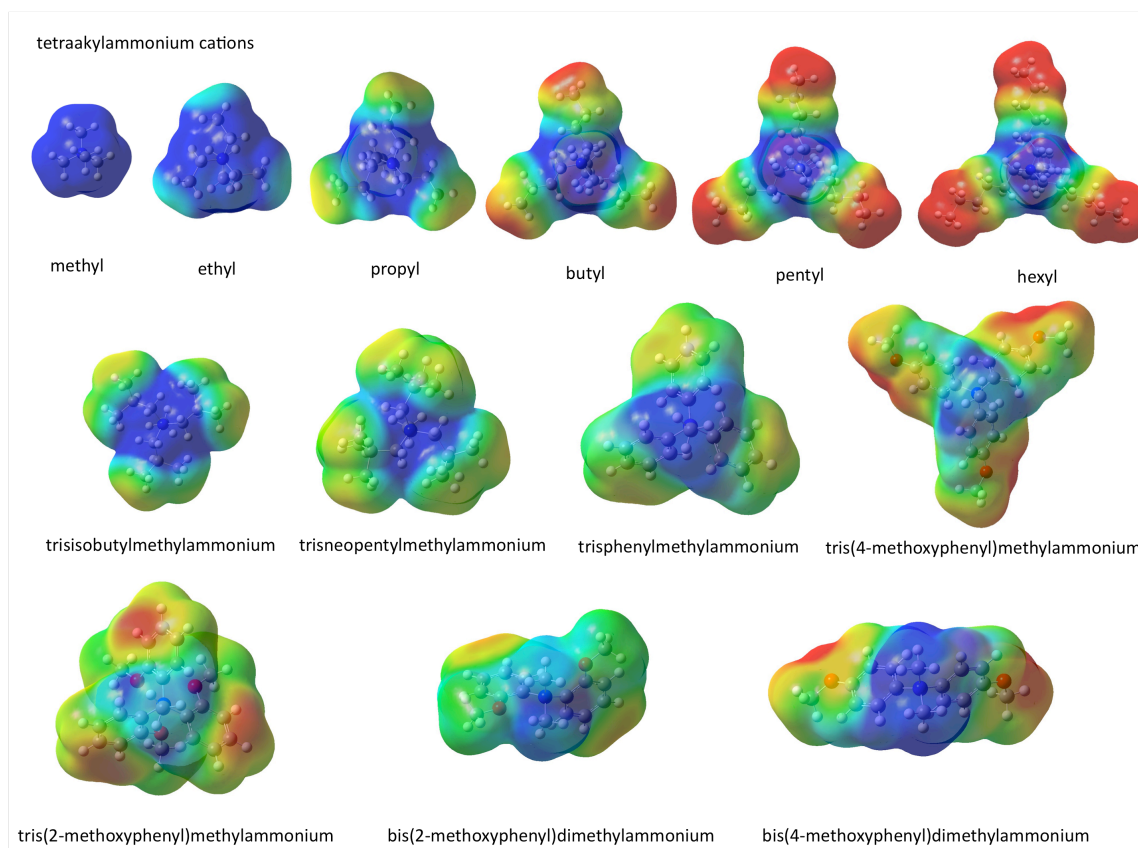


**Figure 1-11** Calculated electrostatic potential maps (B3LYP/6-311G+(d)) for selected tetrasubstituted ammonium cations.

A series of tertiary amines were conveniently converted to their corresponding ammonium triflate salts by direct alkylation with alkyltriflate in dry benzene. The salts thus formed precipitated readily from the solution and were filtered and dried over high vacuum before subjected to ion exchange with TBAF. Sterically hindered amines like tris(4-methoxyphenyl)amine and N,N,N',N'-tetrakis(isobutyl)-1,4-phenylenediamine require prolonged heating for the alkylation to take place, while tris(2-

methoxyphenyl)amine refused to react with methyl triflate under the conditions we tried.

A list of cations synthesized and/or used for this study can be found in Figure 1-12.

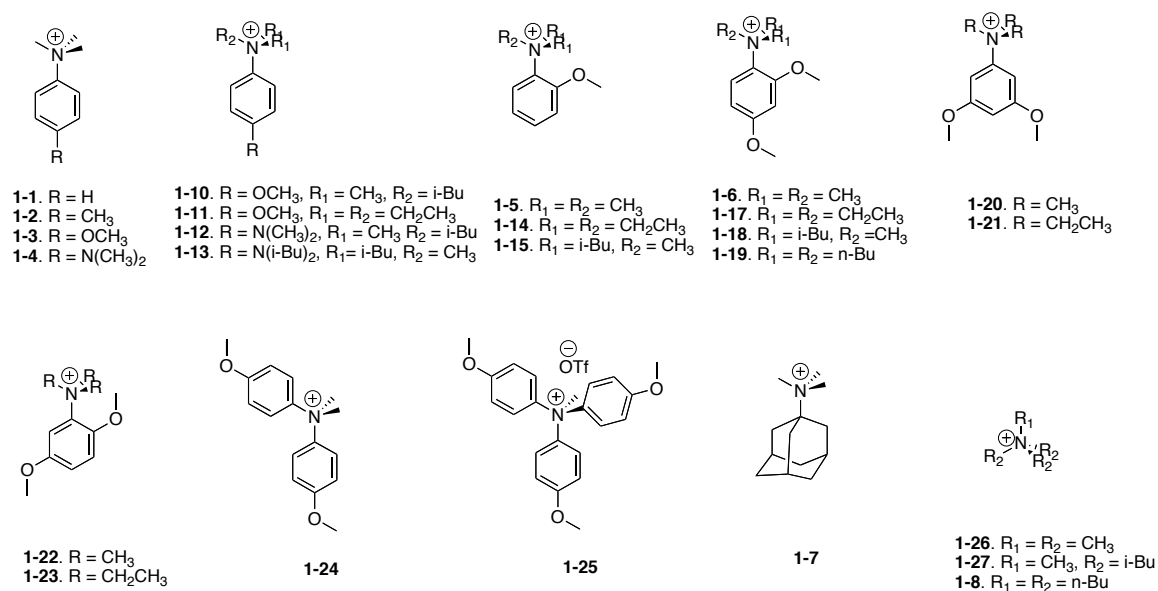


**Figure 1-12** List of cations made and/or used in the stability study.

The triflate salts were subjected to treatment with TBAF for <sup>1</sup>H-<sup>19</sup>F HOESY affinity studies. However, upon mixing with 1 equivalent of TBAF in DMSO (0.4 mM total ionic strength), some of the cations immediately underwent decomposition via either E2 (Hofmann elimination) or S<sub>N</sub>2 (demethylation) mechanisms, thereby preventing a direct measure of their fluoride affinities.

Among all salts decomposed by S<sub>N</sub>2 mechanism, cation **1-25** was the least stable, which decomposed completely to give the tris(4-methoxyphenyl)amine and methylfluoride in less than 5 minutes. Diaryldimethylammonium and trimethylanilinium salts were also decomposed by fluoride via an S<sub>N</sub>2 mechanism over time. The rate of decomposition was found to decrease with the number of aryl substituents. Most

trimethylanilinium fluorides were stable enough to allow the  $^1\text{H}$ - $^{19}\text{F}$  HOESY measurements and results were reported in the previous section.

Decomposition of six representative cations via the demethylation pathway is shown in Figure 1-13; among the trimethylanilinium cations tested, cation **1-4** was the most stable. This stands to reason since the *para*-dimethylamino group is the strongest electron donor, and the most effective in delocalizing the positive charge. All other substituted trimethylanilinium cations (including cations **1-1**, **1-2**, and **1-3**, for which rates were not monitored by NMR) decomposed at similar rates, with the exception of cation **1-22**, which decomposes at an appreciably higher rate.

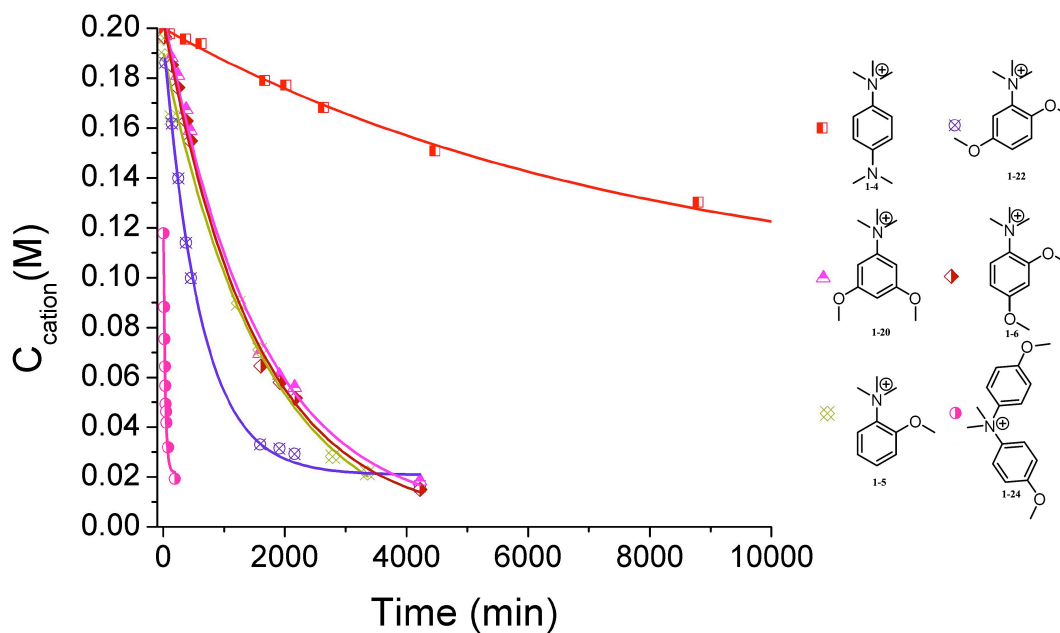


**Figure 1-13** Decomposition of tetrasubstituted ammonium salts by fluoride via demethylation pathway.

Trialkylanilinium cations bearing  $\beta$ -hydrogens that are susceptible to Hofmann elimination decompose in the presence of fluoride at much faster rates compared to tetraalkylammonium salts. Such salts with ethyl substituents (cations **1-11**, **1-14**, **1-17**, **1-21**, and **1-23**) decompose too fast for rate measurements by NMR to be practical (the reaction was completed in less than 5 minutes at room temperature). The increased susceptibility of these cations can be explained by two reasons: 1) statistically, ethyl substituents have the highest number of  $\beta$ -hydrogens; 2) and these  $\beta$  hydrogens are all easily accessible to fluoride anion.

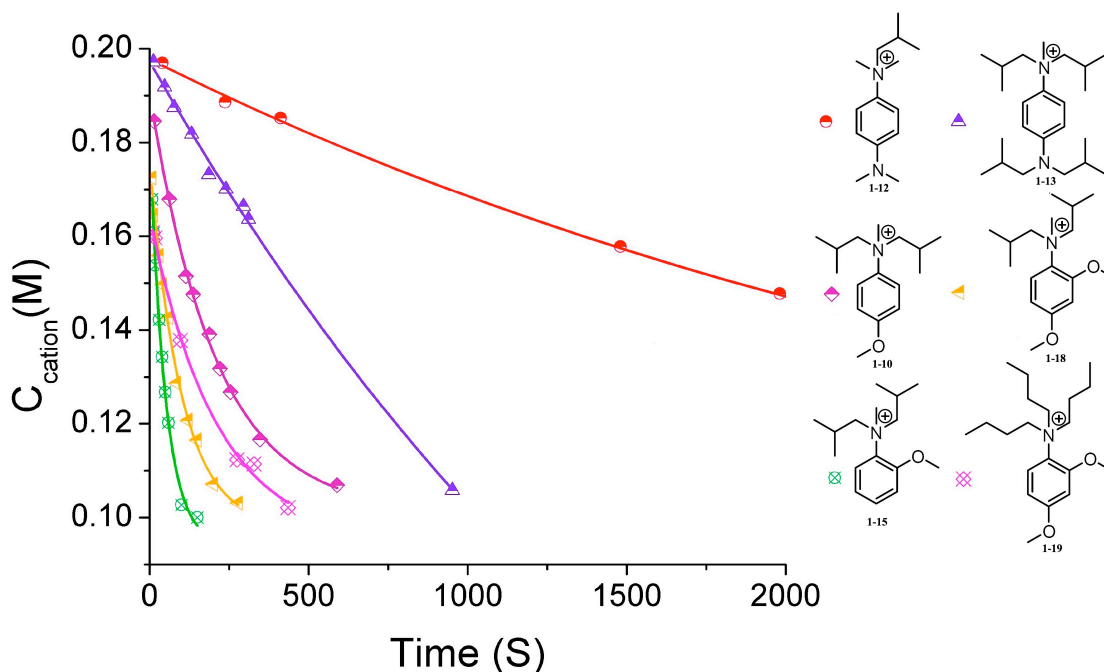


**Figure 1-14** Decomposition of tetrasubstituted ammonium cations by fluoride via Hofmann elimination pathway.

When both decomposition pathways are possible for a given cation, E2 always dominates over the  $S_N2$  pathway. Figure 1-14 listed the decomposition of six cations by

fluoride via mainly E2 pathway. Hydrogen bifluoride, the corresponding alkene and aniline are the observed product. Note that since two equivalents of fluoride are consumed by each cation, half of the initial cation remained intact at the end-point of the decomposition.

Tetraalkylammonium cations were the most stable among the ones studied. At room temperature, the decomposition of anhydrous TMAF (**1-26**) in DMSO is not detectable; trimethyladamantylammonium fluoride (**1-7**) is slightly less stable with less than 5 % decomposition in a week; both TBAF (**1-8**) and tris(isobutyl)methylammonium fluoride (**1-27**) have half-lives of more than 20 days. Direct half-life comparison of 14 different fluorides can be found in Figure 1-15.

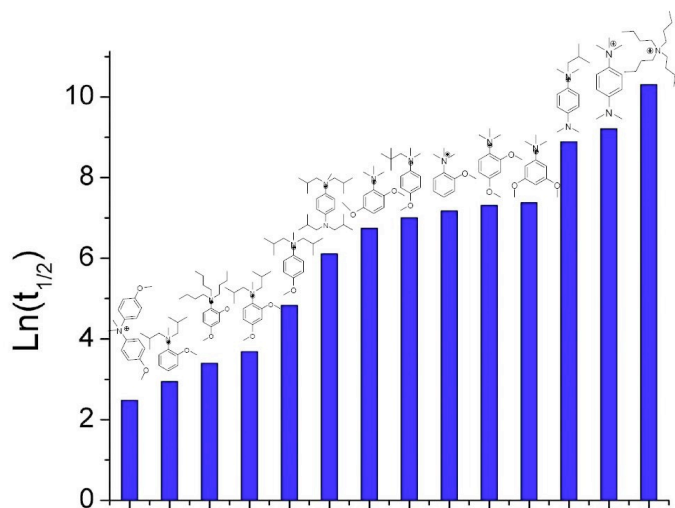


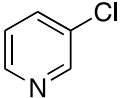
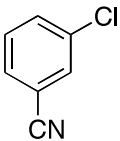
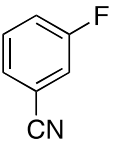
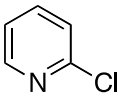
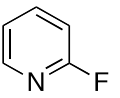
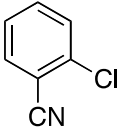

**Figure 1-15 Half lives for the decomposition of tetrasubstituted cations by fluoride in  $d_6$ -DMSO.**

In conclusion, by comparing the decomposition rates of various tetrasubstituted ammonium cations by fluoride, it was found that: 1) in general, rates of E2

decomposition is faster than the  $S_N2$  pathway, indicative of a lower activation barrier for the E2 process; 2) aryl substituents increases the nucleofugacity of; 3) release of steric strain tends to accelerate the decomposition. With that in mind, in searching for novel, low fluoride affinity cations it is reasonable to avoid tetrasubstituted ammonium cations with aryl substituents and/or alkyl substituents bearing  $\beta$ -hydrogens.

#### 1.4 Synthesis of anhydrous trineopentylmethyllammonium fluoride as a stable nucleophilic fluorinating reagent compatible with high temperature applications

**Table 1-3 Helax reactions of selective unactivated chloroaromatic compounds by TBAF\*.<sup>22</sup>**

Entry	Substrate	Conditions	Product	% Yield <sup>a</sup>
1		4 eq. TBAF* 14 d	No reaction.	0
2		1.5 eq. TBAF* 5 d		2
3		4 eq. TBAF* 4 d		80
4		1.5 eq. TBAF* 18 h		>95

<sup>a</sup> All yields are calculated from integration of  $^1\text{H}$  and  $^{19}\text{F}$  NMR signals in comparison to an added internal standard.

Even with the superior fluorinating power of TBAF\*, direct nucleophilic fluorination of chloroarenes requires activation by strong electron-withdrawing groups. For example, as shown in Table 1-3, little or no fluorination occurred for 3-

chloropyridine and 3-chlorobenzonitrile at room temperature, even with a gross excess of TBAF\*. For 2-chloropyridine, fluorination took up to 2 weeks to reach 80 % conversion with 4 equivalent of TBAF\* at room temperature. In these cases, heating may be required to overcome the activation barrier and accelerate the fluorinating process.

Although TBAF is stable in polar solvent such as DMSO and acetonitrile for days at room temperature, fast decomposition by E2 mechanism occurs upon heating. The instability of the TBAF upon heating limits its use at elevated temperatures. Anhydrous TMAF, on the other hand has better stability but fluoride nucleophilicity is attenuated due to the high fluoride affinity of TMA cation. Therefore, we sought to synthesize nucleophilic fluorinating reagents featuring cations more stable than TBA but with comparably weak fluoride affinities.

From the stability study described in the previous section, we know that aryl substitution significantly accelerates both the  $S_N2$  and E2 decomposition pathways; therefore aryl substitution was excluded in our design. To shut off the  $\beta$  hydrogen elimination pathway, alkyl groups with  $\beta$  hydrogens should also be avoided. As the smallest alkyl substituent to bear no  $\beta$  hydrogen except for the methyl group, the neopentyl group appears to be an ideal choice. Its bulkiness would also make the  $S_N2$  decomposition unlikely to occur. Since it is not synthetically practical to make tetraneopentylammonium salts, we settled on making trineopentylmethylammonium salts instead. Following a reported procedure,<sup>26</sup> we were able to synthesize trineopentylamine in good yield from pivaloyl chloride and neopentylamine. Trineopentylamine was

quaternized effectively with methyl triflate to give the novel trineopentylmethylammonium triflate in good yield (see experimental section for details).

A computational study showed that two possible binding mode (Figure 1-16) of similar ion-pair energies exist for the TNPMA-fluoride ion pair. To be specific, fluoride interacts with TNPMA cation according to the “three C-H bond” criterion; the three protons are either all from the methyl substituent (front binding) or from three different neopentyl groups (back binding).

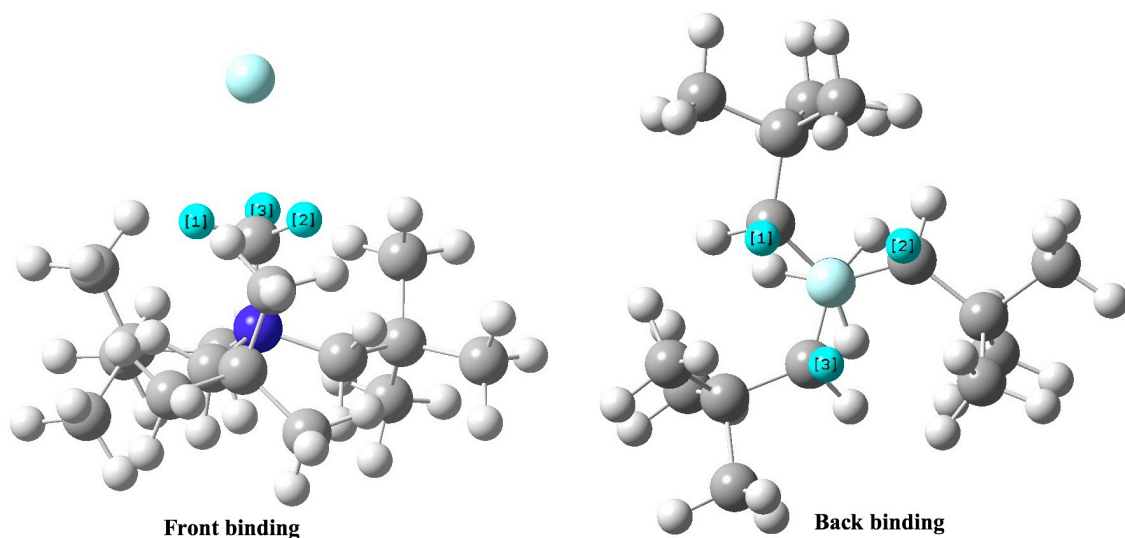


**Figure 1-16** Calculated (B3LYP/6-311G++(d,p))structures of TNPMA-fluoride ion pair.

Competitive fluoride binding was observed for the mixture of 1:1 TBAF\*/TNPMAOTf in  $d_6$ -DMSO. Cross peaks arising from fluoride and  $\alpha$ -protons on both cations were present in the  $^1\text{H}$ - $^{19}\text{F}$  HOESY spectrum (Figure 1-17), indicating that the two cations have comparable fluoride affinity. The two predicted fluoride binding mode for TNPMA cation were also confirmed; and even the cross peak from  $\beta$ -methyl groups on TNPMA caused by back binding were clearly observable. On the other hand,



cross peaks from  $\beta$ -,  $\gamma$ -, and  $\delta$ -protons on TBA were reduced to almost nonexistence, indicating the fluoride-affinity of TBA is slightly lower than that of TNPMA.

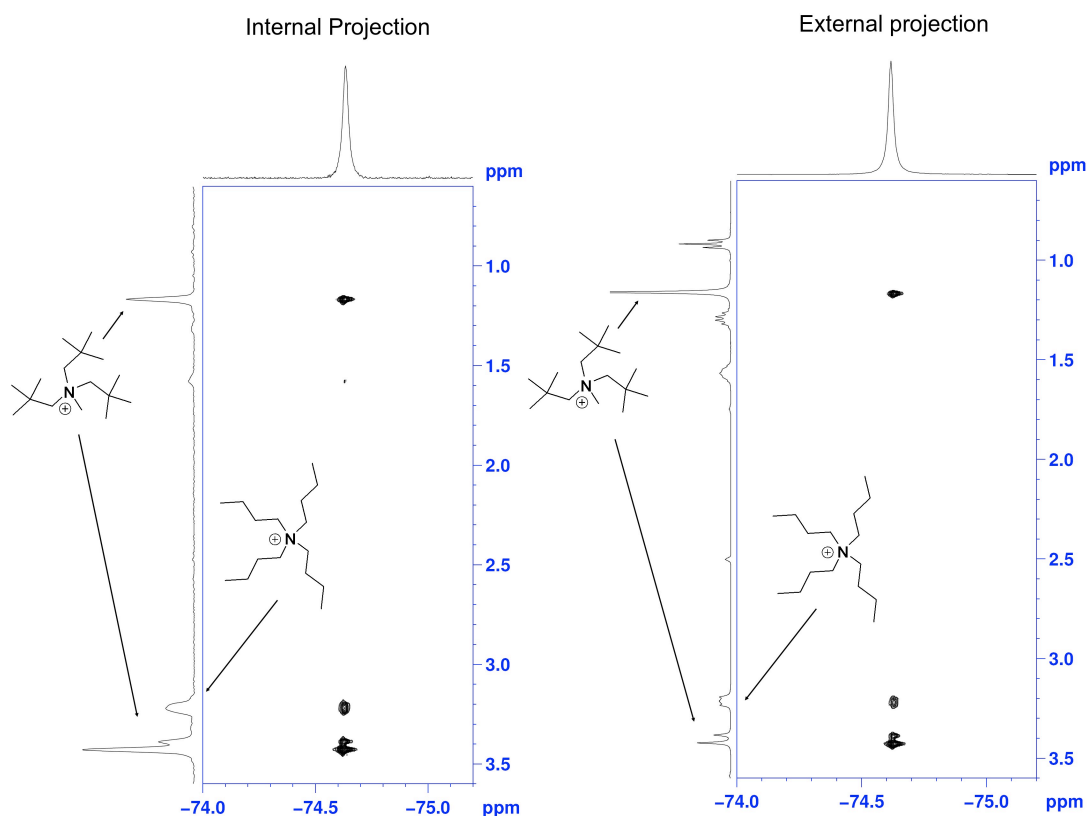


**Figure 1-17 Competitive fluoride binding indicated by  $^1\text{H}$ - $^{19}\text{F}$  HOESY spectra of 1:1 mixture of TNPMAOTf and TBAF\* in  $\text{d}_6$ -DMSO.**

The different solubility of TBAF\* and anhydrous TNPMAF (TNPMAF\*) in THF allowed us to make anhydrous TNPMAF by a simple metathesis reaction. To the solution of freshly made TBAF\* in THF was added one equivalent of dry TNPMAOTf, the mixture was chilled to  $-40\text{ }^\circ\text{C}$ , filtered and washed with cold THF to yield TNPMAF\* as a white solid ( $\sim 60\%$  yield). The salt thus obtained contains less than 1 % of TBA cation

and about 2 % of the triflate anion. It was suitable for use as highly reactive fluorinating agent without further purifications.

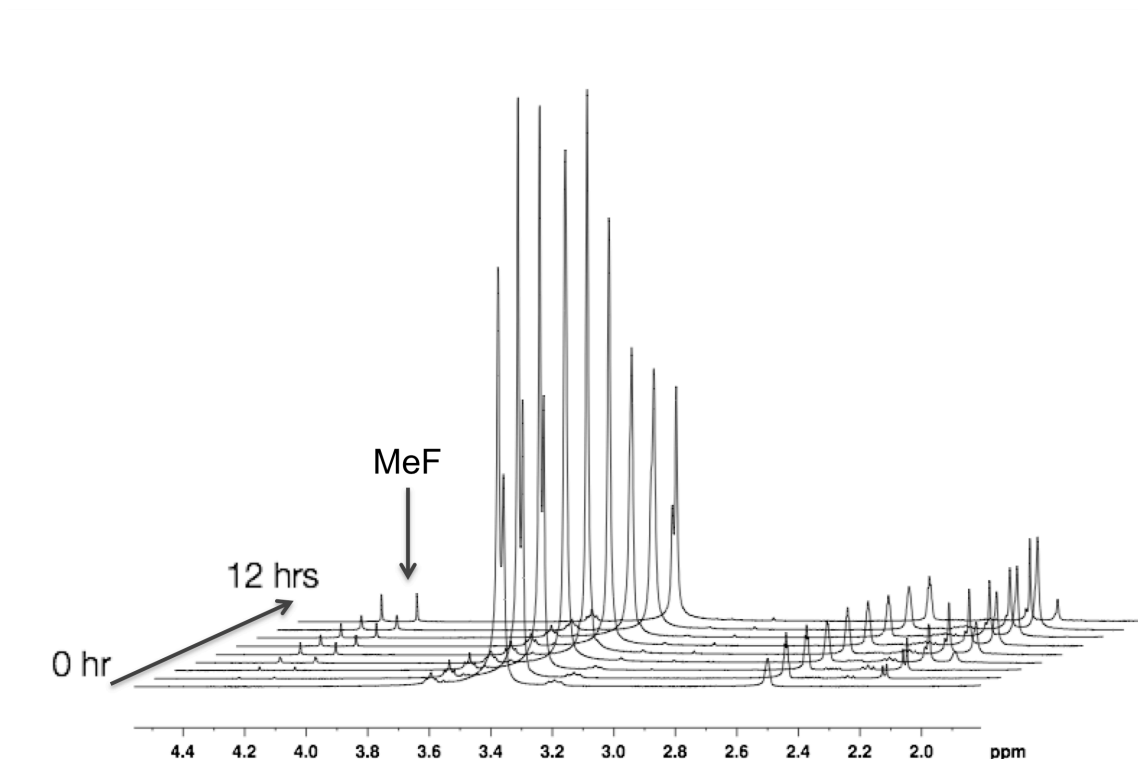


**Figure 1-18 Decomposition of TNPMAF\* @ 80 °C monitored by  $^1\text{H}$  NMR.**

To test the thermal stability of TNPMAF\*, a solution of 0.2 mM of TNPMAF\* in DMSO was heated to 85 °C. Successive  $^1\text{H}$  NMR spectra of the solution taken at 60 minute intervals showed that less than 10 % of the cation decomposed to give methyl fluoride and trineopentylamine after 12 hours of heating (Figure 1-18). Under the same conditions, half of the TBAF\* completely decomposed (all fluoride was consumed) in less than 100 minutes. For direct stability comparison of TNPMA and TBA cation, mixture of TNPMAF\* and TBAF\* in DMSO was heated to 130 °C.  $^1\text{H}$  NMR showed that TBA cation completely decomposed in 10 min, while TNPMA cation remained

intact. These experiments demonstrate the superior thermal stability of TNPMA compared to TBA.

Halogen exchange (Halex) reactions of chloro aromatics and TNPMAF\* were carried out at 145 °C in DMSO. For 2-chlorobenzonitrile and 2-chloropyridine, the reaction time can be significantly shortened compared to the corresponding reaction using TBAF\* at room temperature (5 min vs. 18 h, 20 min vs. 4 days). Thus, TNPMAF\* can replace TBAF\* for fluorination of relatively unactivated substrates when short reaction times are required. Another advantage of TNPMA cation is that it reacts with fluoride by nucleophilic substitution, thus only one equivalent of fluoride is consumed during the decomposition reaction. (Compared to the two equivalent of fluoride trapped as  $\text{HF}_2^-$  in the case of TBA decomposition.) Thus, substitution of TBA with TNPMA as the counterion for fluoride will help minimize the amount of the fluorinating agent needed for a specific reaction.

In summary, despite the fact the TNPMA interacts with fluoride slightly more strongly than TBA, its higher thermostability and better decomposition profile make TNPMA superior to TBA as a counterion for anhydrous fluoride. However, fluorination of 3-chlorobenzonitrile and 3-chloropyridine was not improved by substituting TBAF\* with TNPMAF\*. It turned out that large amount of bifluoride formed upon prolonged heating, which was accompanied by the disappearance of the most acidic proton at position 2 on the aromatic ring in  $^1\text{H}$  NMR spectra. This can be understood given that the fluoride is such a strong base that is able to deprotonate the proton at position 2 to form bifluoride, which is of much less nucleophilicity. Hence, direct fluorination of

unactivated aromatic compounds bearing acidic protons is still not practical, and an alternative route is needed to obtain the corresponding fluoro aromatics. The fluorination of unactivated aromatic compounds will be addressed later in this thesis.

## 1.5 Experimental

**General:** All materials were obtained from commercial sources and used as received unless otherwise noted. Methyl triflate and ethyl triflate were purchased from Aldrich and used without further purification, butyl triflate was freshly made from n-butanol and triflate anhydride. Acetonitrile and acetonitrile- $d_3$  were heated at reflux over  $P_2O_5$ , distilled into flame-dried storage tubes, transferred to the glove box, and were stored there over  $CaH_2$ . Benzene and benzene- $d_6$  were heated at reflux over  $CaH_2$  overnight and distilled directly into flame-dried storage tubes under dry nitrogen. Tetrahydrofuran (THF) was dried over Na/benzophenone and distilled into a flame dried storage flask under dry nitrogen. All glassware, syringes, and NMR tubes were oven dried (140 °C) for more than 24 h before they were transferred into the glove box for use. TBAF was synthesized according to our previously reported method<sup>18</sup>. All NMR experiments reported here were performed using a 400 MHz (QNP probe) Bruker NMR spectrometer in the NMR laboratory at the University of Nebraska-Lincoln.

**Calculations:** All calculations were performed using the Gaussian03 suite of programs and visualization was performed with GaussView03.<sup>27</sup> Structures were optimized and their energies calculated using DFT B3LYP/6311G++(d,p) methods. Frequency

calculations on minimized structures were performed to make the zero point energy and thermal corrections.

**General procedure for synthesis substituted dialkylanilines:** Under an atmosphere of N<sub>2</sub>, potassium carbonate (4.14 g, 30 mmol) and an appropriate iodoalkane (30 mmol) were added to a solution of substituted aniline (10 mmol) in acetonitrile (20 mL). The stirred reaction mixture was heated at reflux for 12 - 36 hours. The progress of the reaction was monitored by thin layer chromatography (TLC, 60 Å silica, hexanes/dichloromethane). After the reaction mixture was allowed to cool to room temperature, it was filtered to remove the inorganic salts, which were washed with dichloromethane (3 × 10 mL). The wash was combined with the filtrate and concentrated to yield the crude product, which was chromatographed (60 Å silica, hexanes/dichloromethane) to give the pure product. Yields range from 40 % to 60 %; except that in the case of permethylation, the trimethylanilinium iodides was isolated in excellent yields (>90 %). The products were characterized by <sup>1</sup>H and <sup>13</sup>C NMR spectroscopy.

**General procedure for the synthesis of trialkylanilinium triflates:** The appropriate alkyl triflate (2 mmol) was added to a solution of appropriate substituted dialkylaniline (2 mmol) in dry benzene (5 mL). The reaction mixture was stirred at room temperature to 45 °C for 72 h. At the conclusion of the reaction the trialkylanilinium triflate separated from the benzene solution as either a white crystalline solid or an immiscible layer of ionic

liquid. The crystalline compounds were isolated by simple filtration followed by washing with dry benzene ( $3 \times 3$  mL). The immiscible ionic liquids were extracted with dry hexanes (3 times) to remove the residual benzene and starting materials, and exposed to dynamic vacuum for 3 days. The products were characterized by  $^1\text{H}$  and  $^{13}\text{C}$  NMR spectroscopy.

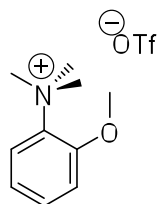
**General procedure for the synthesis of triethylanilinium iodides:** Ethyl iodide (7 mmol) and potassium carbonate (10 mmol) were added to a solution of appropriate substituted aniline (2 mmol) in dry acetonitrile (15 mL). The reaction mixture was heated at reflux for 24 h. At the conclusion of the reaction, the solvent was evaporated and the product was washed with water and recrystallized from DCM/Hexane. The products were characterized by  $^1\text{H}$  and  $^{13}\text{C}$  NMR spectroscopy.

**General procedure for the pairwise HOESY experiments:** In a nitrogen charged glove box, TBAF\* (0.1 mmol, 26.2 mg) was added to a solution of two appropriate tetrasubstituted ammonium triflates (0.1 mmol of each) in  $d_6$ -DMSO (0.5 mL). The solution was transferred into an NMR tube; the tube was sealed with a rubber septum and parafilm, and removed from the glove box.  $^1\text{H}$ ,  $^{19}\text{F}$ , and  $^1\text{H}$ - $^{19}\text{F}$ -HOESY (aliphatic and aromatic region were investigated separately) spectra were obtained for the sample. The acquisition parameters for the HOESY spectra were:  $D_8 = 0.5$  s,  $\text{SW (F)} = 4$  ppm,  $\text{SW (P)} = 3$  ppm,  $\text{td} = 4\text{k}$ . For cations having a fluoride affinity similar to that of TBA, a head-to-head comparison was made. (The DMSO solution contained only two cations, not three.)

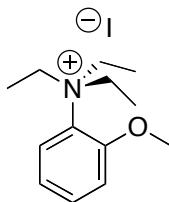
**General procedure for the decomposition study:** In a nitrogen charged glove box, TBAF\* (0.1 mmol, 26.2 mg) was added to a solution of an appropriate tetrasubstituted ammonium triflate (0.1 mmol) in  $d_6$ -DMSO (0.5 mL). The solution was transferred into an NMR tube; the tube was sealed with a rubber septum and parafilm, and removed from the glove box. The decomposition of the cation was followed by  $^1\text{H}$  NMR until no further change was observed. The concentration of the cation was calculated by integrating the corresponding peaks against a standard (solvent peak or one of the TBA peaks) and plotted against time.

**General procedure for fluorination reactions with trineopentylmethylammonium fluoride:** In a nitrogen charged glove box, anhydrous TNPMAF (0.1 mmol, 26.2 mg) was added to a solution of appropriate chloro-aromatic precursor (0.1 mmol) in  $d_6$ -DMSO (0.5 mL). The solution was transferred into a J-Young NMR tube, sealed, and the NMR tube was removed from the glove box. Initial  $^1\text{H}$  and  $^{19}\text{F}$  NMR spectra were gathered before the NMR tube was placed into a 140 °C oil bath. The progress of the reaction was monitored by  $^{19}\text{F}$  NMR until the fluoride peak disappeared completely. Yields were determined by integrating final  $^1\text{H}$  and  $^{19}\text{F}$  NMR spectra.

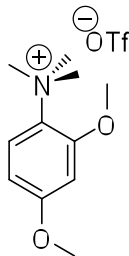
### Characterization of quaternary ammonium salts



**N,N,N-Trimethyl-2-methoxyanilinium triflate:**  $^1\text{H}$  NMR ( $\text{d}_6$ -DMSO, 400 MHz, 25 °C):  $\delta$  7.78 (d,  $J$  = 8 Hz, 1 H), 7.59 (t,  $J$  = 8 Hz, 1 H), 7.40 (d,  $J$  = 8 Hz, 1 H), 7.17 (t,  $J$  = 8 Hz, 1 H), 4.02 (s,  $-\text{OCH}_3$ , 3 H), 3.66 (s,  $-\text{CH}_3$ , 9 H);  $^{13}\text{C}$  NMR ( $\text{d}_6$ -DMSO, 100 MHz, 25 °C):  $\delta$  151.68, 133.55, 131.99, 120.71(q, OTf), 121.7, 121.19, 115.00, 56.62, 55.14;  $^{19}\text{F}$  NMR ( $\text{d}_6$ -DMSO, 376 MHz, 25 °C):  $\delta$  -77.74.



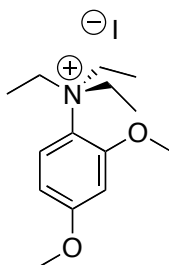
**N,N,N-Triethyl-2-methoxyanilinium iodide:**  $^1\text{H}$  NMR ( $\text{CD}_3\text{CN}$ , 400 MHz, 25 °C):  $\delta$  7.64 (d,  $J$  = 8 Hz, 1 H), 7.59 (t,  $J$  = 8 Hz, 1 H), 7.32 (d,  $J$  = 8 Hz, 1 H), 7.16 (t,  $J$  = 8 Hz, 1 H), 3.98 (s, 3 H), 3.97 (q,  $J$  = 7.2 Hz, 6 H), 1.09 (t,  $J$  = 7.2 Hz, 9 H);  $^{13}\text{C}$  NMR ( $\text{CD}_3\text{CN}$ , 100 MHz, 25 °C):  $\delta$  153.44, 133.23, 128.91, 125.88, 122.59, 115.97, 57.61, 55.41, 9.15.



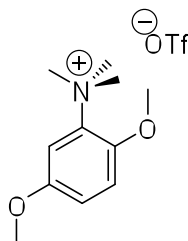
**N,N,N-Trimethyl-2,4-dimethoxyanilinium triflate:**  $^1\text{H}$  NMR ( $\text{d}_6$ -DMSO, 400 MHz, 25 °C):  $\delta$  7.67 (d,  $J$  = 9.4 Hz, 1 H), 6.87 (d,  $J$  = 2.6 Hz, 1 H), 6.68 (dd,  $J_1$  = 9.4 Hz,  $J_2$  = 2.6



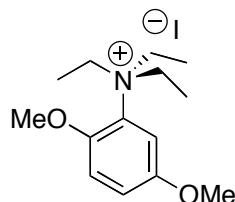
Hz, 1 H), 4.00 (s, -OCH<sub>3</sub>, 3 H), 3.84 (s, -OCH<sub>3</sub>, 3 H), 3.61 (s -CH<sub>3</sub>, 9 H); <sup>13</sup>C NMR (d<sub>6</sub>-DMSO, 100 MHz, 25 °C): δ 161.46, 152.86, 127.01, 122.67, 120.68 (q, OTf), 105.10, 101.37, 56.72, 55.85, 55.39; <sup>19</sup>F NMR (d<sub>6</sub>-DMSO, 376 MHz, 25 °C): δ -77.75.



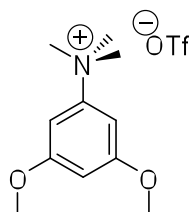
**N,N,N-Triethyl-2,4-dimethoxyanilinium iodide:** <sup>1</sup>H NMR (CD<sub>3</sub>CN, 400 MHz, 25 °C): δ 7.55 (d, J = 9.4 Hz, 1 H), 6.76 (d, J = 2.7 Hz, 1 H), 6.65 (dd, J<sub>1</sub> = 9.4 Hz, J<sub>1</sub> = 2.7 Hz, 1 H), 3.95 (s, -OCH<sub>3</sub>, 3 H), 3.91 (q, J = 7.3 Hz, 6 H), 3.84 (s, 3 H), 1.08 (t, J = 7.3 Hz, 9 H); <sup>13</sup>C NMR (CD<sub>3</sub>CN, 100 MHz, 25 °C): δ 163.05, 154.61, 126.99, 121.95, 106.39, 102.48, 57.83, 57.00, 55.52, 9.13.



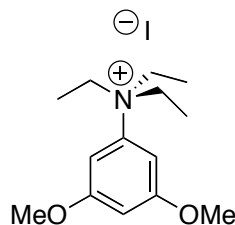
**N,N,N-Trimethyl-2,5-dimethoxyanilinium triflate:** <sup>1</sup>H NMR (d<sub>6</sub>-DMSO, 400 MHz, 25 °C): δ 7.34(d, J = 9.1 Hz, 1 H), 7.28 (d, J = 2.7 Hz, 1 H), 7.19 (dd, J<sub>1</sub> = 9.1 Hz, J<sub>2</sub> = 2.7, 1 H), 3.96 (s, -OCH<sub>3</sub>, 3 H), 3.81 (s, -OCH<sub>3</sub>, 3 H), 3.64 (s, -CH<sub>3</sub>, 9 H); <sup>13</sup>C NMR (d<sub>6</sub>-DMSO, 100 MHz, 25 °C): δ 125.88, 145.46, 133.88, 120.68 (q, OTf), 115.99, 115.53, 109.52, 56.90, 56.01, 55.11; <sup>19</sup>F NMR (d<sub>6</sub>-DMSO, 376 MHz, 25 °C): δ -77.73.



**N,N,N-Triethyl-2,5-dimethoxyanilinium iodide:**  $^1\text{H}$  NMR ( $\text{CD}_3\text{CN}$ , 400 MHz, 25  $^\circ\text{C}$ ):  $\delta$  7.26 (d,  $J$  = 9.1 Hz, 1 H), 7.15 (dd,  $J_1$  = 9.1 Hz,  $J_2$  = 2.7 Hz, 1 H), 7.11 (d,  $J$  = 2.7 Hz, 1 H), 3.95 (q,  $J$  = 7.2 Hz, 6 H), 3.93 (s,  $-\text{OCH}_3$ , 3 H), 3.82 (s,  $-\text{OCH}_3$ , 3 H), 1.10 (t,  $J$  = 7.2 Hz, 9 H);  $^{13}\text{C}$  NMR ( $\text{CD}_3\text{CN}$ , 100 MHz, 25  $^\circ\text{C}$ ):  $\delta$  154.82, 147.22, 129.53, 116.85, 116.79, 113.09, 57.79, 57.10, 55.23, 9.00.

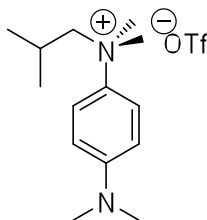


**N,N,N-Trimethyl-3,5-dimethoxyanilinium triflate:**  $^1\text{H}$  NMR ( $\text{d}_6\text{-DMSO}$ , 400 MHz, 25  $^\circ\text{C}$ ):  $\delta$  7.06 (d,  $J$  = 1.8 Hz, 2 H), 6.72 (t,  $J$  = 1.8 Hz, 1 H), 3.84 (s,  $-\text{OCH}_3$ , 6 H), 3.57 (s -  $\text{CH}_3$ , 9 H);  $^{13}\text{C}$  NMR ( $\text{d}_6\text{-DMSO}$ , 100 MHz, 25  $^\circ\text{C}$ ):  $\delta$  161.11, 148.90, 120.72 (q, OTf), 100.77, 99.58, 56.35, 56.02;  $^{19}\text{F}$  NMR ( $\text{d}_6\text{-DMSO}$ , 376 MHz, 25  $^\circ\text{C}$ ):  $\delta$  -77.73.

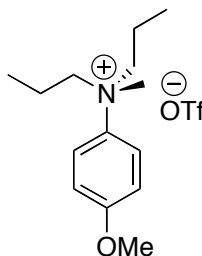


**N,N,N-Triethyl-3,5-dimethoxyanilinium iodide:**  $^1\text{H}$  NMR ( $\text{CD}_3\text{CN}$ , 400 MHz, 25  $^\circ\text{C}$ ):  $\delta$  6.80 (d,  $J$  = 1.8 Hz, 2 H), 6.66 (t,  $J$  = 1.8 Hz, 1 H), 3.86 (s,  $-\text{OCH}_3$ , 6 H), 3.81 (q,  $J$  = 7.4

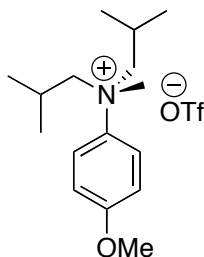
Hz, 6 H), 1.10 (t,  $J = 7.4$  Hz, 9 H);  $^{13}\text{C}$  NMR ( $\text{CD}_3\text{CN}$ , 100 MHz, 25 °C):  $\delta$  163.10, 148.17, 102.40, 102.07, 57.25, 57.04, 8.52.



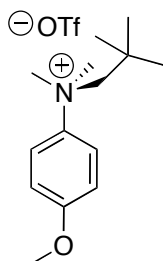
**N,N-Dimethyl-N-isobutyl-4-(dimethylamino)anilinium triflate:**  $^1\text{H}$  NMR ( $\text{d}_6\text{-DMSO}$ , 400 MHz, 25 °C):  $\delta$  7.66 (d,  $J = 9.3$  Hz, 2 H), 6.79 (d,  $J = 9.3$  Hz, 2 H), 3.71 (d,  $J = 4.9$  Hz, 2 H), 3.51 (s,  $-\text{CH}_3$ , 6 H), 2.96 (s,  $-\text{CH}_3$ , 6 H), 1.79 (m,  $-\text{CH}-$ , 1 H), 0.72 (d,  $J = 6.6$  Hz, 6 H);  $^{13}\text{C}$  NMR ( $\text{d}_6\text{-DMSO}$ , 100 MHz, 25 °C):  $\delta$  150.3, 132.85, 121.79, 111.67, 75.13, 75.13, 54.39, 23.87, 21.79;  $^{19}\text{F}$  NMR ( $\text{d}_6\text{-DMSO}$ , 376 MHz, 25 °C):  $\delta$  -77.71.



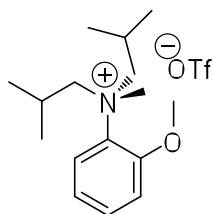
**N,N-Dipropyl-N-methyl-4-methoxyanilinium triflate:**  $^1\text{H}$  NMR ( $\text{d}_6\text{-DMSO}$ , 400 MHz, 25 °C):  $\delta$  7.73 (d,  $J = 9.4$  Hz, 2 H), 7.14 (d,  $J = 9.4$  Hz, 2 H), 3.85 (td,  $J_1 = 12.4$  Hz,  $J_2 = 4.6$  Hz, 2 H), 3.83 (s,  $-\text{CH}_3$ , 3 H), 3.67 (td,  $J_1 = 12.4$  Hz,  $J_2 = 4.6$  Hz, 2 H), 3.47 (s,  $-\text{OCH}_3$ , 3 H), 1.61 (m,  $-\text{CH}_2-$ , 2 H), 1.11 (m,  $-\text{CH}_2-$ , 2 H), 0.81 (t,  $J = 7.4$  Hz, 6 H);  $^{13}\text{C}$  NMR ( $\text{d}_6\text{-DMSO}$ , 100 MHz, 25 °C):  $\delta$  159.53, 134.55, 123.12, 115.01, 69.16, 55.69, 47.22, 15.86, 10.23, 21;  $^{19}\text{F}$  NMR ( $\text{d}_6\text{-DMSO}$ , 376 MHz, 25 °C):  $\delta$  -77.72.



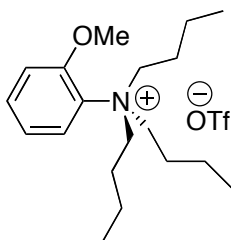
**N,N-Diisobutyl-N-methyl-4-methoxyanilinium triflate:**  $^1\text{H}$  NMR ( $\text{d}_6$ -DMSO, 400 MHz, 25 °C):  $\delta$  7.82 (d,  $J$  = 9.4 Hz, 2 H), 7.14 (d,  $J$  = 9.4 Hz, 2 H), 3.88 (dd,  $J_1$  = 13.4 Hz,  $J_2$  = 6.1 Hz, 2 H), 3.83 (s,  $-\text{CH}_3$ , 3 H), 3.60 (dd,  $J_1$  = 13.4 Hz,  $J_2$  = 4.4 Hz, 2 H), 3.52 (s,  $-\text{OCH}_3$ , 3 H), 1.82 (m,  $-\text{CH}-$ , 2 H), 0.94 (d,  $J$  = 6.8 Hz, 6 H), 0.49 (d,  $J$  = 6.8 Hz, 6 H);  $^{13}\text{C}$  NMR ( $\text{d}_6$ -DMSO, 100 MHz, 25 °C):  $\delta$  159.73, 134.55, 123.84, 114.69, 76.01, 55.70, 46.53, 23.38, 22.47, 21.59;  $^{19}\text{F}$  NMR ( $\text{d}_6$ -DMSO, 376 MHz, 25 °C):  $\delta$  -77.72.



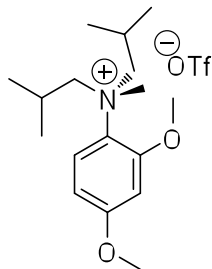
**N,N-Dimethyl-N-neopentyl-4-methoxyanilinium triflate:**  $^1\text{H}$  NMR ( $\text{CD}_3\text{CN}$ , 400 MHz, 25 °C):  $\delta$  7.68 (d,  $J$  = 9.6 Hz, 2 H), 7.09 (d,  $J$  = 9.6 Hz, 2 H), 3.85 (s,  $-\text{OCH}_3$ , 3 H), 3.75 (s,  $-\text{CH}_2-$ , 2 H), 3.53 (s,  $-\text{CH}_3$ , 6 H), 0.83 (s,  $-\text{C}(\text{CH}_3)_3$ , 9 H);  $^{13}\text{C}$  NMR ( $\text{CD}_3\text{CN}$ , 100 MHz, 25 °C):  $\delta$  161.60, 138.10, 123.62, 115.96, 80.15, 57.92, 56.70, 34.21, 29.50;  $^{19}\text{F}$  NMR ( $\text{CD}_3\text{CN}$ , 376 MHz, 25 °C):  $\delta$  -77.72.



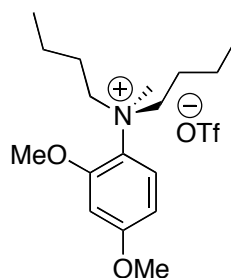
**N,N-Diisobutyl-N-methyl-2-methoxyanilinium triflate:**  $^1\text{H}$  NMR ( $\text{d}_6$ -DMSO, 400 MHz, 25 °C): 7.73 (d,  $J$  = 8 Hz, 1 H), 7.62 (t,  $J$  = 8 Hz, 1 H), 7.35 (d,  $J$  = 8 Hz, 1 H), 7.19 (t,  $J$  = 8 Hz, 1 H), 4.28 (dd,  $J_1$  = 13.4 Hz,  $J_2$  = 4.4 Hz, 2 H), 3.99 (s,  $-\text{OCH}_3$ , 3 H), 3.60 (s,  $-\text{CH}_3$ , 3 H), 3.48 (dd,  $J_1$  = 13.4 Hz,  $J_2$  = 6.1 Hz, 2 H), 1.77 (m,  $-\text{CH}-$ , 2 H), 0.93 (d,  $J$  = 6.8 Hz, 6 H), 0.50 (d,  $J$  = 6.8 Hz, 6 H);  $^{13}\text{C}$  NMR ( $\text{d}_6$ -DMSO, 100 MHz, 25 °C):  $\delta$  152.37, 132.48, 127.80, 124.51, 121.43, 114.28, 72.93, 56.35, 49.38, 23.73, 22.8, 21.09;  $^{19}\text{F}$  NMR ( $\text{d}_6$ -DMSO, 376 MHz, 25 °C):  $\delta$  -77.71.



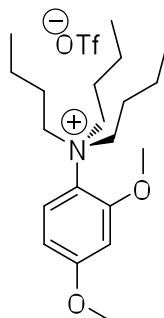
**N,N,N-Tributyl-2-methoxyanilinium triflate:**  $^1\text{H}$  NMR ( $\text{d}_6$ -DMSO, 400 MHz, 25 °C):  $\delta$  7.73 (d,  $J$  = 8 Hz, 1 H), 7.61 (t,  $J$  = 8 Hz, 1 H), 7.40 (d,  $J$  = 8 Hz, 1 H), 7.18 (t,  $J$  = 8 Hz, 1 H), 3.99 (s,  $-\text{OCH}_3$ , 3 H), 3.89 (m,  $-\text{CH}_2$ , 6 H), 1.40 (m,  $-\text{CH}_2$ , 6 H), 1.30 (m,  $-\text{CH}_2$ , 6 H), 0.86 (t,  $J$  = 7.9 Hz, 9 H);  $^{13}\text{C}$  NMR ( $\text{d}_6$ -DMSO, 100 MHz, 25 °C):  $\delta$  151.91, 132.02, 128.65, 124.59, 121.47, 119.09, 114.98, 59.08, 56.64, 24.36, 18.99, 13.33;  $^{19}\text{F}$  NMR ( $\text{d}_6$ -DMSO, 376 MHz, 25 °C):  $\delta$  -77.74.



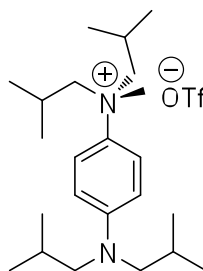
**N,N-Diisobutyl-N-methyl-2,4-dimethoxyanilinium triflate:**  $^1\text{H}$  NMR ( $\text{d}_6$ -DMSO, 400 MHz, 25 °C):  $\delta$  7.60 (d,  $J$  = 9.2 Hz, 1 H), 6.82 (d,  $J$  = 2.8 Hz, 1 H), 6.70 (dd,  $J_1$  = 9.2 Hz,  $J_2$  = 2.8 Hz, 1 H), 4.20 (dd,  $J_1$  = 13.4 Hz,  $J_2$  = 4.4 Hz, 2 H), 3.97 (s,  $-\text{OCH}_3$ , 3 H), 3.85 (s,  $-\text{OCH}_3$ , 3 H), 3.54 (s,  $-\text{CH}_3$ , 3 H), 3.43 (dd,  $J_1$  = 13.4 Hz,  $J_2$  = 6.2 Hz, 2 H), 1.78 (m,  $-\text{CH}_2-$ , 2 H), 0.93 (d,  $J$  = 6.8 Hz, 6 H), 0.50 (d,  $J$  = 6.8 Hz, 6 H);  $^{13}\text{C}$  NMR ( $\text{d}_6$ -DMSO, 100 MHz, 25 °C):  $\delta$  153.49, 125.47, 120.91, 107.32, 105.24, 100.90, 73.04, 67.58, 56.46, 55.83, 49.50, 23.68, 22.50, 21.20;  $^{19}\text{F}$  NMR ( $\text{d}_6$ -DMSO, 376 MHz, 25 °C):  $\delta$  -77.71.



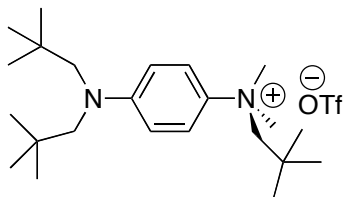
**N,N-Dibutyl-N-methyl-2,4-dimethoxyanilinium triflate:**  $^1\text{H}$  NMR ( $\text{CD}_3\text{CN}$ , 400 MHz, 25 °C):  $\delta$  7.38 (d,  $J$  = 9.2 Hz, 1 H), 6.69 (d,  $J$  = 2.8 Hz, 1 H), 6.63 (dd,  $J_1$  = 9.2 Hz,  $J_2$  = 2.8 Hz, 1 H), 4.28 (td,  $J_1$  = 12.4 Hz,  $J_2$  = 4.4 Hz, 2 H), 3.95 (s,  $-\text{OCH}_3$ , 3 H), 3.84 (s,  $-\text{OCH}_3$ , 3 H), 3.48 (dd,  $J_1$  = 12.1 Hz,  $J_2$  = 5.2 Hz, 2 H), 3.40 (s,  $-\text{CH}_3$ , 3 H), 1.56 (m,  $-\text{CH}_2-$ , 2 H), 1.26 (m,  $-\text{CH}_2-$ , 4 H), 1.07 (m,  $-\text{CH}_2-$ , 2 H), 0.84 (t,  $J$  = 7.3 Hz, 6 H);  $^{13}\text{C}$  NMR ( $\text{CD}_3\text{CN}$ , 100 MHz, 25 °C):  $\delta$  162.29, 153.44, 128.32, 124.96, 122.78, 121.22, 119.59, 104.99, 101.13, 66.21, 56.30, 55.70, 49.45, 24.94, 19.06, 12.68;  $^{19}\text{F}$  NMR ( $\text{CD}_3\text{CN}$ , 376 MHz, 25 °C):  $\delta$  -77.73.



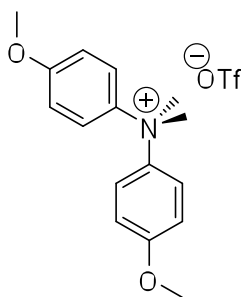
**N,N,N-Tributyl-2,4-dimethoxyanilinium triflate:**  $^1\text{H}$  NMR ( $\text{d}_6$ -DMSO, 400 MHz, 25  $^\circ\text{C}$ ):  $\delta$  7.65 (d,  $J = 9.2$  Hz, 1 H), 6.89 (d,  $J = 2.8$  Hz, 1 H), 6.73 (dd,  $J_1 = 9.2$  Hz,  $J_2 = 2.8$  Hz, 1 H), 3.96 (s,  $-\text{OCH}_3$ , 3 H), 3.85 (s,  $-\text{OCH}_3$ , 3 H), 3.83 (m,  $-\text{CH}_2-$ , 6 H), 1.40 (m,  $-\text{CH}_2-$ , 6 H), 1.31 (m,  $-\text{CH}_2-$ , 6 H), 0.87 (t,  $J = 7.8$  Hz, 9 H);  $^{13}\text{C}$  NMR ( $\text{d}_6$ -DMSO, 100 MHz, 25  $^\circ\text{C}$ ):  $\delta$  161.33, 152.99, 125.53, 121.68, 105.40, 101.34, 59.14, 56.61, 55.66, 24.26, 18.97, 13.26;  $^{19}\text{F}$  NMR ( $\text{d}_6$ -DMSO, 376 MHz, 25  $^\circ\text{C}$ ):  $\delta$  -77.70.



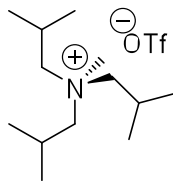
**N,N-Diisobutyl-N-methyl-(4-diisobutylamino)anilinium triflate:**  $^1\text{H}$  NMR ( $\text{d}_6$ -DMSO, 400 MHz, 25  $^\circ\text{C}$ ):  $\delta$  7.54 (d,  $J = 9.4$  Hz, 2 H), 6.75 (d,  $J = 9.4$  Hz, 2 H), 3.80 (dd,  $J_1 = 13.4$  Hz,  $J_2 = 4.4$  Hz, 2 H), 3.54 (dd,  $J_1 = 13.4$  Hz,  $J_2 = 6.1$  Hz, 2 H), 3.45 (s,  $-\text{CH}_3$ , 3 H), 3.21 (d,  $-\text{CH}_2-$ , 4 H), 1.96 (m,  $-\text{CH}-$ , 2 H), 1.84 (m,  $-\text{CH}-$ , 2 H), 0.94 (d,  $J = 6.8$  Hz, 6 H), 0.85 (d,  $J = 6.8$  Hz, 12 H), 0.53 (d,  $J = 6.8$  Hz, 6 H);  $^{13}\text{C}$  NMR ( $\text{d}_6$ -DMSO, 100 MHz, 25  $^\circ\text{C}$ ):  $\delta$  148.31, 128.79, 122.72, 120.69 (q, OTf), 111.78, 75.68, 58.57, 46.36, 26.10, 23.34, 22.48, 21.56, 19.87;  $^{19}\text{F}$  NMR ( $\text{d}_6$ -DMSO, 376 MHz, 25  $^\circ\text{C}$ ):  $\delta$  -77.73.



**N,N-Dimethyl-N-neopentyl-(4-dineopentylamino)anilinium triflate:**  $^1\text{H}$  NMR ( $\text{d}_6$ -DMSO, 400 MHz, 25 °C):  $\delta$  7.56 (d,  $J$  = 9.4 Hz, 2 H), 7.08 (d,  $J$  = 9.4 Hz, 2 H), 3.77 (s, -CH<sub>2</sub>-, 2 H), 3.54 (s, -CH<sub>3</sub>, 6 H), 3.39 (s, -CH<sub>2</sub>-, 4 H), 0.82 (s, -CH<sub>3</sub>, 18 H) 0.75(s, -CH<sub>3</sub>, 9 H);  $^{13}\text{C}$  NMR ( $\text{d}_6$ -DMSO, 100 MHz, 25 °C):  $\delta$  150.81, 132.13, 1221.21, 115.00, 77.76, 60.69, 55.96, 54.83, 36.26, 32.79, 28.52;  $^{19}\text{F}$  NMR ( $\text{d}_6$ -DMSO, 376 MHz, 25 °C):  $\delta$  -77.72.



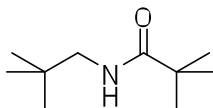
**Bis(4-methoxyphenyl)dimethylammonium triflate:**  $^1\text{H}$  NMR ( $\text{d}_6$ -DMSO, 400 MHz, 25 °C):  $\delta$  7.59 (4 H, d, Ar- H), 7.11 (4 H, d, Ar- H), 4.01 (6 H, s, -OCH<sub>3</sub>), 3.82 (6 H, s, CH<sub>3</sub>);  $^{13}\text{C}$  NMR ( $\text{d}_6$ -DMSO, 100 MHz, 25 °C):  $\delta$  159.59, 141.81, 123.00, 114.79, 57.81, 55.79;  $^{19}\text{F}$  NMR ( $\text{d}_6$ -DMSO, 376 MHz, 25 °C):  $\delta$  -77.71.



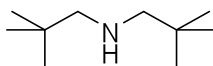


**Trisisobutylmethyammonium triflate:**  $^1\text{H}$  NMR ( $\text{d}_6\text{-DMSO}$ , 400 MHz, 25  $^\circ\text{C}$ ):  $\delta$  3.19 (d,  $J$  = 4.9 Hz, 6 H), 3.03 (s  $-\text{CH}_3$ , 3 H) 2.22 (m,  $-\text{CH}-$ , 3 H), 1.03 (d,  $J$  = 6.5, 18 H);  $^{13}\text{C}$  NMR ( $\text{d}_6\text{-DMSO}$ , 100 MHz, 25  $^\circ\text{C}$ ):  $\delta$  120.67 (q, OTf) 69.49, 48.26, 22.83, 22.55;  $^{19}\text{F}$  NMR ( $\text{d}_6\text{-DMSO}$ , 376 MHz, 25  $^\circ\text{C}$ ):  $\delta$  -77.77.

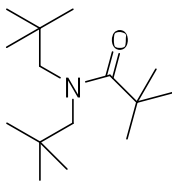
### Preparation of anhydrous TNPMAF and its precursors



**Neopentylpivalamide:** Neopentylamine (6.06 mL, 50 mmol), triethylamine (7 mL, 50 mmol), and 50 mL of chloroform were added to a two-neck flask equipped with a condenser and a Teflon stir bar. The mixture was stirred under an atmosphere of  $\text{N}_2$ , and chilled to 0  $^\circ\text{C}$ . Pivaloyl chloride (6 mL, 50 mmol) was added slowly and the mixture was brought to reflux. After 16 h at reflux, the mixture was allowed to cool to room temperature before 30 mL of water was added. The organic layer was separated, washed, dried over  $\text{NaSO}_4$ , and the solvent was evaporated under reduced pressure to afford 8.55 g (97 %) of neopentylpivalamide, which was sufficiently pure to carry through to the next step.  $^1\text{H}$  NMR ( $\text{CDCl}_3$ , 400 MHz, 25  $^\circ\text{C}$ ):  $\delta$  5.70 (broad s, N-H, 1 H), 3.03 (d,  $J$  = 6.0 Hz,  $-\text{CH}_2$ , 2 H), 1.19 (s, t-Bu, 9 H), 0.87 (s, t-Bu, 9 H);  $^{13}\text{C}$  NMR ( $\text{CDCl}_3$ , 100 MHz, 25  $^\circ\text{C}$ ):  $\delta$  178.1 (C=O), 49.7 ( $-\text{CH}_2$ ), 40.1 ( $-\text{CCH}_3$ ), 33.2 ( $-\text{CCH}_3$ ), 29.1 ( $-\text{CH}_3$ ), 27.9 ( $-\text{CH}_3$ ); HRMS (HRFAB): calcd. for  $\text{C}_{10}\text{H}_{22}\text{ON}^+$   $[\text{M} + \text{H}]^+$  172.1701 found 172.1711.

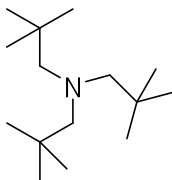


**Dineopentylamine:** Neopentylpivalamide (8.3 g, 48.5 mmol) was added to a suspension of  $\text{LiAlH}_4$  (4.15 g, 109 mmol) in THF under  $\text{N}_2$ . The suspension was stirred at room temperature for 0.5 h and then heated at reflux for 24 h. The mixture was allowed to cool to room temperature and 20 mL of degassed water was added in a dropwise fashion under  $\text{N}_2$ . The hot mixture was cooled and the aluminum salts removed by filtration. The solution was extracted with  $\text{CH}_2\text{Cl}_2$  ( $3 \times 60$  mL). The organic layers were combined, dried over  $\text{NaSO}_4$ , and filtered. The remaining solvent was removed under reduced pressure to afford the crude dineopentylamine (6.74 g, 88 %) as a pale yellow oil. This product was sufficiently pure to be used directly for the next step.  $^1\text{H}$  NMR ( $\text{CDCl}_3$ , 400 MHz, 25 °C):  $\delta$  2.31 (s,  $-\text{CH}_2$ , 4 H), 0.88 (s, t-Bu, 18 H), 0.63 (broad s, N-H, 1 H);  $^{13}\text{C}$  NMR ( $\text{CDCl}_3$ , 100 MHz, 25 °C):  $\delta$  50.2 ( $-\text{CH}_2$ ), 32.9 ( $-\text{CCH}_3$ ), 27.7 ( $-\text{CH}_3$ ); HRMS (HRFAB): calcd. for  $\text{C}_{10}\text{H}_{24}\text{N}^+$   $[\text{M} + \text{H}]^+$  158.1909 found 158.1913. (lit. b.p. 150°C-153°C; Anal. For  $\text{C}_{10}\text{H}_{23}\text{N}$ : C 76.35, H 14.74, N 8.90, found 76.45, 14.73, 8.99.)<sup>28</sup>



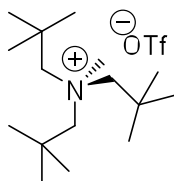
**Dineopentylpivalamide:** Dineopentylamine (6.74 g, 42.6 mmol), triethylamine (6 mL, 42.6 mmol) and 50 mL of chloroform were added to a two-necked flask equipped with a condenser and a stir bar. The mixture was stirred under an atmosphere of  $\text{N}_2$ , and chilled to 0 °C. Pivaloyl chloride (5.11 mL, 42.6 mmol) was added slowly and the mixture was brought to reflux. After 24 h the mixture was cooled to room temperature and 30 mL of water was added. The organic layer was separated, washed, dried over  $\text{NaSO}_4$ , and

filtered. The solvent was removed under reduced pressure to afford 6.98 g (68 %) of dineopentylpivalamide, which was used directly for the next step.  $^1\text{H}$  NMR ( $\text{CDCl}_3$ , 400 MHz, 25 °C):  $\delta$  3.48 (broad s,  $-\text{CH}_2$ , 4 H), 1.32 (s, t-Bu, 9 H), 1.02-0.91 (two broad s, t-Bu, 18 H);  $^{13}\text{C}$  NMR ( $\text{CDCl}_3$ , 100 MHz, 25 °C):  $\delta$  179.9 (C=O), 59.3 ( $-\text{CH}_2$ ), 55.2 ( $-\text{CH}_2$ ), 40.3 ( $-\text{CCH}_3$ ), 35.0 ( $-\text{CCH}_3$ ), 33.6 ( $-\text{CCH}_3$ ), 30.1 ( $-\text{CH}_3$ ), 30.0 ( $-\text{CH}_3$ ), 28.8 ( $-\text{CH}_3$ ); HRMS (HRFAB): calcd. for  $\text{C}_{15}\text{H}_{32}\text{ON}^+ [\text{M} + \text{H}]^+$  242.2484 found 242.2490.

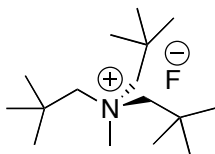


**Trineopentylamine:** Under an atmosphere of  $\text{N}_2$ , dineopentylpivalamide (6.98 g, 29 mmol) was added to a suspension of  $\text{LiAlH}_4$  (1.1 g, 29 mmol) in THF. The suspension was stirred at room temperature for 0.5 h and then heated at reflux for 4 h. The mixture was cooled to temperature and 15 mL of degassed water was added dropwise under  $\text{N}_2$ . The hot mixture was cooled and the precipitate removed by filtration. The remaining solution was extracted with  $\text{CH}_2\text{Cl}_2$  ( $3 \times 60$  mL). The organic layers were combined, dried over  $\text{NaSO}_4$ , and filtered. The solvent evaporated under reduced pressure to afford the crude trineopentylamine (6.31 g, 96 %), which was purified by column chromatography (60 Å silica, hexane,  $R_f = 0.35$ ). The solvent was removed by rotary evaporation and the last traces of solvent were removed from the remaining colorless oil under dynamic vacuum (12 h). Yield 5.85 g (89 %).  $^1\text{H}$  NMR ( $\text{CDCl}_3$ , 400 MHz, 25 °C):  $\delta$  2.19 (s,  $-\text{CH}_2$ , 6 H), 0.96 (s, t-Bu, 27 H);  $^{13}\text{C}$  NMR ( $\text{CDCl}_3$ , 100 MHz, 25 °C):  $\delta$  71.7 ( $-\text{CH}_2$ ), 33.1 ( $-\text{CCH}_3$ ), 28.0 ( $-\text{CH}_3$ ); HRMS (HRFAB): calcd. for  $\text{C}_{15}\text{H}_{34}\text{N}^+ [\text{M} + \text{H}]^+$

228.2691 found 228.2697. (lit.  $^1\text{H}$  NMR ( $\text{CD}_2\text{Cl}_2$ )  $\delta$  0.93 (27 H, s), 2.21 (6 H, s); MS  $m/e$  227 ( $\text{M}^+$ ), 212, 170, 100, 71.)<sup>26</sup>



**Trineopentylmethylammonium triflate:** Trineopentylamine (5.68 g, 25 mmol) and methyl triflate (4.17 g, 25 mmol) were added to a 50 mL glass storage tube equipped with a Teflon stir bar under  $\text{N}_2$ . The tube was sealed with a PTFE closure and the mixture was stirred at 85 °C for 3 days. After the reaction mixture was cooled to room temperature, a colorless crystalline material formed. This salt was isolated by filtration and recrystallized from DCM/hexanes to yield 6.99 g (71 %) of pure trineopentylmethylammonium triflate.  $^1\text{H}$  NMR ( $\text{CD}_3\text{CN}$ , 400 MHz, 25 °C):  $\delta$  3.29 (s, - $\text{CH}_2$ , 6 H), 3.17 (s, - $\text{CH}_3$ , 3 H), 1.21 (s, t-Bu, 27 H);  $^{13}\text{C}$  NMR ( $\text{CD}_3\text{CN}$ , 100 MHz, 25 °C):  $\delta$  127.9 (q,  $J$  = 321 Hz, - $\text{CF}_3$ ), 78.0 (t,  $J$  = 1.6 Hz, - $\text{CH}_2$ ), 51.8 (t,  $J$  = 5.7 Hz, - $\text{CH}_3$ ), 34.8 (- $\text{CCH}_3$ ), 30.6 (- $\text{CH}_3$ ); HRMS (HRFAB): calcd. for  $\text{C}_{16}\text{H}_{36}\text{N}^+$  [ $\text{M} - \text{OTf}$ ] $^+$  242.2848 found 242.2857. (lit.  $^1\text{H}$  NMR ( $\text{CDCl}_3$ )  $\delta$  1.25 (27 H, s), 3.32 (3 H, s), 3.44 (6 H, s); mp 234-237°C dec.)<sup>26</sup>



**Trineopentylmethylammonium fluoride (anhydrous):** In a nitrogen charged glove box, dry TNPMAOTf (10 mmol, 3.91 g) was added to the solution of freshly made TBAF\* in THF (10 mmol). The mixture was chilled to -40 °C to precipitate TNPMAF, and the

white precipitate was isolated by filtration and washed with cold THF to yield 1.57 g anhydrous TNPMAF (60 % yield). The sample prepared in this manner contained less than 1 % of the TBA cation and less than 2 % of the triflate anion.  $^1\text{H}$  NMR ( $\text{d}_6$ -DMSO, 400 MHz, 25 °C):  $\delta$  3.43 (s,  $-\text{CH}_2$ , 6 H), 3.39 (s,  $-\text{CH}_3$ , 3 H), 1.15 (s, t-Bu, 27 H);  $^{13}\text{C}$  NMR ( $\text{d}_6$ -DMSO, 100 MHz, 25 °C):  $\delta$  75.9 ( $-\text{CH}_2$ ), 50.8 ( $-\text{CH}_3$ ), 33.4 ( $-\text{C}(\text{CH}_3)_3$ ), 30.2 ( $-\text{CH}_3$ );  $^{19}\text{F}$  NMR ( $\text{d}_6$ -DMSO, 376 MHz, 25 °C):  $\delta$  -74.5.

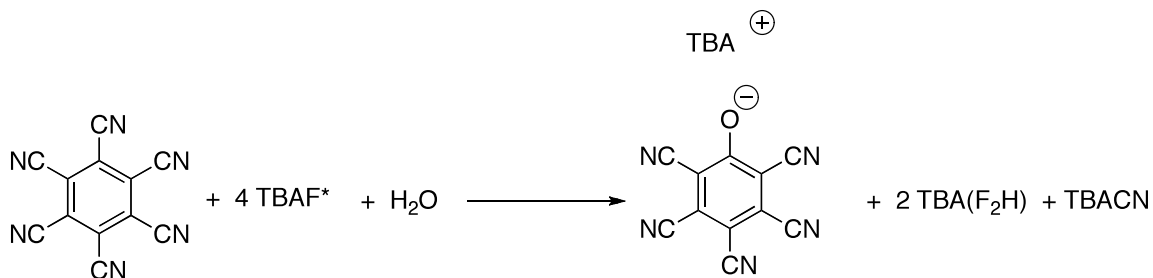
## CHAPTER 2

### REMOVAL OF SMALL AMOUNT OF WATER AND ALTERNATIVE AQUAMETRY BASED ON I(III) CHEMISTRY

#### 2.1 Introduction

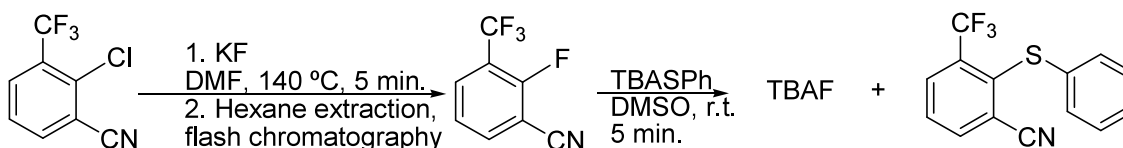
As was demonstrated by the experiments described in the previous chapter, exclusion of moisture greatly enhances the nucleophilicity of fluoride. As a result, faster and more efficient  $S_N2$  and  $S_NAr$  fluorination reactions occur with these reagents and conditions. This is only one of many examples in modern synthetic chemistry where dehydration procedures are performed to enhance yield or to ensure experimental reproducibility. Often, significant effort may be spent to exclude moisture from solvents and reagents, particularly when trace amounts of water have a significant impact on reaction efficiency.

Our original procedure<sup>22</sup> to prepare anhydrous TBAF\* relied on the  $S_NAr$  reaction between hexafluorobenzene and anhydrous TBACN. Concurrent with this preparative  $S_NAr$  reaction, cogenerated hexacyanobenzene scavenges residual water to form tetrabutylammonium pentacyanophenoxide and two equivalents of TBAHF<sub>2</sub> (Scheme 2-1). Thus, the anhydrous fluoride reagents prepared by this procedure and used *in situ* are exceptionally dry. Upon isolation of the fluoride salts for storage, the dehydrating agent is removed leaving the reagents susceptible to trace water contamination from solvents and vessels when the salts are dissolved for synthetic chemistry.



**Scheme 2-1** *In situ* removal of water by hexacyanobenzene in the presence of fluoride.

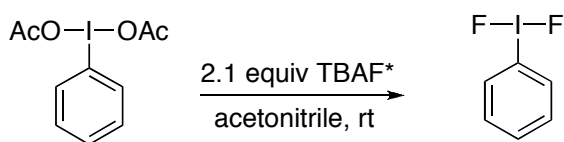
To make anhydrous fluoride reagents more accessible to medicinal chemists and radiochemists, and to make the procedure less hazardous for synthetic chemists, the DiMagno laboratory also developed a F-relay method (Scheme 2-2) and cyanide-free preparation of TBAF\* using thiophenoxide and phenoxide nucleophiles. One major drawback to use these nucleophiles instead of cyanide is that no dehydrating polycyanoaromatic compounds are generated during the reaction. Since water is not removed during the synthesis, trace water contamination in the solvents becomes a problem.



**Scheme 2-2** Generation of anhydrous TBAF via F-relay and cyanide-free method with thiophenoxide as the nucleophile.

Due to water's ubiquity, solubility, and propensity to physisorb on reaction vessel surfaces, experimentalists often have to question if putatively anhydrous conditions actually are. In order to obtain high quality TBAF\* via the F-relay and/or cyanide-free methods, either a fluoride compatible dehydrating agent needs to be introduced or careful drying and frequent checking of the solvents and reagents need to be performed.

Our research with hypervalent iodine compounds enabled us to discover that the reagent combination TBAF\*/PhI(OAc)<sub>2</sub> serves as a convenient dehydrating agent for anhydrous fluoride salts. PhI(OAc)<sub>2</sub> belongs to the class of compounds known as [bis(acyloxy)iodo]arenes (BAI). These iodanes can be regarded as either as mixed anhydrides of carboxylic acids and the hypothetical acids ArI(OH)<sub>2</sub> or as bisacyloxy derivatives of iodo arenes (ArI). Except for the oxidizable formic acid, virtually any carboxylic acid is capable of participating in forming BAI.<sup>29-31</sup> Ligand exchange in these compounds using either metal carboxylates or acids is a convenient way to obtain various BAI. The method can be extended to include the preparation of other monoaryl-λ<sup>3</sup>-iodanes (ArIL<sub>2</sub>, L = Cl, F, CN, SCN, etc.)



**Scheme 2-3 Preparation of PhIF<sub>2</sub> by ion exchange under anhydrous basic conditions.**

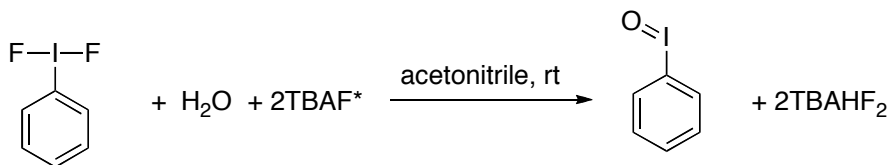
We have found that difluoro-phenyl-λ<sup>3</sup>-iodane (PhIF<sub>2</sub>) can be made simply and directly from PhI(OAc)<sub>2</sub> by ion exchange under anhydrous basic conditions (Scheme 2-3). Previously, difluoro-aryl-λ<sup>3</sup>-iodanes (ArIF<sub>2</sub>) were prepared from ArIX<sub>2</sub> compounds and aqueous HF,<sup>32</sup> by oxidation of iodoarenes with electrophilic fluorine sources (F<sub>2</sub>,<sup>33, 34</sup> XeF<sub>2</sub>,<sup>35-41</sup> ClF,<sup>42</sup> Selectfluor®<sup>43</sup>) and by treatment of iodosoarenes or bis(trifluoroacetoxy)iodo arenes with SF<sub>4</sub>.<sup>44</sup> These compounds are recognized as being hard to isolate and handle due to their remarkable water sensitivity under basic conditions.<sup>29</sup> We have found that, in the presence of excess TBAF\*, PhIF<sub>2</sub> is able to so effectively scavenge water, that the nucleophilicity of the fluoride is not compromised,



aside from the consumption of fluoride to form  $\text{HF}_2^-$ . In addition, in conjunction with  $^{19}\text{F}$  NMR spectroscopy, the reagent combination  $\text{TBAF}^*/\text{PhI}(\text{OAc})_2$  can be used as a rapid, convenient, general, and exquisitely sensitive (100 ng detection limit) aquametry method.<sup>45</sup>

## 2.2 Water sensitivity of $\text{PhIF}_2$

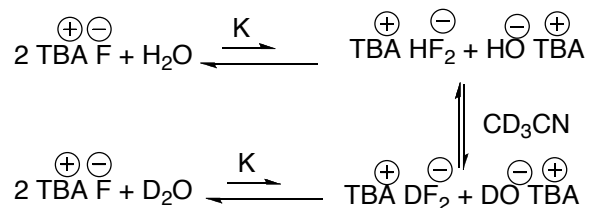
When a  $\text{CD}_3\text{CN}$  solution of carefully dried  $\text{PhI}(\text{OAc})_2$  is treated with anhydrous TBAF at room temperature, an instantaneous ion exchange occurs to form  $\text{PhIF}_2$  and TBAOAc in nearly quantitative yield (Scheme 2-3). If excess added fluoride is present, it associates with  $\text{PhIF}_2$  to form the complex anion  $\text{PhIF}_3^-$ , as is indicated by a broad and shifting signal in the  $^{19}\text{F}$  NMR spectrum. If a slight molar excess of fluoride is present, the signal resonates at approximately -13 ppm; further additions of TBAF shift the fluoride signal upfield. (All  $^{19}\text{F}$  chemical shift values are referenced to  $\delta = 0$  for  $\text{CFCl}_3$ , used as an external standard.) Analyses of the  $^{19}\text{F}$ ,  $^{13}\text{C}$  and  $^1\text{H}$  NMR spectra of  $\text{PhIF}_2$  ( $^{19}\text{F}$  NMR:  $\delta = -172$  ppm) reaction mixture solutions indicated that small amounts (1-2 %) of bifluoride ion ( $^1\text{H}$  NMR:  $\delta = 16.4$  ppm, t;  $^{19}\text{F}$  NMR:  $\delta = -146.5$  ppm, d,  $J_{\text{H-F}} = 121$  Hz) and iodosobenzene ( $\text{PhIO}$ ) were also formed. We suspected that these impurities arose from trace water contamination (Scheme 2-4), and sought to investigate and exploit the water sensitivity of  $\text{PhIF}_2$  under these conditions.



**Scheme 2-4 Reaction of  $\text{PhIF}_2$  with water in the presence of excess fluoride.**

PhIF<sub>2</sub> reacts with water slowly under acidic or neutral conditions, in consistent with the observation that difluoro-aryl-λ<sup>3</sup>-iodanes can be prepared with aqueous HF. However, NMR titration experiments with water (Figure 2-1 and Figure 2-2) revealed that PhIF<sub>2</sub> is hydrolyzed immediately and quantitatively to form HF<sub>2</sub><sup>-</sup> and iodosobenzene (PhIO) in the presence of basic fluoride reagents.

Upon standing, TBAF\* is able to deprotonate deuterated acetonitrile over time and fluoride is consumed to form DF<sub>2</sub><sup>-</sup> in the process. The presence of water contamination catalyzes this H-D exchange process possibly via small amount of hydroxide that results from deprotonation of water by fluoride.<sup>18</sup> Deuterium exchange occurs without a detectable increase in the total bifluoride ion concentration, suggesting that the deprotonation of water by TBAF is thermodynamically unfavorable. Scheme 2-5 shows a simplified scheme for the hydroxide catalyzed H-D exchange process. For a solution of carefully made TBAF\* in d<sub>3</sub>-acetonitrile, the ratio of DF<sub>2</sub><sup>-</sup> to HF<sub>2</sub><sup>-</sup> grows over a span of several hours; while for slightly wet TBAF solution, the H-D exchange is complete within 5 minutes (the time needed to prepare sample and record an NMR spectrum). Therefore, it is possible to obtain a qualitative estimate of the amount of residual water in TBAF\* simply by looking at the <sup>19</sup>F NMR spectrum of its d<sub>3</sub>-acetonitrile solution.



**Scheme 2-5 Simplified scheme for hydroxide catalyzed deuterium exchange.**

The  $^{19}\text{F}$  NMR spectrum of  $\text{PhIF}_2/\text{TBAF}^*$  mixture in  $\text{d}_3$ -acetonitrile (Figure 2-2) shows no evidence of H-D exchange (formation of  $\text{DF}_2^-$ ) even after the addition of 1800 micrograms of water. The apparent elimination of H-D exchange under these anhydrous conditions indicates that anhydrous solutions of  $\text{TBAPhIF}_3$  are significantly less basic than TBAF solutions. Because 1) the TBA cation is susceptible to E2 elimination in  $\text{d}_3$ -acetonitrile by fluoride upon long standing, and 2) this elimination reaction is suppressed by the weakly basic  $\text{PhIF}_3^-$  complex anion, and the dehydrating reagent is best prepared with a 1:1  $\text{PhIF}_2:\text{TBAF}^*$  stoichiometry.

Despite the fact the excess fluoride in  $\text{PhIF}_2/\text{TBAF}^*$  mixture forms complex with the I(III) species, and is no longer “free”, its nucleophilicity is only reduced marginally. Direct fluorination via  $\text{S}_{\text{N}}\text{Ar}$  mechanism works just as well for  $\text{PhI}(\text{OAc})_2$ -added  $\text{TBAF}^*$ . In other words, the reagent combination of  $\text{PhIF}_2/\text{TBAF}^*$  can be used as a convenient and effective dehydrating agent for anhydrous fluoride salt.

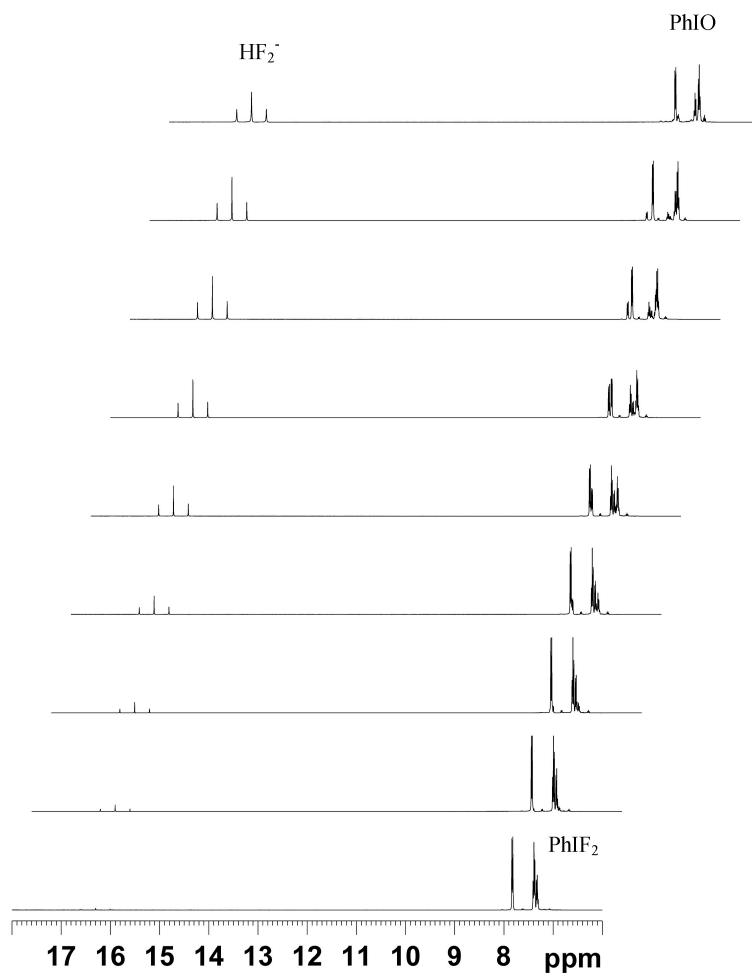


**Figure 2-1** Changes in the  $^1\text{H}$  NMR spectra obtained during the water titration of a 0.5 ml  $\text{PhIF}_2$  (0.2 M) and  $\text{TBAF}^*$  (0.2 M) acetonitrile- $\text{d}_3$  solution. Successive spectra (bottom to top) were taken at approximately 10 minute intervals. This interval was the time required to remove the sample from the magnet, inject the appropriate amount of water, replace the sample, and gather the  $^1\text{H}$  and  $^{19}\text{F}$  NMR (Figure 2-2) spectra. From bottom to top, the spectra correspond to the addition of 0, 100, 200, 400, 700, 1000, 1300, 1500, and 1800 micrograms of water.

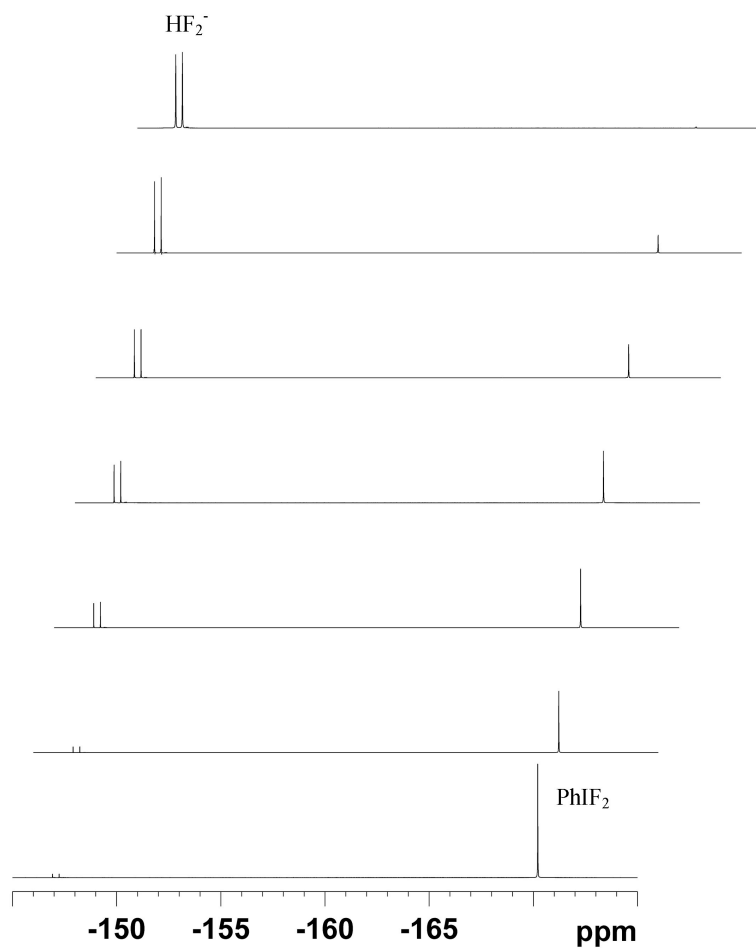


**Figure 2-2 Successive  $^{19}\text{F}$  NMR spectra obtained during the addition of water to a 0.5 ml  $\text{PhIF}_2$  (0.2 M) and  $\text{TBAF}^*$  (0.2 M) acetonitrile- $\text{d}_3$  solution; this is the identical experiment to that shown in Figure 2-1. Note that there is no evidence for  $\text{DF}_2^-$  in these spectra, as is discussed in the text.**

### 2.3 Alternative aquametry to Karl Fisher titration

Since the hydrolysis of  $\text{PhIF}_2$  is fast and quantitative under the conditions discussed above, we were able to design a general aquametry method based on this reaction. The method allows us to directly and quantitatively assay and remove trace amounts of water in solutions. Accurate determination of trace water contamination at the  $\mu\text{g}$  level is devilishly difficult. Existing physical and chemical aquametry methods for quantitative measurement of water in organic solvents ( $\text{GC}^{46-49}$ ,  $\text{IR}^{50-54}$ , and Karl Fischer titration<sup>55, 56</sup>) are not well suited for rapid trace water analysis at the scale (1 mL total solvent volume) or under the conditions used for fluorination. (Sample preparation in an inert atmosphere glove box further complicates aquametry.)

In order to quantify the amount of bifluoride in the reaction mixture, we chose to use  $\text{TBABF}_4$  as an internal standard because the characteristic  $^{19}\text{F}$  NMR signal of  $\text{HF}_2^-$  ( $\delta = -146$  ppm) resonates near that of the  $\text{BF}_4^-$  ion ( $\delta = -151$  ppm). Comparative integration of the  $\text{TBABF}_4$  and  $\text{TBAHF}_2$  signals allows water-generated bifluoride ion to be quantified easily. The long  $T_1$  relaxation time for  $\text{BF}_4^-$  ion (up to 32 seconds) necessitated single scan acquisitions. If better signal to noise ratios are required, a fluorinated benzene can be used as the internal reference.

To test the accuracy and reproducibility of the  $\text{TBAF}^*/\text{PhI}(\text{OAc})_2$  method for water determination, we constructed specialized reaction vessels by fusing crimp-top autosampler vials (2.0 mL, borosilicate glass, PTFE/silicone/PTFE septum seal) to the open ends of standard (5 mm) NMR tubes (Figure 2-3). These customized tubes were charged with  $\text{PhI}(\text{OAc})_2$ ,  $\text{TBAF}$ ,  $\text{TBABF}_4$  (internal standard) and  $\text{CD}_3\text{CN}$ , sealed, and

baseline  $^{19}\text{F}$  NMR spectra of the samples were obtained. For titration experiments involving large amounts of added water (100 to 2000  $\mu\text{g}$ ), NMR spectra were gathered and analyzed after multiple measured additions of standardized water solutions through the septum cap of a single tube. The time elapsed between injection and completion of each NMR data acquisition was less than 10 minutes. The change in the integrated peak areas for the  $\text{BF}_4^-$  and  $\text{HF}_2^-$  signals confirmed that 2 equivalents of  $\text{HF}_2^-$  were generated for each equivalent of added  $\text{H}_2\text{O}$  (Figure 2-4).

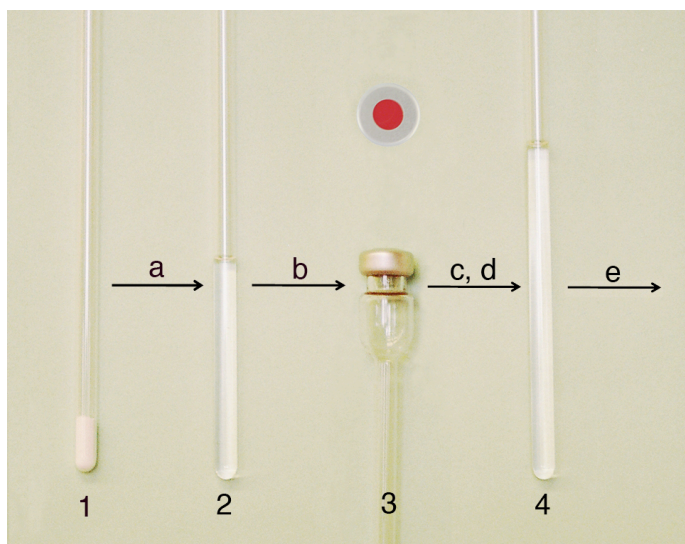


**Figure 2-3 Graphical representation of the water determination experiment. From left to right: 1) TBAF/ $\text{PhI}(\text{OAc})_2$ / $\text{TBABF}_4$  mixture in a reaction tube; 2) assay mixture in  $\text{CD}_3\text{CN}$ ; 3) side (bottom) and top (top) views of a customized 5 mm NMR tube featuring a fused crimp cap vial septum seal; 4) tube containing solid reagents (TBAF,  $\text{TBABF}_4$ ,  $\text{PhI}(\text{OAc})_2$ ),  $\text{CD}_3\text{CN}$  and sample after the addition of the solvent being tested. The process arrows indicate a) addition of  $\text{CD}_3\text{CN}$ , b) installation of the cap, c) collection of the background  $^{19}\text{F}$  NMR spectrum, d) injection of the solvent being tested, e) collection of the final  $^{19}\text{F}$  NMR spectrum.**

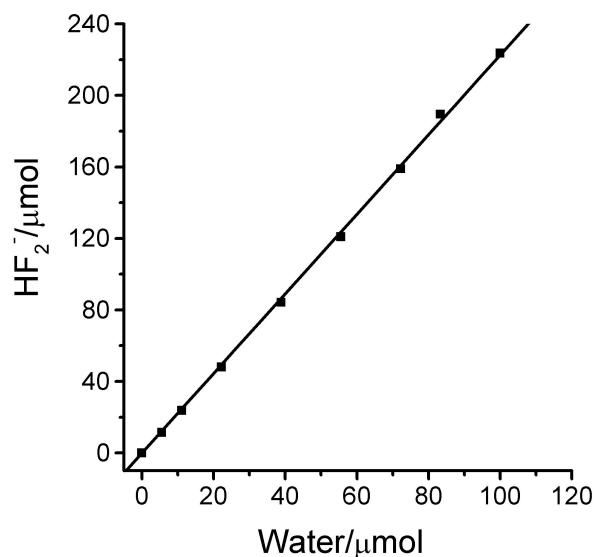


**Figure 2-4 Results from the titration of a  $\text{PhIF}_2/\text{CD}_3\text{CN}$  solution with standardized aqueous acetonitrile.**

For solutions containing very low water concentrations (less than 10 ppm), we were concerned that sample manipulation could introduce significantly more water than that being measured; thus we sought to develop a reproducible “single injection” method. The rationale for this method is that if the septum is only pierced once, all operations may be performed under the inert atmosphere conditions required for very careful work. In the single injection method, the  $\text{PhI}(\text{OAc})_2/\text{TBAF}/\text{TBABF}_4$  reagent is prepared in  $\text{d}_3$ -acetonitrile in a glove box and tube is sealed with a crimp top cap and a new septum seal. The tube is removed from the glove box and a baseline  $^{19}\text{F}$  NMR spectrum is recorded to establish the amount of background bifluoride ion present. (Figure 2-5 bottom spectrum. Background bifluoride ion arises from traces of water in the NMR solvent, salts, and from physisorbed water on the glass vessel.) The sample solution to be tested (either



within or outside of the glove box) is then injected and a second  $^{19}\text{F}$  NMR spectrum is obtained (Figure 2-5 upper spectrum).



**Figure 2-5 Single injection water determination by  $^{19}\text{F}$  NMR: bottom, background spectrum before the addition of “dry”  $\text{CH}_3\text{CN}$ ; top, spectrum collected after the injection of a  $\text{CH}_3\text{CN}$  sample containing 49  $\mu\text{g}$  of  $\text{H}_2\text{O}$ .**

To illustrate and test the reproducibility of the single injection technique, a series of sample tubes was prepared, baseline spectra were gathered, and each tube was treated with a weighed amount of commercially obtained “dry” acetonitrile (measured  $[\text{H}_2\text{O}] = 180$  ppm). Figure 2-5 shows the result of a single injection water determination experiment involving the addition of 49  $\mu\text{g}$  of water.

To test the reproducibility and accuracy of the measurement technique, we measured water concentrations in 15 samples by conventional coulometric Karl Fischer

titration and by  $^{19}\text{F}$  NMR spectroscopy. For the NMR procedure, the reproducibility was equal to that of Karl Fischer titration ( $\pm 3\%$ ) for samples involving measurement of 70  $\mu\text{g}$  of water. Because the NMR method permitted sample preparation in an inert atmosphere glove box, sample handling errors for Karl Fischer titration were larger than those intrinsic to the NMR experiments. Notably, for “dry” commercial THF we were able to measure easily and accurately the addition of 5  $\mu\text{g}$  of water to a sample. In contrast, the detection limit for coulometric Karl Fischer titration using typical commercial equipment is 10  $\mu\text{g}$  of added water.

Reasonable system stability is required for practical application of this water determination method. Because precise evaluation of water concentration relies on an accurate determination of bifluoride ion concentration, it is important to minimize any side reactions that might generate  $\text{HF}_2^-$ . Control experiments showed that the  $\text{PhI}(\text{OAc})_2/\text{TBAF}$  reagent is stable in  $\text{d}_3$ -acetonitrile solution for several hours, long enough for baseline and sample NMR spectra to be gathered. After this time, small amounts of cation decomposition produce detectable amounts of  $\text{HF}_2^-$ . The long term stability of the system can be improved substantially if more robust cations, such as tetramethylammonium (TMA) or trineopentylmethylammonium (TNPMA), or hexamethylpiperidinium are used instead of TBA.

Conveniently, the  $\text{TBAF}^*/\text{PhI}(\text{OAc})_2/\text{TBABF}_4$  salt mixture can be weighed and sealed in the NMR tube so that deuterated solvent and liquid samples can be added through the septum subsequently (Figure 2-3, left). Like TBAF itself, the reagent mixture is stable in the solid state for months at  $-40\text{ }^\circ\text{C}$  under an inert atmosphere. Using typical

instrumentation (Bruker Avance 400 MHz, QNP probe) and a single scan acquisition, the signal to noise ratio is sufficient to measure accurately the addition of 3  $\mu\text{g}$  of water ( $[\text{H}_2\text{O}] = 3 \text{ ppm}$ ).  $^{19}\text{F}$  NMR sensitivity is sufficient for submicrogram (100 ng) water detection ( $[\text{H}_2\text{O}] = 0.1 \text{ ppm}$ ) with more sophisticated equipment (600 MHz spectrometer, dedicated H/F probe) and a longer acquisition time, however we have found it be a significant challenge to prepare  $\text{TBAF}^*/\text{PhI}(\text{OAc})_2/\text{TBABF}_4$  solutions that are sufficiently dry ( $[\text{H}_2\text{O}] < 1 \text{ ppm}$ ) to provide the low background necessary for submicrogram water detection.

The scope of the NMR aquametry technique is relatively broad, although it is limited by the basicity and nucleophilicity of weakly coordinated fluoride ion under these conditions. Halogenated alkanes and enolizable ketones and aldehydes are incompatible with these conditions, but measurement of trace water contamination in a wide range of alcohols, aprotic solvents (DMF,  $\text{CH}_3\text{CN}$ , DMSO, benzene, toluene, ether, THF, pyridine, etc.) is possible. Although it may seem surprising that the water content in alcohols can be measured by this technique, the iodonium ligand exchange reaction of an alcohol for fluoride is strongly disfavored. It is only the formation of the  $\text{I}=\text{O}$  double bond that drives the dehydration reaction under basic conditions.

In conclusion we have found that the  $\text{TBAF}^*/\text{PhI}(\text{OAc})_2/\text{TBABF}_4$  reagent combination removes water quantitatively from organic solvents and generates the easily detectable bifluoride ion in the process.  $^{19}\text{F}$  NMR spectroscopy of these solutions permits water concentration to be assessed sensitively and accurately for a relatively broad range of solvents. The aquametry technique is compatible with glove box and inert atmosphere

work; it is relatively rapid, and it needs no calibration other than the acquisition of a baseline  $^{19}\text{F}$  NMR spectrum. Moreover, it can be performed with dried, commercially available salts and NMR solvents. The difluoro-aryl- $\lambda^3$ -iodane-based procedure is a convenient alternative to Karl Fischer titration wherever NMR infrastructure is available.

## 2.4 Experimental

**Materials:** Iodobenzene diacetate (Aldrich), tetramethylammonium fluoride (TMAF, Aldrich), and tetrabutylammonium tetrafluoroborate (TBABF<sub>4</sub>, Fluka) were dried at 60–80 °C in a drying pistol (charged with P<sub>2</sub>O<sub>5</sub>) under dynamic vacuum for one week. D<sub>3</sub>-acetonitrile was refluxed with P<sub>2</sub>O<sub>5</sub> overnight, distilled directly into a flame-dried storage tube under dry nitrogen, and was stored over CaH<sub>2</sub> inside an inert atmosphere glove box. All glassware, syringes, and NMR tubes were oven-dried (140 °C) for more than 24 h before they were transferred into the glove box for use. TBAF was synthesized according to our previously reported method<sup>18</sup>. All other reagents were purchased from commercial sources and were used as received.

**General:** Crimp top vials (National Scientific, C4000-1W with 11 mm Fisherbrand PTFE/Silicone/PTFE seals) were fused to standard 5 mm NMR tubes. These tubes were sealed using a crimping tool (National Scientific) and the rubber seals. In addition to providing a readily sealed, reusable reactor for these experiments, the wide mouth at the top of the vial permitted solids to be introduced easily. All NMR experiments were performed using a Bruker Avance 400 MHz NMR spectrometer with the QNP probe tuned to  $^{19}\text{F}$  channel. (The sample spinner was turned off.) In order to obtain an accurate

integration of the  $^{19}\text{F}$  NMR signals of  $\text{HF}_2^-$  and  $\text{BF}_4^-$ , a single scan was used for each acquisition. Signal averaging (the collection of multiple scans) is possible provided the relaxation time is  $> 30$  seconds. Karl Fischer titrations were performed with a Metrohm 831 KF coulometer at the Novartis Corporation's research facility in Lincoln, Nebraska.

**Protocol for a typical water determination experiment:** a solution of iodobenzene diacetate (0.1 mmol) in  $\text{CD}_3\text{CN}$  (0.5 mL) was transferred to a small vial containing anhydrous TBAF (0.3 mmol). Upon dissolution of the solid, the solution was transferred into a modified NMR tube (see Figure 1), the tube was weighed, and an aliquot of standardized  $\text{TBABF}_4$  in acetonitrile- $\text{d}_3$  (108  $\mu\text{mol}$  /g solution) was added by syringe. The tube was reweighed to determine the precise amount of  $\text{TBABF}_4$  added, and the aluminum crimp cap and PTFE-lined silicon rubber septum were installed. The NMR tube was removed from the glove box and a baseline  $^{19}\text{F}$  NMR spectrum was obtained (within 15 min). Subsequently, a sample to be assayed was injected into the NMR tube by microsyringe. This operation was conducted outside the glove box for samples that contained more than 50  $\mu\text{g}$  of dissolved water, and inside the glove box (for low water concentration samples). The tared NMR tube was reweighed to determine the exact amount of sample added. A  $^{19}\text{F}$  NMR spectrum was taken within 15 minutes after sample introduction. The mass of added water was determined by measuring the increase in the area of the bifluoride signal (with respect to that of the  $\text{TBABF}_4$  internal standard signal) upon sample injection.

**Preparation of solid samples for multiple or future analysis:** If a large number of samples are to be assayed over an extended period of time, it is convenient to prepare a large number of sample tubes in advance. The only critical parameter for advanced preparation is that the amount of TBABF<sub>4</sub> standard in each tube must be known precisely. To accomplish this task, we used a technique similar to that given in the above protocol: the empty tube was weighed, an aliquot of standardized TBABF<sub>4</sub> in acetonitrile-d<sub>3</sub> (108  $\mu$ mol /g solution) was added by syringe, and the tube was reweighed to determine the precise amount of TBABF<sub>4</sub> added. The tubes were placed in a 100 mL Schlenk tube and the solvent was evaporated in vacuo. After the solvent was removed, iodobenzene diacetate (approximately 0.1 mmol) and anhydrous TBAF (approximately 0.3 mmol) were weighed directly into the tube. (The actual amounts are not critical for the experiment, but the molar ratio should be 1:2.5-3.0 for PhI(OAc)<sub>2</sub>:TBAF.) The aluminum crimp cap and PTFE-lined silicon rubber septum are installed and the tubes are stored in the glove box freezer for subsequent use. The stored samples are stable for at least one month.

**Use of <sup>1</sup>H NMR for water detection:** The change in the integrated area of the characteristic bifluoride ion <sup>1</sup>H NMR resonance ( $\delta$  = 15.7 ppm, Figure 2-1 ) can also be used to quantify added water. The main limitation to using <sup>1</sup>H NMR is that a reference signal is required as integration standard. If large amounts of solvents to be tested are added to the NMR tube, the signal to noise ratio of the bifluoride ion and integration standard degrades in a simple 1-D experiment. This problem can be surmounted by the

use of solvent suppression algorithms, but care must be exercised to use the appropriate power level so that the integrated areas of the bifluoride and integration standard signals remain unaffected.

## CHAPTER 3

### FLUORINATION OF ELECTRON-RICH AROMATICS VIA REDUCTIVE ELIMINATION OF DIARYL IODONIUM SALTS AND THE APPLICATION OF DIARYLIODONIUM SALTS IN RADIOTRACER SYNTHESIS

#### 3.1 Introduction

Modern Positron Emission Tomography (PET) is a functional imaging technique of high sensitivity and specificity, which is based on the coincident detection of two 511 keV photons, emitted upon positron annihilation in nearly opposite directions (Figure 3-1). It has become one of the most important and innovative clinical applications in oncology, cardiology and neurology.<sup>57</sup> PET also represents the method of choice to assess the distribution, pharmacokinetics and dynamics of a drug *in vivo* and can therefore play a key-role in drug discovery and development.<sup>58</sup>

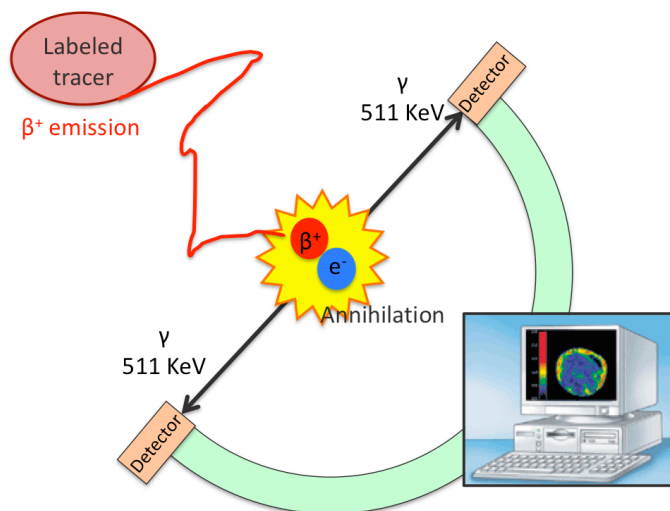


**Figure 3-1 Illustration of Positron Emission Tomography (PET).**



Imaging with PET requires the preparation of a positron-emitting radiolabeled probe also known as a radiotracer. The most widely used, short-lived positron-emitting isotopes are  $^{11}\text{C}$ ,  $^{13}\text{N}$ ,  $^{15}\text{O}$ , and  $^{18}\text{F}$ .<sup>59</sup> Some essential properties of these positron-emitting isotopes can be found in Table 3-1.

**Table 3-1 Nuclear properties of commonly used positron emitters. (Data taken from Browne and Firestone 1986 and from Brookhaven National Laboratory internet data base, BNL 2003.)**

Isotope	Half-life	Decay mode	$E_{\beta^+}^{\text{avg.}}$ [keV]	Maximum (average) range in $\text{H}_2\text{O}$ [mm]	Maximum specific activity [ $\text{GBq } \mu\text{mol}^{-1}$ ]
$^{11}\text{C}$	20.39 min	$\beta^+$ (99.8 %) EC (0.24 %)	385	3.8 (1)	$3.4 \times 10^5$
$^{13}\text{N}$	9.965 min	$\beta^+$ (99.8 %) EC (0.2 %)	491	5 (1.5)	$7.0 \times 10^5$
$^{15}\text{O}$	122.24 s	$\beta^+$ (99.9 %) EC (0.01 %)	735	7.6 (2.7)	$3.4 \times 10^6$
$^{18}\text{F}$	109.77 min	$\beta^+$ (96.73 %) EC (3.3 %)	242	2.2 (0.3)	$6.3 \times 10^4$

Among these radionuclides, fluorine-18 is thought to have excellent nuclear properties for PET applications. Its relatively low positron emission energy (633.5 keV) results in the shortest positron linear range in tissue (2.3 mm), and the highest resolution. A half-life of almost two hours is long enough for relatively extended imaging protocols and it permits multi-step synthetic approaches for the radiotracer. Last but not least, fluorine-18 can be reliably and routinely produced at the multi-Curie level from (p, n) nuclear reaction on an oxygen-18-enriched water target using a relatively low-energy

proton beam (e.g. 18 MeV). These advantages permit the use of fluorine-18-labeled radiotracers at “satellite” PET centers orbiting a central cyclotron production facility.

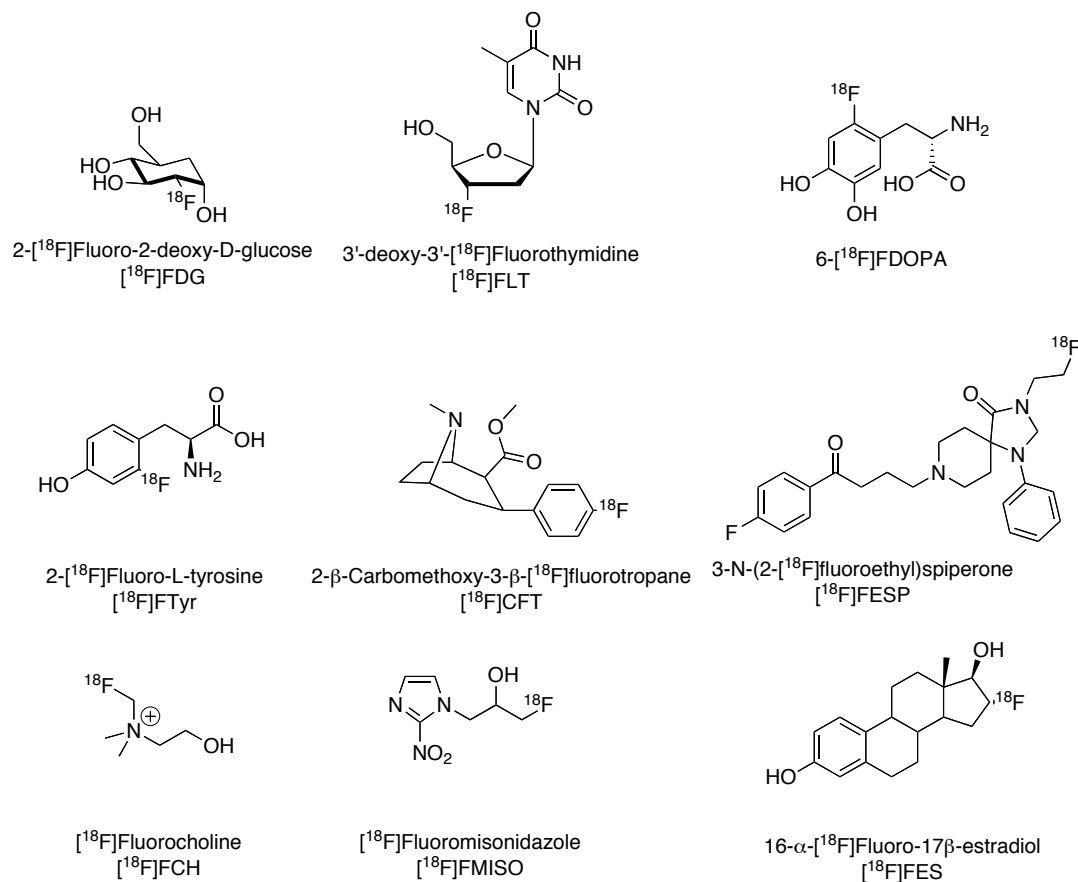


**Figure 3-2 Structures of  $^{18}\text{F}$ -labeled radiopharmaceuticals for clinical use or under preclinical studies.**

In contrast to a broad spectrum of drugs with defined *in vivo* behavior useful for  $^{11}\text{C}$ -,  $^{13}\text{N}$ - or  $^{15}\text{O}$ -labeling, fluorine-containing drugs comprise a somewhat smaller class. Most  $^{18}\text{F}$ -labeled radiotracers developed so far have  $^{18}\text{F}$ -labels replacing C-H or C-O bonds. Some are designed especially for PET imaging. Since alteration of pharmacokinetic and pharmacodynamics cannot be excluded for  $^{18}\text{F}$ -compounds that closely resemble the parent structure, evaluation using *in vitro* and *in vivo* models is

necessary, prior to the human application. The most widely used PET radiotracer is  $^{18}\text{F}$ -2-fluoro-2-deoxy-D-glucose or simply  $[^{18}\text{F}]\text{FDG}$ . FDG is a very good general metabolic indicator, and it is easily available via nucleophilic fluorination. Figure 3-2 shows the structures of  $[^{18}\text{F}]\text{FDG}$  and other promising  $[^{18}\text{F}]$ -labeled radiotracers. Note that most of these radiotracers are easily accessible by nucleophilic aliphatic fluorination by displacement of a tosylate or triflate group on the precursors. Compounds like  $[^{18}\text{F}]\text{FDOPA}$ ,  $[^{18}\text{F}]\text{FTyr}$  and  $[^{18}\text{F}]\text{CFT}$  are examples of non-activated aromatic systems for nucleophilic fluorination, and their syntheses remain a significant challenge for radiochemists; these synthetic challenges greatly limit the application of these aromatic radiotracers in PET imaging.

**Table 3-2 Production routes to  $[^{18}\text{F}]\text{fluoride}$  and  $[^{18}\text{F}]\text{fluorine}$ .<sup>60</sup>**

Nuclear reaction	$^{18}\text{O}(\text{p},\text{n})^{18}\text{F}$	$^{16}\text{O}(^3\text{He},\text{n})^{18}\text{F}$	$^{20}\text{Ne}(\text{d},\alpha)^{18}\text{F}$	$^{18}\text{O}(\text{p},\text{n})^{18}\text{F}$
Target	$\text{H}_2^{18}\text{O}$	$\text{H}_2\text{O}$	Ne (0.1~0.2 % $\text{F}_2$ , 18 atm)	$^{18}\text{O}_2$ , 20 atm
Energy range of bombarding particle [MeV]	$16 \longrightarrow 0$	$36 \longrightarrow 0$	$11.2 \longrightarrow 0$	$10 \longrightarrow 0$
Chemical form	$[^{18}\text{F}]\text{F}_{\text{aq}}^-$	$[^{18}\text{F}]\text{F}_{\text{aq}}^-$	$[^{18}\text{F}]\text{F}_2$	$[^{18}\text{F}]\text{F}_2$
Thick target yield [MBq $\mu\text{A}^{-1}\text{h}^{-1}$ ]	2.200	250	350 – 450	~ 350
Specific activity [GBq $\mu\text{mol}^{-1}$ ]	$40 \times 10^3$	$40 \times 10^3$	0.04 – 0.4	0.04 – 2

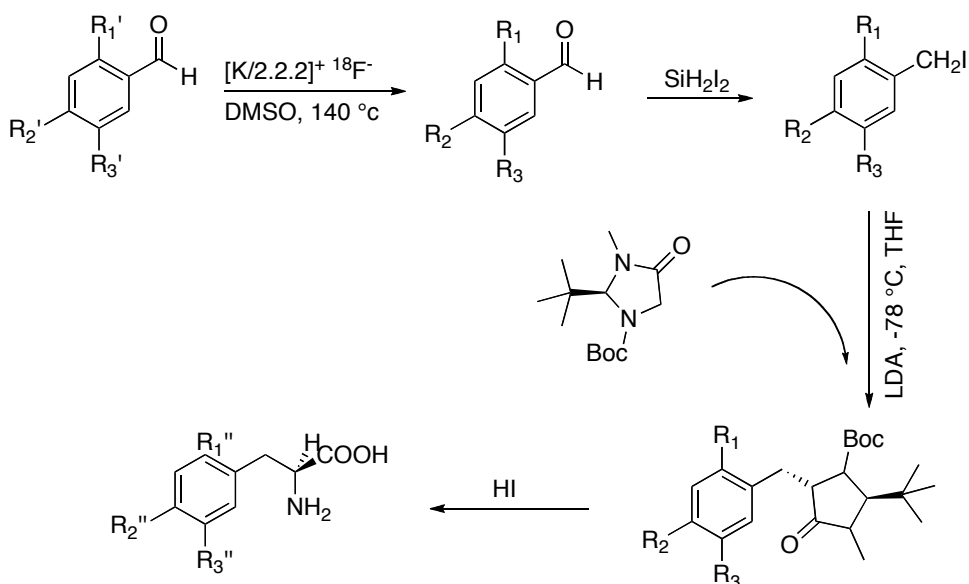
Four commonly used production routes for  $^{18}\text{F}$  nuclei are listed in Table 3-2. It is easy to recognize that the  $^{18}\text{O}(\text{p},\text{n})^{18}\text{F}$  nuclear reaction on highly enriched  $\text{H}_2^{18}\text{O}$  is the

most effective way to generate  $^{18}\text{F}$ . The  $^{18}\text{F}$ -fluoride ( $[^{18}\text{F}]\text{F}_{\text{aq}}^-$ ) generated is of high specific activity and suitable for nucleophilic substitution.<sup>61</sup> In contrast,  $[^{18}\text{F}]\text{F}_2$ , the primary species for electrophilic fluorination, can only be obtained in low specific activities and low thick target yields. (Thick target yield is a measurement of radioisotope formation rate). Therefore, the versatility of labeling strategies to produce high specific  $^{18}\text{F}$ -radiotracers is greatly restricted. To be specific, the inability to directly functionalize electron-rich arenes with  $^{18}\text{F}$ -fluoride narrows the substrate scope and increases the expense of practical  $^{18}\text{F}$ -labeled radiotracers for PET.<sup>62</sup>

Efforts to circumvent this arene fluorination problem are ongoing. In a procedure described by Bergman and Solin (1997),<sup>63</sup>  $[^{18}\text{F}]\text{CH}_3\text{F}$  was synthesized from  $[^{18}\text{F}]\text{F}^-$  in a inert neon matrix.  $[^{18}\text{F}]\text{F}_2$  was obtained following an electric discharge, a rearrangement and  $^{18}\text{F}$ -for- $^{19}\text{F}$  exchange.  $[^{19}\text{F}]\text{F}_2$  was used as a carrier and the  $[^{18}\text{F}]\text{CH}_3\text{F}/[^{18}\text{F}]\text{F}_2$  conversion efficiency topped at 60 % when 500 nmol or more carrier fluorine was used, while the discharge time was set to be 10 sec. Starting from 37 GBq  $[^{18}\text{F}]\text{F}^-$ , more than 7.5 GBq  $[^{18}\text{F}]\text{F}_2$  can be produced with a specific activity up to 55 GBq  $\mu\text{Mol}^{-1}$ , which was over 100 times higher compared to the typical specific activity of  $[^{18}\text{F}]\text{F}_2$  obtained through direct bombardment of  $^{20}\text{Ne}$  or  $[^{18}\text{O}]\text{O}_2$ , yet still two orders of magnitude lower than the specific activity of n.c.a.  $[^{18}\text{F}]\text{F}^-$ .

“Nucleophilic routes” toward unactivated arene functionalization have been investigated with the aim of introducing the  $^{18}\text{F}$  label.<sup>64-66</sup> The idea is to include accessory activating groups that will enable nucleophilic aromatic substitution. The accessory group is then removed, or otherwise converted to a desired functionality during a multistep

synthesis. Figure 3-3 summarizes the asymmetric synthesis of [ $^{18}\text{F}$ ]FTyr, 6-[ $^{18}\text{F}$ ]FDOPA, and 4-[ $^{18}\text{F}$ ]Fluoro-*meta*-L-tyrosine (4-[ $^{18}\text{F}$ ]FmTyr) starting with nucleophilic aromatic fluorodenitration of the appropriate aldehydes.<sup>67</sup> The fluorobenzaldehydes were reduced to corresponding benzyl iodides and subsequently alkylated with (S)-1-Boc-2-*tert*-butyl-3-methyl-4-imidazolidinone (S-Boc-BMI). Finally, hydrolysis with hydrogen iodide led to the expected tracers. The conversion was completed within 125 min with 11-16 % decay corrected radiochemical yield (RCY). Overall, the multistep method offers only limited improvement over the one-step electrophilic demetalation procedure.

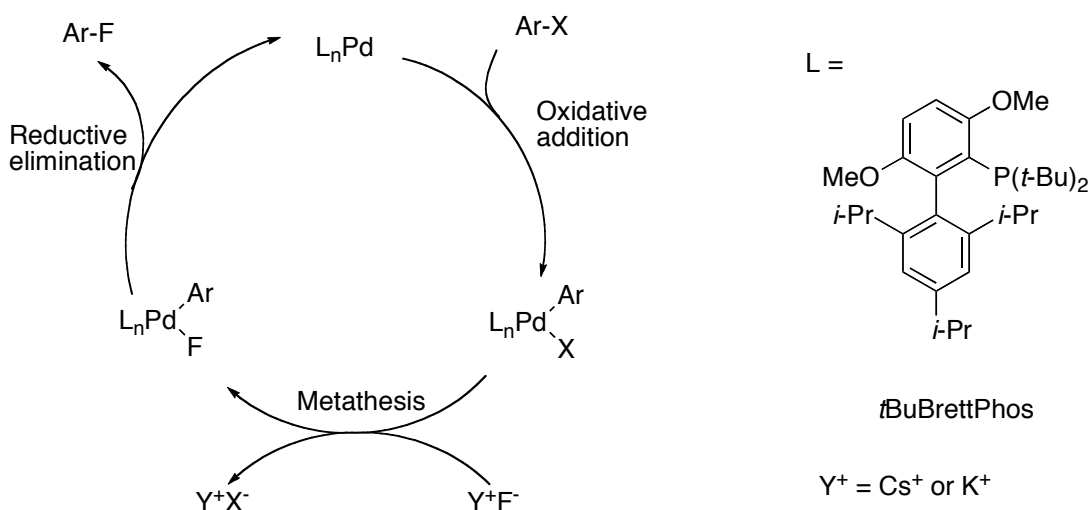


[ $^{18}\text{F}$ ]FTyr : R<sub>1</sub>' = NO<sub>2</sub> or Me<sub>3</sub>N<sup>+</sup>SO<sub>3</sub>CF<sub>3</sub><sup>-</sup>, R<sub>1</sub> = R<sub>1</sub>'' = <sup>18</sup>F, R<sub>2</sub> = R<sub>2</sub>' = OMe, R<sub>2</sub>'' = OH, R<sub>3</sub> = R<sub>3</sub>' = R<sub>3</sub>'' = H;  
 [ $^{18}\text{F}$ ]FDOPA: R<sub>1</sub>' = NO<sub>2</sub> or Me<sub>3</sub>N<sup>+</sup>SO<sub>3</sub>CF<sub>3</sub><sup>-</sup>, R<sub>1</sub> = R<sub>1</sub>'' = <sup>18</sup>F, R<sub>2</sub> = R<sub>2</sub>' = R<sub>3</sub> = R<sub>3</sub>' = OMe, R<sub>2</sub>'' = R<sub>3</sub>'' = OH;  
 4-[ $^{18}\text{F}$ ]FmTyr: R<sub>2</sub>' = NO<sub>2</sub> or Me<sub>3</sub>N<sup>+</sup>SO<sub>3</sub>CF<sub>3</sub><sup>-</sup>, R<sub>2</sub> = R<sub>2</sub>'' = <sup>18</sup>F, R<sub>3</sub> = R<sub>3</sub>' = OMe, R<sub>3</sub>'' = OH, R<sub>1</sub> = R<sub>1</sub>' = R<sub>1</sub>'' = H

**Figure 3-3** Multistep synthesis of n.c.a. [ $^{18}\text{F}$ ]FTyr, [ $^{18}\text{F}$ ]FDOPA and 4-[ $^{18}\text{F}$ ]FmTyr.<sup>67</sup>

Two other fluoride-based approaches to <sup>18</sup>F-labeled, electron-rich fluoroarenes have been heavily investigated of late: 1) transition-metal-catalyzed fluorination,<sup>68-70</sup> and 2) elimination of aryl fluorides from diaryliodonium salts.<sup>71</sup>

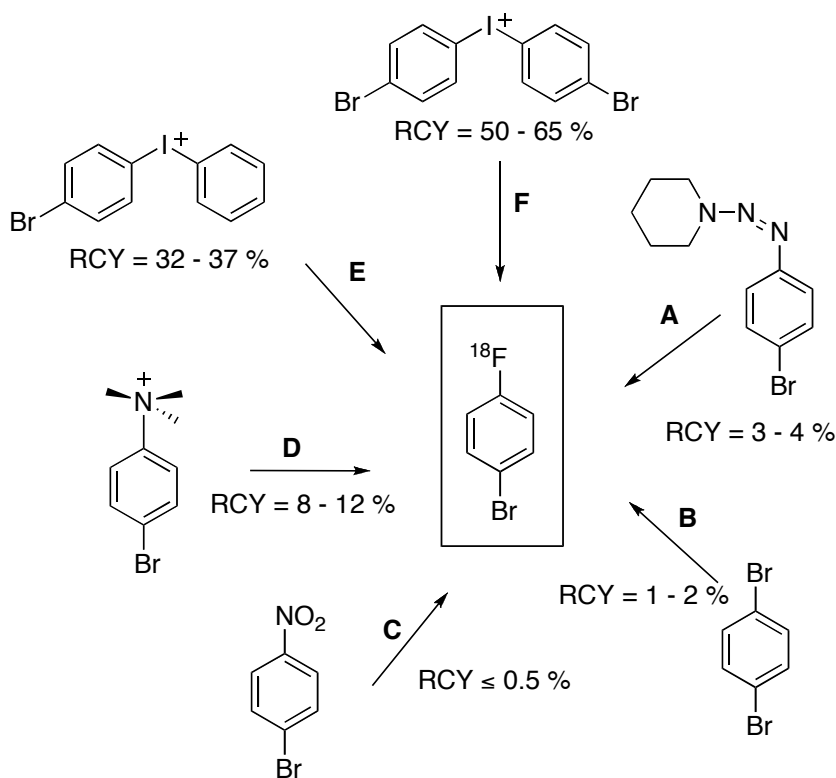
For metal mediated C-F bond formation to create ArF, reductive elimination is the most difficult step. Buchwald and colleagues<sup>69</sup> reasoned that dimer formation of fluoro-Palladium complexes may impede reductive elimination of ArF and prepared the monomeric complex  $\text{LPd(II)Ar(F)}$ , which finally enabled the sought-after reductive elimination step and delivered ArF as the product. The authors show that *t*BuBrettPhos (structure shown in Scheme 3-1) is the ideal ligand for fluorinating aryl triflates with CsF or spray-dried KF as the fluoride source. The steric size of *t*BuBrettPhos may also help to induce reductive elimination of ArF by compressing the Ar-Pd-F angle. Therefore, the correct choice of ligand is key to the success of metal-mediated fluorination.



**Scheme 3-1 Pd-catalyzed aromatic fluorination utilizing *t*BuBrettPhos as the ligand.<sup>69</sup>**

The Buchwald chemistry worked well to provide fluorinated heteroaromatics and various aromatics with electron-withdrawing substituents, while electron-rich aromatics required higher temperatures. In some cases, this led to unexpected formation of regioisomeric products, especially for reactions done in toluene. The mechanism leading to the formation of the regioisomers is not well understood but replacing toluene with

cyclohexane was found to effectively suppress this undesirable pathway. Nevertheless, for electron-rich aromatics more reduction products (ArH) were formed resulting in lower overall yields. Also, *ortho*-positioned Lewis basic groups are not compatible with the method. Despite these limitations, the method is a breakthrough in metal-mediated C-F bond formation. However, it is still not practical for accessing  $^{18}\text{F}$  aryl fluorides (6 equivalent of CsF was used).



**Scheme 3-2 One-step methods to n.c.a. 1-bromo-4-[ $^{18}\text{F}$ ]fluorobenzene.<sup>72</sup>**

Compared to the metal catalyzed approach, successful fluorination via decomposition of diaryliodonium salts has been known since the 1980's.<sup>73-75</sup> Pike and colleagues<sup>71</sup> were the first to introduce this method to  $^{18}\text{F}$ -PET tracer synthesis. The reaction was initially assumed to be  $\text{S}_{\text{N}}2$ -like with iodoarenes as super leaving-groups;

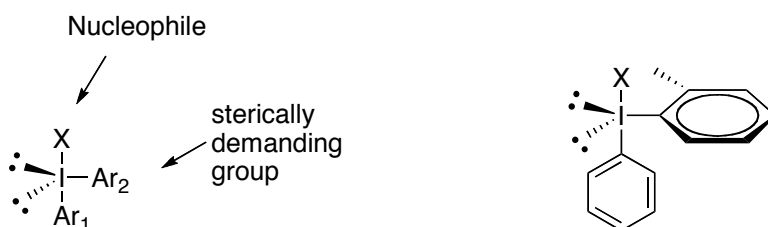
and polar solvents such as acetonitrile and DMAF were thought to be most appropriate for these reactions. The method is considered to be advantageous for being one-step and of high RCY. After comparing six methods (Scheme 3-2) for the one-step synthesis of n.c.a. 1-bromo-4-[ $^{18}\text{F}$ ]fluorobenzene, Ermert and colleagues<sup>72</sup> reached the conclusion that decomposition of symmetrically substituted 4-bromophenyliodonium salt far outperformed other methods to give the highest RCY of up to 65 %. The unsymmetrically substituted (4-bromophenyl)phenyl-iodonium salt resulted in lower RCY of 32 -37 % because it has the drawback of forming [ $^{18}\text{F}$ ]fluorobenzene (30 %) as byproduct. It is obvious that using a symmetrically substituted iodonium precursor would maximize the radiochemical yield, yet synthesis of such precursors for drugs with complicated structures is not practical. An effort has been made to improve the regioselectivity on fluorination of unsymmetrically substituted iodonium precursors so that better RCY can be achieved.

It is known that the nucleophilic attack (including the attack by fluoride) on diaryliodonium salt occurs preferably at the more electron-deficient ring<sup>76</sup>. This is because the attack of nucleophile leads to build-up of negative charge attacked ring in the transition state. Electron-rich aryl substituents such as 4-methoxyphenyl<sup>72</sup> and 2-thienyl<sup>77</sup> are typically incorporated in precursors as “dummy” or “directing” ligands to allow  $^{18}\text{F}$ -labeling of electron-rich aromatics.

A steric influence of substituents, known as the “ortho effect”<sup>78, 79</sup> also influences the regioselectivity of arene functionalization during diaryliodonium(III) decomposition reactions. The current explanation for the “ortho effect” states that the more sterically



demanding ortho-substituted ring occupies the so-called equatorial position and is preferentially attacked by the nearby nucleophile, which occupies one of the axial positions (Scheme 3-3). Despite being well accepted in the field, the theory does not adequately explain all of the reported results,<sup>80</sup> suggesting that the outcome of the reaction may be governed by more complicated factors.



**Scheme 3-3 More stable complex formed by diaryliodonium cation and the nucleophile with the sterically demanding aryl group occupying the equatorial position (left); Structure proposed by Lancer to explain the observed “ortho effect” for decomposition of (2-methylphenyl)phenyliodonium by nucleophiles (right).**

The incorporation of [ $^{18}\text{F}$ ] into target arenes was reported to work reasonably well for a variety of simple aromatic model compounds. Due to the extremely small scale of these  $^{18}\text{F}$  fluorination reactions, it is impossible to identify the  $^{18}\text{F}$ -labeled products with conventional spectrometric methods. Therefore, radio HPLC or radio TLC was used for product identification and yield determination. Although the radio-chromatographic methods are highly reliable, caution must be exercised to ensure that the labeled compound does not coelute with a contaminant or isomer. That this error can be made was demonstrated in a study of the radiofluorination of 2-thienyliodonium salts. An initial  $^{18}\text{F}$  study showed that no 2-fluorothiophene was formed, suggesting the 2-thienyl group causes the process to be regiospecific.<sup>77, 81</sup> However, closer examination of the

reaction mixture revealed that the process was not as selective as would appear from the fluoroarene products only.<sup>82</sup> Another problem with the studies dealing with [<sup>18</sup>F]fluorination is that optimized conditions were sometimes highly divergent among different research groups. For example: Zhang and colleagues<sup>83</sup> claimed that DMSO was favorable over acetonitrile, THF, and DMF as a solvent for [<sup>18</sup>F]fluorination; while according to Ermert,<sup>72</sup> no labeling reaction was observed in DMSO and DMF led to the highest RCY.

So far, the approach to <sup>18</sup>F-labeling through diaryliodonium salt decomposition has been investigated mainly for simple, readily prepared diaryliodonium model compounds.<sup>62</sup> Only a few applications to prepare specific radiotracers<sup>83</sup> have emerged. Without an understanding of the detailed mechanism of the process, it is impossible to make the method generally applicable. Since it is hard to gain useful information about the true mechanism of the reaction by investigating [<sup>18</sup>F] fluoride chemistry alone, model reactions with [<sup>19</sup>F]fluoride (“cold” reactions) need to be studied systematically. Of the few such “cold” fluorination studies reported<sup>84</sup>, incorporation of fluoride was rather inefficient (less than 30 % of total fluoride added), leaving ample room for improvement. Therefore, we decided to take advantage of our access to highly reactive anhydrous fluoride salts<sup>18, 22, 85</sup> and systematically investigate the decomposition of diaryliodonium salts by [<sup>19</sup>F]fluoride.

### 3.2 Decomposition of diaryliodonium salts by fluoride

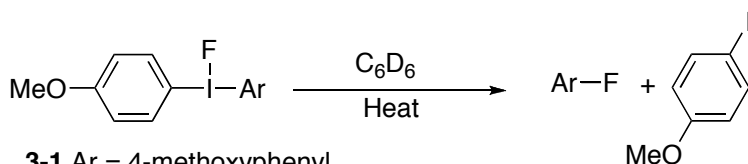
We showed in CHAPTER 2 that difluoro-aryl- $\lambda^3$ -iodanes are stable in benzene, but slowly decompose to give bifluoride and the corresponding iodoarene, upon standing

at room temperature in acetonitrile and DMSO. Knowing that polar solvents stabilize higher oxidation states, we suspected solvent-promoted disproportionation was the cause of the unwanted decomposition.

Diaryliodonium fluoride should be susceptible to a similar decomposition pathway in polar solvents. Thus, we began our studies by examining the most simple diaryliodonium fluoride, diphenyliodonium fluoride. Indeed, at room temperature, a solution of diphenyliodonium nitrate and 1 equivalent of TBAF\* gave rise to iodobenzene and TBAHF<sub>2</sub> upon standing in acetonitrile or DMSO. No fluorobenzene was detected in the reaction mixture. Heating the same reaction mixture to 80 °C resulted in formation of fluorobenzene in up to 30 % yield; the remainder of the fluoride ended up as bifluoride and tetrafluoroborate (by reacting with borosilicate glass). The low efficiency of the fluoride incorporation agrees with a previous literature report.<sup>84</sup> Addition of extra fluoride was detrimental to the reaction and further lowered the yield of fluorobenzene to 18 %. Suppressing the suspected disproportionation pathway by switching to non-polar solvents, such as benzene, led to a significant improvement in the yield of fluorobenzene (almost quantitative). Under these conditions, no bifluoride or tetrafluoroborate was detected by the <sup>19</sup>F NMR spectroscopy.

Encouraged by these preliminary results, we set out to investigate the decomposition of a set of diaryliodonium salts by fluoride. Figure 3-4 shows a list of the diaryliodonium fluoride salts investigated in this study. These salts all feature the electron-rich 4-methoxyphenyl ring as one of the aryl substituents on the I(III) center. This ligand is considered to be an excellent “directing group” for arene functionalization.

Salts **3-1** through **3-8** conveniently allowed us to study electronic and steric effects on the regioselectivity of the reductive elimination process; and compounds **3-9** and **3-10** are suitably protected precursors of previously investigated radiotracers  $^{18}\text{F}$ -6-fluorodopamine<sup>86</sup> and  $^{18}\text{F}$ -2-fluoroestradiol<sup>87</sup> respectively. For comparison, the decomposition was run in both benzene and acetonitrile, with and without additional salts (from making the iodonium fluoride).



- 3-1** Ar = 4-methoxyphenyl  
**3-2** Ar = 3,4-dimethoxyphenyl  
**3-3** Ar = 2-methoxyphenyl  
**3-4** Ar = 2-methyl-4,5-dimethoxyphenyl  
**3-5** Ar = 2,6-dimethoxyphenyl  
**3-6** Ar = Ph  
**3-7** Ar = m- $\text{CF}_3$ Ph  
**3-8** Ar = m-CNPh

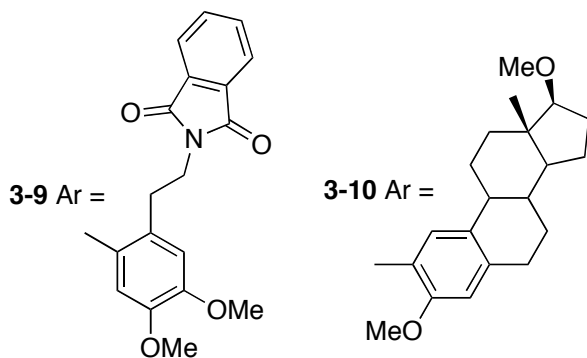


**Figure 3-4** List of diaryliodonium fluorides made and studied.

The diaryliodonium hexafluorophosphate precursors to compounds **3-1** through **3-10** were made by two established methods<sup>88, 89</sup> (detailed synthetic procedures and characterization for the compounds can be found in the experimental section of this chapter): precursors **3-1**, **3-7** and **3-8** were prepared by  $\text{H}_2\text{SO}_4$  catalyzed electrophilic

aromatic substitution of anisole by  $\text{ArI}(\text{OAc})_2$  followed by ion exchange. The rest of the hexafluorophosphate precursors were prepared from the corresponding tributylstannanes and  $p\text{-OMePhI}(\text{OH})(\text{OTs})$ .<sup>90</sup> The clean diaryliodonium fluorides **3-2** through **3-10** were synthesized by mixing the corresponding  $\text{PF}_6$  salts and anhydrous  $\text{TMAF}$ <sup>91</sup> in acetonitrile, evaporation of the solvent, treatment with anhydrous benzene, and filtration to remove the insoluble  $\text{TMAPF}_6$ . Owing to its insolubility, **3-1** was precipitated from dry THF by treatment of the trifluoroacetate salt with TBAF\*. Preparations of aryl fluorides from compounds **3-1** through **3-8** in  $\text{d}_6$ -benzene and  $\text{CD}_3\text{CN}$  solutions (140 °C, 15 min) were performed in sealed NMR tubes. Yields were determined by  $^1\text{H}$  NMR spectroscopy and confirmed by GC analysis (Table 3-3). Decomposition of compound **3-9** and **3-10** was only performed in  $\text{d}_6$ -benzene without added salt.

**Table 3-3 Observed yields of ArF from the decomposition of 3-1 through 3-8.**

#	No added salt		1 equiv. added $\text{TMAPF}_6$	
	$\text{C}_6\text{D}_6$	$\text{CD}_3\text{CN}$	$\text{C}_6\text{D}_6$	$\text{CD}_3\text{CN}$
	(ArF + 4FA)	(ArF + 4FA)	(ArF + 4FA)	(ArF + 4FA)
<b>3-1</b>	86 (-)*	43 (-)	76 (-)	17 (-)
<b>3-2</b>	91 (77+14)	38 (30+8)	78 (59+19)	3 (2+1)
<b>3-3</b>	72 (49+23)	60 (40+20)	84 (59+25)	3 (2+1)
<b>3-4</b>	90 (78+12)	81 (49+32)	90 (76+14)	3 (2+1)
<b>3-5</b>	70 (32+38)	34 (7+27)	67 (28+39)	3 (1+2)
<b>3-6</b>	77 (57+20)	55 (40+15)	51 (41+10)	4 (3+1)
<b>3-7</b>	95 (85+10)	68 (68+0)	86 (86+0)	33 (33+0)
<b>3-8</b>	89 (89+0)	78 (78+0)	98 (93+5)	0

\* Yield does not include the regioisomer 3-fluoroanisole formed, total fluoride incorporation > 95 %

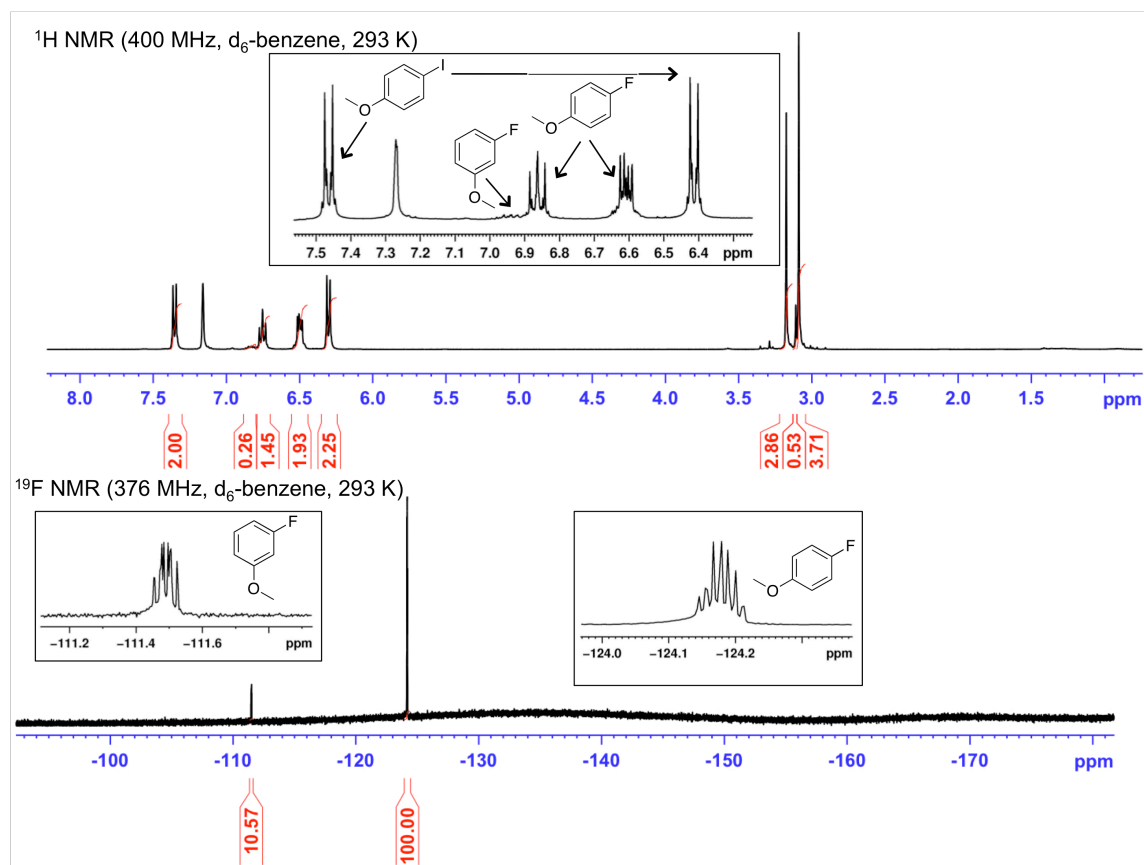


**Figure 3-5**  $^1\text{H}$  and  $^{19}\text{F}$  NMR spectra of **3-1** decomposition mixture in benzene.

For symmetrically substituted diaryliodonium salt **3-1**, the incorporation of fluoride was greater than 95 % in dry benzene (NMR spectra of the reaction mixture shown in Figure 3-5). However, both the expected 4-fluoroanisole and its regioisomer 3-fluoroanisole were formed in a 9:1 ratio. A change of the reaction condition resulted in change in the ratio of the fluorinated products. Solvent polarity is a decisive factor in determining the regioisomer ratio. Polar solvents tend to minimize the formation of regioisomer, 3-fluoroanisole. For example, when acetonitrile or DMSO was used as the reaction solvent, no 3-fluoroanisole was detected. When dichlorobenzene saturated with

TMAOTf was used as solvent, the ratio of 4-fluoroanisole to 3-fluoroanisole increased to 40:1.

Similar regioisomer formation was observed by Buchwald for reductive elimination of arylPd(II) fluoride species.<sup>69</sup> They also reported a strong dependence of product ratio on solvent polarity. However, in that case, non-polar solvents seemed to suppress the formation of undesired regioisomer. The mechanism leads to the formation of 3-fluoroanisole is not well understood, though we suspect the intermediacy of benzyne in the I(III) reaction. Grushin<sup>92</sup> reported the formation of fluoroarenes through aryne intermediates in the reaction of bromoarenes with TMAF at elevated temperature. With the positively charged iodanyl group being strongly  $\sigma$ -withdrawing, the *ortho* proton becomes more acidic and is likely abstracted to yield an aryne species. The GC spectrum (Figure 3-6) of the reaction mixture revealed that anisole was also formed as a minor product.

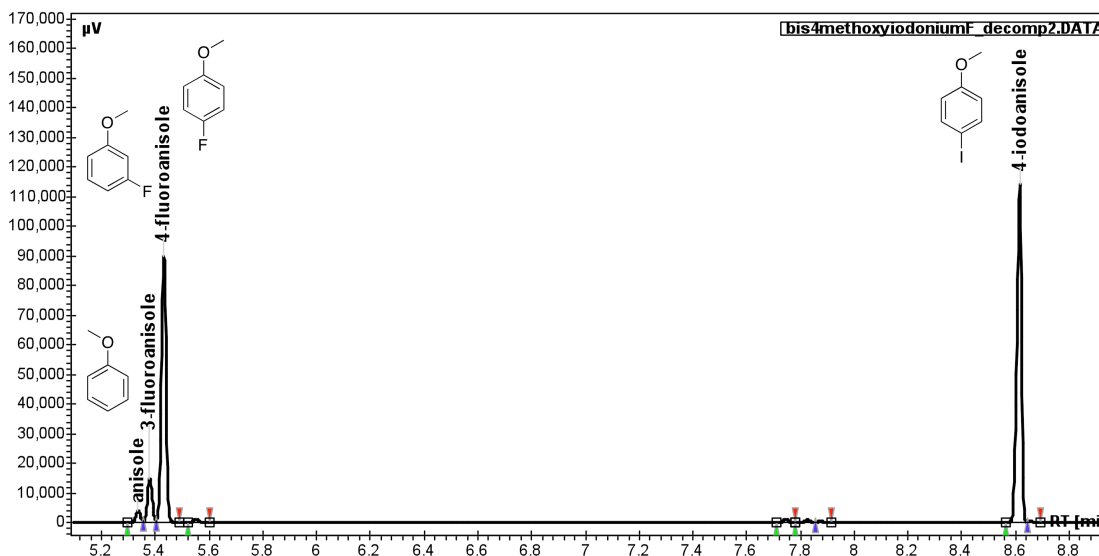


**Figure 3-6** GC spectrum: reaction mixture of 3-1 decomposition in dry benzene.

Inspection of the results of thermal decomposition of compound **3-2** through **3-8** shows that, as expected, the 4-methoxyphenyl group directs the fluoride nucleophile to the electron-poor aromatic ring.<sup>62</sup> The 2,6-dimethoxyphenyl group on compound **3-5** features two *ortho*-methoxy substituents, which makes it more electron-rich than the 4-methoxyphenyl “directing group”. As a result, 4-fluoroanisole was the main product formed. The so-called “*ortho*” effect, in which *ortho* substituents promote functionalization is not observed OR groups (**3-3** and **3-5**). In contrast, the *ortho*-methyl substituent on **3-4** did result in a marginally higher selectivity for the fluorination reaction in benzene. Formation of rearranged products, which we attribute to benzyne formation, was only observed for electron-rich rings (compound **3-2** through **3-5**). In all cases, the percentage of the misfluorinated regioisomer was no more than 5 % of the expected fluoroarene.

Compounds **3-9** and **3-10** are suitably protected precursors of the previously investigated radiotracers <sup>18</sup>F-6-fluorodopamine<sup>86</sup> and <sup>18</sup>F-2-fluoroestradiol,<sup>87</sup> respectively. They were decomposed to the corresponding fluorinated arenes in excellent (80 % for **3-9**) and fair (39 % for **3-10**) yields in benzene. The reduced fluorination yield for the latter compound is accompanied by a concomitant increase in the amount of 4-fluoroanisole produced, consistent with the similar “directing group” abilities of the 2-methoxy and 4-methoxy substituents.

As is expected, the observed yields of arene fluorination are generally improved if the reaction is performed in benzene. For slightly activated systems (compounds **3-7** and **3-8**), decomposition of pure iodonium fluoride salts was not affected by solvent polarity.



In contrast, for complexes that undergo reductive elimination more reluctantly (compound **3-3** and **3-5**), the yields of fluoroarenes was significantly higher in benzene. Importantly, if added salt is present, as is always the case when  $^{18}\text{F}$  fluoride is used, the yields of fluoroarenes decrease precipitously in acetonitrile.

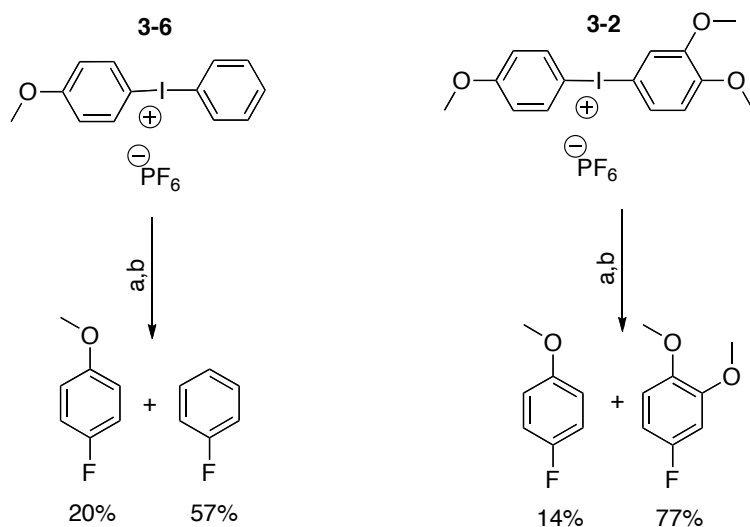
Again, the formation of bifluoride and a small amount of  $\text{BF}_4^-$  (from the borosilicate NMR tube) was observed in acetonitrile reactions, whereas no inorganic fluoride byproducts were seen when benzene was employed as the reaction solvent. The presence of salts may further increase the polarity of solvent and accelerate the undesired decomposition pathway. These observations suggest that disproportionation may be responsible, in part, for the poor yields of fluorinated reductive elimination products frequently observed from electron rich fluorodiaryl- $\lambda^3$ -iodane precursors. Alternatively, the added salt may facilitate fluoride ligand exchange reactions.

In conclusion, our studies suggest that the reductive elimination process for diaryliodonium fluoride resembles that for aryl transition metal fluorides in that both are compromised by disproportionation reactions. Use of non-polar solvents, such as benzene, suppresses disproportionation and leads to significant improvements in total fluorination yields in thermal decomposition reactions of diaryliodonium fluorides.

### 3.3 Fluoride promoted aryl-swapping of the diaryliodonium cations

Electronic substituent effects offer the greatest control of regioselectivity in diaryliodonium salt decomposition. In general, the more electron-poor ring is functionalized selectively. During the course of our work with diaryliodonium salts we observed this trend in regioselectivity, however, we were also struck by the fact that

regioselectivity was not strongly correlated to the electronic character of the two rings. As a result, the yield of relatively electron-rich arylfluorides remains low despite the use of highly electron-rich 4-methoxyphenyl substituent as the directing group. For example, the diaryliodonium salt **3-6**, which features an electron-rich 4-methoxyphenyl substituent paired with a relatively electron-poor aryl substituent, gave surprisingly poor regioselectivity (Scheme 3-4). Also of interest was that the regioselectivity became increasingly worse as the reaction progressed. The observation of the surprisingly better regioselectivity for fluorination of **3-2**, and the intriguing time course of the regioselectivity of **3-6** led us to investigate in detail the reaction of fluoride ion with diaryliodonium salts. These studies led us to discover the remarkably facile, fluoride-promoted aryl ligand exchange reactions of these compounds.



**Scheme 3-4** Observed regioselectivity for **3-6**(PF<sub>6</sub>) (featuring the relatively electron-poor phenyl substituent) is worse than that of **3-2**(PF<sub>6</sub>) (featuring relatively electron-rich 3,4-dimethoxyphenyl group.) a. TMAF/CH<sub>3</sub>CN, evaporation of solvent, addition of d<sub>6</sub>-benzene, filtration; b. 140 °C, 15 minutes.

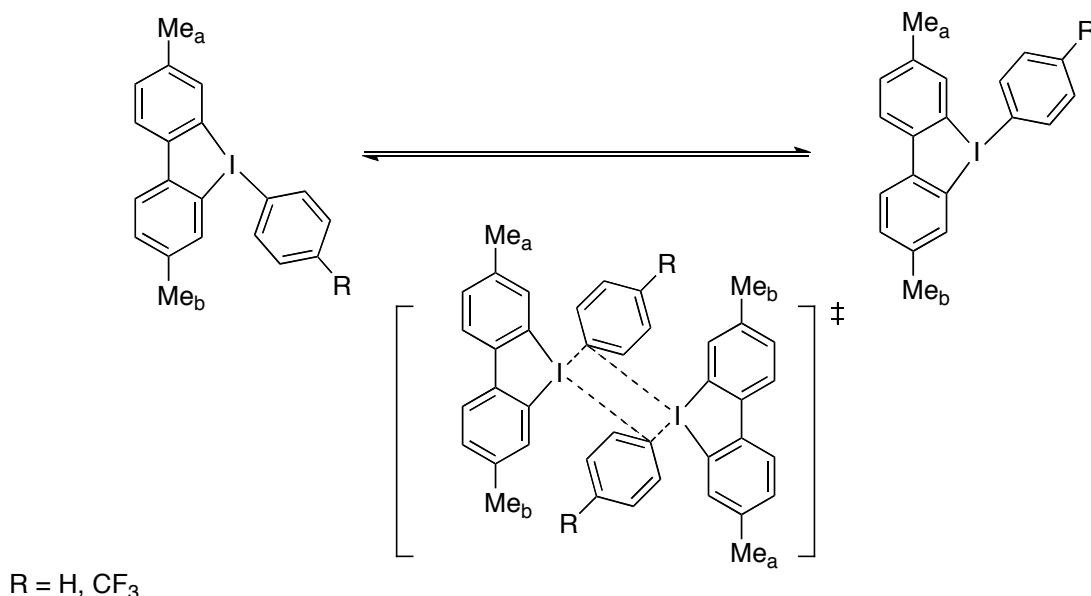


**Figure 3-7 Proposed exchange in 5-aryl-3,7-dimethyl-5H-dibenziodoles.<sup>93</sup>**

Aryl transfer from organometallic reagents (Sn,<sup>88, 94</sup> Si,<sup>90, 95</sup> B,<sup>96, 97</sup> and Li<sup>98, 99</sup>) to monoaryliodine(III) species is commonly used to prepare diaryliodine(III) compounds. These compounds, in turn, are used as arylating reagents to either directly transfer one of the aryl ligand to organic<sup>100-104</sup> or inorganic nucleophiles,<sup>105, 106</sup> or do so via transition metal catalysis<sup>107-114</sup>. The exchange of aryl ligands on I(III) centers is in line with the general tendency of these compounds to engage in reactions typical of organometallic complexes. Though it has not previously been observed directly, exchange of aryl ligands among I(III) centers in diaryliodonium salts has been posited in a few studies. Reutov and colleagues<sup>115</sup> observed isotope exchange between diaryliodonium tetrafluoroborates and [<sup>131</sup>I]-labeled aryl iodides at the melting temperatures of the salts. Reich and Cooperman<sup>93</sup> have shown that 5-aryl-3,7-dimethyl-5H-dibenziodoles shows temperature dependent NMR spectra. At low temperatures, two methyl groups appear as singlets at  $\delta$  2.24 and 2.41 ppm, which coalesce as the temperature is raised. The line shape changes

are reversible and consistent with degenerate thermal isomerization of the aryl ligand about the T-shaped iodine. The observation of large negative entropies of activation and irreproducible rate constants for the isomerization of the same compound at the same temperature were interpreted as evidence against a unimolecular and in favor of an intermolecular ligand exchange isomerization mechanism (Figure 3-7). Although previous reports have suggested aryl ligand exchange in these compounds, here we show for the first time that mildly basic ligands, such as fluoride, catalyze facile aryl swapping among diaryliodonium(III) species at room temperature.

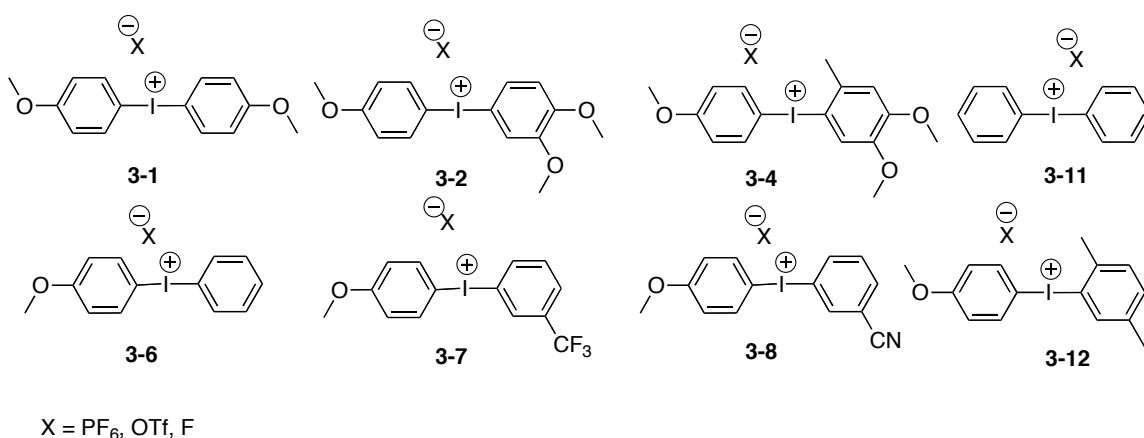


**Figure 3-8** Diaryliodonium salts discussed in this section. Throughout the text, the particular counterion of interest (X = PF<sub>6</sub>, OTf, F) is denoted in parentheses following the compound number (i.e. **3-1**(PF<sub>6</sub>)).

Compounds shown in Figure 3-8 were prepared by established methods<sup>103, 116, 117</sup> and used for this study. Treatment of the symmetrical diaryliodonium hexafluorophosphates **3-1**(PF<sub>6</sub>) and **3-11**(PF<sub>6</sub>) with tetramethylammonium fluoride (TMAF) in CD<sub>3</sub>CN gave rise to ion exchange to the corresponding fluoride salts, **3-1**(F)

and **3-11(F)**, as was evidenced by the appearance of a broad singlet in the downfield region of the  $^{19}\text{F}$  NMR spectra ( $\delta = -17.9$  ppm for **3-1(F)**,  $\delta = -13.0$  ppm for **3-11(F)**) and a concomitant sharpening of the signals for the  $\text{PF}_6$  anion at  $\delta = -72.8$  ppm. A general upfield shift of the signals in the aromatic region was also noted in the  $^1\text{H}$  NMR spectrum (Figure 3-9). In contrast, treatment of the unsymmetrically substituted diaryliodonium salt **3-6(PF<sub>6</sub>)** with TMAF under the same conditions led to a complex change in the spectrum (Figure 3-9) with an apparent doubling of the number of signals in the aromatic region.

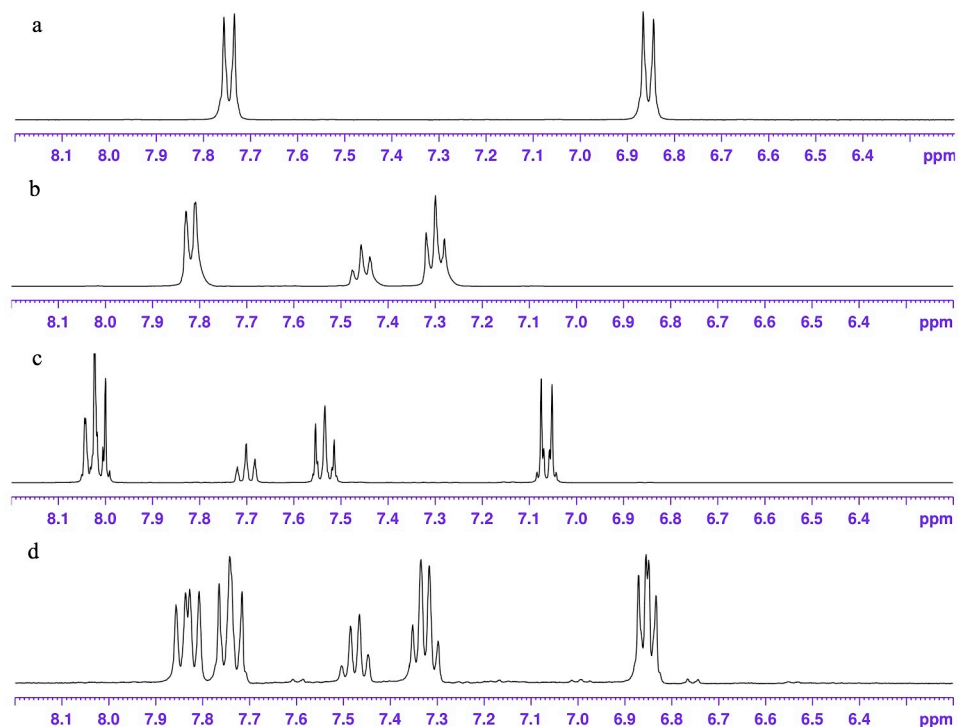
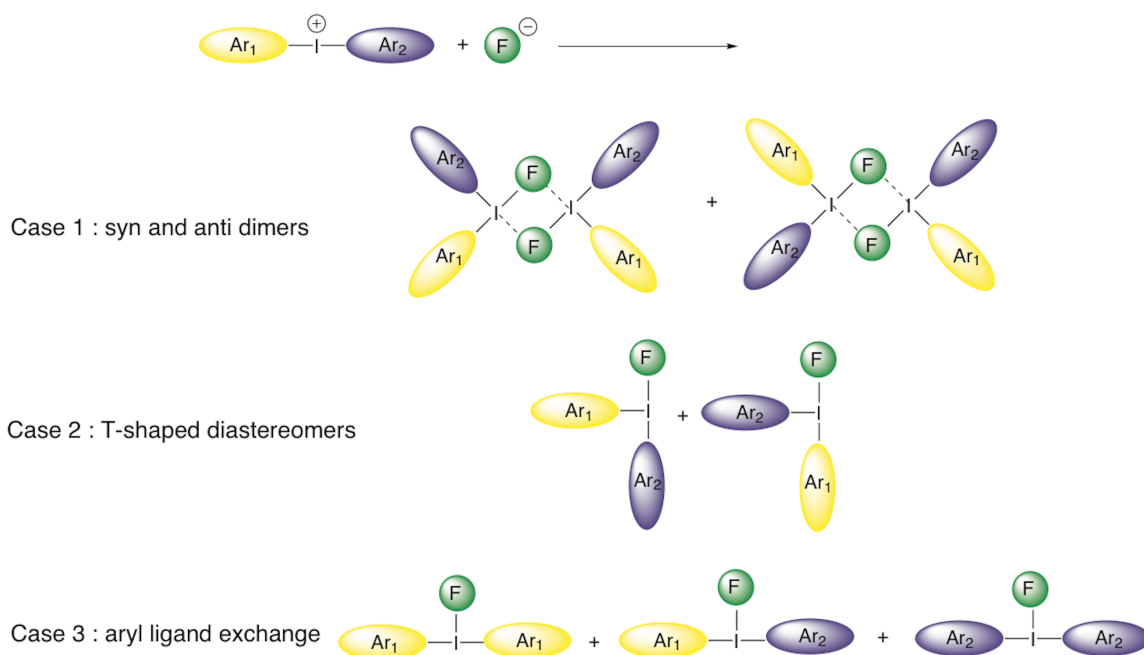


**Figure 3-9**  $^1\text{H}$  NMR spectra in  $\text{CD}_3\text{CN}$  of a) **3-1(F)**, b) **3-11(F)**, c) **3-6(PF<sub>6</sub>)**, and d) **3-6(PF<sub>6</sub>)** after it was treated with TMAF in  $\text{CH}_3\text{CN}$ , desalted with benzene, and dissolved in  $\text{CD}_3\text{CN}$ . Only the aromatic regions are displayed for clarity.

Such an increase in complexity could arise from several causes (Scheme 3-5), including dimerization into syn- and anti- dimers, different T-shaped geometries with aryl groups occupying the axial positions, or fast ligand exchange promoted by the addition of fluoride ion.



**Scheme 3-5 Possible origins of the additional complexity observed in the  $^1\text{H}$  NMR spectrum of **3-6**( $\text{PF}_6$ ) after addition of fluoride.**

To test whether the addition of fluoride ion was promoting the formation of bridged dimers, the fluoride salt obtained by treatment of **3-6**( $\text{PF}_6$ ) with TMAF was further treated with TMS triflate to generate the I(III) triflates and to remove the fluoride in the form of  $\text{TMSF}$ . Even after all traces of fluoride were removed, the  $^1\text{H}$  NMR spectrum remained complex and distinct from that of an independently synthesized **3-6**( $\text{OTf}$ ). Thus, the formation of dimers as a possible origin of the observed spectral complexity could be excluded. To examine whether the addition of fluoride had

promoted formation of two different T-shaped diastereomers, we independently synthesized **3-6(OTf)**, **3-1(OTf)**, and **3-11(OTf)** and subjected them to ES-MS analysis. The pure salt **3-6(OTf)** gave a single clean molecular ion peak at  $M = 310.7$  ( $M^+ (-OTf)$ ). Similarly **3-1(OTf)** and **3-11(OTf)** gave molecular ion peaks at 280.7 and 340.7 daltons, respectively, indicating that these three compounds flew cleanly and did not undergo any exchange reactions during the electrospray ionization process in the mass spectrometer. In contrast, a preparation of the triflate salt of **3-6(OTf)** that had been exposed previously to fluoride ion gave three molecular ion peaks at 280.7, 310.7, and 340.7 daltons, indicating formation of three distinct diaryliodonium salts (Figure 3-10).

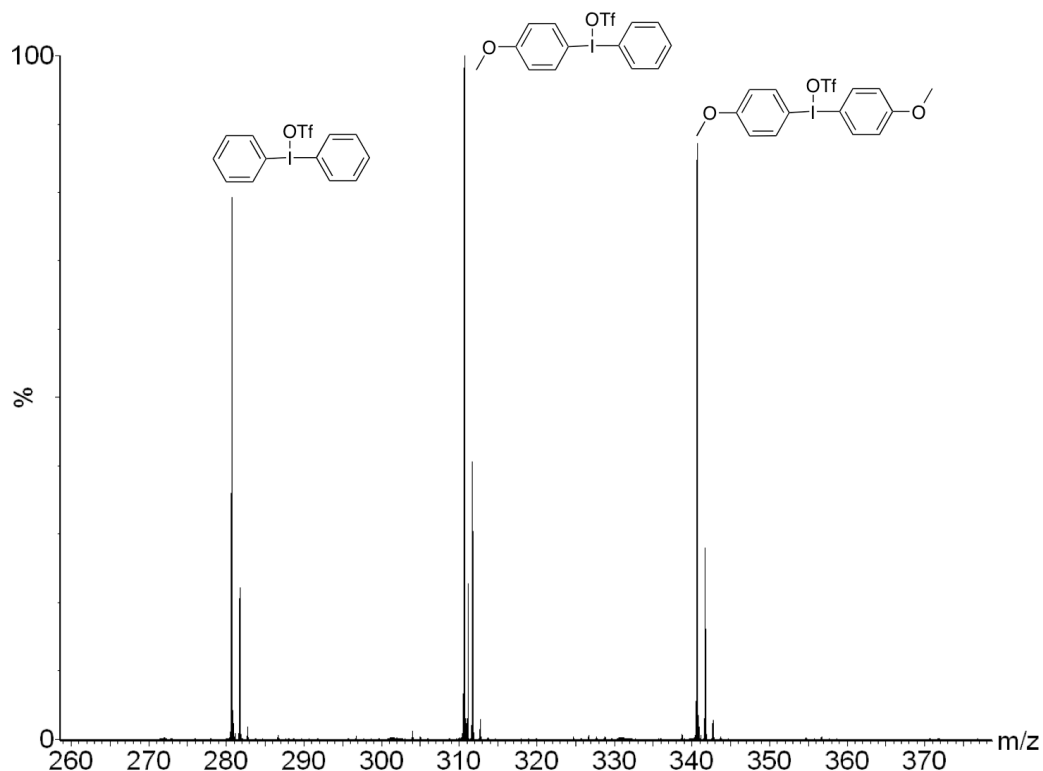
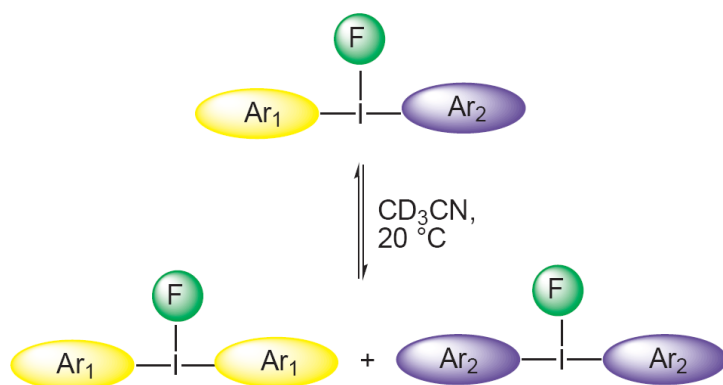


**Figure 3-10** ES-MS spectrum of **3-6(OTf)** that had previously converted to the fluoride salt and exchanged back to the triflate.

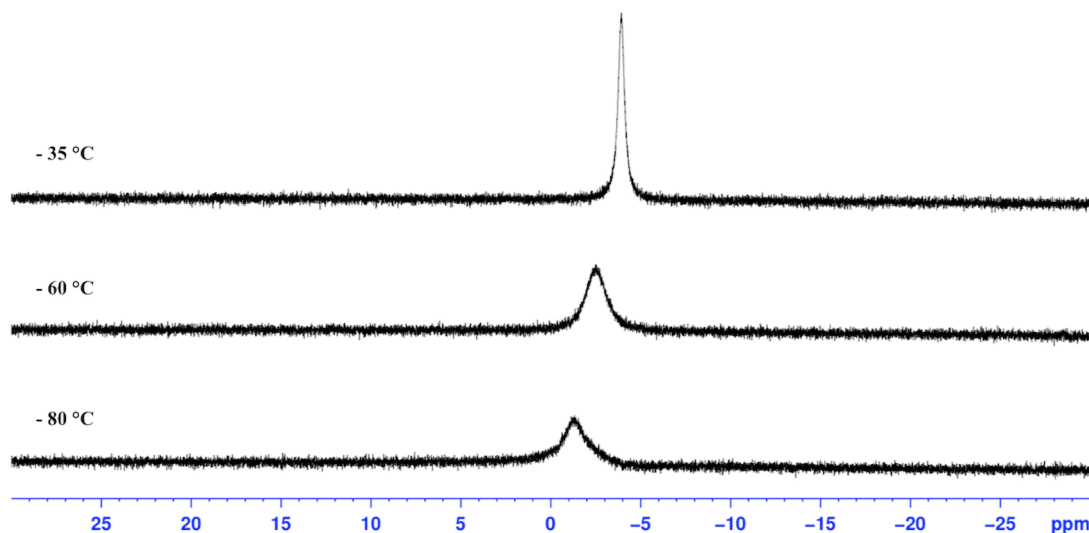
MS-MS analysis of each of these ions indicated that the principal decomposition product was the corresponding biphenyl, formed by extrusion of iodine. The ES-MS data are consistent with the formation of three different diaryliodonium compounds upon treatment of unsymmetrical diaryliodonium salts with fluoride in solution, and definitively exclude formation of different T-shaped diastereomers as a possible origin of the complexity observed by NMR spectroscopy. All data support a remarkably rapid, fluoride-catalyzed aryl exchange reaction for unsymmetrically substituted diaryliodonium salts, and the presence of an equilibrium mixture of three distinct diaryliodonium fluorides in solution (Scheme 3-6).



**Scheme 3-6 Fluoride-catalyzed aryl exchange of diaryliodonium salts.**

Despite the existence of three separate diaryliodonium fluorides in solution,  $^{19}\text{F}$  NMR spectra of the mixture in  $\text{CD}_3\text{CN}$  display one broad singlet at -12.3 ppm. This observation is consistent with a fast exchange of fluoride among the three I(III) species. We sought to slow the exchange rate by removing excess salts, switching to a nonpolar solvent ( $d_8$ -toluene) and lowering the temperature, but under no circumstances could we reach the coalescence temperature for the exchange. Representative low-temperature (-35 °C, -60 °C, and -80 °C)  $^{19}\text{F}$  NMR spectra are shown in Figure 3-11.

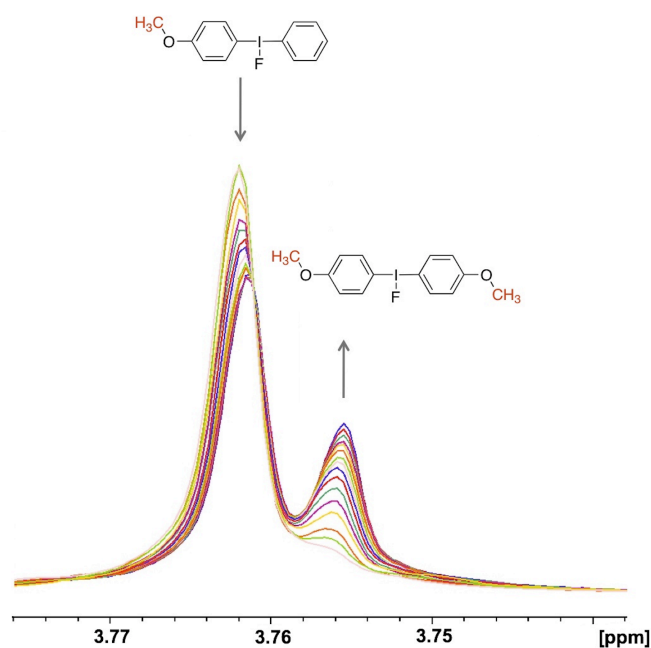




**Figure 3-11**  $^{19}\text{F}$  NMR spectra of **1(F)**, **3(F)** and **4(F)** in  $d_8$ -toluene at various temperatures.

Since radiotracer synthesis is typically conducted with nanograms of fluoride ion and a million-fold excess of potential substrate, we decided to probe the rate of the aryl exchange process as a function of fluoride ion concentration. As was seen above, adding one equivalent of TMAF to a solution of **3-6(PF<sub>6</sub>)** in dry CD<sub>3</sub>CN allowed the aryl exchange reaction to reach equilibrium before the first  $^1\text{H}$  NMR data could be obtained (approximately 8 minutes). This rapid equilibration implies a first order rate constant for the process of at least  $1.2 \times 10^{-3} \text{ s}^{-1}$ . (The simple kinetic model used to determine this rate constant is  $-\text{d}[\text{Ar}_1\text{-I-Ar}_2]/\text{dt} = k([\text{Ar}_1\text{-I-Ar}_2] - [\text{Ar}_1\text{-I-Ar}_2]_{\text{eq}})$  where  $[\text{Ar}_1\text{-I-Ar}_2]_{\text{eq}}$  is the concentration of the remaining heterogeneously substituted diaryliodonium salt once an equilibrium has been established). In contrast, when the TMAF concentration was only halved, aryl exchange became so slow ( $t_{1/2} > 24 \text{ h}$ ) that the rate could not be determined accurately since it was on the same timescale as decomposition processes. With 0.89

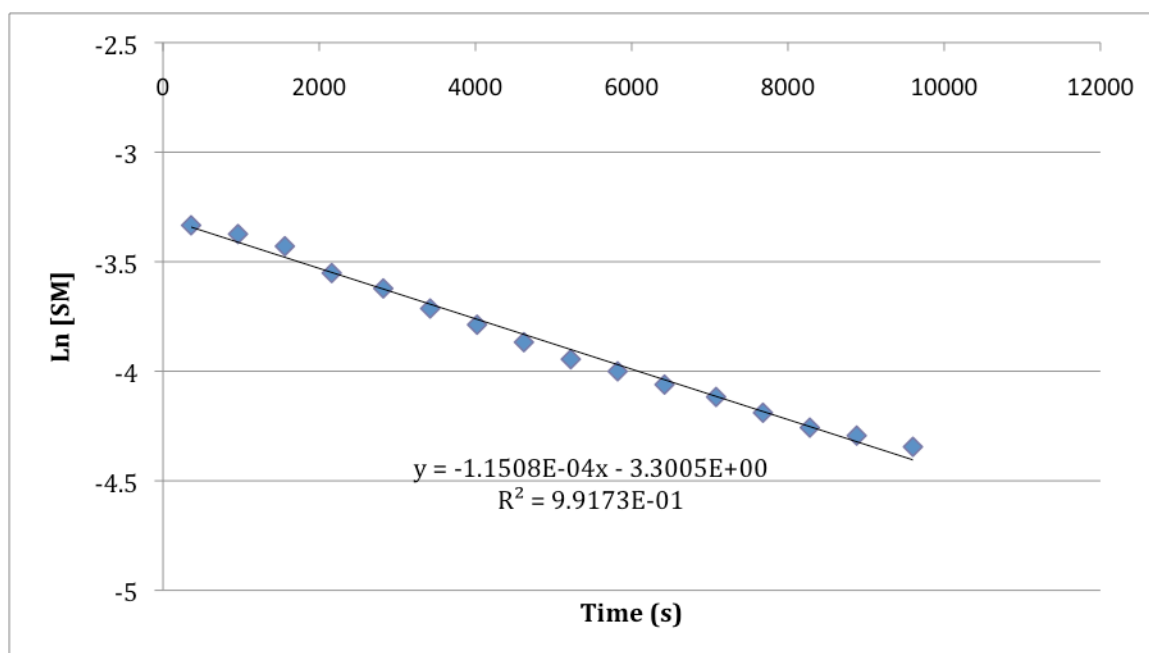
equivalents of added TMAF, the reaction rate was in an intermediate range convenient for performing a kinetic study by  $^1\text{H}$  NMR spectroscopy.



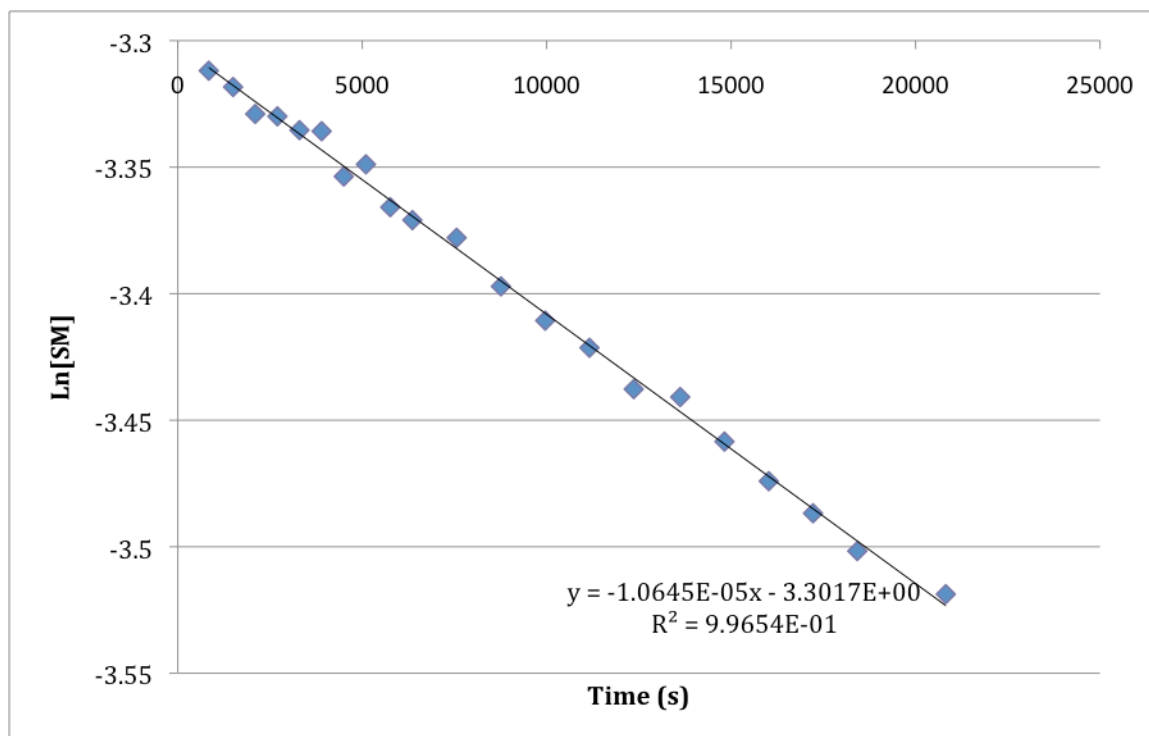
**Figure 3-12** Stacked  $^1\text{H}$  NMR spectra (detail showing the *p*-methoxy region) of **3-6**(PF<sub>6</sub>) and 0.89 equiv of TMAF. Elapsed time = 160 min.

Figure 3-12 shows a set of stacked  $^1\text{H}$  NMR spectra taken over the initial 160 min for the reaction of **3-6**(PF<sub>6</sub>) and 0.89 equivalent of TMAF in dry acetonitrile. (The reaction took 8 hours to reach equilibrium.) A first order plot ( $\ln[\text{Ar}_1\text{-I-Ar}_2]/[\text{Ar}_1\text{-I-Ar}_2]_{\text{eq}}$  vs. time) of these data yielded a rate constant  $1.15 \times 10^{-4} \text{ s}^{-1}$  (Figure 3-13). The rate of the aryl exchange process was found to be a very sensitive, nonlinear function of fluoride ion concentration. When the amount of added TMAF corresponded to 0.81 equivalents (9% less compared to 0.89 equiv) the equilibration rate dropped about 10 fold; the observed rate constant was  $1.06 \times 10^{-5} \text{ s}^{-1}$  (Figure 3-14). These observations suggest that the

majority of the fluoride remains bound to the iodine(III) center, and that a small amount of dissociated fluoride is responsible for catalyzing the aryl exchange process. With a substoichiometric amount of added fluoride, the concentration of dissociated “free” fluoride is low, leading to a drastic decrease in the rate of aryl group exchange. These results suggest that fluoride-catalyzed aryl exchange may not be a significant concern under the conditions used typically for PET radiotracer synthesis where fluoride ion concentration is very low, and also that this catalyzed exchange reaction could have synthetic potential.



**Figure 3-13 Plot of  $\ln[\text{Ar}_1\text{-I-Ar}_2]/[\text{Ar}_1\text{-I-Ar}_2]_{\text{eq}}$  vs. time for aryl-swapping of 1(PF<sub>6</sub>) with 0.89 equiv added fluoride.**



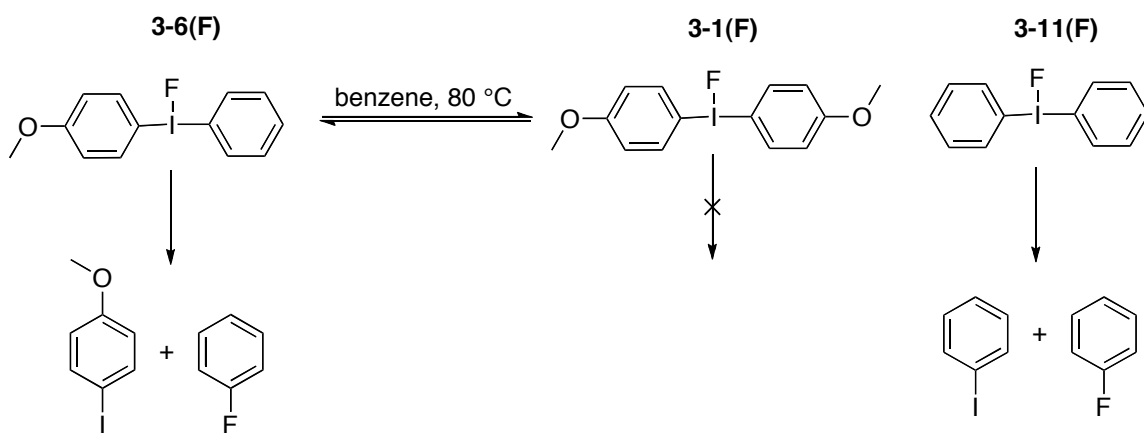
**Figure 3-14 Plot of  $\ln[\text{Ar}_1\text{-I-Ar}_2]/[\text{Ar}_1\text{-I-Ar}_2]_{\text{eq}}$  vs. time for aryl-swapping of **1**(PF<sub>6</sub>) with 0.81 equiv added fluoride.**

In the previous section, we found that the presence of excess salts, even seemingly benign salts such as TMAPF<sub>6</sub>, could have a profound and negative impact upon the amount of fluoroarene produced during the reductive elimination process. The mechanism by which excess salt promotes deleterious side reactions remains obscure, but a reasonable hypothesis is that these additional ions serve to balance charge during ligand exchange reactions, and that ligand exchange reactions are related to the formation of I(III) species of differing redox potentials. Accordingly, we investigated whether excess salt, namely, the TMAPF<sub>6</sub> formed from the ion exchange reaction, facilitated the aryl ligand exchange process. We precipitated and isolated **3-1(F)** by treating **3-1(PF<sub>6</sub>)** with TBAF in THF. <sup>1</sup>H and <sup>19</sup>F NMR analyses indicated that no TBAPF<sub>6</sub> remained in the

sample after this desalting procedure. When **3-1(F)** was mixed with one equivalent of similarly desalted **3-11(F)** in acetonitrile, an aryl exchange reaction ensued which reached equilibrium in less than 10 minutes. Since a full equivalent of fluoride was present and TMAPF<sub>6</sub> was not, this experiment indicates that the fluoride ion concentration is a much more important determinant of the aryl exchange rate than the concentration of spectator salts. Similarly, when one equivalent of **3-1(F)** was mixed with one equivalent of **3-11(PF<sub>6</sub>)** in CD<sub>3</sub>CN solution (to give a total of 0.5 equivalents of fluoride ion), aryl exchange did not proceed to an observable extent within 24 hours. These results support the conclusion that added TMA salts of weakly coordinating anions do not play a significant role in the aryl exchange reactions of diaryliodonium salts in CD<sub>3</sub>CN.

To investigate the propensity of aryl ligand exchange to occur under the high temperature conditions used for aromatic fluoridation, we examined the thermal decomposition of diaryliodonium salts in the presence of substoichiometric amounts of fluoride at 80 °C in d<sub>6</sub>-benzene. In a typical experiment 0.05 mmol of **3-6(PF<sub>6</sub>)** was dissolved in 0.3 mL of dry acetonitrile and 0.025 mmol of anhydrous TMAF in 0.3 mL acetonitrile was introduced. The solvent was removed *in vacuo*, dry d<sub>6</sub>-benzene was added to the remaining salts, and the mixture was shaken and filtered into a J-Young NMR tube equipped with a screw top PTFE closure. <sup>1</sup>H and <sup>19</sup>F NMR revealed that very little, if any aryl exchange occurred during the sample preparation. The sample was heated to 80 °C, and the reaction progress was monitored by NMR spectroscopy. At this temperature both reductive elimination and aryl exchange were evident. During the

course of the reaction only three decomposition products were formed: fluorobenzene, iodobenzene and iodoanisole. Importantly, the amount of fluorobenzene formed equaled the sum of the amounts of iodobenzene and 4-iodoanisole that formed. This observation indicates that fluoridation of benzene occurred by reductive elimination reactions of two different salts (Scheme 3-7).



**Scheme 3-7 Mechanism for the generation of iodobenzene during the thermal decomposition of 3-6(F).**

It is noteworthy that the regioselectivity for fluorobenzene formation was perfect; no 4-fluoroanisole was formed under these conditions (0.5 equivalents of fluoride). Instead, the symmetrical diaryliodonium salt **3-1(PF<sub>6</sub>)** accumulated during the course of the reaction. (An independently prepared sample of **3-1(PF<sub>6</sub>)** treated 0.5 equivalents of TMAF could only be coaxed to undergo reductive elimination at appreciable rates at temperatures significantly higher than 80 °C.) The highly selective formation of fluorobenzene observed in this case contrasts dramatically with the results obtained when a full equivalent of fluoride was used (Table 3-3). Under stoichiometric conditions a relatively large amount of fluoroanisole was generated. In addition, the time course of the

reaction **3-6(PF<sub>6</sub>)** with 1 equivalent of TMAF showed exceptionally high selectivity for fluorobenzene formation at low conversion at early times, and only at a much longer reaction time did fluoroanisole begin to form. This study makes clear that aryl exchange and thermal decomposition are in competition at high temperature, even when substoichiometric amounts of fluoride are in solution. If fluoride is still present when no phenyl-substituted diaryliodonium salts remain, **3-1(F)** begins to decompose to 4-fluoroanisole, albeit at an appreciably slower rate that fluorobenzene is formed. Thus, the true “directing group abilities” of aryl substituents in diaryliodonium salt fluoridation reactions can only be determined when the fluoride is present at low concentration and the reaction is monitored to determine which aryl iodides and which salts are generated during the course of the functionalization process. Alternatively, the true ability of aryl ligands on I(III) to direct regioselective functionalization can be assessed using other nucleophiles that do not promote aryl ligand exchange. Such nucleophiles include soft, relatively nonbasic anions such as azide or thiophenoxide.

It seems clear from these data that fluoride-promoted aryl exchange reactions may not play an important role in the preparation of [<sup>18</sup>F]-labeled radiotracers because the miniscule amount of <sup>18</sup>F-fluoride added is unlikely to catalyze aryl ligand exchange. However, fluoride is not the only anion capable of promoting aryl swapping in diaryliodonium species. Fluoride is just one of many hard, basic, and strongly coordinating anions; we found that others, including hydroxide, ethoxide, and phenoxide also catalyze aryl exchange reactions of diaryliodonium salts. This exchange process may

be responsible, in part, for the fact that hydrolysis reactions of unsymmetrical diaryliodonium salts are reported to be insensitive to electronic effects.<sup>118</sup>

**Table 3-4<sup>a</sup> Equilibrium populations of symmetrically and unsymmetrically substituted diaryliodonium fluorides.**

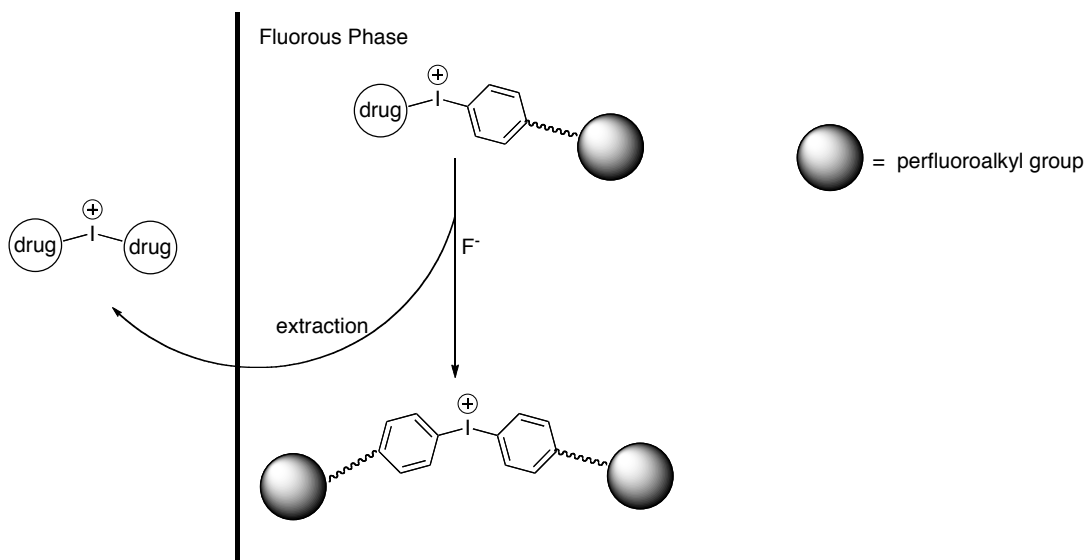
#	Ar <sub>1</sub> -I-Ar <sub>2</sub> (%)	Ar <sub>1</sub> -I-Ar <sub>1</sub> (%)	Ar <sub>2</sub> -I-Ar <sub>2</sub> (%)
<b>3-2</b>	50	25	25
<b>3-6</b>	56	22	22
<b>3-7</b>	74	13	13
<b>3-8</b>	>98	<1	<1
<b>3-4</b>	64	18	18
<b>3-12</b>	62	19	19

[a] Ratios measured by integration of <sup>1</sup>H NMR spectra. Equilibration was performed treating the corresponding PF<sub>6</sub> salts with one equivalent of TMAF in acetonitrile. The solvent was evaporated and the remainder dissolved in d<sub>6</sub>-benzene (60 mM total concentration) for NMR analysis.

The fluoride-catalyzed aryl exchange reaction provides a means by which the relative solution stabilities of various diaryliodonium salts can be interrogated directly for the first time. Inspection of Table 3-4, which lists the relative populations of symmetrically and unsymmetrically substituted diaryliodonium salts at equilibrium in benzene for variously substituted I(III) compounds, indicates that the unsymmetrically substituted diaryliodonium salt becomes increasingly more stable as the electronic disparity between the two rings increases. In the absence of competing steric effects, if two relatively electron-rich rings are bonded to an I(III) center, as in **3-2(F)**, the observed distribution is simply statistical at equilibrium; in contrast, when an electron-rich and an electron-poor aromatic substituents are present, as in **3-8(F)**, the unsymmetrically



substituted diaryliodonium salt predominates. In the case of *ortho*-methylation of one of the aryl substituents (as in **3-4(F)** and **3-12(F)**), the additional steric demand in the vicinity of iodine shifts the equilibrium toward the unsymmetrically substituted salt, even when other strong electron-donating substituents are on the ring. These observations are consistent with an explanation that invokes steric destabilization of symmetrical diaryliodonium salts bearing *ortho*-substituents.



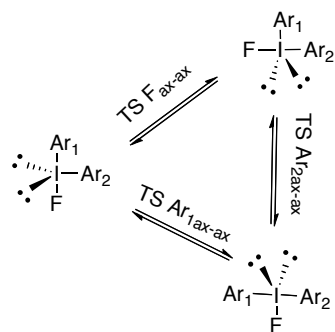
**Scheme 3-8 Proposed utilization of aryl-swapping in bis-drug iodonium salts synthesis.**

In conclusion, we have shown that diaryliodonium species undergo aryl-ligand exchange in the presence of fluoride and other strongly coordinating, hard anions. The data seem to support a mechanism by which a small amount of dissociated “free” fluoride is responsible for catalyzing the aryl ligand exchange among I(III) complexes. Aryl exchange reactions are fast if fluoride is present in nearly stoichiometric amounts, and become precipitously slower as fluoride concentration is diminished. Aryl exchange lowers the apparent regioselectivity of aryl-fluoride extrusion from diaryliodonium

fluorides under stoichiometric conditions, but this problem disappears at low fluoride ion concentration. The fluoride-catalyzed exchange reaction is an interesting mechanistic tool for measuring relative solution stabilities of various diaryliodonium species directly. It is also possible that this reaction may be useful to prepare novel and currently inaccessible mixed or symmetrically substituted diaryliodonium salts by inducing aryl ligand exchange in solutions containing more easily obtained precursors (Scheme 3-8).

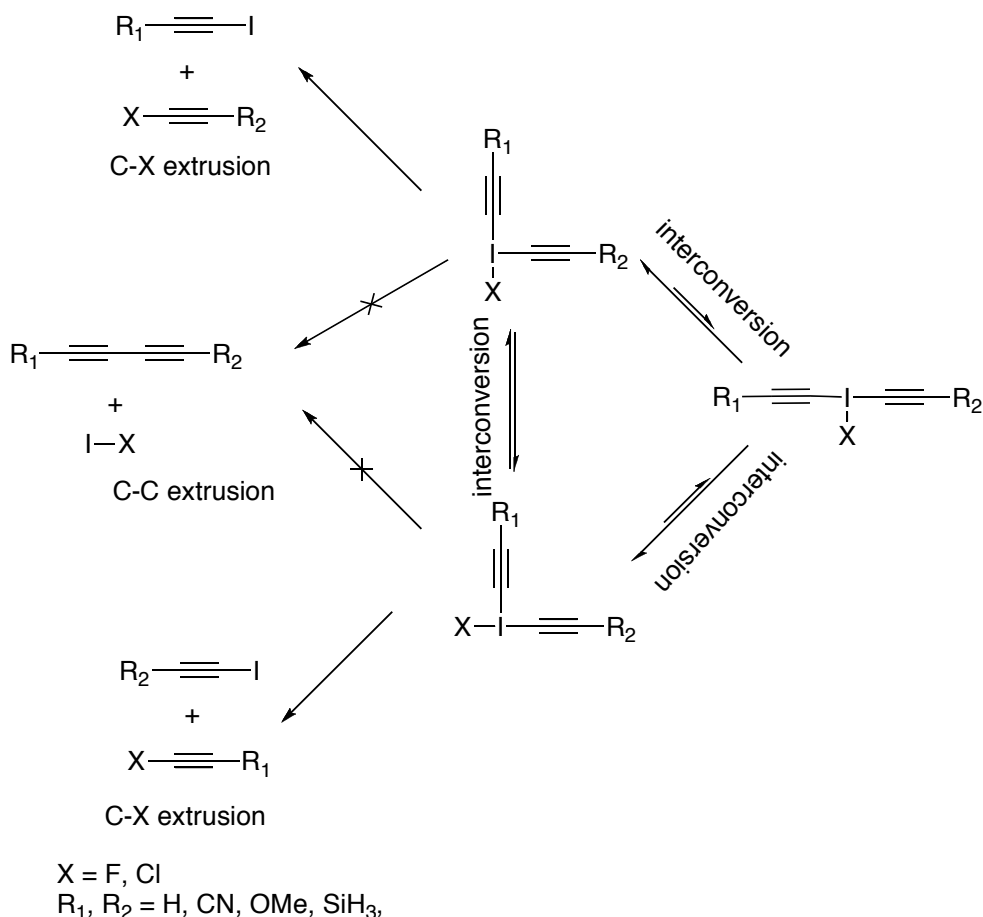
### 3.4 Computational approach to address the regioselectivity of reductive elimination on diaryliodonium salts: an explanation for the “ortho effect”

For  $^{18}\text{F}$ -labeling of electron rich aromatics via reductive elimination of diaryliodonium precursors, the ability to control and predict the regiochemical outcome of the aryl-fluoride extrusion process is key to the general practicality. Experimental observations suggest that it is the interplay of steric demand, the so-called “ortho effect”, and the electronic property of the aromatic rings that determines the outcome of the reductive elimination process. In effort to rationalize the observed regioselectivity, it has been proposed that the T-shaped fluoro(diaryl)- $\lambda^3$ -iodane species are fluxional and the fluoride is transferred to the aryl group that occupies the equatorial position.<sup>119, 120</sup>



**Scheme 3-9** Fluxional geometry of T-shaped fluoro(diaryl)- $\lambda^3$ -iodanes.<sup>120</sup>

Grushin's fluxional model did not specify whether the elimination process was controlled thermodynamically or kinetically. In attempt to gain insight of the reactivity and to predict the regiochemical outcome of the elimination process, Pike and colleagues<sup>80, 81, 121</sup> conducted computational studies of the extrusion reactions for such R<sub>2</sub>-IF iodine(III) species. To minimize computational requirement, they used substituted dialkynylhalonium models. According to these authors, for iodonium species, the fluxional interconversion that places the nucleophile X on the equatorial position is strongly disfavored (Scheme 3-10). The calculated energies of extrusion reactions are significantly higher than interconversion, suggesting that the fluxional behavior represents a pre-equilibrium to the rate determining extrusion steps. The barriers for C-C extrusion are significantly higher than C-X extrusion, which is consistent with the experimental observation that C-C extrusion is a very minor process. The outcome of the reaction is determined only by the energy difference between the two transition states for the C-X extrusions. The calculated reaction barriers suggest that reaction proceeds by attack on the most electron-deficient alkynyl group placed on the equatorial position, which agrees well with experimental observations. However, the dialkynyliodonium model is obviously not suitable to study the "*ortho* effect" in aryl substituents.



**Scheme 3-10 Reaction pathways for monomeric dialkynylidonium species.**

We decided to model the extrusion reactions using substituted diaryliodonium species to gain information about both electronic and steric control of the process. The calculations were based on the assumption of a concerted reductive elimination transition state. To establish a reliable computational procedure, we first the prototypic unsubstituted  $Ph_2IF$  at various levels of theories. The results are summarized in Table 3-5. RHF and MP2 calculations gave slightly higher activation barriers than the density function theory (B3LYP) calculation. Among B3LYP calculations, Midix seemed to give

results consistent with those obtained using a larger basis set (DGDZVP). Therefore, we decided to use B3LYP/Midix for the rest of the study.

**Table 3-5 Energies (hartree), activation barriers (kcal/mol), and transition normal mode for Ph<sub>2</sub>IF (ZPE corrected).**

Level of theory	GS	TS for extrusion	Activation barrier	$\nu_1$	Average time per cycle <sup>*</sup>
RHF/3-21G	-7444.1279	-7444.0834	27.92	500.4 <i>i</i>	6 min
B3LYP/3-21G	-7450.3662	-7450.3un353	19.33	322.1 <i>i</i>	24 min
B3LYP/3-21G(d)	-7450.4787	-7450.4374	25.86	371.4 <i>i</i>	27 min
B3LYP/Lanl2DZ	-574.2231	-574.1962	16.90	325.0 <i>i</i>	26 min
B3LYP/Midix	-7449.7836	-7449.7463	23.37	389.1 <i>i</i>	34 min
B3LYP/DGDZVP	-7482.8320	-7482.8000	20.09	365.2 <i>i</i>	93 min
MP2/3-21G(d)	-7445.5527	-7445.5058	29.41	436.5 <i>i</i>	322 min

<sup>\*</sup> Determined for transition state calculations.

Intrinsic reaction coordinate (IRC) calculations were performed to confirm the geometry of the C-F extrusion transition state. As is shown in Figure 3-15, the ground state of the diphenyliodonium fluoride exists in a T-shaped structure, with fluoride and one of the phenyl groups occupying the axial positions. The phenyl group that occupies the equatorial position lies perpendicular to the plane formed by the other phenyl and the fluoride, one of its *ortho* protons reaches out to strongly interact with the fluoride. The distance between this *ortho* proton and the fluoride measures 1.89 Å, which is much smaller than the sum of the Van Der Waals radii of hydrogen and fluorine (2.67 Å). Movement from the ground state to the transition state is accompanied by ipso carbon rehybridization, rotation of the equatorial phenyl ring to make way for the approaching

fluoride, and deflection of iodobenzene out of the plane. The ring rotation results in the breaking of the H-F interaction and accounts for part of the activation barrier.

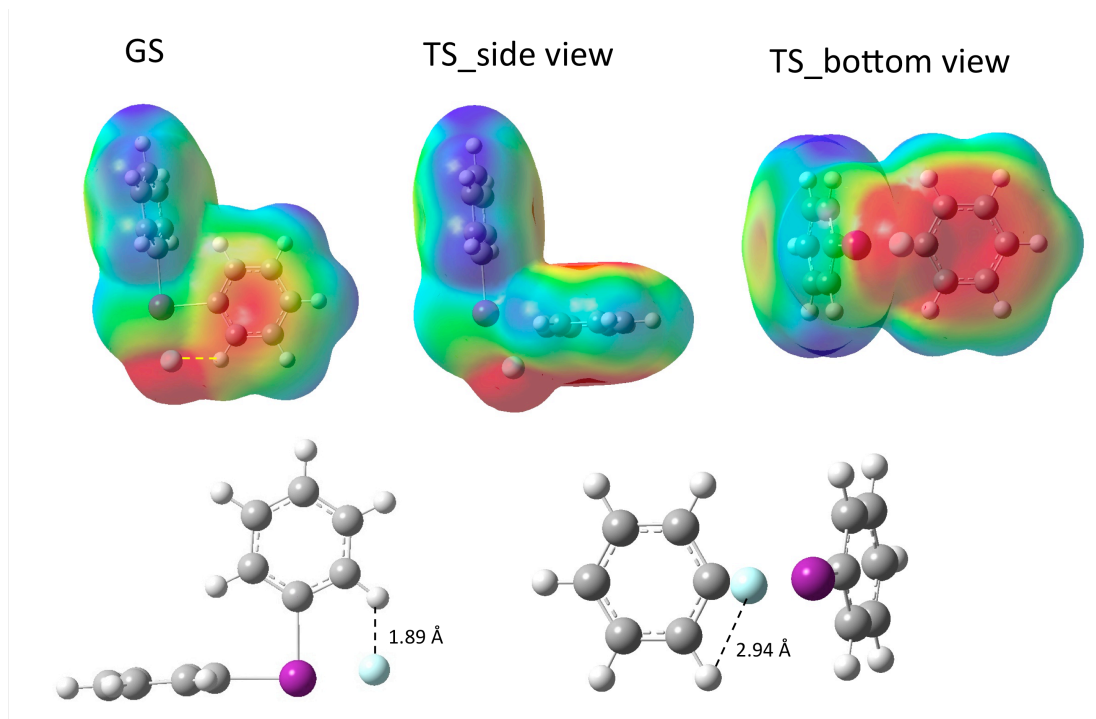


**Figure 3-15** Calculated geometries of ground state and transition state of monomeric diphenyliodonium fluoride with (above) and without (bottom) mapped surface potentials.

Based on reported crystal structures, dimer formation is common for diaryliodonium salts. Our calculation (Figure 3-16) shows that the ground state of diphenyliodonium fluoride dimer features an unsymmetrical bridge. The two contributing monomers may exchange fluoride through stretching of the I-F bonds. For the unsymmetrically substituted monomer, this provides a pathway for interconversion of the two different T-shaped ground state monomers (Scheme 3-11). We modeled the I-F stretching for PhIF<sub>2</sub> dimer, and found that the barrier (9.2 kcal/mol) lay below the barrier for C-F extrusion (23.4 kcal/mol). This finding is consistent with Pike's conclusions of

alkynyl models; he showed that fluxional interconversion represents a pre-equilibrium to the rate determining C-F extrusion step. The relative energy difference in ground state geometry is irrelevant to the outcome of the reaction. In other words, the particular equilibrium disposition (equatorial and syn- or anti- to the fluoride ligand) of the aryl group is irrelevant to whether or not the ring ends up being functionalized. This is a classic Curtin Hammett situation in which the product preference is only determined by relative transition state energies for reductive elimination.

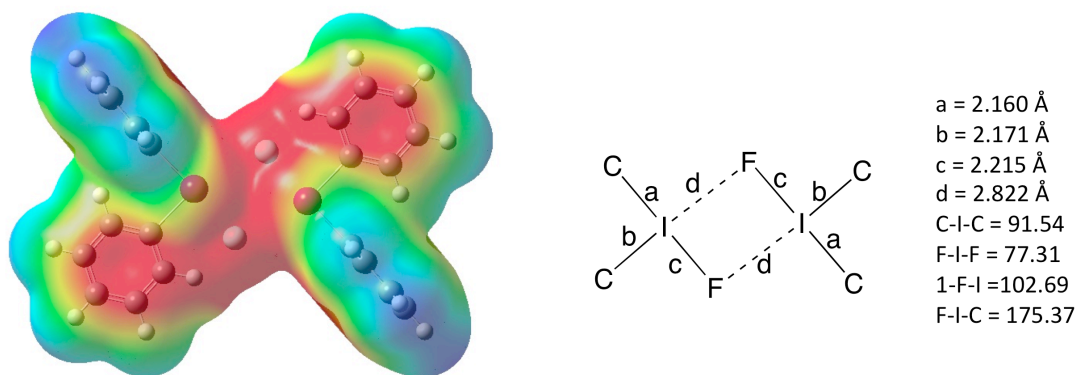
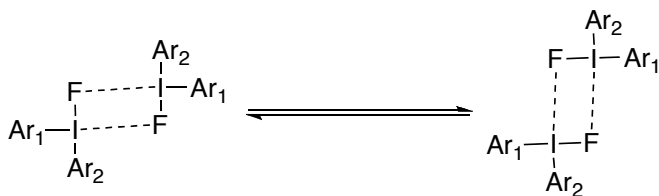


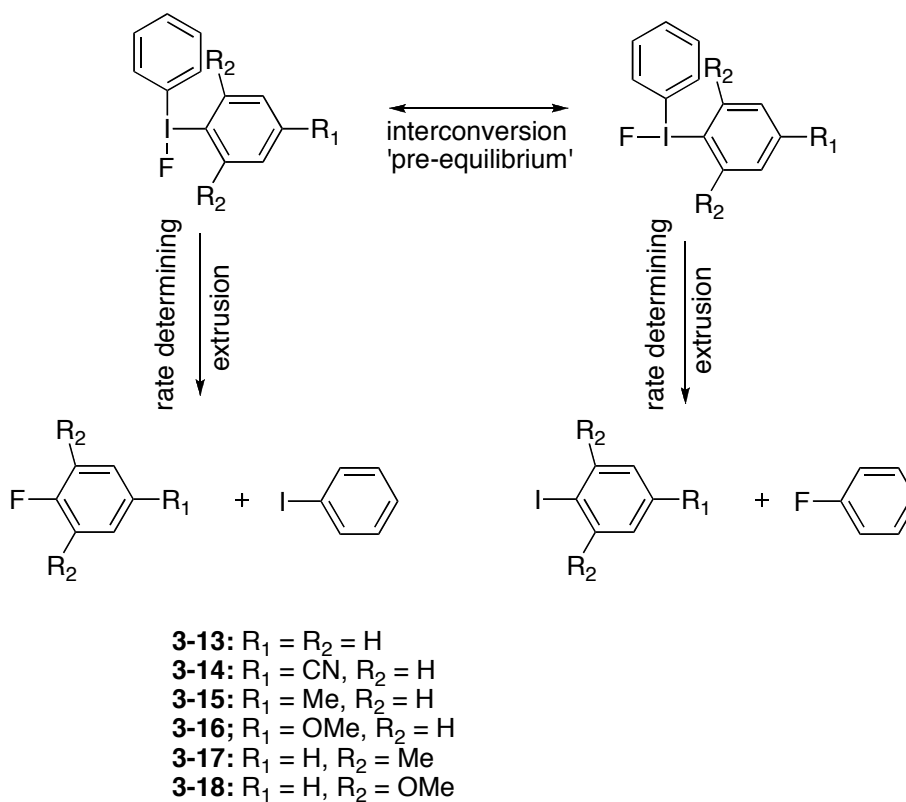
**Figure 3-16** Calculated ground state of  $\text{Ph}_2\text{IF}$  dimer (B3LYP/Midix).



**Scheme 3-11** Interconversion of the two different T-shaped monomers through I-F stretching in dimer.

We then proceeded to model 5 unsymmetrically substituted diaryliodonium fluorides **3-14** through **3-18**. Scheme 3-12 demonstrates that two sets of elimination

products may result from these salts. Compound **3-14** through **3-18** feature a phenyl moiety as one of the aryl substituents, so that the barrier for reductively eliminating Ph-F can be used as a reference to compare substituent effects directly. Compound **3-14**, **3-15**, and **3-16** were picked to study the electronic effect, while compounds **3-17** and **3-18** were targeted at steric “*ortho* effect”.



**Scheme 3-12** Reaction pathways for monomeric diaryliodonium fluorides.

Inspection of the results shown in Table 3-6 reveals that, in contradiction to the hypothesis that sterically demanding aryl groups prefer to occupy the equatorial position syn to the fluoride, the more stable ground states for compound **3-17** and **3-18** actually feature an equatorial phenyl group.



The effect of electronic substituent on the ground state stability of the two low energy stereoisomers remains unclear. *Para*-cyano (**3-14**) and methyl (**3-15**) substitution seem to have little impact; the difference between the energies of the two diastereomers is less than 1.5 kcal/mol differences in energy between two ground states. In contrast, placement of a *para*-methoxy substituted phenyl at the equatorial position (**3-16**) results in a stabilization of 2.9 kcal/mol.

**Table 3-6 Energies and activation barriers (kcal/mol) for ArPhIF (calculated at B3LYP/6-31G(d,p) level, ZPE corrected).**

Compound	GS <sub>1</sub> (Ar = eq)	GS <sub>2</sub> (Ph = eq)	TS <sub>1</sub> (Ar = eq)	TS <sub>2</sub> (Ph = eq)	$\Delta\Delta G_1$ (TS <sub>1</sub> - GS <sub>lower</sub> )	$\Delta\Delta G_2$ (TS <sub>2</sub> - GS <sub>lower</sub> )
<b>3-13</b>	-7449.7836	-	-7449.7463	-	<b>23.37</b>	-
<b>3-14</b>	-7541.5117	<b>-7541.5119</b>	-7541.4776	-7541.4735	<b>21.46</b>	24.03
<b>3-15</b>	-7488.8450	<b>-7488.8474</b>	-7488.8064	-7488.8098	25.70	<b>23.54</b>
<b>3-16</b>	<b>-7563.6250</b>	-7563.6203	-7563.5846	-7563.5889	25.33	<b>22.68</b>
<b>3-17</b>	-7527.9023	<b>-7527.9050</b>	-7527.8760	-7527.8657	<b>18.41</b>	24.64
<b>3-18</b>	-7677.4604	<b>-7677.4724</b>	-7677.4261	-7677.4261	29.00	<b>24.21</b>

Despite the seemingly ambiguity of the relevance of the substituents' impact on the GS structure, the calculated lowest energy transition states is the one that leads to the extrusion of less electron-rich aryl fluorides for compound **3-14** through **3-16**. For compound **3-17**, the calculations show that placing the 2,6-dimethylphenyl at the equatorial position is not favored in ground state. Nevertheless, the corresponding transition state for formation of 2,6-dimethylfluorobenzene lies much lower (6.2 kcal/mol) in energy compared to its counterpart. Close inspection of the calculated structures of the

lower transition state (Figure 3-17) reveals that two protons on the *ortho* methyl substituents interact with the fluoride. The H-F distance measures 2.42 Å, which is slightly smaller than the sum of the Van der Waals radii (2.67 Å). This C-H...F electrostatic interaction is responsible for stabilizing the transition state, making functionalization of the 2,6-dimethylphenyl moiety favored. We believe that C-H...F stabilization is a plausible explanation for “*ortho* effect”.

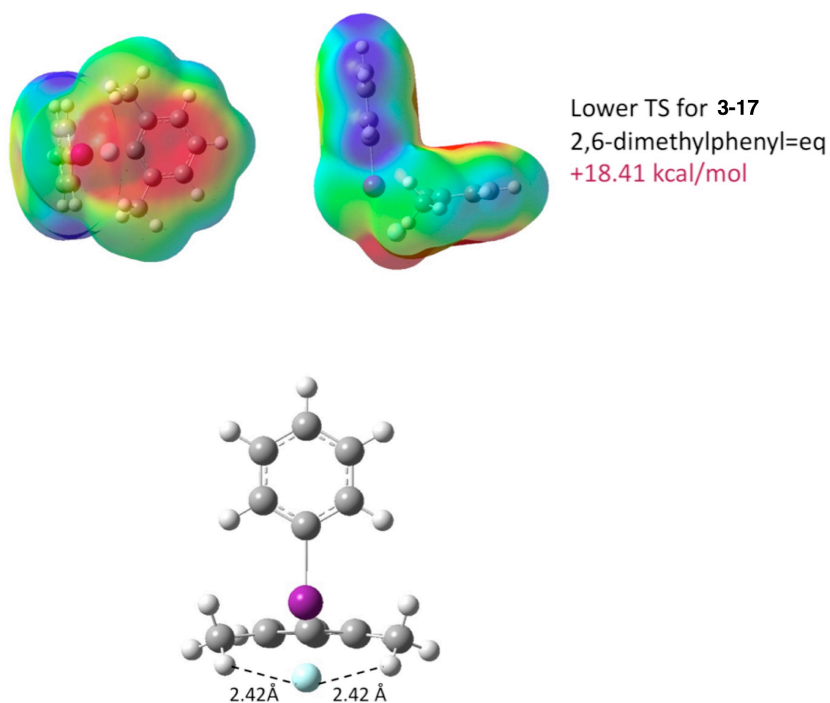


**Figure 3-17** Transition state leads to 2,6-dimethylfluorobenzene formation is lower in energy for compound **3-17** due to two C-H...F stabilization.

In fact, the proper name for this regiochemical trend should be the “*ortho* methyl effect” because the stabilization is not evident with other substituents. For example, despite featuring two *ortho* methoxy substituents, compound **3-18** preferably decomposed to form fluorobenzene rather than 2,6-dimethoxyfluorobenzene. The transition state that

leads to 2,6-dimethoxyfluorobenzene formation lies 4.8 kcal/mol above the one leads to fluorobenzene. No C-H...F stabilization is presence in either case, and the strong electron donating ability of the methoxy groups accounts for the destabilization.

In conclusion, we have studied the extrusion of aryl fluoride from diaryliodonium fluoride complexes using DFT calculations at the B3LYP/Midix level. The results agree well with experiments in that 1) the outcome of the reductive elimination from iodine(III) is determined by electronic effects; the preferred functionalization of *ortho*-substituted moiety is only true for methyl substitution. In general, transition state with the more electron deficient aryl group occupying the equatorial position is lower in energy and leads to the major products. The “*ortho effect*” can be understood as a special case, where the corresponding transition state gets extra stabilization from two additional H-F interactions. It should be called the “ortho methyl effect” because it cannot be generalized to include other electron-donating *ortho* substituents such as the methoxy group (for electron-withdrawing substituents, it is impossible to tell if the regiospecificity results solely from electronic effects).

### 3.5 Application in PET chemistry: Synthesis of [ $^{18}\text{F}$ ]-DOPA

Dihydroxyphenylalanine (DOPA) is an intermediate in the catecholamine synthesis pathway. In the body, DOPA is produced after hydroxylation of the amino acid tyrosine, which may enter the cell from outside. It can be decarboxylated to dopamine by amino acid decarboxylase (AADC). It can also be converted by catechol-O-methyl-transferase to 3,4-dihydroxyphenylacetic acid. DOPA can be radiolabeled with  $^{18}\text{F}$  in various locations, among which 6-L- $^{18}\text{F}$ -fluorodihydroxyphenylalanine ( $^{18}\text{F}$ -DOPA) is clinically

used. The affinity of radioactive  $^{18}\text{F}$ -DOPA for catechol-O-methyltransferase metabolization appears to be low compared to the affinity for AADC conversion.<sup>122</sup> Since the first publication on the application of  $^{18}\text{F}$ -DOPA to imaging of the dopaminergic system in the striatum, numerous studies have been performed to study the applicability in patients with Parkinson's disease and related diseases.<sup>123-126</sup> Because intermediates formed in the catecholamine pathway are also involved in the biosynthesis of melanin,  $^{18}\text{F}$ -DOPA and analogs have also been applied in melanoma imaging.<sup>127-130</sup>

More recently,  $^{18}\text{F}$ -DOPA has emerged as a metabolic PET tracer allowing imaging of neuroendocrine tumors (NET),<sup>131-139</sup> which generally show low uptake of  $^{18}\text{F}$ -FDG. This application is based on the unique property of neuroendocrine tumors to require the uptake of large amount of metabolic aromatic amino acid precursors. It has been demonstrated that, for carcinoid tumors,  $^{18}\text{F}$ -DOPA PET has outstanding sensitivity and detects significantly more disease than all other currently applied modalities.

However, the complex aspects of its synthesis have limited the use of  $^{18}\text{F}$ -DOPA in PET.  $^{18}\text{F}$ -DOPA can be produced by either nucleophilic fluorination or electrophilic fluorination. Regioselective electrophilic fluorination with  $^{18}\text{F}$ -acetylhypofluorite or  $^{18}\text{F}$ - $\text{F}_2$  is done through fluorodemetalation reactions. In these reactions, regioselectivity is achieved by prior functionalization of the aromatic ring followed by fluorination. Currently, the most commonly used synthetic method for routine production of  $^{18}\text{F}$ -DOPA is regioselective fluorodestannylation.<sup>140-143</sup> The  $^{18}\text{F}$  source,  $[^{18}\text{F}]\text{F}_2$  is generated from the nuclear reactions  $^{20}\text{Ne}(\text{d}, \alpha)^{18}\text{F}$  and  $^{18}\text{O}(\text{p}, \text{n})^{18}\text{F}$ , both of which require the addition of  $[^{19}\text{F}]\text{F}_2$  as the carrier which leads to attenuation of the specific radioactivity.

On the other hand, carrier-free nucleophilic substitution<sup>144</sup> using [<sup>18</sup>F]F<sup>-</sup> offers specific radioactivity several magnitudes higher, but the synthesis itself is a time-consuming, multi-step procedure and it's hard to achieve sufficiently high enantiomeric purity.

In our previous study, we have achieved reasonably good yield in fluorination of an analogue of DOPA, namely 1-methyl-3,4-dimethoxybenzene, (compound **3-4** Table 3-3) as well as dopamine (compound **3-9** Table 3-3) via reductive elimination of iodoanisole from the corresponding diaryliodonium precursors. Here we show that the methodology can be successfully applied for FDOPA synthesis.

It became apparent that the selection of protecting groups for the amino functionality is crucial to the success of DOPA fluorination. Because of the strong basicity of the TMAF as the fluorinating agent, it's necessary to replace both protons on the primary amino functionality. In our model study, dopamine (compound **3-9** Table 3-3) was protected with phthalimidyl group, whose removal requires harsh conditions incompatible with the racemizable  $\alpha$  carbon in L-DOPA. Therefore, we sought a more easily removed protecting group for the amino functionality of DOPA.

Dibenzyl, benzilidene, diphenylmethylene, and a combination of benzyl and Boc (benzyl-Boc) were used to protect DOPA. Benzilidene and diphenylmethylene were not compatible with the stannylation step, and their use was abandoned. Dibenzyl and benzyl-Boc protected DOPA were stannylated and transferred successfully to the corresponding iodonium precursors. Upon ion exchange to fluoride and heating, the dibenzyl protected precursor failed to yield any FDOPA. This is probably because the reducing tertiary amine leads to redox reactions during the attempted reductive

elimination. Coordination of the amine to iodine(III) may also be a factor heading to poor yields of fluoroarene. With the electron-withdrawing Boc functionality, the reductive elimination of iodoanisole occurred smoothly to yield protected FDOPA in good yield (85%).

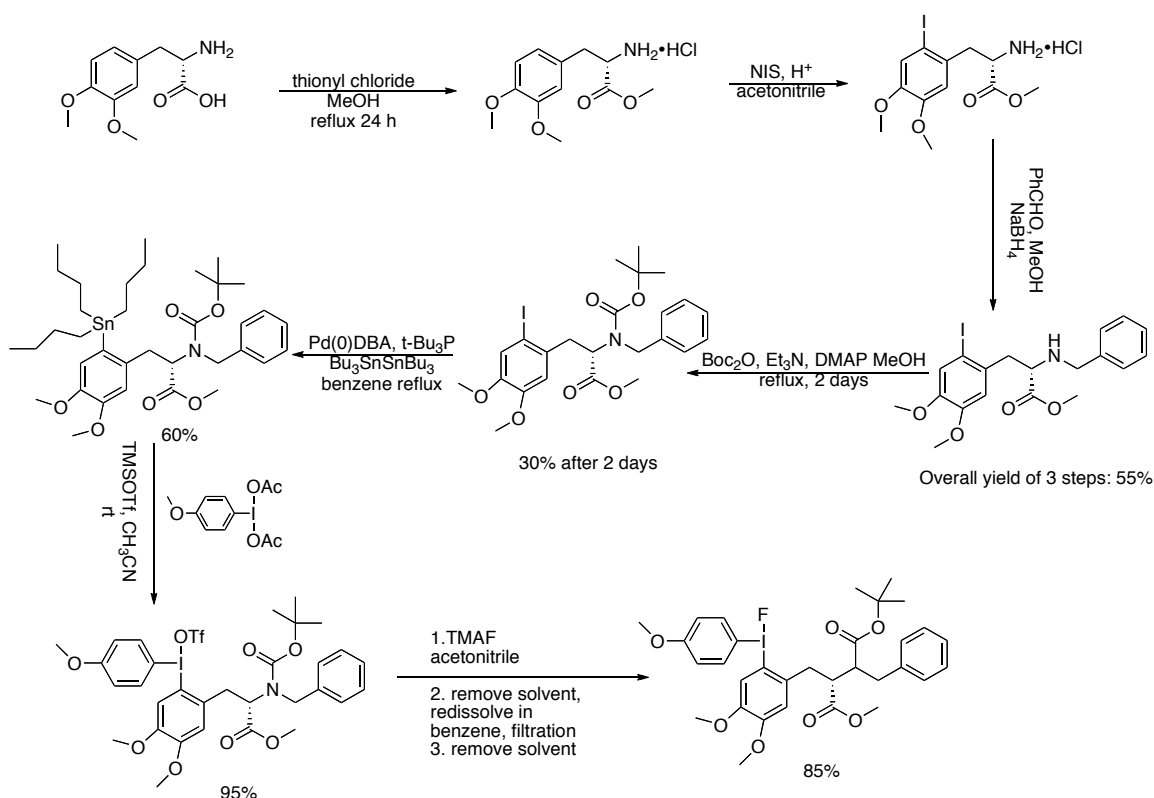


**Figure 3-18 Synthesis of benzyl-Boc protected iodonium fluoride precursor of 6-fluoro-DOPA.**

Figure 3-18 shows the synthesis of the iodonium fluoride precursor of 6-fluoro-DOPA. The yields are generally acceptable except for the Boc protection step (30 % conversion in 2 days). This is likely due to the steric congestion around the benzyl-protected nitrogen center. Evidence supporting the hindered nature of the amine could be seen in the <sup>1</sup>H NMR spectrum, where hindered rotation was observed for the Boc group

and the all of the protons in the vicinity of the Boc protected amine. In the final ion exchange step in Figure 3-18, iodonium fluoride salt was prepared by treatment of the triflate salt with TMAF in acetonitrile. The solvent was evaporated, and the remaining solid was dissolved in benzene, filtered to remove TMAOTf, and the solution was evaporated. No more than one equivalent of TMAF was used for the exchange process to minimize the disproportionation and aryl exchange reactions in acetonitrile. Thus, the iodonium fluoride made in this way contains a small amount of the iodonium triflate and the protected 6-iodo-DOPA (as a non-volatile hexane soluble by-product formed via disproportionation). No further purification was made to the iodonium fluoride salts before it was subject to decomposition. The iodonium fluoride was taken up in dry  $d_6$ -benzene under inert atmosphere conditions; the solution was transferred into a J-Young NMR tube and heated to 140 °C in a silicon oil bath. The progress of the reductive elimination reaction was monitored by  $^1\text{H}$  NMR; fully conversion of the iodonium salt was achieved in 30 minutes. The regioselectivity of this salt was similar to that observed for (2-methyl-4,5-dimethoxyphenyl)(4'-methoxyphenyl)-iodonium fluoride and the dopamine iodonium derivative; the fluoride was preferably transferred to the DOPA aromatic ring. The excellent selectivity can be attributed to the additive effects of the *ortho* substitution and the *meta*-withdrawing effect of the 5-methoxy group. Figure 3-19 shows the  $^1\text{H}$  NMR spectra for this reaction prior to and after heating. The major products of the reaction were the benzyl-Boc protected 6-fluoro-DOPA and iodoanisole.

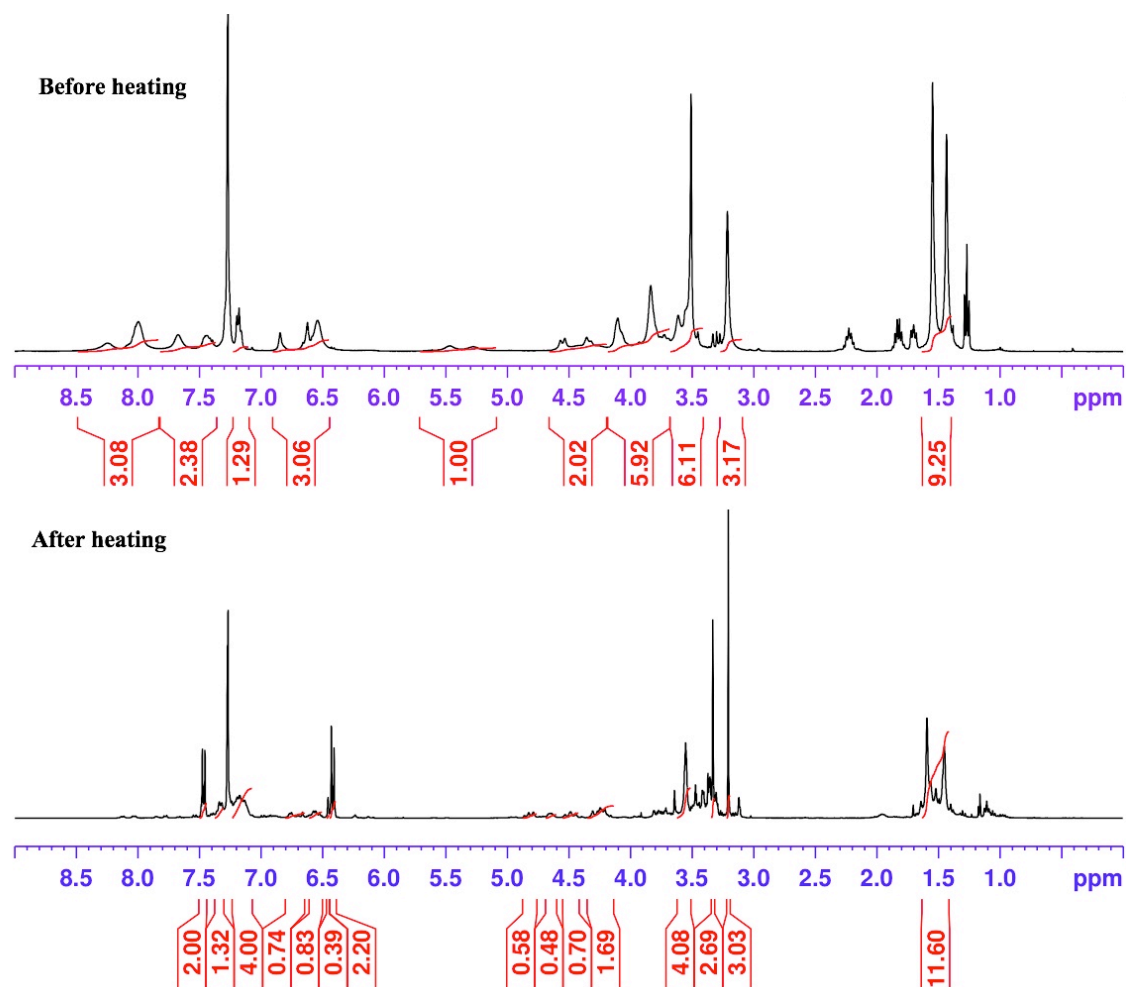


**Figure 3-19**  $^1\text{H}$  NMR showing the decomposition of benzyl-Boc DOPA iodonium fluoride.

The benzyl-Boc protected FDOPA product was purified by column chromatography using 20 % dichloromethane in hexanes as eluent. The small amount of protected 6-iodo-DOPA could not be separated effectively. The identity of the product was confirmed by  $^1\text{H}$  and  $^{19}\text{F}$  NMR spectroscopy (Figure 3-20), and MS analysis. The purified sample was passed through a chiral HPLC column to determine its enantiomeric purity. Because no racemic standard was available, a sample of L-FDOPA was racemized by sodium hexamethyldisilazide to provide HPLC standard (Scheme 3-13). The



chromatograms (Figure 3-21) showed that without racemization, the product was mainly composed of L-FDOPA. Therefore, it was confirmed that the stereochemistry was retained during both preparation of the iodonium precursor and the reductive elimination.

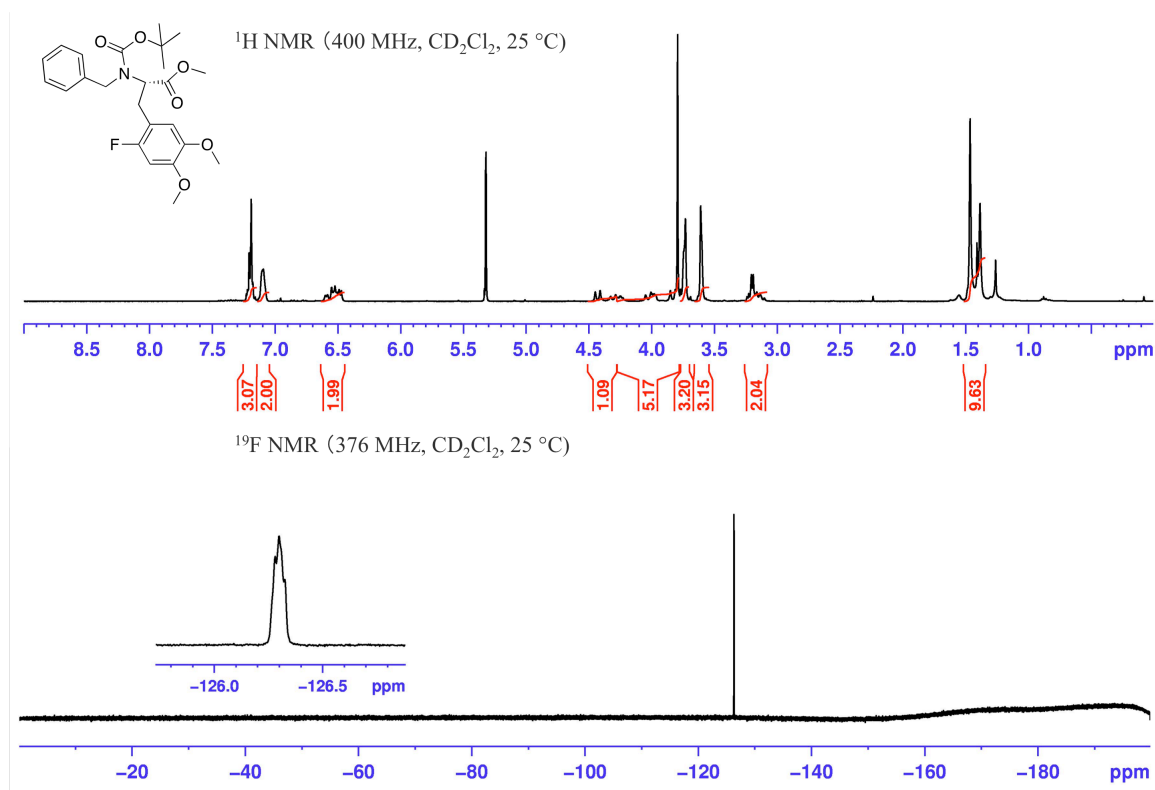
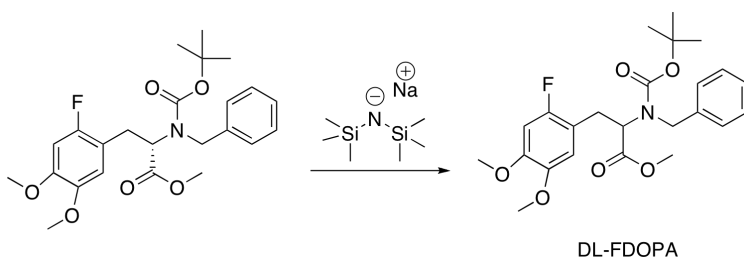


**Figure 3-20 <sup>1</sup>H and <sup>19</sup>F NMR spectra of isolated benzyl-Boc protected FDOPA.**

With the viability of the method confirmed, we tried to fluorinate DOPA with cyclotron generated [<sup>18</sup>F]-fluoride through collaborations with UCLA Medical Center. The preliminary results of the “hot” reactions showed that up to 30 % RCY could be obtained using the benzyl-Boc protected DOPA iodonium precursor. Although the results are only marginally better than the current “state of the art” method (25 ± 3 %),<sup>143</sup> conditions are yet to be optimized to achieve comparable high yield with the “cold”

reactions. And the time of the experiment is significantly shorter than the multistep synthesis currently employed.



**Scheme 3-13 Racemization of L-FDOPA derivative using sodium hexamethyldisilazide.**

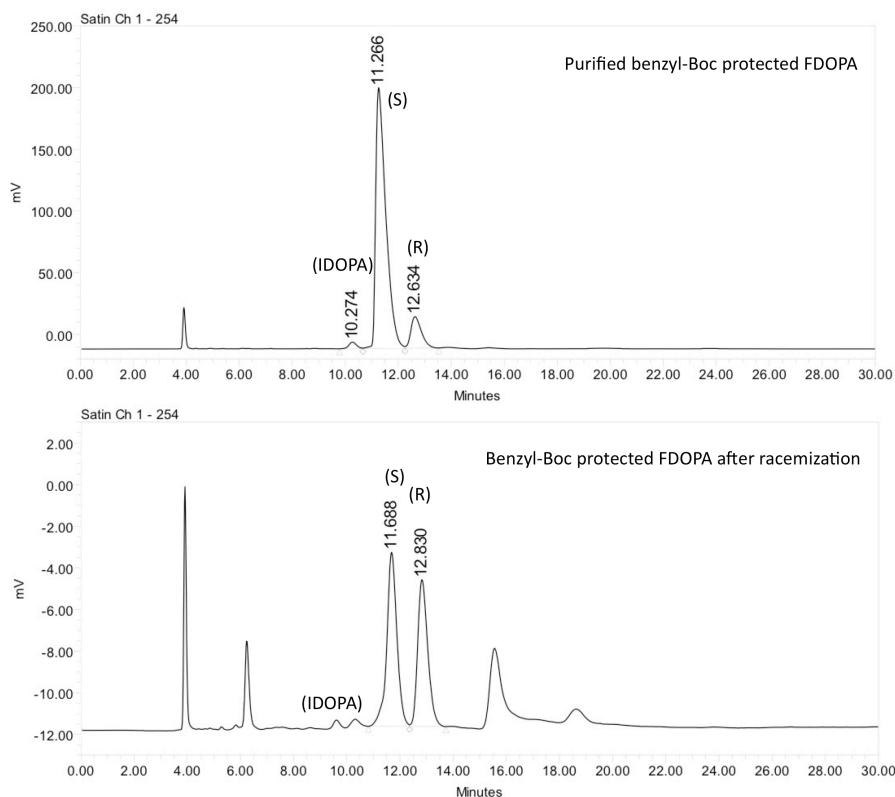


**Figure 3-21 Chiral HPLC chromatograms of benzyl-Boc protected FDOPA.**

A problem with benzyl-Boc protected DOPA derivative is that the N-benzyl group cannot be removed easily with the rest of the protecting groups via heating with

strong acid (HI, HBr etc). Therefore, we also synthesized N,N-diBoc protected DOPA derivatives to solve this deprotection problem. The fluorination reaction went smoothly to give comparable (80 %) yield of diBoc protected F-DOPA. Control experiments showed that all the protection groups can be removed easily by heating with HI or HBr at 140 °C for 10 min. An unexpected bonus of using diBoc protection was that the NMR spectra of all the diBoc protected derivatives show clean and sharp peaks that are much easier to identify compared to the benzyl-Boc protected compounds. Radiofluorination studies of this compound are currently undergoing at the National Institution of Health.

### 3.6 Experimental

**General:** All materials were obtained from commercial sources and used as received unless otherwise noted. Tetramethylammonium fluoride (TMAF) and diphenyliodonium nitrate were dried at 60-80 °C in a drying pistol (charged with P<sub>2</sub>O<sub>5</sub>) under dynamic vacuum for one week. Hexabutyldistannane and chlorotributylstannane were distilled *in vacuo* into flame-dried storage tubes and stored under dry nitrogen. Zinc triflate was dried *in vacuo* before use. Diethyl ether was distilled under reduced pressure from sodium/benzophenone. Acetonitrile and acetonitrile-d<sub>3</sub> were heated at reflux over P<sub>2</sub>O<sub>5</sub>, distilled into flame-dried storage tubes, transferred to the glove box, and were stored there over CaH<sub>2</sub>. Benzene and benzene-d<sub>6</sub> were heated at reflux over CaH<sub>2</sub> overnight and distilled directly into flame-dried storage tubes under dry nitrogen. Tetrahydrofuran (THF) was dried over Na/benzophenone and distilled into a flame dried storage flask under dry nitrogen. Iodonium salts were shielded from the light during all operations. All glassware, syringes, and NMR tubes were oven dried (140 °C) for more than 24 h before they were

transferred into the glove box for use. TBAF was synthesized according to our previously reported method.<sup>18</sup> All NMR experiments reported here were performed using 400 MHz (QNP probe) and 500 MHz (CP TXI Cryoprobe) Bruker NMR spectrometers in the NMR laboratory at the University of Nebraska-Lincoln. A Q-TOF I tandem mass spectrometer (Micromass, now Waters) with electrospray ionization was used to analyze the samples. Samples were infused in solution at 5  $\mu$ L/min by means of a syringe pump. The data were acquired using a mass range of  $m/z$  100 to 1500. The instrument was operated at a mass resolution of 5000.

**General procedure for generating and isolating aryl-(4-methoxyphenyl)-fluoro- $\lambda^3$ -iodanes:** In a nitrogen atmosphere glove box, 0.5 mmol of an appropriate aryl(4-methoxyphenyl)-iodonium hexafluorophosphate was dissolved in 1.5 mL of dry acetonitrile. A solution of 0.5 mmol of TMAF in dry acetonitrile was added slowly. The mixture was transferred into a Schlenk flask, capped, and taken out of the glove box. The solvent was evaporated and the flask was taken back into the glove box. Dry benzene (5 mL) was added to dissolve only the fluoro- $\lambda^3$ -iodane formed. The solution was passed through a 0.2 mm membrane filter and benzene was removed to yield the expected aryl(4-methoxyphenyl)-fluoro- $\lambda^3$ -iodane.

**General procedure for fluorination of diaryliodonium salts in benzene or acetonitrile (salt-free):** In a nitrogen atmosphere glove box, 0.03 mmol of the appropriate aryl(4-methoxyphenyl)-fluoro- $\lambda^3$ -iodane was dissolved in 0.6 mL of dry  $d_6$ -

benzene or dry  $d_3$ -acetonitrile. The solution was transferred into a J-Young NMR tube, sealed, and taken out of the glove box. The tube was wrapped in aluminum foil and placed in a 140 °C oil bath. The progress of the reaction was monitored by  $^1\text{H}$  NMR spectroscopy until no starting material was observable.

**General procedure for fluorination of diaryliodonium salts in benzene:** In a nitrogen atmosphere glove box, 0.03 mmol of the appropriate aryl(4-methoxyphenyl)-fluoro- $\lambda^3$ -iodane and 0.03 mmol of TMAOTf were dissolved in 0.6 mL of dry  $d_6$ -benzene. The solution was transferred into a J-Young NMR tube, sealed, and taken out of the glove box. The tube was wrapped in aluminum foil and placed in a 140 °C oil bath. The progress of the reaction was monitored by  $^1\text{H}$  NMR spectroscopy until no starting material was observable.

**General procedure for fluorination of diaryliodonium salts in acetonitrile:** In a nitrogen atmosphere glove box, 0.03 mmol of the appropriate aryl(4-methoxyphenyl)-iodonium hexafluorophosphate and 0.03 mmol of TMAF were dissolved in 0.6 mL of dry acetonitrile. The solution was transferred into a J-Young NMR tube, sealed, and taken out of the glove box. The tube was wrapped in aluminum foil and placed in a 140 °C oil bath. The progress of the reaction was monitored by  $^1\text{H}$  NMR spectroscopy until no starting material was observable.

**General procedure for aryl ligand exchange reactions in acetonitrile:** In a Nitrogen atmosphere glove box, 0.05 mmol of the appropriate diaryliodonium

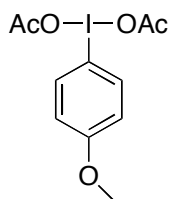
hexafluorophosphate was dissolved in 0.3 mL of dry acetonitrile. A measured amount of a freshly made stock solution of TMAF in dry acetonitrile (0.2 M) was added slowly. The solution was transferred into a J-Young NMR tube, sealed, and taken out of the glove box. The progress of the reaction was monitored by  $^1\text{H}$  NMR spectroscopy.

**Aryl ligand exchange kinetic study in acetonitrile:** To a solution of phenyl(4-methoxyphenyl)-iodonium hexafluorophosphate (0.05 mmol in 0.3 mL of  $\text{d}_3$ -acetonitrile) was slowly added a solution of TMAF (0.05 mmol) in  $\text{d}_3$ -acetonitrile (amount varied). The resulting solution was mixed well and transferred into an NMR tube equipped with a Teflon screw cap closure. The progress of the reaction was monitored by  $^1\text{H}$  NMR spectroscopy; rates were back calculated based upon the areas of the deconvoluted peak areas (deconvolution was performed using the Bruker Topspin software).

**Calculations:** All calculations were performed using the Gaussian03 suite of programs; and visualization was performed with GaussView03.<sup>27</sup> Input geometries of all ground state species were entered using the GaussView03 program. They are first pre-optimized at RHF/3-21G(d) level then optimized at B3LYP/6-31G(d) level. Frequency calculations on minimized structures were performed to make the zero point energy and thermal corrections. Geometries of all putative saddle points were determined by scanning the energy potential surface of the reaction pathway at RHF/3-21G(d) level followed by optimization at B3LYP/6-31G(d) level, and in the case of the prototypical diphenyliodonium

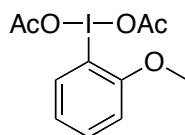
fluoride, confirmed by calculating the intrinsic reaction coordinate along the first normal mode direction.

### Preparative procedures and characterization of compounds



**Bis(acetyloxy)-(4-methoxyphenyl)- $\lambda^3$ -iodane:** 4-Iodoanisole (2.34 g, 10 mmol) was dissolved in 90 mL of glacial acetic acid and the stirred solution was warmed to 40 °C. Sodium perborate tetrahydrate (13.6 g, 110 mmol) was added in portions over the course of one hour. After the addition was complete, the temperature of the reaction mixture was maintained at 40 °C for 8 h before it was allowed to cool to room temperature. Half of the acetic acid (~ 45 mL) was removed by distillation at reduced pressure. The remaining solution was treated with 100 mL of deionized water and the aqueous layer was extracted (3  $\times$  40 mL) with dichloromethane. The combined organic fractions were dried over sodium sulfate, and the solvent was removed by rotary evaporation to give 2.25 g (64 %) of 1-(diacetoxyiodo)-4-methoxybenzene. This compound was dried *in vacuo* and used without further purification.  $^1\text{H}$  NMR ( $\text{CD}_3\text{CN}$ , 400 MHz, 25 °C):  $\delta$  8.055 (d,  $J$  = 9.1 Hz, 2 H, H2/H6), 7.053 (d,  $J$  = 9.1 Hz, 2 H, H3/H5), 3.861 (s, 3 H, OMe), 1.905 (s, 6 H,  $(\text{OCOCH}_3)_2$ );  $^{13}\text{C}$  NMR ( $\text{CD}_3\text{CN}$ , 100 MHz, 25 °C)  $\delta$  177.73 (CO), 163.73 (C4), 138.75 (C2/C6), 118.00, (C3/C5), 111.97 (C1), 56.85 (OMe), 20.76  $((\text{OCOCH}_3)_2)$ ; HRMS: (HRFAB) calcd. for  $\text{C}_{14}\text{H}_{13}\text{NO}_4\text{I}$   $[\text{M} - 2\text{OAc} + 3\text{-NBA}]^+$  385.9889 found 385.9885. (lit.<sup>145</sup>,

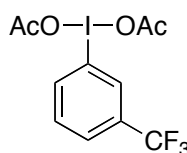
$^{146} \text{ }^{13}\text{C}$  NMR ( $\text{CDCl}_3$ , 50 MHz, 20 °C)  $\delta$  162.0 (C4), 137.0 (C2/C6), 116.5 (C3/C5), 111.4 (C1).);  $^{13}\text{C}$  NMR ( $\text{CDCl}_3$ , 75 MHz, 25 °C)  $\delta$  176.31 (CO), 111.64 (C1), 20.36 (( $\text{OCOCH}_3$ )<sub>2</sub>).)



**Bis(acetyloxy)-(2-methoxyphenyl)- $\lambda^3$ -iodane:** 2-Iodoanisole (2.34 g, 10 mmol) was dissolved in 90 mL of glacial acetic acid and the stirred solution was warmed to 40 °C. Sodium perborate tetrahydrate (13.6 g, 110 mmol) was added in portions over the course of one hour. After the addition was complete, the temperature of the reaction mixture was maintained at 40 °C for 8 h before it was allowed to cool to room temperature. Half of the acetic acid (~ 45 mL) was removed by distillation at reduced pressure. The remaining solution was treated with 100 mL of deionized water and the aqueous layer was extracted (3  $\times$  40 mL) with dichloromethane. The combined organic fractions were dried over sodium sulfate, and the solvent was removed by rotary evaporation to give 2.29 g (65 %) of 1-(diacetoxyiodo)-2-methoxybenzene. This compound was dried *in vacuo* and used without further purification.  $^1\text{H}$  NMR ( $\text{CD}_3\text{CN}$ , 400 MHz, 25 °C):  $\delta$  8.175 (d,  $J$  = 8.0 Hz, 1 H, H6), 7.690 (dd,  $J_1$  = 7.6,  $J_2$  = 8.2 Hz 1 H, H5), 7.313 (d,  $J$  = 8.2 Hz, 1 H, H3), 7.085 (dd,  $J_1$  = 8.0,  $J_2$  = 7.6 Hz, 1 H, H4), 3.958 (s, 3 H, OMe), 1.884 (s, 6 H, ( $\text{OCOCH}_3$ )<sub>2</sub>);  $^{13}\text{C}$  NMR ( $\text{CD}_3\text{CN}$ , 100 MHz, 25 °C)  $\delta$  178.00 (CO), 157.72 (C2), 139.09 (C6), 136.34 (C4), 124.17 (C3), 113.91 (C1), 113.87 (C5), 58.20 (OMe), 20.71 (( $\text{OCOCH}_3$ )<sub>2</sub>); HRMS (HRFAB): calcd. for  $\text{C}_{14}\text{H}_{13}\text{NO}_4\text{I}$  [ $\text{M} - 2\text{OAc} + 3\text{-NBA}$ ] $^+$  385.9889 found 385.9874. lit.<sup>84</sup>  $^1\text{H}$  NMR  $\delta$  (270 MHz,  $\text{CDCl}_3$ ) 8.10 (1 H, d, H6  $J$  = 8 Hz), 7.56 (1 H, t, H5  $J$  = 8 Hz), 7.13

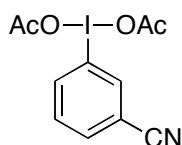


(1H, d, H3, J = 8 Hz), 7.00 (1 H, t, H4 J = 8 Hz), 3.95 (3 H, s, OCH<sub>3</sub>), 1.93 (6 H, s, (OCOCH<sub>3</sub>)<sub>2</sub>); <sup>13</sup>C NMR (68 MHz; CDCl<sub>3</sub>) δ 176.7 (CO), 156.3 (C3), 137.8, 134.6, 122.9, 113.4 (C1), 112.1, 57.0 (OMe), 20.5 ((OCOCH<sub>3</sub>)<sub>2</sub>).

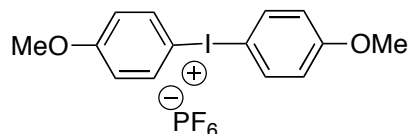


**Bis(acetyloxy)-(3-(trifluoromethyl)phenyl)-λ<sup>3</sup>-iodane:** 3-Iodobenzotrifluoride (2.72 g, 10 mmol) was dissolved in 90 mL of glacial acetic acid and the stirred solution was warmed to 40 °C. Sodium perborate tetrahydrate (13.6 g, 110 mmol) was added in portions over the course of one hour. After the addition was complete, the temperature of the reaction mixture was maintained at 40 °C for 8 h before it was allowed to cool to room temperature. Half of the acetic acid (~ 45 mL) was removed by distillation at reduced pressure. The remaining solution was treated with 100 mL of deionized water and the aqueous layer was extracted (3 × 40 mL) with dichloromethane. The combined organic fractions were dried over sodium sulfate, and the solvent was removed by rotary evaporation to give 2.12 g (80 %) 1-(Diacetoxyiodo)-3-(trifluoromethyl)benzene. <sup>1</sup>H NMR (CD<sub>3</sub>CN, 400 MHz, 25 °C): δ 8.492 (s, H1, H2), 8.397 (d, J = 8.3 Hz, 1 H, H6), (d, J = 7.9 Hz, 1 H, H4), (dd, J<sub>1</sub> = 8.3 Hz, J<sub>2</sub> = 7.9 Hz, 1 H, H5), 1.939 (s, 6 H, (OCOCH<sub>3</sub>)<sub>2</sub>); <sup>13</sup>C NMR (CD<sub>3</sub>CN, 100 MHz, 25 °C) δ 178.03 (CO), 140.25 (C6), 133.45 (q, J = 33.5 Hz, C3), 133.24 (q, J = 3.9 Hz, C2), 133.14 (C5), 130.07 (q, J = 3.7 Hz, C4), 123.96 (q, J = 273.1 Hz, CF<sub>3</sub>), 122.02 (C1), 20.73 ((OCOCH<sub>3</sub>)<sub>2</sub>); <sup>19</sup>F NMR (CD<sub>3</sub>CN, 376MHz, 25 °C) δ -63.255 (<sup>1</sup>J<sub>C-F</sub> = 273.1 Hz, <sup>2</sup>J<sub>C-F</sub> = 33.5 Hz); HRMS (HRFAB): calcd. for C<sub>14</sub>H<sub>10</sub>NO<sub>3</sub>IF<sub>3</sub> [M

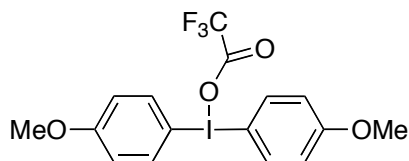
– 2OAc+3-NBA]<sup>+</sup> 423.9657 found 423.9645. lit.<sup>147</sup> : <sup>1</sup>H NMR (300 MHz, CDCl<sub>3</sub>) δ 2.03 (s, 6 H, (OCOCH<sub>3</sub>)<sub>2</sub>), 7.65 (t, J = 7.9 Hz, 1 H, ArH), 7.85 (d, J = 7.9 Hz, 1 H, ArH), 8.28 (d, J = 7.9 Hz, 1 H, ArH), 8.33 (s, 1 H, ArH); <sup>13</sup>C NMR (75 MHz, CDCl<sub>3</sub>) δ 176.5, 138.1, 132.9 (q, J<sub>CF</sub> = 33.4 Hz, CCF<sub>3</sub>), 131.7 (q, J<sub>CF</sub> = 3.7 Hz, CCF<sub>3</sub>), 131.2, 128.4 (q, J<sub>CF</sub> = 3.7 Hz, CCF<sub>3</sub>), 122.7 (q, J<sub>CF</sub> = 270.8 Hz, CF<sub>3</sub>), 120.9, 20.2.)



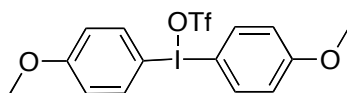
**Bis(acetyloxy)-(3-cyanophenyl)-λ<sup>3</sup>-iodane:** 3-Iodobenzonitrile (2.29 g, 10 mmol) was dissolved in 90 mL of glacial acetic acid and the stirred solution was warmed to 40 °C. Sodium perborate tetrahydrate (13.6 g, 110 mmol) was added in portions over the course of one hour. After the addition was complete, the temperature of the reaction mixture was maintained at 40 °C for 8 h before it was allowed to cool to room temperature. Half of the acetic acid (~ 45 mL) was removed by distillation at reduced pressure. The remaining solution was treated with 100 mL of deionized water and the aqueous layer was extracted (3 × 40 mL) with dichloromethane. The combined organic fractions were dried over sodium sulfate, and the solvent was removed by rotary evaporation to give 2.43 g (70 %). <sup>1</sup>H NMR (CD<sub>3</sub>CN, 400 MHz, 25 °C): δ 8.515 (s, 1 H, H2), 8.406 (d, J = 8.1 Hz, 1 H, H6), 7.866 (d, J = 8.1 Hz, 1 H, H4), 7.711 (t, J = 8.1 Hz, 1 H, H5), 1.954 (s, 6 H, (OCOCH<sub>3</sub>)<sub>2</sub>); <sup>13</sup>C NMR (CD<sub>3</sub>CN, 100 MHz, 25 °C) δ 178.25 (CO), 140.65 (C6), 139.69 (C2), 136.88 (C5), 132.95 (C4), 121.84 (C3), 115.82 (CN), 109.99 (C1); HRMS (HRFAB): calcd. for C<sub>14</sub>H<sub>10</sub>N<sub>2</sub>O<sub>3</sub>I [M – 2OAc+3-NBA]<sup>+</sup> 380.9736 found 380.9722. lit.<sup>148</sup> <sup>1</sup>H NMR (CDCl<sub>3</sub>, 200 MHz) δ 7.61-8.39(4 H, m, ArH), 2.02(6 H, s, MeCO<sub>2</sub>).)



**Bis(4-methoxyphenyl)-iodonium hexafluorophosphate:** In a nitrogen atmosphere glove box, 1-(diacetoxyiodo)-4-methoxybenzene (352 mg, 1 mmol) was weighed into a glass vial and 1.5 mL of dry acetonitrile was added. A solution of *p*-toluenesulfonic acid monohydrate (190 mg, 1 mmol) in 1.5 mL of dry acetonitrile was added by syringe. Upon completion of the addition, anisole (neat, 0.11 mL, 1 mmol) was added and the vial was sealed and taken out of the glove box; the mixture was allowed to stir at room temperature for 2 h. Water (10 mL) was added and the mixture was transferred to a separatory funnel and extracted ( $3 \times 5$  mL) with hexanes. The reserved aqueous layer was treated with 502 mg (3 mmol) of NaPF<sub>6</sub>. The white precipitate was filtered, dried in vacuo, and recrystallized in a mixture of diethyl ether/dichloromethane to give 391 mg of bis(4-methoxyphenyl)-iodonium hexafluorophosphate (80.5 %). <sup>1</sup>H NMR (CD<sub>3</sub>CN, 400 MHz, 25 °C):  $\delta$  7.973 (d, *J* = 9.1 Hz, 4 H, H<sub>2</sub>/H<sub>2</sub>'/H<sub>6</sub>/H<sub>6</sub>'), 7.046 (d, *J* = 9.1 Hz, 4 H, H<sub>3</sub>/H<sub>3</sub>'/H<sub>5</sub>/H<sub>5</sub>'), 3.833 (s, 6 H, OMe); <sup>13</sup>C NMR (CD<sub>3</sub>CN, 100 MHz, 25 °C)  $\delta$  164.61 (C<sub>4</sub>/C<sub>4</sub>'), 138.55 (C<sub>2</sub>/C<sub>2</sub>'/C<sub>6</sub>/C<sub>6</sub>'), 119.42 (C<sub>3</sub>/C<sub>3</sub>'/C<sub>5</sub>/C<sub>5</sub>'), 103.36 (C<sub>1</sub>/C<sub>1</sub>'), 57.06 (OMe); <sup>19</sup>F NMR (CD<sub>3</sub>CN, 376 MHz, 25 °C)  $\delta$  -72.833 (d, <sup>1</sup>*J*<sub>P-F</sub> = 707.3 Hz, PF<sub>6</sub><sup>-</sup>); HRMS (HRFAB): calcd. for C<sub>14</sub>H<sub>14</sub>O<sub>2</sub>I [M – PF<sub>6</sub>]<sup>+</sup> 341.0038 found 341.0036.

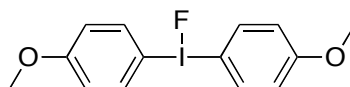


**Bis(4-methoxyphenyl)-trifluoroacetoxy- $\lambda^3$ -iodane:** In a nitrogen flushed Schlenk tube equipped with a magnetic stir bar and a rubber septum seal, 1-(diacetoxyiodo)-4-methoxybenzene (1.41 g, 4 mmol) was dissolved in 30 mL of dry dichloromethane and the solution was cooled to -30 °C. Trifluoroacetic acid (0.61 mL, 8 mmol) was added and the solution was allowed to warm slowly to room temperature and stirred for 30 min. Subsequently, the solution was cooled to -30 °C and anisole (0.44 mL, 4 mmol) was added dropwise by syringe. When the addition was complete, the mixture was allowed to warm to room temperature and stirred for an additional 1 h. The solvent was removed by rotary evaporation and the residual solid was recrystallized from diethyl ether/dichloromethane to give 1.53 g (71 %) of bis(4-methoxyphenyl)-trifluoroacetoxy- $\lambda^3$ -iodane.  $^1\text{H}$  NMR ( $\text{CD}_3\text{CN}$ , 400 MHz, 25 °C):  $\delta$  7.951 (d,  $J$  = 9.1 Hz, 4 H, H2/H2'/H6/H6'), 6.981 (d,  $J$  = 9.1 Hz, 4 H, H3/H3'/H5/H5'), 3.805 (s, 6 H, OMe);  $^{13}\text{C}$  NMR ( $\text{CD}_3\text{CN}$ , 100 MHz, 25 °C)  $\delta$  163.84 (C4/C4'), 138.14 (C2/C2'/C6/C6'), 118.69 (C3/C3'/C5/C5'), 106.64 (C1/C1'), 56.86 (OMe);  $^{19}\text{F}$  NMR ( $\text{CD}_3\text{CN}$ , 376 MHz, 25 °C)  $\delta$  -75.436 ( $\text{CF}_3^-$ ,  $^1J_{\text{C-F}}$  = 297.3 Hz,  $^1J_{\text{C-F}}$  = 33.3 Hz).



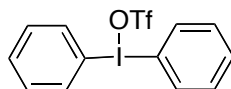
**Bis(4-methoxyphenyl)-trifluoromethanesulfonyl- $\lambda^3$ -iodane:** In a flame-dried 25 mL Schlenk flask charged with  $\text{N}_2$ , 1-(diacetoxyiodo)-4-methoxybenzene (753.0 mg, 2.13 mmol) was dissolved in 7 mL dry methylene chloride. With stirring, anisole (0.93 mL, 8.52 mmol) was added by syringe. The solution was cooled to -10 °C in a sodium chloride-ice bath. To this solution, triflic acid (0.21 mL, 2.34 mmol) was added dropwise

over the course of 10 minutes by syringe. A deep blue color developed immediately upon addition. After the addition was complete, the solution was allowed to warm slowly to room temperature over 12 h. The volatiles were removed *in vacuo* to obtain a crude solid. The solid was dissolved in methylene chloride and precipitated with a 10% solution of ether in hexanes to yield bis(4-methoxyphenyl)-trifluoromethanesulfonyl- $\lambda^3$ -iodane as a colorless solid (729.6 mg, 69.5%).  $^1\text{H}$  NMR (400 MHz,  $\text{CD}_3\text{CN}$ , 25 °C):  $\delta$  7.981 (d,  $J$  = 8.8 Hz, 2H, H2/H2'/H6/H6'), 7.038 (d,  $J$  = 8.8 Hz, 2H, H3/H3'/H5/H5'), 3.829 (s, 3H, OMe).  $^{13}\text{C}$  NMR (100 MHz,  $\text{CD}_3\text{CN}$ , 25 °C):  $\delta$  164.258 (C4/C4'), 138.280 (C2/C2'/C6/C6'), 122.148 (q,  $J$  = 320.8 Hz,  $\text{CF}_3\text{SO}_3^-$ ), 119.066 (C3/C3'/C5/C5'), 103.383 (C1/C1'), 56.772 (OMe).  $^{19}\text{F}$  NMR (376 MHz,  $\text{CD}_3\text{CN}$ , 25 °C):  $\delta$  -79.249 (s,  $\text{CF}_3\text{SO}_3^-$ ).

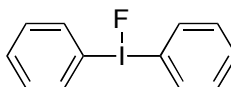


**Bis(4-methoxyphenyl)-fluoro- $\lambda^3$ -iodane:** In a nitrogen atmosphere glove box, a mixture of 454 mg (1 mmol) bis(4-methoxyphenyl)-iodonium trifluoroacetate and 262 mg (1 mmol) anhydrous tetrabutylammonium fluoride (TBAF) was treated with 1 mL of dry THF. The solution was allowed to stand for 1 h, the white precipitate was collected and washed ( $3 \times 0.5$  mL) with THF. Calculated yield: 288.7 mg (80.2 %).  $^1\text{H}$  NMR (saturated solution in  $\text{CD}_3\text{CN}$ , 400 MHz, 25 °C):  $\delta$  7.739 (d,  $J$  = 8.9 Hz, 4 H, H2/H2'/H6/H6'), 6.853 (d,  $J$  = 8.9 Hz, 4 H, H3/H3'/H5/H5'), 3.769 (s, 6 H, OMe);  $^{13}\text{C}$  NMR ( $\text{CD}_3\text{CN}$ , 100 MHz, 25 °C)  $\delta$  162.43 (C4/C4'), 136.98 (C2/C2'/C6/C6'), 117.52

(C3/C3'/C5/C5'), 113.20 (C1/C1'), 56.55 (OMe);  $^{19}\text{F}$  NMR ( $\text{CD}_3\text{CN}$ , 376 MHz, 25 °C)  $\delta$  -17.9 (broad s, I-F).

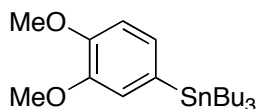


**Diphenyl-trifluoromethanesulfonyl- $\lambda^3$ -iodane:** To a stirred suspension of diacetoxyiodobenzene (660 mg, 2.05 mmol) in 10 mL dry methylene chloride at 0 °C under  $\text{N}_2$ , triflic acid (0.36 mL, 4.10 mmol) was added dropwise via syringe. The mixture was stirred at 0 °C for 5 min and then at room temperature for 1 h. The resulting clear yellow solution was cooled to 0 °C and benzene (0.37 mL, 4.10 mmol) was added dropwise via syringe. The resulting solution was stirred at 0 °C for 5 min and then at room temperature for 30 min. The volatiles were removed *in vacuo* to obtain a crude brown solid, which was triturated with diethyl ether. The solid was collected by filtration and washed with diethyl ether to yield diphenyl-trifluoromethanesulfonyl- $\lambda^3$ -iodane as a light brown flaky crystalline solid (726 mg, 82.4%).  $^1\text{H}$  NMR (500 MHz,  $\text{CD}_3\text{CN}$ , 25 °C):  $\delta$  8.091 (d,  $J$  = 8.2 Hz, 4H, H2/H2'/H6/H6'), 7.710 (t,  $J$  = 7.6 Hz, 2H, H4/H4'), 7.540 (t,  $J$  = 7.9 Hz, 4H, H3/H3'/H5/H5').  $^{13}\text{C}$  NMR (125 MHz,  $\text{CD}_3\text{CN}$ , 25 °C):  $\delta$  136.75 (C2/C2'/C6/C6'), 134.33 (C4/C4'), 133.76 (C3/C3'/C5/C5'), 122.34 (q,  $J_{\text{C-F}}$  = 321.0 Hz,  $\text{CF}_3\text{SO}_3^-$ ), 114.84 (C1/C1').  $^{19}\text{F}$  NMR (376 MHz,  $\text{CD}_3\text{CN}$ , 25 °C):  $\delta$  -79.33 (s,  $\text{CF}_3\text{SO}_3^-$ ).



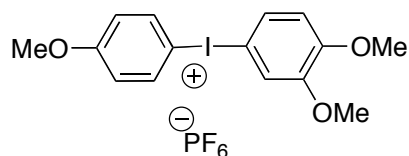
**Diphenyl-fluoro- $\lambda^3$ -iodane:** In a nitrogen atmosphere glove box, a mixture of 343 mg (1 mmol) diphenyliodonium nitrate and 262 mg (1 mmol) anhydrous tetrabutylammonium fluoride (TBAF) was treated with 1 mL of dry THF. The solution was allowed to stand

for 1 h, the white precipitate was collected and washed ( $3 \times 0.5$  mL) with THF. Calculated yield: 210 mg (70 %).  $^1\text{H}$  NMR (saturated solution in  $\text{CD}_3\text{CN}$ , 400 MHz, 25  $^\circ\text{C}$ ):  $\delta$  7.819 (d,  $J = 7.5$  Hz, 4 H, H2/H2'/H6/H6'), 7.457 (t,  $J = 7.5$  Hz, 2 H, H4/H4'), 7.299 (t,  $J = 7.5$  Hz, 4 H, H3/H3'/H5/H5');  $^{13}\text{C}$  NMR ( $\text{CD}_3\text{CN}$ , 100 MHz, 25  $^\circ\text{C}$ )  $\delta$  135.29 (C2/C2'/C6/C6), 131.62 (C3/C3'/C5/C5'), 131.21 (C4/C4'), 122.91 (C1/C1');  $^{19}\text{F}$  NMR ( $\text{CD}_3\text{CN}$ , 376 MHz, 25  $^\circ\text{C}$ )  $\delta$  -13.0 (broad s, I-F).



**3,4-Dimethoxyphenyltributyltin:** In a nitrogen atmosphere glove box, 4-bromoveratrole (1.085 g, 5 mmol) and  $\text{Pd}(\text{PPh}_3)_4$  (289 mg, 0.25 mmol) were dissolved in 15 mL of dry toluene. The solution was transferred into a storage tube equipped with PTFE chemcap seal, and hexabutylditin (3.19 g, 5 mmol) was added. The tube was sealed, taken out of the glove box, and heated at 120  $^\circ\text{C}$  for 48 h. The reaction mixture was allowed to cool to room temperature and diluted with hexane (15 mL) before saturated aqueous KF solution (15 mL) was added. The mixture was stirred for 30 min, filtered through celite, and the organic layer was separated. The solvent was removed *in vacuo* to give the crude product as a yellow oil. The crude product was purified by column chromatography ( $R_f = 0.4$ , hexane/dichloromethane 98/2, basic alumina) to give 1.69 g (79.1 %) of 3,4-dimethoxyphenyltributyltin.  $^1\text{H}$  NMR ( $\text{C}_6\text{D}_6$ , 400 MHz, 25  $^\circ\text{C}$ ):  $\delta$  7.097 (d,  $J = 7.7$  Hz, 1 H, H6), 7.074 (s, 1 H, H2), 6.744 (d,  $J = 7.7$  Hz, 1 H, H5), 3.557 (s, 3 H, 3-OMe), 3.443 (s, 3 H, 4-OMe), 1.632 (m, 6 H,  $\beta\text{CH}_2$ ), 1.384 (m, 6 H,  $\gamma\text{CH}_2$ ), 1.117 (m, 6 H,  $\alpha\text{CH}_2$ ), 0.912 (t,  $J = 7.6$  Hz, 9 H,  $\text{CH}_3$ ), (coupling to  $^{117}\text{Sn}$  and  $^{119}\text{Sn}$  observed,  $J$  ranged from 10.7

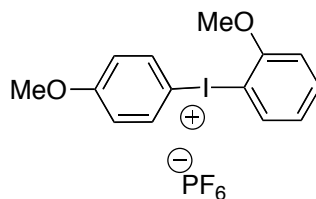
– 41.3 Hz);  $^{13}\text{C}$  NMR ( $\text{C}_6\text{D}_6$ , 100 MHz, 25 °C)  $\delta$  151.21 (C4), 150.66 (C6), 132.35 (C1), 130.13 (C3), 120.75 (C5), 113.12 (C2), 56.21 (3-OMe), 55.75 (4-OMe), 29.87 ( $\gamma\text{C}$ ), 28.16 ( $\beta\text{C}$ ), 14.31 ( $\delta\text{C}$ ), 10.32 ( $\alpha\text{C}$ ), (coupling to  $^{117}\text{Sn}$  and  $^{119}\text{Sn}$  observed, J ranged from 1.0 – 320.8 Hz); HRMS (HRFAB): calcd. for  $\text{C}_{20}\text{H}_{37}\text{O}_2\text{Sn}$   $[\text{M} + \text{H}]^+$  429.1815 found 429.1799. lit.<sup>149</sup>  $^1\text{H}$  NMR ( $\text{CDCl}_3$ ):  $\delta$  6.7 - 7.3 (m, 3 H, Ar-H), 3.89 (s, 3 H, OMe), 3.86 (s, 3 H, OMe), 1.1-1.8 (m, 18 H,  $9 \times \text{CH}_2$ ), 0.89 (s, 9 H,  $3 \times \text{CH}_3$ ); b.p. 166-172 °C /0.4 mm Hg.)



**(3,4-Dimethoxyphenyl)(4'-methoxyphenyl)-iodonium hexafluorophosphate:** In a nitrogen atmosphere glove box, 1-(diacetoxyiodo)-4-methoxybenzene (352 mg, 1 mmol) was dissolved in 1.5 mL of dry acetonitrile and a solution of p-toluenesulfonic acid monohydrate (190 mg, 1 mmol) in 1.5 mL of dry acetonitrile was added. 3,4-dimethoxyphenyltributyltin, (427 mg, 1 mmol) was added and the mixture was allowed to react at room temperature for 2 h. Water (10 mL) was added and the mixture was extracted ( $3 \times 5$  mL) with hexanes. The aqueous layer was treated with  $\text{NaPF}_6$  (502 mg, 3 mmol) and the white precipitate was filtered, dried in vacuo, and recrystallized with diethyl ether/dichloromethane to give 370 mg (71.7 %) of (3,4-dimethoxyphenyl)(4'-methoxyphenyl)-iodonium hexafluorophosphate.  $^1\text{H}$  NMR ( $\text{CD}_3\text{CN}$ , 400 MHz, 25 °C):  $\delta$  7.986 (d,  $J = 9.1$  Hz, 2 H,  $\text{H}_{2'}/\text{H}_{6'}$ ), 7.647 (dd,  $J_1 = 8.9$  Hz,  $J_2 = 2.2$  Hz, 1 H,  $\text{H}_6$ ), 7.558 (d,  $J = 2.2$  Hz, 1 H,  $\text{H}_2$ ), 7.049 (d,  $J = 9.1$  Hz, 2 H,  $\text{H}_{3'}/\text{H}_{5'}$ ), 7.022 (d,  $J = 8.9$  Hz, 1 H,  $\text{H}_5$ ),

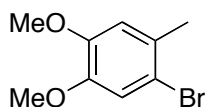


3.845 (s, 3 H, 3-OMe), 3.843 (s, 3 H, 4'-OMe), 3.834 (s, 3 H, 4-OMe);  $^{13}\text{C}$  NMR ( $\text{CD}_3\text{CN}$ , 100 MHz, 25 °C)  $\delta$  164.58 (C4'), 154.62 (C4), 152.50 (C3), 138.49 (C2'/C6'), 130.65 (C6), 119.38 (C2), 119.13 (C3'/C5'), 115.52 (C5), 103.37 (C1), 102.64 (C1'), 57.49 (3-OMe), 57.14 (4'-OMe), 57.05 (4-OMe);  $^{19}\text{F}$  NMR ( $\text{CD}_3\text{CN}$ , 376 MHz, 25 °C)  $\delta$  -72.786 (d,  $^1J_{\text{P-F}} = 705.8$  Hz,  $\text{PF}_6^-$ ); HRMS (HRFAB): calcd. for  $\text{C}_{15}\text{H}_{16}\text{O}_3\text{I}$   $[\text{M} - \text{PF}_6]^+$  371.0144 found 371.0156.

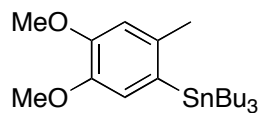


**(2-Methoxyphenyl)(4'-methoxyphenyl)-iodonium hexafluorophosphate:** In a nitrogen atmosphere glove box, 1-(diacetoxyiodo)-2-methoxybenzene, (352 mg, 1 mmol) was weighed into a glass vial and 1.5 mL of dry acetonitrile was added. A solution of *p*-toluenesulfonic acid monohydrate (190 mg, 1 mmol) dissolved in 1.5 mL of dry acetonitrile was added by syringe. Upon completion of the addition, 4-iodoanisole (neat, 0.11 mL, 1 mmol) was added. The vial was sealed and taken out of the glove box; the mixture was allowed to stir at room temperature for 2 h. Water (10 mL) was added and the mixture was transferred to a separatory funnel and extracted ( $3 \times 5$  mL) with hexanes. The reserved aqueous layer was treated with 502 mg (3 mmol) of  $\text{NaPF}_6$ . The white precipitate was filtered, dried in vacuo, and recrystallized in a mixture of diethyl ether/dichloromethane to give 405 mg (83.3 %) of (2-methoxyphenyl)(4'-methoxyphenyl)-iodonium hexafluorophosphate.  $^1\text{H}$  NMR ( $\text{CD}_3\text{CN}$ , 400 MHz, 25 °C):  $\delta$  7.988 (d,  $J = 9.2$  Hz, 2 H, H2'/H6'), 7.878 (d,  $J = 8.4$  Hz, 1 H, H6), 7.659 (td,  $J_1 = 8.4$  Hz,

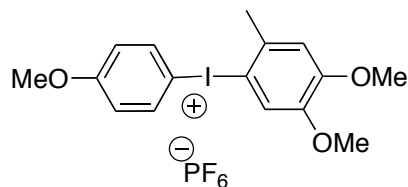
$J_2 = 1.3$  Hz, 1 H, H4), 7.232 (dd,  $J_1 = 8.4$  Hz,  $J_2 = 1.3$  Hz, 1 H, H5), 7.063 (td,  $J_1 = 8.4$  Hz,  $J_2 = 1.3$  Hz, 1 H, H3), 7.051 (d,  $J = 9.2$ , 2 H, H3'/H5'), 3.970 (s, 3 H, 2-OMe), 3.841 (s, 3 H, 4'-OMe);  $^{13}\text{C}$  NMR ( $\text{CD}_3\text{CN}$ , 100 MHz, 25 °C)  $\delta$  164.73 (C4'), 157.90 (C2), 139.52 (C2'/C6'), 137.08 (C4), 136.79 (C6), 125.36 (C3), 119.44 (C3'/C5'), 114.70 (C5), 104.69 (C1), 100.92 (C1'), 58.40 (2-OMe), 57.06 (4'-OMe);  $^{19}\text{F}$  NMR ( $\text{CD}_3\text{CN}$ , 376 MHz, 25 °C)  $\delta$  -72.675 (d,  $^1J_{\text{P-F}} = 706.2$  Hz,  $\text{PF}_6^-$ ); HRMS (HRFAB): calcd. for  $\text{C}_{14}\text{H}_{14}\text{O}_2\text{I} [\text{M} - \text{PF}_6]^+$  341.0038 found 341.0035.



**1-Bromo-4,5-dimethoxy-2-methylbenzene:** To a stirred solution of 3,4-dimethoxytoluene (3.6 mL, 25 mmol) in 125 mL of acetonitrile was added N-bromosuccinimide (4.9 g, 27.5 mmol). The mixture was stirred at room temperature for 2 h, the solvent was removed by rotary evaporation, and 100 mL of  $\text{CCl}_4$  was added. The solid was succinimide was removed by filtration, the solvent was removed by rotary evaporation, and the crude product was recrystallized from hexane to afford 5.2 g (90 %) of 1-bromo-4,5-dimethoxy-2-methylbenzene.  $^1\text{H}$  NMR ( $\text{CD}_3\text{CN}$ , 400 MHz, 25 °C):  $\delta$  7.022 (s, 1 H, H6), 6.822 (s, 1 H, H3), 3.752 (s, 3 H, OMe), 3.744 (s, 3 H, OMe), 2.269 (s, 3 H, Me);  $^{13}\text{C}$  NMR ( $\text{CD}_3\text{CN}$ , 100 MHz, 25 °C)  $\delta$  149.91 (C5), 149.33 (C4), 130.73 (C2), 116.73 (C6), 115.35 (C3), 115.12 (C1); HRMS (HRCI): calcd. for  $\text{C}_9\text{H}_{12}\text{O}_2\text{Br} [\text{M} + \text{H}]^+$  231.0021, 233.0000 found 231.0011, 233.0013. lit.<sup>150</sup> :  $^1\text{H}$  NMR ( $\text{CDCl}_3$ , 300 MHz):  $\delta$  7.000 (s, 1 H, Ar-H), 6.731 (s, 1 H, Ar-H), 3.874 (s, 3 H, -OMe), 3.843 (s, 3 H, OMe), 2.327 (s, 3 H, -Me.)

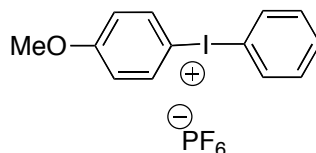


**(4,5-Dimethoxy-2-methylphenyl)tributyltin:** In a nitrogen atmosphere glove box, 1-bromo-4,5-dimethoxy-2-methylbenzene (1.155 g, 5 mmol) and  $\text{Pd}(\text{PPh}_3)_4$  (289 mg, 0.25 mmol) were dissolved in 15 mL of dry toluene. The solution was transferred into a storage tube equipped with PTFE chemcap seal and hexabutylditin (3.19 g, 5 mmol) was added. The tube was sealed, removed from the glove box, and heated at 120 °C for 48 h. The reaction mixture was allowed to cool to room temperature and diluted with hexane (15 mL) before saturated aqueous KF solution (15 mL) was added. The mixture was stirred for 30 min, filtered through celite, and the organic layer was separated. The solvent was removed to give the crude product as a yellow oil. The crude product was purified by column chromatography ( $R_f = 0.4$ , hexane/dichloromethane 98/2, basic alumina) to give 1.68 g (76.2 %) of (4,5-dimethoxy-2-methyl-phenyl)tributyltin.  $^1\text{H}$  NMR ( $\text{C}_6\text{D}_6$ , 400 MHz, 25 °C):  $\delta$  7.048 (s, 1 H, H6), 6.661 (s, 1 H, H3), 3.593 (s, 3 H, 3-OMe), 3.458 (s, 3 H, 4-OMe), 2.358 (s, 3 H, 2-Me), 1.615 (m, 6 H,  $\beta\text{CH}_2$ ), 1.384 (m, 6 H,  $\gamma\text{CH}_2$ ), 1.143 (m, 6 H,  $\alpha\text{CH}_2$ ), 0.910 (t,  $J = 7.6$  Hz, 9 H,  $\text{CH}_3$ ), (coupling to  $^{117}\text{Sn}$  and  $^{119}\text{Sn}$  observed,  $J$  ranged from 5.4 – 45.6 Hz);  $^{13}\text{C}$  NMR ( $\text{C}_6\text{D}_6$ , 100 MHz, 25 °C)  $\delta$  151.11 (C4), 148.36 (C2), 137.98 (C5), 131.85 (C1), 121.44 (C3), 114.65 (C6), 56.53 (3-OMe), 55.78 (4-OMe), 30.04 ( $\gamma\text{C}$ ), 28.18 ( $\beta\text{C}$ ), 25.04 (2-Me), 14.28 ( $\delta\text{C}$ ), 10.77 ( $\alpha\text{C}$ ), (coupling to  $^{117}\text{Sn}$  and  $^{119}\text{Sn}$  observed,  $J$  ranged from 1.0 – 326.2 Hz); HRMS (HRFAB): calcd. for  $\text{C}_{21}\text{H}_{39}\text{O}_2\text{Sn}$   $[\text{M} + \text{H}]^+$  443.1972 found 443.1982.

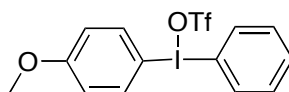


**(4,5-Dimethoxy-2-methylphenyl)(4'-methoxyphenyl)-iodonium hexafluorophosphate:**

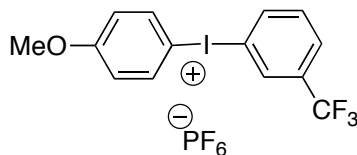
In a nitrogen atmosphere glove box, 1-(diacetoxyiodo)-4-methoxybenzene (352 mg, 1 mmol) was dissolved in 1.5 mL of dry acetonitrile. A solution of *p*-toluenesulfonic acid monohydrate (190 mg, 1 mmol) in 1.5 mL of dry acetonitrile was added by syringe. Upon completion of the addition, (4,5-dimethoxy-2-methylphenyl)tributyltin (441 mg, 1 mmol) was added. The vial was sealed and taken out of the glove box and the mixture was allowed to stir at room temperature for 2 h. Water (10 mL) was added and the mixture was transferred to a separatory funnel and extracted ( $3 \times 5$  mL) with hexanes. The reserved aqueous layer was treated with 502 mg (3 mmol) of NaPF<sub>6</sub>. The white precipitate was filtered, dried in vacuo, and recrystallized in a mixture of diethyl ether/dichloromethane to give 397 mg (75 %) of (4,5-dimethoxy-2-methylphenyl)(4'-methoxyphenyl)-iodonium hexafluorophosphate. <sup>1</sup>H NMR (CD<sub>3</sub>CN, 400 MHz, 25 °C): δ 7.939 (d, *J* = 9.2 Hz, 2 H, H2'/H6'), 7.593 (s, 1 H, H6), 7.055 (d, *J* = 9.2 Hz, 2 H, H3'/H5'), 7.026 (s, 1 H, H5), 3.835 (s, 6 H, 3/4'-OMe), 3.828 (s, 3 H, 4-OMe), 2.550 (s, 3 H, 2-Me); <sup>13</sup>C NMR (CD<sub>3</sub>CN, 100 MHz, 25 °C) δ 164.45 (C4'), 154.63 (C4), 150.46 (C5), 138.28 (C2'/C6'), 136.71 (C2), 120.59 (C6), 119.41 (C3'/C5'), 115.28 (C3), 107.01 (C1), 102.58 (C1'), 57.51 (3-OMe), 57.14 (4'-OMe), 57.04 (4-OMe); <sup>19</sup>F NMR (CD<sub>3</sub>CN, 376 MHz, 25 °C) δ -72.735 (d, <sup>1</sup>*J*<sub>P-F</sub> = 706.9 Hz, PF<sub>6</sub><sup>-</sup>); HRMS (HRFAB): calcd. for C<sub>16</sub>H<sub>18</sub>O<sub>3</sub>I [M – PF<sub>6</sub>]<sup>+</sup> 3385.0301 found 3385.0313.



**Phenyl(4-methoxyphenyl)-iodonium hexafluorophosphate:** In a nitrogen atmosphere glove box, diacetoxyiodobenzene (322 mg, 1 mmol) was weighed into a glass vial and 1.5 mL of dry acetonitrile was added. A solution of *p*-toluenesulfonic acid monohydrate (190 mg, 1 mmol) in 1.5 mL of dry acetonitrile was added by syringe. Upon completion of the addition, anisole (neat, 0.11 mL, 1 mmol) was added and the vial was sealed and taken out of the glove box; the mixture was allowed to stir at room temperature for 2 h. Water (10 mL) was added and the mixture was transferred to a separatory funnel and extracted ( $3 \times 5$  mL) with hexanes. The reserved aqueous layer was treated with 502 mg (3 mmol) of NaPF<sub>6</sub>. The white precipitate was filtered, dried in vacuo, and recrystallized in a mixture of diethyl ether/dichloromethane to give 355 mg (77.9 %) of phenyl(4-methoxyphenyl)-iodonium hexafluorophosphate. <sup>1</sup>H NMR (CD<sub>3</sub>CN, 400 MHz, 25 °C): δ 8.022 (d, *J* = 7.6 Hz, 2 H, H<sub>2</sub>/H<sub>6</sub>), 8.011 (d, *J* = 9.4 Hz, 2 H, H<sub>2</sub>'/H<sub>6</sub>'), 7.701 (t, *J* = 7.6 Hz, 1 H, H<sub>4</sub>), 7.734 (t, *J* = 7.6 Hz, 2 H, H<sub>3</sub>/H<sub>5</sub>), 7.063 (d, *J* = 9.4 Hz, 2 H, H<sub>3</sub>'/H<sub>5</sub>'), 3.839 (s, 6 H, OMe); <sup>13</sup>C NMR (CD<sub>3</sub>CN, 100 MHz, 25 °C) δ 164.77 (C<sub>4</sub>'), 139.04 (C<sub>2</sub>'/C<sub>6</sub>'), 136.22 (C<sub>2</sub>/C<sub>6</sub>), 134.27 (C<sub>4</sub>), 133.77 (C<sub>3</sub>/C<sub>5</sub>), 119.58 (C<sub>3</sub>'/C<sub>5</sub>'), 115.29 (C<sub>1</sub>), 102.50 (C<sub>1</sub>'), 57.09 (OMe); <sup>19</sup>F NMR (CD<sub>3</sub>CN, 376 MHz, 25 °C) δ -72.754 (d, <sup>1</sup>*J*<sub>P-F</sub> = 707.7 Hz, PF<sub>6</sub><sup>-</sup>); HRMS (HRFAB): calcd. for C<sub>13</sub>H<sub>12</sub>OI [M – PF<sub>6</sub>]<sup>+</sup> 310.9925 found 310.9932.

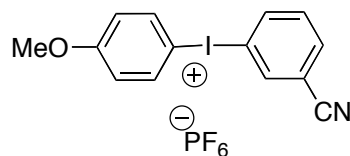


**Phenyl(4-methoxyphenyl)-trifluoromethanesulfonyl- $\lambda^3$ -iodane:** To a stirred suspension of diacetoxyiodobenzene (660 mg, 2.05 mmol) in 10 mL dry methylene chloride at 0 °C under N<sub>2</sub>, triflic acid (0.36 mL, 4.10 mmol) was added dropwise via syringe. The mixture was stirred at 0 °C for 5 min and then at room temperature for 1 h. The resulting clear yellow solution was cooled to 0 °C and anisole (0.25 mL, 2.30 mmol) was added drop wise via syringe. The resulting blue colored solution was stirred at 0 °C for 5 min and then at room temperature for 30 min. The volatiles were removed *in vacuo* to obtain a dark brown oil which was triturated with diethyl ether. The solvent was removed *in vacuo* to obtain an off white solid which was triturated with diethyl ether. The solid was collected by filtration and washed with diethyl ether to yield phenyl(4-methoxyphenyl)-trifluoromethanesulfonyl- $\lambda^3$ -iodane as a colorless, finely powdered solid (651 mg, 70.7%). <sup>1</sup>H NMR (500 MHz, CD<sub>3</sub>CN, 25 °C):  $\delta$  8.042 (d, J = 8.5 Hz, 2H, H2/H6), 8.017 (d, J = 9.1 Hz, 2H, H2'/H6'), 7.690 (t, J = 7.6 Hz, 1H, H4), 7.524 (t, J = 8.0 Hz, 2H, H3/H5), 7.055 (d, J = 9.1 Hz, 2H, H3'/H5'), 3.835 (s, 3H, OMe). <sup>13</sup>C NMR (125 MHz, CD<sub>3</sub>CN, 25 °C):  $\delta$  164.67 (C4'), 139.02 (C2'/C6'), 136.23 (C2/C6), 134.14 (C4), 133.66 (C3/C5), 122.37 (q, J<sub>C-F</sub> = 320.9 Hz, CF<sub>3</sub>SO<sub>3</sub><sup>-</sup>), 119.47 (C3'/C5'), 115.49 (C1), 102.80 (C1'), 57.06 (OMe). <sup>19</sup>F NMR (376 MHz, CD<sub>3</sub>CN, 25 °C):  $\delta$  -79.29 (s, CF<sub>3</sub>SO<sub>3</sub><sup>-</sup>).

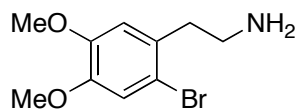


**(3-(Trifluoromethyl)phenyl)(4'-methoxyphenyl)-iodonium hexafluorophosphate:** In a nitrogen atmosphere glove box, 1-(diacetoxyiodo)-3-(trifluoromethyl)-benzene (390 mg,

1 mmol) was weighed into a glass vial and 1.5 mL of dry acetonitrile was added. A solution of *p*-toluenesulfonic acid monohydrate (190 mg, 1 mmol) in 1.5 mL of dry acetonitrile was added by syringe. Upon completion of the addition, anisole (neat, 0.11 mL, 1 mmol) was added and the vial was sealed and taken out of the glove box; the mixture was allowed to stir at room temperature for 2 h. Water (10 mL) was added and the mixture was transferred to a separatory funnel and extracted ( $3 \times 5$  mL) with hexanes. The reserved aqueous layer was treated with 502 mg (3 mmol) of NaPF<sub>6</sub>. The white precipitate was filtered, dried in vacuo, and recrystallized in a mixture of diethyl ether/dichloromethane to give 503 mg (96.1 %) of (3-(trifluoromethyl)phenyl)(4'-methoxyphenyl)-iodonium hexafluorophosphate. <sup>1</sup>H NMR (CD<sub>3</sub>CN, 400 MHz, 25 °C):  $\delta$  8.384 (s, 1 H, H<sub>2</sub>), 8.266 (d, *J* = 8.1 Hz, 1 H, H<sub>6</sub>), 8.056 (d, *J* = 9.2 Hz, 2 H, H<sub>2</sub>'/H<sub>6</sub>'), 7.996 (d, *J* = 8.1 Hz, 1 H, H<sub>4</sub>), 7.716 (t, *J* = 8.1 Hz, 1 H, H<sub>5</sub>), 7.083 (d, *J* = 9.2, 2 H, H<sub>3</sub>'/H<sub>5</sub>'), 3.847 (s, 3 H, 4'-OMe); <sup>13</sup>C NMR (CD<sub>3</sub>CN, 100 MHz, 25 °C)  $\delta$  164.99 (C4'), 139.99 (C6), 139.38 (C2'/C6'), 134.44 (C5), 134.281 (q, *J* = 33.6 Hz, C3), 133.08 (q, *J* = 3.7 Hz, C2), 133.05 (q, *J* = 3.7 Hz, C4), 124.11 (q, *J* = 272.8 Hz, CF<sub>3</sub>), 119.71 (C3'/C5'), 114.83 (C1), 102.54 (C1'), 57.13 (4'-OMe); <sup>19</sup>F NMR (CD<sub>3</sub>CN, 376 MHz, 25 °C)  $\delta$  -63.420 (*J*<sub>1(F-C)</sub> = 272.8 Hz, *J*<sub>2(F-C)</sub> = 33.6 Hz, CF<sub>3</sub>), -72.625 (d, *J*<sub>1(P-F)</sub> = 707.1 Hz, PF<sub>6</sub><sup>-</sup>); HRMS (HRFAB): calcd. for C<sub>14</sub>H<sub>11</sub>OIF<sub>3</sub> [M – PF<sub>6</sub>]<sup>+</sup> 378.9807 found 378.9817.

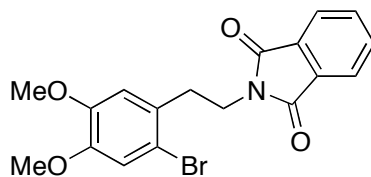


**(3-Cyanophenyl)(4'-methoxyphenyl)-iodonium hexafluorophosphate:** In a nitrogen atmosphere glove box, 3-(diacetoxyiodo)benzonitrile (347 mg, 1 mmol) was weighed into a glass vial and 1.5 mL of dry acetonitrile was added. A solution of *p*-toluenesulfonic acid monohydrate (190 mg, 1 mmol) in 1.5 mL of dry acetonitrile was added by syringe. Upon completion of the addition, anisole (neat, 0.11 mL, 1 mmol) was added and the vial was sealed and taken out of the glove box. The mixture was allowed to stir at room temperature for 2 h. Water (10 mL) was added and the mixture was transferred to a separatory funnel and extracted ( $3 \times 5$  mL) with hexanes. The reserved aqueous layer was treated with 502 mg (3 mmol) of NaPF<sub>6</sub>. The white precipitate was filtered, dried in vacuo, and recrystallized in a mixture of diethyl ether/dichloromethane to give 354 mg (73.7 %) of (3-cyanophenyl)(4'-methoxyphenyl)-iodonium hexafluorophosphate. <sup>1</sup>H NMR (CD<sub>3</sub>CN, 400 MHz, 25 °C):  $\delta$  8.389 (t, *J* = 1.6 Hz, 1 H, H<sub>2</sub>), 8.273 (dd, *J*<sub>1</sub> = 8.2 Hz, *J*<sub>2</sub> = 1.6 Hz, 1 H, H<sub>6</sub>), 8.038 (d, *J* = 9.4 Hz, 2 H, H<sub>2</sub>'/H<sub>6</sub>'), 8.017 (dd, *J*<sub>1</sub> = 8.2 Hz, *J*<sub>2</sub> = 1.6 Hz, 1 H, H<sub>4</sub>), 7.665 (t, *J* = 8.2 Hz, 1 H, H<sub>5</sub>), 7.082 (d, *J* = 9.4, 2 H, H<sub>3</sub>'/H<sub>5</sub>'), 3.850 (s, 3 H, 4'-OMe); <sup>13</sup>C NMR (CD<sub>3</sub>CN, 100 MHz, 25 °C)  $\delta$  165.04 (C4'), 140.40 (C6), 139.50 (C2), 139.47 (C2'/C6'), 137.79 (C5), 134.13 (C4), 119.75 (C3'/C5'), 117.63 (C3), 116.75 (CN), 114.53 (C1), 102.56 (C1'), 57.16 (4'-OMe); <sup>19</sup>F NMR (CD<sub>3</sub>CN, 376 MHz, 25 °C)  $\delta$  -72.675 (d, <sup>1</sup>*J*<sub>P-F</sub> = 707.5 Hz, PF<sub>6</sub><sup>-</sup>); HRMS (HRFAB): calcd. for C<sub>14</sub>H<sub>11</sub>NOI [M – PF<sub>6</sub>]<sup>+</sup> 335.9885 found 335.9876.

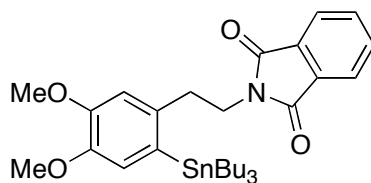




**2-(2-Bromo-4,5-dimethoxyphenyl)ethanamine:** A solution of bromine (1.1 mL, 22 mmol) in acetic acid (10 mL) was added slowly to a vigorously stirred solution of 2-(3,4-dimethoxyphenyl)ethanamine (3.4 mL, 20 mmol) in 50 mL of acetic acid. The mixture was stirred for two hours, filtered, and the isolated solid was washed with dichloromethane ( $3 \times 10$  mL) and petroleum ether ( $3 \times 10$  mL). The remaining solid was in water and the pH was adjusted to 10 with aqueous KOH solution. The aqueous solution was extracted with dichloromethane ( $3 \times 10$  mL) and the combined organic layers were evaporated to give 4.12g (78 %) of 2-(2-bromo-4,5-dimethoxyphenyl)ethanamine. The crude product was dried under dynamic vacuum overnight and used without further purification.  $^1\text{H}$  NMR ( $\text{CD}_3\text{CN}$ , 400 MHz, 25 °C):  $\delta$  7.00 (s, 1 H, H6), 6.73 (s, 1 H, H3), 3.85 (s, 3 H, OMe), 3.84 (s, 3 H, OMe), 2.94 (t,  $J = 7.17$  Hz, 2 H,  $\text{CH}_2$ ), 2.81 (t,  $J = 7.17$  Hz, 2 H,  $\text{CH}_2$ ), 1.24 (s, 2 H,  $\text{NH}_2$ );  $^{13}\text{C}$  NMR ( $\text{CD}_3\text{CN}$ , 100 MHz, 25 °C):  $\delta$  148.34 (C5), 148.07 (C4), 131.09 (C2), 115.66 (C6), 114.33 (C1), 113.43 (C3), 56.15 (OMe), 42.40 ( $\text{CH}_2$ ), 39.92 ( $\text{CH}_2$ ); HRMS (HRFAB): calcd. for  $\text{C}_{10}\text{H}_{14}\text{O}_2\text{NBr}$   $[\text{M} + \text{H}]^+$  262.0266, 260.0286 found 262.0262, 260.0276. lit.<sup>151</sup> :  $^1\text{H}$  NMR  $\delta$  1.38, s,  $\text{NH}_2$ ; 2.8-2.9, m,  $\text{CH}_2\text{Ar}$ ; 2.9-3.0, m,  $\text{CH}_2\text{N}$ ; 3.85, s,  $\text{OCH}_3$ ; 3.86, s,  $\text{OCH}_3$ ; 6.74, s, 1 H;  $^{13}\text{C}$  NMR  $\delta$  39.8,  $\text{CH}_2$ ; 42.3,  $\text{CH}_2$ ; 56.1,  $2 \times \text{OCH}_3$ ; 113.4, C3 or C6; 114.3, C-Br; 115.6, C6 or C3; 131.0, C1; 148.0, C4 or C5; 148.3, C5 or C4. MS (CI,  $\text{NH}_3$ )  $m/z$  262 (MH, 98 %), 260 (MH, 100), 182 (20), 180 (14).)

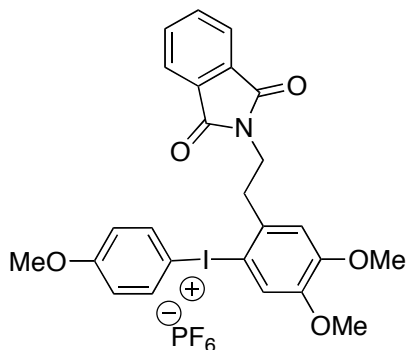


**2-Bromo-4, 5-dimethoxyl-1-(2-phthalimidoethyl)benzene:** 2-(2-Bromo-4,5-dimethoxyphenyl)ethanamine (3.5 g, 13.2 mmol) was dissolved in 50 mL of dry acetonitrile and phthaloyl dichloride (2.14 mL, 14.5 mmol) and diisopropylethylamine (7 mL, 39.6 mmol) were added. This mixture was stirred at room temperature for 14 h. The acetonitrile was removed by rotary evaporation and the remaining material was taken up in dichloromethane and washed with alkaline water (pH = 11). The aqueous wash was extracted with dichloromethane ( $3 \times 15$  mL), and the organic fractions were combined and dried over sodium sulfate. The solvent was removed by rotary evaporation to give a colorless solid. This crude product was dissolved in dichloromethane and loaded on top of a silica gel column (60 Å silica) and the purified product was eluted with dichloromethane ( $R_f = 0.2$ ). The solvent was removed by rotary evaporation to give 2-Bromo-4, 5-dimethoxyl-1-(2-phthalimidoethyl)benzene (1.8 g, 34 %).  $^1\text{H}$  NMR ( $\text{CDCl}_3$ , 400 MHz, 25 °C):  $\delta$  7.83 (m, 2 H, phthalimide), 7.71 (m, 2 H, phthalimide), 7.00 (s, 1 H, H6), 6.68 (s, 1 H, H3), 3.96 (t,  $J = 7.02$  Hz, 2 H,  $\text{CH}_2$ ), 3.84 (s, 3 H, OMe), 3.72 (s, 3 H, OMe), 3.08 (t, 2 H,  $J = 7.02$  Hz,  $\text{CH}_2$ );  $^{13}\text{C}$  NMR ( $\text{CDCl}_3$ , 100 MHz, 25 °C)  $\delta$  168.17 (CO), 148.35 (C5), 148.30 (C4), 133.97 (C3'/C6'), 132.04 (C1'/C2'), 129.30 (C2), 123.24 (C4'/C5'), 115.54 (C6), 114.50 (C1), 113.20 (C3), 56.08 (OMe), 55.95 (OMe), 37.65 ( $\text{CH}_2$ ), 34.40 ( $\text{CH}_2$ ); HRMS (ESI): calcd. for  $\text{C}_{18}\text{H}_{16}\text{O}_4\text{NBr}$   $[\text{M} + \text{Na}]^+$  412.0160, 414.0140 found 412.0173, 414.0143. lit.<sup>152</sup>:  $^1\text{H}$  NMR ( $\text{CDCl}_3$ , 200MHz):  $\delta$  2.99 (2 H, dd, H- $\beta$ ); 3.63 (3 H, s,  $\text{OCH}_3$ ); 3.75 (3 H, s,  $\text{OCH}_3$ ); 3.88 (2 H, dd, H- $\alpha$ ); 6.65 (1 H, s, H-3), 6.91 (1 H, s, H-6); 7.64 (2 H, tt, H-5', H-6'); 7.75 (2 H, dddd, H-4', H-7').)



**(4,5-Dimethoxy-2-(2-phthalimido)phenyl)tributyltin:** In a nitrogen atmosphere glove box, 1.945 g (5 mmol) 2-bromo-4,5-dimethoxy-1-(2-phthalimidoethyl)benzene and 289 mg (0.25 mmol) Pd(0)(PPh<sub>3</sub>)<sub>4</sub> was dissolved in 15 mL of dry toluene. The solution was transferred into a storage tube equipped with a PTFE chemcap seal and hexabutylditin (3.19 g, 5 mmol) was added. The tube was sealed, removed from the glove box, and heated to at 120 °C for 48 h. The reaction mixture was allowed to cool to room temperature and diluted with hexane (15 mL) before saturated aqueous KF solution (15 mL) was added. The mixture was stirred for 30 min, filtered through celite, and the organic layer was separated. The solvent was removed to give the crude product as a yellow oil. The crude product was purified by column chromatography ( $R_f$  = 0.4, hexane/dichloromethane 95/5, basic alumina) to give 0.68 g (22.6 %) of (4,5-dimethoxy-2-(2-phthalimido)phenyl)tributyltin. <sup>1</sup>H NMR (C<sub>6</sub>D<sub>6</sub>, 400 MHz, 25 °C): δ 7.41 (m, 2 H, phthalimide), 7.10 (s, 1 H, H3), 7.01 (s, 1 H, H6), 6.84 (m, 2 H, phthalimide), 3.93 (t, J = 8.14 Hz, 2 H, CH<sub>2</sub>), 3.56 (s, 3 H, OMe), 3.43 (s, 3 H, OMe), 3.12 (t, J = 8.14 Hz, 2 H, CH<sub>2</sub>), 1.73 (m, 6 H, βCH<sub>2</sub>), 1.44 (m, 6 H, γCH<sub>2</sub>), 1.35 (m, 6 H, αCH<sub>2</sub>), 0.960 (t, J = 7 Hz, 9 H, CH<sub>3</sub>), (coupling to <sup>117</sup>Sn and <sup>119</sup>Sn observed, J ranged from 8.14 – 50.48 Hz); <sup>13</sup>C NMR (C<sub>6</sub>D<sub>6</sub>, 100 MHz, 25 °C) δ 167.64 (CO), 150.70 (C4), 147.40 (C2), 137.95 (C5), 133.21 (C3'/C6'), 132.39 (C1'/C2'), 132.00 (C1), 122.73 (C4'/C5'), 120.50 (C6), 55.64 (OMe), 55.05 (OMe), 39.90 (CH<sub>2</sub>), 37.71 (CH<sub>2</sub>), 29.54 (γC), 27.66 (βC), 13.76 (δC),

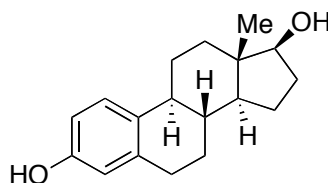
10.66 ( $\alpha$ C), (coupling to  $^{117}\text{Sn}$  and  $^{119}\text{Sn}$  observed, J ranged from 1.0 – 322.00 Hz); HRMS (HRCI): calcd. for  $\text{C}_{30}\text{H}_{43}\text{O}_4\text{NSn}$   $[\text{M} + \text{H}]^+$  602.2292, found 602.2281.



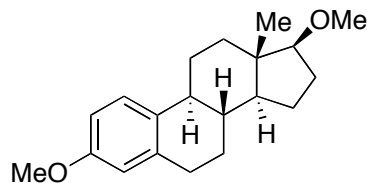
**(4,5-Dimethoxy-2-(2-phthalimidoethyl)phenyl)(4'-methoxyphenyl)-iodonium**

**hexafluorophosphate:** In a nitrogen atmosphere glove box, 1-(diacetoxyiodo)-4-methoxybenzene (352 mg, 1 mmol) was dissolved in 1.5 mL of dry acetonitrile. A solution of *p*-toluenesulfonic acid monohydrate (190 mg, 1 mmol) in 1.5 mL of dry acetonitrile was added by syringe. Upon completion of the addition, (4,5-dimethoxy-2-(2-phthalimido)phenyl)tributyltin (601 mg, 1 mmol) was added and the mixture was allowed to stir at room temperature for 2 h outside the glove box. Water (10 mL) was added and the mixture was transferred to a separatory funnel and extracted ( $3 \times 5$  mL) with hexanes. The reserved aqueous layer was treated with 502 mg (3 mmol) of  $\text{NaPF}_6$ . The white precipitate was filtered, dried in vacuo, and recrystallized in a mixture of diethyl ether/dichloromethane to give 379 mg (4,5-dimethoxy-2-(2-phthalimidoethyl)phenyl)(4'-methoxyphenyl)-iodonium hexafluorophosphate (55 %).  $^1\text{H}$  NMR ( $\text{CD}_3\text{CN}$ , 400 MHz, 25  $^\circ\text{C}$ ):  $\delta$  8.00 (d,  $J = 9.15$  Hz, 2 H,  $\text{H}_{2''}/\text{H}_{6''}$ ), 7.81 (m, 4 H, phthalimide), 7.61 (s, 1 H,  $\text{H}_6$ ), 7.37 (s, 1 H,  $\text{H}_3$ ), 7.00 (d,  $J = 9.15$  Hz, 2 H,  $\text{H}_{3''}/\text{H}_{5''}$ ), 3.87 (t,  $J = 7.52$  Hz,  $\text{CH}_2$ ), 3.85 (s, 3 H, OMe), 3.81 (s, 3 H, OMe), 3.78 (s, 3 H, OMe), 3.20 (t,  $J = 7.52$  Hz,  $\text{CH}_2$ );  $^{13}\text{C}$

NMR (CD<sub>3</sub>CN, 100 MHz, 25 °C)  $\delta$  168.21 (CO), 163.08 (C4''), 153.25 (C4), 149.95 (C5), 136.80 (C2''/C6''), 135.06 (C2), 134.41 (C3'/C6'), 132.01 (C1'/C2'), 123.06 (C4'/C5'), 119.54 (C3), 118.06 (C3''/C5''), 113.73 (C6), 106.01 (C1), 101.80 (C1''), 56.22 (OMe), 55.85 (OMe), 55.69 (OMe), 38.04 (CH<sub>2</sub>), 36.67 (CH<sub>2</sub>); <sup>19</sup>F NMR (CD<sub>3</sub>CN, 376 MHz, 25 °C)  $\delta$  -72.785 (d, <sup>1</sup>J<sub>P-F</sub> = 706.59 Hz, PF<sub>6</sub><sup>-</sup>); HRMS (HRFAB): calcd. for C<sub>25</sub>H<sub>23</sub>O<sub>5</sub>NPF<sub>6</sub>I [M – PF<sub>6</sub>]<sup>+</sup> 544.0621, found 544.0615.

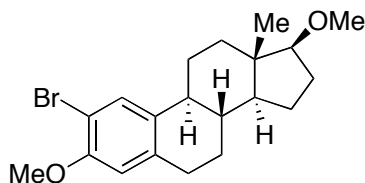


**$\beta$ -Estradiol:**<sup>153</sup> A solution of estrone (2.60 g, 9.62 mmol) in 130 mL of methanol was treated with concentrated aqueous NaOH (1.14 g, 28.5 mmol) and added to a stirred solution of NaBH<sub>4</sub> (0.97 g, 25.53 mmol) in 130 mL of methanol. H<sub>2</sub> evolution ceased after about 45 min, and the mixture was poured into 200 mL of water and neutralized with 3 M HCl. The precipitate was filtered, washed with water and recrystallized from hot aqueous methanol to give  $\beta$ -estradiol 2.54 g (97 %). <sup>1</sup>H NMR (DMSO-d<sub>6</sub>, 400 MHz, 25 °C):  $\delta$  8.983 (s, 1 H), 7.044 (d, J = 8.4 Hz, 1 H), 6.500 (d, J = 8.4 Hz, 1 H), 6.428 (s, 1 H), 4.496 (d, J = 4.8 Hz, 1 H), 3.52 (m, 1 H), 2.697 (m, 2 H), 2.229 (m, 1 H), 2.065 (m, 1 H), 1.94-1.73 (m, 3 H), 1.582 (m, 1 H), 1.43-1.05 (m, 7 H), 0.665 (s, 3 H); <sup>13</sup>C NMR (DMSO-d<sub>6</sub>, 100 MHz, 25 °C):  $\delta$  154.89, 137.14, 130.42, 126.05, 114.91, 112.71, 80.06, 49.52, 43.54, 42.82, 38.70, 36.60, 29.90, 29.17, 26.96, 26.09, 22.79, 11.28; HRMS (ESI) calcd. for C<sub>18</sub>H<sub>24</sub>O<sub>2</sub>Na [M + Na]<sup>+</sup> 295.1674 found 295.1668.



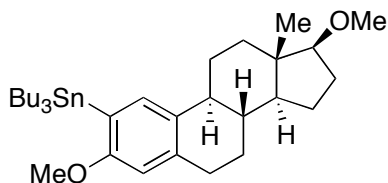
**3,17-Dimethoxy- $\beta$ -estra-1,3,5(10)-triene:**<sup>154</sup> A previously reported procedure was improved upon slightly.  $\beta$ -Estradiol (2.54 g, 9.32 mmol) was dissolved in 125 mL of dry THF under  $N_2$  and cooled to 0 °C. Sodium hydride (1.07 g, 44.58 mmol) was added, and the reaction mixture was stirred for 15 min.  $CH_3I$  (5.40 mL, 86.48 mmol) was added by syringe, and the turbid reaction mixture was stirred overnight and allowed to warm slowly to room temperature. The reaction mixture was poured carefully into ice-water. After the effervescence ceased, the organic product was extracted into ethyl acetate (3 x 125 mL), washed with aqueous  $NaHCO_3$  (125 mL), and dried over anhydrous  $MgSO_4$ . The solvent was removed *in vacuo* to afford 3,17-dimethoxy- $\beta$ -estra-1,3,5(10)-triene 2.33 g (83 %) as an off-white solid.  $^1H$  NMR ( $CDCl_3$ , 400 MHz, 25 °C):  $\delta$  7.218 (d,  $J$  = 8.6 Hz, 1 H), 6.722 (dd,  $J_1$  = 8.6 Hz,  $J_2$  = 2.6 Hz, 1 H), 6.640 (d,  $J$  = 2.6 Hz, 1 H), 3.787 (s, 3 H), 3.391 (s, 3 H), 3.327 (t,  $J$  = 8.3 Hz, 1 H), 2.861 (m, 2 H), 2.297 (m, 1 H), 2.20 (m, 1 H), 2.15-2.00 (m, 2 H), 1.94-1.84 (m, 1 H), 1.76-1.64 (m, 1 H), 1.58-1.15 (m, 7 H), 0.80 (s, 3 H);  $^{13}C$  NMR ( $CDCl_3$ , 100 MHz, 25 °C):  $\delta$  157.61, 138.19, 132.89, 126.55, 113.97, 111.66, 91.01, 58.13, 55.41, 50.49, 44.13, 43.43, 38.81, 38.27, 30.04, 27.98, 27.44, 26.67, 23.26, 11.76; HRMS (ESI) calcd. for  $C_{20}H_{28}O_2Na$   $[M + Na]^+$  323.1987 found 323.1994. Lit.<sup>155</sup>:  $^1H$  NMR ( $CDCl_3$ ):  $\delta$  7.18 (d,  $J$  = 8.63 Hz, 1 H), 6.68 (d,  $J$  = 8.54 Hz, 1 H), 6.60 (s, 1 H), 3.75 (s, 3 H), 3.36 (s, 3 H), 3.29 (t,  $J$  = 16.62 Hz, 1 H), 2.84 (m, 2 H), 2.25 (m, 1 H),

2.15 (t,  $J = 21.87$  Hz, 1 H), 2.02 (m, 2 H), 1.84 (m, 1 H), 1.66 (m, 1 H), 1.52-1.17 (m, 7 H), 0.77 (s, 3 H); LRMS (CI):  $m/z$  (rel intensity) 301 ( $MH^+$ , 100).)



**2-Bromo-3,17-dimethoxy- $\beta$ -estra-1,3,5(10)-triene:**<sup>156</sup> A solution of N-bromosuccinimide (1.51 g, 8.5 mmol) in  $CH_3CN$  (30 mL) was added to a  $CCl_4$  solution (70 mL) of dimethoxy- $\beta$ -estra-1,3,5(10)-triene (2.32 g, 7.72 mmol), and the resulting mixture was stirred at room temperature protected from light for 2.5 h. The solvent was removed *in vacuo* to obtain a residual mixture of a yellow oil and a white solid.  $CCl_4$  was added and the solution was filtered and evaporated to give a yellow oil. The oil was triturated in warm methanol to yield a crude solid, which was determined by  $^1H$ -NMR to be an 80:20 mixture of the 2-bromo and the 4-bromo estradiol dimethyl ethers (2.30 g, 78.5 %). Recrystallization of the crude product mixture from hot methanol (1<sup>st</sup> crop) gave 2-Bromo-3,17-dimethoxy- $\beta$ -estra-1,3,5(10)-triene 1.40g (48 %) as a white solid in 95 % purity, with the 4-bromo isomer as a trace impurity. The solid was carried forward to the next step without further purification.  $^1H$  NMR ( $CDCl_3$ , 400 MHz, 25 °C):  $\delta$  7.434 (s, 1 H), 6.615 (s, 1 H), 3.860 (s, 3 H), 3.385 (s, 3 H), 3.319 (t,  $J = 8.4$  Hz, 1 H), 2.820 (m, 2 H), 2.29-2.01 (m, 4 H), 1.93-1.85 (m, 1 H), 1.75-1.64 (m, 1 H), 1.58-1.15 (m, 7 H), 0.796 (s, 3 H);  $^{13}C$  NMR ( $CDCl_3$ , 100 MHz, 25 °C):  $\delta$  153.70, 137.40, 134.47, 130.44, 112.50, 108.74, 90.89, 58.13, 56.40, 50.38, 43.90, 43.39, 38.53, 38.10, 29.82, 27.96, 27.26, 26.63,

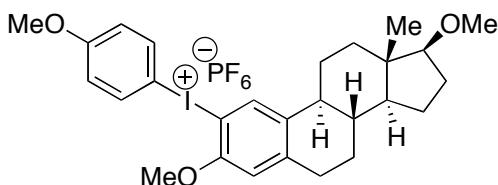
23.23, 11.34; HRMS (FAB) calcd. for  $C_{20}H_{27}O_2Br$   $[M]^+$  378.1194, 380.1174 found 378.1149, 380.1174.



**2-Tributylstannyl-3,17-dimethoxy- $\beta$ -estra-1,3,5(10)-triene:**<sup>157</sup> A THF solution of 2-Bromo-3,17-dimethoxy- $\beta$ -estra-1,3,5(10)-triene (0.7 g, 1.84 mmol in 20 mL) was cooled to  $-78^\circ\text{C}$  under  $N_2$ .  $n\text{-BuLi}$  (2.47 M in hexanes, 0.78 mL, 1.93 mmol) was added dropwise with stirring, and the resulting solution was stirred at  $-78^\circ\text{C}$  for 30 min.  $\text{Bu}_3\text{SnCl}$  (0.52 mL, 1.93 mmol) was then added dropwise at  $-78^\circ\text{C}$ , and the resultant mixture allowed to room temperature over 12 h. Diethyl ether (50 mL) was added to the reaction mixture and the organic solvents were washed with water (3 x 50 mL). The organic layer was mixed with KF (0.1 g in 1 mL EtOH) and stirred for a few minutes to remove any residual  $\text{Bu}_3\text{SnCl}$ . The mixture was washed with water, and the organic layer was dried over anhydrous  $\text{MgSO}_4$ . The solvent was removed *in vacuo* to obtain 2-tributylstannyl-3,17-dimethoxy- $\beta$ -estra-1,3,5(10)-triene as a colorless, viscous oil 0.87 g (80 %).  $^1\text{H}$  NMR ( $\text{CD}_2\text{Cl}_2$ , 400 MHz,  $25^\circ\text{C}$ ):  $\delta$  7.229 (s,  $^3J_{\text{Sn-H}} = 46.4$  Hz, 1 H), 6.521 (s,  $^4J_{\text{Sn-H}} = 17.4$  Hz, 1 H), 3.705 (s, 3 H), 3.330 (s, 3 H), 3.292 (t,  $J = 8.3$  Hz, 1 H), 2.92-2.74 (m, 2 H), 2.306 (m, 1 H), 2.188 (m, 1 H), 2.10-1.96 (m, 2 H), 1.93-1.82 (m, 1 H), 1.72-1.16 (m, 8 H,  $H_{\text{alicyclic}}$  on steroid overlapping with m centered  $\sim \delta$  1.52, 6 H,  $\beta\text{CH}_2$  and m centered  $\sim \delta$  1.32, 6 H,  $\gamma\text{CH}_2$ ), 1.001 (m, 6 H,  $\alpha\text{CH}_2$ ), 0.878 (t,  $J = 7.3$  Hz, 9 H,  $\text{CH}_3$ ), 0.763 (s, 3 H);  $^{13}\text{C}$  NMR ( $\text{CD}_2\text{Cl}_2$ , 100 MHz,  $25^\circ\text{C}$ ):  $\delta$  162.48, 138.91, 134.41, 133.16,



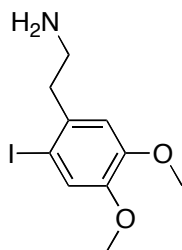
127.03, 109.82, 91.27, 58.07, 55.56, 50.79, 44.69, 43.79, 39.42, 38.68, 30.68, 29.76, 28.25, 27.95, 27.86, 27.14, 23.58, 14.06, 11.95, 10.26; HRMS (FAB) calcd. for  $C_{32}H_{54}O_2Sn [M]^+$  590.3146 found 590.3130.



**(3,17-Dimethoxy-β-estra-1,3,5(10)-trien-2-yl)(4'-methoxyphenyl)-iodonium**

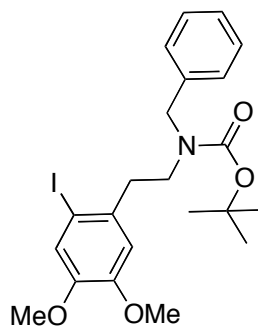
**hexafluorophosphate:** In a nitrogen atmosphere glove box,  $CH_3CN$  solutions of 1-(diacetoxyiodo)-4-methoxybenzene (65 mg, 0.19 mmol in 1 mL) and tosylic acid monohydrate (35 mg, 0.19 mmol in 1 mL) were mixed together to generate a Koser's type reagent. The yellow reagent mixture was added to a THF solution of 2-tributylstannyl-3,17-dimethoxy-β-estra-1,3,5(10)-triene (112 mg, 0.19 mmol in 1 mL), and the resultant pale yellow reaction mixture was stirred overnight protected from light. The reaction mixture was brought out of the box, and the solvent was removed *in vacuo* to obtain a white solid residue, which was first washed with hexanes, and then dissolved in  $CH_3CN$  and extracted with hexanes to remove the alkyltin byproducts. Solvent was removed from the  $CH_3CN$  layer to obtain a colorless oil. The oil was dissolved in about 5 mL of  $CH_3CN$  and water (25 mL) and  $NaPF_6$  (96 mg, 0.57 mmol) were added; the solution turned into a milky suspension. The mixture was extracted with  $CH_2Cl_2$  and the organic solvents were removed *in vacuo* to obtain a colorless oil. The oil was triturated twice with hexanes to afford a pale brown solid. The solid was separated and dissolved in  $CH_3CN$  and filtered. The solvent was removed *in vacuo* and the sticky solid was

trituated again with hexane to give (3,17-dimethoxy- $\beta$ -estra-1,3,5(10)-trien-2-yl)(4'-methoxyphenyl)-iodonium hexafluorophosphate (84 mg, 65 %) as a pale brown solid.  $^1\text{H}$  NMR ( $\text{CD}_3\text{CN}$ , 400 MHz, 25  $^\circ\text{C}$ ):  $\delta$  7.953 (d,  $J$  = 8.8 Hz, 2 H), 7.826 (s, 1 H), 7.018 (d,  $J$  = 8.8 Hz, 2 H), 6.933 (s, 1 H), 3.895 (s, 3 H), 3.828 (s, 3 H), 3.36-3.23 (s overlapping with t, 4 H), 2.918 (m, 2 H), 2.28-2.12 (m, 2 H), 2.12-1.81 (m overlapping with solvent, 3 H), 1.672 (m, 1 H), 1.52-1.14 (m, 7 H), 0.743 (s, 3 H);  $^{13}\text{C}$  NMR ( $\text{CD}_3\text{CN}$ , 100 MHz, 25  $^\circ\text{C}$ ):  $\delta$  164.52, 155.71, 147.38, 139.13, 138.45, 134.81, 119.23, 114.65, 101.98, 101.67, 91.59, 58.27, 58.23, 57.03, 51.15, 44.94, 44.29, 39.15, 38.81, 30.92, 28.69, 27.60, 27.44, 24.01, 12.35;  $^{19}\text{F}$  NMR ( $\text{CD}_3\text{CN}$ , 376 MHz, 25  $^\circ\text{C}$ ):  $\delta$  -72.876 (d,  $^1J_{\text{P-F}}$  = 706.9 Hz,  $\text{PF}_6^-$ );  $^{31}\text{P}$  NMR ( $\text{CD}_3\text{CN}$ , 162 MHz, 25  $^\circ\text{C}$ ):  $\delta$  -144.525 (septet,  $^1J_{\text{P-F}}$  = 706.9 Hz,  $\text{PF}_6^-$ ); HRMS (FAB) calcd. for  $\text{C}_{27}\text{H}_{34}\text{IO}_3$   $[\text{M} - \text{PF}_6]^+$  533.1553 found 533.1561.



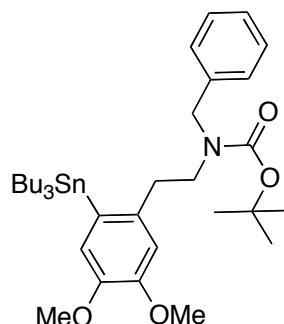
**2-(2-Iodo-4,5-dimethoxyphenyl)ethanamine:** To a solution of N-iodosuccinimide (NIS) (4.95 g, 22 mmol) in dry acetonitrile (50 mL) was added 2-(3,4-dimethoxyphenyl)ethanamine (3.32 mL, 20 mmol) and trifluoroacetic acid (3.85 mL, 50 mmol) with stirring. The mixture was stirred at room temperature in dark for another two hours. The acetonitrile was removed and the remaining solid was taken up in water. The water solution was treated with saturated sodium bisulfite aqueous solution until the purple color disappeared and the PH was adjusted to 11. The neutralized aqueous solution

was extracted with dichloromethane (50 mL, 3 times). The organic layers were combined and dried over sodium sulfate. The solvent was evaporated to yield 4.3 g (70 %) 2-(2-iodo-4,5-dimethoxyphenyl)ethananamine. The crude product was dried under dynamic vacuum overnight and used without further purification.  $^1\text{H}$  NMR ( $\text{CD}_2\text{Cl}_2$ , 400 MHz, 25  $^\circ\text{C}$ ):  $\delta$  7.21 (s, H6, 1 H), 6.77 (s, H3, 1 H), 3.79 (s, OMe, 3 H), 3.77 (s, OMe, 3 H), 3.08 (broad s,  $\text{NH}_2$ , 2 H), 2.89 (t,  $J = 6.7$  Hz,  $\text{CH}_2$ , 2 H), 2.81 (t,  $J = 6.7$  Hz,  $\text{CH}_2$ , 2 H);  $^{13}\text{C}$  NMR ( $\text{CD}_2\text{Cl}_2$ , 100 MHz, 25  $^\circ\text{C}$ ):  $\delta$  150.0 (C4), 148.8 (C5), 135.2 (C2), 122.4 (C6), 113.5 (C3), 88.5 (C1), 56.6 (5-OMe), 56.3 (4-OMe), 43.9 ( $\text{CH}_2$ ), 42.7 ( $\text{CH}_2$ ); HRMS (HRFAB): calcd. for  $\text{C}_{10}\text{H}_{15}\text{O}_2\text{NI}^+$   $[\text{M} + \text{H}]^+$  308.0147, 309.0181 found 308.0152, 309.0195. (lit<sup>158</sup>: MS (CI):  $m/z$  ( %) 308 (M+1, 100), 278 (13), 180 (67), 164 (53), 152 (45);  $^1\text{H}$  NMR:  $\delta = 7.22$  and  $6.75$  (2s, 2 arom H), 3.86 and 3.85 (2s, 2OCH<sub>3</sub>), 2.93 and 2.82 (2t, each  $J = 7.0$  Hz, benzyl-CH and N-CH), 1.40 (br s, NH) ppm.)



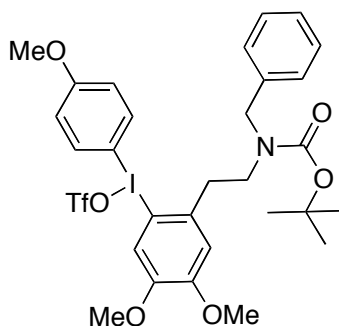
***tert*-Butyl-benzyl-(2-iodo-4,5-dimethoxyphenethyl)carbamate:** To a solution of 2-(2-iodo-4,5-dimethoxyphenyl)ethananamine (4g, 13.1 mmol) in 60 mL of dry benzene were added benzaldehyde (1.73 mL, 17 mmol) and sodium sulfate (10 g) with stirring. The reaction was kept at room temperature with stirring for 2 hour and the sodium sulfate was filtered off. Benzene was removed and 20 mL of ethanol was added to the remaining

solid. Sodium hydroborate (1.23 g, 32 mmol) was added slowly in portions to the ethanol solution with stirring. The reaction mixture was stirred for 2 hours before quenched with 1 N HCl. The PH was adjusted to 8 and ethanol was removed. Dichloromethane was added and the insoluble solid was filtered off and washed by more dichloromethane. The organic wash was combined and dried over sodium sulfate. The solvent was evaporated and the white crystalline solid was dissolved in 20 mL of dry ethanol. Sodium perborate (1.23 g, 32 mmol) and triethylamine (7.3 mL, 52 mmol) was added to the solution followed by di-*tert*-butyl dicarbonate (4.36 g, 20 mmol). The reaction was stirred at room temperature and monitored by TLC. After one hour of stirring, 100 mL of water was added to the reaction mixture. The solution was extracted with dichloromethane (50 mL, 3 times). The organic layers were combined and dried with sodium sulfate. The solvent was evaporated to give an oily crude product, which was chromatographed (60Å silica, 30 % ether in hexanes,  $R_f = 0.3$ ) to yield 5 g (78 %) *tert*-Butyl-benzyl-(2-iodo-4,5-dimethoxyphenethyl)carbamate as a white solid.  $^1\text{H}$  NMR ( $\text{CD}_2\text{Cl}_2$ , 400 MHz, 25 °C):  $\delta$  7.36-7.20 (m, H6 and PhCH<sub>2</sub>, 6 H), 6.77-6.64 (two broad s, H3, 1 H), 4.40-4.34 (two broad s, PhCH<sub>2</sub>, 2 H), 3.80-3.78 (broad s, OMe, 6 H), 3.37-3.32 (m, -CH<sub>2</sub>, 2 H), 2.91-2.72 (m, -CH<sub>2</sub>, 2 H), 1.48-1.46 (two broad s, Boc, 9 H);  $^{13}\text{C}$  NMR ( $\text{CD}_2\text{Cl}_2$ , 100 MHz, 25 °C):  $\delta$  156.0 (C=O), 150.2 (C4), 149.3 (C5), 139.3 (C2), 135.1 (C1'), 128.9 (C2'/C6'), 127.6 (C3'/C5'), 127.3 (C4'), 122.3 (C6), 113.5 (C3), 88.2 (C1), 80.0 (Boc), 56.6 (5-OMe), 56.3 (4-OMe), 51.2 (CH<sub>2</sub>Ph), 47.5 (CH<sub>2</sub>), 39.3 (CH<sub>2</sub>), 28.7 (Boc); HRMS (HRFAB): calcd. for C<sub>22</sub>H<sub>28</sub>INO<sub>4</sub> [M + H]<sup>+</sup> 497.1063, 498.1141 found 497.1063, 498.1137.



***tert*-Butyl-benzyl-(2-(tributylstannyl)-4,5-dimethoxyphenethyl)carbamate:** In a nitrogen atmosphere glove box, Pd<sub>2</sub>DBA<sub>3</sub> (20 mg, 2.5 mol %), *tert*-butyl-benzyl-(2-iodo-4,5-dimethoxyphenethyl)carbamate (496 mg, 1 mmol), and tri(*tert*-butyl)phosphine (20 mg, 10 mol %) were dissolved in 10 mL of dry benzene, the solution was transferred into a storage tube equipped with Teflon stirrer and Teflon chemcap seal; hexabutylditin (1.2 g, 2 mmol) was added. The tube was sealed, taken out of the glove box, heated to, and kept at kept at 90°C for 72 h. The reaction mixture was allowed to cool to room temperature, diluted with 15 mL hexane. 15 mL of saturated aqueous KF solution was added and the mixture was stirred for 30 min followed by filtration through celite. The organic layer was separated; solvent was removed to give the crude product as a yellow oil. The crude was purified by column chromatography ( $R_f$  =, hexane/diethyl ether 7/3, 60 Å silica pretreated with triethylamine) to give 660 mg (50 %) *tert*-butyl-benzyl-(2-(tributylstannyl)-4,5-dimethoxyphenethyl)carbamate. <sup>1</sup>H NMR (CD<sub>3</sub>CN, 400 MHz, 25 °C): δ 7.33-7.21 (broad m, Ph, 5 H), 6.86 (s, H<sub>6</sub>, 1 H), 6.75 (broad s, H<sub>3</sub>, 1 H), 4.39 (s, PhCH<sub>2</sub>, 2 H), 3.76 (s, OMe, 6 H), 3.41 (t,  $J$  = 7.2 Hz, -CH<sub>2</sub>, 2 H), 2.73 (t,  $J$  = 7.2 Hz, -CH<sub>2</sub>, 2 H), 1.44 (s, Boc, 9 H), 1.54-0.83 (m, Bu, 27 H); <sup>13</sup>C NMR (CD<sub>3</sub>CN, 100 MHz, 25 °C): δ 156.4 (C=O), 150.6 (C<sub>5</sub>), 148.2 (C<sub>4</sub>), 140.2 (C<sub>1'</sub>), 139.8 (C<sub>2</sub>) 129.5 (C<sub>2'</sub>/C<sub>6'</sub>),

128.1 (C3'/C5'), 128.0 (C4'), 127.8 (C1), 120.5 (C6), 113.6 (C3), 80.2 (Boc), 61.9 (CH), 56.4 (5-OMe), 56.1 (4-OMe), 51.5 (CH<sub>2</sub>Ph), 50.2 (CH<sub>2</sub>), 38.4 (CH<sub>2</sub>), 30.0 ( $\beta$ -C on *n*-Bu), 28.7 (Boc), 28.1 ( $\gamma$ -C on *n*-Bu), 14.1 ( $\delta$ -C on *n*-Bu), 11.1 ( $\alpha$ -C on *n*-Bu); HRMS (HRFAB): calcd. for C<sub>34</sub>H<sub>56</sub>NO<sub>4</sub>Sn [M + H]<sup>+</sup> 662.3231 found 662.3233.

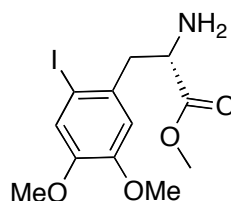


**(2-(2-(Benzyl-(*tert*-butoxycarbonyl)amino)ethyl-4,5-dimethoxy)phenyl)(4'-**

**methoxyphenyl)-iodonium triflate:** In a nitrogen atmosphere glove box, 1-(diacetoxyiodo)-4-methoxybenzene (93.5 mg, 0.27 mmol) was dissolved in 1.5mL of dry acetonitrile. *tert*-Butyl-benzyl-(2-(tributylstannyl)-4,5-dimethoxyphenethyl)carbamate (175 mg, 0.27 mmol) was added to the solution followed by trimethylsilyl triflate (59 mg, 0.27 mmol). The mixture was allowed to react at room temperature for 2 h. The solvent and trimethylsilyl acetate were removed by vacuum. The remaining solid was washed by hexanes (3  $\times$  5 mL) followed by recrystallization from dichloromethane/hexanes to give (2-(2-(benzyl-(*tert*-butoxycarbonyl)amino)ethyl-4,5-dimethoxy)phenyl)(4'-

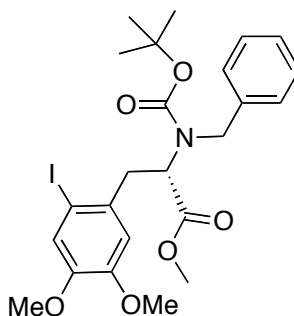
methoxyphenyl)-iodonium triflate (175 mg, 83 %) as a white solid. <sup>1</sup>H NMR (CD<sub>2</sub>Cl<sub>2</sub>, 400 MHz, 25 °C):  $\delta$  7.82-7.62 (m, H2'/H6', 2 H), 7.40 (s, H6, 1 H), 7.37-7.23 (m, Ph, 5 H), 6.97-6.90 (m, H3'/H5', 2 H), 6.80 (s, H3, 1 H), 4.40 (s, CH<sub>2</sub>Ph, 2 H), 3.84-3.81 (m, OMe, 9 H), 3.46-2.42 (m, -CH<sub>2</sub>, 2 H), 2.97 (broad s, -CH<sub>2</sub>, 2 H), 1.62-1.44 (two broad s,

Boc, 9 H);  $^{13}\text{C}$  NMR ( $\text{CD}_2\text{Cl}_2$ , 100 MHz, 25 °C):  $\delta$  163.6 (C4'), 156.4 (C=O), 150.5 (C5), 149.2 (C4), 138.8 (C2'/C6'), 137.3 (C2), 137.1 (C1''), 129.6 (C2''/C6''), 128.5 (C4''), 128.0 (C3''/C5''), 118.7 (C6), 118.5 (C3'/C5'), 114.2 (C3), 106.9 (C1), 102.2 (C1'), 81.0 (Boc), 57.1 (5-OMe), 56.7 (4-OMe), 56.4 (4'-OMe), 53.2 ( $\text{CH}_2\text{Ph}$ ), 48.2 ( $\text{CH}_2$ ), 37.8 ( $\text{CH}_2$ ), 28.6 (Boc); HRMS (HRFAB): calcd. for  $\text{C}_{29}\text{H}_{35}\text{INO}_5$  [ $\text{M} - \text{OTf}$ ] $^+$  604.1560 found 604.1556.



**(S)-3-(2-Iodo-4,5-dimethoxyphenyl)-1-methoxy-1-oxopropan-2-amine:** To a solution of N-iodosuccinimide (8.3 g, 37 mmol) in 80 mL of dry acetonitrile were added trifluoroacetic acid (2.7 mL, 37 mmol) and (S)-3-(3,4-dimethoxyphenyl)-1-methoxy-1-oxopropan-2-amine hydrochloride (4.63 g, 16.8 mmol) with stirring. The reaction mixture was stirred at room temperature in dark for 2 and half hours. The acetonitrile was removed and the remaining solid was taken up in water. The water solution was treated with saturated sodium bisulfite aqueous solution until the purple color disappeared and the PH was adjusted to 8. The neutralized aqueous solution was extracted with dichloromethane (50 mL, 3 times). The organic layers were combined and dried over sodium sulfate. The solvent was evaporated to yield 4.97 g (81 %) (S)-3-(2-iodo-4,5-dimethoxyphenyl)-1-methoxy-1-oxopropan-2-amine as a pale yellow oil, which was dried over dynamic vacuum overnight and used without further purification.  $^1\text{H}$  NMR ( $\text{C}_6\text{D}_6$ , 400 MHz, 25 °C):  $\delta$  7.12 (s, H6, 1 H), 6.75 (s, H3, 1 H), 3.90 (t, -CH, 1 H), 3.41 (s,

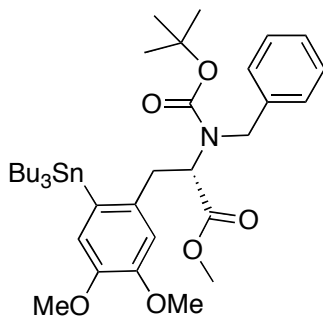
OMe, 3 H), 3.34 (s, COOMe, 3 H), 3.24 (dd, -CH<sub>2</sub>, 1 H), 3.16 (s, OMe, 3 H), 2.98 (dd, -CH<sub>2</sub>, 1 H), 2.69 (broad s, NH<sub>2</sub>, 2 H); <sup>13</sup>C NMR (C<sub>6</sub>D<sub>6</sub>, 100 MHz, 25 °C): δ 175.3 (C=O), 150.6 (C5), 149.8 (C4), 140.7 (C2), 122.8 (C6), 114.9 (C3), 89.5 (C1), 61.8 (C H), 55.9 (5-OMe), 55.8 (4-OMe), 51.6 (COOMe), 44.6 (CH<sub>2</sub>); HRMS (HRFAB): calcd. for C<sub>12</sub>H<sub>17</sub>INO<sub>4</sub> [M + H]<sup>+</sup> 366.0202, 367.0236 found 366.0221, 367.0248.



**Methyl (S)-2-(benzyl-(*tert*-butoxycarbonyl)amino)-3-(2-iodo-4,5-dimethoxyphenyl)propanoate:** To a solution of (S)-3-(2-iodo-4,5-dimethoxyphenyl)-1-methoxy-1-oxopropan-2-amine (4.97 g, 13.6 mmol) in 70 mL of dry benzene were added benzaldehyde (1.8 mL, 17.7 mmol) and sodium sulfate (10 g) with stirring. The reaction was kept at room temperature with stirring for 2 hour and the sodium sulfate was filtered off. Benzene was removed and 40 mL of methanol was added to the remaining solid. Sodium hydroborate (1.23 g, 34 mmol) was added slowly in portions to the methanol solution with stirring. The reaction mixture was stirred for 2 hours before quenched with 1 N HCl. The PH was adjusted to 8 and methanol was removed. Dichloromethane was added and the insoluble solid was filtered off and washed by more dichloromethane. The organic wash was combined and dried over sodium sulfate. The solvent was evaporated and the white crystalline solid was dissolved in 50 mL of dry acetonitrile. Sodium

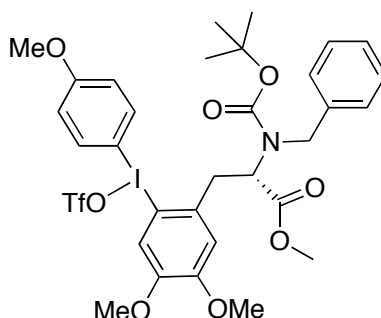


bicarbonate (1.7 g, 20 mmol) and dimethylaminopyridine (DMAP) (24 mg, 0.2 mmol) was added to the solution followed by di-*tert*-butyl dicarbonate (4.36 g, 20 mmol). The reaction was stirred at room temperature and monitored by TLC. After 2 and half hours of stirring, 100 mL of water was added to the reaction mixture. The solution was extracted with dichloromethane (50 mL, 3 times). The organic layers were combined and dried with sodium sulfate. The solvent was evaporated to give an oily crude product, which was chromatographed (60Å silica, 40 % ether in hexanes,  $R_f = 0.35$ ) to yield methyl (S)-2-(benzyl-(*tert*-butoxycarbonyl)amino)-3-(2-iodo-4,5-dimethoxyphenyl)-propanoate as a pale yellow viscous oil (3.15g, 41 %).  $^1\text{H}$  NMR ( $\text{CD}_2\text{Cl}_2$ , 400 MHz, 25 °C):  $\delta$  7.18-7.08 (m, H6 and  $\text{PhCH}_2$ , 6 H), 6.66-6.55 (two broad s, H3, 1 H), 4.43-4.25 (two broad d,  $\text{PhCH}_2$ , 1 H), 4.10-4.06 (broad m, -CH, 1 H), 3.86-3.55 (two broad d,  $\text{PhCH}_2$ , 1 H), 3.80 (s, OMe, 3 H), 3.76 (s, COOMe, 3 H), 3.63 (s, OMe, 3 H), 3.41-3.24 (m, -CH<sub>2</sub>, 2 H), 1.49-1.42 (two broad s, Boc, 9 H);  $^{13}\text{C}$  NMR ( $\text{CD}_2\text{Cl}_2$ , 100 MHz, 25 °C):  $\delta$  171.6 (C=O), 155.6 (C=O), 150.0 (C5), 149.1 (C4), 137.8 (C2), 133.3 (C1'), 129.1 (C2'/C6'), 128.5 (C3'/C5'), 127.5 (C4'), 122.2 (C6), 110.6 (C3), 88.6 (C1), 81.1 (Boc), 59.9 (CH), 56.5 (5-OMe), 56.2 (4-OMe), 54.5 ( $\text{CH}_2\text{Ph}$ ), 52.6 (COOMe), 40.1 ( $\text{CH}_2$ ), 28.7 (Boc); HRMS (HRFAB): calcd. for  $\text{C}_{24}\text{H}_{31}\text{INO}_6$   $[\text{M} + \text{H}]^+$  556.1196, 557.1230 found 556.1217, 557.1249.



**Methyl (S)-2-(benzyl-(*tert*-butoxycarbonyl)amino)-3-(2-(tributylstannyl)-4,5-dimethoxyphenyl)-propanoate:** In a nitrogen atmosphere glove box, methyl (S)-2-(benzyl-(*tert*-butoxycarbonyl)amino)-3-(2-iodo-4,5-dimethoxyphenyl)-propanoate (1.16 g, 2.1 mmol), Pd<sub>2</sub>DBA<sub>3</sub> (42 mg, 2.5 mol %) and tri(*tert*-butyl)phosphine (42 mg, 10 mol %) were dissolved in 15 mL of dry benzene, the solution was transferred into a storage tube equipped with Teflon stirrer and Teflon chemcap seal; hexabutylditin (5 g, 8.4 mmol) was added. The tube was sealed, taken out of the glove box, heated to, and kept at 80 °C for 72 h. The reaction mixture was allowed to cool to room temperature, diluted with 15 mL hexane. 15 mL of saturated aqueous KF solution was added and the mixture was stirred for 30 min followed by filtration through celite. The organic layer was separated; solvent was removed to give the crude product as a yellow oil. The crude was purified by column chromatography ( $R_f$  = 0.4, hexane/diethyl ether 7/3, 60 Å silica pretreated with triethylamine) to give 903 mg (60 %) methyl (S)-2-(benzyl-(*tert*-butoxycarbonyl)amino)-3-(2-(tributylstannyl)-4,5-dimethoxyphenyl)-propanoate as a colorless oil. <sup>1</sup>H NMR (CD<sub>2</sub>Cl<sub>2</sub>, 400 MHz, 25 °C): δ 7.19-7.06 (broad m, Ph, 5 H), 6.96-6.47 (m, H6 and H3, 2 H), 4.61-4.41 (broad m, PhCH<sub>2</sub>, 1 H), 4.16-3.81 (broad m, -CH, 1 H), 3.72-3.25 (broad m, PhCH<sub>2</sub>, 1 H), 3.83 (s, OMe, 3 H), 3.80 (s, COOMe, 3 H), 3.61 (s, OMe, 3 H), 3.28-3.03

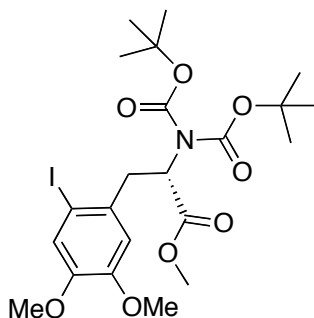
(m, -CH<sub>2</sub>, 2 H), 1.48-1.40 (two broad s, Boc, 9 H), 1.62-0.84 (m, Bu, 27 H); <sup>13</sup>C NMR (CD<sub>2</sub>Cl<sub>2</sub>, 100 MHz, 25 °C): δ 171.7 (C=O), 155.6 (C=O), 150.0 (C5), 147.9 (C4), 138.1 (C1'), 128.9 (C2'/C6'), 128.5 (C3'/C5'), 128.1 (C2), 127.6 (C4'), 127.4 (C1), 120.1 (C6), 113.8 (C3), 81.2 (Boc), 61.9 (CH), 56.3 (5-OMe), 56.0 (4-OMe), 52.5 (CH<sub>2</sub>Ph), 52.2 (COOMe), 38.9 (CH<sub>2</sub>), 29.6 (β-C on *n*-Bu), 28.7 (Boc), 27.9 (γ-C on *n*-Bu), 13.9 (δ -C on *n*-Bu), 10.8 (α-C on *n*-Bu); HRMS (HRFAB): calcd. for C<sub>36</sub>H<sub>58</sub>NO<sub>6</sub>Sn [M + H]<sup>+</sup> 720.3286, 718.3280, 719.3358 found 720.3273, 718.3242, 719.3293.



**(S)-2-(2-(Benzyl-(*tert*-butoxycarbonyl)amino)-3-methoxy-3-oxopropyl)-4,5-**

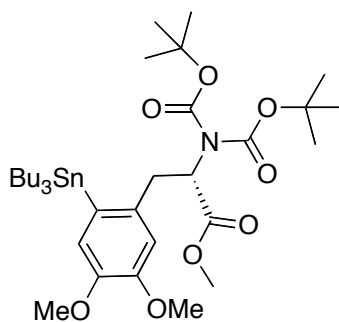
**dimethoxyphenyl)(4'-methoxyphenyl)-iodonium triflate:** In a nitrogen atmosphere glove box, 1-(diacetoxyiodo)-4-methoxybenzene (352 mg, 1 mmol) was dissolved in 1.5mL of dry acetonitrile. Methyl (S)-2-(benzyl-(*tert*-butoxycarbonyl)amino)-3-(2-(tributylstannyl)-4,5-dimethoxyphenyl)-propanoate (717 mg, 1 mmol) was added to the solution followed by trimethylsilyl triflate (195mg, 1 mmol). The mixture was allowed to react at room temperature for 2 h. The solvent and trimethylsilyl acetate were removed by vacuum. The remaining solid was washed by hexanes (3 × 5 mL) followed by recrystallization from dichloromethane/hexanes to give 774 mg (95.3 %) (S)-2-(2-(Benzyl-(*tert*-butoxycarbonyl)amino)-3-methoxy-3-oxopropyl)-4,5-

dimethoxyphenyl)(4'-methoxyphenyl)-iodonium triflate as a white solid.  $^1\text{H}$  NMR ( $\text{CD}_2\text{Cl}_2$ , 400 MHz, 25 °C):  $\delta$  7.85 (d,  $J$  = 8.8 Hz,  $\text{H}_2'/\text{H}_6'$ , 2 H), 7.35-7.14 (broad m, Ph, 5 H), 7.14-7.06 (two broad s,  $\text{H}_6$ , 1 H), 6.96 (d,  $J$  = 8.8 Hz,  $\text{H}_3'/\text{H}_5'$ , 2 H), 6.43-6.06 (2 broad s,  $\text{H}_3$ , 1 H) 4.97-4.67 (2 broad d,  $\text{CH}_2\text{Ph}$ , 1 H), 4.23-3.81 (2 broad d,  $\text{CH}_2\text{Ph}$ , 1 H), 4.19-4.11 (broad m,  $-\text{CH}$ , 1 H), 3.83 (s, 4'-OMe, 3 H), 3.75-3.72 (two s, 4-OMe, 3 H), 3.69 (s, 5-OMe, 3 H), 3.68-3.63 (two, s, COOMe, 3 H), 3.54-2.96 (m,  $-\text{CH}_2$ , 2 H), 1.53-1.49 (two broad s, Boc, 9 H);  $^{13}\text{C}$  NMR ( $\text{CD}_2\text{Cl}_2$ , 100 MHz, 25 °C):  $\delta$  172.9 (C=O), 163.6 ( $\text{C}_4'$ ), 155.8 (C=O), 153.4 ( $\text{C}_5$ ), 150.5 ( $\text{C}_4$ ), 137.5 ( $\text{C}_2'/\text{C}_6'$ ), 134.6 ( $\text{C}_2$ ), 129.5 ( $\text{C}_2''/\text{C}_6''$ ), 129.1 ( $\text{C}_3''/\text{C}_5''$ ), 128.5 ( $\text{C}_4''$ ), 118.5 ( $\text{C}_3'/\text{C}_5'$ ), 118.1 ( $\text{C}_6$ ), 113.6 ( $\text{C}_3$ ), 108.5 ( $\text{C}_1$ ), 108.0 ( $\text{C}_1'$ ), 82.3 (Boc), 61.5 (CH), 56.9 (5-OMe), 56.6 (4-OMe), 56.4 (4'-OMe), 54.7 ( $\text{CH}_2\text{Ph}$ ), 53.2 (COOMe), 40.8 ( $\text{CH}_2$ ), 28.7 (Boc); HRMS (HRFAB): calcd. for  $\text{C}_{31}\text{H}_{37}\text{INO}_7$   $[\text{M} - \text{OTf}]^+$  662.1615, 663.1648 found 662.1607, 663.1649.



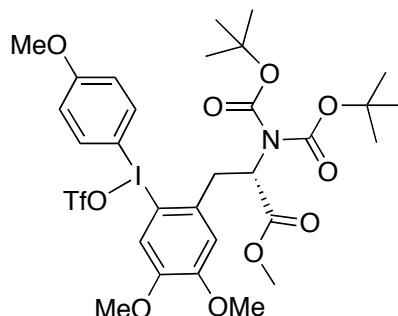
**Methyl (S)-2-(di-tert-butoxycarbonyl)amino-3-(2-iodo-4,5-dimethoxyphenyl)propanoate:** To a suspension of (S)-3-(2-iodo-4,5-dimethoxyphenyl)-1-methoxy-1-oxopropan-2-amine (2.84 g, 19.8 mmol) in THF: water (2 : 1, 45 mL), sodium carbonate (8.4 g, 79.2 mmol) was added portion wise. At 0 °C, di-tert-butyl dicarbonate (8.6 g, 39.6 mmol) was added and the reaction mixture was stirred at room temperature for 2 hours.

The organic layer was extracted with ethyl acetate, washed with saturated  $\text{NH}_4\text{Cl}$  solution, water and brine, dried, and concentrated. The concentrate was dissolved in acetonitrile and treated with DMAP (2.42 g, 19.8 mmol) and di-*tert*-butyl dicarbonate (13 g, 60 mmol). The mixture was stirred at room temperature for 12 hours followed by removal of the solvent. The crude was diluted with ethyl acetate and washed with saturated  $\text{NH}_4\text{Cl}$  solution, water and brine. The organic layer was dried and concentrated. Chromatographic purification afforded 9.3 g (82 %) methyl (*S*)-2-(di-*tert*-butoxycarbonyl)amino)-3-(2-iodo-4,5-dimethoxyphenyl)-propanoate.  $^1\text{H}$  NMR ( $\text{CD}_2\text{Cl}_2$ , 400 MHz, 25 °C):  $\delta$  7.19 (s, H6, 1 H), 6.62 (s, H3, 1 H), 5.13 (dd,  $J_1 = 11.2$  Hz,  $J_2 = 4.3$  Hz, CH, 1 H), 3.77 (s, 5- $\text{OCH}_3$ , 3 H), 3.76 (s, 4- $\text{OCH}_3$ , 3 H), 3.74 (s,  $-\text{COOCH}_3$ , 3 H), 3.44 (dd,  $J_1 = 14.1$  Hz,  $J_2 = 4.3$  Hz,  $-\text{CH}_2$ , 1 H), 3.30 (dd,  $J_1 = 14.1$  Hz,  $J_2 = 11.2$  Hz,  $-\text{CH}_2$ , 1 H), 1.36 (s, Boc, 18 H);  $^{13}\text{C}$  NMR ( $\text{CD}_2\text{Cl}_2$ , 100 MHz, 25 °C):  $\delta$  170.9 (C=O), 152.3 (C=O), 149.9 (C4), 149.1 (C5), 133.1 (C2), 122.3 (C6), 114.5 (C3), 89.2 (C1), 83.4 (C=O), 58.3 ( $\alpha$ -C), 56.6 (4- $\text{OCH}_3$ ), 56.2 (5- $\text{OCH}_3$ ), 52.7 ( $\text{COOCH}_3$ ), 40.6 ( $\beta$ -C), 28.1 (Boc); HRMS (HRFAB): calcd. for  $\text{C}_{22}\text{H}_{32}\text{INO}_8$   $\text{M}^+$  565.1173 found 565.1168, calcd. for  $\text{C}_{22}\text{H}_{33}\text{INO}_8$   $[\text{M} + \text{H}]^+$  566.1251 found 566.1230.



**Methyl (S)-2-(di-*tert*-butoxycarbonyl)amino)-3-(2-(tributylstannyl)-4,5-dimethoxyphenyl)-propanoate:** In a nitrogen atmosphere glove box, methyl (S)-2-(di-*tert*-butoxycarbonyl)amino)-3-(2-iodo-4,5-dimethoxyphenyl)-propanoate (1.5 g, 2.7 mmol), Pd<sub>2</sub>DBA<sub>3</sub> (54 mg, 2.5 mol %) and tri(*tert*-butyl)phosphine (54 mg, 10 mol %) were dissolved in 15 mL of dry benzene, the solution was transferred into a storage tube equipped with Teflon stirrer and Teflon chemcap seal; hexabutyliditin (4.2 g, 7 mmol) was added. The tube was sealed, taken out of the glove box, heated to, and kept at 80 °C for 72 h. The reaction mixture was allowed to cool to room temperature, diluted with 15 mL hexane. After filtration through a membrane filter, the solvent was removed to give the crude product as a yellow oil. The crude was purified by column chromatography (*R<sub>f</sub>* = 0.3, hexane/diethyl ether 3/1, 60 Å silica pretreated with triethylamine) to give methyl (S)-2-(di-*tert*-butoxycarbonyl)amino)-3-(2-(tributylstannyl)-4,5-dimethoxyphenyl)-propanoate (1.5 g, 78 %) as a pale yellow oil. <sup>1</sup>H NMR (CD<sub>2</sub>Cl<sub>2</sub>, 400 MHz, 25 °C): δ 6.86 (s, H<sub>6</sub>, 1 H), 6.60 (s, H<sub>3</sub>, 1 H), 4.89 (dd, *J*<sub>1</sub> = 11.2 Hz, *J*<sub>2</sub> = 4.3 Hz, CH, 1 H), 3.78 (s, -OCH<sub>3</sub>, 6 H), 3.74 (s, -COOCH<sub>3</sub>, 3 H), 3.27 (dd, *J*<sub>1</sub> = 14.3 Hz, *J*<sub>2</sub> = 11.2 Hz, -CH<sub>2</sub>, 1 H), 3.17 (dd, *J*<sub>1</sub> = 14.3 Hz, *J*<sub>2</sub> = 4.3 Hz, -CH<sub>2</sub>, 1 H), 1.53 (m, 1.36, β-CH<sub>2</sub>, 6 H), 1.36 (s, Boc, 18 H), 1.35 (m, γ-CH<sub>2</sub>, 6 H), 1.08 (m, α-CH<sub>2</sub>, 6 H), 0.89 (t, δ-CH<sub>3</sub>, 9 H), (coupling to <sup>117</sup>Sn and <sup>119</sup>Sn observed); <sup>13</sup>C NMR (CD<sub>2</sub>Cl<sub>2</sub>, 100 MHz, 25 °C): δ 171.2 (C=O), 152.5 (C=O), 149.6 (C<sub>4</sub>), 147.8 (C<sub>5</sub>), 137.9 (C<sub>2</sub>), 133.3 (C<sub>1</sub>), 120.2 (C<sub>6</sub>), 114.0 (C<sub>3</sub>), 83.3 (Boc), 60.6 (α-C), 56.4 (4-OCH<sub>3</sub>), 55.7 (5-OCH<sub>3</sub>), 52.7 (COOCH<sub>3</sub>), 38.6 (β-C), 29.7 (γ'-C), 28.1 (Boc), 28.0 (β'-C), 14.0 (δ'-C), 10.8 (α'-C), (coupling to <sup>117</sup>Sn and <sup>119</sup>Sn

observed); HRMS (HRFAB): calcd. for  $C_{34}H_{60}NO_8Sn$   $[M + Li]^+$  736.3423 found 736.3405.



**(S)-(2-(2-(di-*tert*-butoxycarbonyl)amino)-3-methoxy-3-oxopropyl)-4,5-**

**dimethoxyphenyl)(4'-methoxyphenyl)-iodonium triflate:** In a nitrogen atmosphere glove box, 1-(diacetoxyiodo)-4-methoxybenzene (145 mg, 0.2 mmol) was dissolved in 1.5mL of dry acetonitrile. Methyl (S)-(di-*tert*-butoxycarbonyl)amino)-3-(2-(tributylstannyl)-4,5-dimethoxyphenyl)-propanoate (70.4 mg, 0.2 mmol) was added to the solution followed by trimethylsilyl triflate (42.2 mg, 0.2 mmol). The mixture was allowed to react at room temperature for 30 min. The solvent and trimethylsilyl acetate were removed by vacuum. The remaining solid was washed by hexanes ( $3 \times 5$  mL) followed by recrystallization from dichloromethane/hexanes to give 130 mg (S)-(di-*tert*-butoxycarbonyl)amino)-3-methoxy-3-oxopropyl)-4,5-dimethoxyphenyl)-(4'-

methoxyphenyl)iodonium triflate as a white solid (80 %).  $^1H$  NMR ( $CD_2Cl_2$ , 400 MHz, 25 °C):  $\delta$  7.94 (d,  $J = 8.8$  Hz,  $H_{2'}/H_{6'}$ , 2 H), 7.30 (s,  $H_6$ , 1 H), 6.99 (d,  $J = 8.8$  Hz,  $H_{3'}/H_{5'}$ , 2 H), 6.93 (s,  $H_3$ , 1 H), 5.10 (dd,  $J_1 = 7.4$  Hz,  $J_2 = 7.3$  Hz, CH, 1 H), 3.85 (s, -OCH<sub>3</sub>, 3 H), 3.84 (s, -OCH<sub>3</sub>, 3 H), 3.76 (s, -OCH<sub>3</sub>, 3 H), 3.74 (s, -COOCH<sub>3</sub>, 3 H), 3.62 (dd,  $J_1 = 14.3$  Hz,  $J_2 = 7.3$  Hz, -CH<sub>2</sub>, 1 H), 3.39 (dd,  $J_1 = 14.3$  Hz,  $J_2 = 7.4$  Hz, -CH<sub>2</sub>, 1 H),

1.44 (s, Boc, 18 H);  $^{13}\text{C}$  NMR ( $\text{CD}_2\text{Cl}_2$ , 100 MHz, 25 °C):  $\delta$  171.0 (C=O), 163.7(C4'), 153.5 (C=O), 152.7 (C4), 150.8 (C5), 137.5 (C2'/C6'), 134.4 (C2), 118.8 (C6), 118.6 (C3'/C5'), 114.6 (C3), 107.6 (C1), 102.7 (C1'), 84.8 (Boc), 58.9 ( $\alpha$ -C), 57.1 (4-OCH<sub>3</sub>), 56.6 (5-OCH<sub>3</sub>), 56.4 (4'-OCH<sub>3</sub>), 53.4 (COOCH<sub>3</sub>), 39.9 ( $\beta$ -C), 28.2 (Boc); HRMS (HRFAB): calcd. for  $\text{C}_{29}\text{H}_{39}\text{INO}_9$   $[\text{M} - \text{OTf}]^+$  672.1670, 673.1703 found 672.1683, 673.1680.



## CHAPTER 4

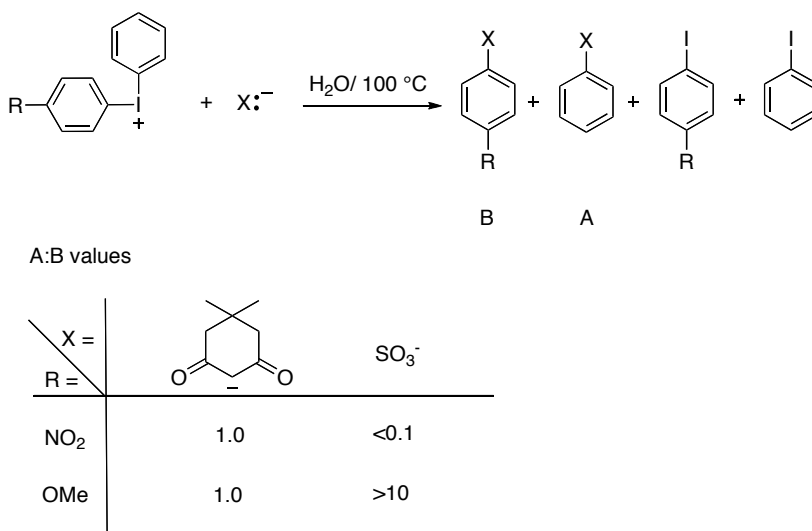
### METAL FREE ARYLATION OF HETEROATOM NUCLEOPHILES VIA DIARYLIODONIUM SALTS

#### 4.1 Background

Diaryl- $\lambda^3$ -iodanes or diaryliodonium salts are useful precursors to functionalize arenes, and their chemistry is the subject of several recent reviews.<sup>31, 159-166</sup> The reductive elimination of aryl iodides is the most important reaction mode of these compounds, which leads to their synthetic application as arylating reagents. A variety of carbon<sup>167-172</sup> and heteroatom nucleophiles<sup>75, 104, 173-178</sup> can be successfully arylated by treatment with symmetrical diaryliodonium salts. Symmetrical salts are used typically so that no regioselectivity issue needs to be addressed. Examples of such transformations, which date back to the 1930's are listed in Table 4-1. The work by Beringer's group in the 50's paved the way for future discoveries by showing a wide range of organic and inorganic nucleophiles including alkoxides, phenoxides, sulfites, sulfinates, and cyanides can be phenylated by diphenyliodonium salts in moderate to good yield.<sup>100, 105, 106, 179, 180</sup> The majority of the recent contributions to this field feature transition metal catalysts. In these metal-catalyzed cross-coupling reactions, the diaryliodonium species act only as the source of the aryl ligands; the actual reductive elimination process leading to product formation involves only the transition metal (Cu, Pd etc.) complexes. These reactions are beyond the scope of this discussion as they involve reductive elimination from an I(III)

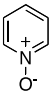
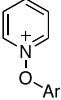
species. Thus we will only focus on metal-free cross-coupling reactions involving diaryliodonium salts. This type of transformation is far less common in the literature.

Most direct arylation reactions by reductive elimination of diaryliodanes are considered to proceed by one of two mechanisms.<sup>163</sup> For nucleophiles that are not easily oxidized (halides, azide etc.), a polar process resembling the classic  $S_NAr$  mechanism is indicated by experimental evidence. On the other hand, those nucleophiles having relatively low oxidation potentials appear to react by a mechanism involving intermediate diaryliodinanyl radicals,  $Ar_2I^\bullet$ . One way to differentiate the polar process from radical mediated process is to examine the regioselective nature of the cleavage process with unsymmetrical substrates. For reactions proceeding via a polar process, the products ratio depends on the electronic nature of the substituents. For radical mediated homolytic decompositions, a 1:1 ratio of products is to be expected regardless of the electronic nature of the substituent (Figure 4-1).



**Figure 4-1 Two different mechanisms of decomposition of diaryliodonium(III) by nucleophiles.**<sup>106</sup>

**Table 4-1 Arylations of nucleophilic species by diaryliodonium salts.**

Substrate(s)	Products	Yield (%)	Reference
NaNO <sub>2</sub>	ArNO <sub>2</sub>	37-88	105
NaN <sub>3</sub>	ArN <sub>3</sub>	95-98	75, 176
NaCN	ArCN	23-58	105, 176, 181
NaSCN	ArSCN (ArNCS)	17-98	75, 176, 182
NaF	ArF	38-96	74, 75
Na <sub>2</sub> SO <sub>3</sub>	ArSO <sub>3</sub> H	Up to 95	105, 106, 183
ROH, RONa	ArOR	20-70	106, 183 181 105, 181, 184
Ar'ONa	ArOAr'	20-90	182
PhCOONa	PhCOOAr	40	105, 180
PhCONHOH	PhCONHOAr	66	185
(RO) <sub>2</sub> P=O <sup>-</sup>	Ph(RO) <sub>2</sub> P=O	98	186
ArSe <sup>-</sup>	PhSeAr	58-75	187
RCOS <sup>-</sup>	PhSCOR	39-72	188-190
R <sub>2</sub> NCS <sub>2</sub> <sup>-</sup>	ArCS <sub>2</sub> NR <sub>2</sub>	50-85	191
Saccharin	N-Phenylsaccharin	75	105
Pyridine	N-Phenylpyridine	88	192
		90-99	193

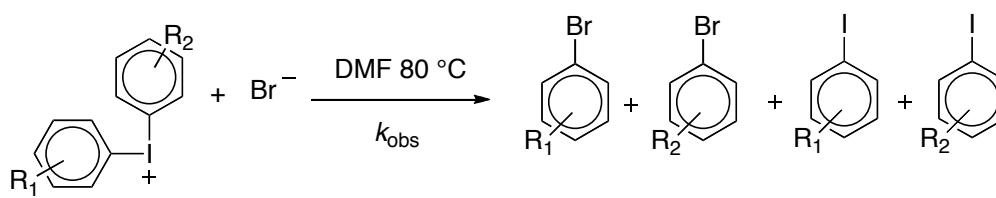
R	A' : B	
	Molten phase	DMF solution
<i>p</i> -MeO	4.24	2.69
H	0.62	0.37
<i>p</i> -Cl	0.67	0.45
<i>m</i> -Cl	0.53	0.24
<i>p</i> -COOH	0.15	0.08
<i>p</i> -NO <sub>2</sub>	0.04	-

**Figure 4-2 Decomposition of aryl(*p*-tolyl)-iodonium bromide at molten phase and in DMF solution.**

It is generally accepted that reactions that proceed to give synthetically useful arylated nucleophiles predominantly involve polar, 2-electron processes rather than radical, single electron processes.<sup>194</sup> Polar solvents such as water, the lower alcohols, acetonitrile, DMF, and DMSO are typically used in these reactions. Solid/molten state pyrolysis reaction of phenyl(*p*-tolyl)-iodonium salts have also been reported; these reactions appear to be less selective than solution phase reactions for nitrite, azide, thiocyanate, and cyanide.<sup>176</sup> Yamada and colleagues studied the cleavage ratios of a series of aryl(*p*-tolyl)-iodonium bromides both in the molten state (235 °C) and in DMF solution at 100 °C. The product ratios for these thermal decomposition reactions are summarized in Figure 4-2. When the competing aryl ligand is phenyl or *p*-anisole, the molten decomposition is more selective; however, for electron deficient aryl ligands, the

solution phase decomposition is more regioselective. The cause of this inconsistency in selectivity has not been explained satisfactorily.

Diaryliodonium salts are sometimes considered to be highly activated species of aryl halides in  $S_NAr$  reactions at the ipso positions. According to this point of view, the high reactivity is attributed to the excellent nucleofugality of the aryliodonio group, which shows a leaving group ability about  $10^6$  times greater than that of triflate.<sup>195</sup> As is expected for  $S_NAr$  reactions, diaryliodonium salts bearing electron-withdrawing groups decompose more rapidly than those with electron-donating groups. However, the  $\log k_{obs}$  values are not related in a linear way to the Hammett substituent constants (Figure 4-3).



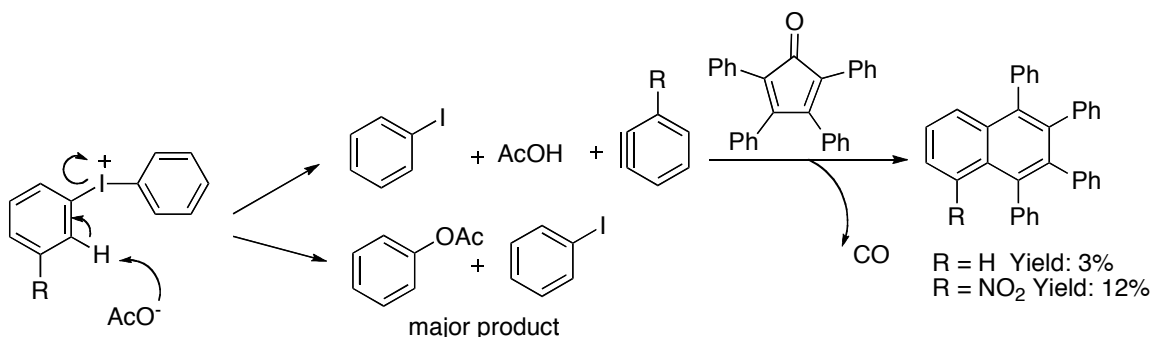
R <sub>1</sub>	$\sigma_x$	R <sub>2</sub>	$\sigma_x$	$k_{obs}, h^{-1}$
<i>m</i> -NO <sub>2</sub>	0.71	<i>m</i> -NO <sub>2</sub>	0.71	19.6
H	0	H	0	10.0
<i>p</i> -Cl	0.23	<i>p</i> -Cl	0.23	7.7
<i>p</i> -Me <sub>3</sub> C	-0.2	<i>p</i> -Me <sub>3</sub> C	-0.2	4.23
<i>p</i> -Me	-0.17	<i>p</i> -Me	-0.17	3.82
<i>p</i> -F	0.06	<i>p</i> -F	0.06	17.3
<i>p</i> -OMe	-0.27	<i>p</i> -OMe	-0.27	0.38
<i>m</i> -NO <sub>2</sub>	0.71	H	0	18.9
<i>p</i> -OMe	-0.27	H	0	5.1

**Figure 4-3** Observed rate constants for thermo decomposition of diaryliodonium bromide in DMF.<sup>196</sup>

The effects of solvent have also been investigated. The reaction of diphenyliodonium ion with phenoxide in 1:1 dioxane: water has been reported to exhibit second-order kinetics over temperature ranging from 45 to 70 °C.<sup>197</sup> In 5:1 dioxane:

water, the kinetic order for the same reaction is 1.5, a result that manifests the increasing importance of ion pair formation in solvents of lower polarity. It is reasonable to argue that the formation of an intermediate ‘molecular complex’ between the nucleophile and the iodonium ion is significant in low polarity media.

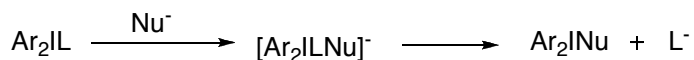
In the previous chapter, we showed that significant improvements in the yield of electron-rich aryl fluorides were achieved in reductive elimination reactions of diaryliodonium fluorides if the thermal decomposition reactions were carried out in nonpolar media. We reasoned that similar improvements could be made for arylating other nucleophile as well. Use of benzene as reaction solvent for decomposition of diaryliodonium salts remains uncommon. In one example, the formation of benzyne intermediate by the thermal decomposition of diaryliodonium acetate in hot benzene was reported.<sup>198</sup> The evidence for this is based on trapping experiments with tetraphenylcyclopentadienone and the isolation of tetraphenylnaphthalenes. It stands to reason that side reactions involving benzyne intermediates will be sensitive to ortho-proton acidity and nucleophile basicity.



**Scheme 4-1 Benzyne formation from diaryliodonium acetate as a competing side reaction for its thermal decomposition.**<sup>198</sup>

Heteroatom ligands on  $\lambda^3$ -iodanes are readily displaced with external nucleophiles. Although a detailed mechanism for ligand exchange on iodine(III) is not known, two mechanistic pathways, associative and dissociative, have been considered for the process (Figure 4-4).<sup>198</sup> There is much evidence supporting the associative mechanism, and little for the dissociative mechanism.<sup>165</sup> This is probably because the dicoordinated [8-I-2] iodonium ion involved in a dissociative passway is a highly energetic species. The ligand exchange process is believed to precede the actual decomposition process to form a tricoordinated I(III) intermediate complex, which is almost never isolated. It is favorable to choose non-coordinating ligands such as tetrafluoroborate, hexafluorophosphate, or triflate counterions for the starting salt to avoid competitive coordination and elimination.

associative pathway



dissociative pathway

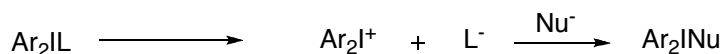
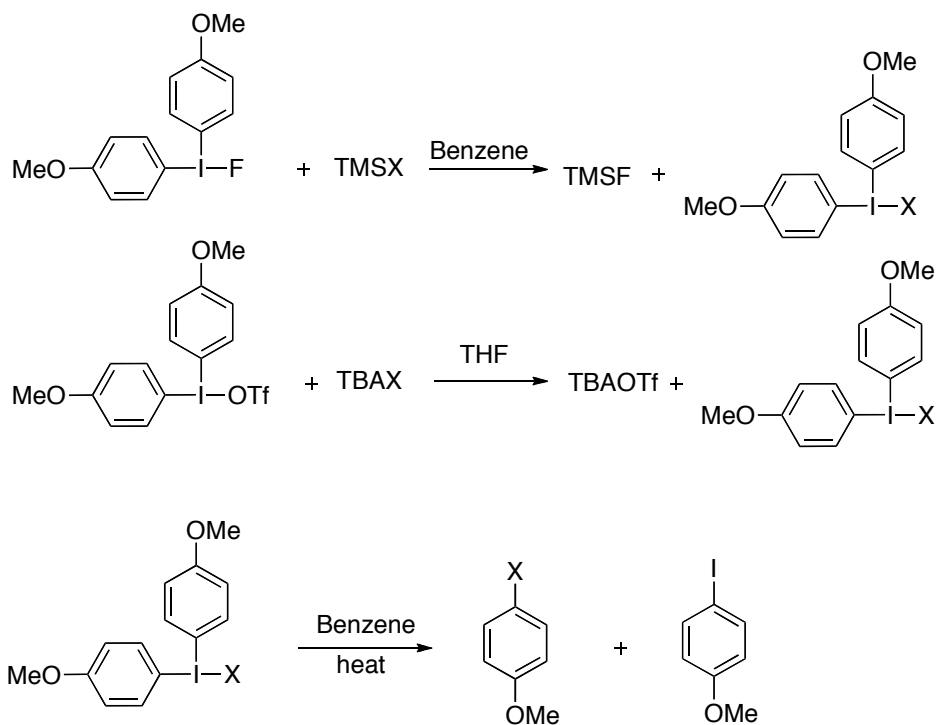


**Figure 4-4 Two possible mechanistic pathway for ligand exchange of diaryl- $\lambda^3$ -iodanes.**

We have learned from the fluorination reactions that having extra salt sometimes reduces the yields of aryl fluorides. Here we report that treatment of diarylfluoro- $\lambda^3$ -iodane with TMS derivatives of the nucleophiles offers a convenient salt-free method to achieve the ligand exchange process leading to diaryl- $\lambda^3$ -iodane featuring the desired nucleophile. We were able to study the reductive elimination of diaryl- $\lambda^3$ -iodanes featuring various heteroatom ligands in benzene under salt-free conditions. Reductive elimination of diarylazido- $\lambda^3$ -iodanes was studied in detail and compared to the

fluorination study. Decomposition by carbon nucleophiles has also been carried out by our group, but this will not be discussed here.

#### 4.2 Decomposition of bis(4-methoxyphenyl)iodonium salts in benzene: reactivity of various nucleophiles.

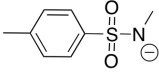
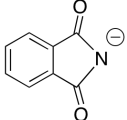
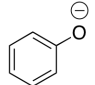
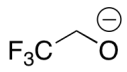
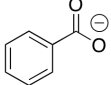
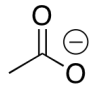
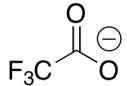
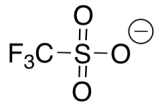
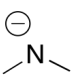
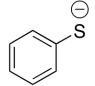
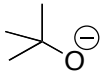


X = Cl, Br, I, OTf, OAc, CF<sub>3</sub>COO, OPh, CF<sub>3</sub>CH<sub>2</sub>O, *t*-BuO, phthalimidyl, CN, NCO, NCS, N<sub>3</sub>, SPh, NMe<sub>2</sub>

**Scheme 4-2** Preparation of bis(4-methoxyphenyl)-λ<sup>3</sup>-iodanes and their decomposition in benzene.



**Table 4-2 Decomposition of bis(4-methoxyphenyl)- $\lambda^3$ -iodanes in benzene.**

X =		X =	
$\text{F}^-$	86 %, (13 % isomer via benzyne pathway)		Multiple products
$\text{Cl}^-$	>99%		Multiple products
$\text{Br}^-$	>99%		>99%
$\text{I}^-$	>85 %		70 % (r.t. reaction)
$\text{N}_3^-$	>99%		>99%
$\text{C}\equiv\text{N}^-$	Multiple products		>99%
$\text{N}=\text{C}=\text{O}^-$	>99% C-N bond formation		>99%
$\text{N}=\text{C}=\text{S}^-$	C-S bond formation as major process (90 %)		>99%
	Multiple products		Quantitative
	Multiple products		

First we set out to investigate the reductive elimination of 4-iodoanisole from various bis(4-methoxyphenyl)- $\lambda^3$ -iodoanes featuring halides, oxygen, sulfur, and nitrogen ligands in benzene. As reported in CHAPTER 3, bis(4-methoxyphenyl)iodonium fluoride can be made conveniently by treating the corresponding trifluoroacetate or hexafluorophosphate with TBAF in THF. Similarly, bis(4-methoxyphenyl)iodonium

halides and pseudohalides can be prepared by the ion exchange of the TBA salts with iodonium triflate in THF. An alternative way to prepare diaryl- $\lambda^3$ -iodane featuring the desired nucleophiles involves treatment of the fluoride salt with TMS derivatives of nucleophiles in benzene. TMS fluoride is formed as by-product, which can be removed easily in vacuo. Sixteen bis(4-methoxyphenyl)- $\lambda^3$ -idoanes were prepared (Scheme 4-2) and subjected to reductive elimination in benzene. Products were analyzed by NMR spectroscopy and results are summarized in Table 4-2.

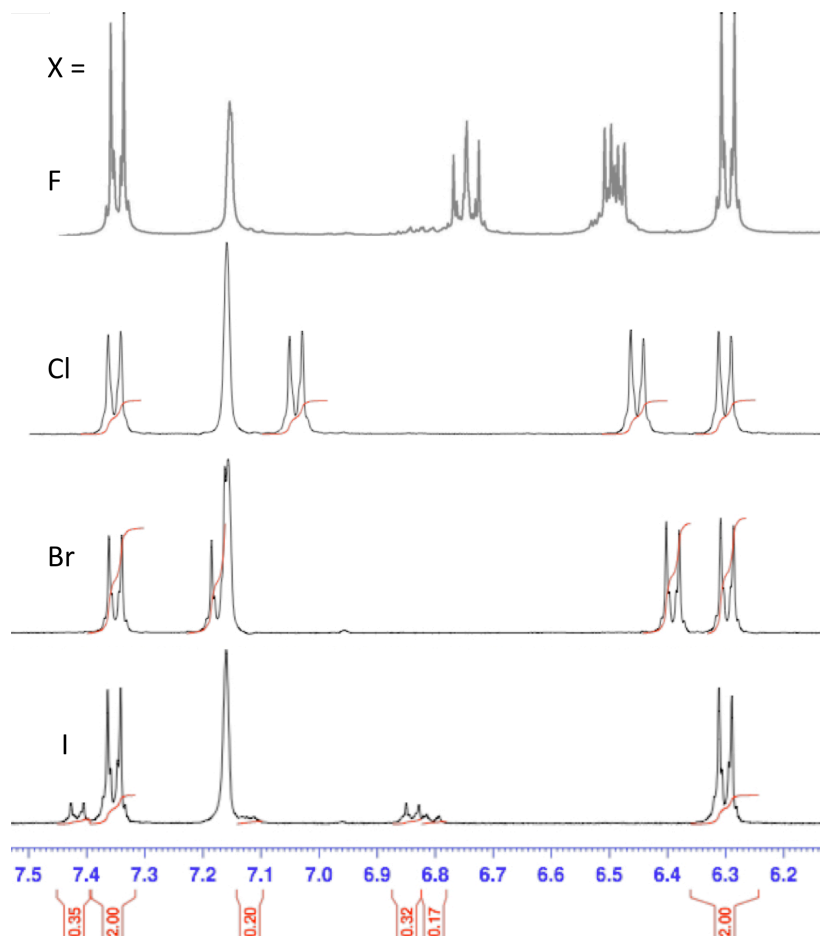


**Figure 4-5**  $^1\text{H}$  NMR spectra of bis(4-methoxyphenyl)-halo- $\lambda^3$ -iodane decomposition mixtures in  $\text{d}_6$ -benzene (only aromatic regions are displayed).

None of the bis(4-methoxyphenyl)-halo- $\lambda^3$ -iodanes have appreciable solubility in benzene; and the heterogeneous conditions make it difficult to compare the reaction rates directly. The observed rate is slowest for chloride, which took more than five days at 120 °C to complete. The iodide decomposes at a rate similar to that of the fluoride (2.5 hours), while the bromide decomposition takes slightly longer to finish (5 hours). The aromatic regions of  $^1\text{H}$  NMR spectra of the post-heat reaction mixtures for bis(4-methoxyphenyl)-halo- $\lambda^3$ -iodanes are shown in Figure 4-5. The fluoro-iodane gives 3-fluoroanisole in addition to the expected 4-fluoroanisole product due to a competing, benzyne-mediated process. Both chloride and bromide react to yield the corresponding 4-haloanisole quantitatively, without forming the 3-halo regioisomers. This can be explained easily; the basicity of chloride and bromide is not high enough to promote benzyne generation through proton abstraction. Unexpectedly, the iodo- $\lambda^3$ -iodane decomposes to yield 4,4'-dimethoxy-biphenyl,  $\text{I}_2$ , and an unidentified arene product in addition to the 4-iodoanisole. The biphenyl and  $\text{I}_2$  result from the C-C extrusion instead of C-I extrusion on the I(III) center.  $\text{I}_2$  is extruded because it is much more stable than the mixed halides.

When soluble diaryliodanes featuring various oxygen ligands were subjected to reductive elimination in benzene, it was found that the reaction rates strongly correlated with the basicity of the ligands. In the case of the weakest base, triflate, heating at 140 °C for 7 days was required to drive the reaction to go to completion; while the alkoxy- $\lambda^3$ -iodanes decompose rapidly (within minutes) at room temperature. It is reasonable to argue that more basic ligand lowers the activation barrier for reductive elimination by destabilizing the ground state of the iodane. This destabilization possibly also opens up

other reaction pathways for the iodane, therefore and the *t*-butoxide gave a mixture of many unidentified products. The cut-off pK<sub>a</sub> value for a clean reaction is in the range 10 – 12.5; phenoxide reacts to yield diarylether quantitatively, while trifluoromethyl aryl ethers were formed only in 70 % yield for the trifluoroethoxide decomposition.

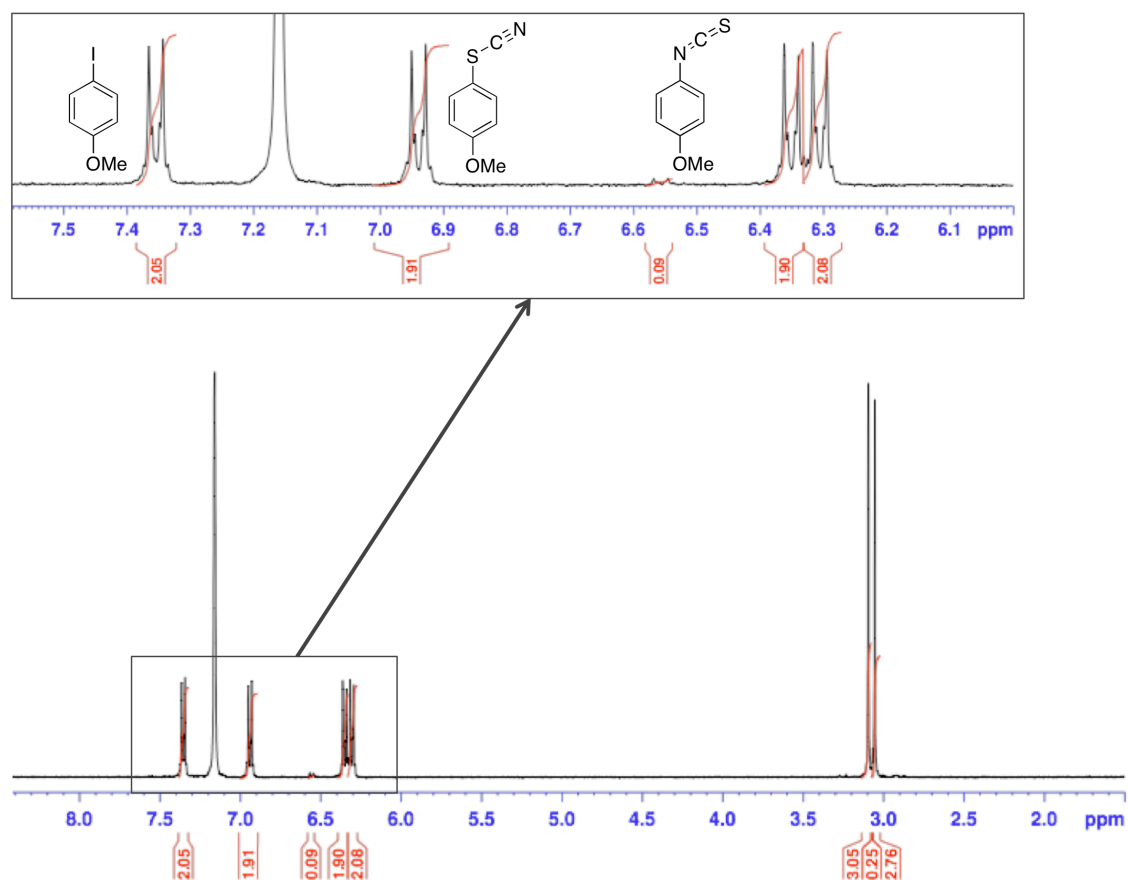


**Figure 4-6** <sup>1</sup>H NMR spectra of the reaction mixture of bis(4-methoxyphenyl)-thiocyanato- $\lambda^3$ -iodane decomposition in d<sub>6</sub>-benzene.

The synthetic value of iodonium decomposition by sulfur nucleophiles is well recognized in literature.<sup>112, 182, 188, 199-202</sup> We studied the decomposition of two bis(4-methoxyphenyl)- $\lambda^3$ -iodanes featuring sulfur ligands. The phenyl thioether was formed quantitatively upon heating of the corresponding iodane in benzene at 120 °C. The decomposition of the

bis(4-methoxyphenyl)-thiocyanato- $\lambda^3$ -iodane yield both 4-methoxyphenyl isothiocyanate and 4-methoxyphenyl thiocyanate (Figure 4-6). Treatment with neopentyl amine revealed 4-methoxyphenyl thiocyanate to be the major product, since only the 5 % 4-methoxyphenyl isothiocyanate reacts to form the corresponding thiourea.

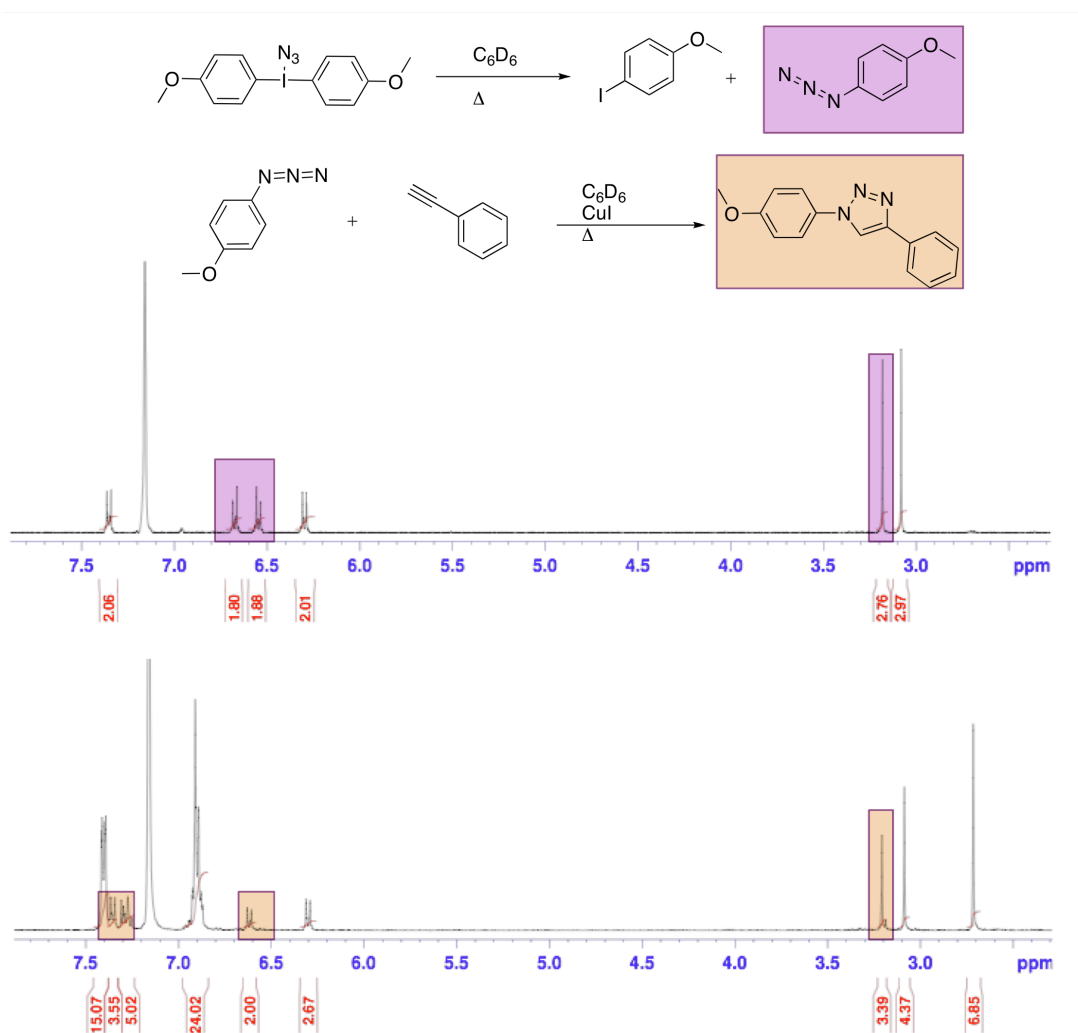


**Figure 4-7** Decomposition of bis(4-methoxyphenyl)-azido- $\lambda^3$ -iodane to form 4-azidoanisole and its coupling with phenyl acetylene to form the corresponding triazole.

Recent efforts to arylate nitrogen nucleophiles using diaryliodonium salts have focused prominently, although not exclusively, on copper catalyzed reactions.<sup>159</sup> Without

a copper catalyst, smooth C-N bond formation by reductive elimination of aryl iodide is not generally observed. Out of the six nitrogen nucleophiles we investigated, only azide and cyanate gave quantitative reductive elimination products. Contrary to the case with thiocyanate decomposition (C-S bond formation) described previously, 4-methoxyphenyl isocyanate was formed exclusively (C-N bond formation) for decomposition of bis(4-methoxyphenyl)-cyano- $\lambda^3$ -iodane. There seems to be a general rule that, in iodine-mediated reactions, coordination of the softer end of the bidentate nucleophiles leads to functionalization. Both azido and isocyanato arenes are valuable precursors in organic synthesis. Figure 4-7 shows the formation of 4-azidoanisole and its tandem coupling to phenyl acetylene (click chemistry).

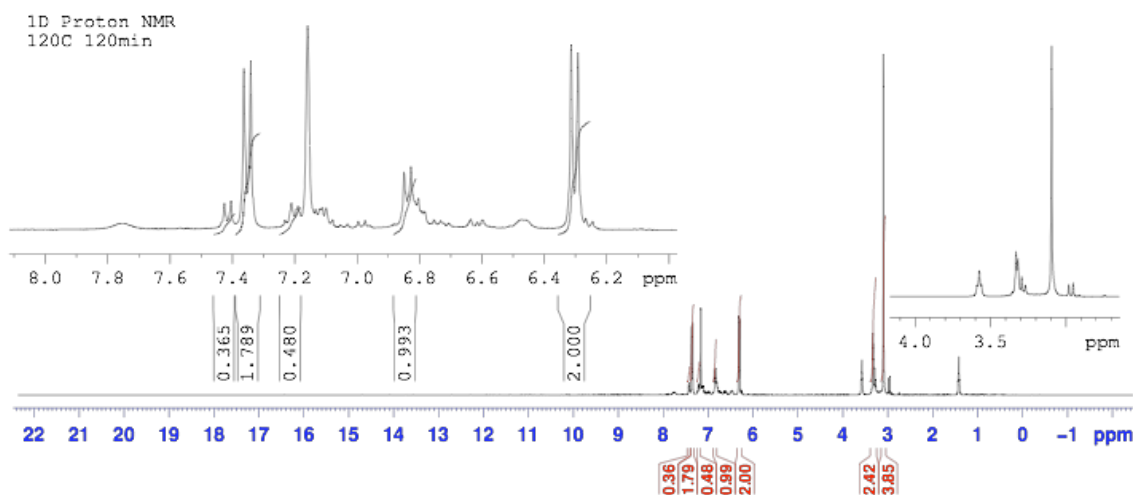


**Figure 4-8**  $^1\text{H}$  NMR spectra of the reaction mixture of bis(4-methoxyphenyl)-cyano- $\lambda^3$ -iodane decomposition in  $\text{d}_6$ -benzene.

Arylation of cyanide via diaryliodonium decomposition typically gives yield of < 40 %. The low yield has been attributed to the ease of homolytic cleavage of the I-CN bond, which results in side reactions involving radical species.<sup>105</sup> In the  $^1\text{H}$  NMR

spectrum of the reaction mixture (Figure 4-8), we were only able to identify 4-iodoanisole, 4,4'-dimethoxy-biphenyl, and anisole (confirmed by GC-MS analysis). The broad peaks seem to indicate the presence of polymeric species, possibly formed by radical chain processes. Similar results were obtained for phthalimide, *p*-tolylsulfonamide, and *N,N*-dimethylamide with multiple unidentified products shown up in the  $^1\text{H}$  NMR spectra of the reaction mixtures. These results suggest that the direct arylation of amines via reductive elimination of I(III)-iodanes is not practical, however azido arenes can be made easily from iodonium precursors and converted to corresponding anilines by Staudinger reduction. The next section of this chapter is dedicated to arylation of azide by decomposition of azido- $\lambda^3$ -iodanes.

### 4.3 Formation of azidoarenes

Aryl azides are valuable intermediate in organic synthesis.<sup>203-206</sup> Their typical synthetic roles include: 1) as protected nitrenes, which can insert into nearby C-H or C=C bond to yield nitrogen containing cyclic compounds; 2) as masked anilines that are relatively insensitive to acidic or basic environment via conversion by Staudinger reduction; and 3) they provide access to heterocycles such as triazoles and tetrazoles through [2+3] cycloadditions. Particularly, the copper(I)-catalyzed 1,2,3-triazole formation from azides and terminal acetylenes is highlighted as a powerful linking reaction in Click chemistry, due to its high reliability. It is virtually quantitative, very robust, insensitive, general, and orthogonal ligation reaction, suitable for even biomolecular ligation<sup>207-210</sup> and in vivo tagging,<sup>211, 212</sup> or as a polymerization reaction for synthesis of long linear polymers.<sup>213-215</sup>

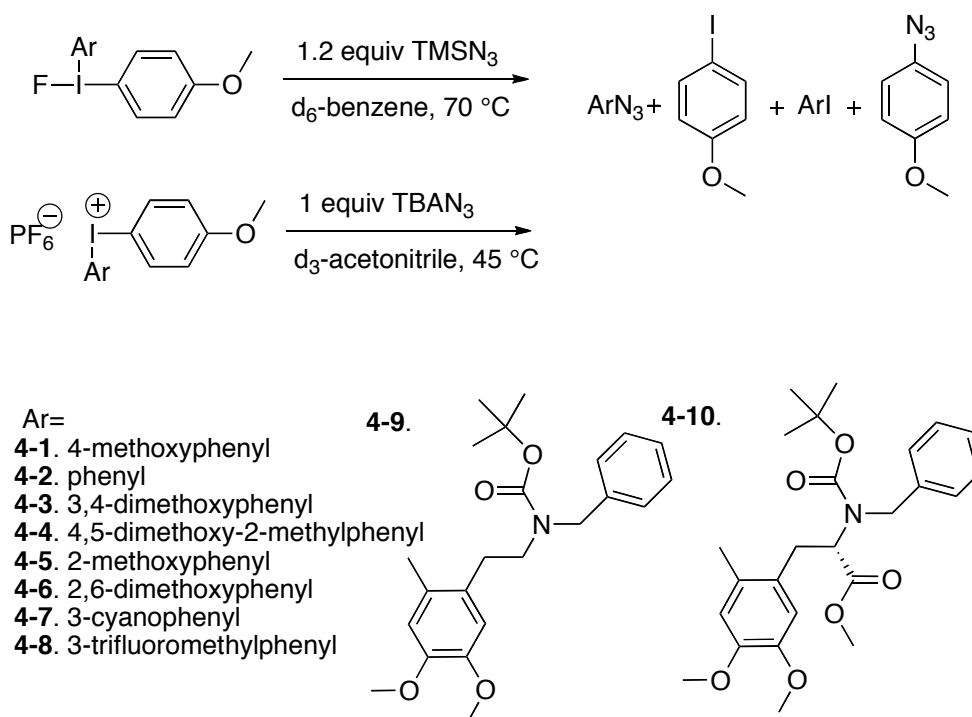
Previously, the most general and widely used preparative method for aryl azide formation was diazotization of the corresponding aniline followed by addition of sodium azide.<sup>216-218</sup> The need to prepare the diazonium salts limits the scope slightly. Alternatively, copper(I) iodide catalyzed substitution of halides with sodium azides has been reported to provide good to excellent yields of aryl and heteroaryl azides.<sup>219-221</sup> However, for unactivated aryl halides the reaction is sluggish and yields are low, presumably due to product decomposition at the elevated temperature that is required for the transformation. Additives such as proline were reported to lower the activation barrier so that the reaction could be performed at lower temperature, hence better yields could be achieved.<sup>222</sup> Aryl azides and heteroaryl azides can also be prepared by the mild reaction of anilines with triflyl azide.<sup>223</sup> The access to aryl azides by reductive elimination of diaryliodonium salts is not well developed in the literature; despite a few examples of nearly quantitative transformation were reported.<sup>75, 176</sup> Monoaryl-azido- $\lambda^3$ -iodanes such as 1-azido-1,2-benziodoxol-3(1H)-one, 1-azido-1,3-dihydro-3,3-dimethyl-1,2-benziodoxole,<sup>224, 225</sup> and phenyl-diazido- $\lambda^3$ -iodane<sup>226-229</sup> (*in situ* generation only) have found their way into organic synthesis as azidation reagents. Homolytic decomposition of the azidoiodanes followed by the addition of azido radicals is believed to be responsible for the formation of products. However, it is obvious that in some cases, diaryl-azido- $\lambda^3$ -iodanes were formed as intermediates.<sup>226</sup> Here we show that diaryl-azido- $\lambda^3$ -iodanes generated from either ion exchange of  $\text{TBAN}_3$  and diaryliodonium hexafluorophosphate, or by ligand exchange between the corresponding fluoroiodanes and  $\text{TMSN}_3$ , undergo reductive elimination upon heating in benzene or acetonitrile to yield aryl azides



quantitatively. This reaction is potentially useful as an alternative synthetic route for aryl azides.

The diaryliodonium model compounds synthesized for our fluorination study (CHAPTER 3) were conveniently used here. The reaction conditions and the structures of the iodanes are shown in Scheme 4-3. The exchange reaction of  $\text{TMSN}_3$  with iodonium fluorides in benzene can be slow at room temperature due to the low solubility of some of the fluoride salts. Heating the reaction mixture to 70 °C promote both the exchange and the subsequent reductive elimination. The yields of the reaction were calculated based on  $^1\text{H}$  NMR spectra of the reaction mixtures. The identities of the products were confirmed by GC-MS. The results are summarized in Table 4-3, where results for decomposition of the fluoroiodanes are also included as comparative benchmarks. In general, reductive eliminations of azidoiodanes are cleaner and higher yielding compared to that of the fluoroiodanes. The benzyne pathway wasn't viable so only azidation of the ipso carbon was observed in all cases. The reactions also seem to be insensitive to solvent; the overall yield in acetonitrile is even better in some cases (**4-4** and **4-6**). The superior efficiency of the azidation reactions compared to fluorination reactions in acetonitrile can be rationalized considering the azide is a superior nucleophile, a weaker base, and can back bond to iodine. For fluorination in acetonitrile, the major by-products are  $\text{HF}_2^-$  and  $\text{DF}_2^-$ . These complex ions are presumably formed from deprotonation of acetonitrile by fluoride dissociated from the I(III) center and etching of the glass by the hydrogen fluoride thus formed. Since the interactions between the iodonium cations and the fluoride ion are stronger in benzene, the reactivity of fluoride as a base was attenuated,

shutting off the side reactions. In addition, the lower yield for the decomposition of electron rich iodonium fluorides in acetonitrile could be due to the fact that fluoride-promoted disproportionation of the I(III) salts was favored in such a polar solvent.



**Scheme 4-3 Reductive elimination of aryl-(4-methoxyphenyl)-azido- $\lambda^3$ -iodanes in benzene and acetonitrile.**

**Table 4-3 Yields and reaction time of reductive elimination of aryl-(4-methoxyphenyl)-azido- $\lambda^3$ -iodanes and aryl-(4-methoxyphenyl)-fluoro- $\lambda^3$ -iodanes in benzene and acetonitrile.**

#	ArN <sub>3</sub> : AnN <sub>3</sub>		ArF: AnF	
	Benzene*	Acetonitrile	Benzene*	Acetonitrile
<b>4-1</b>	>99:-	>99:-	86:-	43:-
<b>4-2</b>	76:22	90:9	57:20	40:15
<b>4-3</b>	58:39	59:41	77:14	30:8
<b>4-4</b>	67:23	74:25	78:12	49:32
<b>4-5</b>	74:25	81:18	49:23	40:20
<b>4-6</b>	27:53	32:59	19:28	7:27
<b>4-7</b>	92:7	98:2	89:0	78:0
<b>4-8</b>	94:5	99:1	85:10	68:0
<b>4-9</b>	45:46	72:24	80:7	66:5
<b>4-10</b>	72:18	39:59	85:10	-

\* Some of the starting iodanes were post-swapping mixtures; product ratios do not reflect the true regioselectivities.

The product ratios for unsymmetrical iodanes (Table 4-3) follow the trend observed for fluorination reactions except for compounds **4-9** and **4-10**, which show reversed selectivities in different solvents. For compounds **4-2** through **4-5**, the regioselectivity appeared to be slightly better in acetonitrile. Initially, it was hard to rationalize these results. However, after we discovered the aryl-swapping process promoted by fluoride, it is clear that the azidoiodanes generated from fluoroiodanes are actually post-swapping mixtures that no longer resemble the initial pure compounds. Since azide does not promote aryl-swapping for diaryliodanes, the product ratios from the

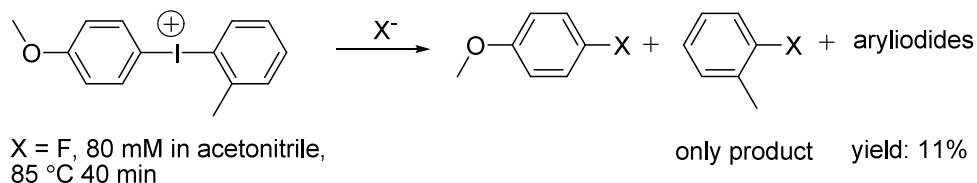
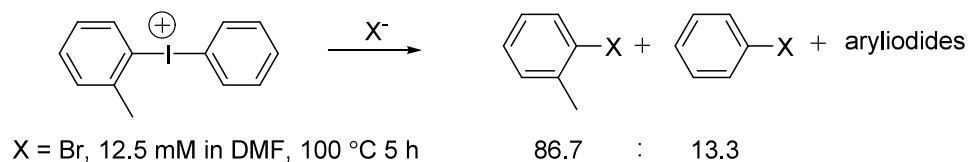
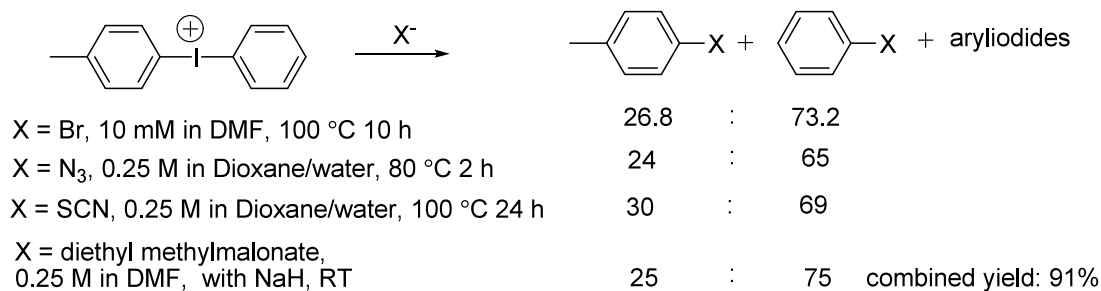
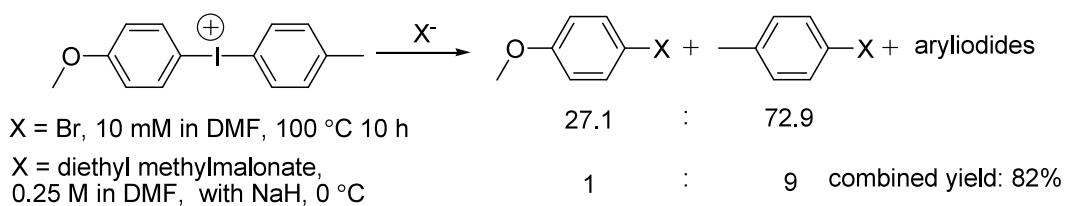
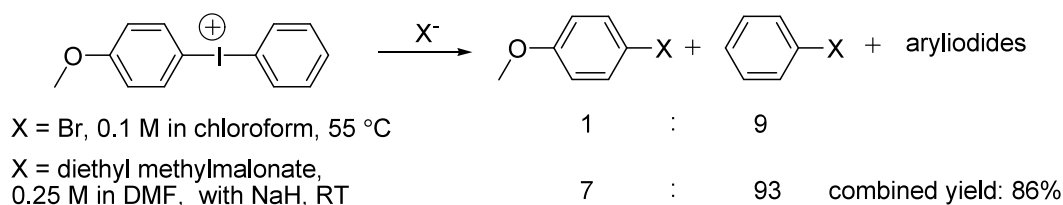
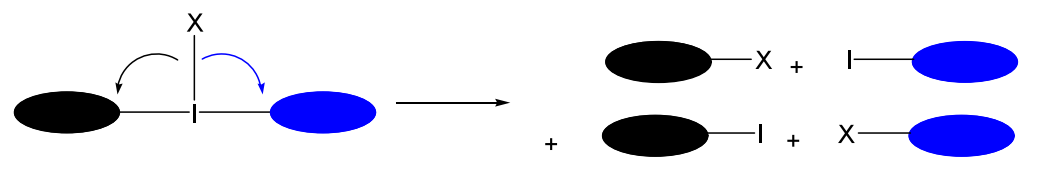
acetonitrile reactions reflect the true regioselectivities. For compounds **4-6** through **4-8**, the observed selectivities are about the same in both solvents, possibly because little or no aryl-swapping occurred. However, the reason for the reversion of regioselectivity for compound **4-9** and **4-10** is still not clear. And since these two examples represent azido functionalization of real drug molecules, the selectivity observed is not good enough for the method to be practical.

In conclusion, we have shown that reductive elimination of diaryliodonium azides offers fast facile access to various azido aromatic compounds. In all the compounds investigated here, we relied on the directing group ability of the electron-rich 4-methoxyphenyl moiety. The selectivity of the process could be improved by introducing a superior directing ligand that strongly disfavors the formation of the anionic transition state. We attempt to address this issue in the following section so that the process can become a useful alternative to access electron-rich azido aromatic compounds.

#### 4.4 Stereoelectronic control of unidirectional reductive elimination (SECURE) of I(III) species

In general, poor regioselectivity for reductive elimination narrows the synthetic scope of diaryliodonium salts as arylations reagents. Efficient conversion is best obtained when the two aryl substituents on I(III) are identical. However, the preparation of symmetrical diaryliodonium salts can be problematic and uneconomical.<sup>62</sup> For relatively complex aromatic molecules, it is usually a substantial challenge to synthesize and protect the oxidized (I(III)) and reduced (organometallic) coupling partners necessary to prepare the symmetrical diaryliodonium salt. In addition, the symmetrical salt approach has another problem that purification of the functionalized product from the reductively eliminated aryl iodide can be difficult.

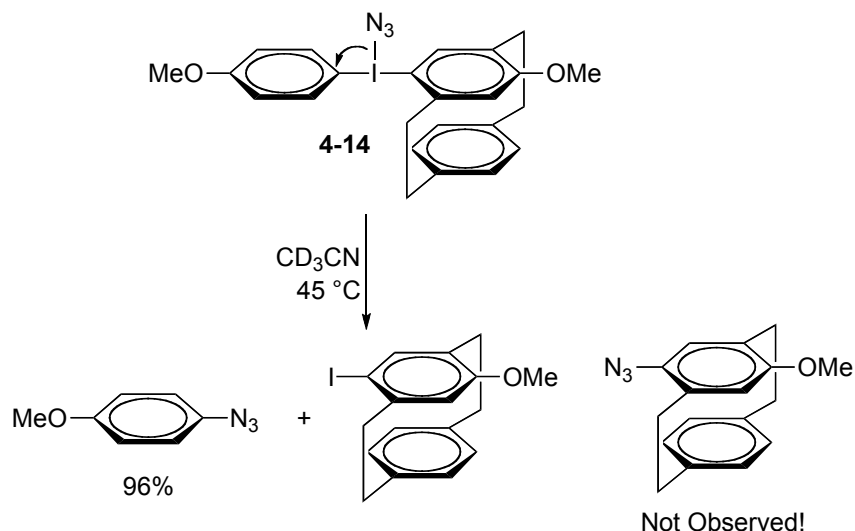
In the thermal decomposition of unsymmetrical diaryliodonium salts, it is typically the electronic effects that govern the identity of the aryl iodide reductively eliminated; the electron-rich aryl iodide and the functionalized electron-poor aromatic compound are formed predominantly (Scheme 4-4). Electron-rich aryls such as 4-methoxyphenyl and 2-thiophenyl were often used to direct the nucleophile to the other ring.<sup>77, 82, 230</sup> However, since extremely electron-rich diaryliodonium salts are prone to side reactions involving redox and inner-sphere electron transfer, there is a limit to using electronic control to achieve regioselectivity.



**Scheme 4-4 Examples of regioselectivities obtained in thermal decomposition reactions of unsymmetrical diaryliodonium salts.** <sup>76, 78, 103, 176, 231, 232</sup>

The impact of steric effects upon reductive elimination in diaryliodonium salts has been investigated in some detail. The “*ortho* effect” states that there is a preference for the *ortho* substituted aryls to be functionalized. The two explanations offered were: 1) the more sterically demanding aromatic ring prefers an equatorial position syn to the nucleophile, and 2) the *ortho*-substituted aromatic is more likely to prefer a conformation in which the  $\pi$ -system is more likely to align with the incoming nucleophile. This rule is marred by exceptions. For example, Ochiai and coworkers have shown that for binaphthyl aryl iodonium salts, *ortho*-substitution coupled with sterically demanding enolate nucleophiles results in alkylation of the less hindered ring.<sup>95</sup> Our computational study using simple diaryliodonium fluorides as models (3.4) had revealed that relative stability of the elimination transition states is key to the regioselectivity and the steric regioselective effect is unique to *ortho* methyl substituents. No example of using the steric effect to control the regioselectivity of diaryliodonium decomposition exists in the literature.

We sought to solve the problem of selective functionalization of the more electron-rich aromatic ring in an unsymmetrical diaryliodonium salt by using a universal “locked” aryl substituent that would result in unidirectional reductive elimination.<sup>233</sup> Since electronic effects cannot be used solely to achieve this end, steric and/or stereoelectronic effects have to be exploited to gain regiocontrol of reductive elimination. Hence we developed the concept of StereoElectronic Control of Unidirectional Reductive Elimination (*SECURE*). Here we show that the use of cyclophane-derived iodonium salts permits regiospecific reductive elimination (Scheme 4-5).



**Scheme 4-5 Regiochemically controlled reductive elimination of an electron-rich, cyclophane-derived diaryliodonium salt.**

Our approach was to generate a highly strained reductive elimination transition state with a designed aryl ligand so to direct reductive elimination. If the mechanistic assumption of a concerted reductive elimination process is adopted, selective destabilization of the transition state requires significant steric congestion above and/or below the aromatic ring and little steric congestion in the plane of the ring. Therefore, we started investigating the SECURE methodology with “strapped” or “capped” aromatic compounds. [2.2]Paracyclophane<sup>234, 235</sup> is a particularly attractive potential iodine(III) ligand because 1) it is commercial available, 2) it has established functionalization chemistry,<sup>236</sup> 3) it features severe out of plane steric congestion, and 4) it allows one to exploit the planar chiral ligand in stereoselective reactions.<sup>237</sup> However, synthesizing the I(III) derivatives of [2.2]paracyclophane was challenging because no such compounds have been reported to date.



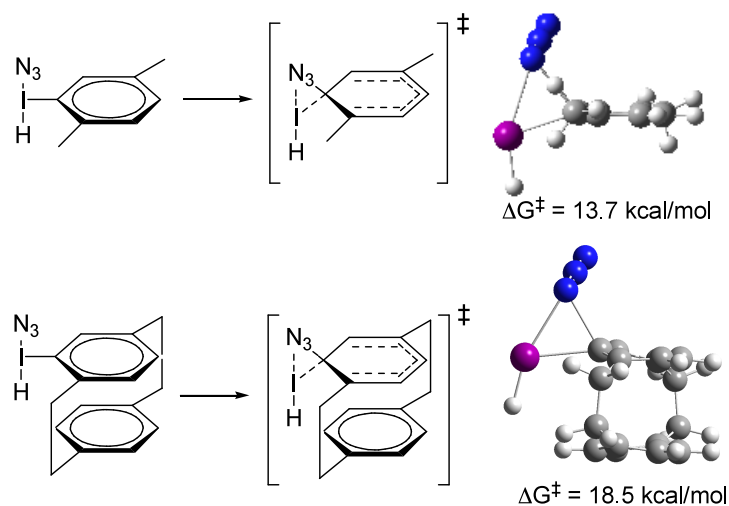


**Figure 4-9** Calculated TS structures and activation barriers for xylyl and cyclophanyl I(III) species.

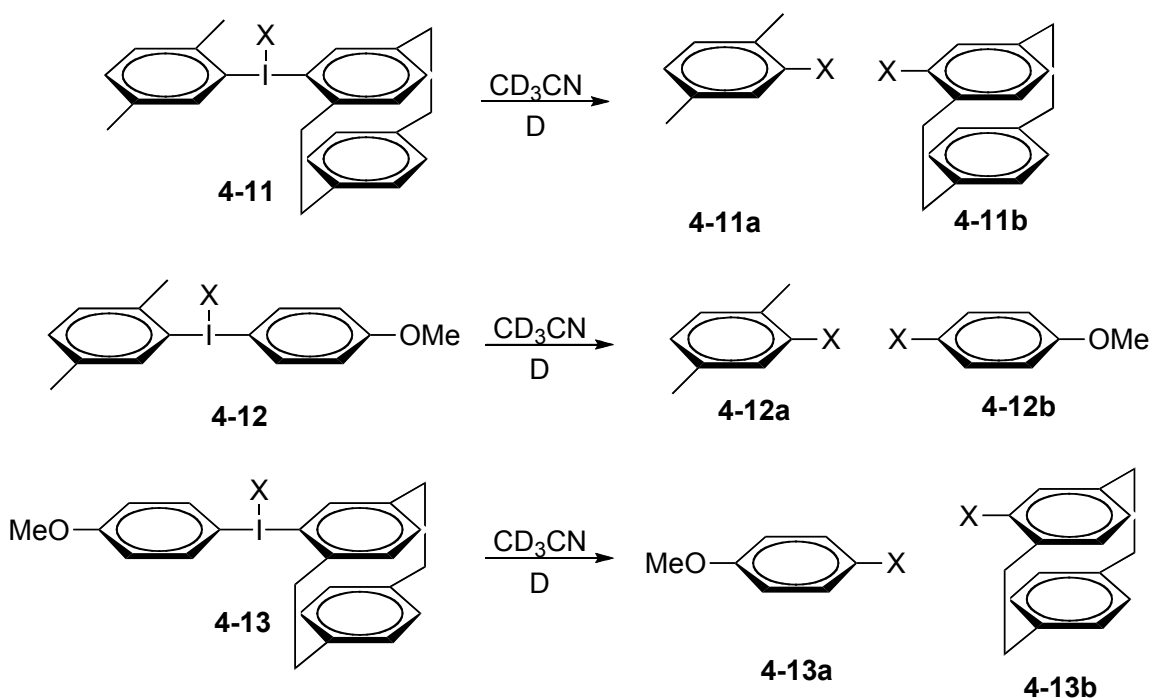
An initial computational study (B3LYP/DGDZVP, ZPE corrected) was performed to explore the *SECURE* concept (results shown in Figure 4-9). We selected azide transfer in diaryliodonium salts for our test reaction since diaryliodonium azides are known to undergo reductive elimination at or near room temperature,<sup>75, 176</sup> and because the small azide nucleophile has a relatively modest steric demand. Ground and transition state energies were calculated for a highly simplified model of azido functionalization, reductive elimination of HI from the  $\text{HIN}_3\text{Ar}$  complexes of *p*-xylene and [2.2]paracyclophane.

The calculated free energy of activation for reductive elimination of HI from the *p*-xylene salt is 13.7 kcal/mol, while the barrier for the cyclophane derivative is 4.8 kcal/mol higher. Inspection of Figure 4-9 reveals that this energetic penalty is associated with the structural difference between the transition states. The movement from the ground state to the transition state geometries for azide substitution is accompanied by

ipso carbon rehybridization and deflection of the HI group out of the plane. For the xylyl derivative the C4-C1-I angle is 161.9°. However, in the [2.2]paracyclophan-4-yl transition state structure the significant steric demand of the second ring in the planar chiral ligand inhibits out of plane movement of the iodine atom (C4-C1-I angle is 167.2°). With this “in silico” confirmative result, we moved on to demonstrate the SECURE concept empirically.

([2.2]Paracyclophan-4-yl)(2',5'-dimethylphenyl)-iodonium hexafluorophosphate (salts **4-11**, structure shown in Scheme 4-6) was synthesized to compare the directing effects of the electronically similar *p*-xylyl and [2.2]paracyclophan-4-yl groups. We started by treating 4-bromo-[2.2]paracyclophane<sup>236, 238</sup> with 2 equivalents of *t*-BuLi (Et<sub>2</sub>O, -78 °C) followed by transmetalation with anhydrous zinc chloride to get [2.2]paracyclophan-4-ylzinc chloride. The ether solvent was removed and the organozinc chloride reagent was treated with 2,5-dimethylphenyliodonium diacetate in acetonitrile at -40 °C. After the mixture was allowed to warm to room temperature, water was added followed by an aqueous solution of sodium hexafluorophosphate. The product was extracted with dichloromethane to give the hexafluorophosphate salt of salt **4-11** in 18 % yield. Typically diaryliodonium salts have been synthesized by coupling monoaryl I(III) precursor with organotin<sup>117</sup> reagents. Here we had to use organozinc reagent because 4-trialkylstannyl[2.2]paracyclophanes do not transfer the cyclophane moiety. A likely explanation for the poor reactivity of the stannane is that the transition state for cyclophane transfer is highly congested and resembles that shown in Figure 4-9. In addition to organotin reagents, organolithium,<sup>239, 240</sup> organoboron,<sup>97</sup> and organosilicon<sup>90</sup>

have also been used in diaryliodonium synthesis. However, to our knowledge this is the first example of the preparation of a diaryliodonium salt from an arylzinc chloride. The organozinc reagent was more reactive than organotin, organoboron, and organosilicon reagents toward I(III) species in that it reacted with the unactivated arylidonium diacetates. We chose to make the hexafluorophosphate salt of **4-11** because, hexafluorophosphate is a weakly interacting non-nucleophilic counterion which permits introduction of a wide range of nucleophiles via their tetraalkylammonium or sodium salts.



**Scheme 4-6 Reductive elimination of compounds 4-11, 4-12, and 4-13 by various nucleophiles in acetonitrile.**

Accordingly, when the hexafluorophosphate salt **4-11** was treated with  $\text{TBAN}_3$  and heated at  $45^\circ\text{C}$  in  $\text{CD}_3\text{CN}$  (0.04 M), conversion of the diaryliodonium azide was

complete within a few hours. In support of the initial hypothesis, the azidoxylene was formed exclusively in excellent yield, and no azidocyclophane was observed at the detection limit of  $^1\text{H}$  NMR spectroscopy. This unidirectional elimination was also observed with thiocyanate, phenoxide, thiophenoxide, trifluoroethoxide, and acetate (Table 4-4). The observed selectivity ( $> 99:1$ ) corresponds to a difference in the free energies of activation ( $\Delta\Delta G^\ddagger$ ) of at least 2.8 kcal/mol. Thus, the validity of the computational model is confirmed.

**Table 4-4 Results for the reductive elimination of salt 4-11, 4-12, and 4-13 with various nucleophiles in acetonitrile.**

X	4-11		4-12		4-12	
	4-11a	4-11b	4-12a	4-12b	4-13a	4-13b
$\text{N}_3^-$	99<	0	99<	0	86	14
$\text{SCN}^-$	99<	0	99<	0	81	18
$\text{OPh}^-$	87	0	96	4	51	40
$\text{SPh}^-$	98	0	95	5	43	52
$\text{OCH}_2\text{CF}_3^-$	82	0	80	0	19	39
$\text{OAc}^-$	85	0	99<	0	68	31

To provide context for the *SECURE* results, arene functionalization by various nucleophiles (X) in (2,5-dimethoxyphenyl)-(4'-methoxyphenyl)-iodonium (salts **4-12**, structure shown in Scheme 4-6) was investigated. It was found that the regioselectivity observed during the reductive elimination of cyclophanyl-substituted diaryliodonium salts mirrors that of 4-methoxyphenyl derivatives. Despite being the most effective, commonly employed directing group in diaryliodonium chemistry,<sup>83, 230, 231</sup> the 4-

methoxyphenyl moiety does not offer perfect regioselectivity for arene functionalization. For the redox active thiophenoxide and phenoxide nucleophiles, some loss of regiocontrol was evident and functionalized anisoles were formed.

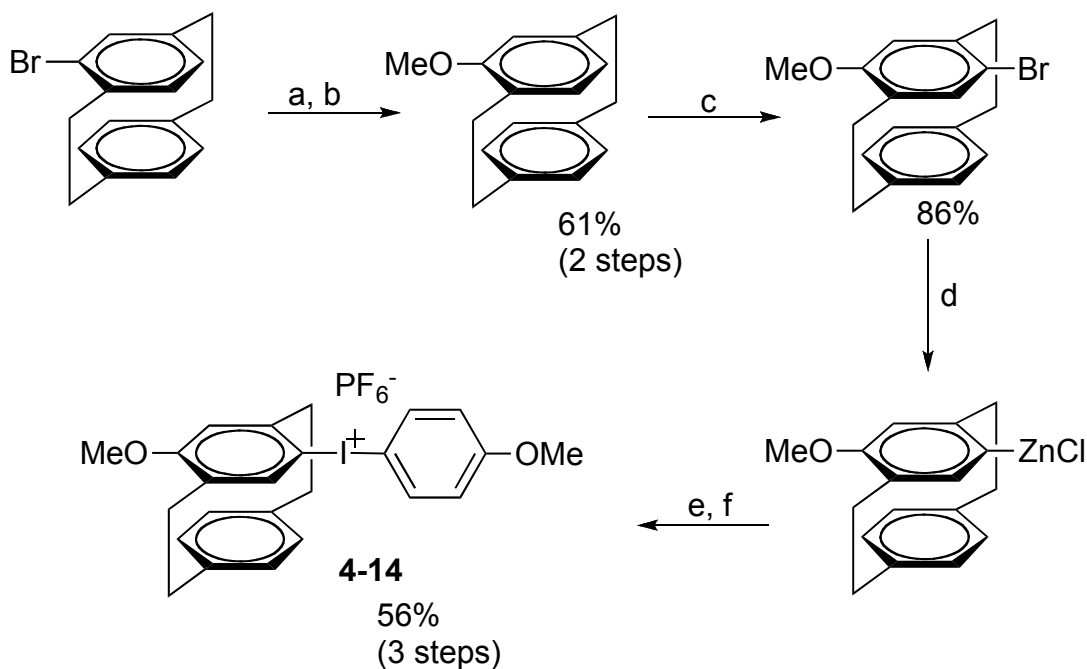
To directly compare the relative directing group abilities of 4-methoxyphenyl and [2.2]paracyclophan-4-yl substituents, we prepared ([2.2]paracyclophan-4-yl)(4'-methoxyphenyl)-iodonium hexafluorophosphate (salt **4-13**, structure shown in Scheme 4-6) from [2.2]paracyclophan-4-ylzinc chloride and 4-methoxyphenyliodonium diacetate using the procedure described above (38 % yield) and examined its thermal decomposition chemistry. More vigorous reaction conditions (80 °C, CD<sub>3</sub>CN) were necessary to promote speedy carbon-heteroatom bond formation with acetate and thiocyanate from **4-13** in comparison to **4-11** or **4-12**. As can be seen from inspection of Table 4-4, the directing group ability of the [2.2]paracyclophane ligand is comparable or slightly superior to that of the 4-methoxyphenyl substituent on I(III).

From the limited data in Table 4-4 it appears that for oxygen or sulphur nucleophiles the directing group ability of the cyclophane ligand diminishes as nucleophile basicity and the driving force for functionalizing the more electron-poor ring increase. Such a trend is consistent with Hammond's postulate and a concerted, reductive elimination mechanism in which less steric strain is developed at the cyclophane ipso carbon atom as the reaction becomes more exergonic.

In order to probe the relative steric and electronic contributions to the observed regioselectivity, we studied the kinetics of aryl azide formation from N<sub>3</sub> salts of **4-11**, **4-12** and **4-13**. The reactions were carried in deuterated acetonitrile at 45 °C. The observed

rate constants for aryl azide formation (azidoxylene for salt **4-11** and **4-12**, azidoanisole for salt **4-13**,) were  $4.2 \times 10^{-4} \text{ s}^{-1}$ ,  $5.5 \times 10^{-5} \text{ s}^{-1}$ , and  $3.3 \times 10^{-6} \text{ s}^{-1}$ , corresponding to free energies of activation of 21.7, 22.9, and 24.6 kcal/mol for the reactions of **4-11**, **4-12** and **4-13**, respectively. The fact that the rate constant for formation of azidoxylene is greater for **4-11** than **4-12** indicates that 4-iodo-[2.2]paracyclophane is a significantly better leaving group than 4-iodoanisole. Since leaving group ability is correlated with the electron density on iodine in the aryl iodide being reductively eliminated, these kinetic data show experimentally that the [2.2]paracyclophane ligand is a significantly more electron-poor aryl substituent than 4-methoxyphenyl. That leaves steric destabilization of the transition state as the only reasonable explanation for the enhanced directing group ability of the [2.2]paracyclophane ligand.

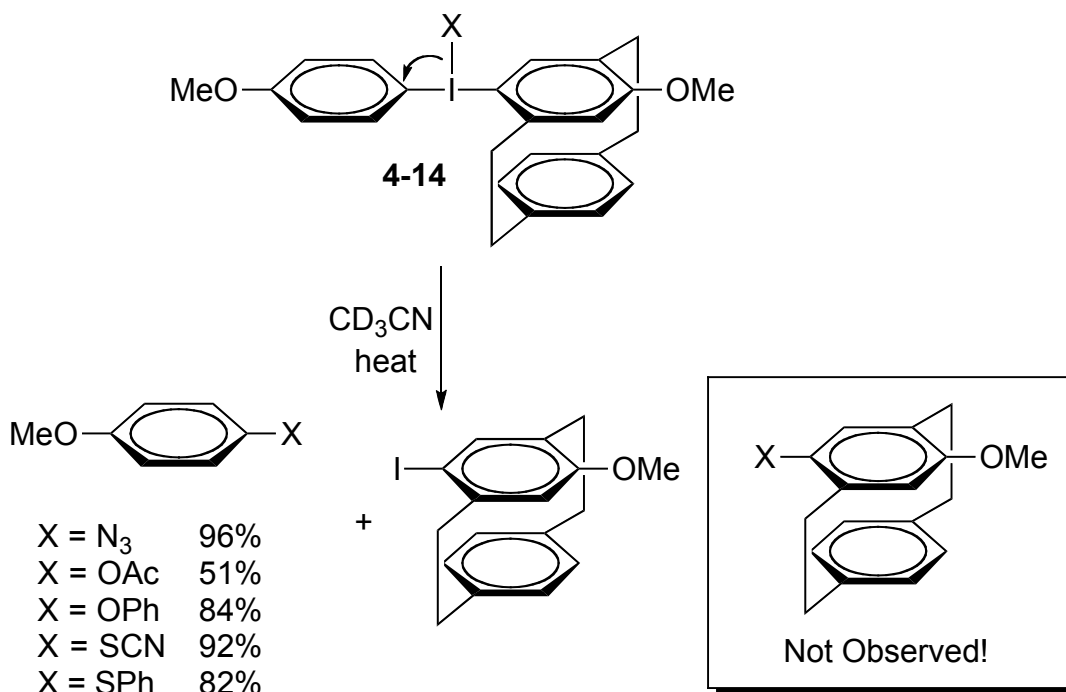
These results validate the *SECURE* concept, but the directing group ability of [2.2]paracyclophan-4-yl group is only marginally better than 4-methoxyphenyl group. The perfect regiochemical control is yet to be realized and functionalizing very electron-rich rings is still challenging. We decided to address this issue by making the cyclophane ligand more electron-rich. (7-Methoxy-[2.2]paracyclophan-4-yl)(4'-methoxyphenyl)-iodonium hexafluorophosphate (salt **4-14**, structure shown in Scheme 4-6) was prepared using the procedure shown in Scheme 4-7. Improved yield in the I(III) transfer reaction was observed (56 %), possibly because the methoxy group enhances the solubility of the cyclophane organozinc chloride reagent.



**Scheme 4-7** Synthesis of (7-methoxy-[2.2]paracyclophan-4-yl)(4'-methoxyphenyl)-iodonium hexafluorophosphate. (a. 1. *t*-BuLi, Et<sub>2</sub>O, -78 °C, 2. B(OMe)<sub>3</sub>, 3. H<sub>2</sub>O<sub>2</sub>, NaOH, H<sub>2</sub>O; b. K<sub>2</sub>CO<sub>3</sub>, CH<sub>3</sub>I, CH<sub>3</sub>CN, 80 °C; c. NBS, CH<sub>2</sub>Cl<sub>2</sub>; d. 1. *t*-BuLi, Et<sub>2</sub>O, -78 °C, 2. ZnCl<sub>2</sub>; e. 1. 4-(OMe)PhI(OAc)<sub>2</sub>, CH<sub>3</sub>CN, -40 °C, f. NaPF<sub>6</sub>, H<sub>2</sub>O.)

In salt **4-14**, both ligands feature electron donating methoxy substituents *para* to the I(III) center, which make them electronically equivalent. The cyclophane ligand has additional directing ability due to its out of plan steric constraint. As expected, salt **4-14** provides excellent regiochemical control for anisole functionalization across the range of nucleophiles investigated here (Scheme 4-8). Only anisole substitution was observed after the thermal decomposition of the azide, acetate, phenoxide, thiocyanate, and thiophenoxide salts. However, a mixture of cyclophane- (30 %) and anisole-substituted (60 %) products was obtained from the arylations of 2,2,2-trifluoroethoxide. Product analysis (<sup>19</sup>F NMR and GC-MS) shows roughly equal amounts of 3- and 4-(2,2,2-

trifluoroethoxy)anisole, as well as roughly equal amounts of the two cyclophane regioisomers were formed. The formation of the regioisomer and the lack of selectivity and distribution of regioisomers can be attributed to a change in mechanism to one involving benzyne intermediates. For this more basic nucleophile, the benzyne reaction pathway becomes competitive when the activation barrier for the reductive elimination of aryl iodide is raised too high. This could be an ultimate limitation in functionalizing electron-rich aromatics via this method.



**Scheme 4-8** Anisole functionalization by thermal decomposition of salt 4-14 in  $\text{CD}_3\text{CN}$ .

In summary, we have shown that an increase in steric demand above the plane of the aromatic ring destabilizes a reductive elimination transition state via computational and experimental data. This effect is sufficiently large to provide stereoelectronic control of unidirectional reductive elimination (*SECURE*). A number of examples are provided to



show that the intrinsic electronic bias in reductive elimination reactions of I(III) compounds can be overcome. Strikingly, even 4-methoxyphenyl groups can be functionalized with perfect regiochemical control. Additionally, since the approach is a general one, it is anticipated that *SECURE* will be useful for controlling reductive elimination from a variety of high valent main group and transition metal ions.

## 4.5 Experimental

**General:** All materials were obtained from commercial sources and used as received unless otherwise noted. Zinc triflate was dried *in vacuo* before use. Diethyl ether and tetrahydrofuran were distilled under reduced pressure from sodium/benzophenone. Tetrabutylammonium azide (TBAN<sub>3</sub>), tetramethylammonium thiocyanate (TBASCN), tetrabutylammonium chloride (TBACl), sodium phenoxide (NaOPh), sodium thiophenoxide (NaSPh), and sodium trifluoroethoxide (NaOCH<sub>2</sub>CF<sub>3</sub>) were dried at room temperature in a drying pistol (charged with P<sub>2</sub>O<sub>5</sub>) under dynamic vacuum for one week. Acetonitrile and d<sub>3</sub>-acetonitrile were heated at reflux over P<sub>2</sub>O<sub>5</sub>, distilled into flame-dried storage tubes, transferred to the glove box. Benzene and d<sub>6</sub>-benzene were heated at reflux over CaH<sub>2</sub> overnight and distilled directly into flame-dried storage tubes under dry nitrogen. Tetrahydrofuran (THF) was dried over Na/benzophenone and distilled into a flame dried storage flask under dry nitrogen. All glassware, syringes, and NMR tubes were oven dried (140 °C) for more than 24 h before they were transferred into the glove box for use. All NMR experiments reported here were performed using a Bruker Avance 400 MHz NMR spectrometer in the NMR laboratory at the University of Nebraska-

Lincoln. Yields from NMR scale reactions were determined by using the residual solvent peak as an internal standard.

**Calculations:** All calculations were performed using the Gaussian03 suite of programs and visualization was performed with GaussView03.<sup>27</sup> Ground state geometries were identified after driving the C-C-I-H dihedral angle through a full range of motion. Structures were optimized and their energies calculated using DFT B3LYP/DGDZVP methods. Frequency calculations on minimized structures were performed to make the zero point energy and thermal corrections. Transition states were optimized at the same computational level.

**General procedure for preparing bis(4-methoxyphenyl)-halo-iodanes:** In a nitrogen atmosphere glove box, 227 mg (0.5 mmol) of bis(4-methoxyphenyl)-iodonium trifluoroacetate was dissolved in 1 mL of dry THF. A solution of 1.05 equivalent TBAX (X = Cl, Br, I, CN) in 1 mL THF was added. The mixture was let stand for 1 hr to allow precipitation formation. The precipitated salt was filtered and washed with 0.2 mL dry THF three times, transferred into a brown vial and pumped under dynamic vacuum for overnight.

**General procedure for decomposition reactions of bis(4-methoxyphenyl)-halo-iodanes in benzene:** In a N<sub>2</sub> nitrogen atmosphere glove box, 0.03 mmol of a proper bis(4-methoxyphenyl)-halo- $\lambda^3$ -iodane was dissolved in 0.6 mL of dry d<sub>6</sub>-benzene. The

solution was transferred into a J-Young NMR tube, sealed, taken out of the glove box and an initial NMR spectrum was obtained. The NMR tube was wrapped with aluminum foil and put into an oil bath of appropriate temperature. The progress of the reaction was monitored by  $^1\text{H}$  NMR until no I(III) species were left.

**General procedure for decomposition reactions of other bis(4-methoxyphenyl)- $\lambda^3$ -iodanes in benzene:** In a nitrogen atmosphere glove box, 10.8 mg (0.03 mmol) of bis(4-methoxyphenyl)-fluoro- $\lambda^3$ -iodane was dissolved in 0.6 mL of dry  $\text{d}_6$ -benzene. 1.05 equivalent of TMSX (X= OAc, OTf,  $\text{CF}_3\text{COO}$ ,  $\text{N}_3$ , NCS, NCO, phthalimidyl, *p*-toluenesulfonamidyl) or NaX (X = *t*-BuO,  $\text{CF}_3\text{CH}_2\text{O}$ , benzoate, phenoxide, thiophenolate) was added and the solution mixture was transferred into a J-Young NMR tube, sealed, taken out of the glove box and an initial NMR spectrum was obtained. The NMR tube was wrapped with aluminum foil and put into a 120 °C oil bath. The progress of the reaction was monitored by  $^1\text{H}$  NMR until no I(III) species were left.

**General procedure for decomposition reactions of aryl-(4-methoxyphenyl)-azido- $\lambda^3$ -iodanes in benzene:** In a nitrogen atmosphere glove box, 0.03 mmol of a proper aryl-(4-methoxyphenyl)-fluoro- $\lambda^3$ -iodane was dissolved in 0.6 mL of dry  $\text{d}_6$ -benzene. 1.05 equivalent of  $\text{TMSN}_3$  was added and the solution mixture was transferred into a J-Young NMR tube, sealed, taken out of the glove box and an initial NMR spectrum was taken. The NMR tube was wrapped with aluminum foil and put into a 70 °C oil bath. The progress of the reaction was monitored by  $^1\text{H}$  NMR until no I(III) species were left.

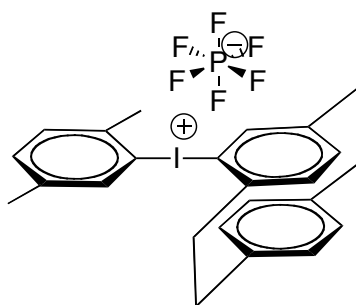
**General procedure for decomposition reactions of aryl-(4-methoxyphenyl)-azido- $\lambda^3$ -iodanes in acetonitrile:** In a nitrogen atmosphere glove box, 0.03 mmol of a proper aryl-(4-methoxyphenyl)-iodonium hexafluorophosphate was dissolved in 0.6 mL of dry  $d_3$ -acetonitrile. 1.05 equivalent of  $TBAN_3$  was added and the solution mixture was transferred into a J-Young NMR tube, sealed, taken out of the glove box and an initial NMR spectrum was obtained. The NMR tube was wrapped with aluminum foil and put into a 45 °C oil bath. The progress of the reaction was monitored by  $^1H$  NMR until no I(III) species were left.

**General procedure for decomposition reactions of compound 4-11, 4-12, 4-13, and 4-14 with  $N_3^-$ ,  $SPh^-$ ,  $OPh^-$ , and  $OCH_2CF_3^-$ :** In a nitrogen atmosphere glove box, 0.025 mmol of salts **4-11** (14.6 mg), **4-12** (12.1 mg), **4-13** (14.7 mg) or **4-14** (15.4 mg) were dissolved in 0.3 mL of dry  $d_3$ -acetonitrile. The solution was combined with 0.3 mL  $d_3$ -acetonitrile solution of 1 equiv. of the appropriate salt ( $TBAN_3$  (7.1 mg),  $TBASPh$  (8.8 mg),  $NaOPh$  (2.9 mg)  $NaOCH_2CF_3$  (3.1 mg)). The mixture was transferred into a J-Young NMR tube, sealed, taken out of the glove box and an initial NMR spectrum was taken. The NMR tube was wrapped with aluminum foil and put into a 45 °C oil bath. The progress of the reaction was monitored by  $^1H$  NMR until no I(III) species were left.

**General procedure for decomposition reactions with  $NCS^-$  and  $OAc^-$ :** In a nitrogen atmosphere glove box, 0.025 mmol of salts **4-11** (14.6 mg), **4-12** (12.1 mg), **4-13** (14.7

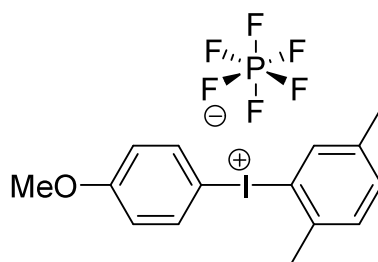
mg) or **4-14** (15.4 mg) were dissolved in 0.3 mL of dry  $d_3$ -acetonitrile. The solution was combined with 0.3 mL  $d_3$ -acetonitrile solution of 1 equiv. of the appropriate salt (TBASCN (7.5 mg), TBAOAc (15 mg)). The mixture was transferred into a J-Young NMR tube, sealed, taken out of the glove box and an initial NMR spectrum was taken. The NMR tube was wrapped with aluminum foil and put into an 80 °C oil bath. The progress of the reaction was monitored by  $^1\text{H}$  NMR until no I(III) species were left.

### Preparation procedures and characterization of compounds



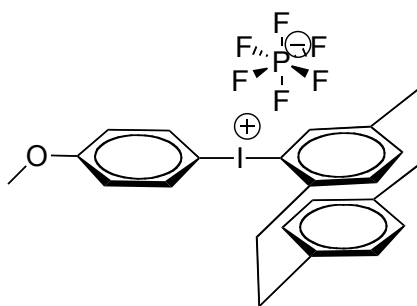
**([2.2]Paracyclophan-4-yl)(2',5'-dimethylphenyl)-iodonium hexafluorophosphate (4-11):** In a 50 mL Schlenk tube under nitrogen, a stirred solution of 4-bromo[2.2]paracyclophane (1 mmol, 282 mg) in 10 mL of anhydrous diethyl ether was cooled to -78 °C. A solution of *t*-BuLi (1.7 M in pentane, 2.3 equiv.) was added dropwise and the resulting mixture was stirred at -78 °C for 20 minutes and then warmed to 0 °C and allowed to stir for an additional 20 min. The reaction mixture was cooled again to -78 °C before a solution of zinc chloride (200 mg, 1.5 mmol) in ether (10 mL) was added dropwise by cannula. After the addition, the reaction mixture was allowed to warm to room temperature over the course of one hour before the solvents were removed in vacuo. The remaining solid was dissolved in anhydrous  $\text{CH}_3\text{CN}$  and the solution was cooled to -

40 °C and added dropwise to precooled (-40 °C) suspension of bis(acetyloxy)-(2,5-dimethylphenyl)- $\lambda^3$ -iodane (350 mg, 1 mmol) in 10 mL of acetonitrile. The mixture was allowed to warm to room temperature over 30 minutes before the solvent was removed in vacuo. The resulting solid was washed with hexanes and then dissolved in aqueous acetonitrile. Addition of an aqueous NaPF<sub>6</sub> solution precipitated the product, which was extracted from the aqueous mixture with CH<sub>2</sub>Cl<sub>2</sub>. The organic layer was evaporated, dissolved in a minimal amount of CH<sub>2</sub>Cl<sub>2</sub>, precipitated with hexanes, filtered and dried *in vacuo* to yield ([2.2]paracyclophane-4-yl)(2',5'-dimethylphenyl)-iodonium hexafluorophosphate (105 mg, 18 % yield). <sup>1</sup>H NMR (CD<sub>3</sub>CN, 400 MHz, 25 °C):  $\delta$  7.93 (s, 1 H), 7.41 (s, 2 H), 7.29 (d, *J* = 1.3 Hz, 1 H), 6.84 (dd, *J*<sub>1</sub> = 7.8 Hz, *J*<sub>2</sub> = 1.3 Hz, 1 H), 6.78 (d, *J* = 7.8 Hz, 1 H), 6.66 (s, 2 H), 6.53 (d, *J* = 7.9 Hz, 1 H), 6.51 (d, *J* = 7.9 Hz, 1 H), 3.04-3.41 (m, 8 H), 2.50 (s, 3 H), 2.33 (s, 3 H); <sup>13</sup>C NMR (CD<sub>3</sub>CN, 100 MHz, 25 °C)  $\delta$  146.5, 143.6, 141.9, 141.1, 140.2, 139.9, 139.5, 138.2, 137.7, 135.6, 134.7, 134.5, 134.1, 133.9, 133.1, 132.5, 120.6, 118.8, 100.8, 38.9, 35.8, 35.5, 35.4, 25.3, 20.6; HRMS: (HRFAB) calcd. for C<sub>24</sub>H<sub>24</sub>I [M]<sup>+</sup> 439.0923, found 439.0907.



**(2,5-Dimethylphenyl)(4'-methoxyphenyl)-iodonium hexafluorophosphate (4-12):** In a nitrogen atmosphere glove box, 1-(diacetoxyiodo)-4-methoxybenzene (352 mg, 1 mmol) was dissolved in 1.5 mL of dry acetonitrile. The solution was combined with a solution of

*p*-toluenesulfonic acid monohydrate (190 mg, 1 mmol) in 1.5 mL of dry acetonitrile. *p*-Xylene (117 mg, 1.1 mmol) was added and the mixture was allowed to stand at room temperature for 2 h. Water (10 mL) was added and the mixture was extracted ( $3 \times 5$  mL) with hexanes. The water layer was treated with NaPF<sub>6</sub> (502 mg, 3 mmol) and the white precipitate was extracted from the aqueous layer with CH<sub>2</sub>Cl<sub>2</sub>. Evaporation of the organic solvent followed by recrystallization with diethyl ether/dichloromethane gave 309 mg (2,5-dimethylphenyl)(4'-methoxyphenyl)-iodonium hexafluorophosphate (65.2 %). <sup>1</sup>H NMR (CD<sub>2</sub>Cl<sub>2</sub>, 400 MHz, 25 °C): δ 7.88 (d, *J* = 9.1 Hz, H2'/H6', 2 H), 7.83 (s, H6, 1 H), 7.41 (s, H3/H4, 2 H), 7.03 (d, *J* = 9.1 Hz, H3'/H5', 2 H), 3.85 (s, 4'-OMe, 3 H), 2.59 (s, 2-Me, 3 H), 2.37 (s, 5-Me, 3 H); <sup>13</sup>C NMR (CD<sub>2</sub>Cl<sub>2</sub>, 100 MHz, 25 °C) δ 164.2 (C4'), 141.7 (C2), 138.5 (C5), 137.8 (C2'/C6'), 137.1 (C6), 135.4 (C4), 132.6 (C3), 119.4 (C3'/C5'), 118.0 (C1), 98.7 (C1'), 56.5 (4'-OMe), 25.3 (2-Me), 20.9 (5-Me); HRMS (HRFAB): calcd. for C<sub>15</sub>H<sub>16</sub>OI [M – PF<sub>6</sub>]<sup>+</sup> 339.0246, 340.0279 found 339.0239, 340.0277.

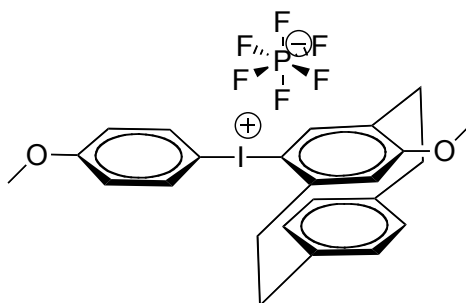


**([2.2]Paracyclophan-4-yl)(4'-methoxyphenyl)-iodonium hexafluorophosphate (4-13):**

In a 50 mL Schlenk tube under nitrogen, a stirred solution of 4-bromo[2.2]paracyclophane (1 mmol, 282 mg) in 10 mL of anhydrous diethyl ether was

cooled to -78 °C. A solution of t-BuLi (1.7 M in pentane, 2.3 equiv.) was added dropwise and the resulting mixture was stirred at -78 °C for 20 minutes and then warmed to 0 °C and allowed to stir for an additional 20 min. The reaction mixture was cooled again to -78 °C before a solution of zinc chloride (200 mg, 1.5 mmol) in ether (10 mL) was added dropwise by cannula. After the addition, the reaction mixture was allowed to warm to room temperature over the course of one hour before the solvents were removed in vacuo. The remaining solid was dissolved in anhydrous CH<sub>3</sub>CN and the solution was cooled to -40 °C and added dropwise to precooled (-40 °C) suspension of bis(acetyloxy)-(4-methoxyphenyl)-λ<sup>3</sup>-iodane (352 mg, 1 mmol) in 10 mL of acetonitrile. The mixture was allowed to warm to room temperature over 30 minutes before the solvent was removed in vacuo. The resulting solid was washed with hexanes and then dissolved in aqueous acetonitrile. Addition of an aqueous NaPF<sub>6</sub> solution precipitated the product, which was extracted from the aqueous mixture with CH<sub>2</sub>Cl<sub>2</sub>. The organic layer was evaporated, dissolved in a minimal amount of CH<sub>2</sub>Cl<sub>2</sub>, precipitated with hexanes, filtered and dried *in vacuo* to yield 225 mg (38.4 %) of ([2.2]paracyclophan-4-yl)(4'-methoxyphenyl)-iodonium hexafluorophosphate). <sup>1</sup>H NMR (CD<sub>3</sub>CN, 400 MHz, 25 °C): δ 8.00 (d, J = 9.1 Hz, 2 H), 7.27 (s, 1 H), 7.08 (d, J = 9.1 Hz, 2 H), 6.83 (d, J = 7.7 Hz, 1 H), 6.76 (d, J = 7.7 Hz, 1 H), 6.65 (s (broad), 2 H), 6.8 (d, J = 7.9 Hz, 1 H), 6.31 (d, J = 7.9 Hz, 1 H), 3.84 (s, 3 H), 3.04-3.35 (m, 8 H); <sup>13</sup>C NMR (CD<sub>3</sub>CN, 100 MHz, 25 °C) δ 164.1, 143.2, 140.9, 139.8, 139.4, 139.2, 138.8, 137.6, 134.3, 134.2, 133.7, 132.4, 120.9, 119.4, 100.8, 56.7, 38.4, 35.6, 35.4, 35.3; HRMS: (HRFAB) calcd. for C<sub>23</sub>H<sub>22</sub>OI [M]<sup>+</sup> 441.07098, found 441.0712.

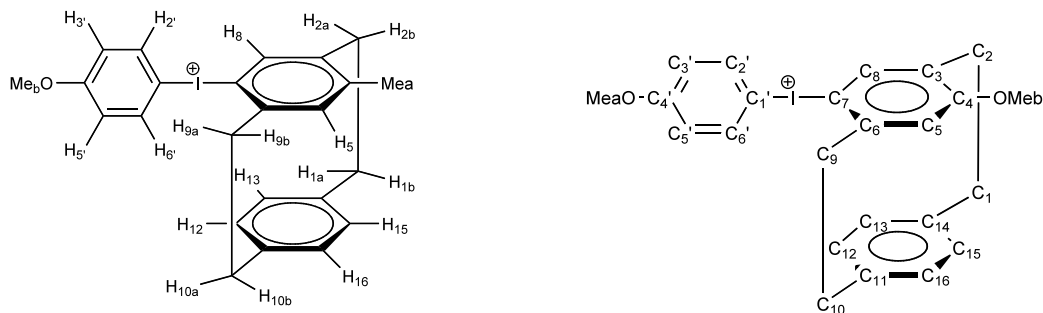




**(7-Methoxy[2.2]paracyclophane-4-yl)(4'-methoxyphenyl)-iodonium**

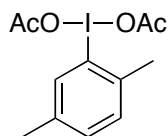
**hexafluorophosphate (4-14):** In a 100 mL Schlenk tube, 4-methoxy-7-bromo[2.2]paracyclophane (1.26 mmol, 400.6 mg) was dissolved in 25 mL of distilled ether and cooled to -78 °C. To the cooled solution, 1.7M t-butyl lithium (3.16 mmol, 1.85 mL) was added dropwise and the stirred solution was held at -78 °C for 1 hour. A solution of anhydrous zinc chloride (1.51 mmol, 206.1 mg) in 10 mL of diethyl ether was added dropwise to the cooled solution. The mixture was allowed to warm to room temperature, and the solvent was removed under reduced pressure. The residual solid (organozinc chloride reagent and lithium salts) was taken up in anhydrous acetonitrile and cooled to -40 °C before a solution of 4-methoxyphenyl iodonium diacetate (1.89 mmol, 665.5 mg) in acetonitrile (10 mL) was added in a dropwise fashion. After 1 hour at -40 °C, the mixture was warmed to room temperature and the solvent was removed under reduced pressure. Deionized water and sodium hexafluorophosphate (410 mg) were added, followed by 50 mL of dichloromethane. The mixture was transferred to a separatory funnel and the organic phase was separated. The solvent was removed by rotary evaporation and the remaining solid was dissolved in 5 mL of dichloromethane and dripped into 150 mL hexanes. The precipitate was aged for one hour, collected by

gravity filtration, and dried *in vacuo* to yield 431.7 mg (55.6 %), (7-methoxy[2.2]paracyclophane-4-yl)(4'-methoxyphenyl)-iodonium hexafluorophosphate.

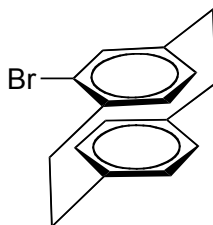


$^1\text{H}$  NMR ( $\text{CD}_3\text{CN}$ , 400 MHz, 25 °C):  $\delta$  8.01 (d,  $J$  = 9.2 Hz, 2 H, H2', H6'), 7.25 (s, 1 H, H8), 7.07 (d,  $J$  = 9.2 Hz, 2 H, H3', H5'), 6.81 (dd,  $J$  = 7.8, 1.8 Hz, 1 H, H15), 6.62 (dd,  $J$  = 7.9, 1.9 Hz, 1 H, H16), 6.29 (dd,  $J$  = 7.9, 1.6 Hz, 1 H, H13), 6.12 (dd,  $J$  = 8.0, 2.0 Hz, 1 H, H12), 6.02 (s, 1 H, H5), 3.83 (s, 3 H, Me<sub>b</sub>), 3.74 (s, 3 H, Me<sub>a</sub>), 3.31 (ddd,  $J$  = 11.6, 9.8, 1.7 Hz, 1 H, H2a), 3.26 (dd,  $J$  = 8.4, 5.7 Hz, 1 H, H9b), 3.23 (dd,  $J$  = 13.9, 4.3 Hz, 1 H, H9a), 3.18 (dd,  $J$  = 12.9, 4.1 Hz, 1 H, H10b), 3.15 (dd,  $J$  = 8.3, 3.0 Hz, 1 H, H10a), 3.05 (ddd,  $J$  = 12.8, 9.9, 6.4 Hz, 1 H, H1a), 3.02 (ddd,  $J$  = 12.8, 9.9, 6.4 Hz, 1 H, H1b), 2.68 (ddd,  $J$  = 13.1, 10.5, 6.4 Hz, 1 H, H2b).  $^{13}\text{C}$  NMR ( $\text{CD}_3\text{CN}$ , 100 MHz, 25 °C):  $\delta$  163.3 (C4), 161.6 (C4'), 146.4 (C6), 140.5 (C8), 139.9 (C11), 137.9 (C14), 137.4 (C2', C6'), 133.2 (C13), 132.4 (C3), 131.4 (C12), 131.3 (C16), 128.8 (C15), 119.8 (C5), 118.2 (C3', C5'), 107.4 (C7), 101.1 (C1'), 55.8 (Me<sub>b</sub>), 54.9 (Me<sub>a</sub>), 37.2 (C9), 34.5 (C10), 32.9 (C1), 30.7 (C2).  $^{19}\text{F}$  NMR ( $\text{CD}_3\text{CN}$ , 376 MHz, 25 °C):  $\delta$  -72.7 (d,  $J$  = 706.7 Hz, 6 F). HRMS:

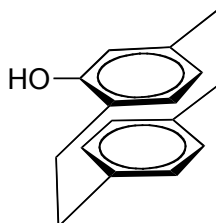
(HRFAB) calcd. for  $C_{24}H_{24}IO_2$   $[M]^+$  471.08210 (100 %), 472.08454 (26 %); found 471.08221 (100 %), 472.08561 (23 %).



**Bis(acetyloxy)-(2,5-dimethylphenyl)- $\lambda^3$ -iodane:** 2,5-Dimethyliodobenzene (2.32 g, 10 mmol) was dissolved in 90 mL of glacial acetic acid and the stirred solution was warmed to 40 °C. Sodium perborate tetrahydrate (13.6 g, 110 mmol) was added in portions over the course of one hour. After the addition was complete, the temperature of the reaction mixture was maintained at 40 °C for 8 h before it was allowed to cool to room temperature. Half of the acetic acid (~ 45 mL) was removed by distillation at reduced pressure. The remaining solution was treated with 100 mL of deionized water and the aqueous layer was extracted ( $3 \times 40$  mL) with dichloromethane. The combined organic fractions were dried over sodium sulfate, and the solvent was removed by rotary evaporation to give 1.44 g (41 %) of 1-(diacetoxyiodo)-2,5-dimethylbenzene. This compound was recrystallized in dry acetonitrile, dried in vacuo, and used without further purification.  $^1H$  NMR ( $CD_2Cl_2$ , 400 MHz, 25 °C):  $\delta$  7.98 (s, 1 H), 7.41 (d,  $J = 7.9$  Hz, 1 H), 7.32 (d,  $J = 7.9$  Hz, 1 H), 2.63 (s, 3 H), 2.37 (s, 3 H), 1.95 (s, 6 H);  $^{13}C$  NMR ( $CD_2Cl_2$ , 100 MHz, 25 °C)  $\delta$  176.4, 138.7, 137.5, 137.4, 133.5, 130.3, 126.3, 24.7, 20.3, 20.0; HRMS: (HRFAB) calcd. for  $C_{15}H_{15}NO_3I$   $[M - 2OAc + 3-NBA]^+$  384.0097, found 384.0096.

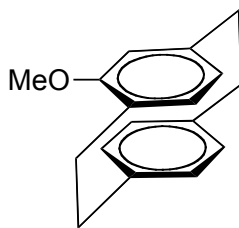


**4-Bromo[2.2]paracyclophane:**<sup>241</sup> N-Bromosuccinimide (890.1 mg, 5.0 mmol) and trifluoroacetic acid (570 mg, 0.385 mL, 5.0 mmol) were dissolved in 40 mL of dichloromethane and added to a CH<sub>2</sub>Cl<sub>2</sub> solution (80 mL) of [2.2]paracyclophane (1.0297 g, 4.9 mmol). The resulting mixture was covered from light and stirred for 4 hours at room temperature. The solution was transferred to a separatory funnel and washed (3 x 50 mL) with 2 M aqueous sodium bicarbonate solution followed by a single deionized water wash. The organic layer was separated, dried over Na<sub>2</sub>SO<sub>4</sub>, and the solvent was evaporated to give 4-bromo[2.2]paracyclophane as a nearly colorless solid (1.061 g, 75 %) that was sufficiently pure to carry forward in the synthesis. <sup>1</sup>H NMR (CDCl<sub>3</sub>, 400 MHz, 25 °C): δ 7.18 (dd, J = 7.8, 1.9 Hz, 1 H), 6.45-6.61 (m, 6 H), 3.45-3.52 (m, 1 H), 2.80-3.26 (m, 7 H); <sup>13</sup>C NMR (CDCl<sub>3</sub>, 100 MHz, 25 °C) δ 141.61, 139.33, 139.11, 137.25, 135.05, 133.31, 133.02, 132.91, 132.25, 131.46, 128.69, 126.97, 35.85, 35.48, 34.82, 33.47.



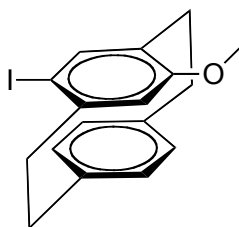
**4-Hydroxy[2.2]paracyclophane:**<sup>242</sup> In a 50 mL Schlenk tube under nitrogen, a stirred, cold (-78 °C) solution of 4-bromo[2.2]paracyclophane (4.0 mmol, 1.14 g) in 50 mL of

anhydrous diethyl ether was treated with t-BuLi (1.7 M in pentane, 2.5 equiv., added dropwise). The resulting mixture was stirred at -78 °C for 20 minutes and held subsequently at 0 °C for 20 min. To this heterogeneous yellow mixture trimethyl borate (831.29 mg, 8.0 mmol) was added dropwise by cannula transfer and the mixture was stirred for 1 hour at room temperature. During this period the solution became homogeneous and dark yellow. Aqueous NaOH (0.5 M, 2 mL) and H<sub>2</sub>O<sub>2</sub> (30 %, 1.5 mL) were added. The resulting mixture was allowed to stir overnight at room temperature. Additional aqueous NaOH solution (0.5 M, 5 mL) was added and the pH of the solution was adjusted to neutral using saturated sodium bicarbonate solution and 1 M HCl. The mixture was extracted (3 x 20 mL) with diethyl ether. The combined ether extracts were washed with 0.5 M sodium bisulfite, separated, and dried over Na<sub>2</sub>SO<sub>4</sub>. Removal of the solvent by rotary evaporation gave 4-hydroxy[2.2]paracyclophane as a light brown solid (844.1 mg, 94.1 %). <sup>1</sup>H NMR (CDCl<sub>3</sub>, 400 MHz, 25 °C): δ 7.01 (dd, J = 7.8, 1.9 Hz, 1 H), 6.56 (dd, J = 7.8, 1.9 Hz, 1 H), 6.46 (dd, J = 7.8, 1.9 Hz, 1 H), 6.38-6.42 (m, 2 H), 6.27 (dd, J = 7.7, 1.6 Hz, 1 H), 5.55 (d, J = 1.6 Hz, 1 H), 3.29-3.39 (m, 1 H), 2.87-3.16 (m, 6 H), 2.62-2.73 (m, 1 H). <sup>13</sup>C NMR (CDCl<sub>3</sub>, 100 MHz, 25 °C): δ 153.7, 142.0, 139.6, 138.8, 133.6, 133.0, 132.8, 131.9, 127.9, 125.4, 125.0, 122.6, 35.3, 34.8, 33.8, 31.1.



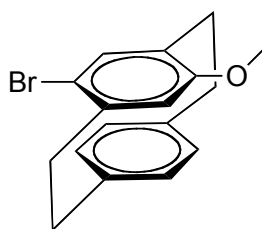
**4-Methoxy[2.2]paracyclophane:**<sup>241</sup> In a 100 mL glass tube sealed with a Teflon screw cap closure, potassium carbonate (1.66 g, 12 mmol) and 4-hydroxy[2.2]paracyclophane

(869.6 mg, 3.87 mmol) were heated to 80 °C in 60 mL of acetonitrile for 30 minutes. Iodomethane (1.7 g, 12 mmol) was added to the mixture, the storage tube was sealed, and the stirred solution was heated at 80 °C for 3 days. The solvent was removed by rotary evaporation and the remaining solid was treated with ethyl acetate and water and transferred to a separatory funnel. The aqueous layer was neutralized with 0.1 M HCl solution, the mixture was shaken, and the organic layer was separated and dried over Na<sub>2</sub>SO<sub>4</sub>. Rotary evaporation of solvent yielded a nearly colorless solid. The somewhat insoluble material was dissolved in hot hexanes and purified via column chromatography (silica gel, hexanes,  $R_f$  = 0.28) to afford 4-methoxy[2.2]paracyclophane as a colorless solid (602.4 mg, 65.4 %). <sup>1</sup>H NMR (CDCl<sub>3</sub>, 400 MHz, 25 °C):  $\delta$  6.76 (dd,  $J$  = 7.8, 1.8 Hz, 1 H), 6.38 – 6.55 (m, 4 H), 6.28 (dd,  $J$  = 7.5, 1.4 Hz, 1 H), 5.67 (d,  $J$  = 1.3, 1 H), 3.71 (s, 3 H), 3.42 – 3.48 (m, 1 H), 2.99 – 3.13 (m, 6 H), 2.59 – 2.66 (m, 1 H). <sup>13</sup>C NMR (CDCl<sub>3</sub>, 100 MHz, 25 °C):  $\delta$  157.6, 142.1, 140.3, 138.8, 135.0, 133.7, 133.1, 131.5, 128.4, 127.5, 124.4, 116.7, 54.3, 35.5, 35.4, 34.1, 31.7.



**4-Methoxy-7-iodo[2.2]paracyclophane:** In a 100 mL round bottom flask, a solution of 4-methoxy[2.2]paracyclophane (0.8 mmol, 192.3 mg) in CH<sub>2</sub>Cl<sub>2</sub> (25 mL) of CH<sub>2</sub>Cl<sub>2</sub> was treated with a solution of N-iodosuccinimide (0.648 mmol, 145.2 mg) and trifluoroacetic acid (0.648 mmol, 75.3 mg) in 25 mL of dichloromethane. The resulting mixture was stirred for 5 minutes and the dark purple color of iodine developed. The solution was

transferred to a separatory funnel and washed (3 x 50 mL) with 2 M aqueous sodium bicarbonate solution followed by a single deionized water wash. The organic layer was separated, dried over Na<sub>2</sub>SO<sub>4</sub>, and the solvent was evaporated to give 4-methoxy-7-iodo[2.2]paracyclophane as an off-white solid (295.0 mg, 99 %). <sup>1</sup>H NMR (CDCl<sub>3</sub>, 400 MHz, 25 °C): δ 7.13 (dd, J = 7.9, 1.8 Hz, 1 H), 6.75 (dd, J = 7.9, 1.8 Hz, 1 H), 6.71 (s, 1 H), 6.46 (dd, J = 7.9, 1.8, 1 H), 6.40 (dd, J = 7.8, 1.8 Hz, 1 H), 5.69 (s, 1 H), 3.68 (s, 3 H), 2.82-3.37 (m, 7 H), 2.43-2.53 (m, 1 H). <sup>13</sup>C NMR (CDCl<sub>3</sub>, 100 MHz, 25 °C): δ 157.9, 144.7, 143.9, 139.9, 138.5, 132.9, 131.5, 129.9, 129.6, 128.9, 117.7, 91.9, 54.3, 39.3, 33.6, 33.2, 31.1.



**4-Methoxy-7-bromo[2.2]paracyclophane:**<sup>243</sup> N-Bromosuccinimide (279.4 mg, 1.57 mmol) and trifluoroacetic acid (179.0 mg, 0.12 mL, 1.57 mmol) were dissolved in 15 mL of CH<sub>2</sub>Cl<sub>2</sub> and added to a solution of 4-methoxy[2.2]paracyclophane (349.7 g, 1.47 mmol) in 30 mL CH<sub>2</sub>Cl<sub>2</sub>. The resulting mixture was covered from light and stirred for 30 minutes at room temperature. The solution was transferred to a separatory funnel and washed (3 x 50 mL) with 2 M aqueous sodium bicarbonate solution followed by a single deionized water wash. The organic layer was separated, dried over Na<sub>2</sub>SO<sub>4</sub>, and the solvent was evaporated to give 4-methoxy-7-bromo[2.2]paracyclophane as a light brown solid (400.6 mg, 86 %). <sup>1</sup>H NMR (CDCl<sub>3</sub>, 400 MHz, 25 °C): δ 7.10 (dd, J = 7.8, 1.8 Hz, 1 H), 6.76 (dd, J = 7.9, 1.9 Hz, 1 H), 6.41 - 6.46 (m, 3 H), 5.69 (s, 1 H), 3.71 (s, 3 H), 3.34 -

3.45 (m, 2 H), 3.18 - 3.25 (m, 1 H), 2.98 – 3.10 (m, 3 H), 2.71 – 2.78 (m, 1 H), 2.46 – 2.54 (m, 1 H);  $^{13}\text{C}$  NMR ( $\text{CDCl}_3$ , 100 MHz, 25 °C)  $\delta$  157.15, 140.81, 139.95, 138.76, 138.65, 133.19, 133.16, 131.83, 130.00, 129.19, 118.54, 117.26, 54.69, 35.89, 33.82, 33.51, 31.29.



## APPENDIX A

### List of Nuclear Magnetic Resonance Spectra

Spectrum 1 $^1\text{H}$ and $^{13}\text{C}$ NMR spectra of N,N-diisobutyl-N-methyl-2-methoxyanilinium triflate in $\text{d}_6\text{-DMSO}$ .....	242
Spectrum 2 $^1\text{H}$ and $^{13}\text{C}$ NMR spectra of N,N-dimethyl-N-neopentyl-4-methoxyanilinium triflate in $\text{CD}_3\text{CN}$ .....	243
Spectrum 3 $^1\text{H}$ and $^{13}\text{C}$ NMR spectra of N,N-dipropyl-N-methyl-4-methoxyanilinium triflate in $\text{d}_6\text{-DMSO}$ .....	244
Spectrum 4 $^1\text{H}$ and $^{13}\text{C}$ NMR spectra of N,N-dibutyl-N-methyl-4-methoxyanilinium triflate in $\text{d}_6\text{-DMSO}$ .....	245
Spectrum 5 $^1\text{H}$ and $^{13}\text{C}$ NMR spectra of N,N,N-tributyl-2-methoxyanilinium triflate in $\text{d}_6\text{-DMSO}$ .....	246
Spectrum 6 $^1\text{H}$ and $^{13}\text{C}$ NMR spectra of N,N,N-trimethyl-2-methoxyanilinium triflate in $\text{d}_6\text{-DMSO}$ .....	247
Spectrum 7 $^1\text{H}$ and $^{13}\text{C}$ NMR spectra of N,N,N-triethyl-2-methoxyanilinium iodide in $\text{CD}_3\text{CN}$ .....	248
Spectrum 8 $^1\text{H}$ and $^{13}\text{C}$ NMR spectra of N,N-diisobutyl-N-methyl-2,4-dimethoxyanilinium triflate in $\text{d}_6\text{-DMSO}$ .....	249
Spectrum 9 $^1\text{H}$ and $^{13}\text{C}$ NMR spectra of N,N,N-tributyl-2,4-dimethoxyanilinium triflate in $\text{d}_6\text{-DMSO}$ .....	250

Spectrum 10 $^1\text{H}$ and $^{13}\text{C}$ NMR spectra of N,N,N-trimethyl-2,4-dimethoxyanilinium triflate in $\text{d}_6$ -DMSO.....	251
Spectrum 11 $^1\text{H}$ and $^{13}\text{C}$ NMR spectra of N,N,N-triethyl-2,4-dimethoxyanilinium iodide in $\text{CD}_3\text{CN}$ .....	252
Spectrum 12 $^1\text{H}$ and $^{13}\text{C}$ NMR spectra of N,N,N-trimethyl-2,5-dimethoxyanilinium triflate in $\text{d}_6$ -DMSO.....	253
Spectrum 13 $^1\text{H}$ and $^{13}\text{C}$ NMR spectra of N,N,N-triethyl-2,5-dimethoxyanilinium iodide in $\text{CD}_3\text{CN}$ .....	254
Spectrum 14 $^1\text{H}$ and $^{13}\text{C}$ NMR spectra of N,N,N-trimethyl-3,5-dimethoxyanilinium triflate in $\text{d}_6$ -DMSO.....	255
Spectrum 15 $^1\text{H}$ and $^{13}\text{C}$ NMR spectra of N,N,N-triethyl-3,5-dimethoxyanilinium iodide in $\text{CD}_3\text{CN}$ .....	256
Spectrum 16 $^1\text{H}$ and $^{13}\text{C}$ NMR spectra of bis(4-methoxyphenyl)-dimethylammonium triflate in $\text{d}_6$ -DMSO.....	257
Spectrum 17 $^1\text{H}$ and $^{13}\text{C}$ NMR spectra of N,N,N',N'-tetraisobutyl-N-methyl-phenylenediammonium triflate .....	258
Spectrum 18 $^1\text{H}$ and $^{13}\text{C}$ NMR spectra of N,N,N',N'-tetramethyl-N-isobutyl-phenylenediammonium triflate in $\text{d}_6$ -DMSO.....	259
Spectrum 19 $^1\text{H}$ and $^{13}\text{C}$ NMR spectra of N,N',N'-trineopentyl-N,N-dimethyl-phenylenediammonium triflate in $\text{d}_6$ -DMSO.....	260
Spectrum 20 $^1\text{H}$ and $^{19}\text{F}$ NMR spectra of trisisobutylmethylammonium triflate in $\text{d}_6$ -DMSO .....	261

Spectrum 21 $^1\text{H}$ and $^{19}\text{F}$ NMR spectra of trineopentylmethyllumonium fluoride in $\text{d}_6$ -DMSO .....	262
Spectrum 22 Pairwise HOESY study: TIBMA vs. TNPMA .....	263
Spectrum 23 Pairwise HOESY study: 4-(dimethylamino)-N,N,N-trimethylanilinium vs. 2-methoxy-N,N,N-trimethylanilinium .....	264
Spectrum 24 Pairwise HOESY study: 4-(dimethylamino)-N,N,N-trimethylanilinium Vs. 2,4-dimethoxy-N,N,N-trimethylanilinium .....	265
Spectrum 25 Pairwise HOESY study: TBA Vs. TNPMA .....	266
Spectrum 26 $^1\text{H}$ and $^{13}\text{C}$ NMR spectra of 2-methoxy-(diacetoxyiodo)benzene in $\text{d}_3$ -acetonitrile .....	267
Spectrum 27 $^1\text{H}$ and $^{13}\text{C}$ NMR spectra of 2,6-dimethoxy-(diacetoxyiodo)benzene in $\text{d}_3$ -acetonitrile .....	268
Spectrum 28 $^1\text{H}$ and $^{13}\text{C}$ NMR spectra of 3-cyano-(diacetoxyiodo)benzene in $\text{d}_3$ -acetonitrile .....	269
Spectrum 29 $^1\text{H}$ and $^{13}\text{C}$ NMR spectra of 3-trifluoromethyl-(diacetoxyiodo)benzene in $\text{d}_3$ -acetonitrile .....	270
Spectrum 30 $^1\text{H}$ and $^{13}\text{C}$ NMR spectra of (2-methoxyphenyl)(4'-methoxyphenyl)-iodonium hexafluorophosphate in $\text{d}_3$ -acetonitrile .....	271
Spectrum 31 $^1\text{H}$ and $^{13}\text{C}$ NMR spectra of (2,6-dimethoxyphenyl)(4'-methoxyphenyl)-iodonium hexafluorophosphate in $\text{d}_3$ -acetonitrile .....	272
Spectrum 32 $^1\text{H}$ and $^{13}\text{C}$ NMR spectra of (2-methyl-4,5-dimethoxyphenyl)(4'-methoxyphenyl)-iodonium hexafluorophosphate in $\text{d}_3$ -acetonitrile .....	273

Spectrum 33 $^1\text{H}$ and $^{13}\text{C}$ NMR spectra of (3,4-dimethoxyphenyl)(4'-methoxyphenyl)- iodonium hexafluorophosphate in $\text{d}_3$ -acetonitrile .....	274
Spectrum 34 $^1\text{H}$ and $^{13}\text{C}$ NMR spectra of phenyl(4-methoxyphenyl)-iodonium hexafluorophosphate in $\text{d}_3$ -acetonitrile .....	275
Spectrum 35 $^1\text{H}$ and $^{19}\text{F}$ NMR spectra of bis(4-methoxyphenyl)-fluoro- $\lambda^3$ -iodane in $\text{d}_3$ - acetonitrile.....	276
Spectrum 36 $^1\text{H}$ and $^{19}\text{F}$ NMR spectra of (3,4-dimethoxyphenyl)(4'-methoxyphenyl)- fluoro- $\lambda^3$ -iodane in $\text{d}_6$ -benzene .....	277
Spectrum 37 $^1\text{H}$ and $^{19}\text{F}$ NMR spectra of (2-methoxyphenyl)(4'-methoxyphenyl)-fluoro- $\lambda^3$ -iodane in $\text{d}_6$ -benzene .....	278
Spectrum 38 $^1\text{H}$ and $^{19}\text{F}$ NMR spectra of (2-methyl-4,5-dimethoxyphenyl)(4'- methoxyphenyl)-fluoro- $\lambda^3$ -iodane in $\text{d}_6$ -benzene.....	279
Spectrum 39 $^1\text{H}$ and $^{19}\text{F}$ NMR spectra of (2,6-dimethoxyphenyl)(4'-methoxyphenyl)- fluoro- $\lambda^3$ -iodane in $\text{d}_3$ -acetonitrile .....	280
Spectrum 40 $^1\text{H}$ and $^{19}\text{F}$ NMR spectra of phenyl(4-methoxyphenyl)-fluoro- $\lambda^3$ -iodane in $\text{d}_6$ -benzene.....	281
Spectrum 41 $^1\text{H}$ and $^{19}\text{F}$ NMR spectra of (3-cyanophenyl)(4'-methoxyphenyl)-fluoro- $\lambda^3$ - iodane in $\text{d}_3$ -acetonitrile .....	282
Spectrum 42 $^1\text{H}$ and $^{19}\text{F}$ NMR spectra of (3-(trifluoromethyl)phenyl)(4'- methoxyphenyl)-fluoro- $\lambda^3$ -iodane in $\text{d}_6$ -benzene.....	283
Spectrum 43 $^1\text{H}$ and $^{19}\text{F}$ NMR spectra of (4,5-dimethoxy-2-(2- phthalimidoethyl)phenyl)(4'-methoxyphenyl)-fluoro- $\lambda^3$ -iodane in $\text{d}_6$ -benzene.....	284

Spectrum 44 $^1\text{H}$ and $^{19}\text{F}$ NMR spectra of (3,17-dimethoxy- $\beta$ -estra-1,3,5(10)-trien-2-yl)(4'-methoxyphenyl)-fluoro- $\lambda^3$ -iodane in $\text{d}_6$ -benzene .....	285
Spectrum 45 $^1\text{H}$ and $^{13}\text{C}$ NMR spectra of (2-(2-(benzyl-( <i>tert</i> -butoxycarbonyl)amino)ethyl-4,5-dimethoxy)phenyl)(4'-methoxyphenyl)-iodonium triflate in $\text{d}_3$ -acetonitrile .....	286
Spectrum 46 $^1\text{H}$ and $^{13}\text{C}$ NMR spectra of (2-(2-(di( <i>tert</i> -butoxycarbonyl)amino)ethyl-4,5-dimethoxy)phenyl)(4'-methoxyphenyl)-iodonium triflate in $\text{d}_3$ -acetonitrile.....	287
Spectrum 47 $^1\text{H}$ NMR spectrum of bis(4-methoxyphenyl)-bromo- $\lambda^3$ -iodane decomposition in $\text{d}_6$ -benzene .....	288
Spectrum 48 $^1\text{H}$ NMR spectrum of bis(4-methoxyphenyl)-chloro- $\lambda^3$ -iodane decomposition in $\text{d}_6$ -benzene .....	289
Spectrum 49 $^1\text{H}$ NMR spectrum of bis(4-methoxyphenyl)-iodo- $\lambda^3$ -iodane decomposition in $\text{d}_6$ -benzene.....	290
Spectrum 50 $^1\text{H}$ NMR spectrum of bis(4-methoxyphenyl)-azido- $\lambda^3$ -iodane decomposition in $\text{d}_6$ -benzene.....	291
Spectrum 51 $^1\text{H}$ NMR spectrum of bis(4-methoxyphenyl)-cyanato- $\lambda^3$ -iodane decomposition in $\text{d}_6$ -benzene .....	292
Spectrum 52 $^1\text{H}$ NMR spectrum of bis(4-methoxyphenyl)-thiocyanato- $\lambda^3$ -iodane decomposition in $\text{d}_6$ -benzene .....	293
Spectrum 53 $^1\text{H}$ NMR spectrum of bis(4-methoxyphenyl)-(2,2,2-trifluoroethoxy)- $\lambda^3$ -iodane decomposition in $\text{d}_6$ -benzene .....	294

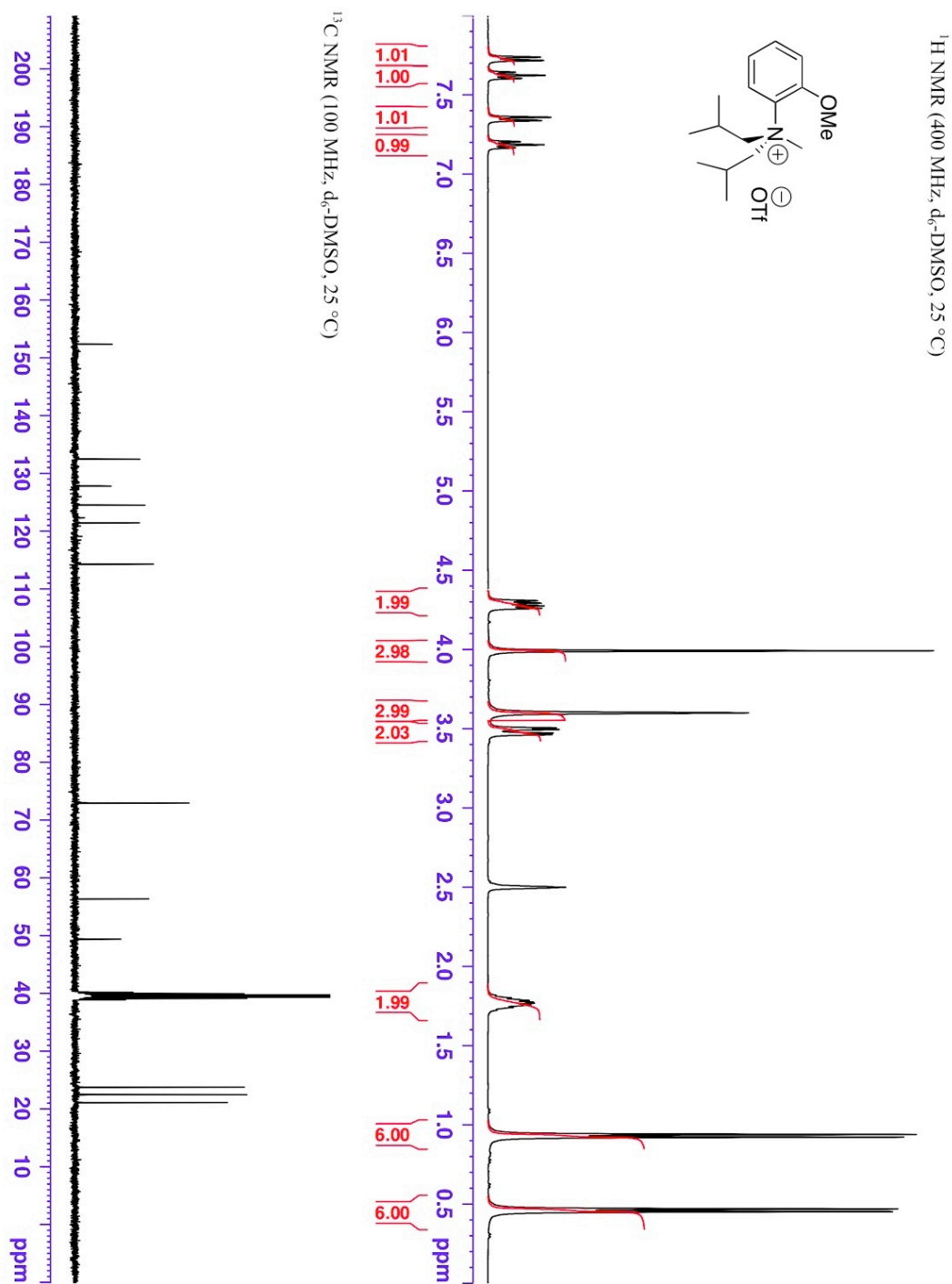
Spectrum 54 $^1\text{H}$ NMR spectrum of bis(4-methoxyphenyl)-phenoxy- $\lambda^3$ -iodane decomposition in $\text{d}_6$ -benzene .....	295
Spectrum 55 $^1\text{H}$ NMR spectrum of bis(4-methoxyphenyl)-phenylthio- $\lambda^3$ -iodane decomposition in $\text{d}_6$ -benzene .....	296
Spectrum 56 $^1\text{H}$ NMR spectrum of bis(4-methoxyphenyl)-acetoxy- $\lambda^3$ -iodane decomposition in $\text{d}_6$ -benzene .....	297
Spectrum 57 $^1\text{H}$ NMR spectrum of bis(4-methoxyphenyl)-(2,2,2-trifluoroacetoxy)- $\lambda^3$ -iodane decomposition in $\text{d}_6$ -benzene .....	298
Spectrum 58 $^1\text{H}$ NMR spectrum of bis(4-methoxyphenyl)-triflyl- $\lambda^3$ -iodane decomposition in $\text{d}_6$ -benzene.....	299
Spectrum 59: $^1\text{H}$ and $^{13}\text{C}$ NMR spectra of (2,5-dimethylphenyl)(4'-methoxyphenyl)-iodonium hexafluorophosphate in $\text{CD}_3\text{CN}$ .....	300
Spectrum 60 $^1\text{H}$ and $^{13}\text{C}$ NMR spectra of ([2.2]paracyclophan-4-yl)(2',5'-dimethylphenyl)-iodonium hexafluorophosphate in $\text{CD}_3\text{CN}$ .....	301
Spectrum 61: $^1\text{H}$ and $^{13}\text{C}$ NMR spectra of ([2.2]paracyclophan-4-yl)(4'-methylphenyl)-iodonium hexafluorophosphate in $\text{CD}_3\text{CN}$ .....	302
Spectrum 62: $^1\text{H}$ and $^{13}\text{C}$ NMR spectra of (7-methoxy-[2.2]paracyclophan-4-yl)(4'-methylphenyl)-iodonium hexafluorophosphate in $\text{CD}_3\text{CN}$ .....	303
Spectrum 63 HMQC spectra of ([2.2]paracyclophan-4-yl)(4'-methylphenyl)-iodonium hexafluorophosphate in $\text{CD}_3\text{CN}$ .....	304
Spectrum 64: COSY spectra of (7-methoxy-[2.2]paracyclophan-4-yl)(4'-methylphenyl)-iodonium hexafluorophosphate in $\text{CD}_3\text{CN}$ .....	305

Spectrum 65: HSQC spectra of (7-methoxy-[2.2]paracyclophan-4-yl)(4'-methylphenyl)- iodonium hexafluorophosphate in CD <sub>3</sub> CN .....	306
Spectrum 66: HSQC spectra of (7-methoxy-[2.2]paracyclophan-4-yl)(4'-methylphenyl)- iodonium hexafluorophosphate in CD <sub>3</sub> CN -aliphatic region.....	307
Spectrum 67: HSQC spectra of (7-methoxy-[2.2]paracyclophan-4-yl)(4'-methylphenyl)- iodonium hexafluorophosphate in CD <sub>3</sub> CN-aromatic region.....	308
Spectrum 68: HMBC-HSQC spectra of (7-methoxy-[2.2]paracyclophan-4-yl)(4'- methylphenyl)-iodonium hexafluorophosphate in CD <sub>3</sub> CN .....	309
Spectrum 69: NOEST spectra of (7-methoxy-[2.2]paracyclophan-4-yl)(4'-methylphenyl)- iodonium hexafluorophosphate in CD <sub>3</sub> CN .....	310
Spectrum 70: NOESY spectra of (7-methoxy-[2.2]paracyclophan-4-yl)(4'- methylphenyl)-iodonium hexafluorophosphate in CD <sub>3</sub> CN- aliphatic Vs aliphatic .....	311
Spectrum 71: NOESY spectra of (7-methoxy-[2.2]paracyclophan-4-yl)(4'- methylphenyl)-iodonium hexafluorophosphate in CD <sub>3</sub> CN-aromatic Vs aliphatic.....	312
Spectrum 72: NEOSY spectra of (7-methoxy-[2.2]paracyclophan-4-yl)(4'- methylphenyl)-iodonium hexafluorophosphate in CD <sub>3</sub> CN-aromatic Vs aromatic.....	313
Spectrum 73: <sup>1</sup> H NMR spectrum of the reaction mixture of salt 1+TBAN <sub>3</sub> (CHAPTER 4) .....	314
Spectrum 74: <sup>1</sup> H NMR spectrum of the reaction mixture of salt 2+TBAN <sub>3</sub> (CHAPTER 4) .....	315
Spectrum 75: <sup>1</sup> H NMR spectrum of the reaction mixture of salt 3+TBAN <sub>3</sub> (CHAPTER 4) .....	316

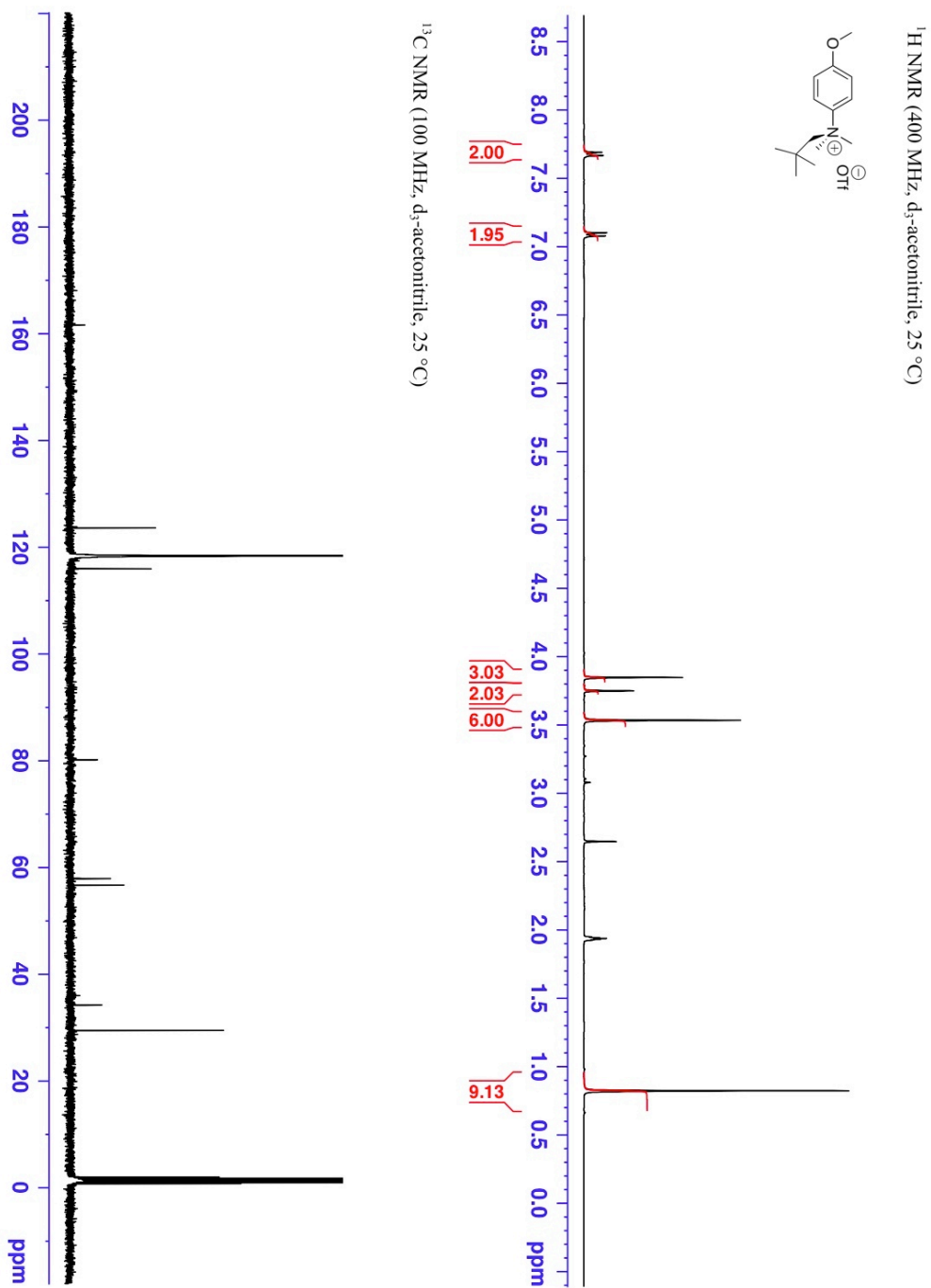
Spectrum 76: $^1\text{H}$ NMR spectrum of the reaction mixture of salt 4+TBAN <sub>3</sub> (CHAPTER 4)	
.....	317
Spectrum 77: $^1\text{H}$ NMR spectrum of the reaction mixture of salt 1+NaOPh (CHAPTER 4)	
.....	318
Spectrum 78: $^1\text{H}$ NMR spectrum of the reaction mixture of salt 2+NaOPh (CHAPTER 4)	
.....	319
Spectrum 79: $^1\text{H}$ NMR spectrum of the reaction mixture of salt 3+NaOPh (CHAPTER 4)	
.....	320
Spectrum 80: $^1\text{H}$ NMR spectrum of the reaction mixture of salt 4+NaOPh (CHAPTER 4)	
.....	321



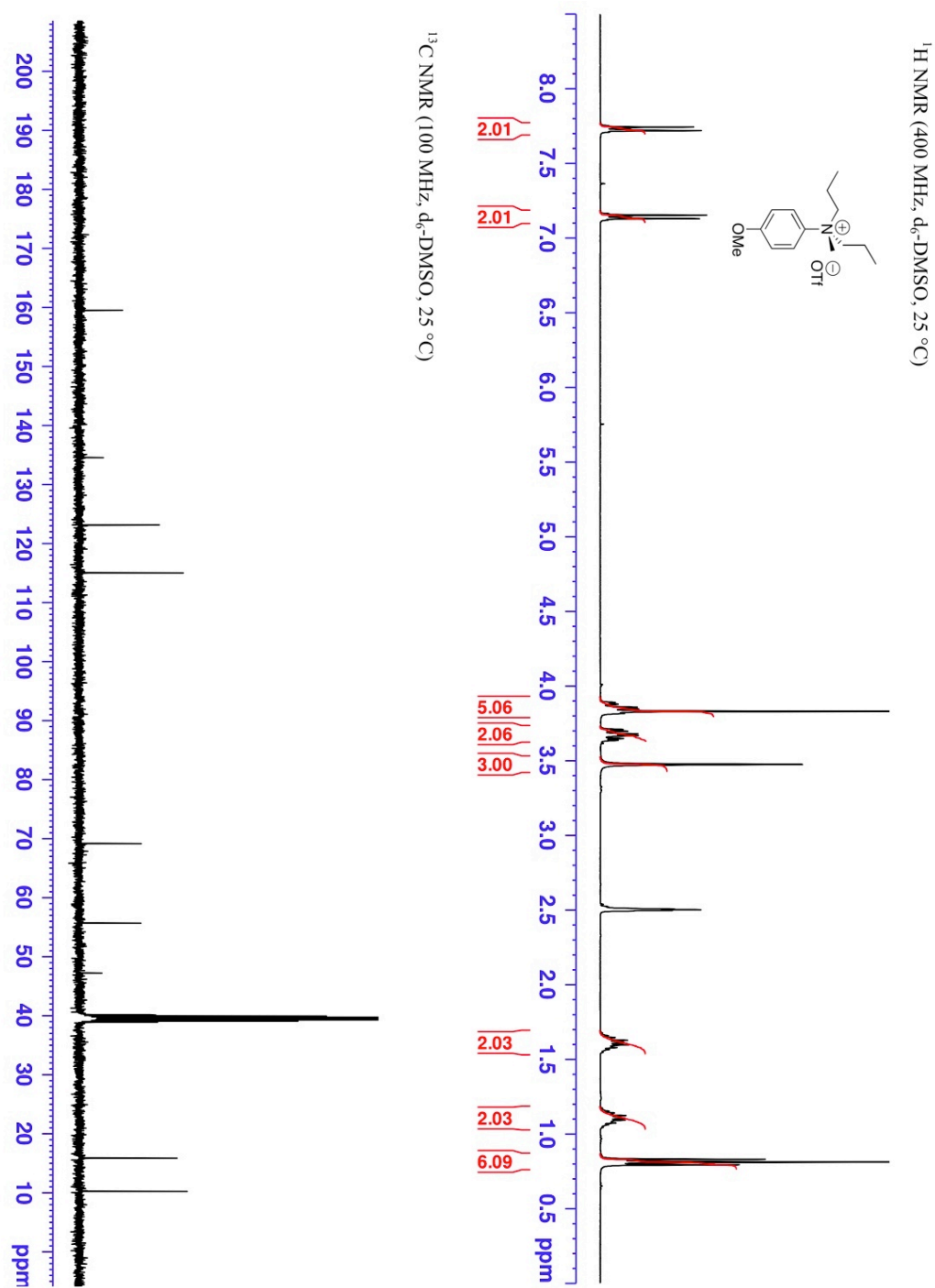
Spectrum 1  $^1\text{H}$  and  $^{13}\text{C}$  NMR spectra of N,N-diisobutyl-N-methyl-2-methoxyanilinium triflate in  $\text{d}_6\text{-DMSO}$



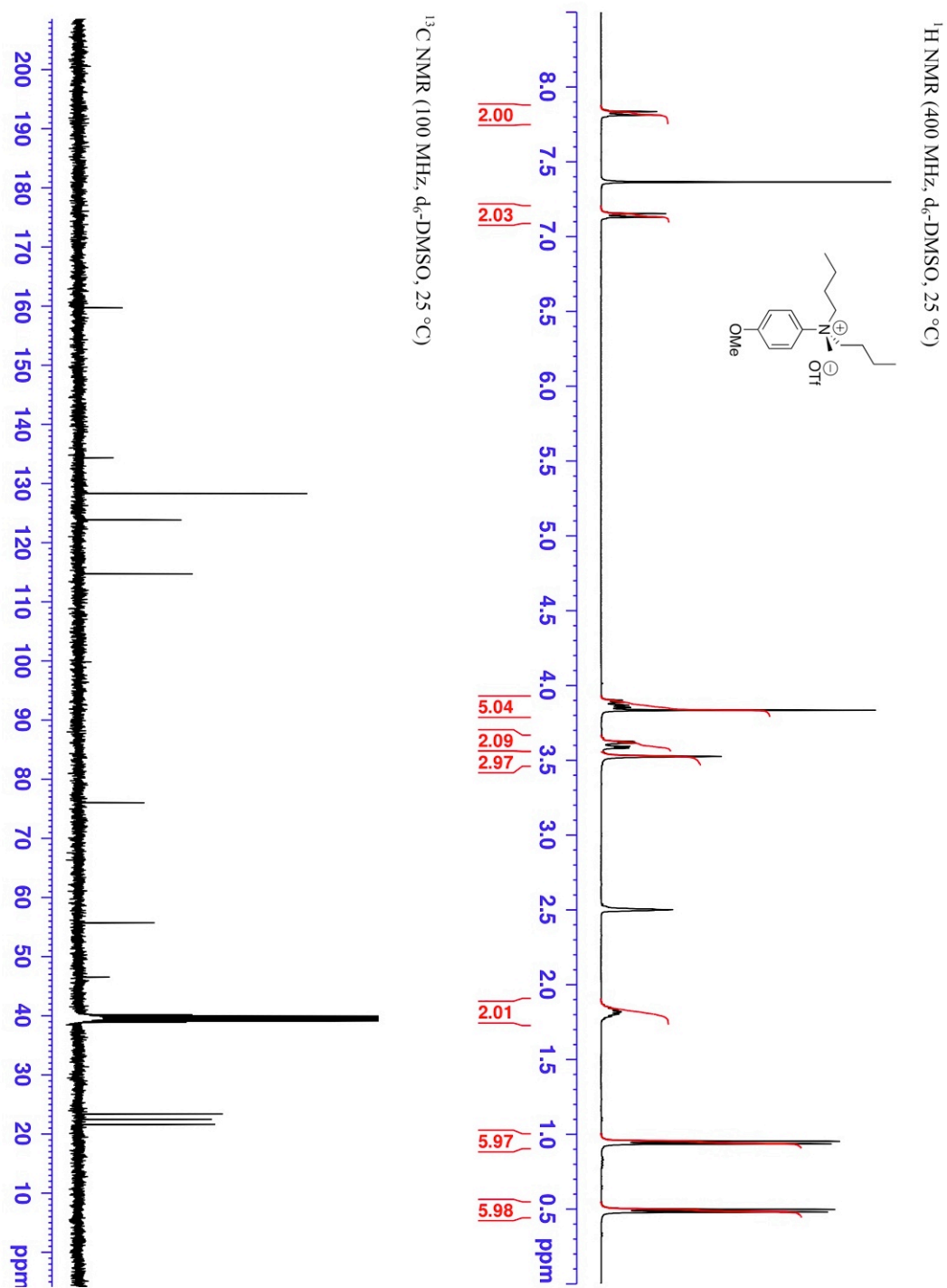
Spectrum 2  $^1\text{H}$  and  $^{13}\text{C}$  NMR spectra of N,N-dimethyl-N-neopentyl-4-methoxyanilinium triflate in  $\text{CD}_3\text{CN}$



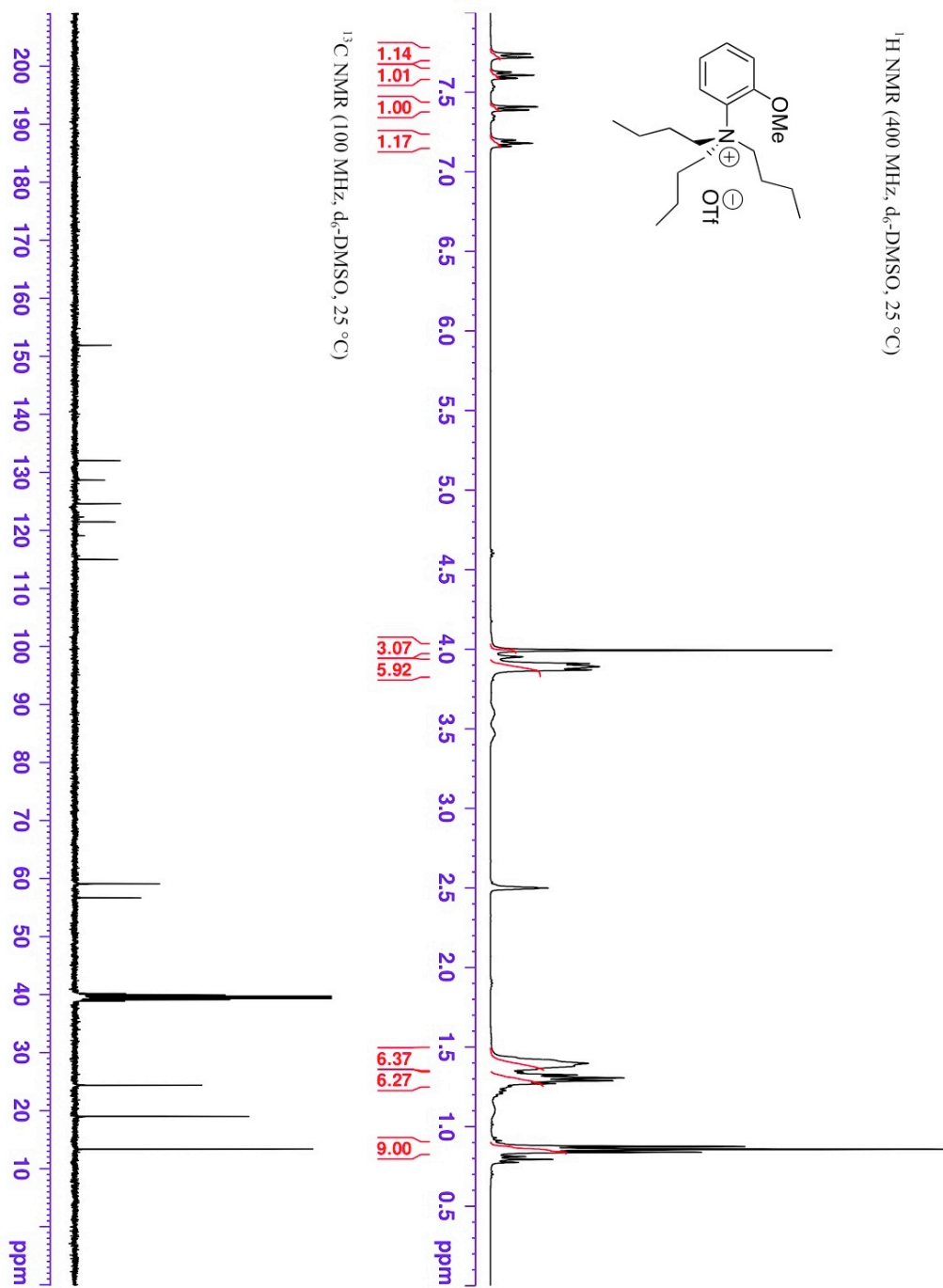
Spectrum 3  $^1\text{H}$  and  $^{13}\text{C}$  NMR spectra of N,N-dipropyl-N-methyl-4-methoxyanilinium triflate in  $\text{d}_6\text{-DMSO}$



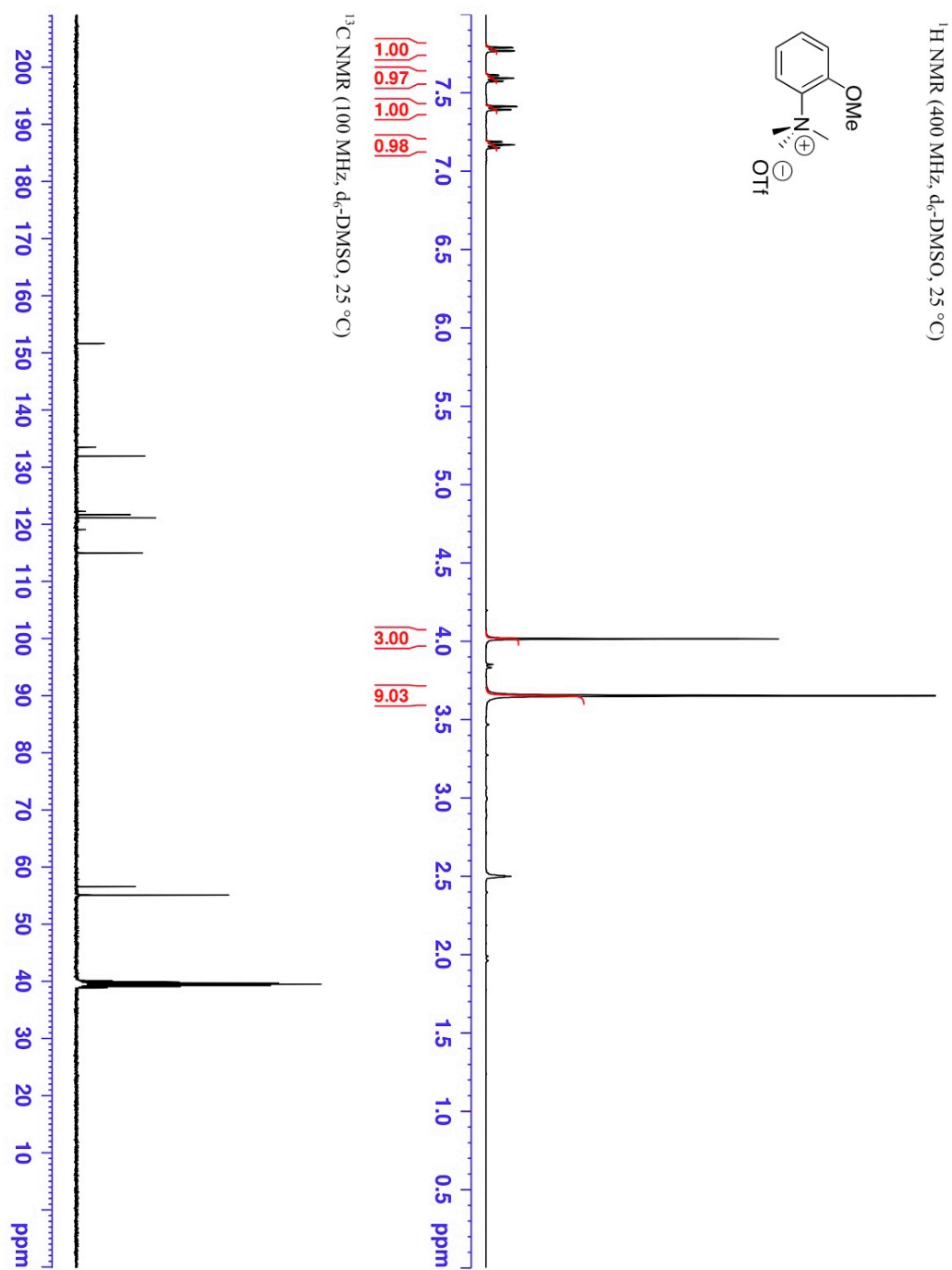
Spectrum 4  $^1\text{H}$  and  $^{13}\text{C}$  NMR spectra of N,N-dibutyl-N-methyl-4-methoxyanilinium triflate in  $\text{d}_6\text{-DMSO}$



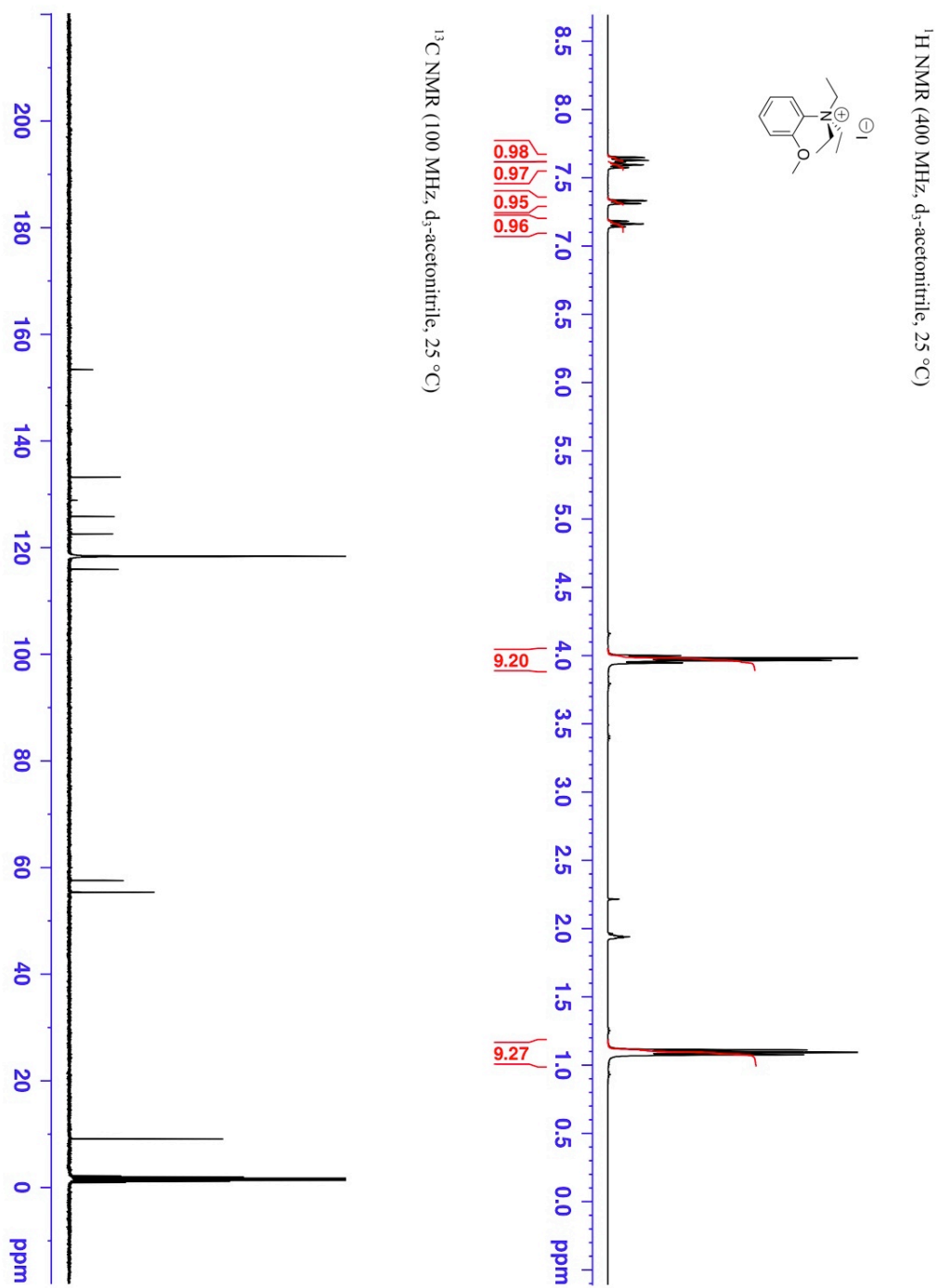
Spectrum 5  $^1\text{H}$  and  $^{13}\text{C}$  NMR spectra of N,N,N-tributyl-2-methoxyanilinium triflate in  $\text{d}_6$ -DMSO



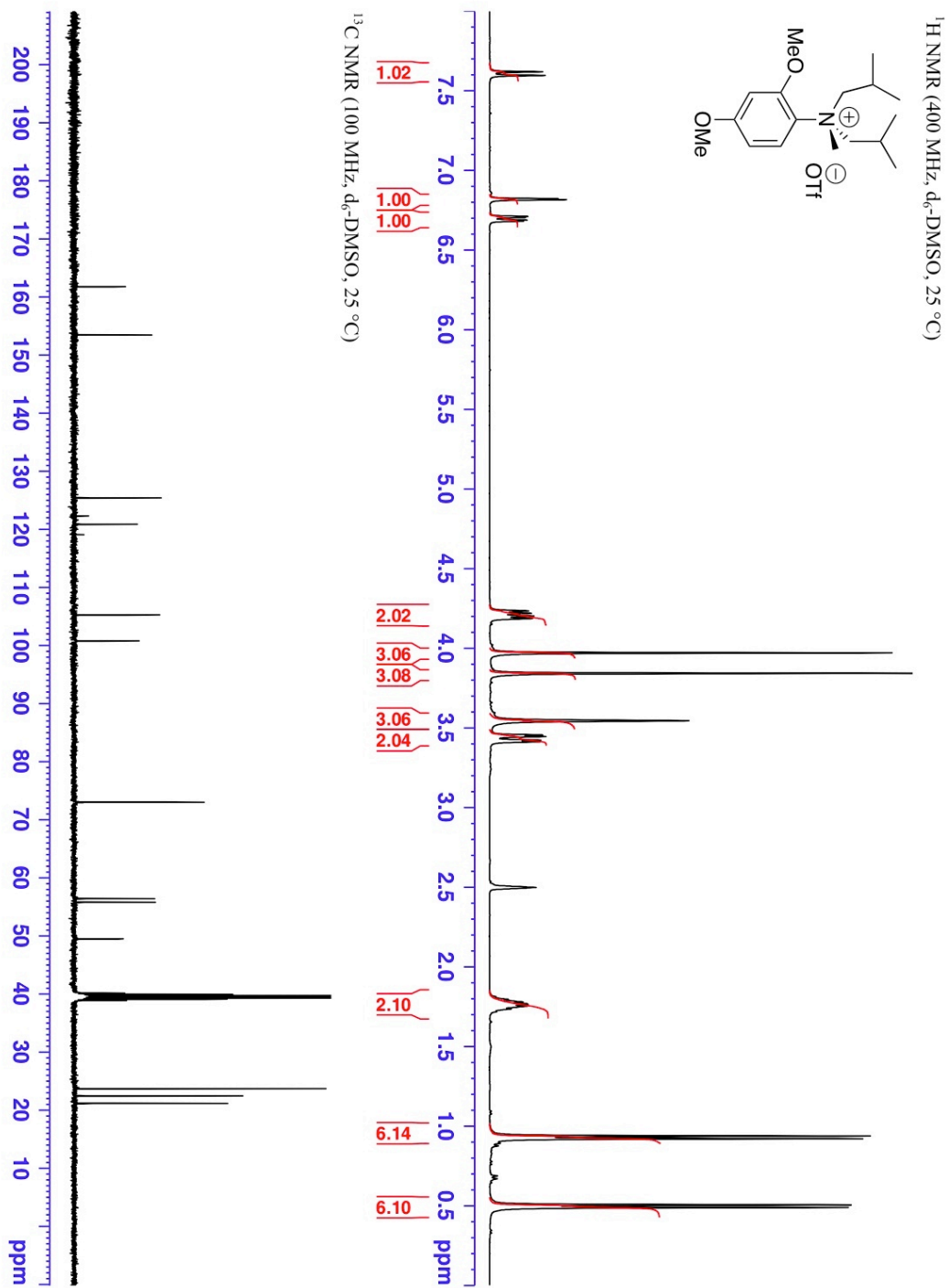
Spectrum 6  $^1\text{H}$  and  $^{13}\text{C}$  NMR spectra of N,N,N-trimethyl-2-methoxyanilinium triflate in  $\text{d}_6$ -DMSO



Spectrum 7  $^1\text{H}$  and  $^{13}\text{C}$  NMR spectra of N,N,N-triethyl-2-methoxyanilinium iodide in  $\text{CD}_3\text{CN}$

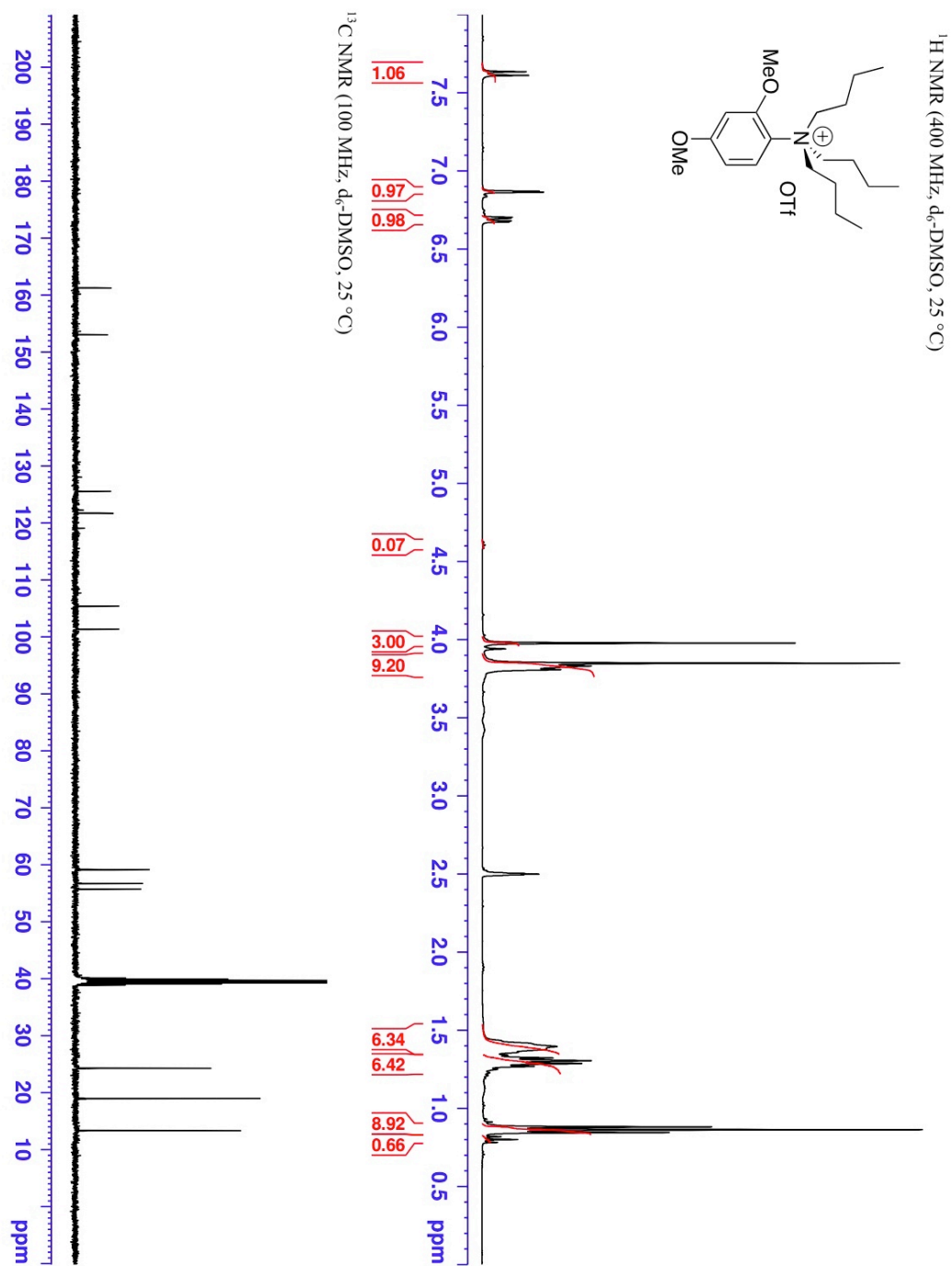


Spectrum 8  $^1\text{H}$  and  $^{13}\text{C}$  NMR spectra of N,N-diisobutyl-N-methyl-2,4-dimethoxyanilinium triflate in  $\text{d}_6\text{-DMSO}$

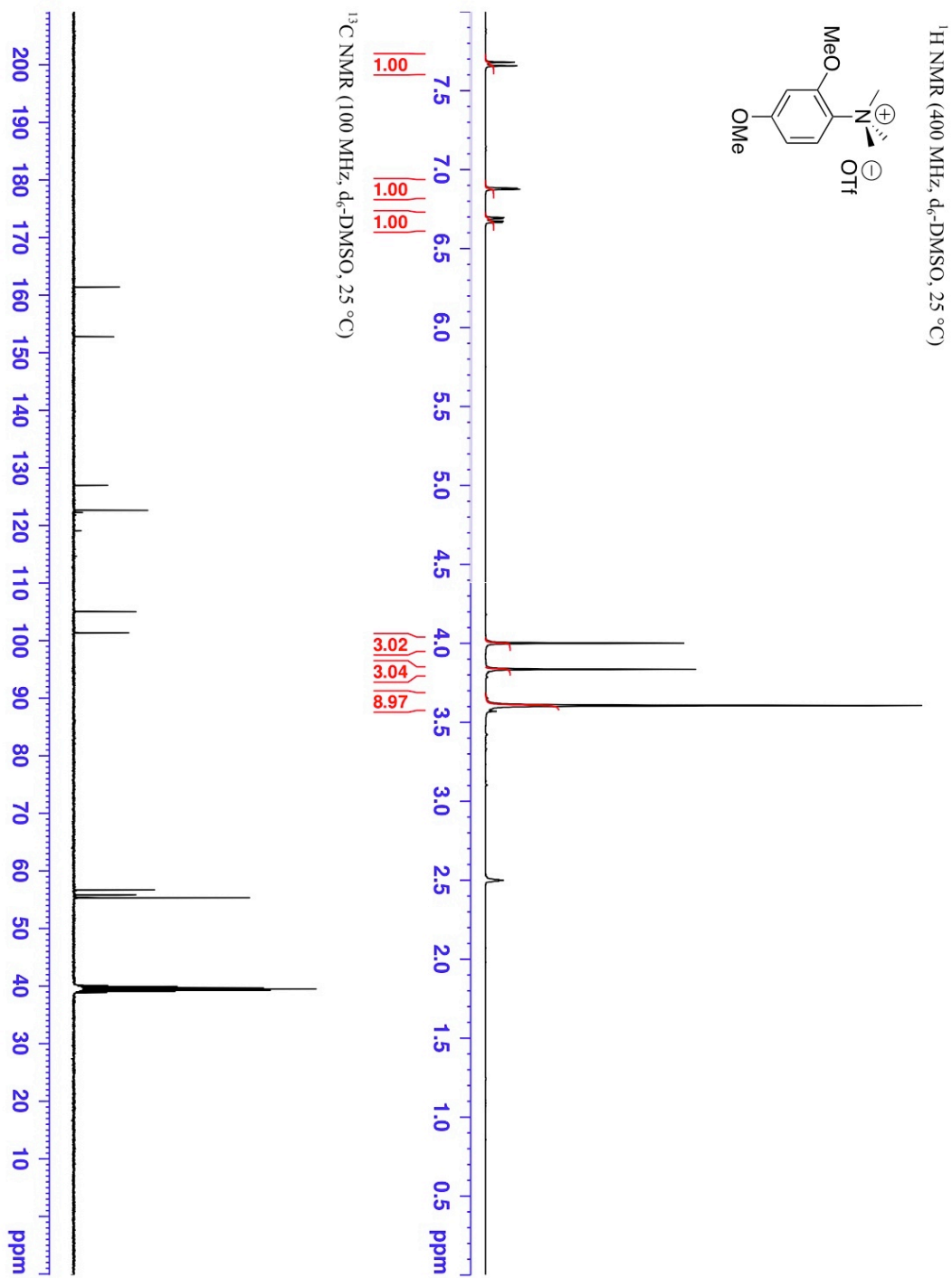


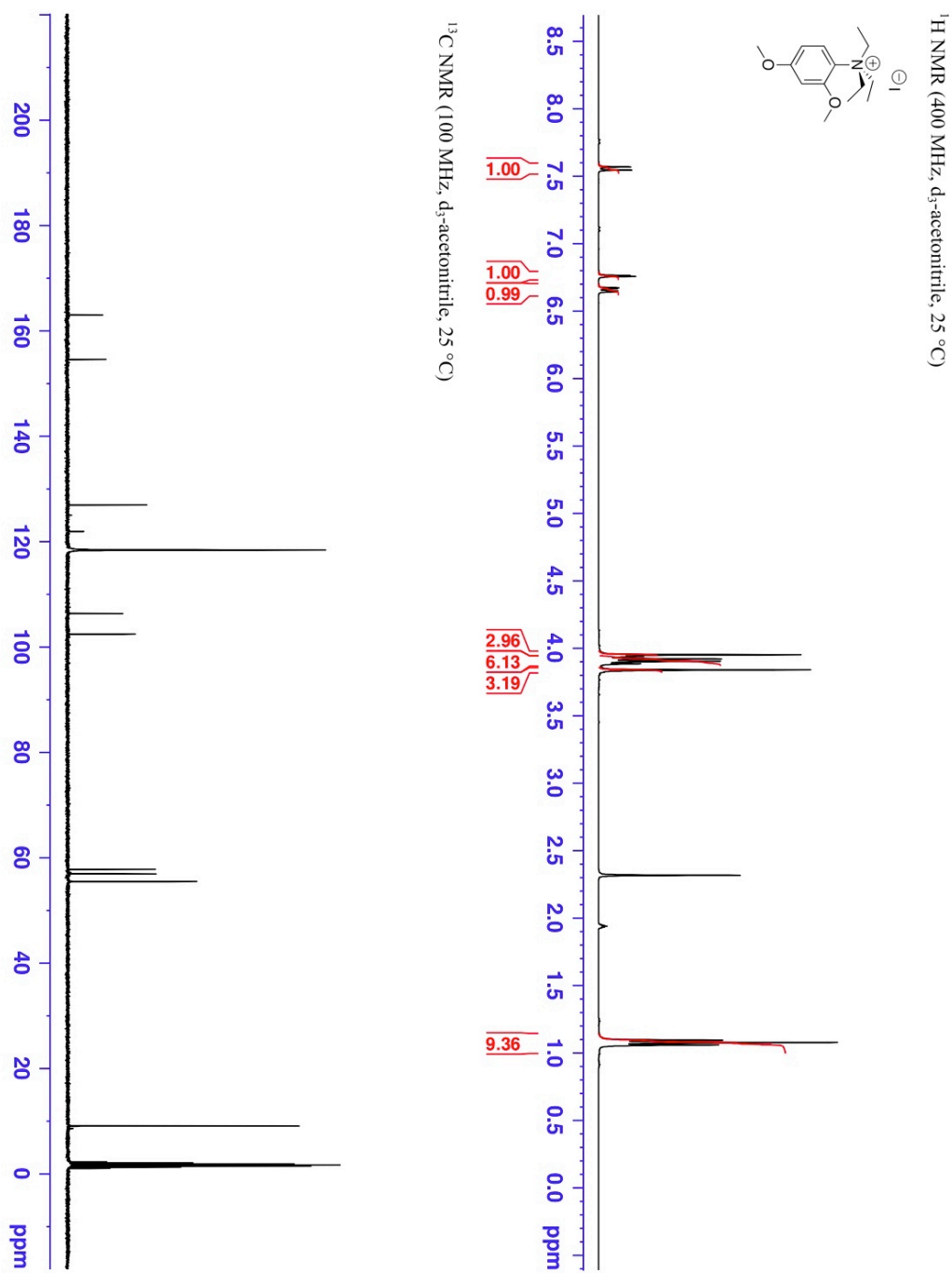


Spectrum 9  $^1\text{H}$  and  $^{13}\text{C}$  NMR spectra of N,N,N-tributyl-2,4-dimethoxyanilinium triflate in  $\text{d}_6\text{-DMSO}$

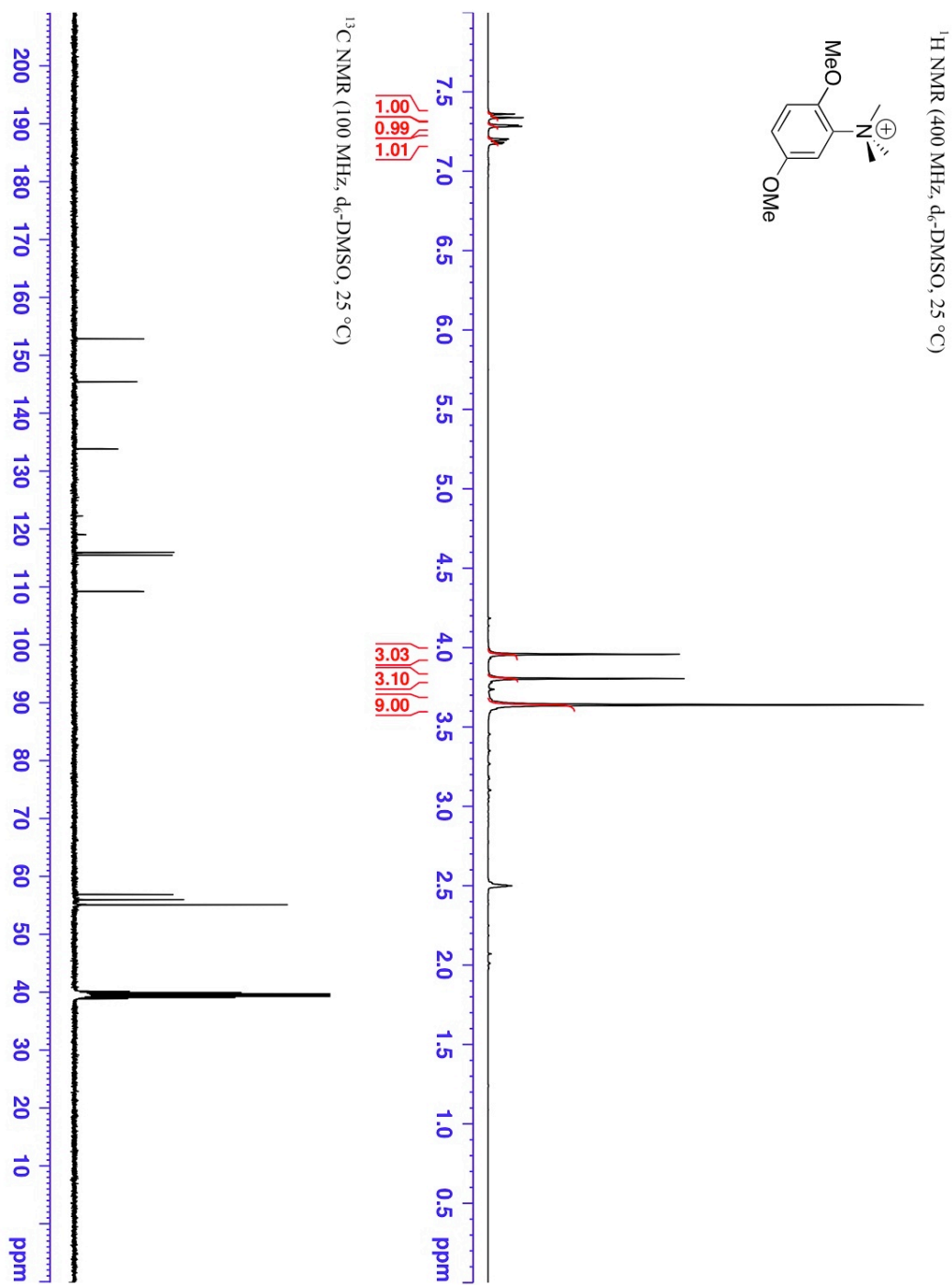


Spectrum 10  $^1\text{H}$  and  $^{13}\text{C}$  NMR spectra of N,N,N-trimethyl-2,4-dimethoxyanilinium triflate in  $\text{d}_6\text{-DMSO}$

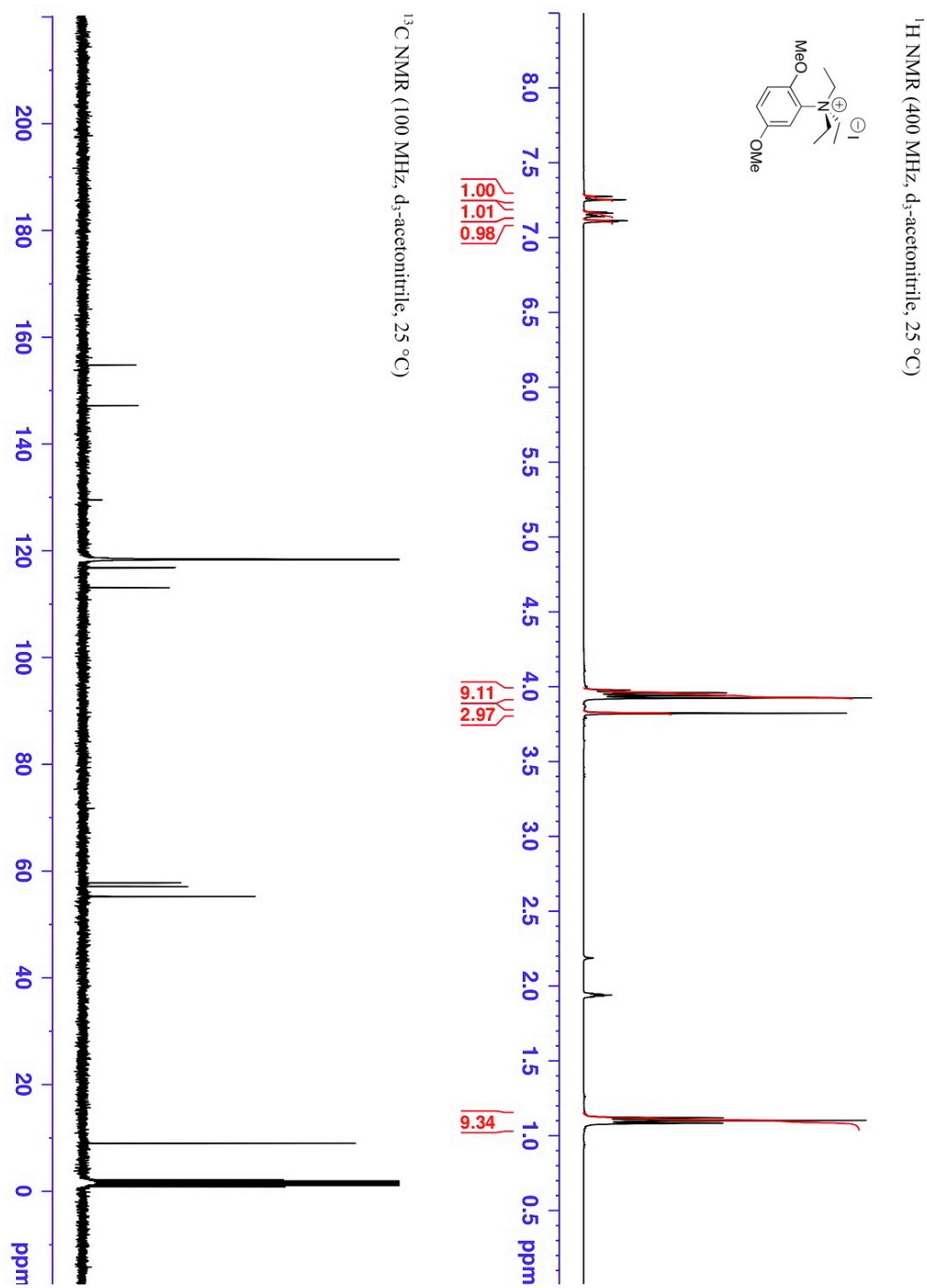




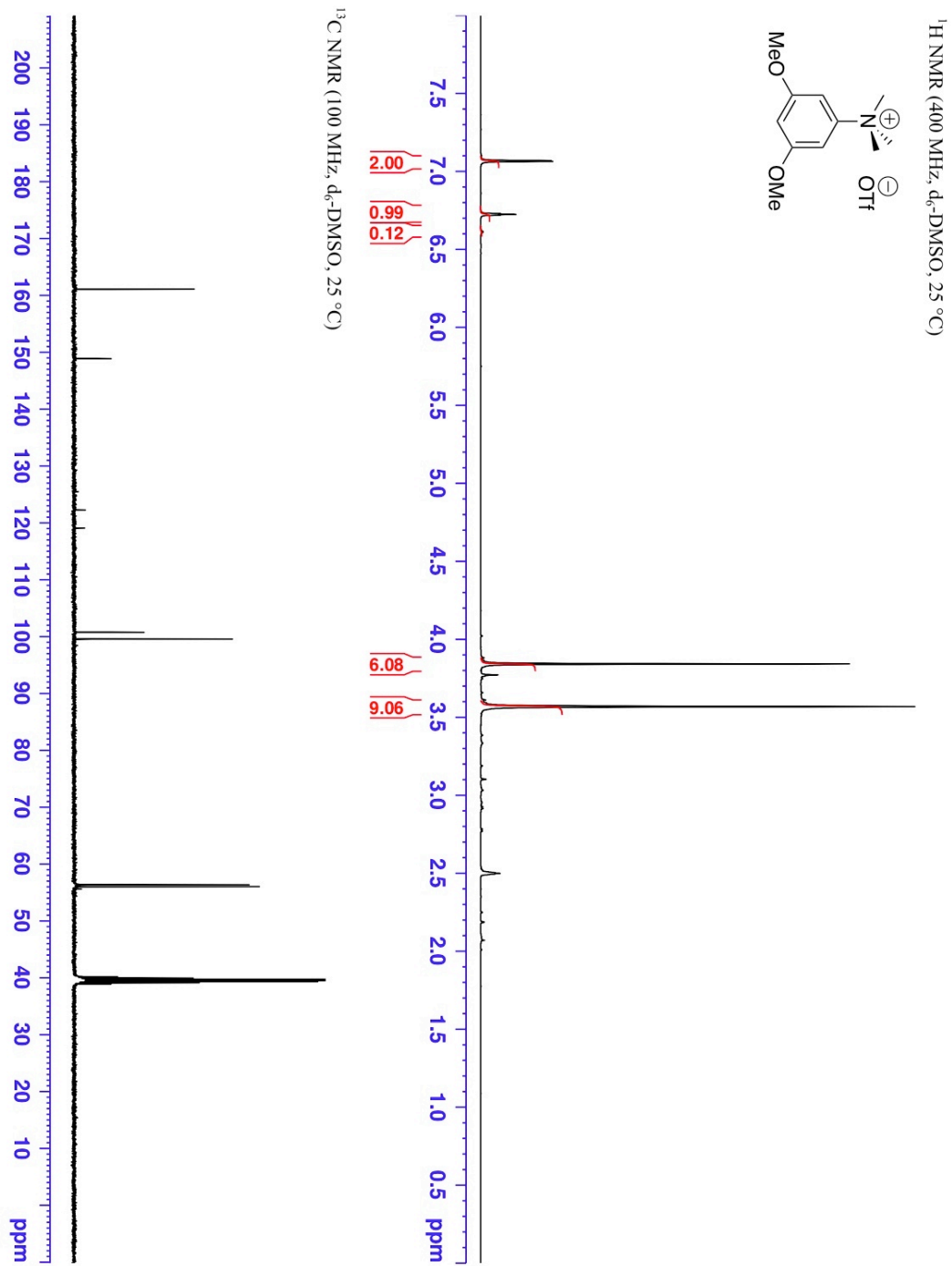
Spectrum 12  $^1\text{H}$  and  $^{13}\text{C}$  NMR spectra of N,N,N-trimethyl-2,5-dimethoxyanilinium triflate in  $\text{d}_6\text{-DMSO}$



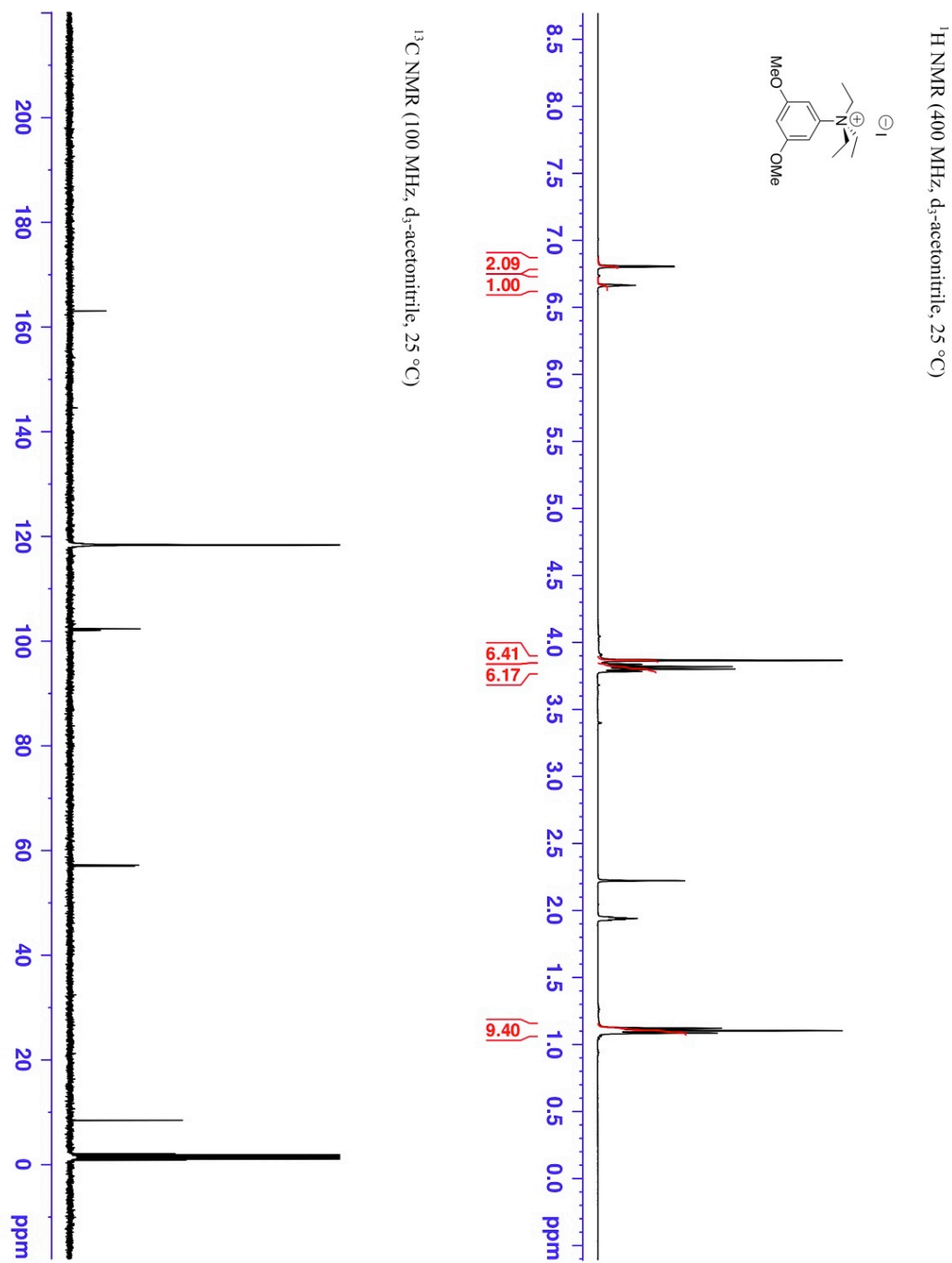
Spectrum 13  $^1\text{H}$  and  $^{13}\text{C}$  NMR spectra of N,N,N-triethyl-2,5-dimethoxyanilinium iodide in  $\text{CD}_3\text{CN}$



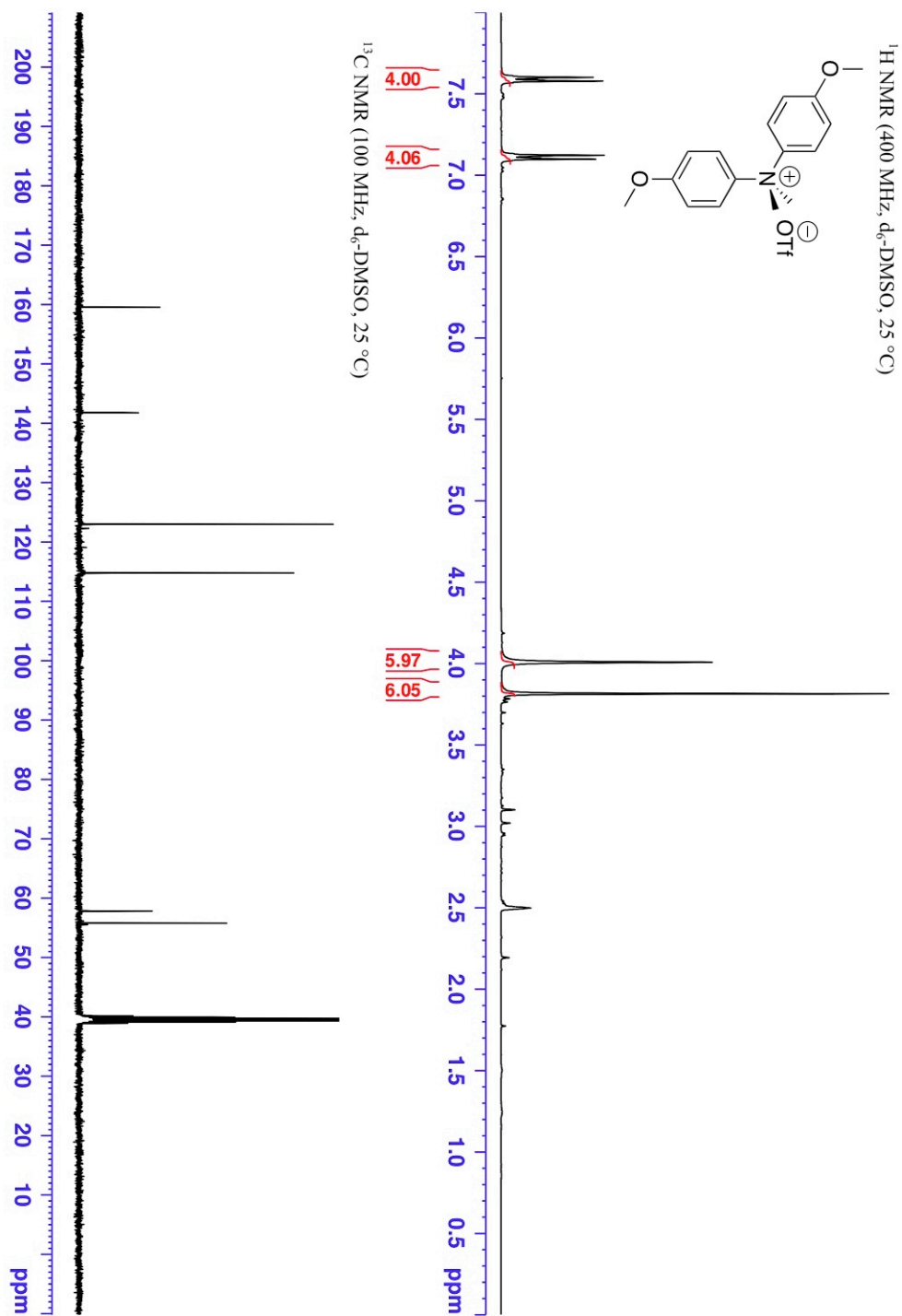
Spectrum 14  $^1\text{H}$  and  $^{13}\text{C}$  NMR spectra of N,N,N-trimethyl-3,5-dimethoxyanilinium triflate in  $\text{d}_6$ -DMSO



Spectrum 15  $^1\text{H}$  and  $^{13}\text{C}$  NMR spectra of N,N,N-triethyl-3,5-dimethoxyanilinium iodide in  $\text{CD}_3\text{CN}$

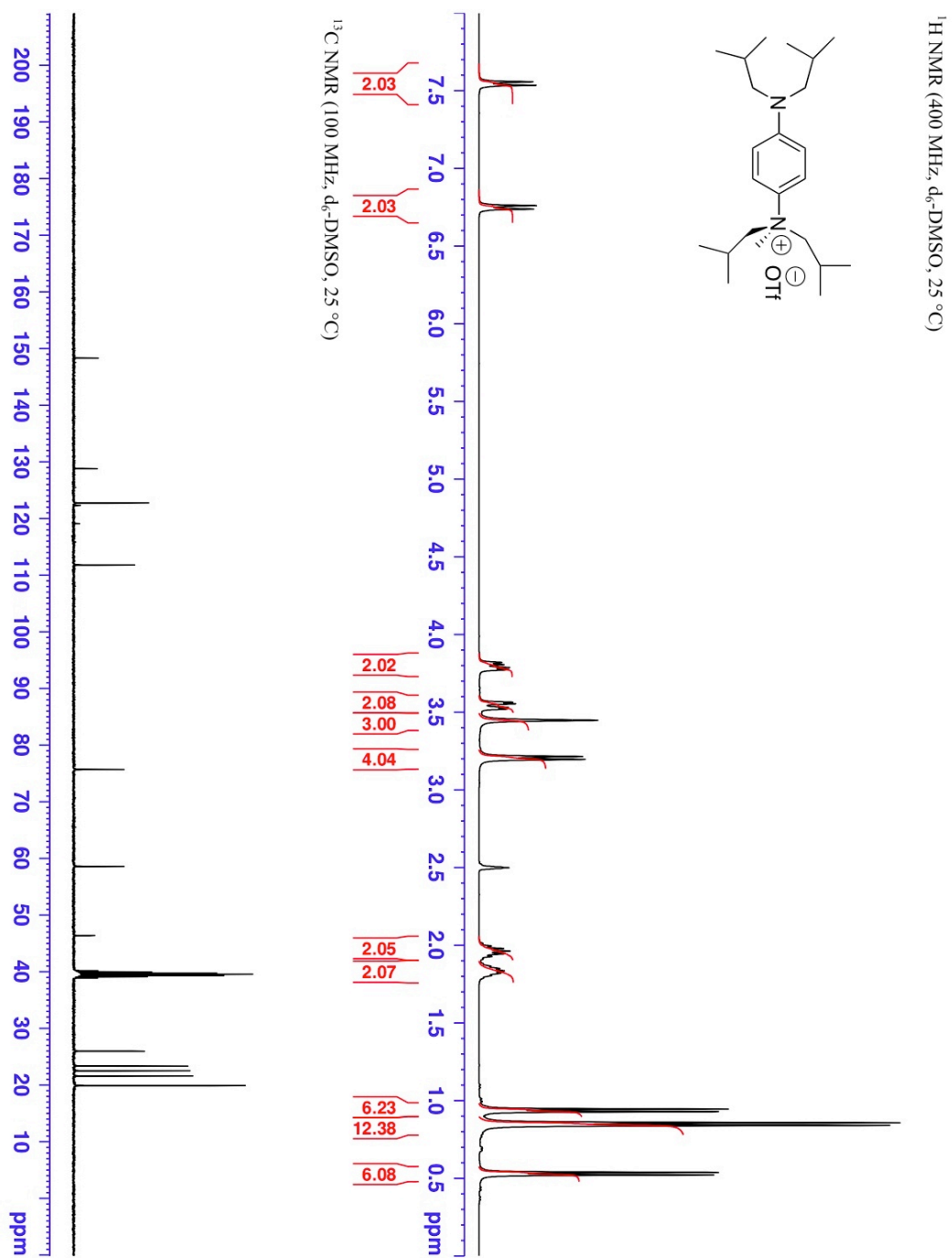


Spectrum 16  $^1\text{H}$  and  $^{13}\text{C}$  NMR spectra of bis(4-methoxyphenyl)-dimethylammonium triflate in  $\text{d}_6$ -DMSO

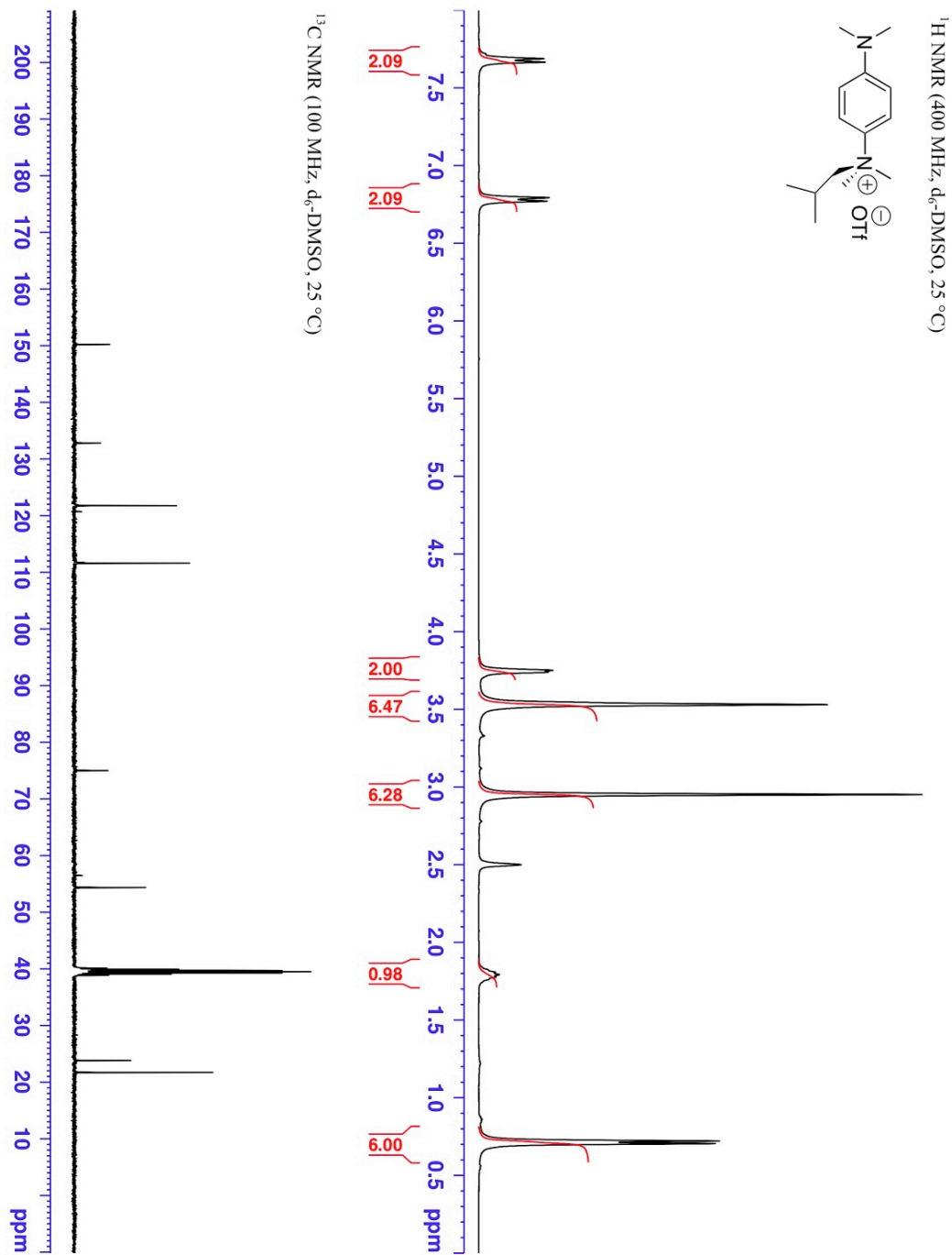




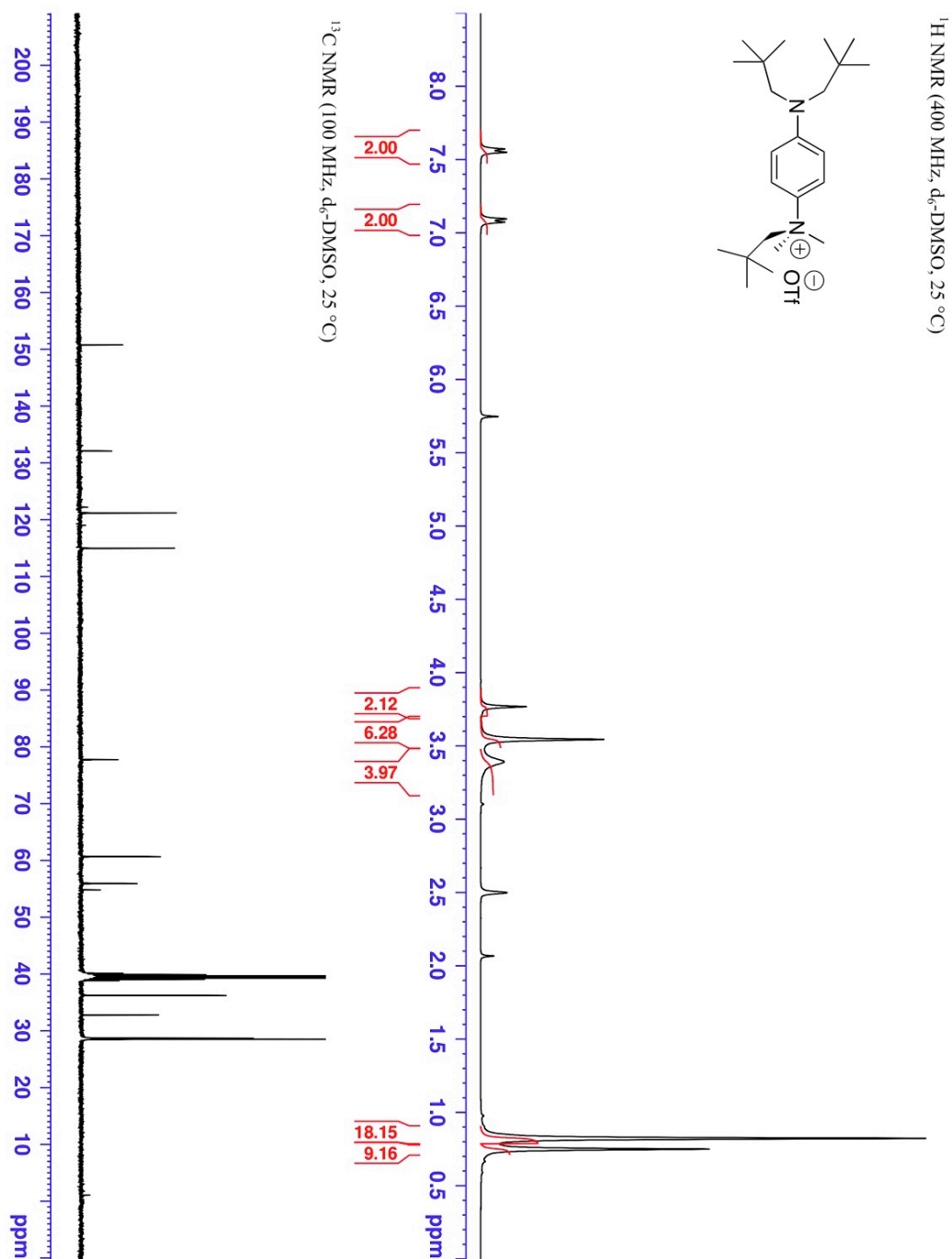
Spectrum 17  $^1\text{H}$  and  $^{13}\text{C}$  NMR spectra of N,N,N',N'-tetraisobutyl-N-methylphenylenediammonium triflate

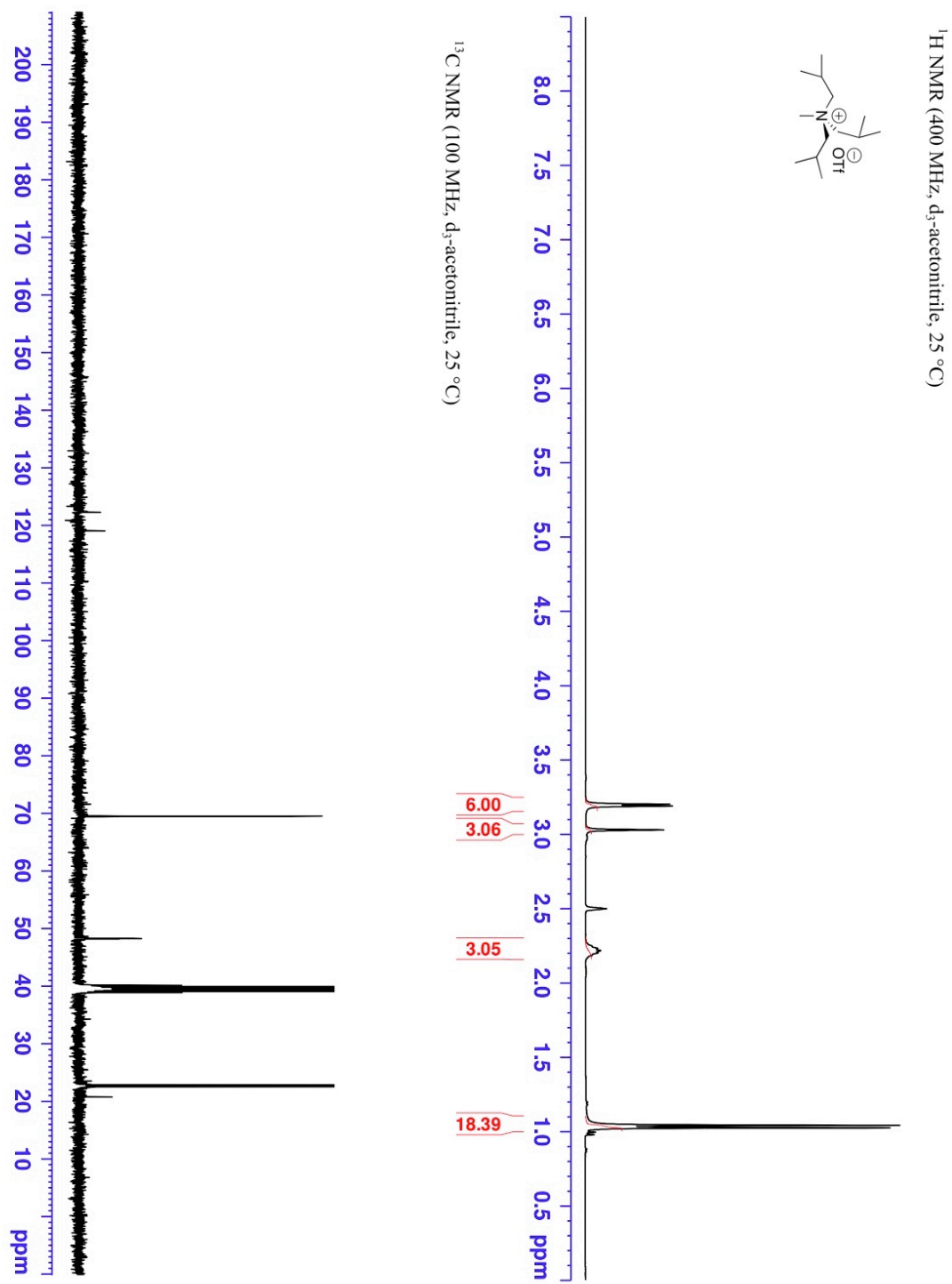


Spectrum 18  $^1\text{H}$  and  $^{13}\text{C}$  NMR spectra of  $N,N,N',N'$ -tetramethyl- $N$ -isobutyl-phenylenediammonium triflate in  $\text{d}_6$ -DMSO

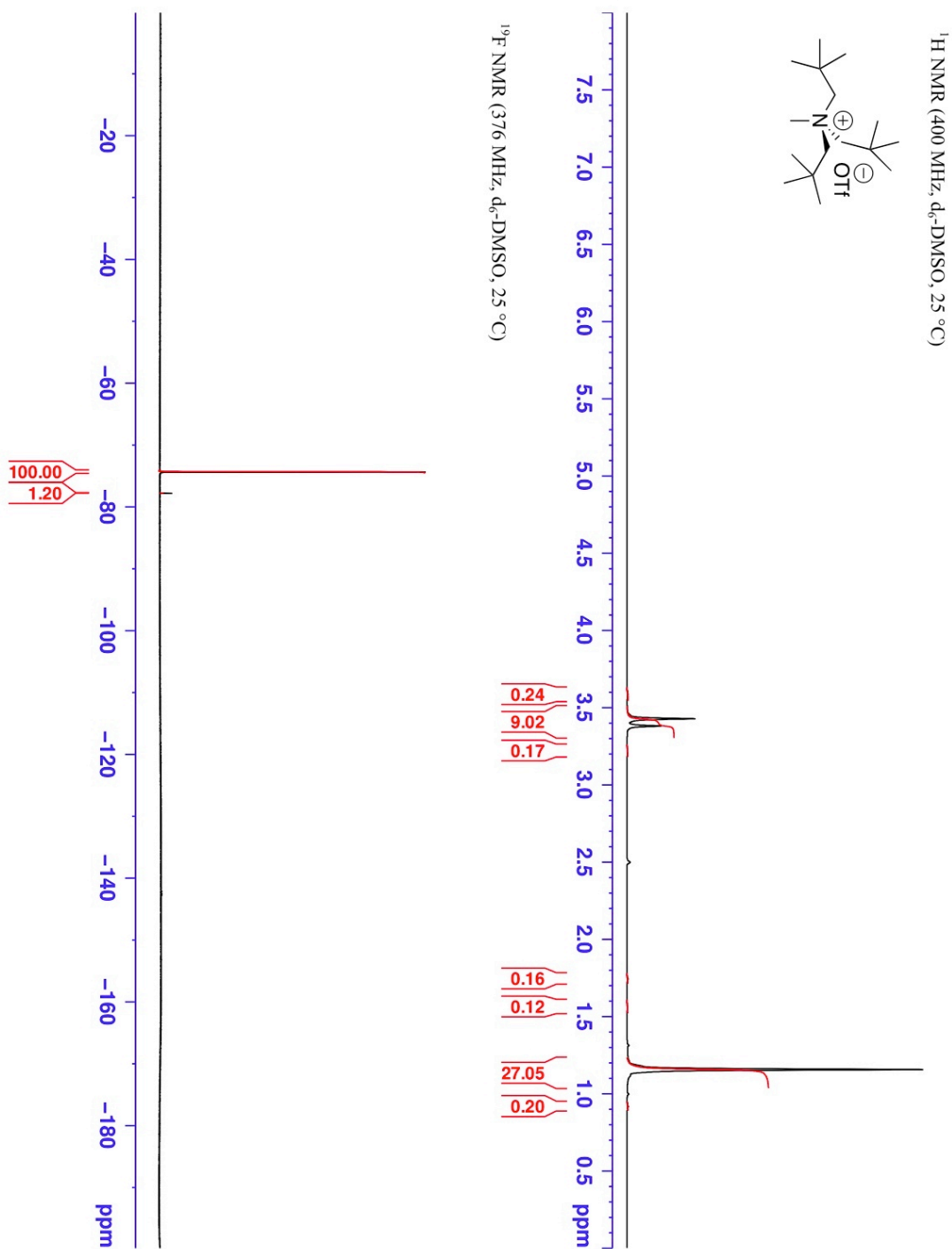


Spectrum 19  $^1\text{H}$  and  $^{13}\text{C}$  NMR spectra of N,N',N'-trineopentyl-N,N-dimethyl-phenylenediammonium triflate in  $\text{d}_6\text{-DMSO}$

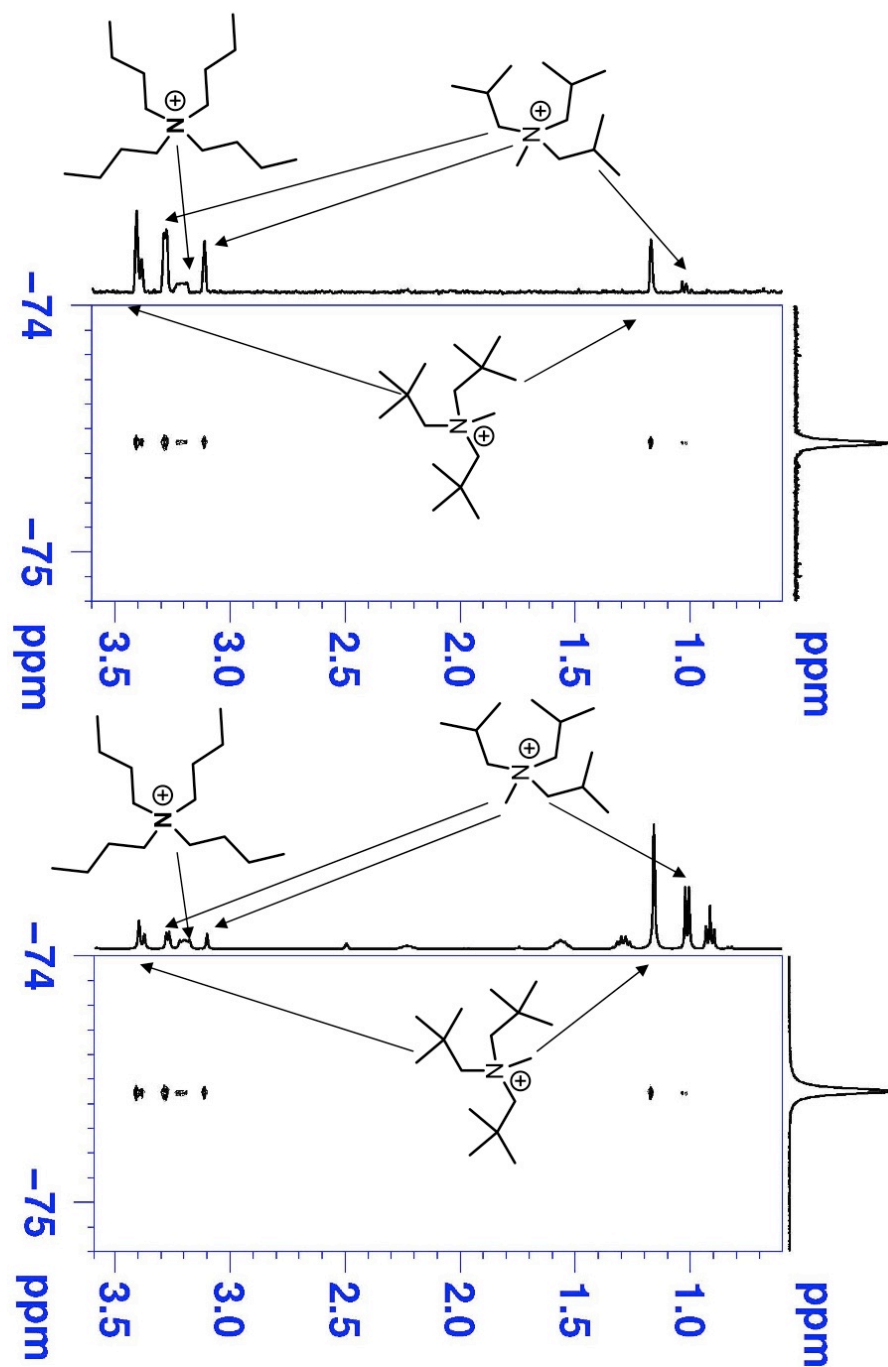


Spectrum 20  $^1\text{H}$  and  $^{19}\text{F}$  NMR spectra of trisisobutylmethylammonium triflate in  $\text{d}_6$ -DMSO

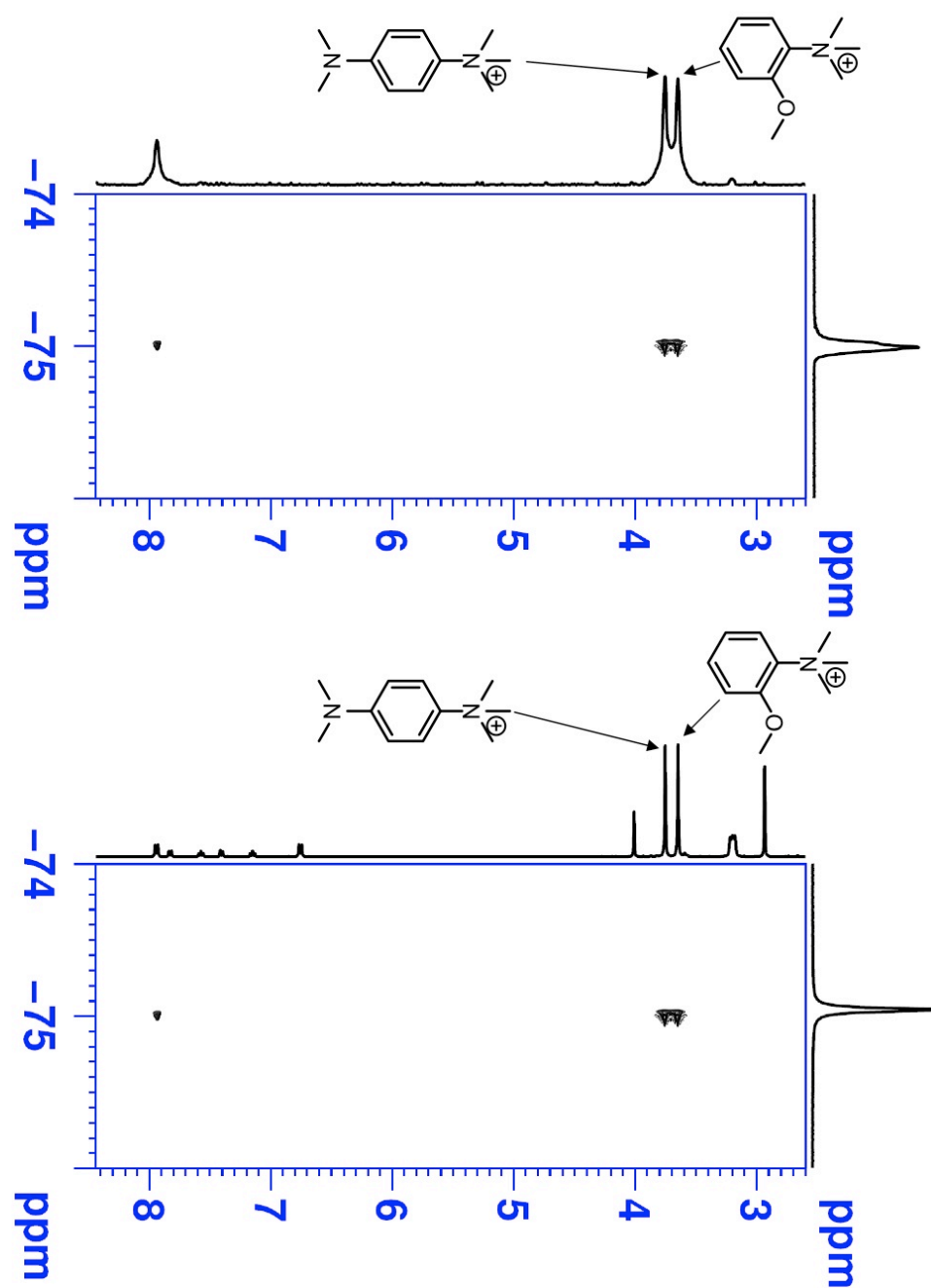
Spectrum 21  $^1\text{H}$  and  $^{19}\text{F}$  NMR spectra of trineopentylmethylammonium fluoride in  $\text{d}_6$ -DMSO



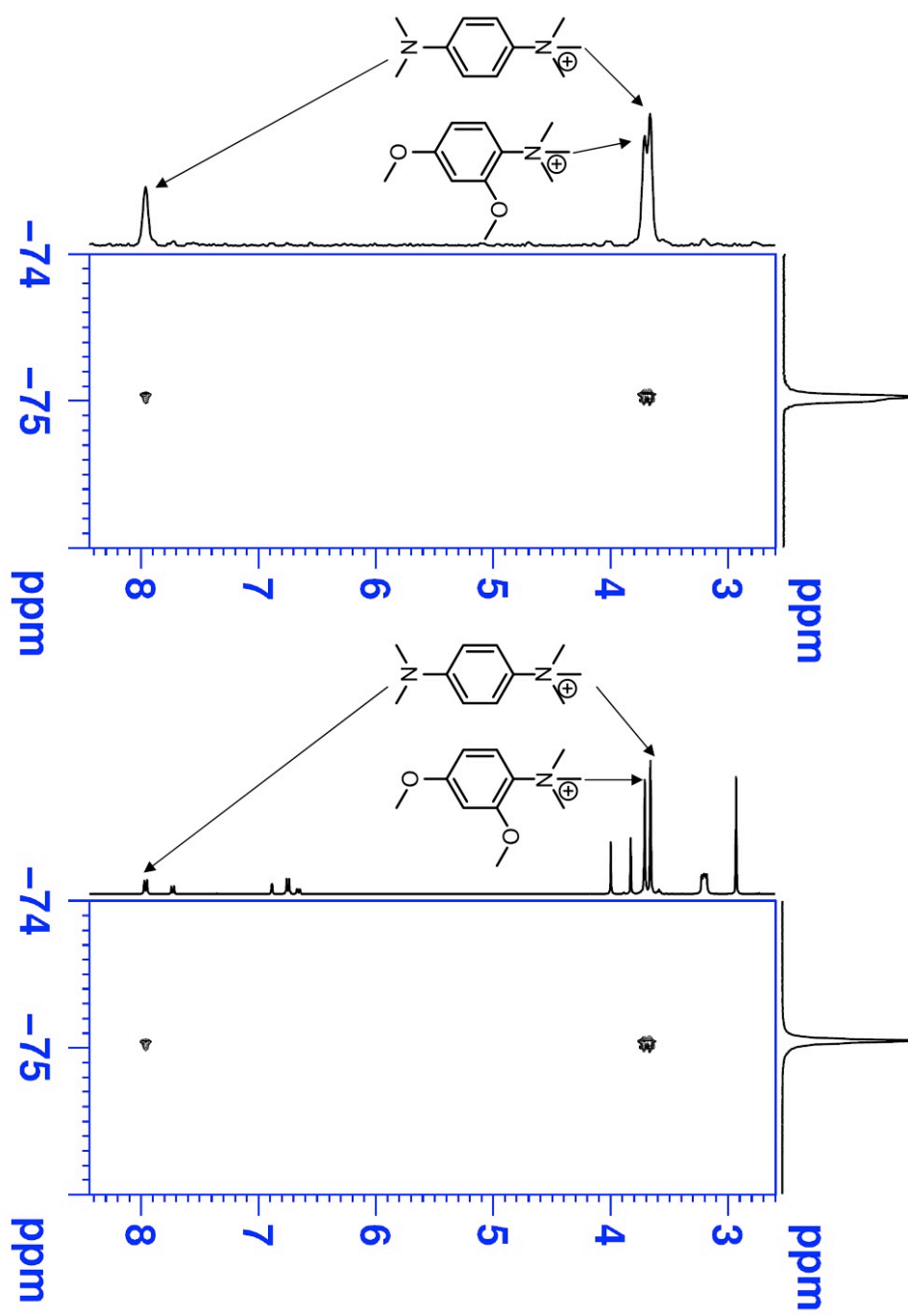
Spectrum 22 Pairwise HOESY study: TIBMA vs. TNPMA



**Spectrum 23** Pairwise HOESY study: 4-(dimethylamino)-N,N,N-trimethylanilinium vs. 2-methoxy-N,N,N-trimethylanilinium

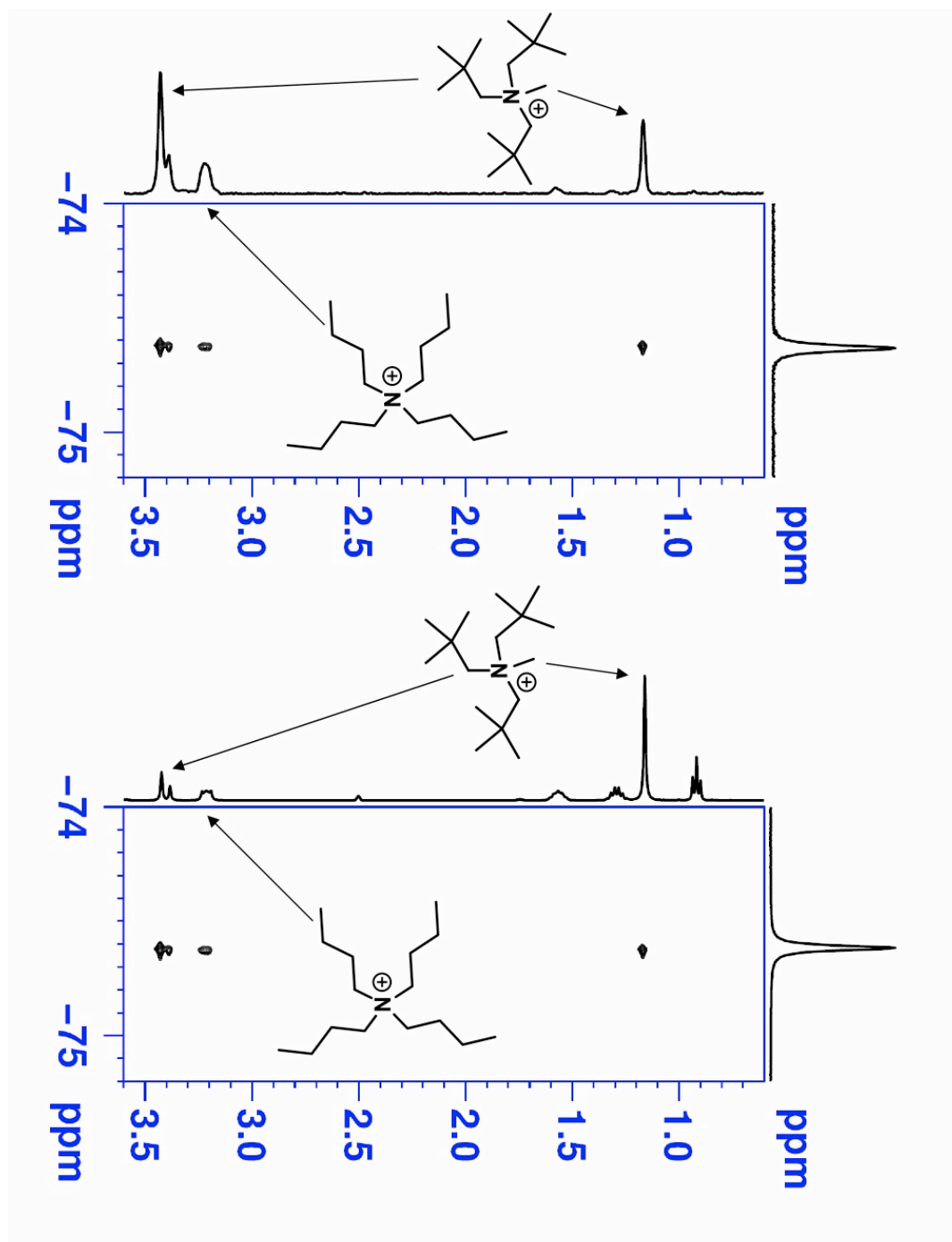


**Spectrum 24** Pairwise HOESY study: 4-(dimethylamino)-N,N,N-trimethylanilinium vs. 2,4-dimethoxy-N,N,N-trimethylanilinium

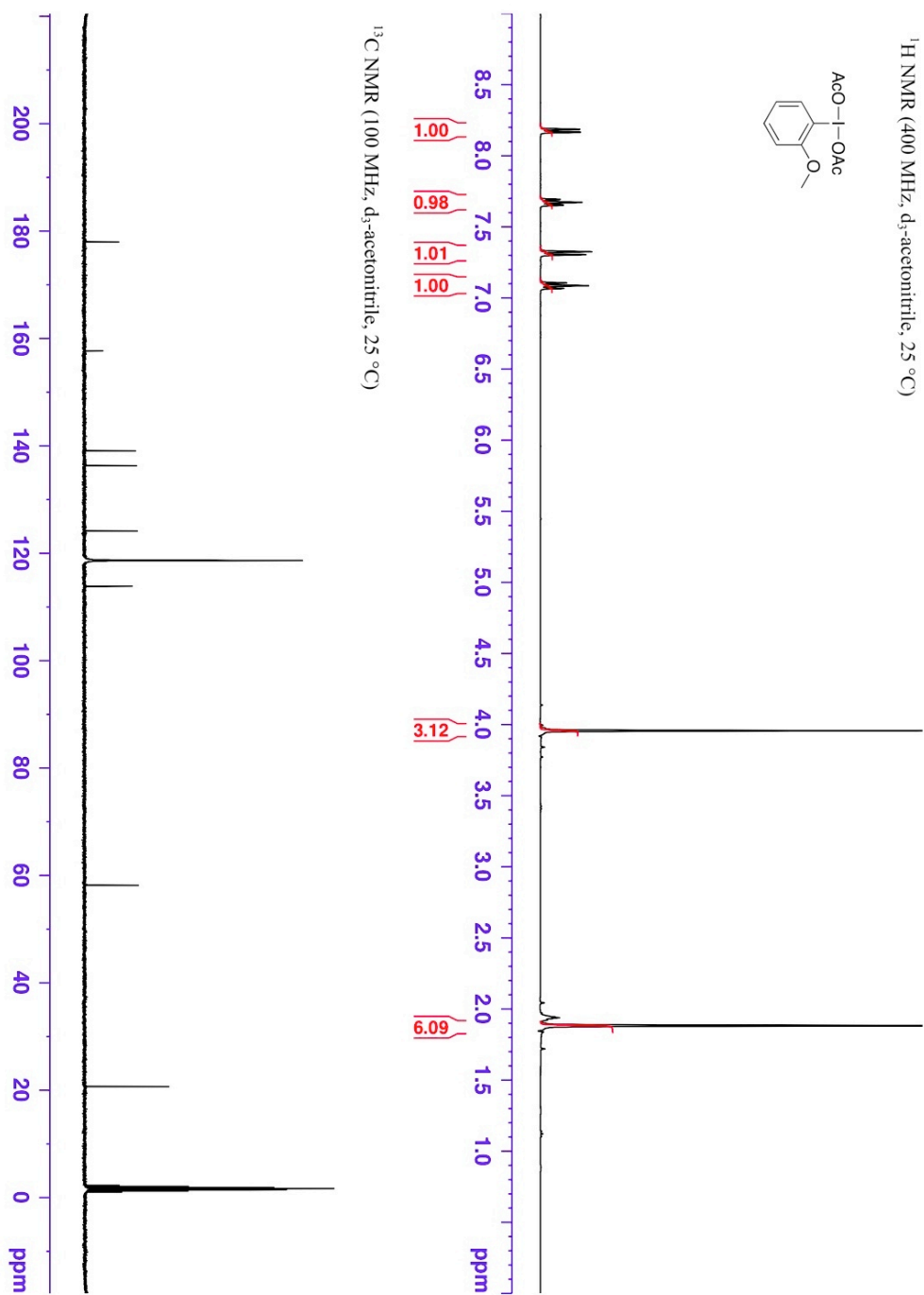




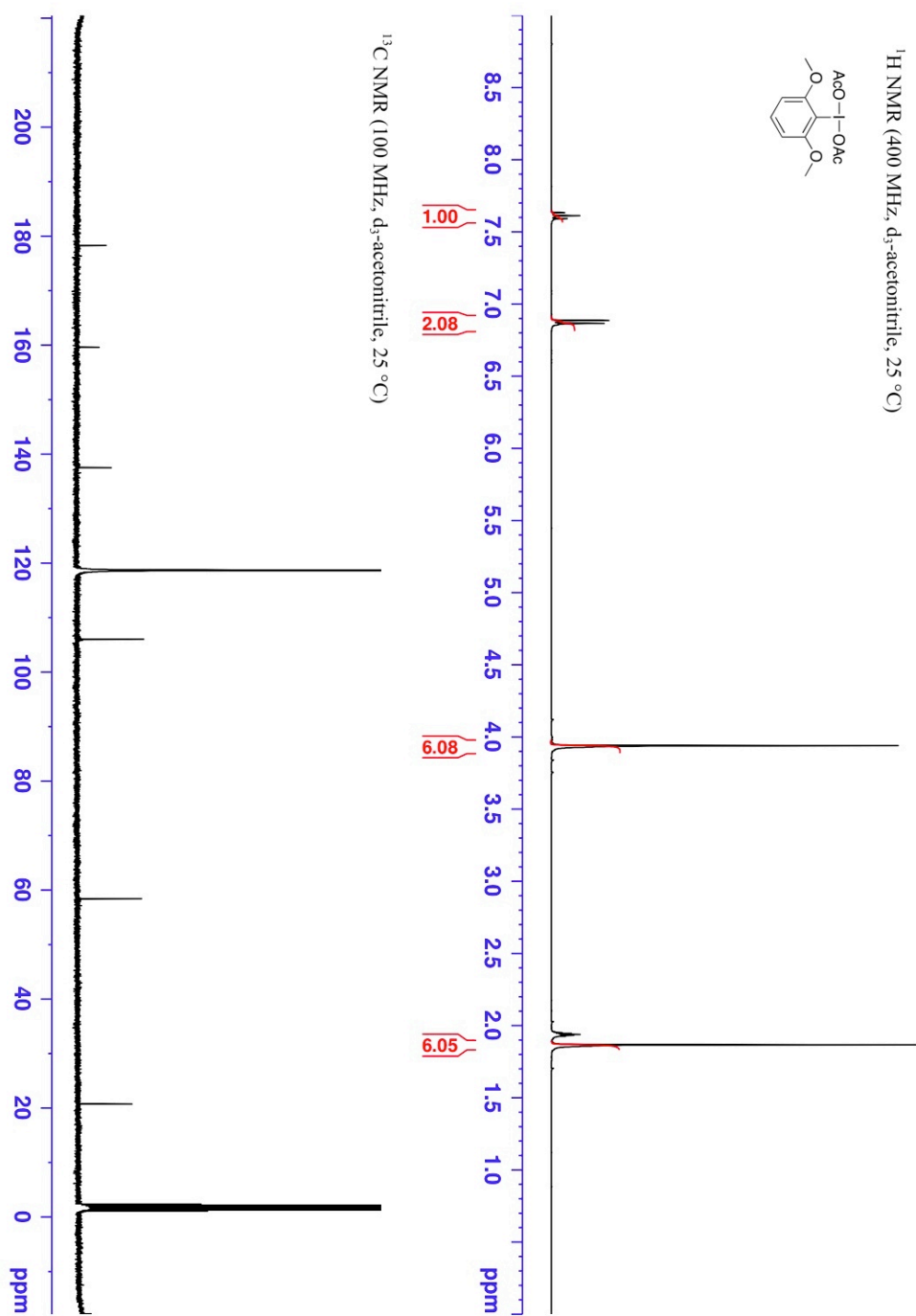
Spectrum 25 Pairwise HOESY study: TBA vs. TNPMA

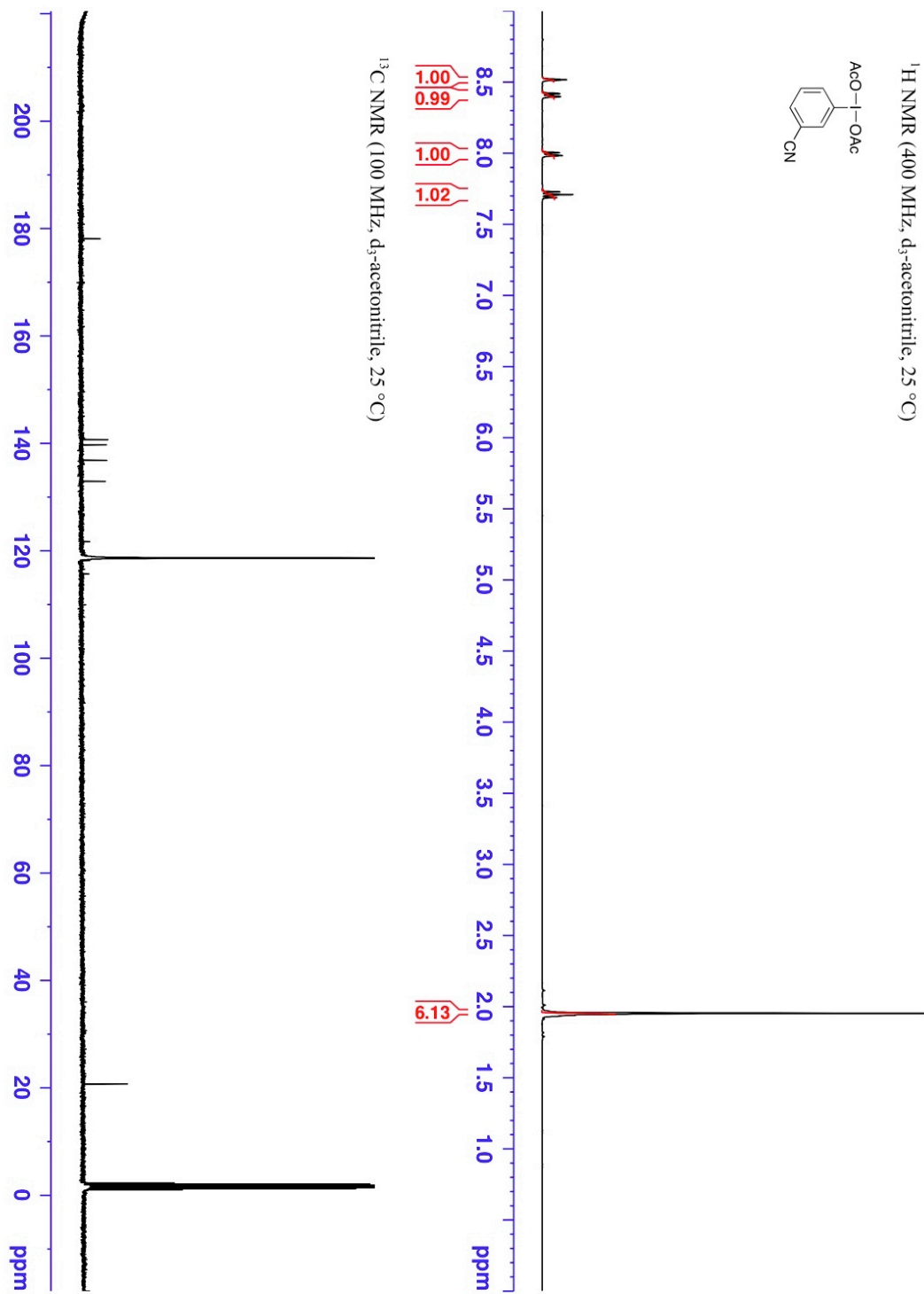


Spectrum 26  $^1\text{H}$  and  $^{13}\text{C}$  NMR spectra of 2-methoxy-(diacetoxyiodo)benzene in  $\text{d}_3$ -acetonitrile

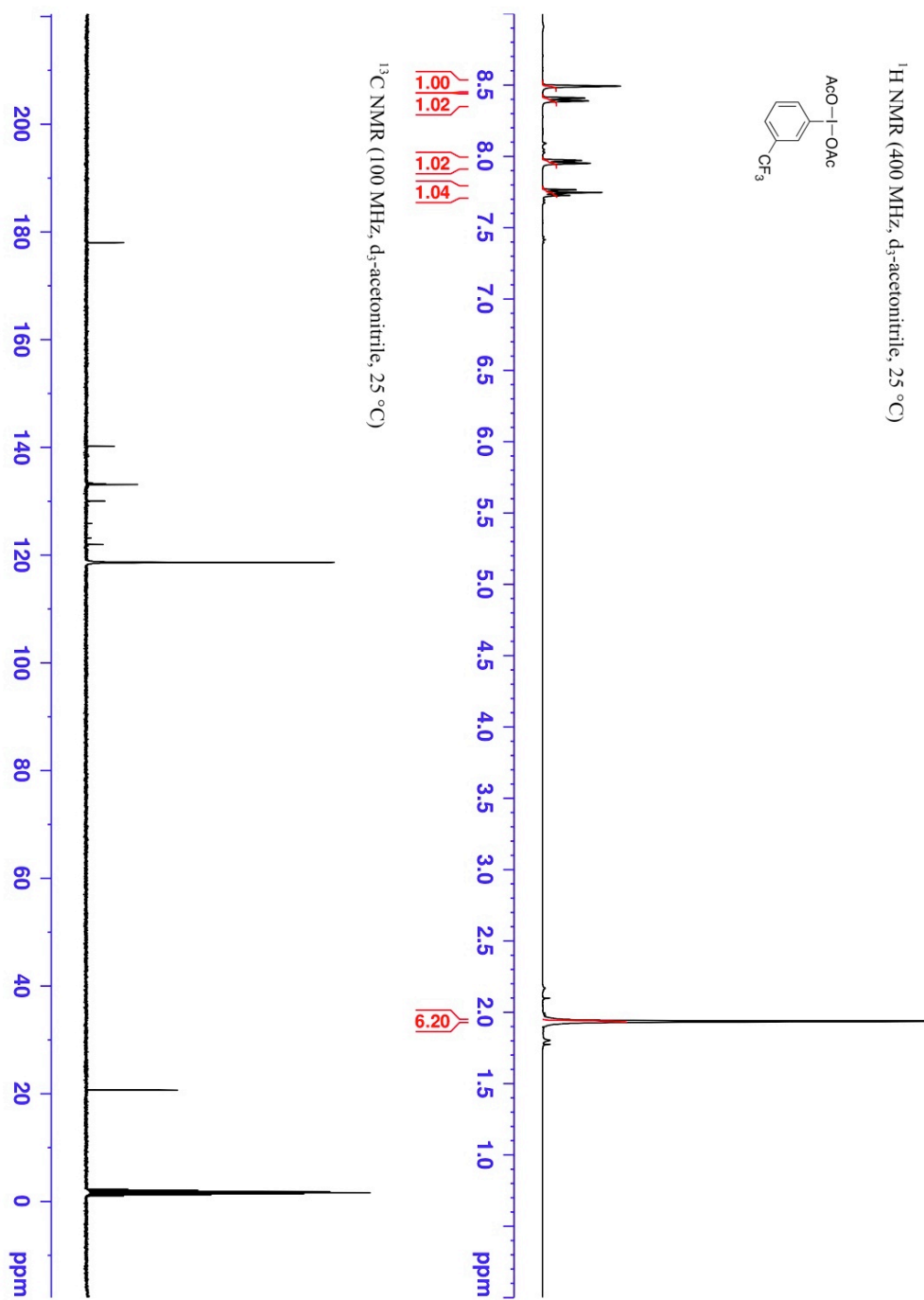


Spectrum 27  $^1\text{H}$  and  $^{13}\text{C}$  NMR spectra of 2,6-dimethoxy-(diacetoxyiodo)benzene in  $\text{d}_3$ -acetonitrile

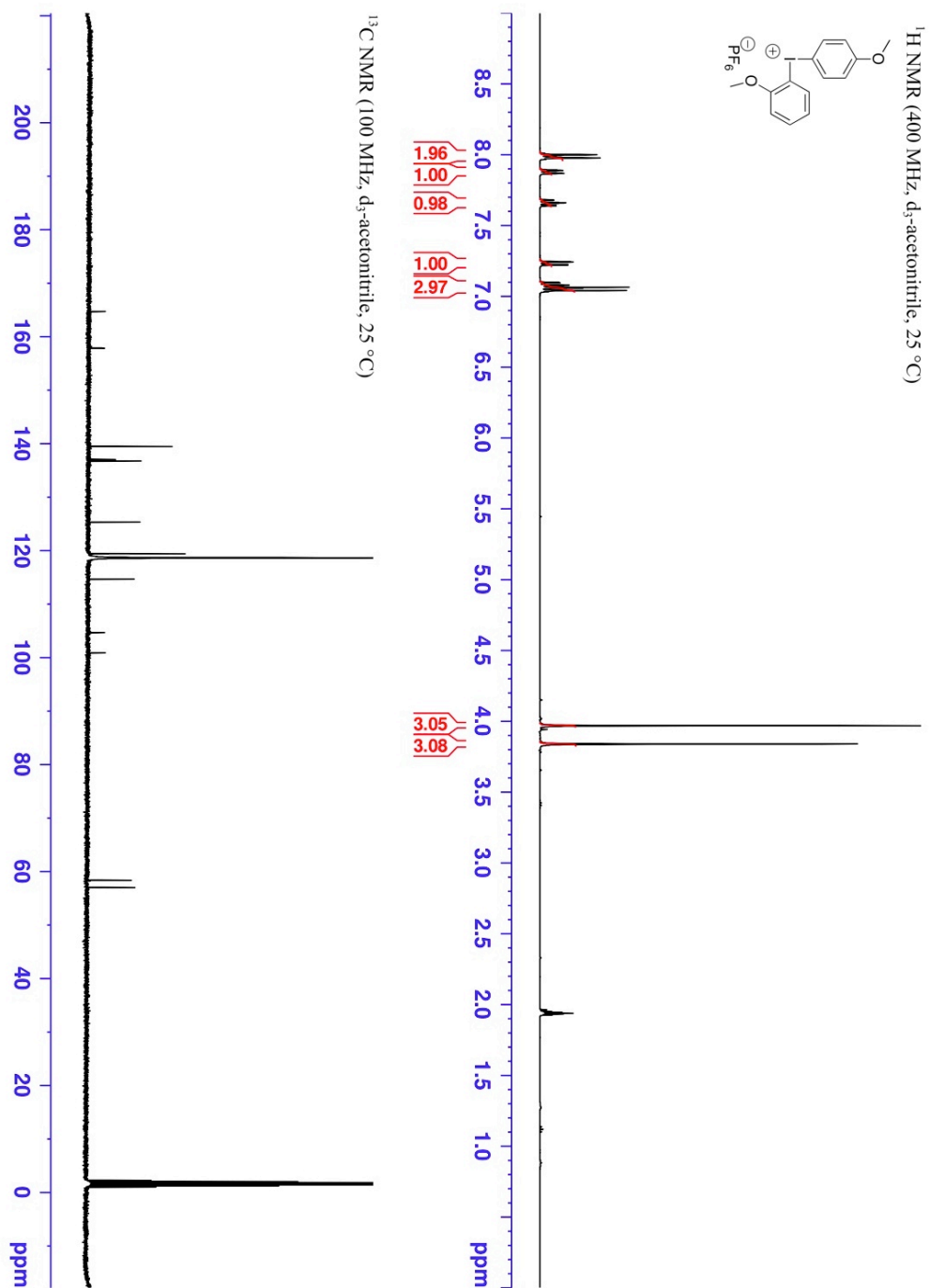


Spectrum 28  $^1\text{H}$  and  $^{13}\text{C}$  NMR spectra of 3-cyano-(diacetoxyiodo)benzene in  $\text{d}_3$ -acetonitrile

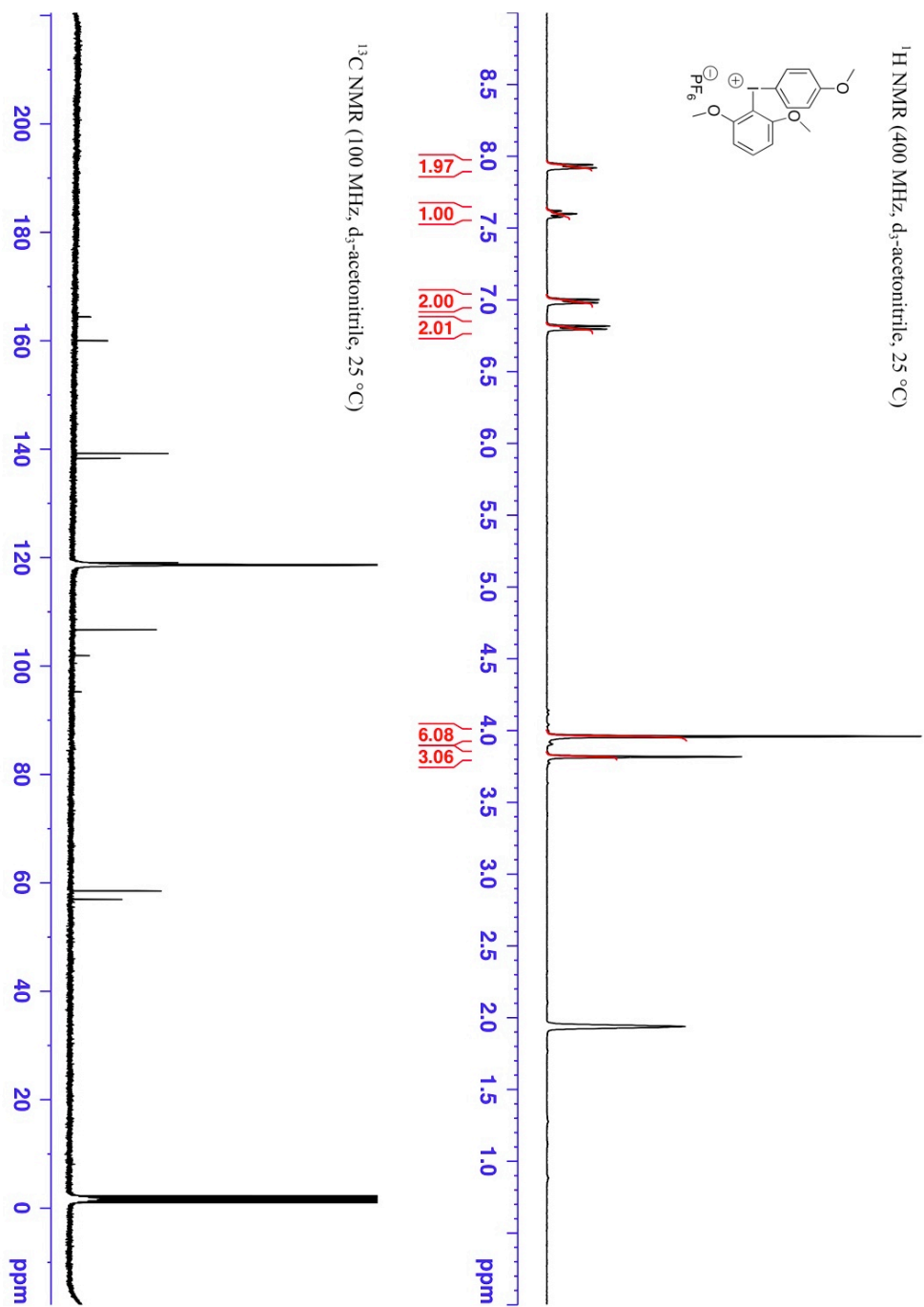
Spectrum 29  $^1\text{H}$  and  $^{13}\text{C}$  NMR spectra of 3-trifluoromethyl-(diacetoxyiodo)benzene in  $\text{d}_3$ -acetonitrile



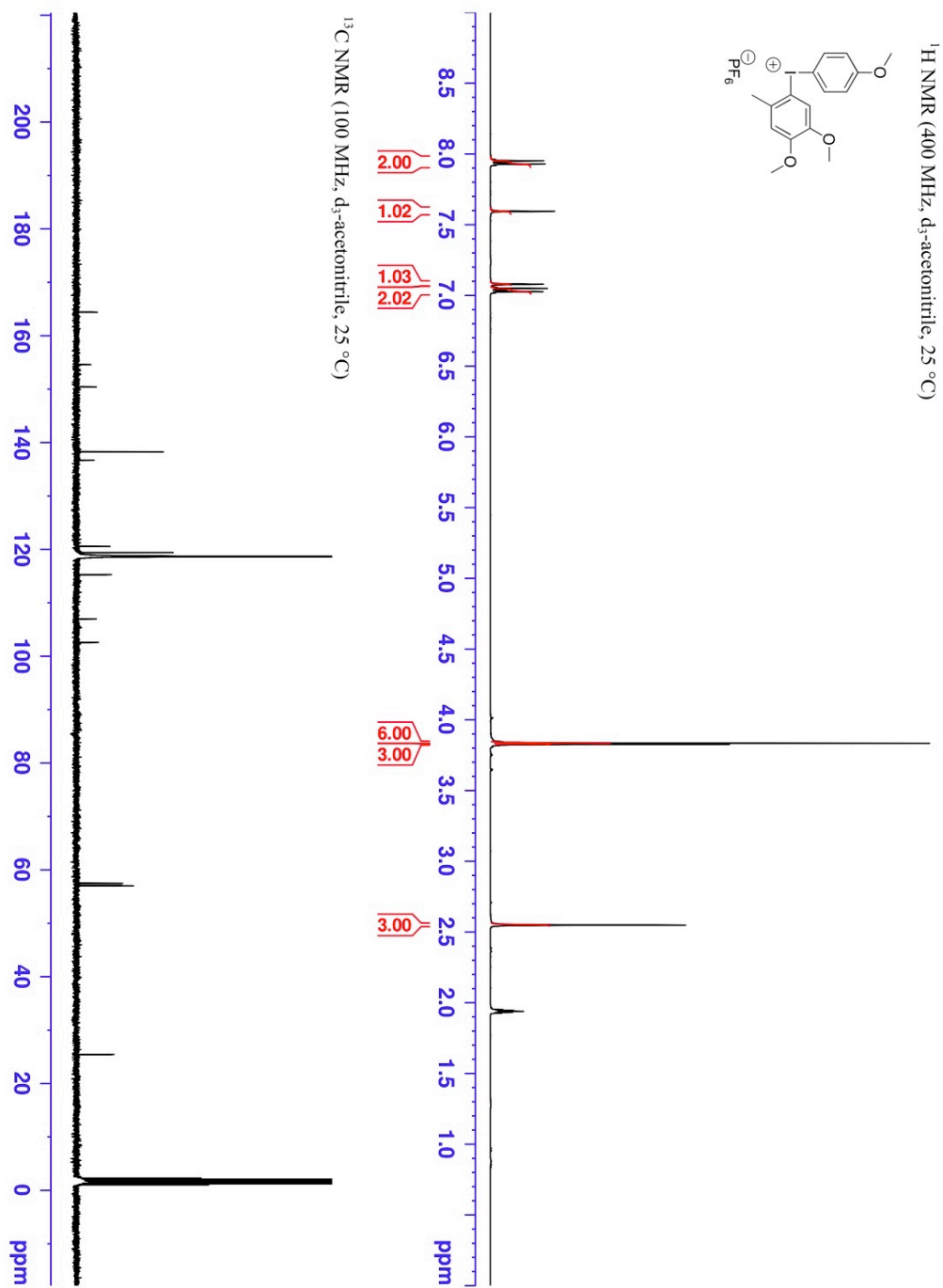
Spectrum 30  $^1\text{H}$  and  $^{13}\text{C}$  NMR spectra of (2-methoxyphenyl)(4'-methoxyphenyl)-iodonium hexafluorophosphate in  $\text{d}_3$ -acetonitrile



Spectrum 31  $^1\text{H}$  and  $^{13}\text{C}$  NMR spectra of (2,6-dimethoxyphenyl)(4'-methoxyphenyl)-iodonium hexafluorophosphate in  $\text{d}_3$ -acetonitrile

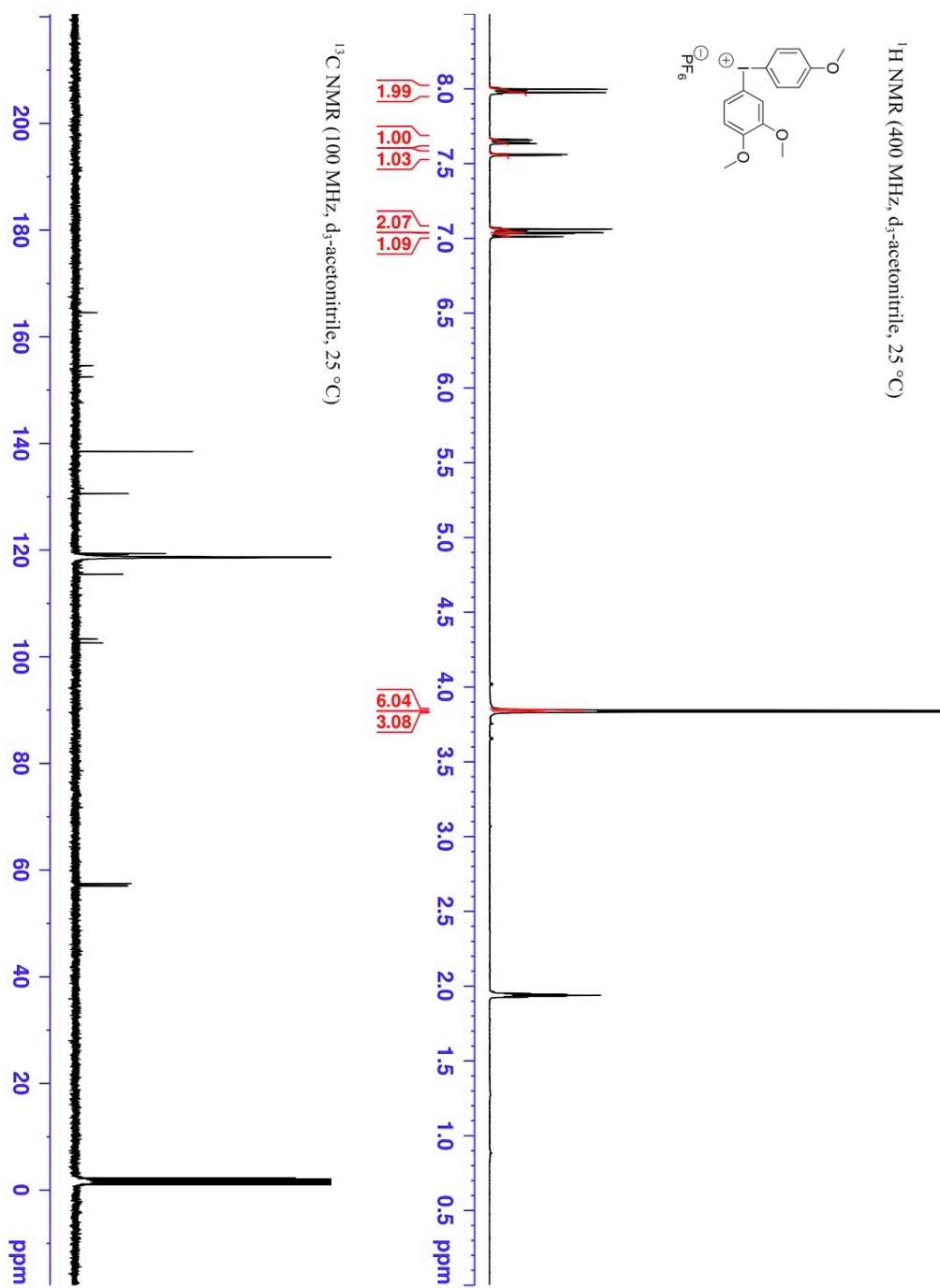


Spectrum 32  $^1\text{H}$  and  $^{13}\text{C}$  NMR spectra of (2-methyl-4,5-dimethoxyphenyl)(4'-methoxyphenyl)-iodonium hexafluorophosphate in  $\text{d}_3$ -acetonitrile

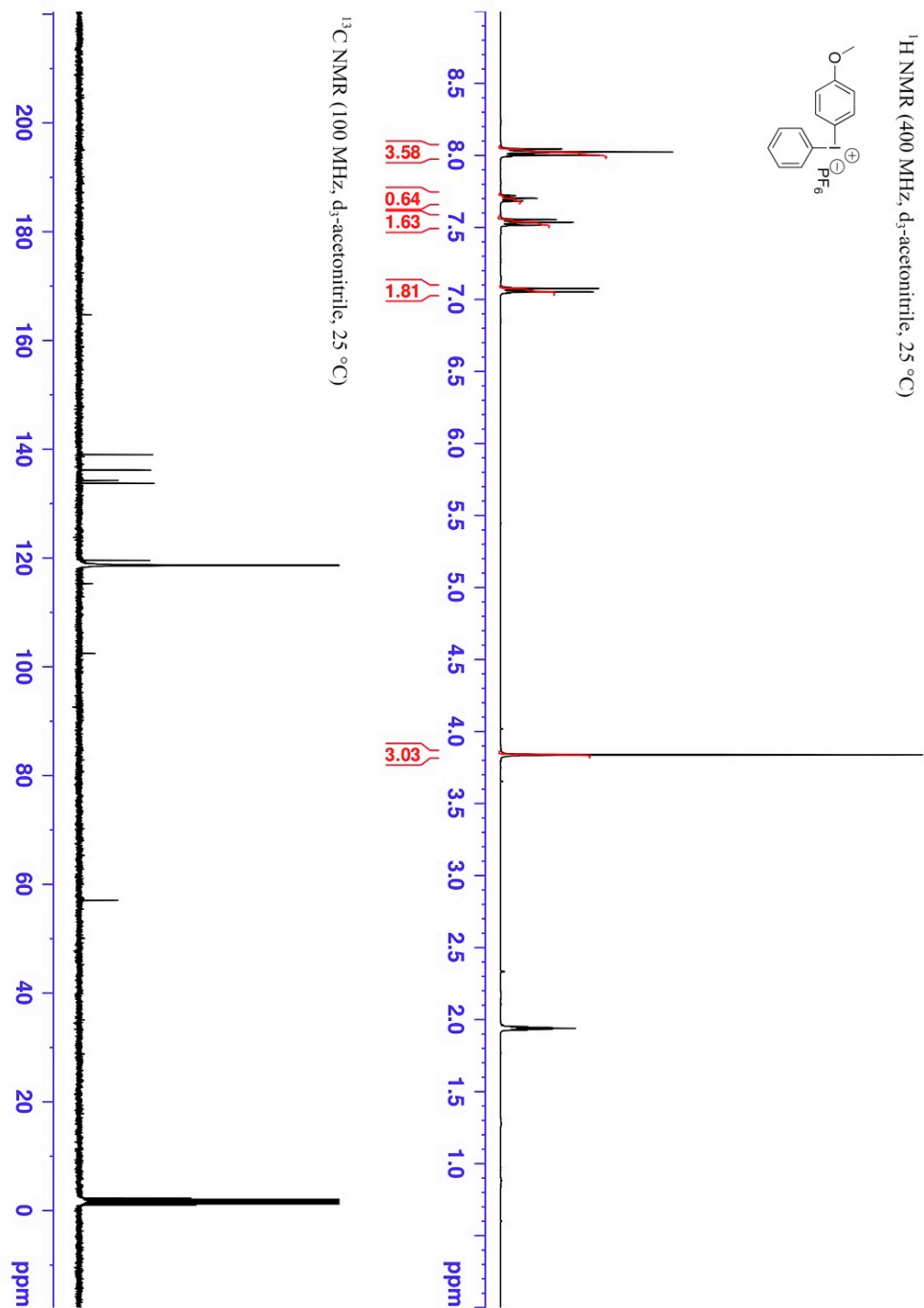




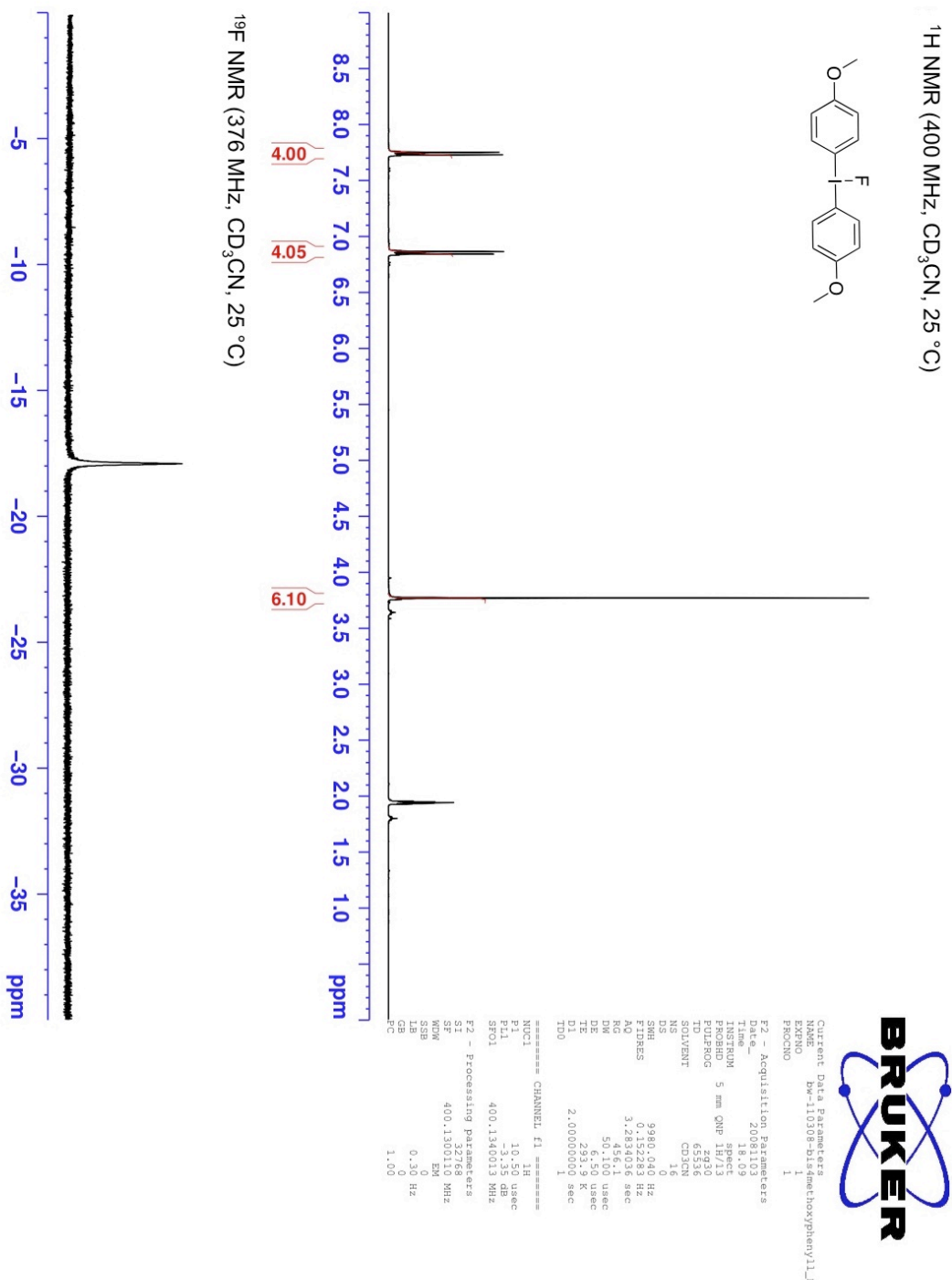
Spectrum 33  $^1\text{H}$  and  $^{13}\text{C}$  NMR spectra of (3,4-dimethoxyphenyl)(4'-methoxyphenyl)-  
iodonium hexafluorophosphate in  $\text{d}_3$ -acetonitrile



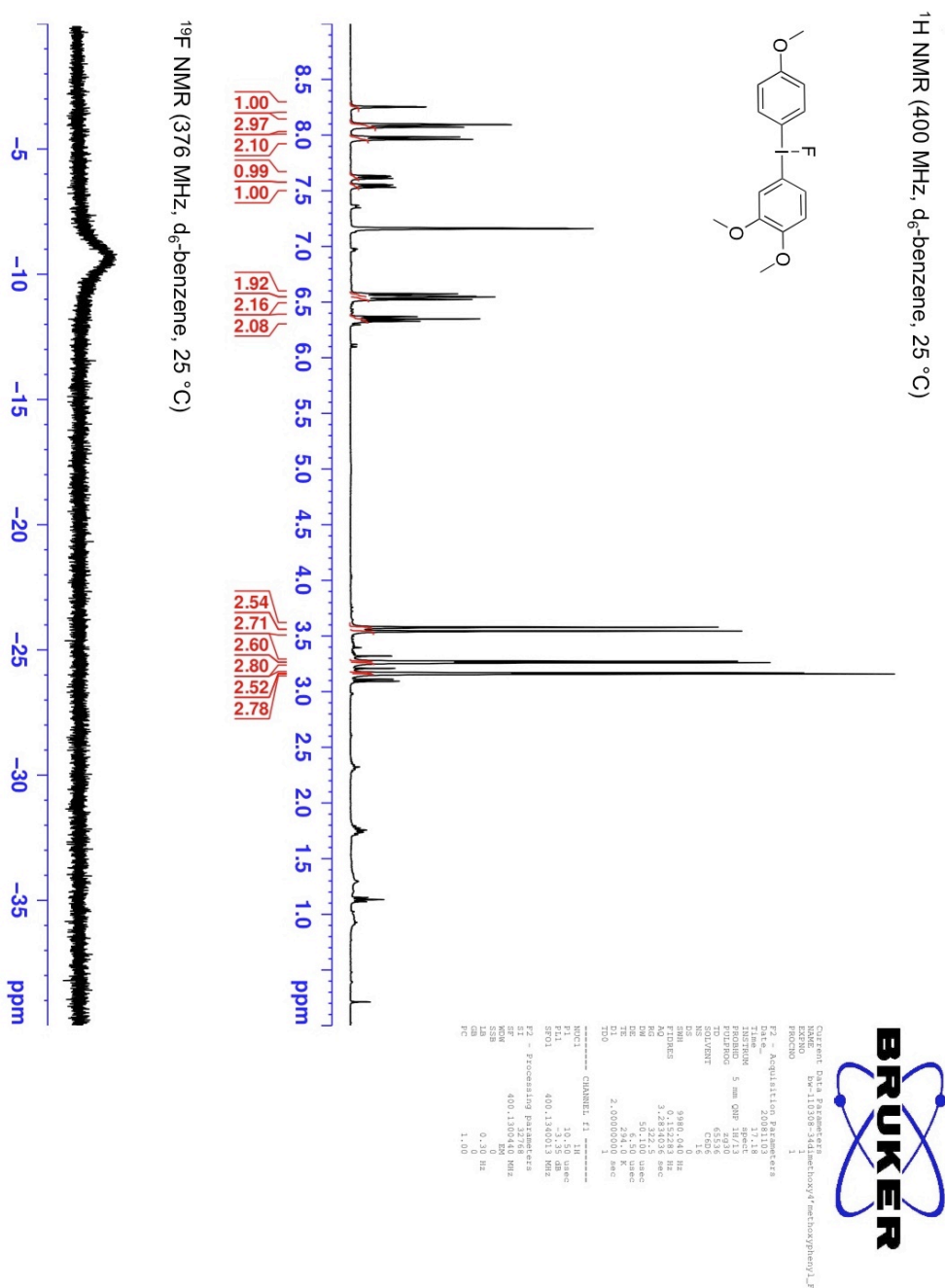
**Spectrum 34**  $^1\text{H}$  and  $^{13}\text{C}$  NMR spectra of phenyl(4-methoxyphenyl)-iodonium hexafluorophosphate in  $\text{d}_3$ -acetonitrile



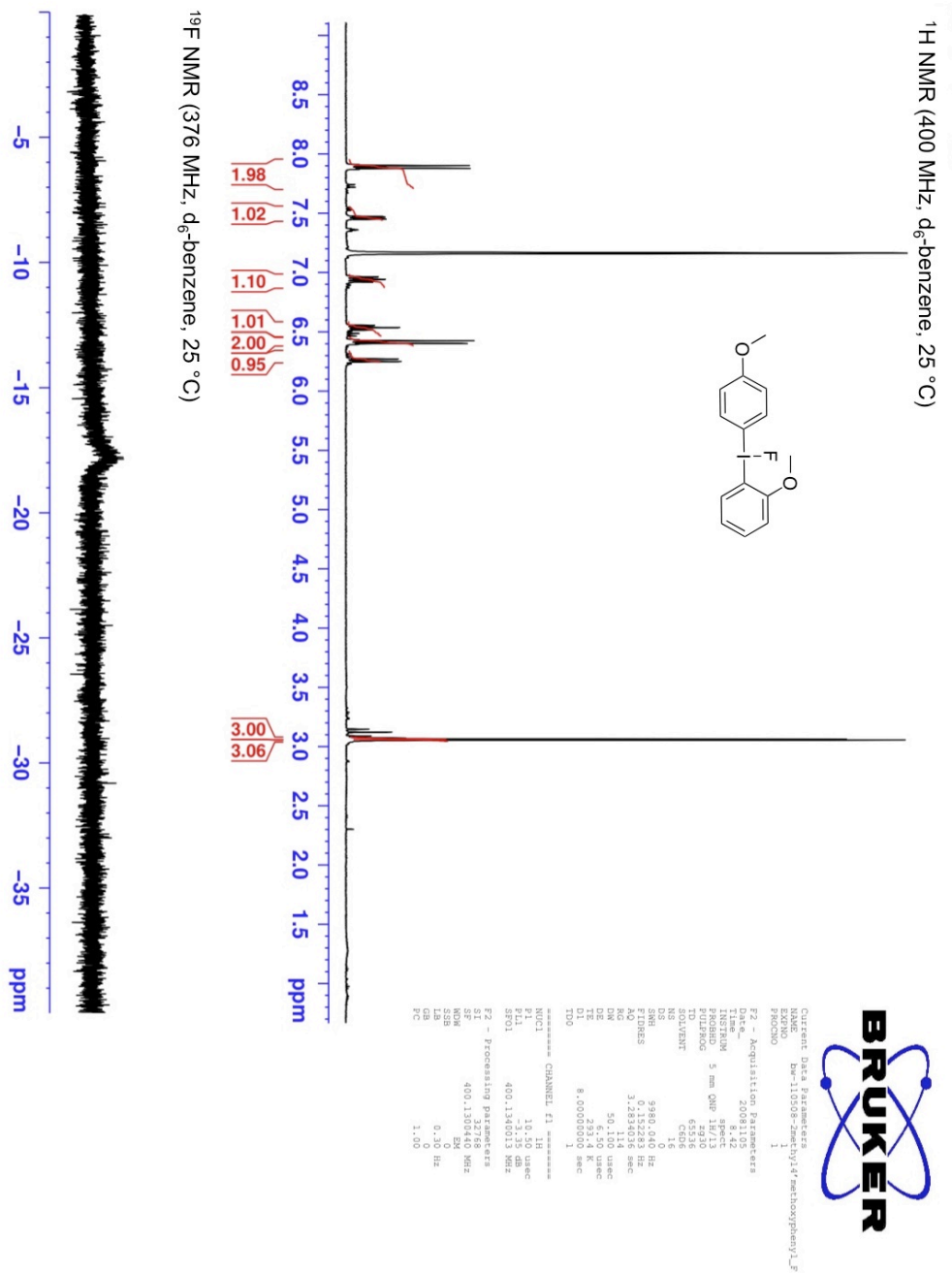
Spectrum 35  $^1\text{H}$  and  $^{19}\text{F}$  NMR spectra of bis(4-methoxyphenyl)-fluoro- $\lambda^3$ -iodane in  $\text{d}_3$ -acetonitrile

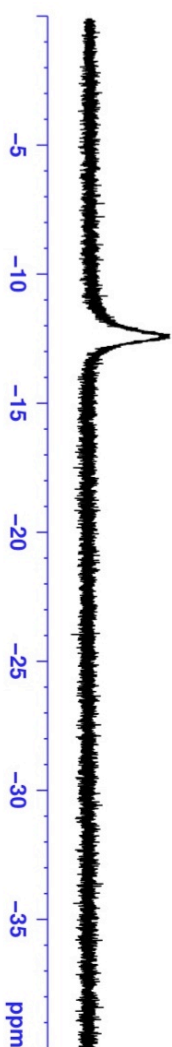
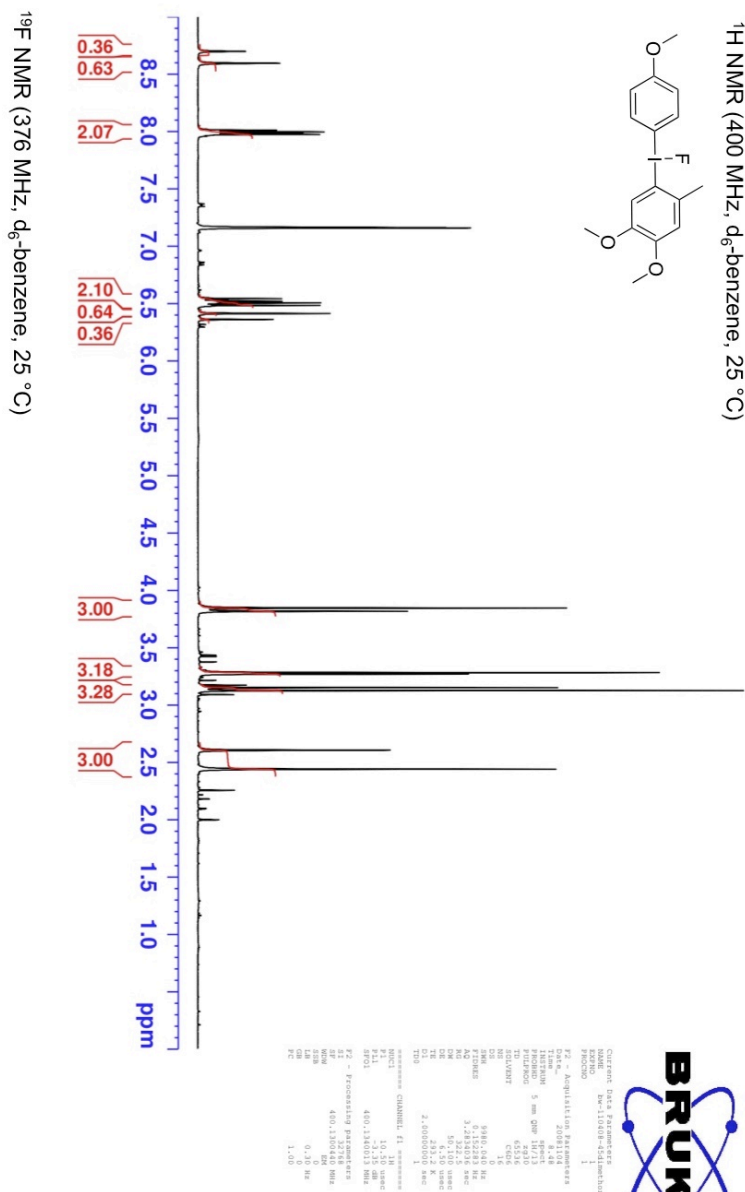


Spectrum 36  $^1\text{H}$  and  $^{19}\text{F}$  NMR spectra of (3,4-dimethoxyphenyl)(4'-methoxyphenyl)-fluoro- $\lambda^3$ -iodane in  $\text{d}_6$ -benzene

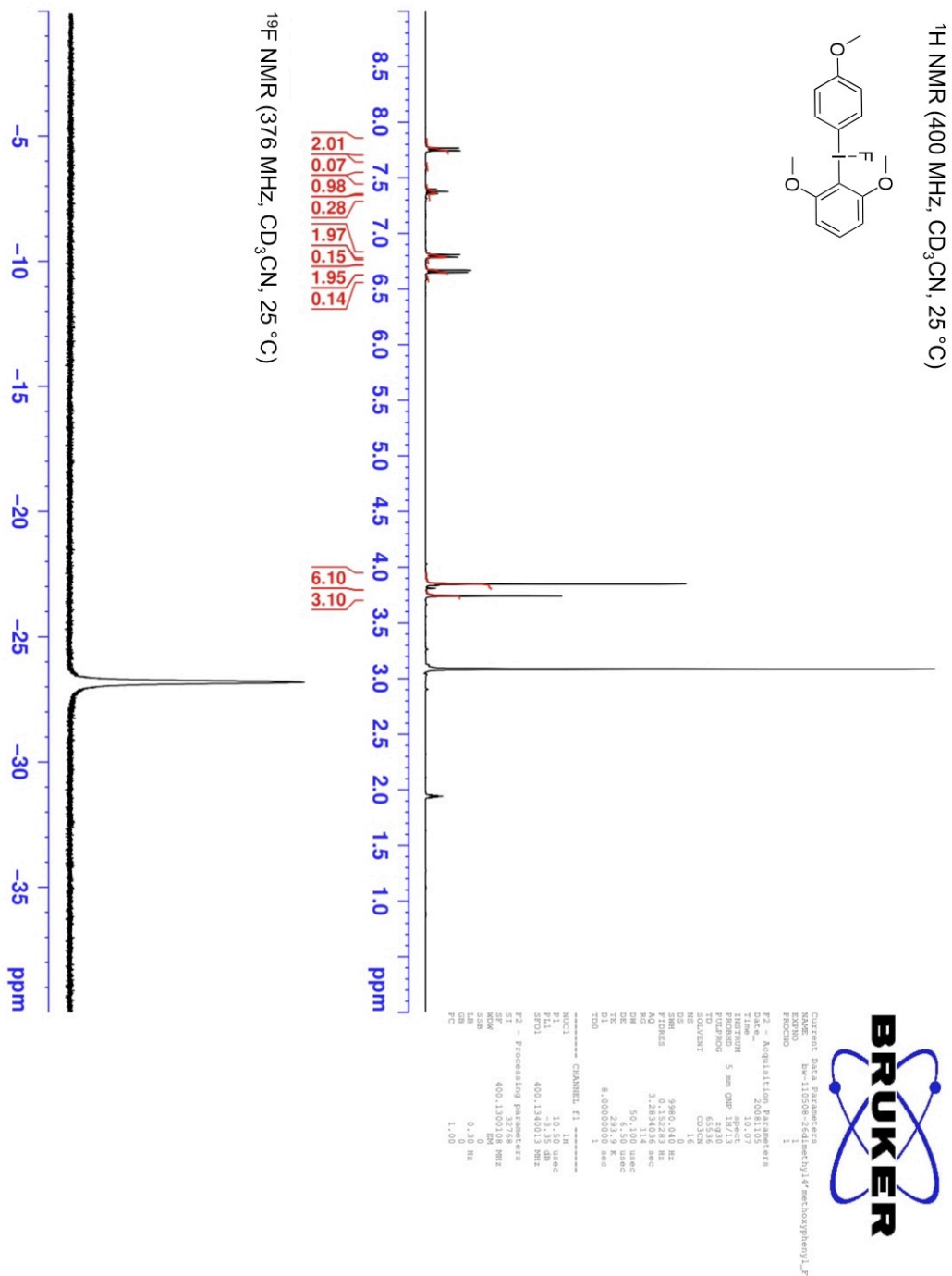


Spectrum 37  $^1\text{H}$  and  $^{19}\text{F}$  NMR spectra of (2-methoxyphenyl)(4'-methoxyphenyl)-fluoro- $\lambda^3$ -iodane in  $\text{d}_6$ -benzene

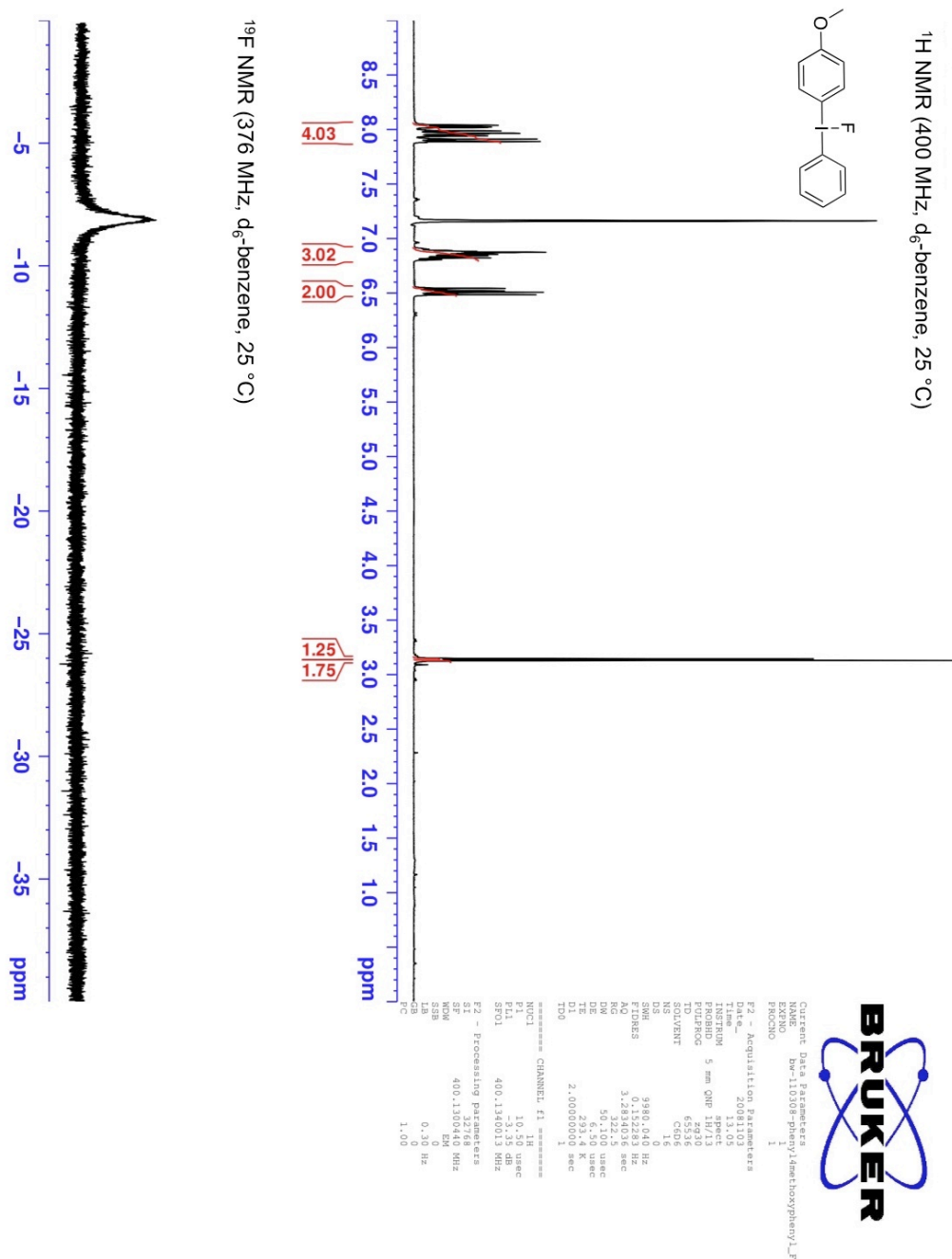




Spectrum 39  $^1\text{H}$  and  $^{19}\text{F}$  NMR spectra of (2,6-dimethoxyphenyl)(4'-methoxyphenyl)-fluoro- $\lambda_3$ -iodane in  $\text{d}_3$ -acetonitrile

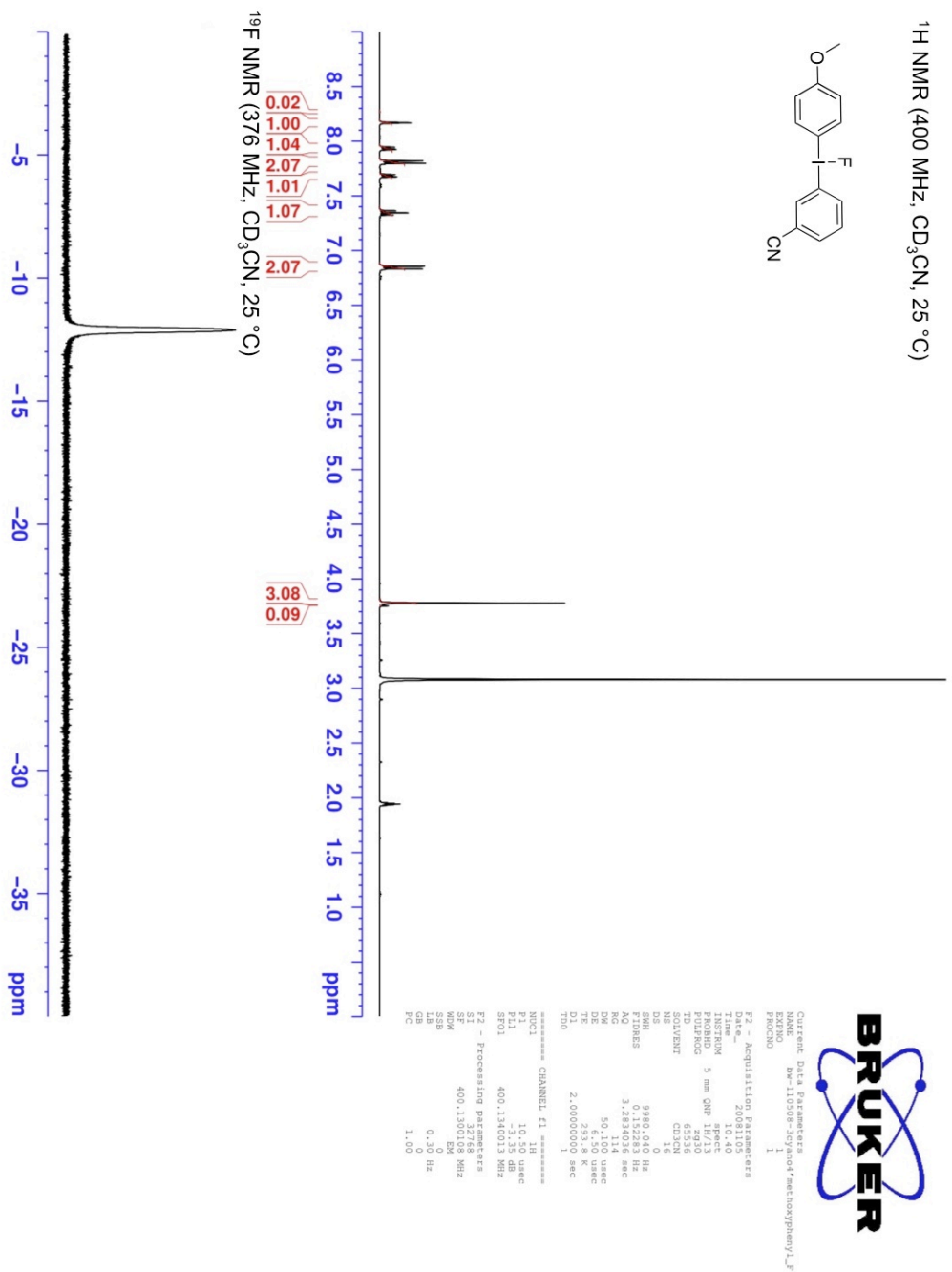


Spectrum 40  $^1\text{H}$  and  $^{19}\text{F}$  NMR spectra of phenyl(4-methoxyphenyl)-fluoro- $\lambda^3$ -iodane in  $\text{d}_6$ -benzene

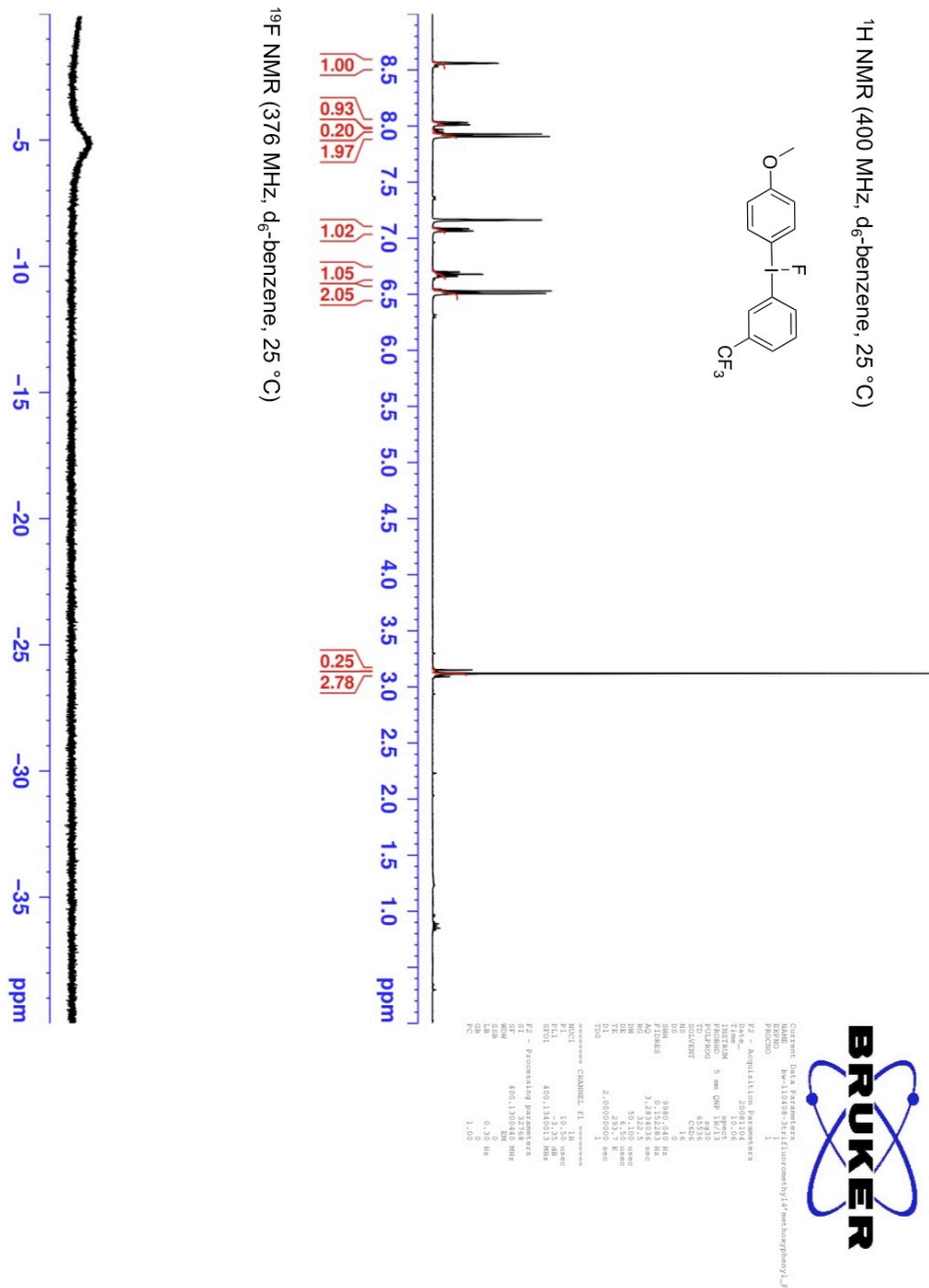




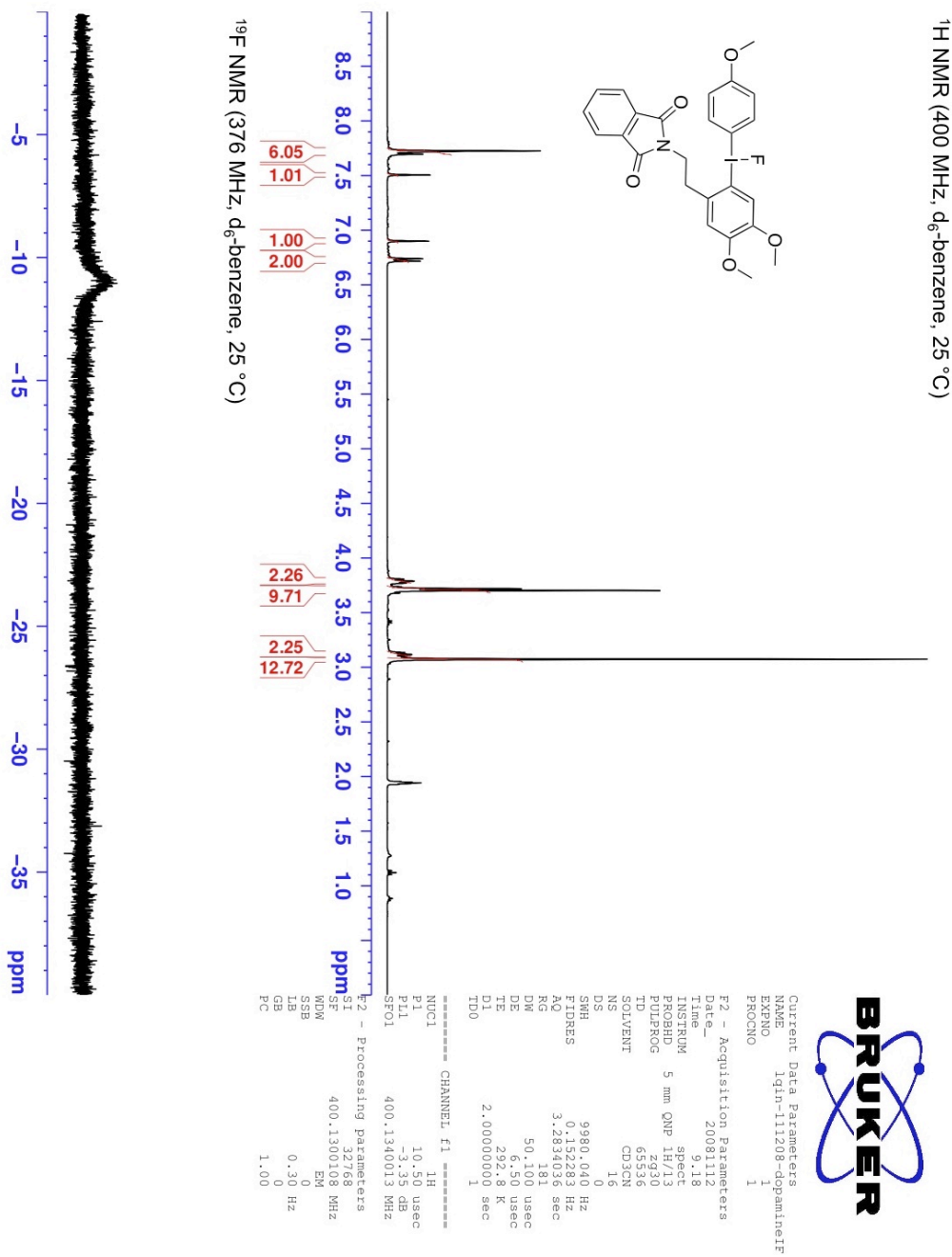
Spectrum 41 <sup>1</sup>H and <sup>19</sup>F NMR spectra of (3-cyanophenyl)(4'-methoxyphenyl)-fluoro-λ<sup>3</sup>-iodane in d<sub>3</sub>-acetonitrile



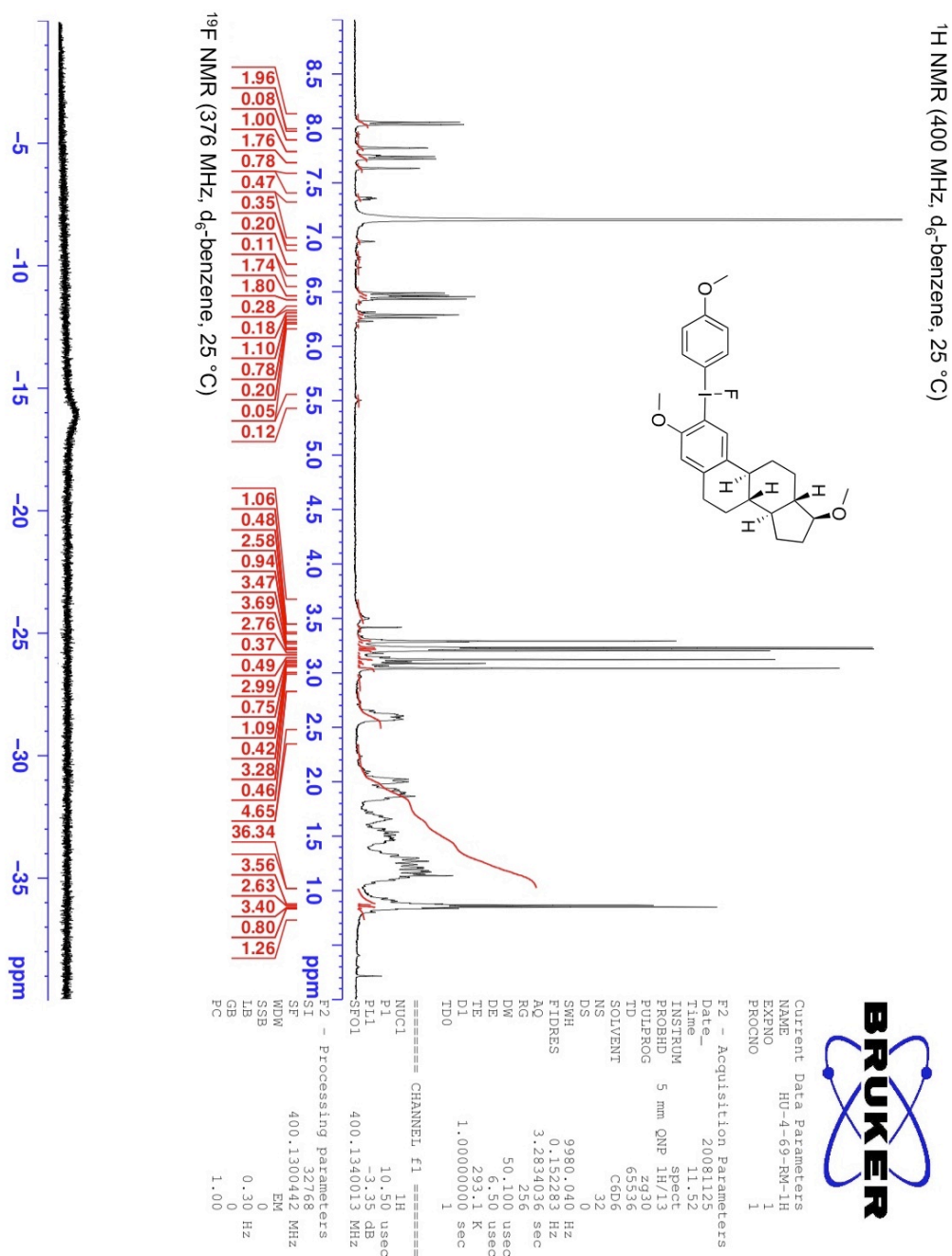
**Spectrum 42  $^1\text{H}$  and  $^{19}\text{F}$  NMR spectra of (3-(trifluoromethyl)phenyl)(4'-methoxyphenyl)-fluoro- $\lambda^3$ -iodane in  $\text{d}_6$ -benzene**



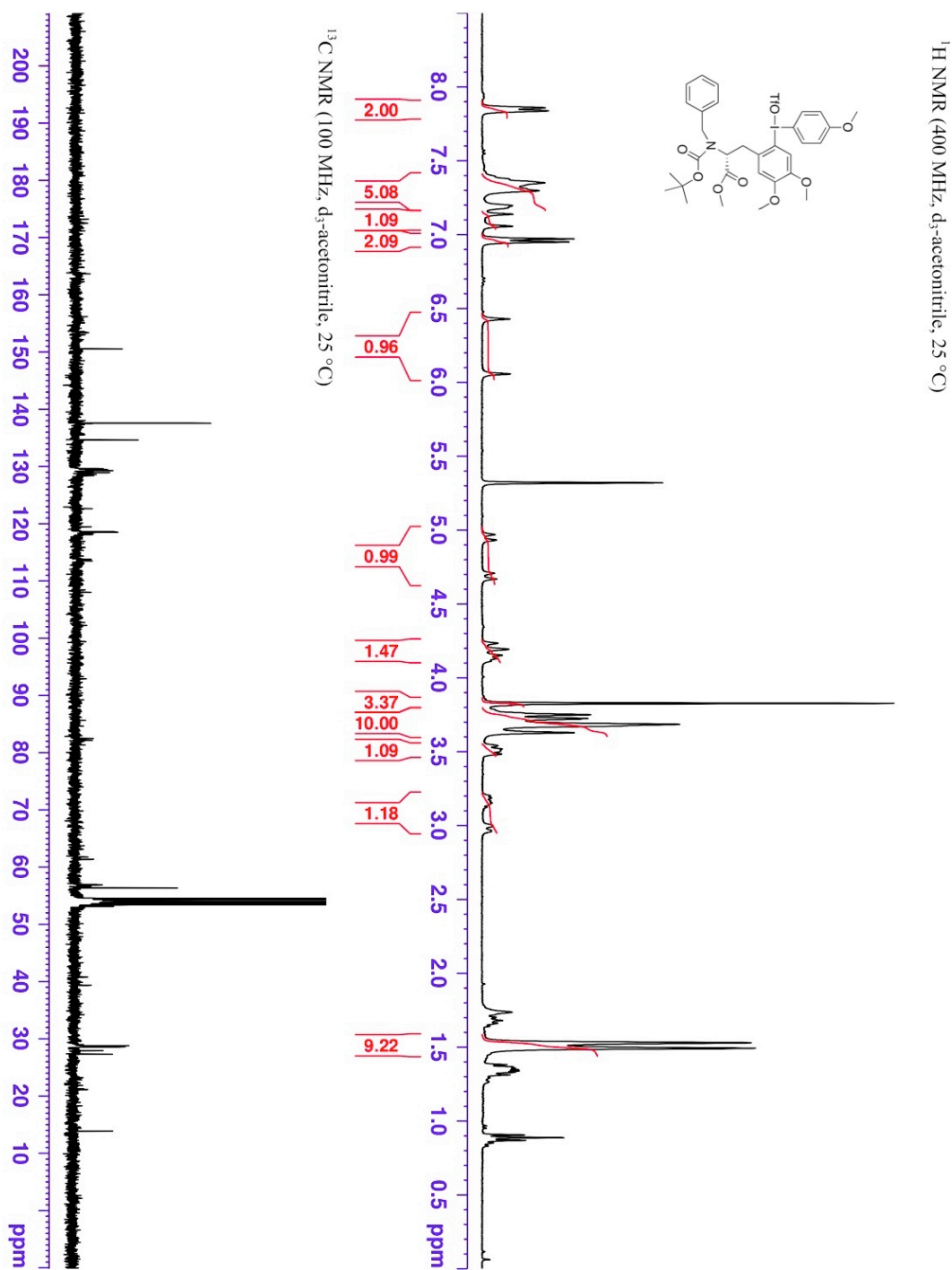
Spectrum 43  $^1\text{H}$  and  $^{19}\text{F}$  NMR spectra of (4,5-dimethoxy-2-(2-phthalimidoethyl)phenyl)(4'-methoxyphenyl)-fluoro- $\lambda^3$ -iodane in  $\text{d}_6$ -benzene

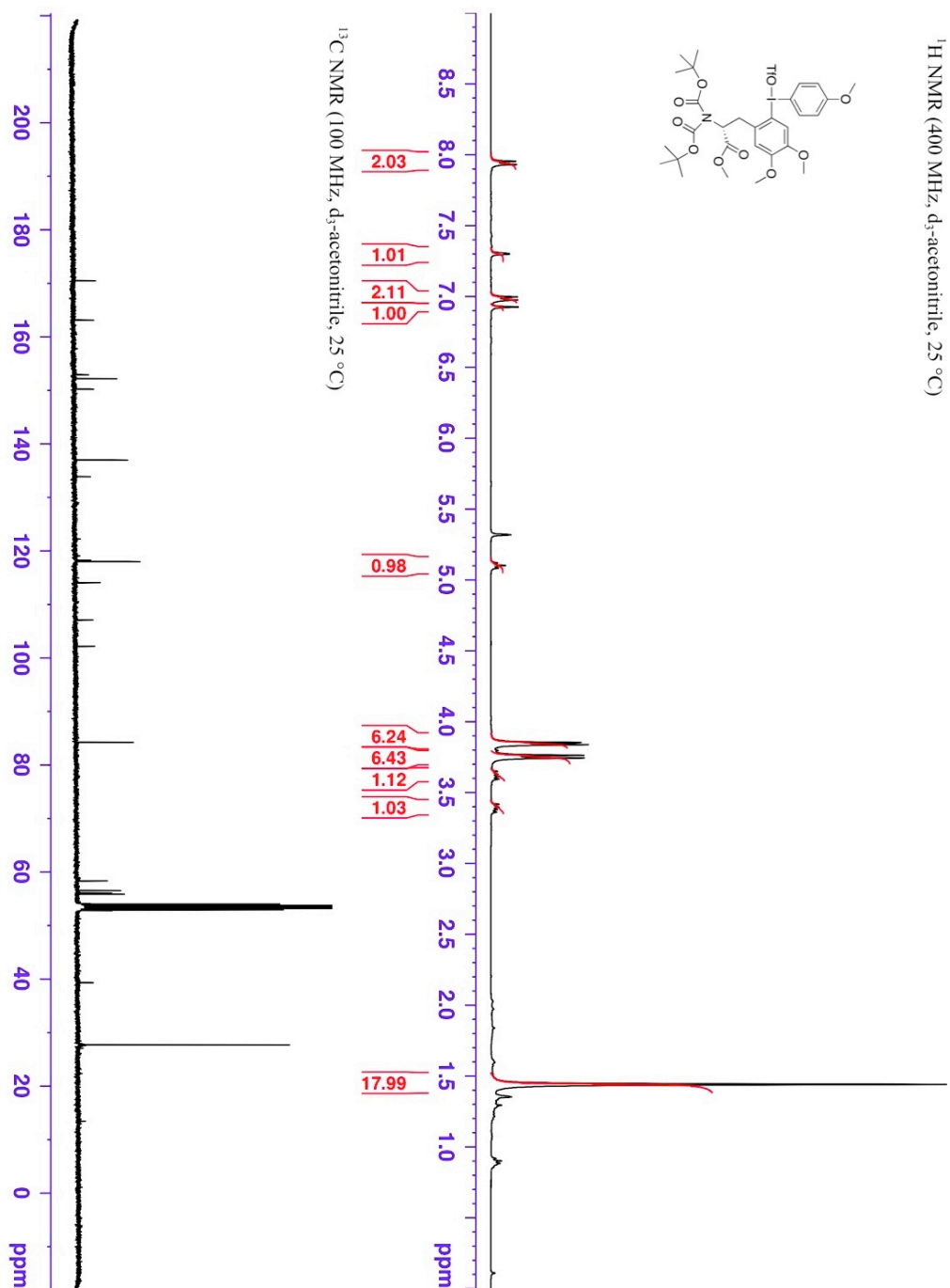


Spectrum 44  $^1\text{H}$  and  $^{19}\text{F}$  NMR spectra of (3,17-dimethoxy- $\beta$ -estra-1,3,5(10)-trien-2-yl)(4'-methoxyphenyl)-fluoro- $\lambda^3$ -iodane in  $\text{d}_6$ -benzene

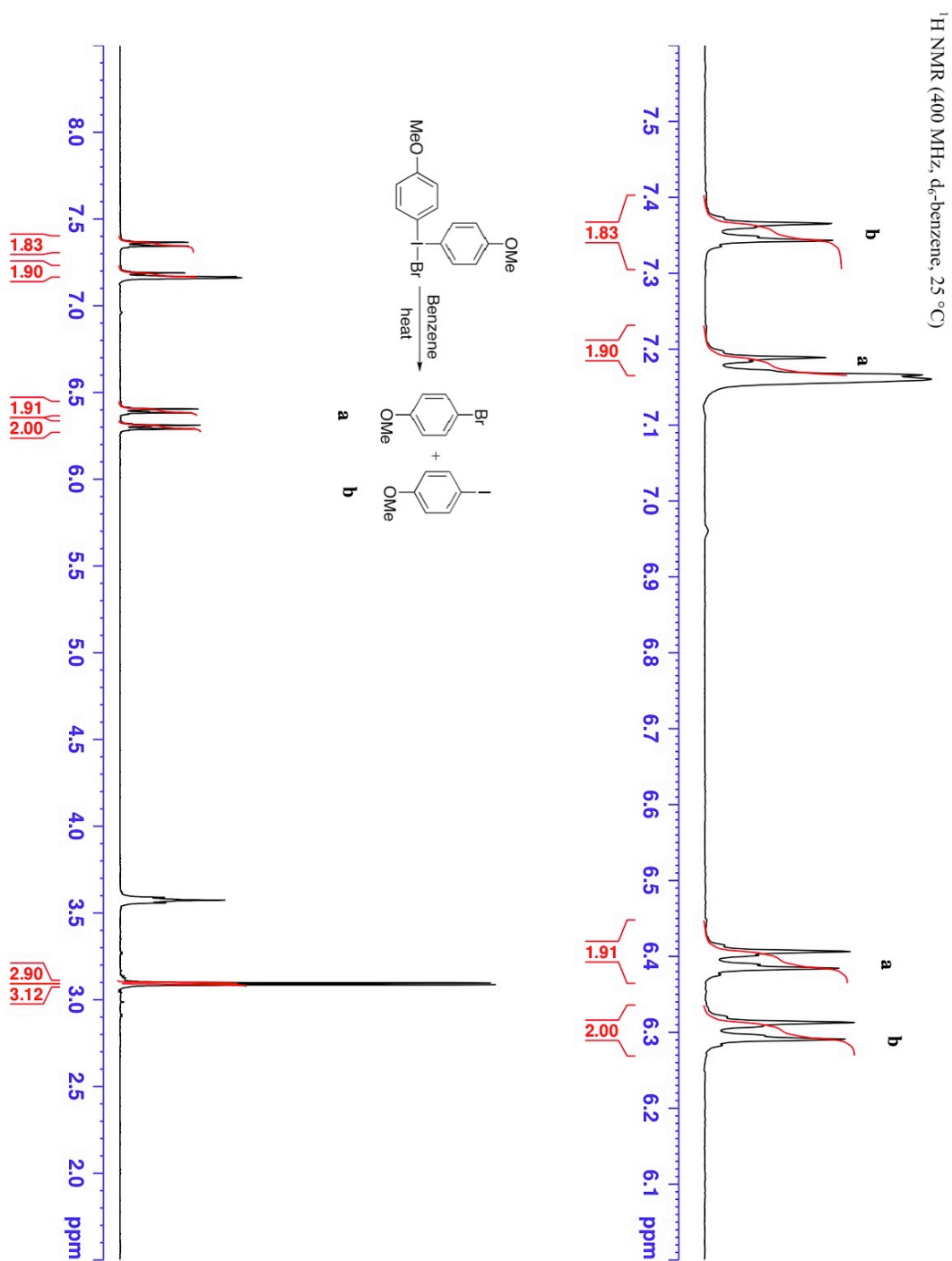


Spectrum 45  $^1\text{H}$  and  $^{13}\text{C}$  NMR spectra of (2-(2-(benzyl-(*tert*-butoxycarbonyl)amino)ethyl-4,5-dimethoxy)phenyl)(4'-methoxyphenyl)-iodonium triflate in  $\text{d}_3$ -acetonitrile

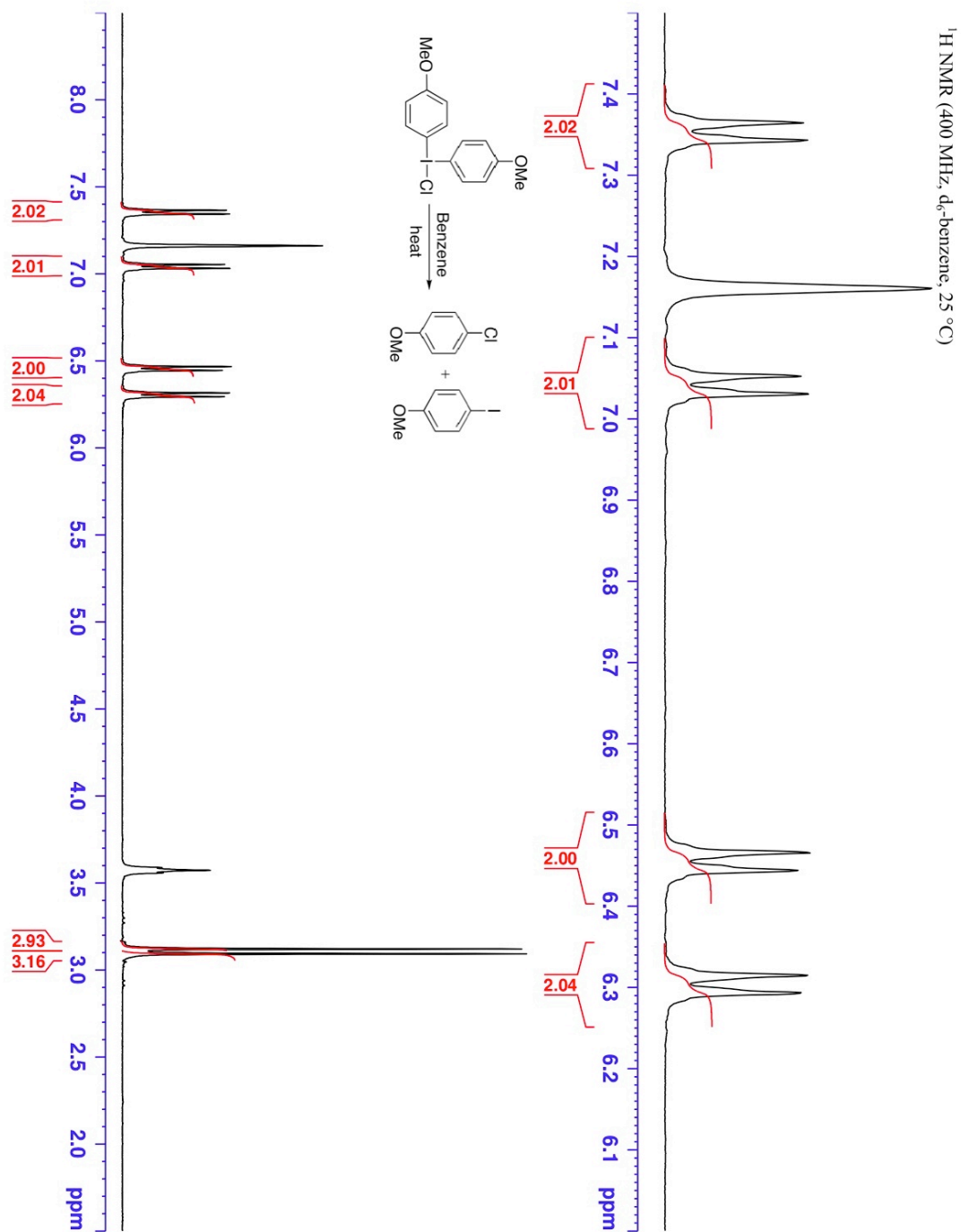




Spectrum 47  $^1\text{H}$  NMR spectrum of bis(4-methoxyphenyl)-bromo- $\lambda^3$ -iodane decomposition in  $\text{d}_6$ -benzene

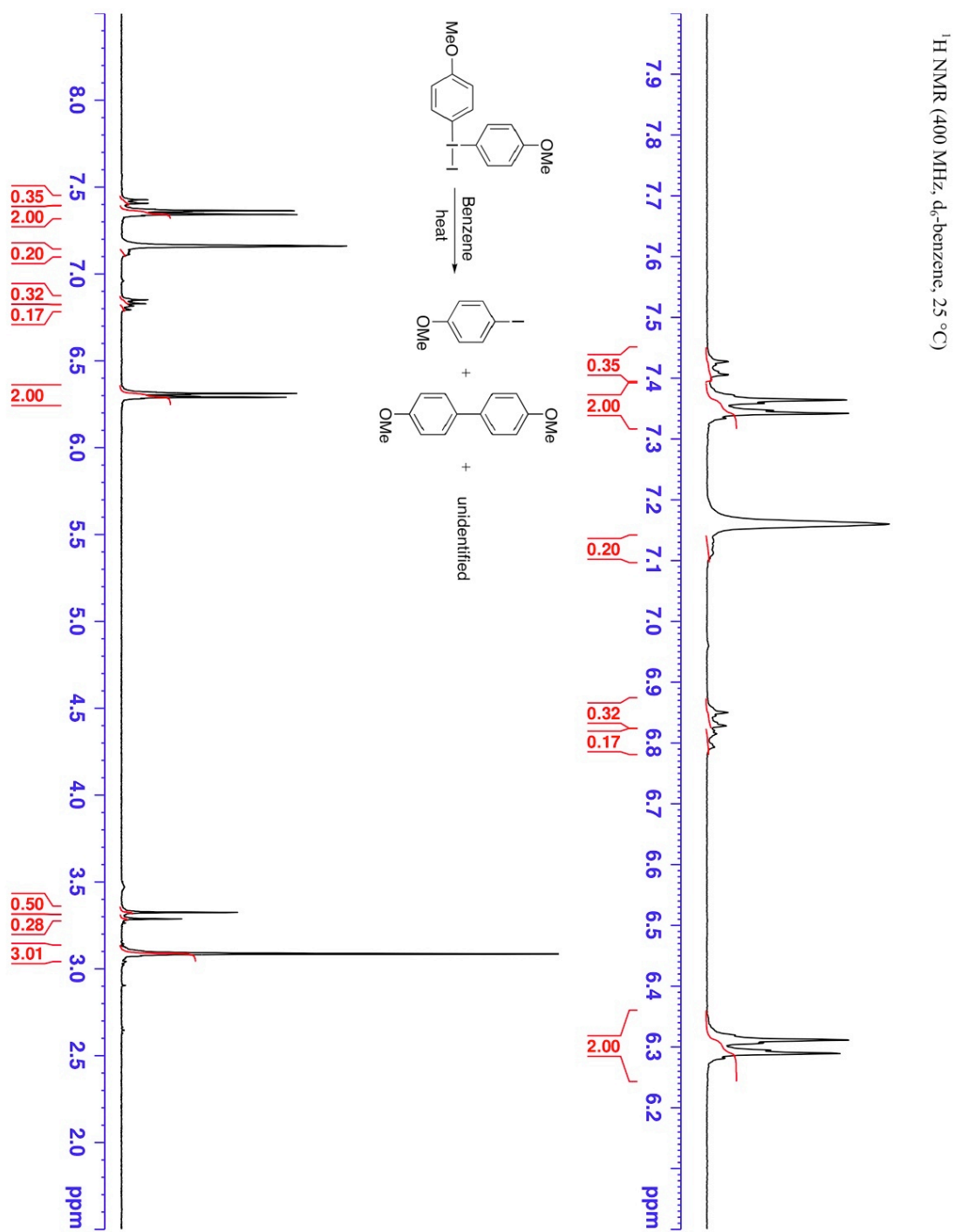


**Spectrum 48**  $^1\text{H}$  NMR spectrum of bis(4-methoxyphenyl)-chloro- $\lambda^3$ -iodane decomposition in  $\text{d}_6$ -benzene

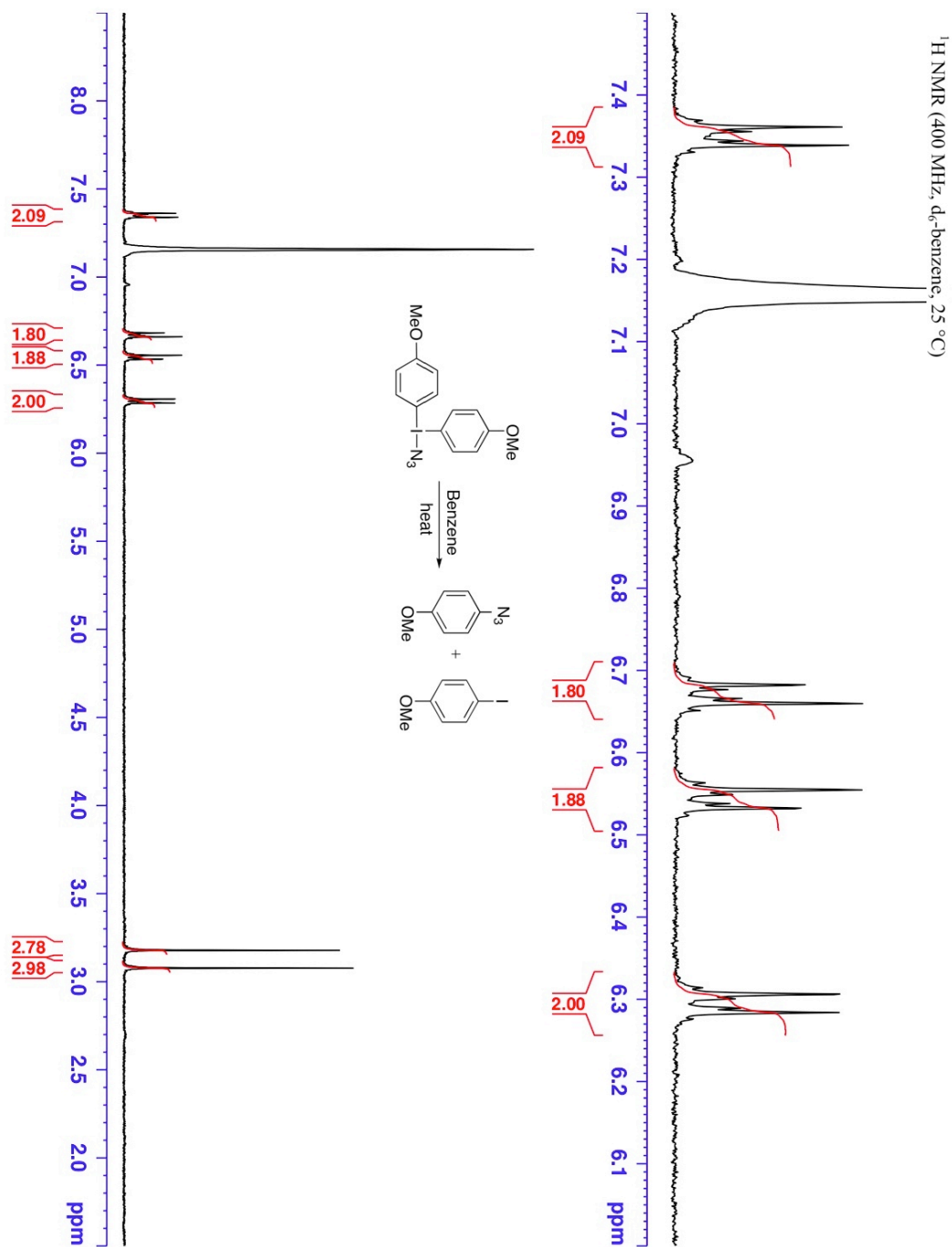




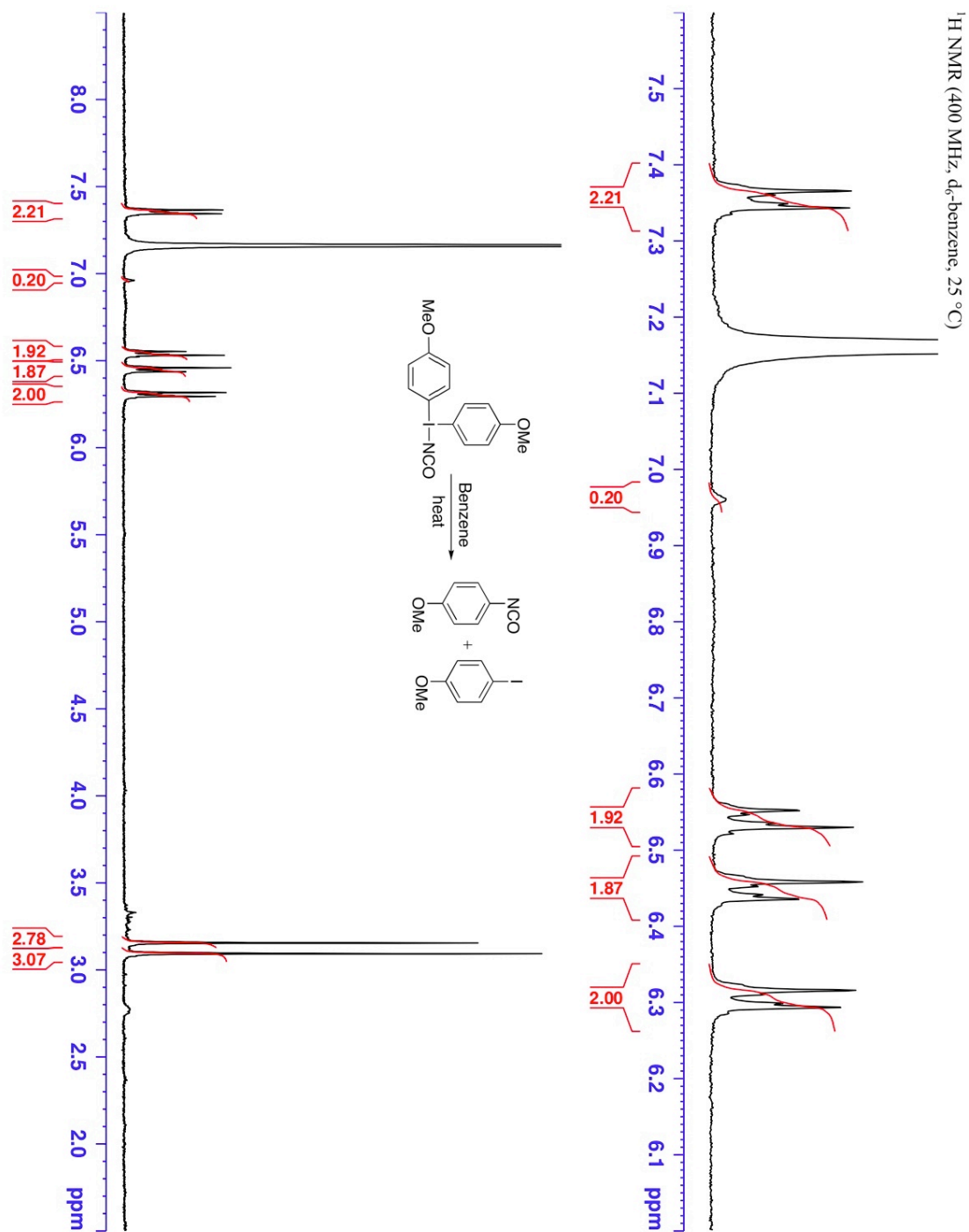
**Spectrum 49**  $^1\text{H}$  NMR spectrum of bis(4-methoxyphenyl)-iodo- $\lambda_3$ -iodane decomposition in  $\text{d}_6$ -benzene



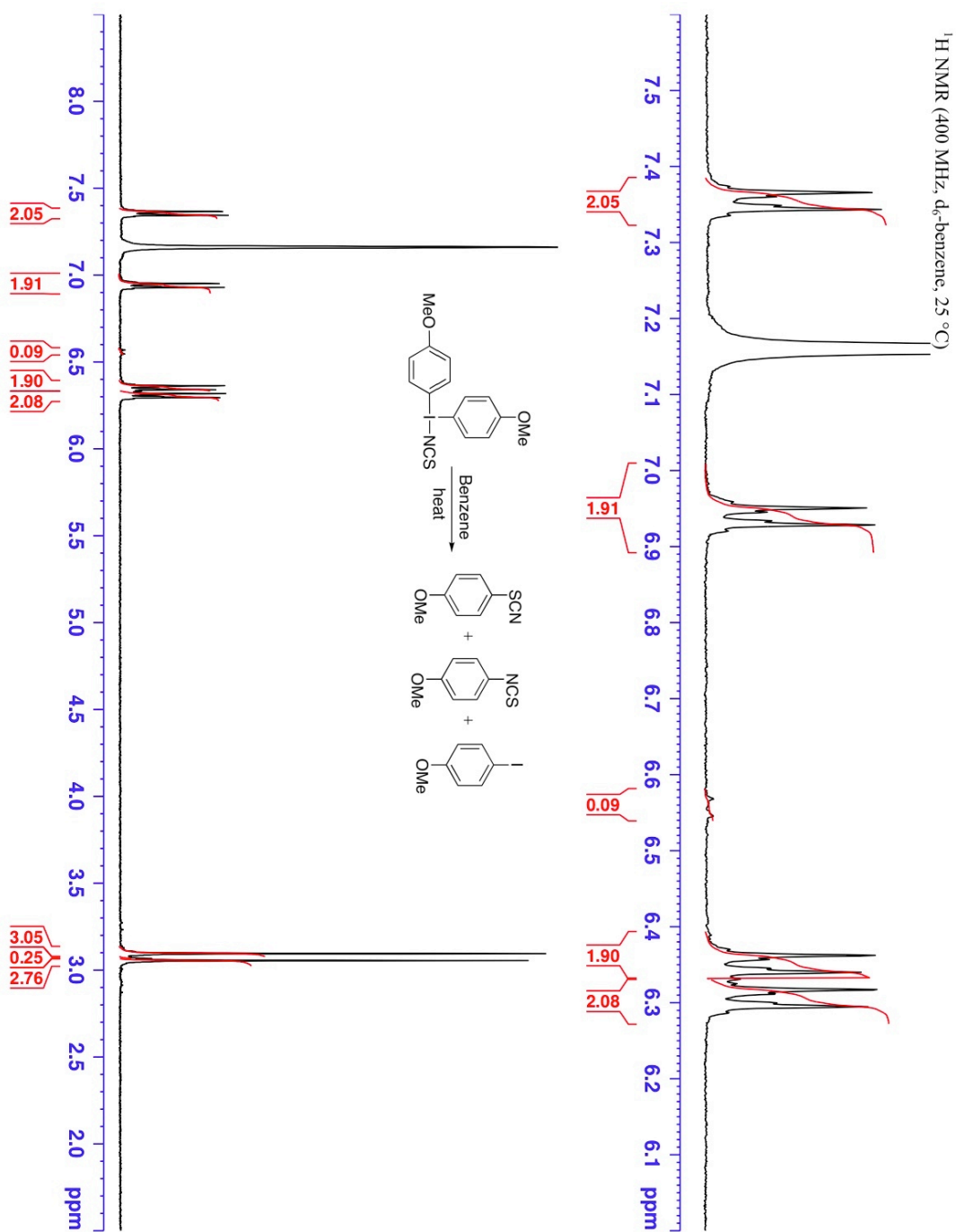
**Spectrum 50**  $^1\text{H}$  NMR spectrum of bis(4-methoxyphenyl)-azido- $\lambda^3$ -iodane decomposition in  $\text{d}_6$ -benzene



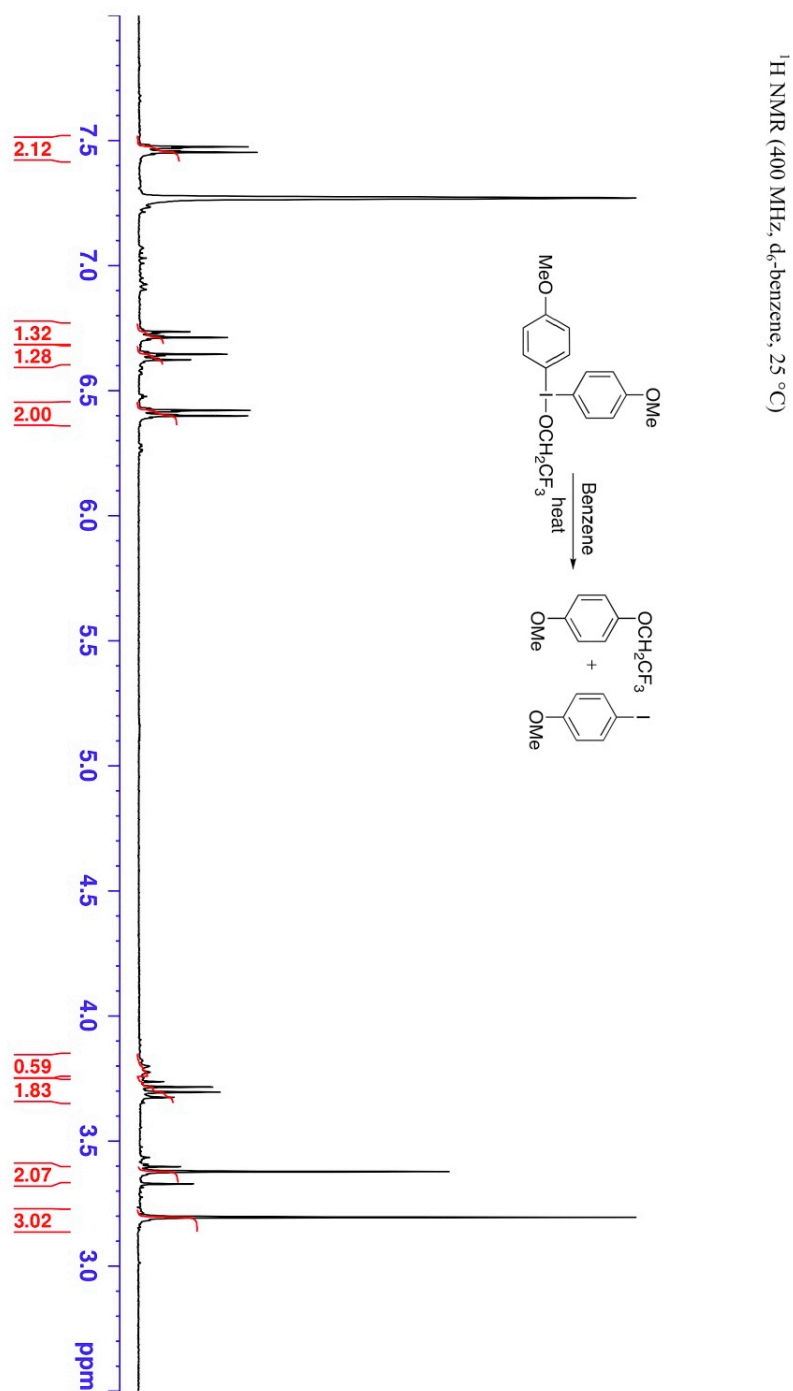
Spectrum 51  $^1\text{H}$  NMR spectrum of bis(4-methoxyphenyl)-cyanato- $\lambda^3$ -iodane decomposition in  $\text{d}_6$ -benzene



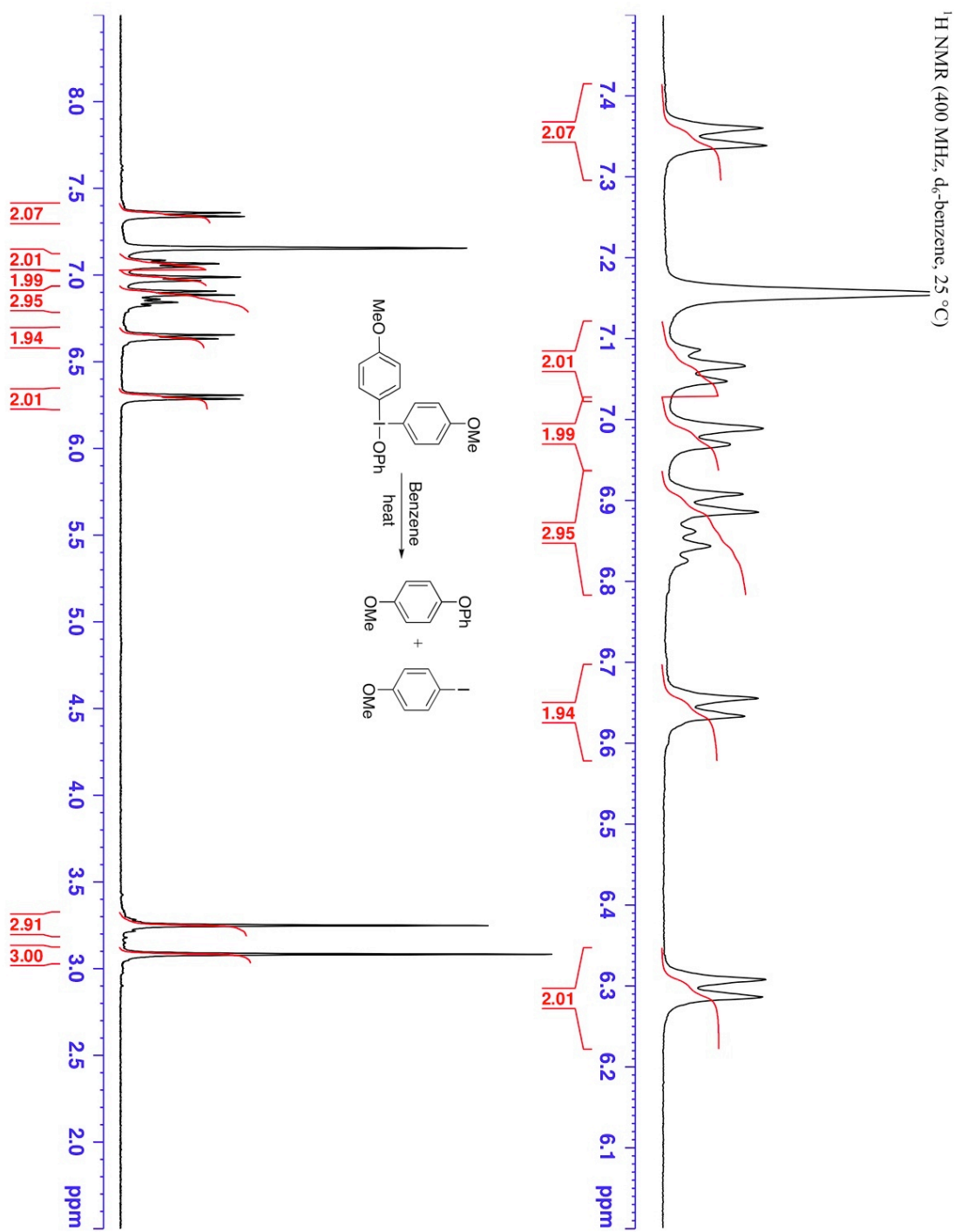
**Spectrum 52**  $^1\text{H}$  NMR spectrum of bis(4-methoxyphenyl)-thiocyanato- $\lambda^3$ -iodane decomposition in  $\text{d}_6$ -benzene



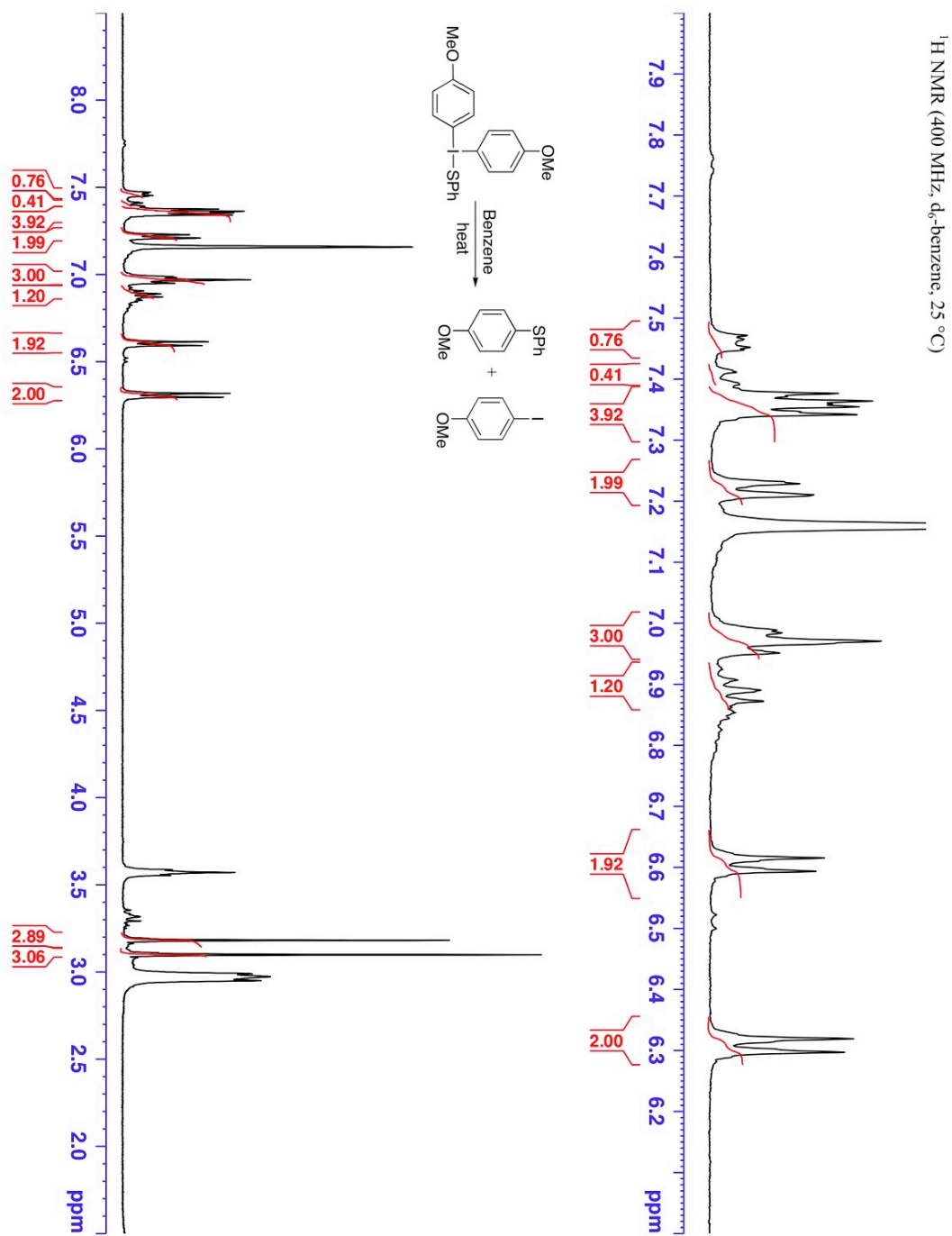
**Spectrum 53**  $^1\text{H}$  NMR spectrum of bis(4-methoxyphenyl)-(2,2,2-trifluoroethoxy)- $\lambda^3$ -iodane decomposition in  $\text{d}_6$ -benzene



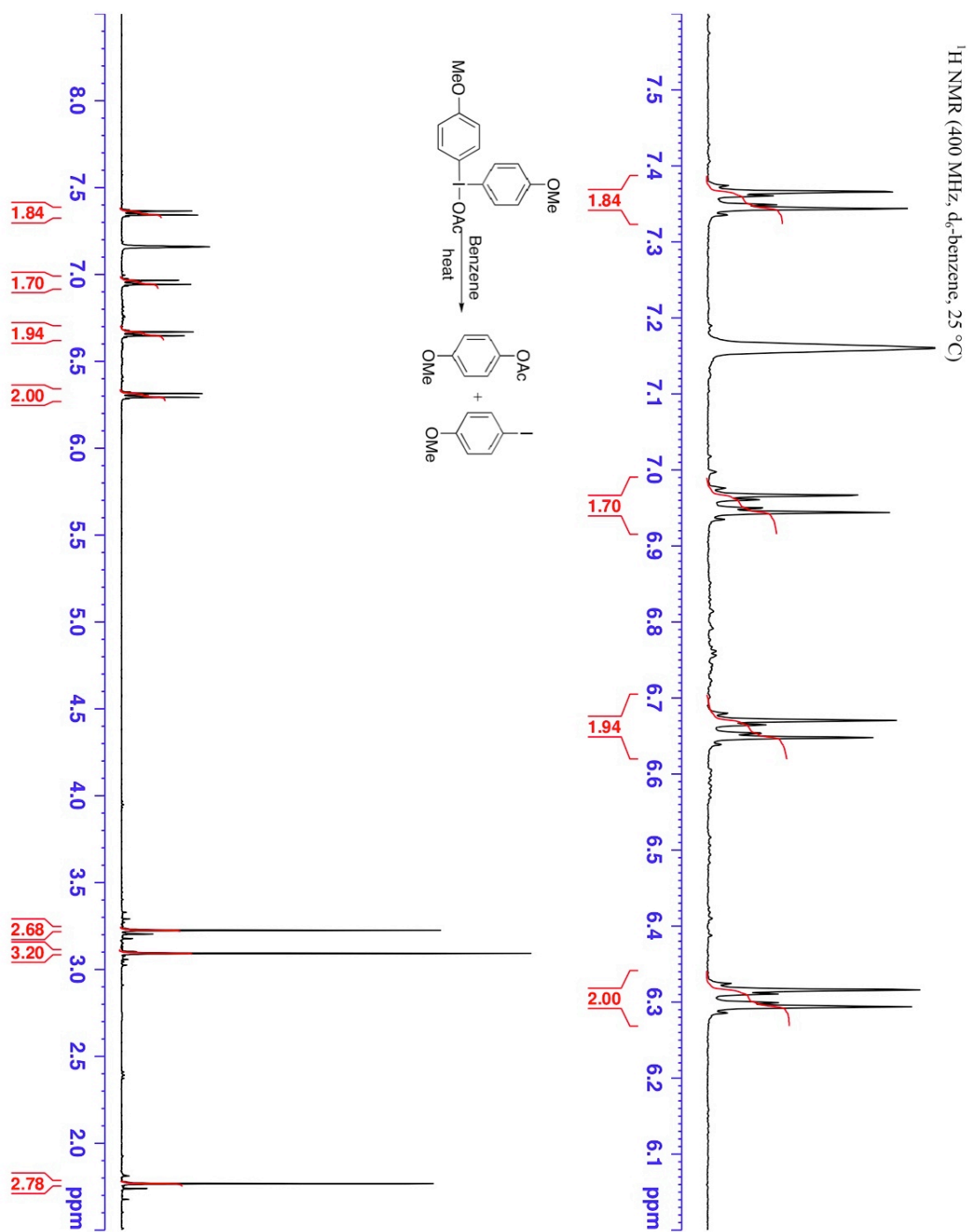
Spectrum 54  $^1\text{H}$  NMR spectrum of bis(4-methoxyphenyl)-phenoxy- $\lambda^3$ -iodane decomposition in  $\text{d}_6$ -benzene



**Spectrum 55**  $^1\text{H}$  NMR spectrum of bis(4-methoxyphenyl)-phenylthio- $\lambda^3$ -iodane decomposition in  $\text{d}_6$ -benzene

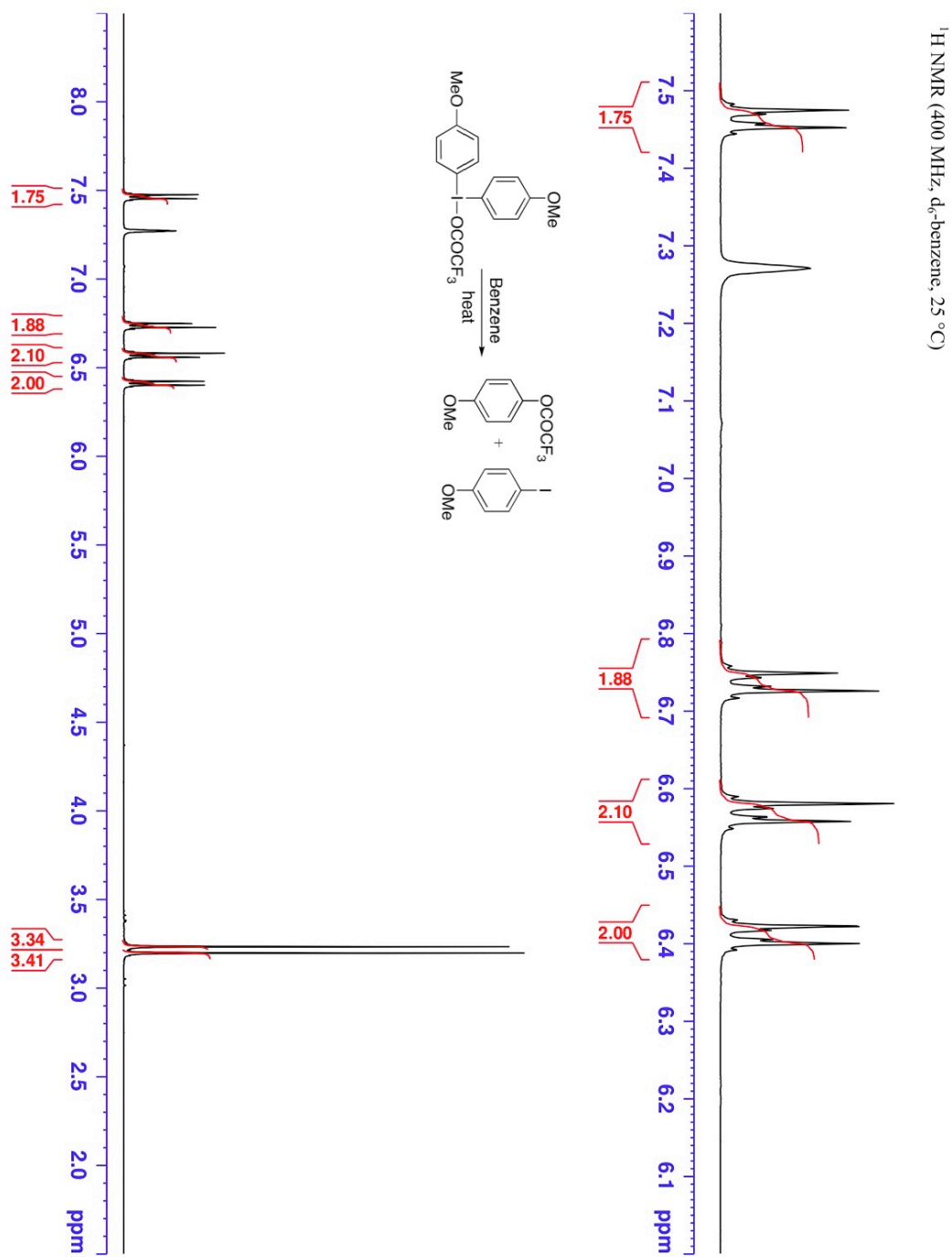


Spectrum 56  $^1\text{H}$  NMR spectrum of bis(4-methoxyphenyl)-acetoxy- $\lambda^3$ -iodane decomposition  
in  $\text{d}_6$ -benzene

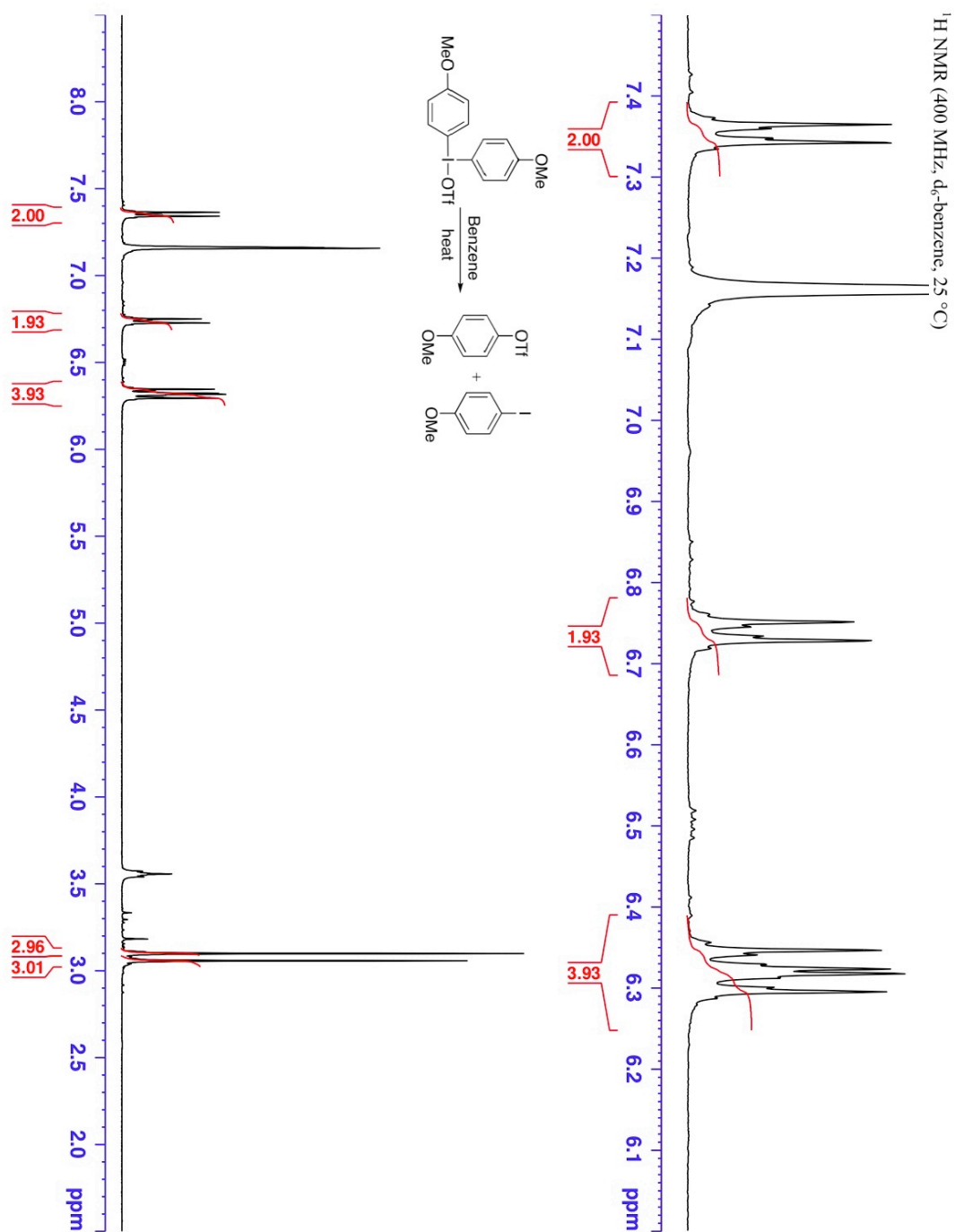




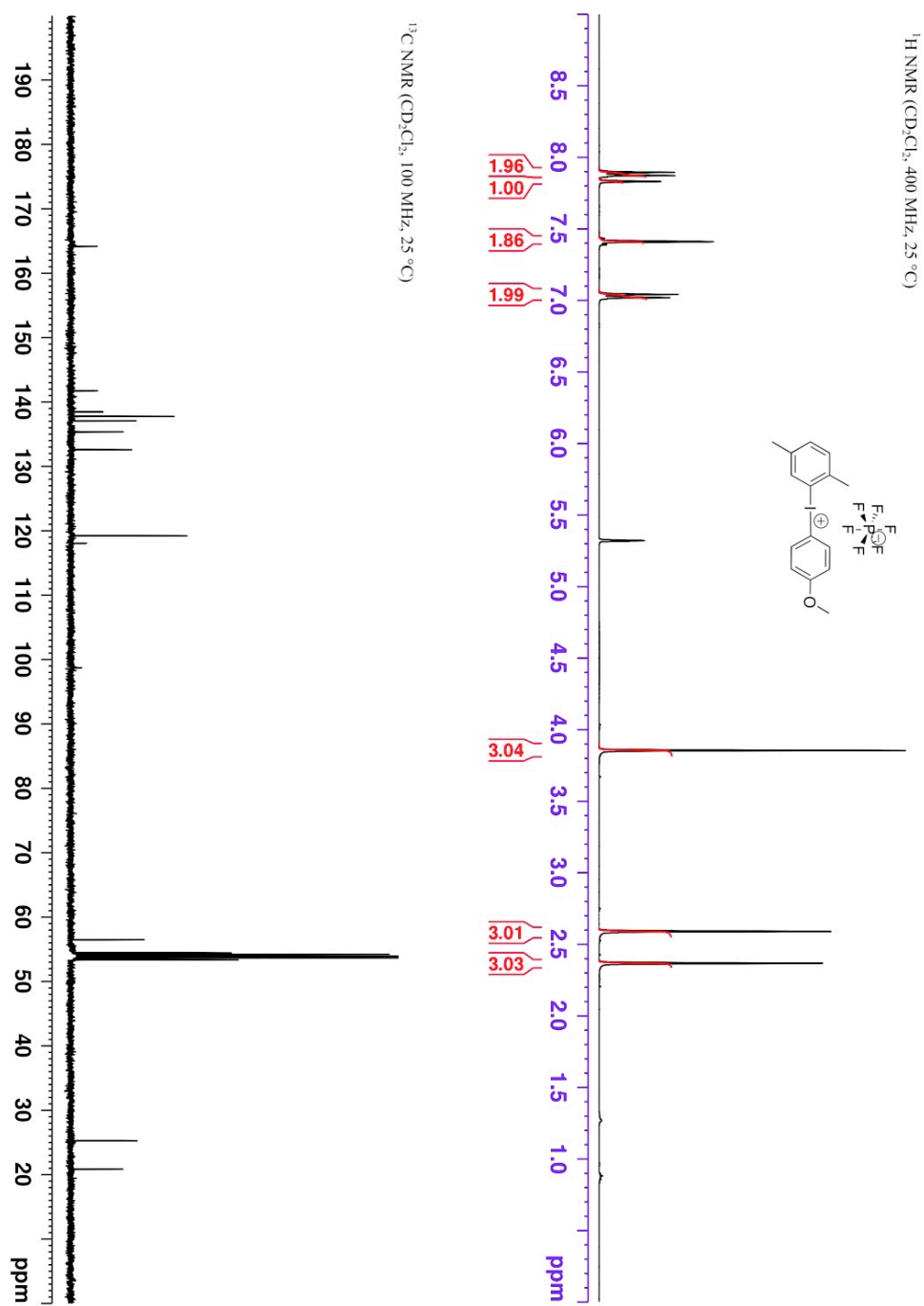
**Spectrum 57**  $^1\text{H}$  NMR spectrum of bis(4-methoxyphenyl)-(2,2,2-trifluoroacetoxy)- $\lambda^3$ -iodane decomposition in  $\text{d}_6$ -benzene



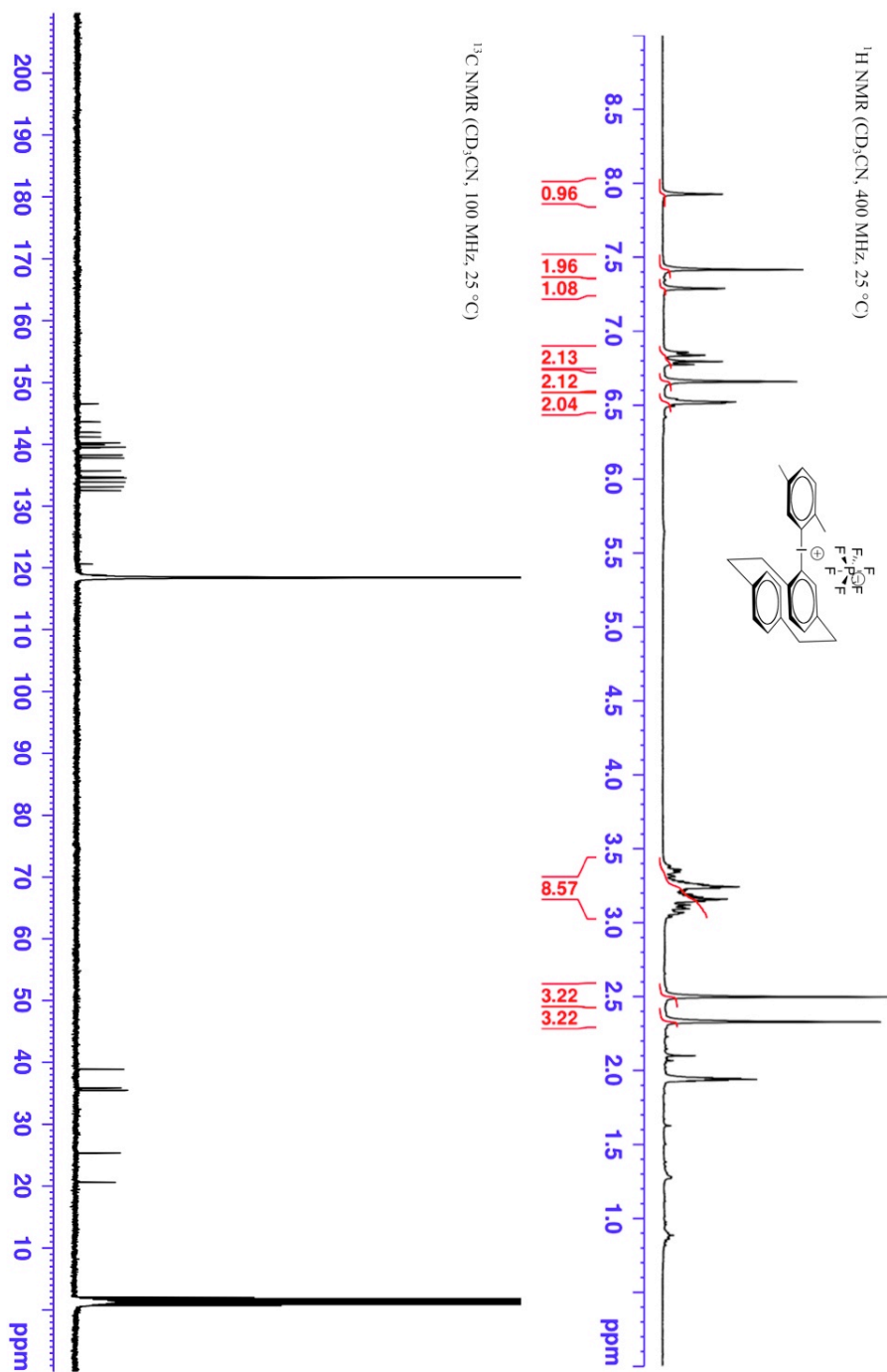
**Spectrum 58**  $^1\text{H}$  NMR spectrum of bis(4-methoxyphenyl)-triflyl- $\lambda^3$ -iodane decomposition in  $\text{d}_6$ -benzene



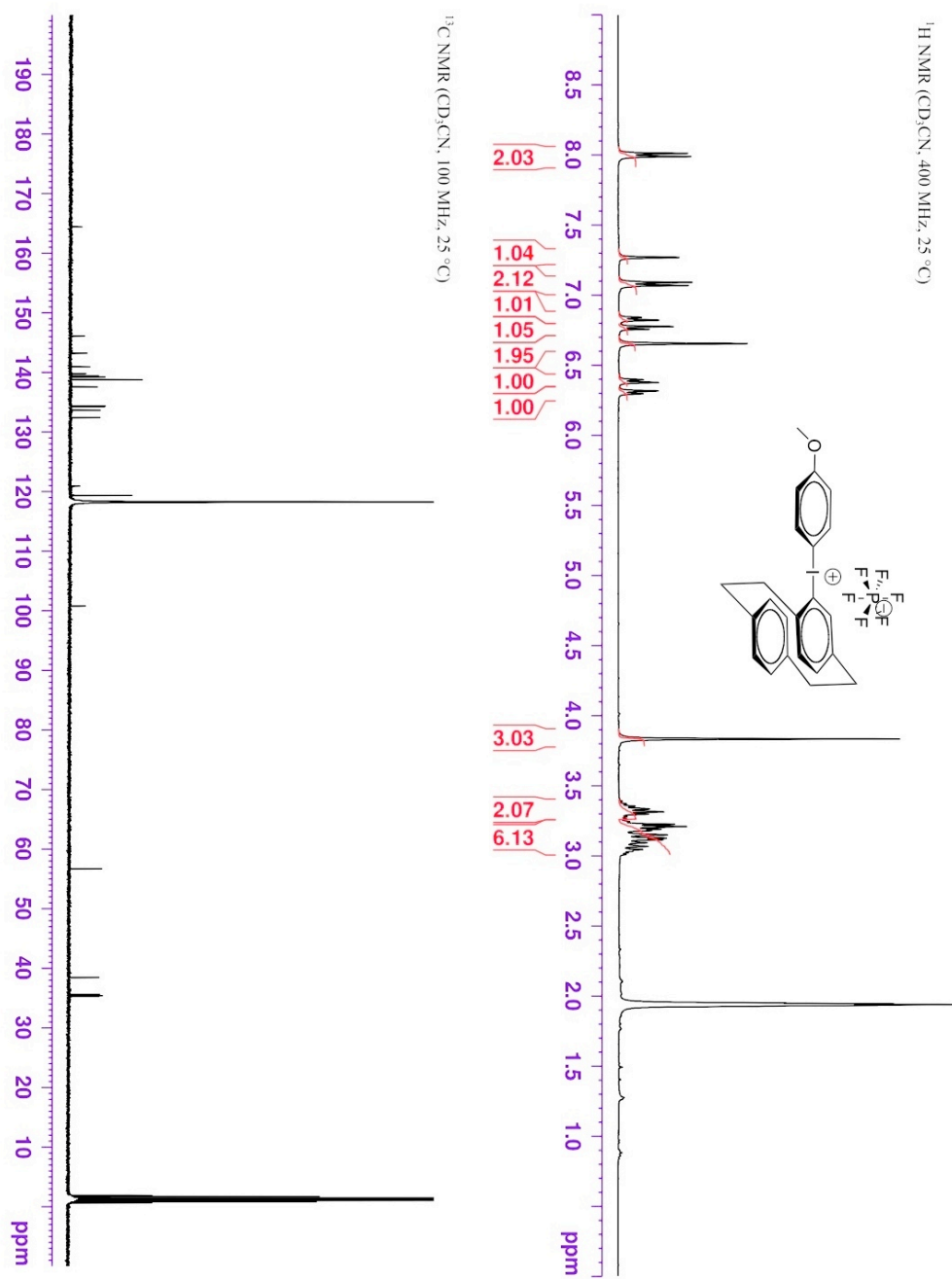
Spectrum 59:  $^1\text{H}$  and  $^{13}\text{C}$  NMR spectra of (2,5-dimethylphenyl)(4'-methoxyphenyl)-  
iodonium hexafluorophosphate in  $\text{CD}_3\text{CN}$



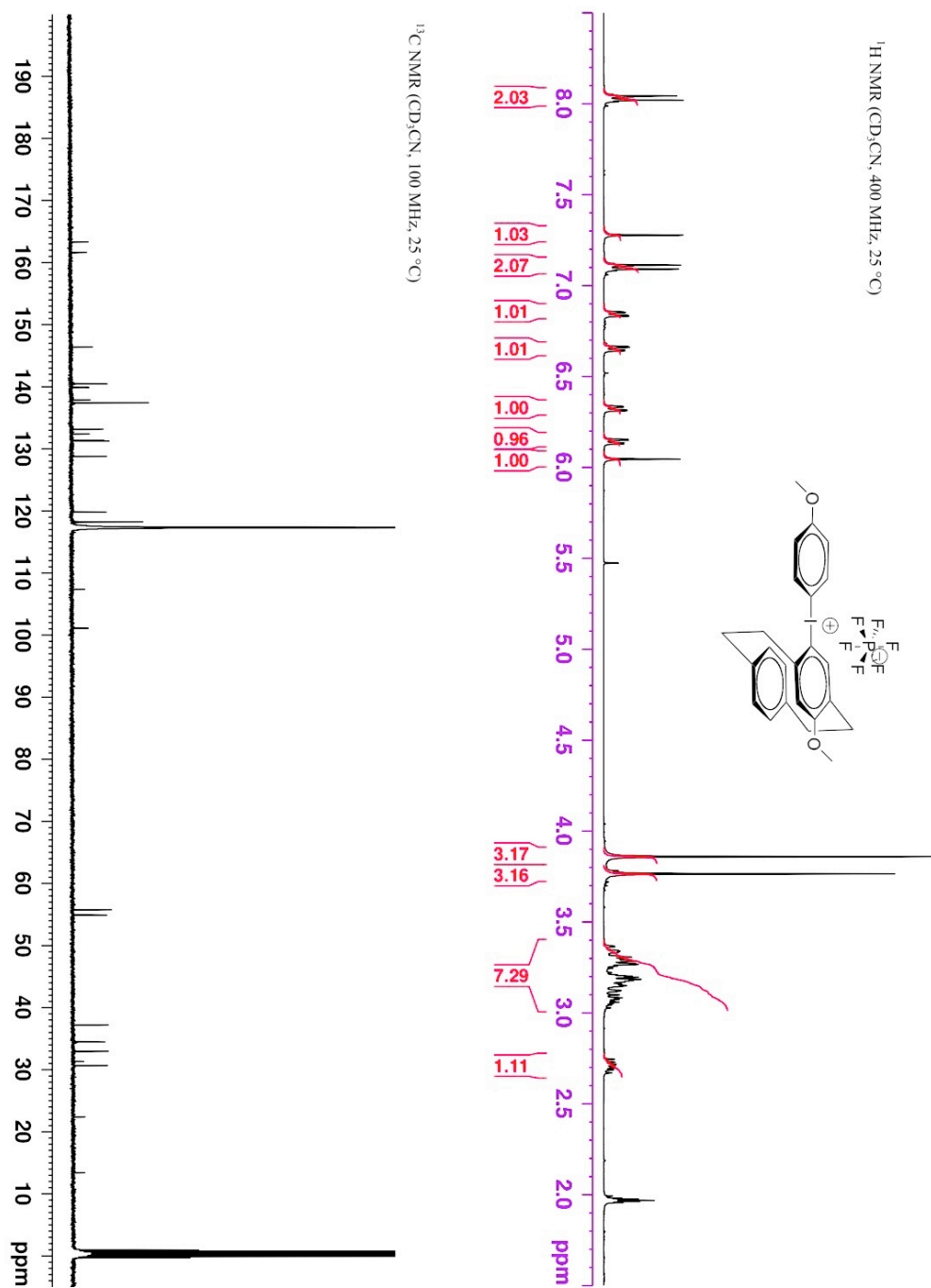
Spectrum 60  $^1\text{H}$  and  $^{13}\text{C}$  NMR spectra of ([2.2]paracyclophan-4-yl)(2',5'-dimethylphenyl)-  
iodonium hexafluorophosphate in  $\text{CD}_3\text{CN}$



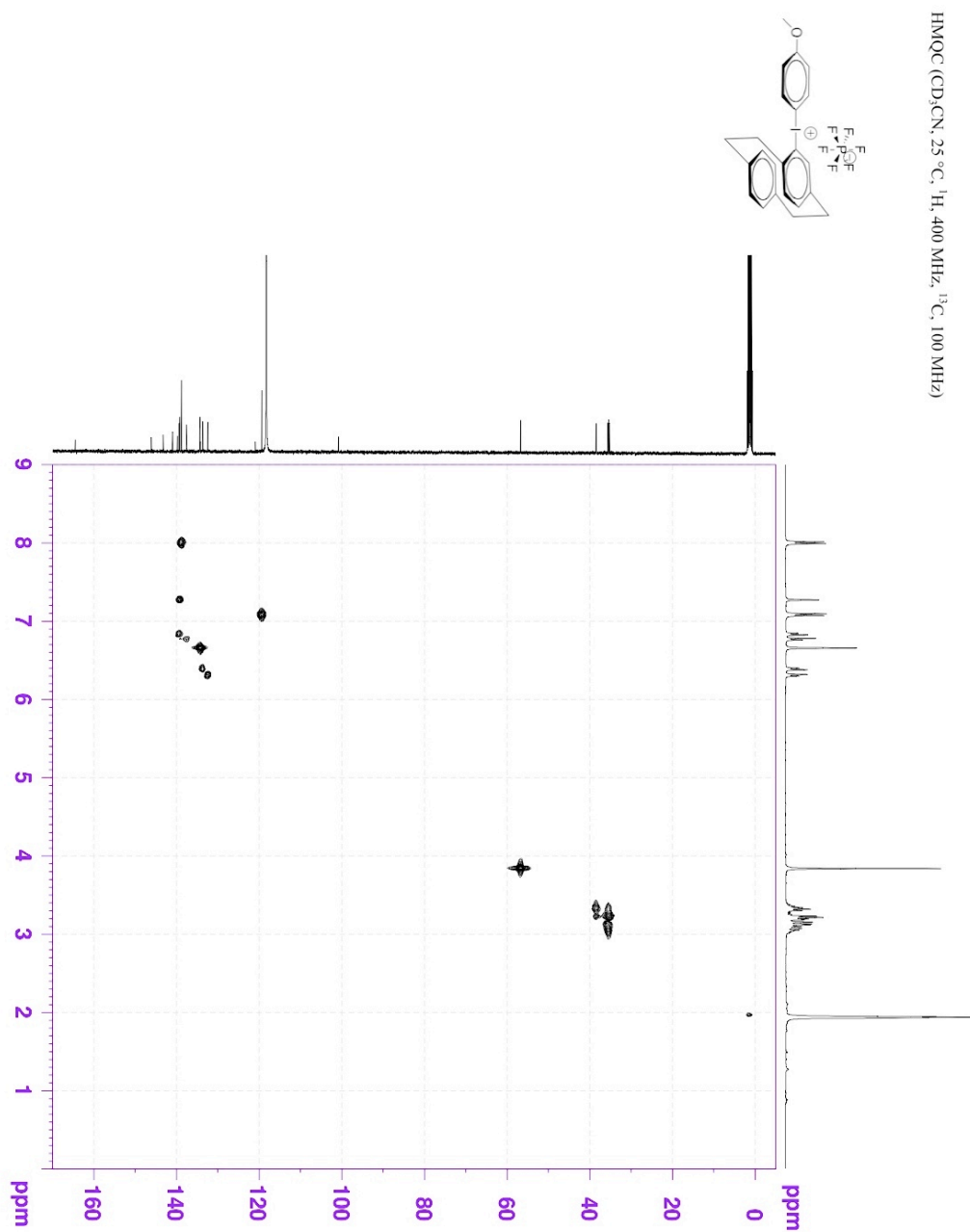
**Spectrum 61:**  $^1\text{H}$  and  $^{13}\text{C}$  NMR spectra of ([2.2]paracyclophan-4-yl)(4'-methoxyphenyl)-  
iodonium hexafluorophosphate in  $\text{CD}_3\text{CN}$



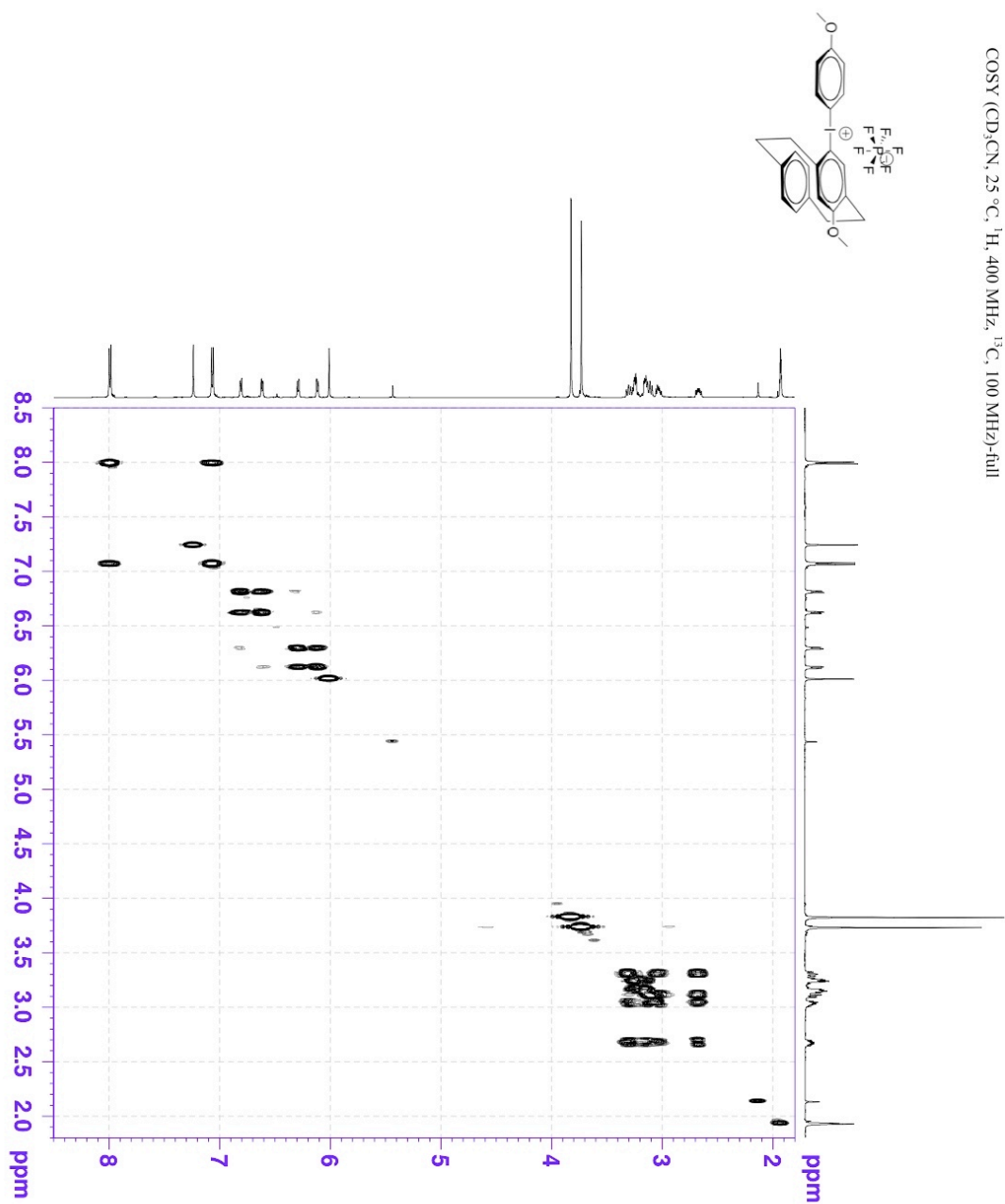
**Spectrum 62:**  $^1\text{H}$  and  $^{13}\text{C}$  NMR spectra of (7-methoxy-[2.2]paracyclophan-4-yl)(4'-methylphenyl)-iodonium hexafluorophosphate in  $\text{CD}_3\text{CN}$



**Spectrum 63** HMQC spectra of ([2.2]paracyclophan-4-yl)(4'-methoxyphenyl)-iodonium hexafluorophosphate in CD<sub>3</sub>CN

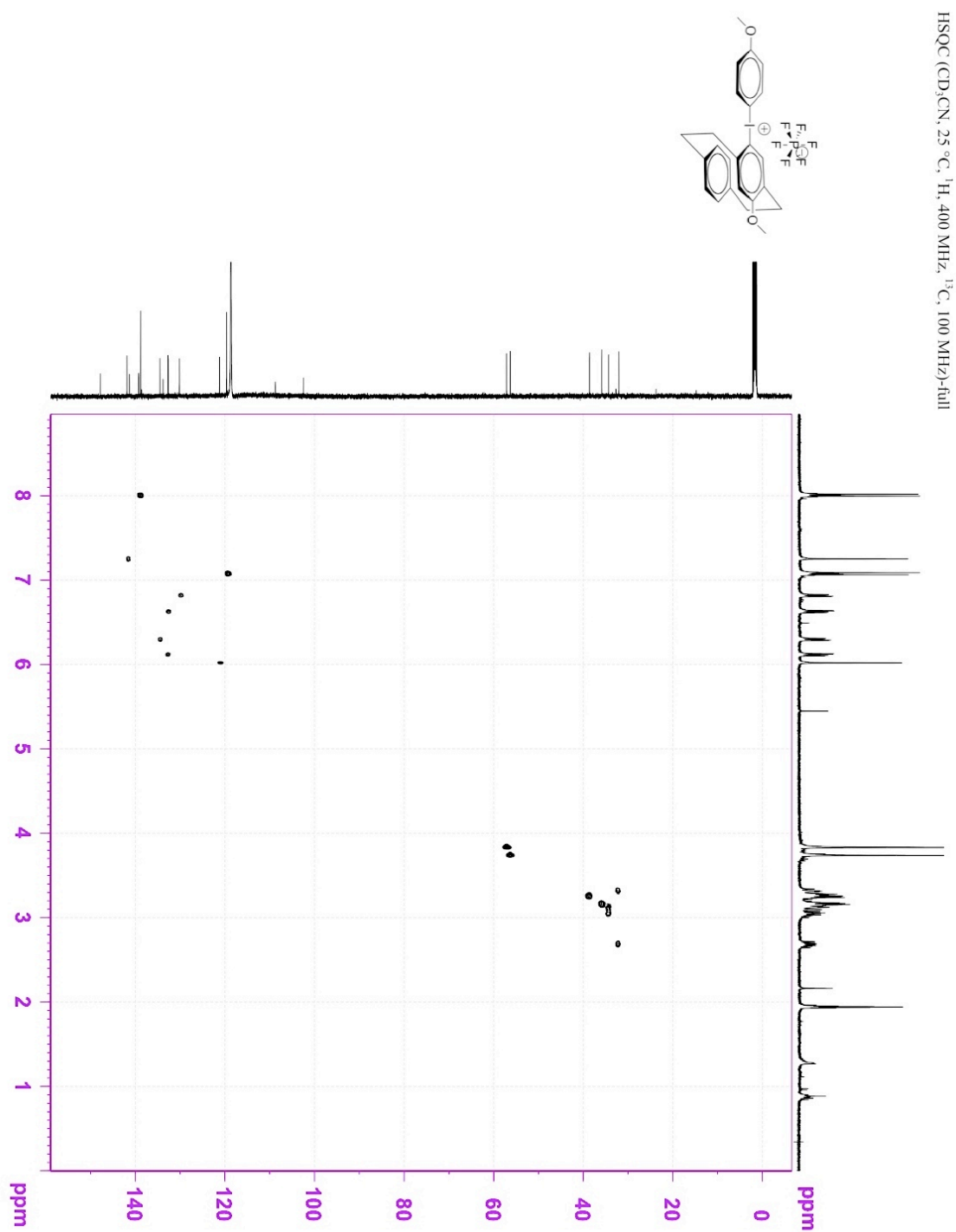


**Spectrum 64:** COSY spectra of (7-methoxy-[2.2]paracyclophan-4-yl)(4'-methylphenyl)-  
iodonium hexafluorophosphate in CD<sub>3</sub>CN

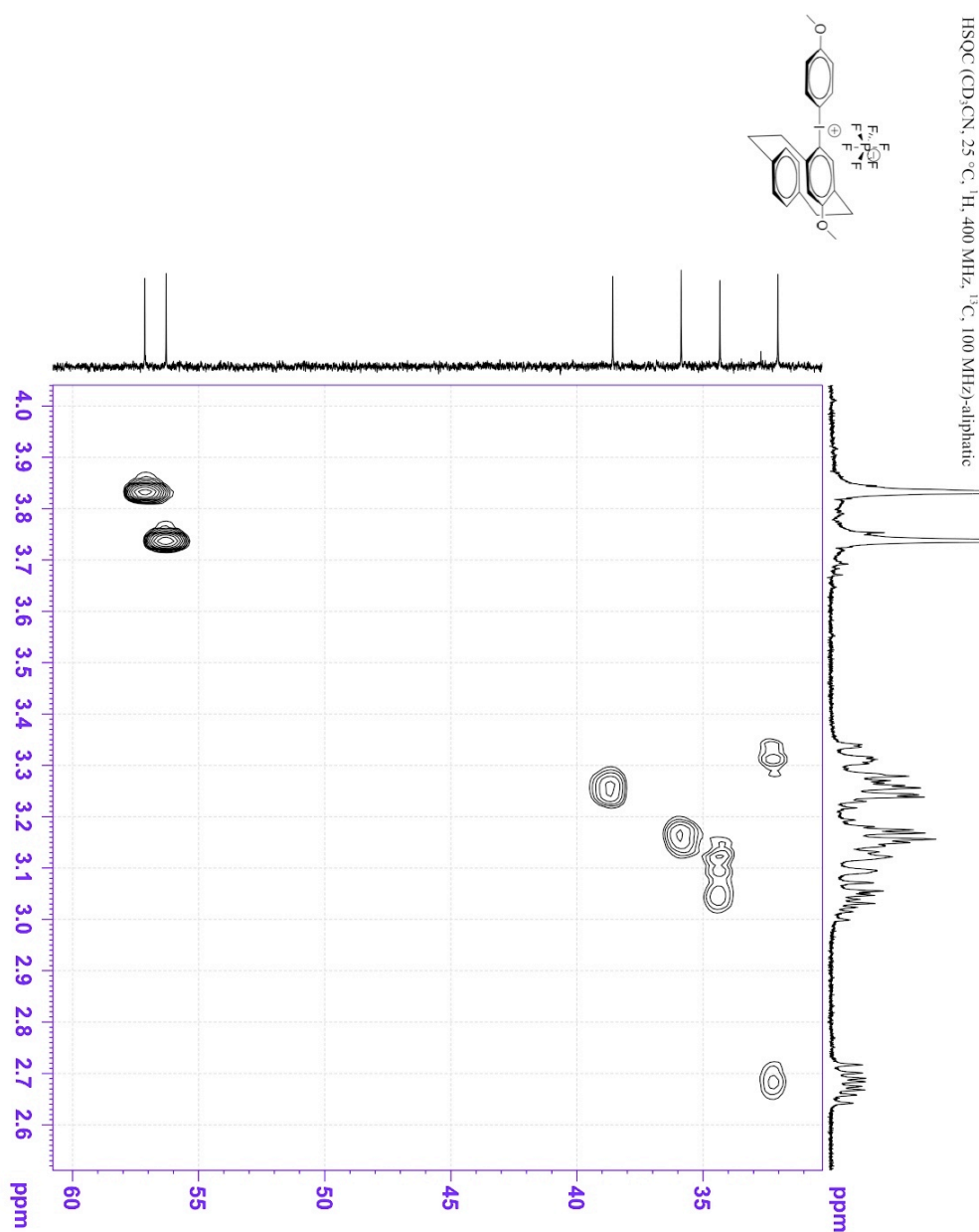




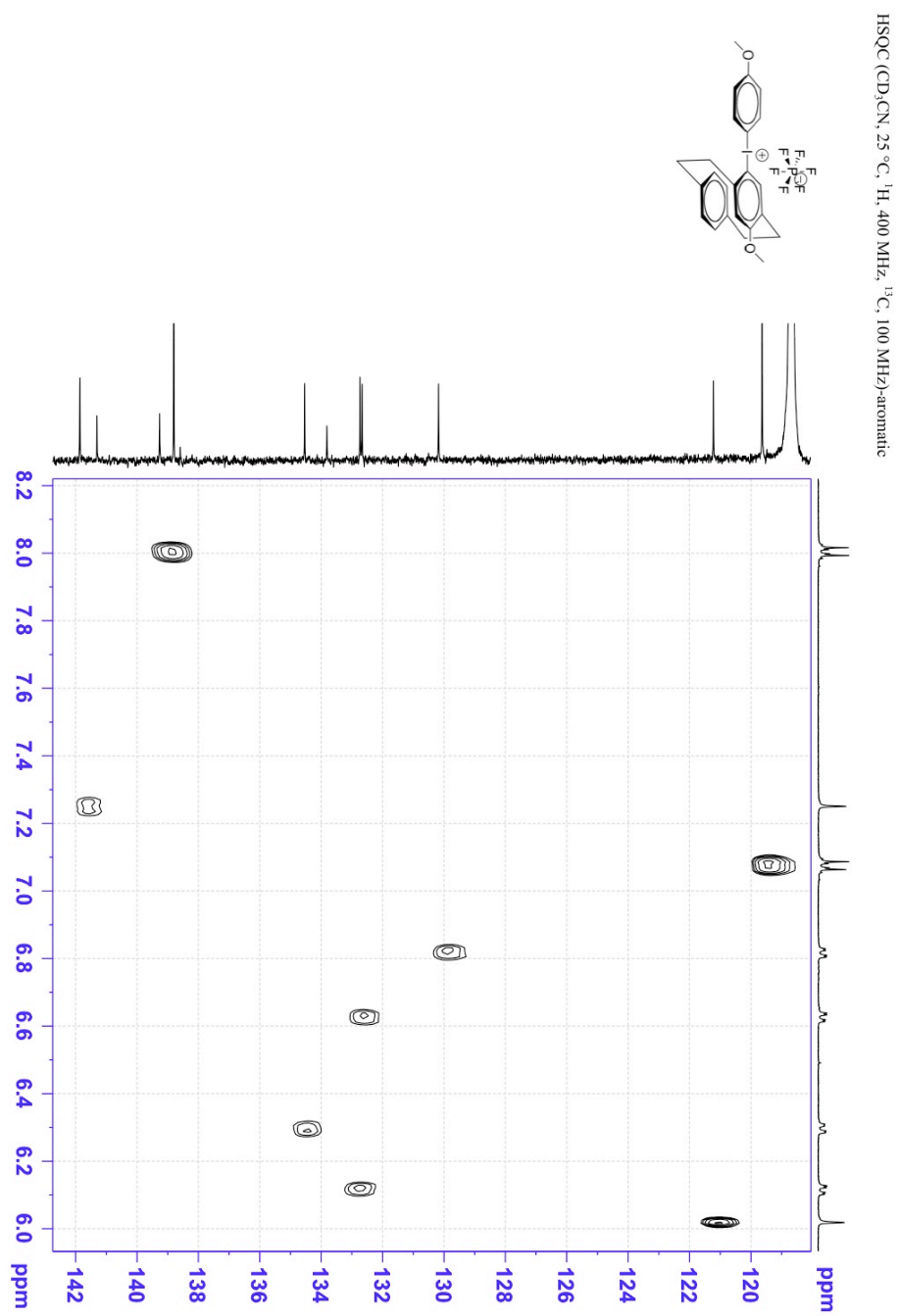
**Spectrum 65: HSQC spectra of (7-methoxy-[2.2]paracyclophan-4-yl)(4'-methylphenyl)-iodonium hexafluorophosphate in CD<sub>3</sub>CN**



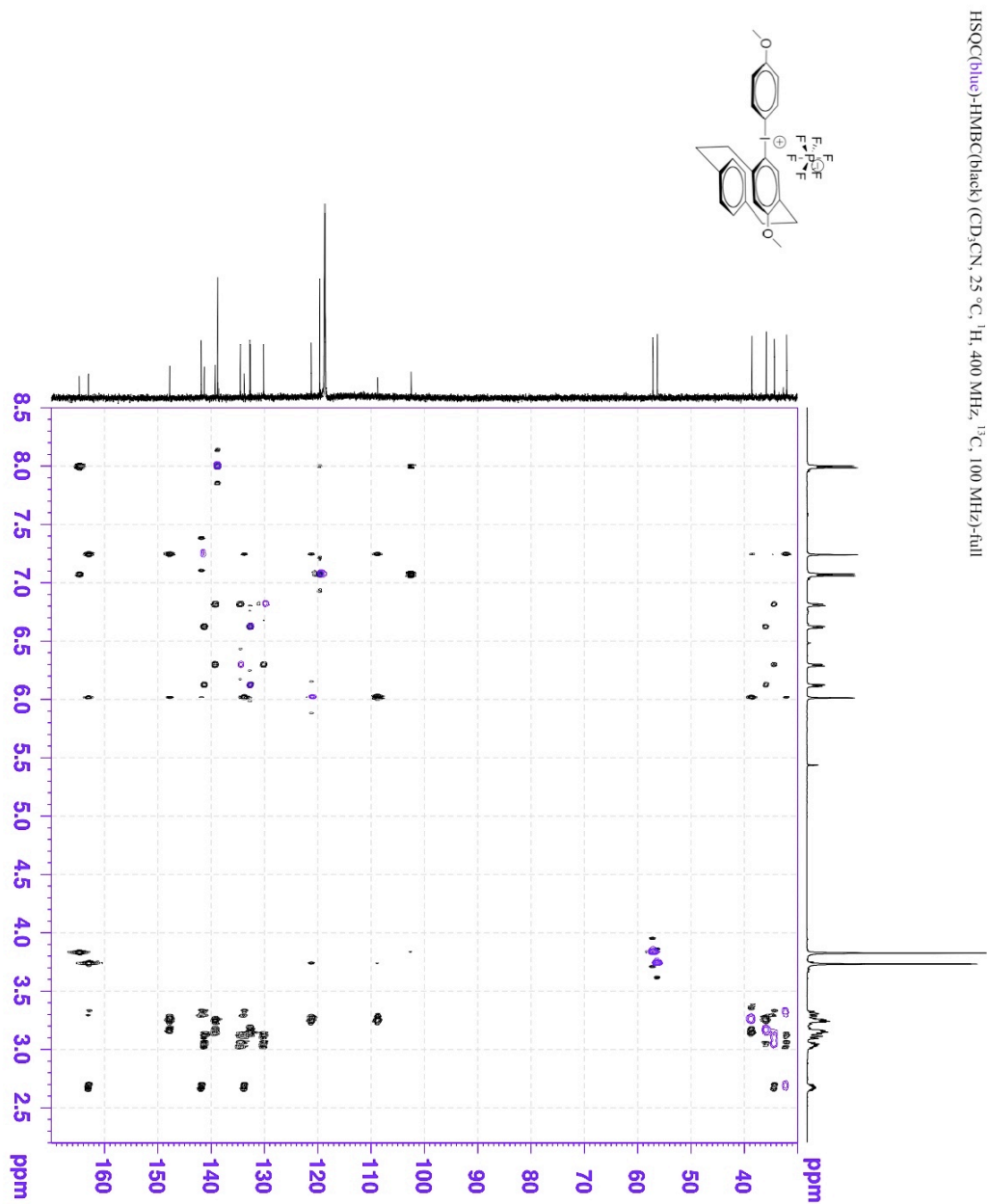
**Spectrum 66: HSQC spectra of (7-methoxy-[2.2]paracyclophan-4-yl)(4'-methylphenyl)-  
iodonium hexafluorophosphate in CD<sub>3</sub>CN -aliphatic region**



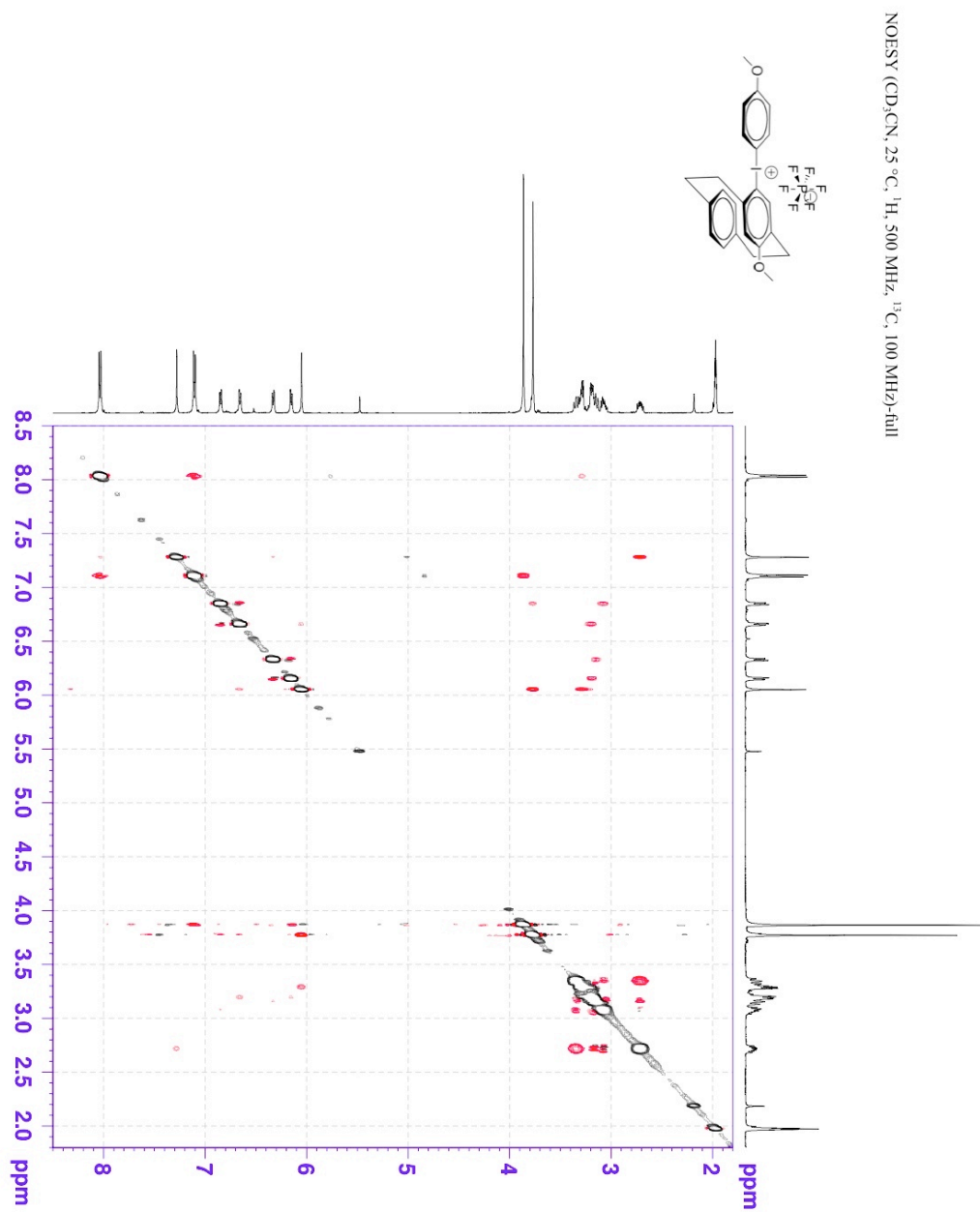
**Spectrum 67: HSQC spectra of (7-methoxy-[2.2]paracyclophan-4-yl)(4'-methylphenyl)-iodonium hexafluorophosphate in CD<sub>3</sub>CN-aromatic region**



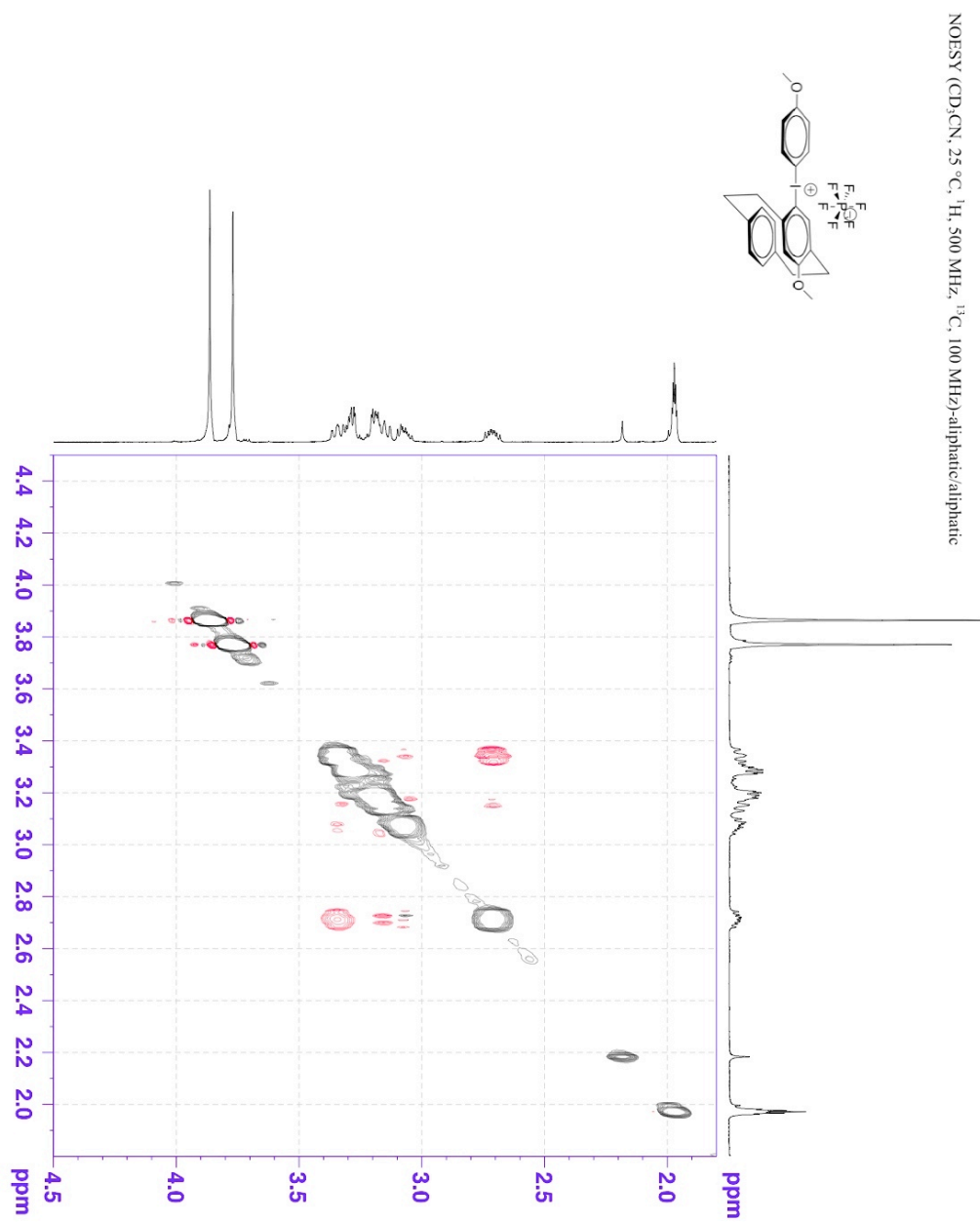
**Spectrum 68: HMBC-HSQC spectra of (7-methoxy-[2.2]paracyclophan-4-yl)(4'-methylphenyl)-iodonium hexafluorophosphate in CD<sub>3</sub>CN**



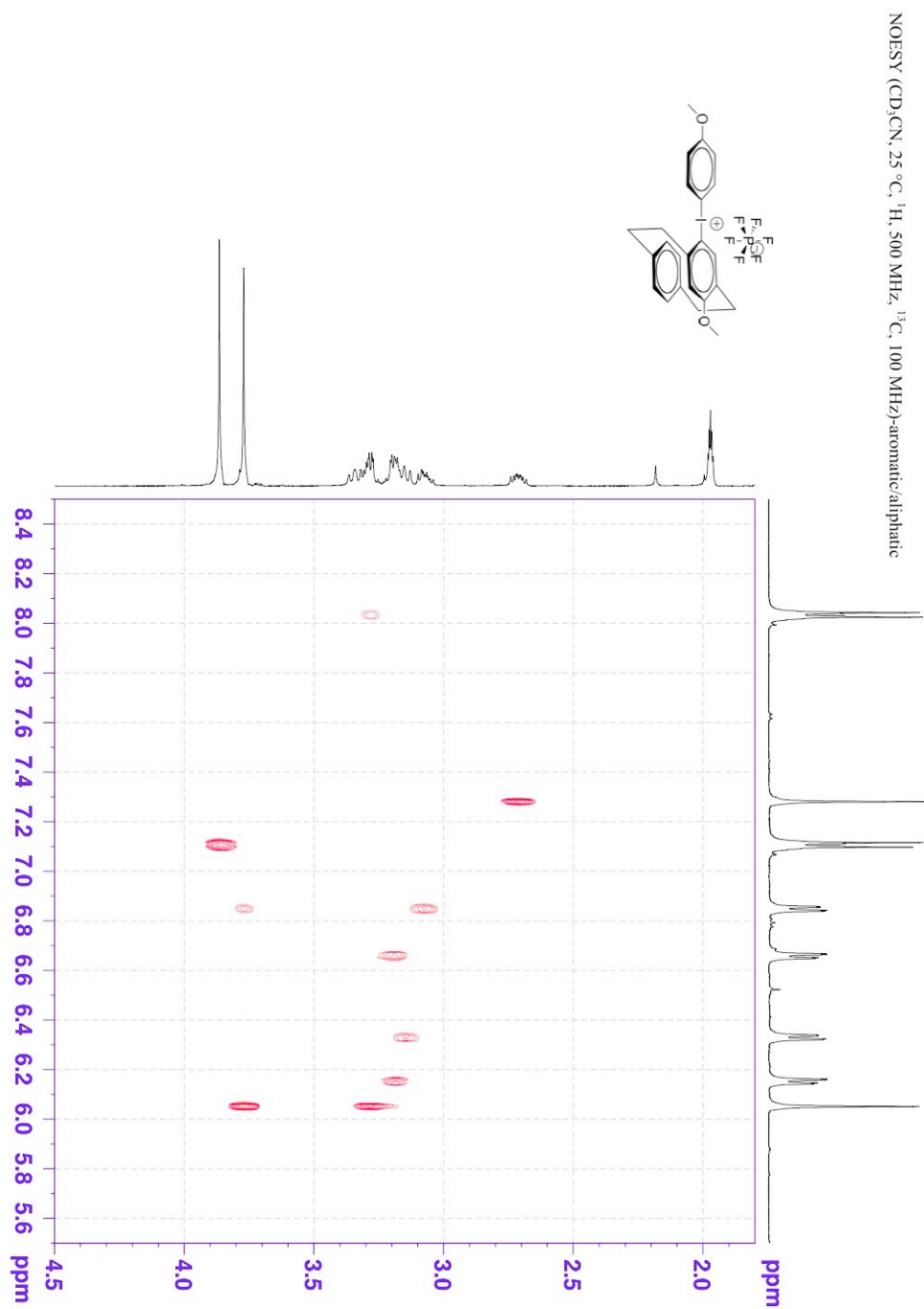
**Spectrum 69:** NOEST spectra of (7-methoxy-[2.2]paracyclophan-4-yl)(4'-methylphenyl)-  
iodonium hexafluorophosphate in CD<sub>3</sub>CN



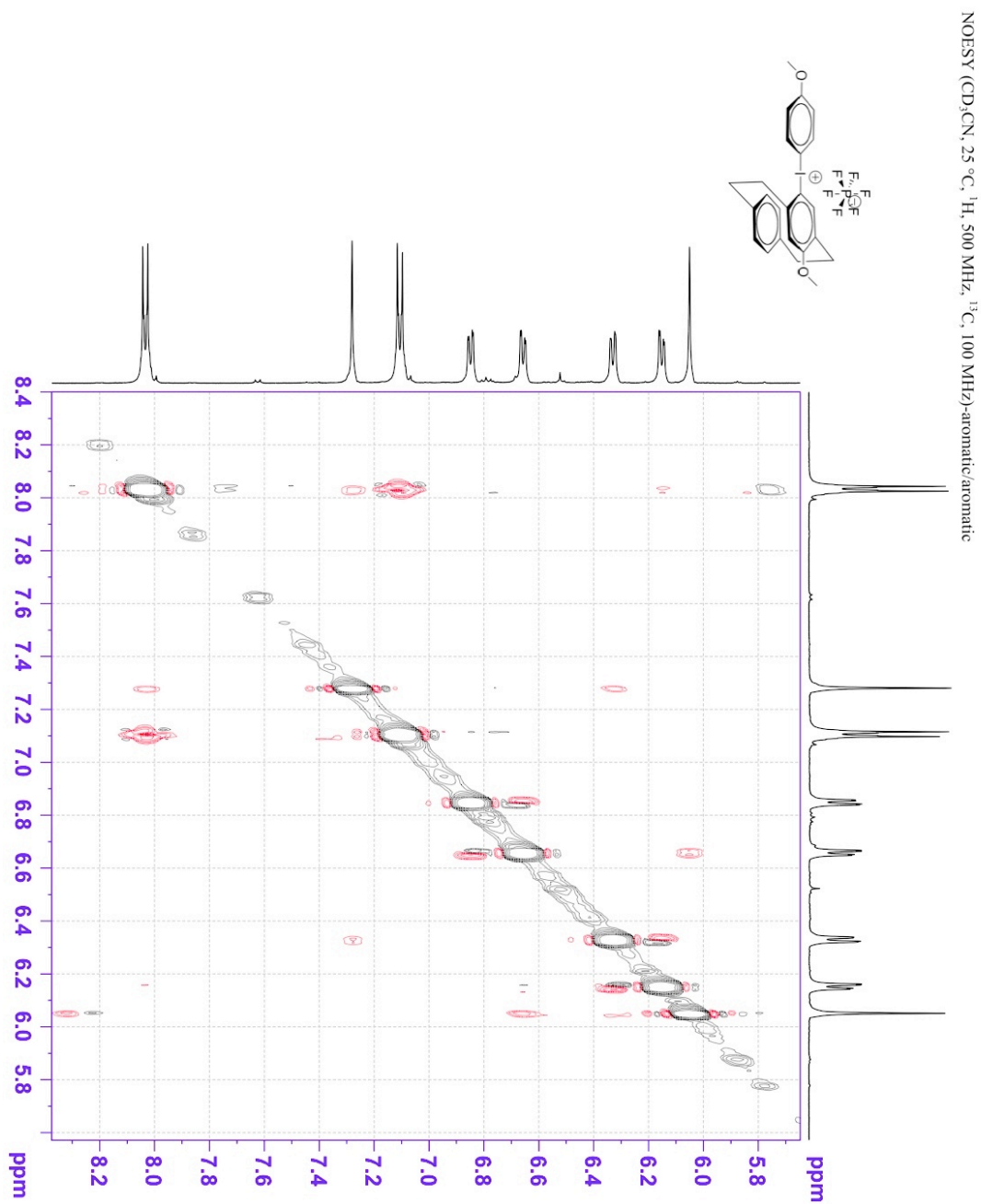
**Spectrum 70:** NOESY spectra of (7-methoxy-[2.2]paracyclophan-4-yl)(4'-methylphenyl)-  
iodonium hexafluorophosphate in CD<sub>3</sub>CN- aliphatic Vs aliphatic



**Spectrum 71: NOESY spectra of (7-methoxy-[2.2]paracyclophan-4-yl)(4'-methylphenyl)-iodonium hexafluorophosphate in CD<sub>3</sub>CN-aromatic Vs aliphatic**

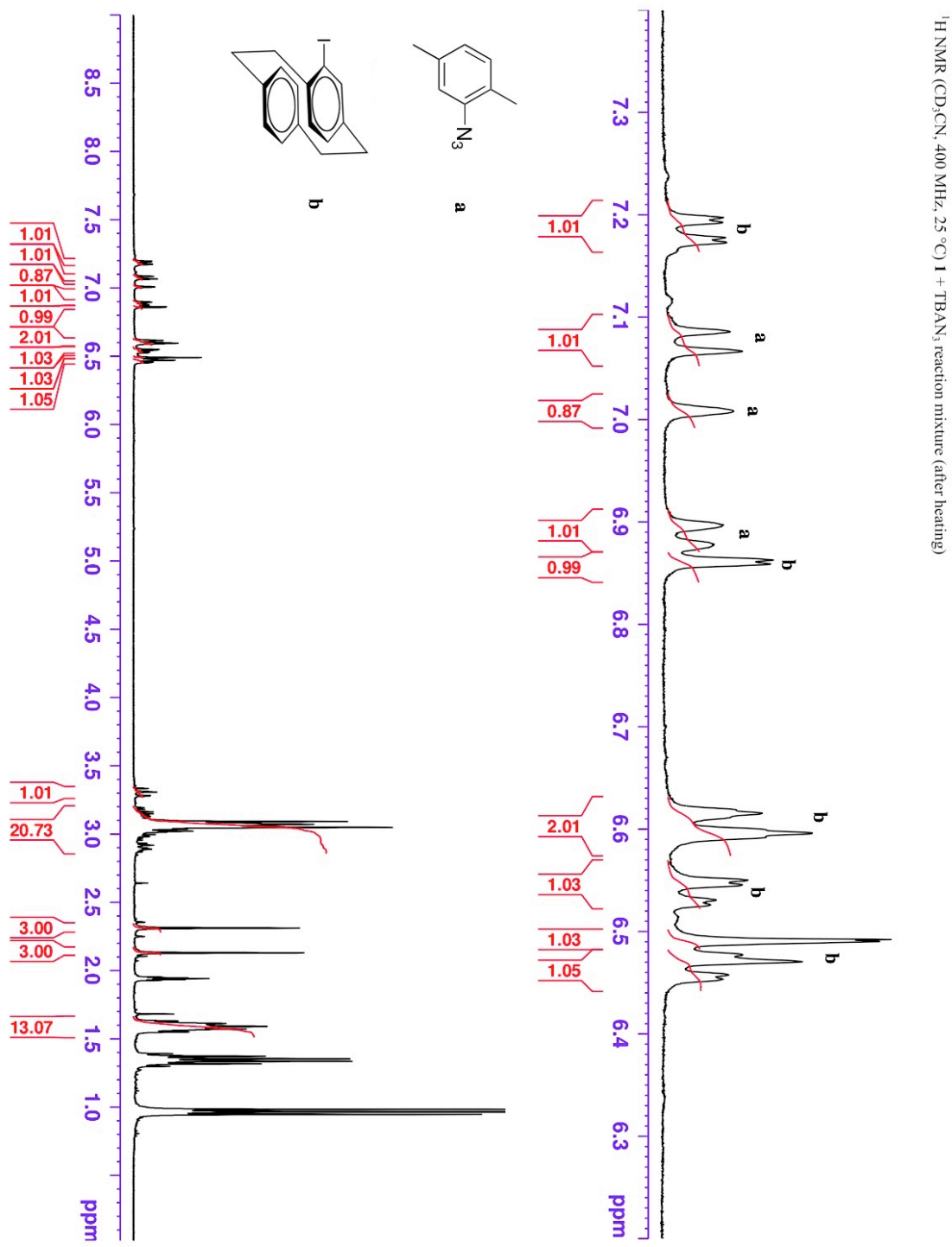


**Spectrum 72: NEOSY spectra of (7-methoxy-[2.2]paracyclophan-4-yl)(4'-methylphenyl)-  
iodonium hexafluorophosphate in CD<sub>3</sub>CN-aromatic Vs aromatic**

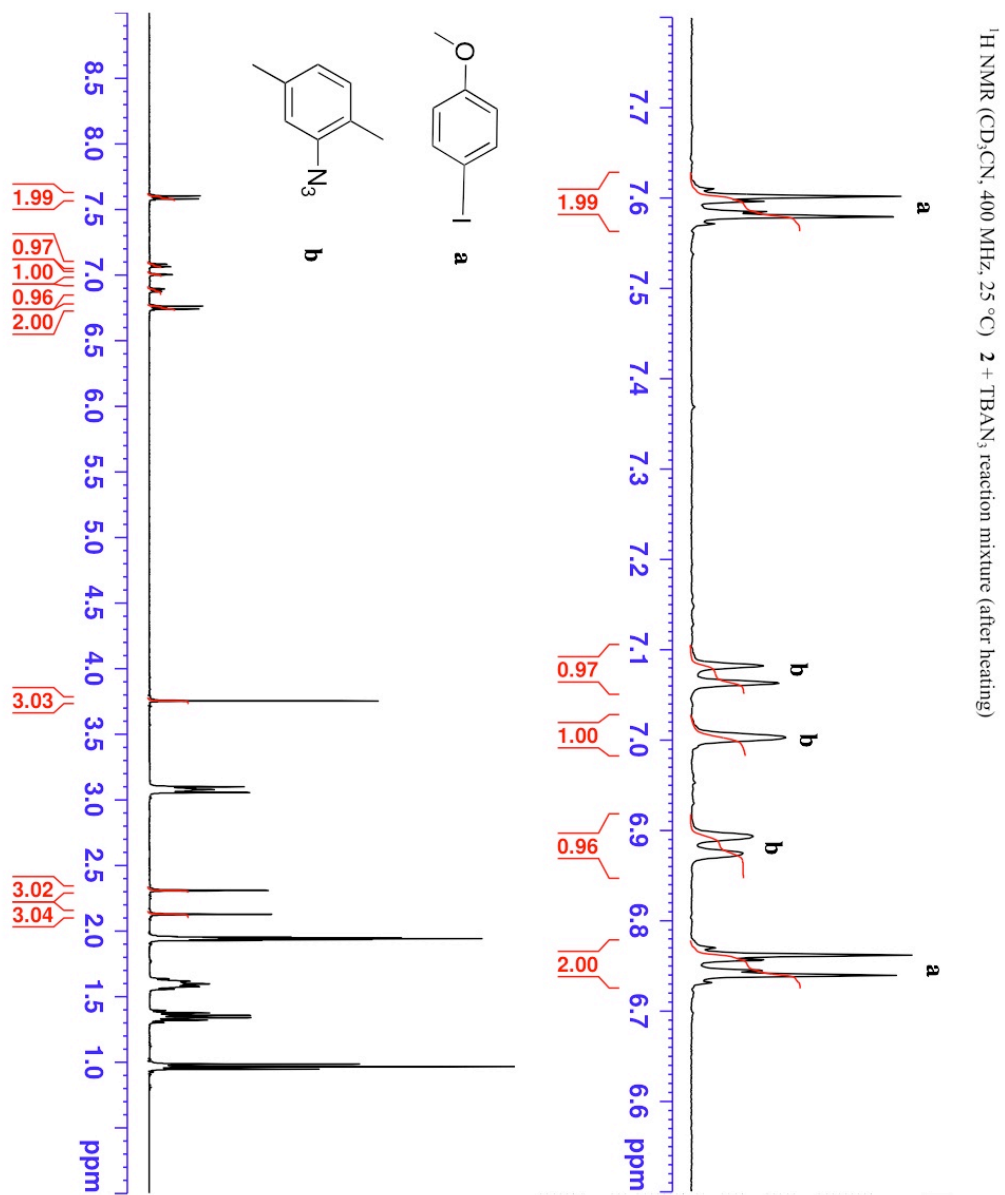




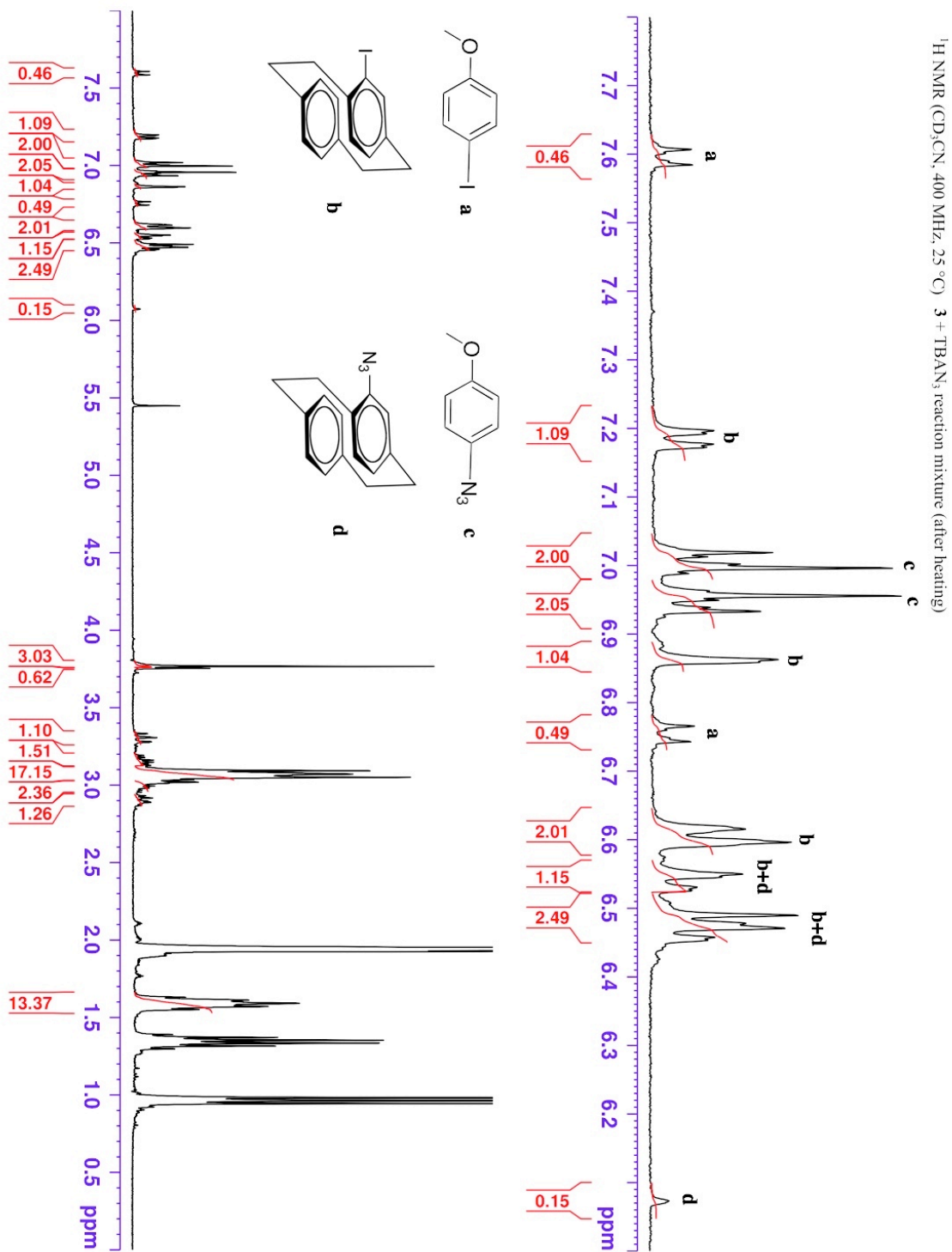
Spectrum 73:  $^1\text{H}$  NMR spectrum of the reaction mixture of salt **1**+TBAN<sub>3</sub> (CHAPTER 4)



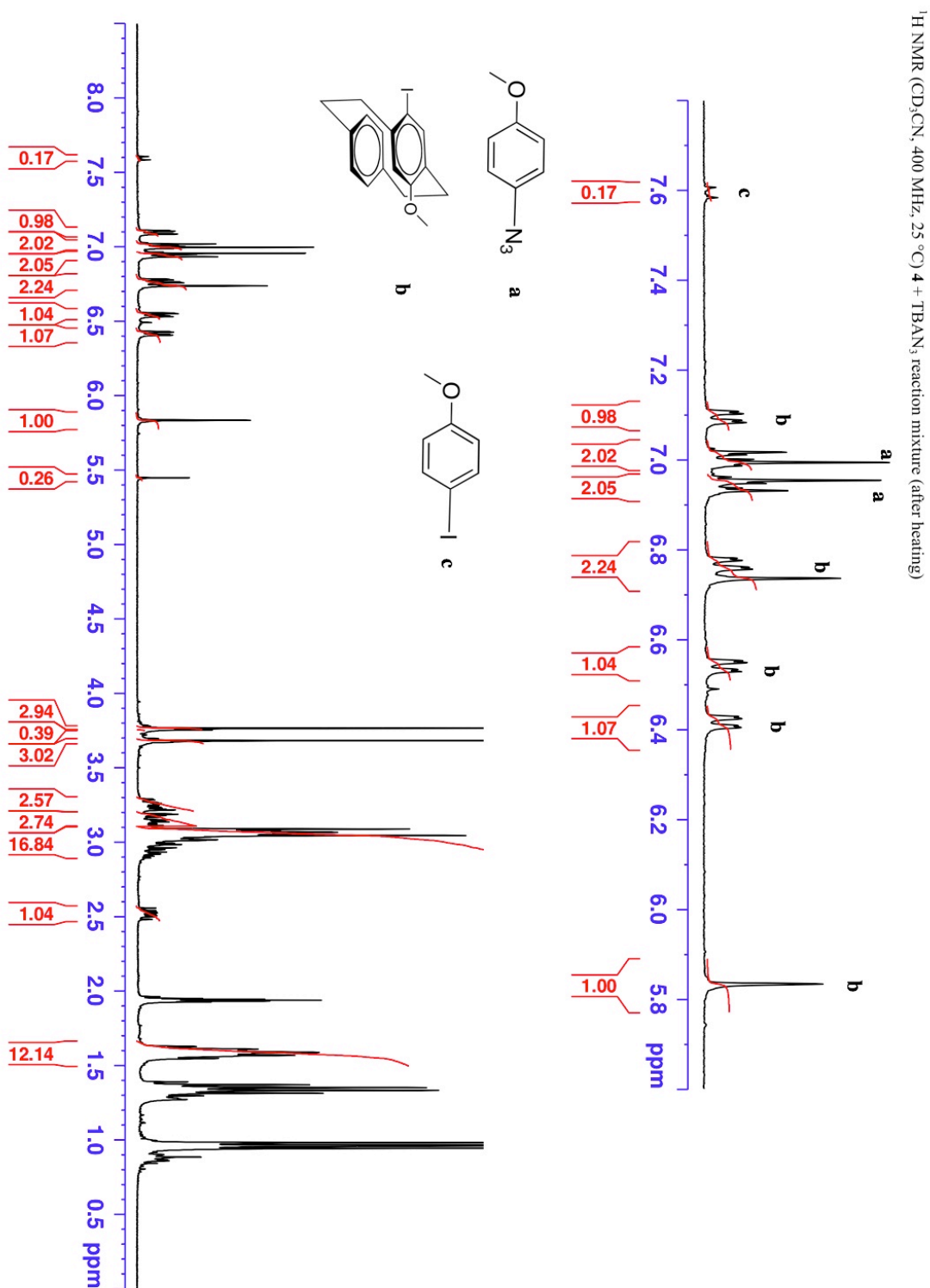
Spectrum 74:  $^1\text{H}$  NMR spectrum of the reaction mixture of salt **2**+TBAN<sub>3</sub> (CHAPTER 4)

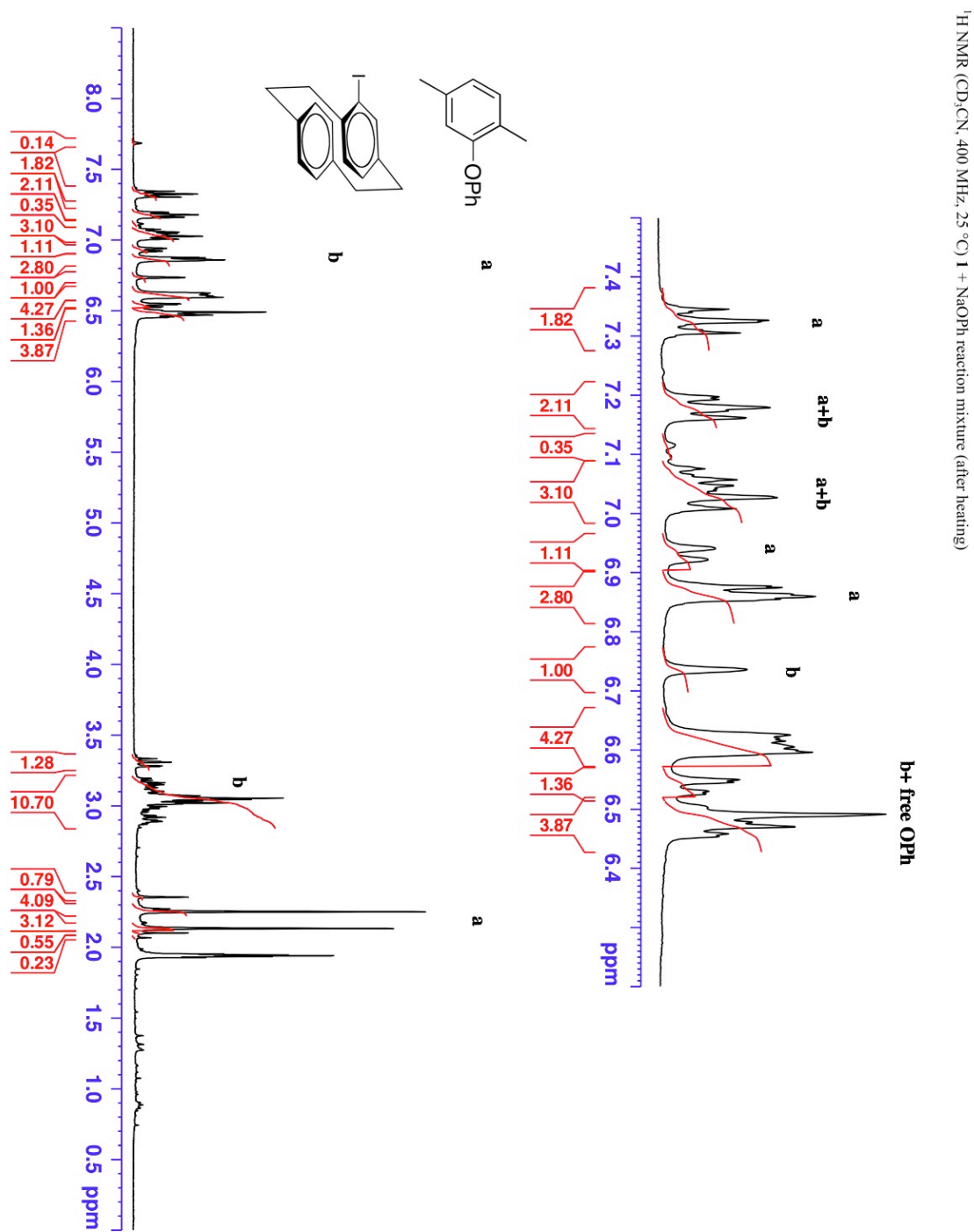


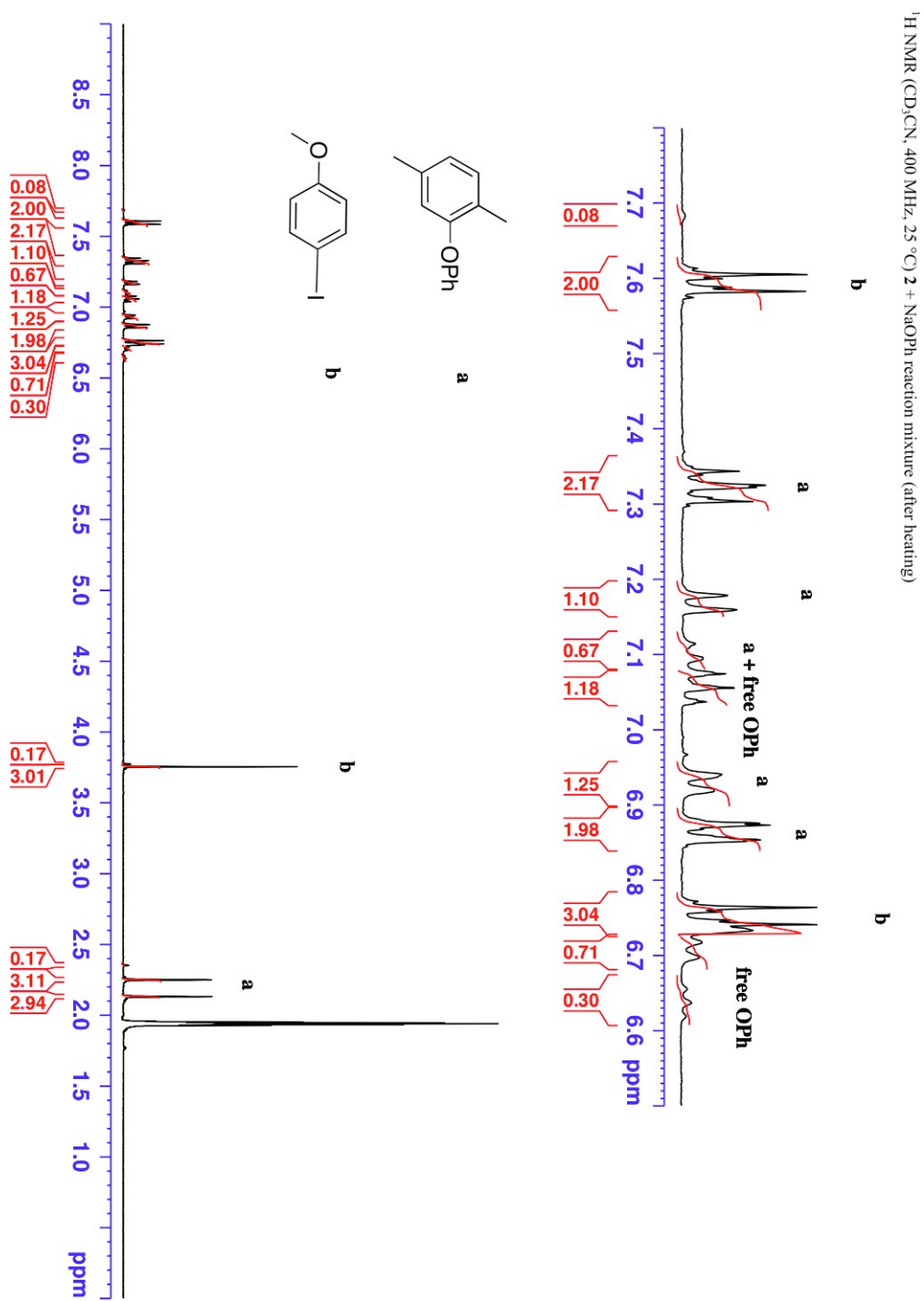
Spectrum 75:  $^1\text{H}$  NMR spectrum of the reaction mixture of salt 3+TBAN<sub>3</sub> (CHAPTER 4)



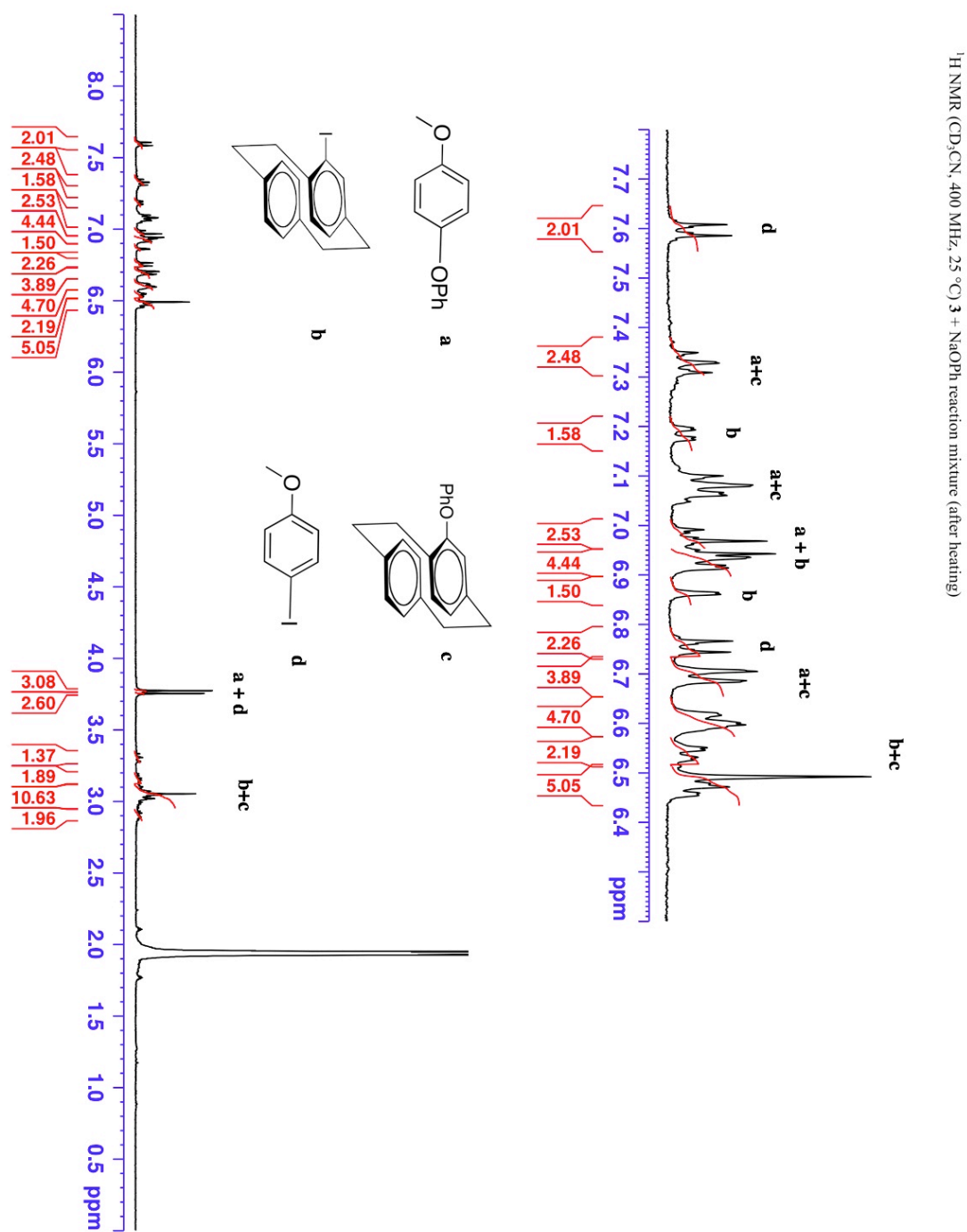
Spectrum 76:  $^1\text{H}$  NMR spectrum of the reaction mixture of salt 4+TBAN<sub>3</sub> (CHAPTER 4)



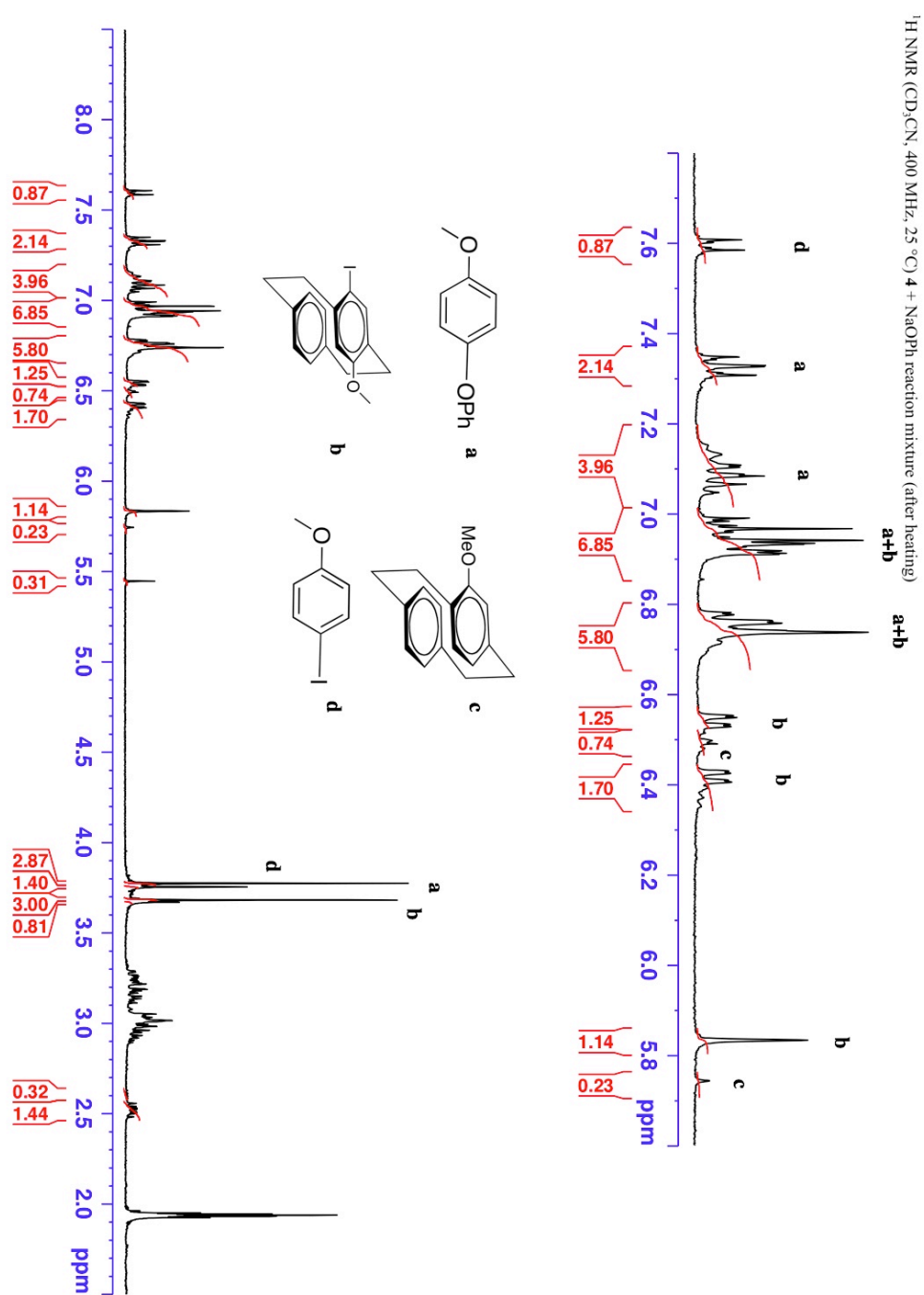
Spectrum 77:  $^1\text{H}$  NMR spectrum of the reaction mixture of salt **1**+NaOPh (CHAPTER 4)

Spectrum 78:  $^1\text{H}$  NMR spectrum of the reaction mixture of salt 2+NaOPh (CHAPTER 4)

Spectrum 79:  $^1\text{H}$  NMR spectrum of the reaction mixture of salt **3**+NaOPh (CHAPTER 4)



Spectrum 80:  $^1\text{H}$  NMR spectrum of the reaction mixture of salt 4+NaOPh (CHAPTER 4)





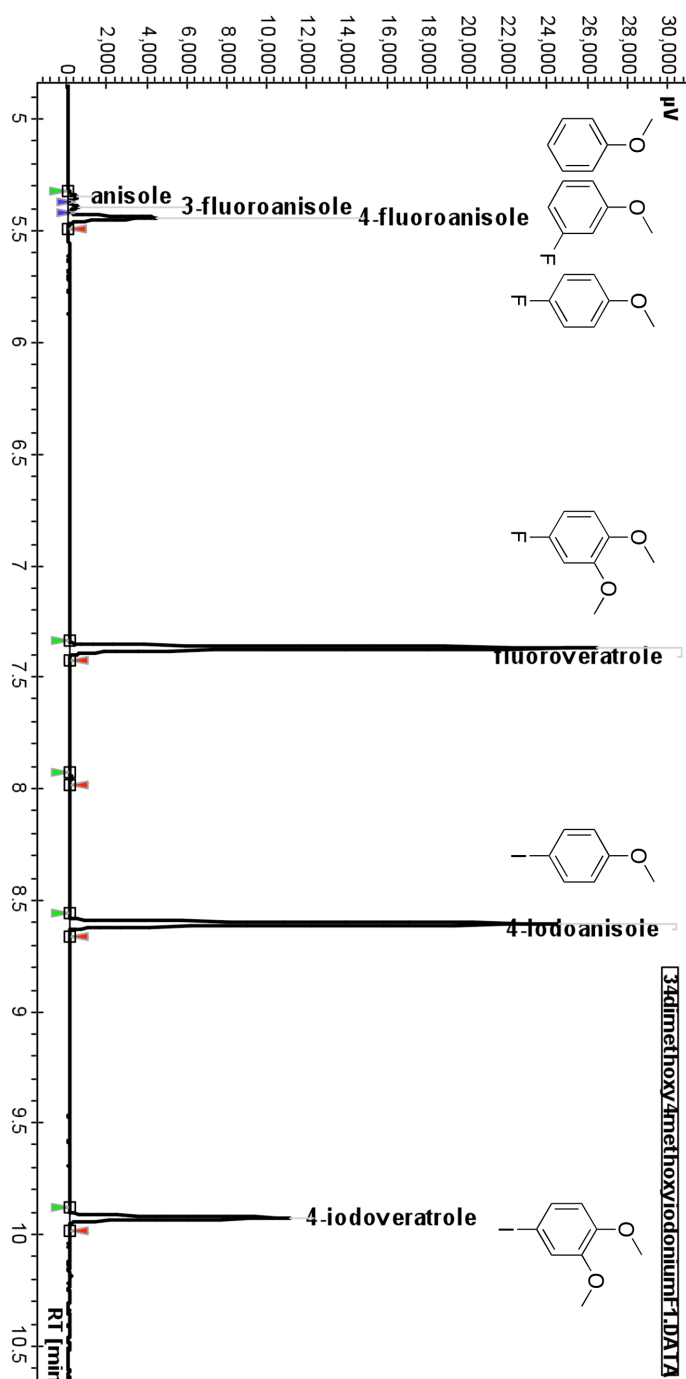
## APPENDIX B

### List of Chromatograms

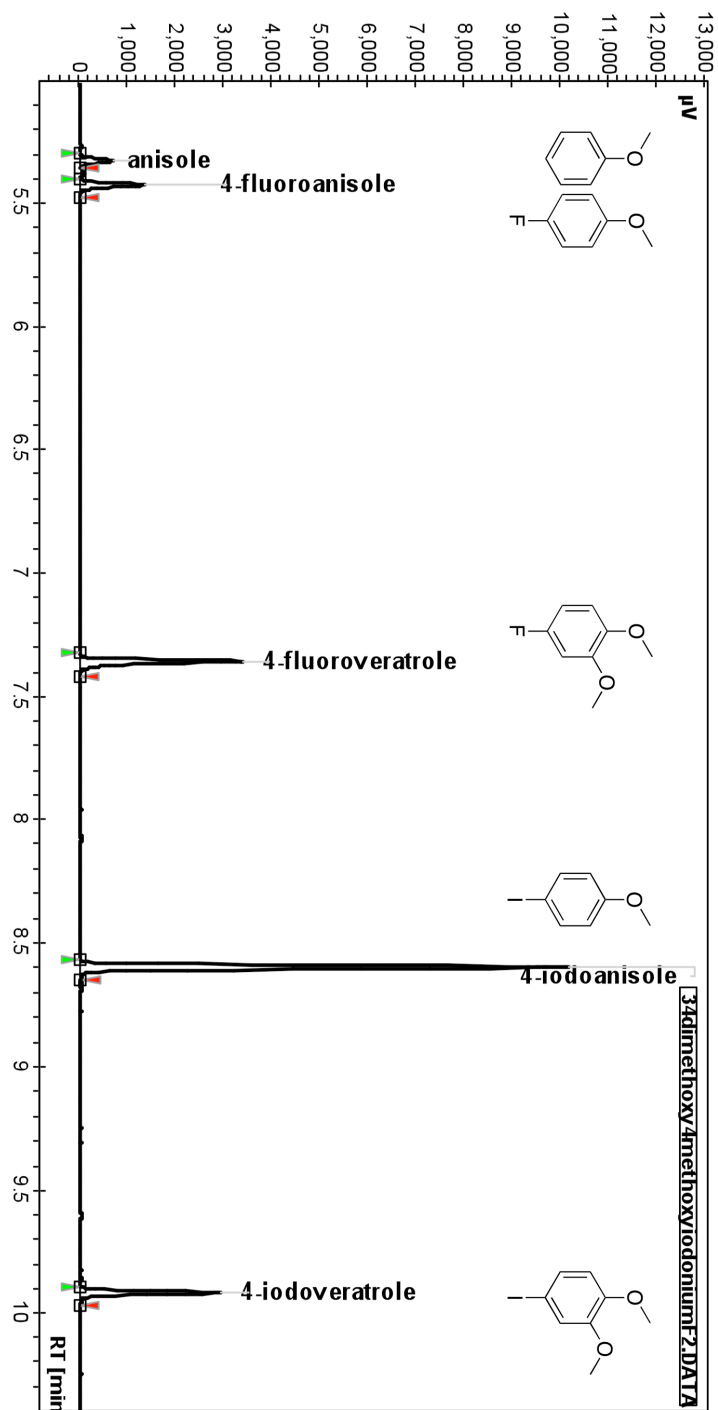
Chromatogram 1 GC chromatogram of (3,4-dimethoxyphenyl)(4'-methoxyphenyl)-fluoro- $\lambda^3$ -iodane decomposition mixture (benzene) .....	324
Chromatogram 2 GC chromatogram of (3,4-dimethoxyphenyl)(4'-methoxyphenyl)-fluoro- $\lambda^3$ -iodane decomposition mixture (acetonitrile) .....	325
Chromatogram 3 GC chromatogram of phenyl(4-methoxyphenyl)-fluoro- $\lambda^3$ -iodane decomposition mixture (benzene).....	326
Chromatogram 4 GC chromatogram of phenyl(4-methoxyphenyl)-fluoro- $\lambda^3$ -iodane decomposition mixture (acetonitrile).....	327
Chromatogram 5 GC chromatogram of (2-methyl-4,5-dimethoxyphenyl)(4'-methoxyphenyl)-fluoro- $\lambda^3$ -iodane decomposition mixture (benzene).....	328
Chromatogram 6 GC chromatogram of (2-methyl-4,5-dimethoxyphenyl)(4'-methoxyphenyl)-fluoro- $\lambda^3$ -iodane decomposition mixture (acetonitrile).....	329
Chromatogram 7 GC chromatogram of (3-cyanophenyl)(4'-methoxyphenyl)-fluoro- $\lambda^3$ -iodane decomposition mixture (benzene) .....	330
Chromatogram 8 GC chromatogram of (3-cyanophenyl)(4'-methoxyphenyl)-fluoro- $\lambda^3$ -iodane decomposition mixture (acetonitrile) .....	331
Chromatogram 9 GC chromatogram of (3-(trifluoromethyl)phenyl)(4'-methoxyphenyl)-fluoro- $\lambda^3$ -iodane decomposition mixture (benzene) .....	332

Chromatogram 10 GC chromatogram of (3-(trifluoromethyl)phenyl)(4'-methoxyphenyl)-fluoro- $\lambda^3$ -iodane decomposition mixture (acetonitrile) .....	333
Chromatogram 11 GC chromatogram of bis(4-methoxyphenyl)-fluoro- $\lambda^3$ -iodane decomposition mixture (benzene).....	334
Chromatogram 12 GC chromatogram of bis(4-methoxyphenyl)-fluoro- $\lambda^3$ -iodane decomposition mixture (acetonitrile).....	335
Chromatogram 13 GC chromatogram of bis(4-methoxyphenyl)-fluoro- $\lambda^3$ -iodane decomposition mixture (wet benzene).....	336
Chromatogram 14 GC chromatogram of bis(4-methoxyphenyl)-fluoro- $\lambda^3$ -iodane decomposition mixture (acetonitrile).....	337
Chromatogram 15 GC chromatogram of bis(4-methoxyphenyl)-fluoro- $\lambda^3$ -iodane decomposition mixture (benzene, with added salt).....	338

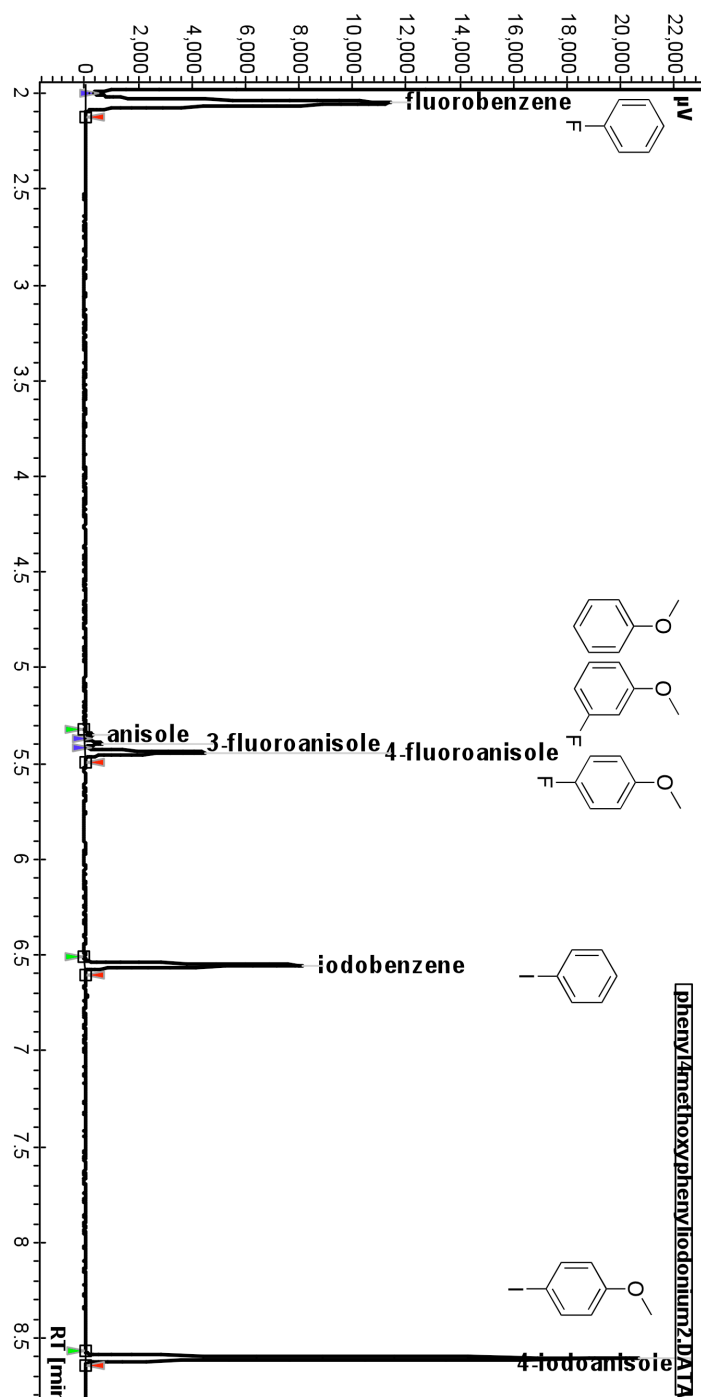
Chromatogram 1 GC chromatogram of (3,4-dimethoxyphenyl)(4'-methoxyphenyl)-fluoro- $\lambda^3$ -iodane decomposition mixture (benzene)



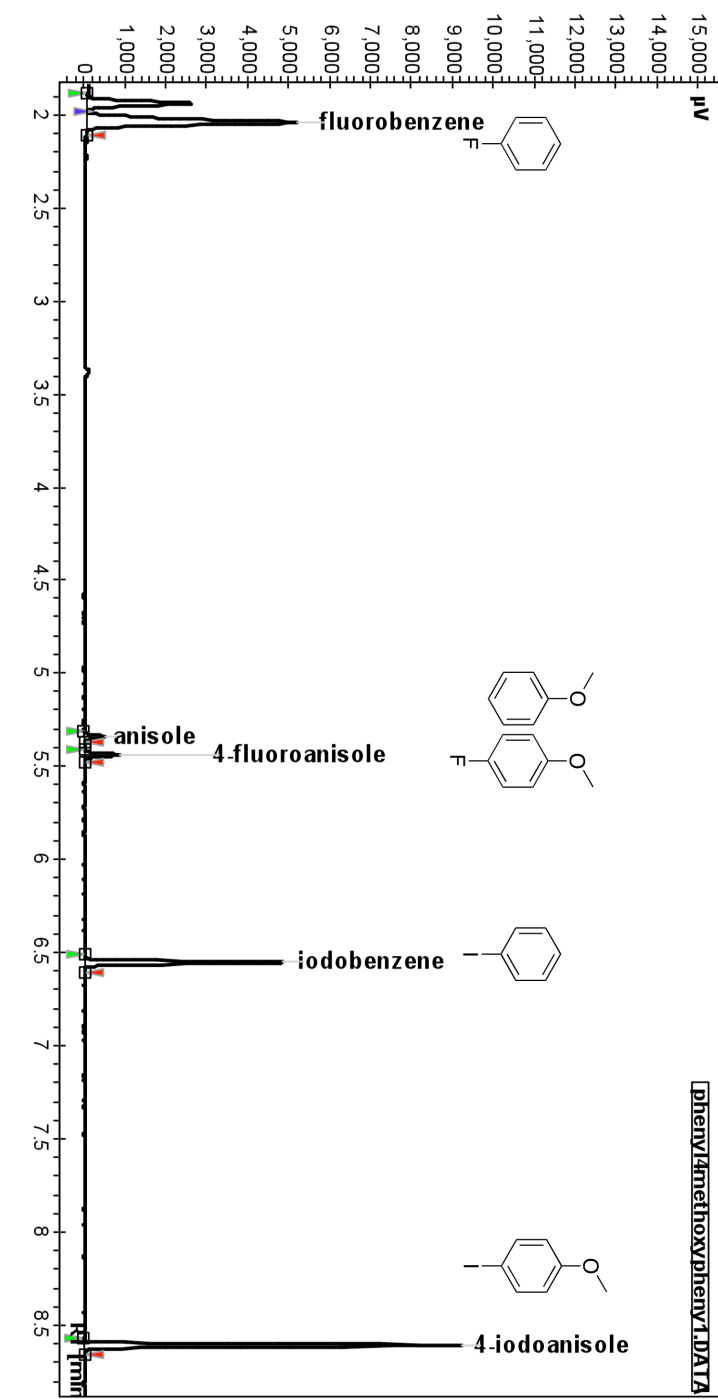
**Chromatogram 2** GC chromatogram of (3,4-dimethoxyphenyl)(4'-methoxyphenyl)-fluoro- $\lambda^3$ -iodane decomposition mixture (acetonitrile)



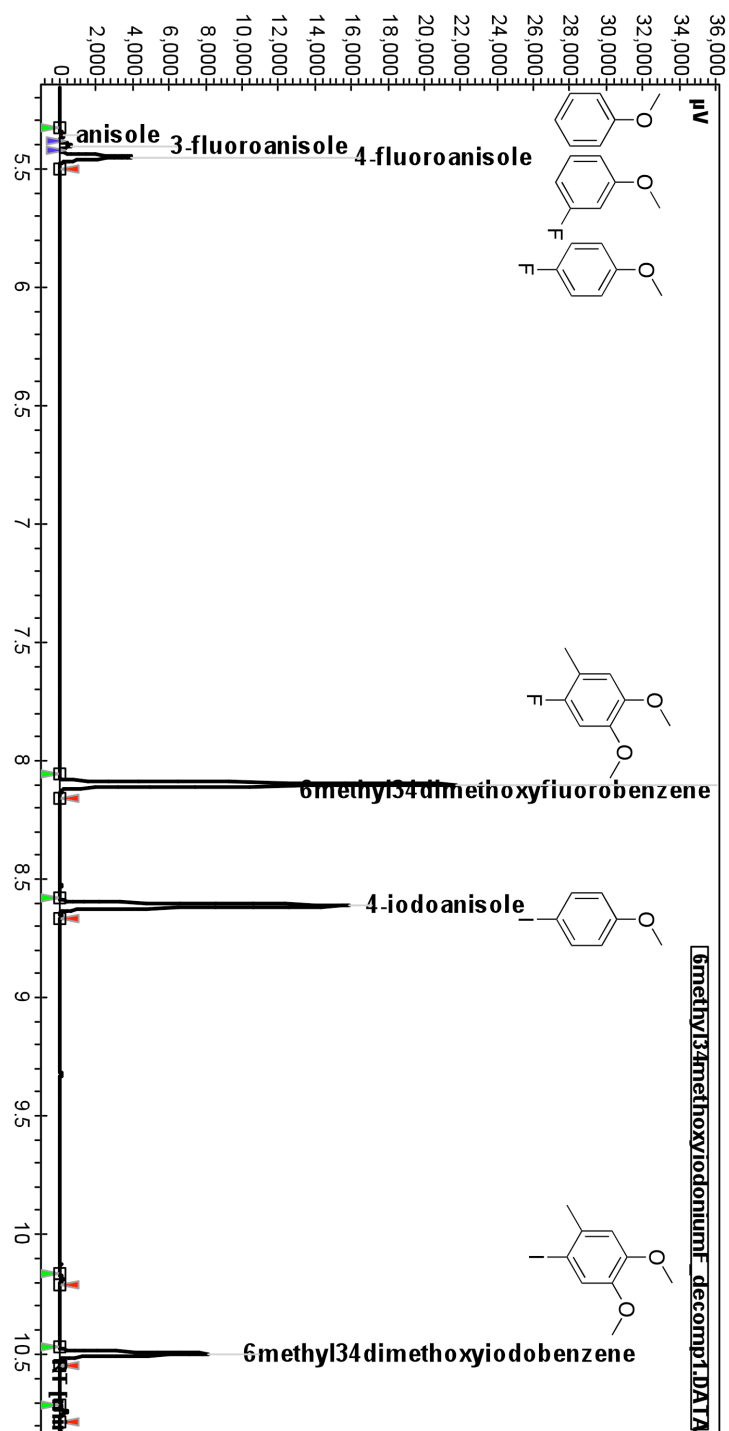
**Chromatogram 3** GC chromatogram of phenyl(4-methoxyphenyl)-fluoro- $\lambda^3$ -iodane decomposition mixture (benzene)



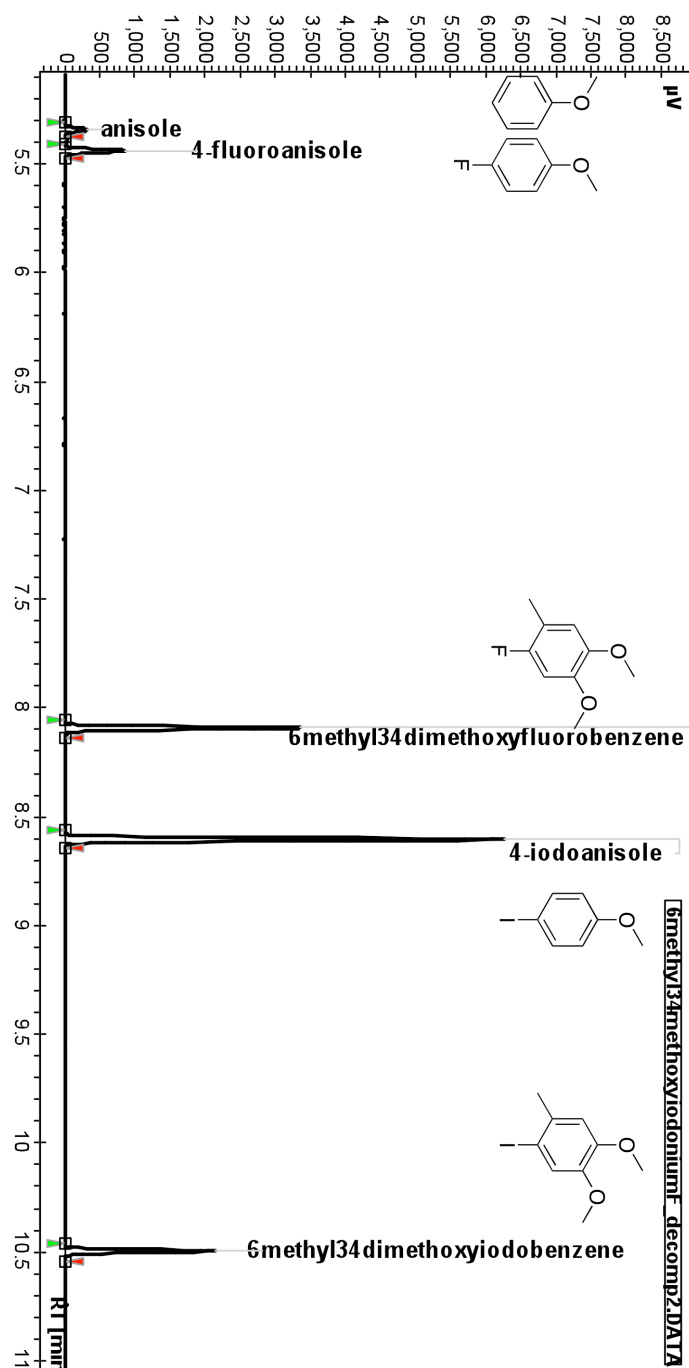
**Chromatogram 4** GC chromatogram of phenyl(4-methoxyphenyl)-fluoro- $\lambda^3$ -iodane decomposition mixture (acetonitrile)



**Chromatogram 5** GC chromatogram of (2-methyl-4,5-dimethoxyphenyl)(4'-methoxyphenyl)-fluoro- $\lambda^3$ -iodane decomposition mixture (benzene)

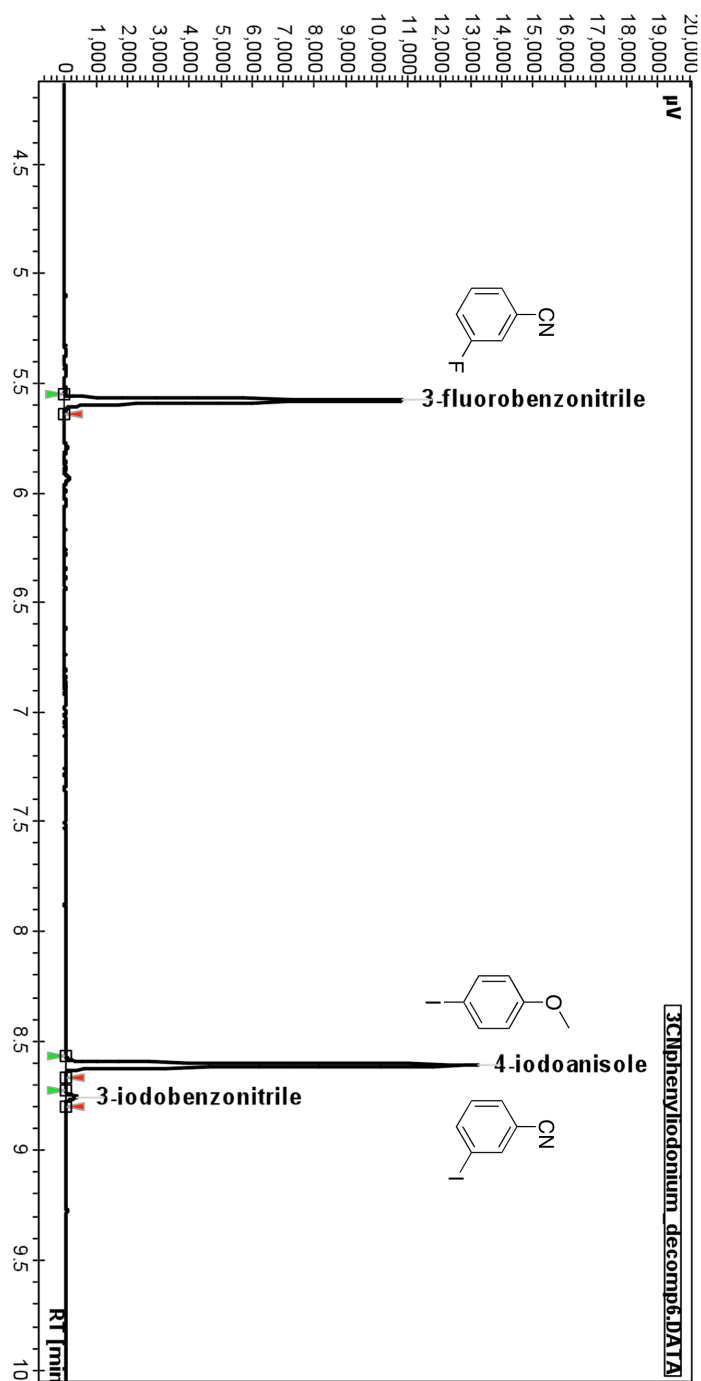


**Chromatogram 6** GC chromatogram of (2-methyl-4,5-dimethoxyphenyl)(4'-methoxyphenyl)-fluoro- $\lambda^3$ -iodane decomposition mixture (acetonitrile)

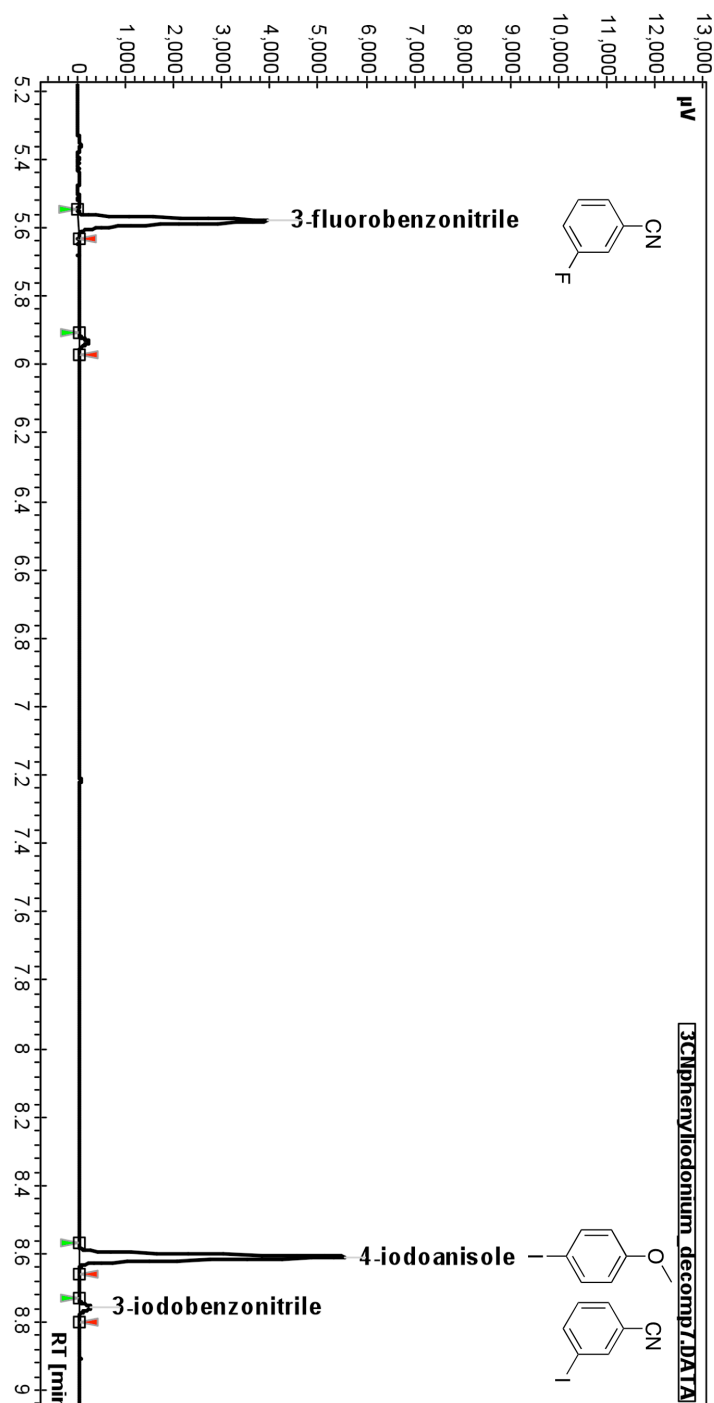




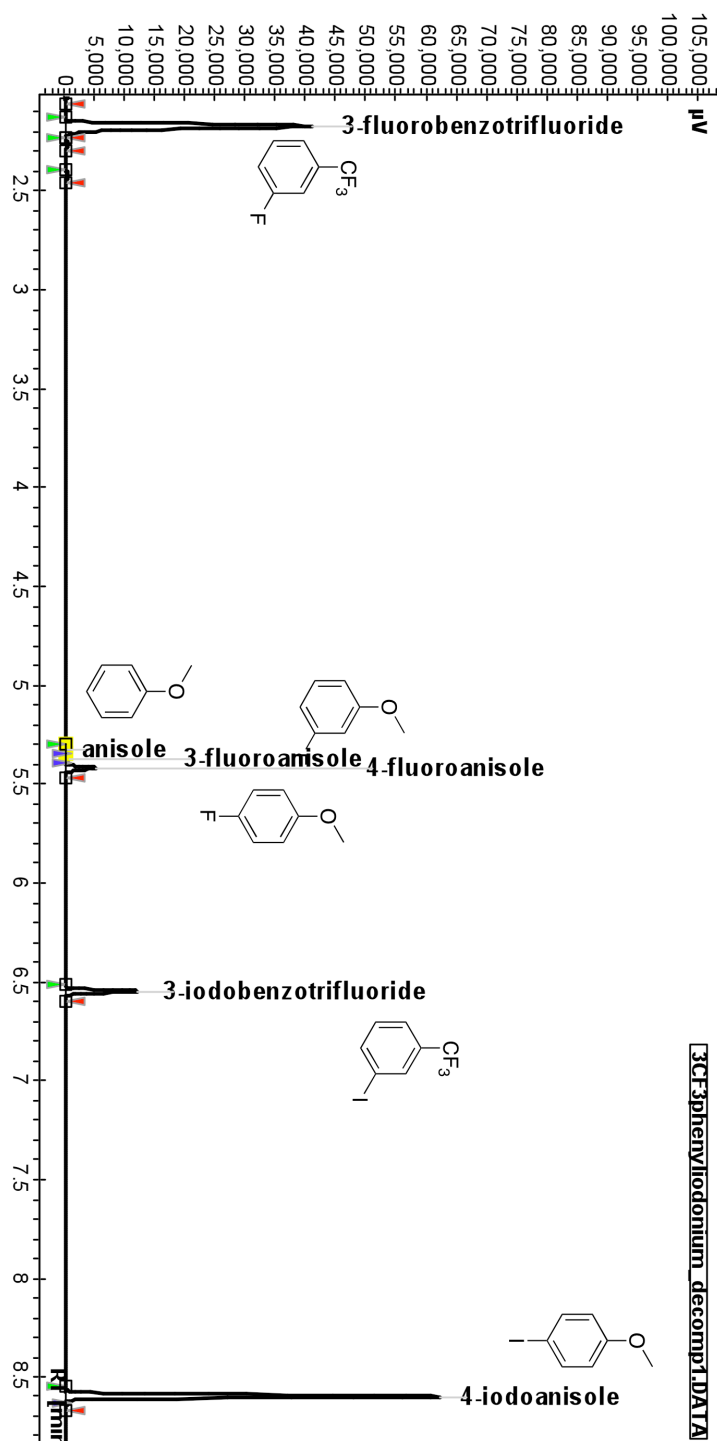
**Chromatogram 7** GC chromatogram of (3-cyanophenyl)(4'-methoxyphenyl)-fluoro- $\lambda^3$ -iodane decomposition mixture (benzene)



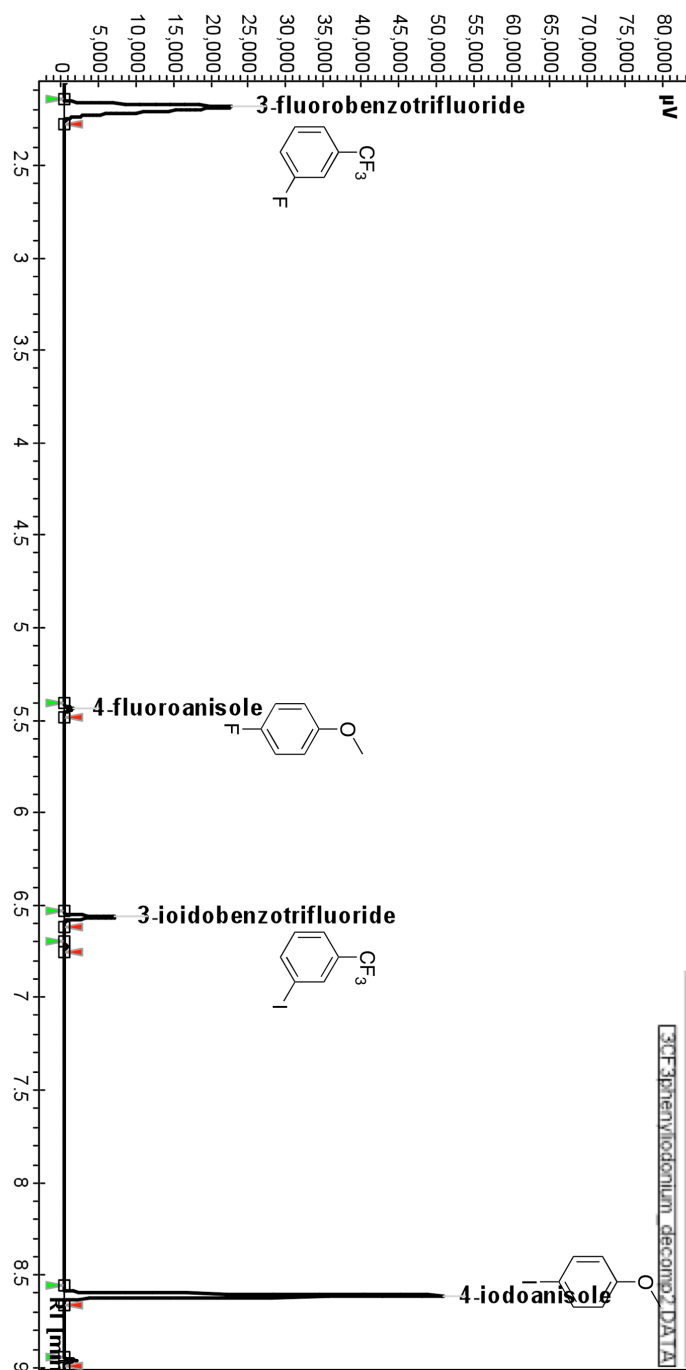
**Chromatogram 8** GC chromatogram of (3-cyanophenyl)(4'-methoxyphenyl)-fluoro- $\lambda^3$ -iodane decomposition mixture (acetonitrile)



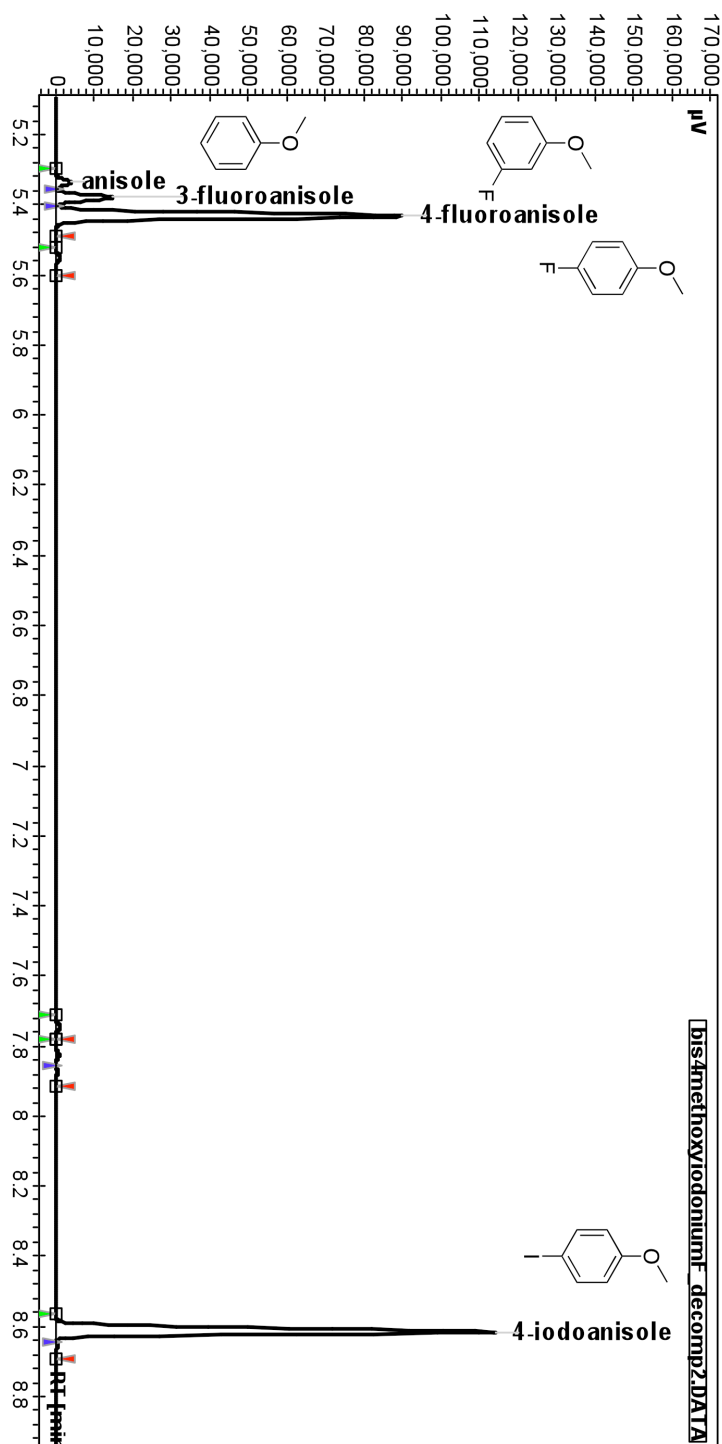
**Chromatogram 9** GC chromatogram of (3-(trifluoromethyl)phenyl)(4'-methoxyphenyl)-fluoro- $\lambda^3$ -iodane decomposition mixture (benzene)



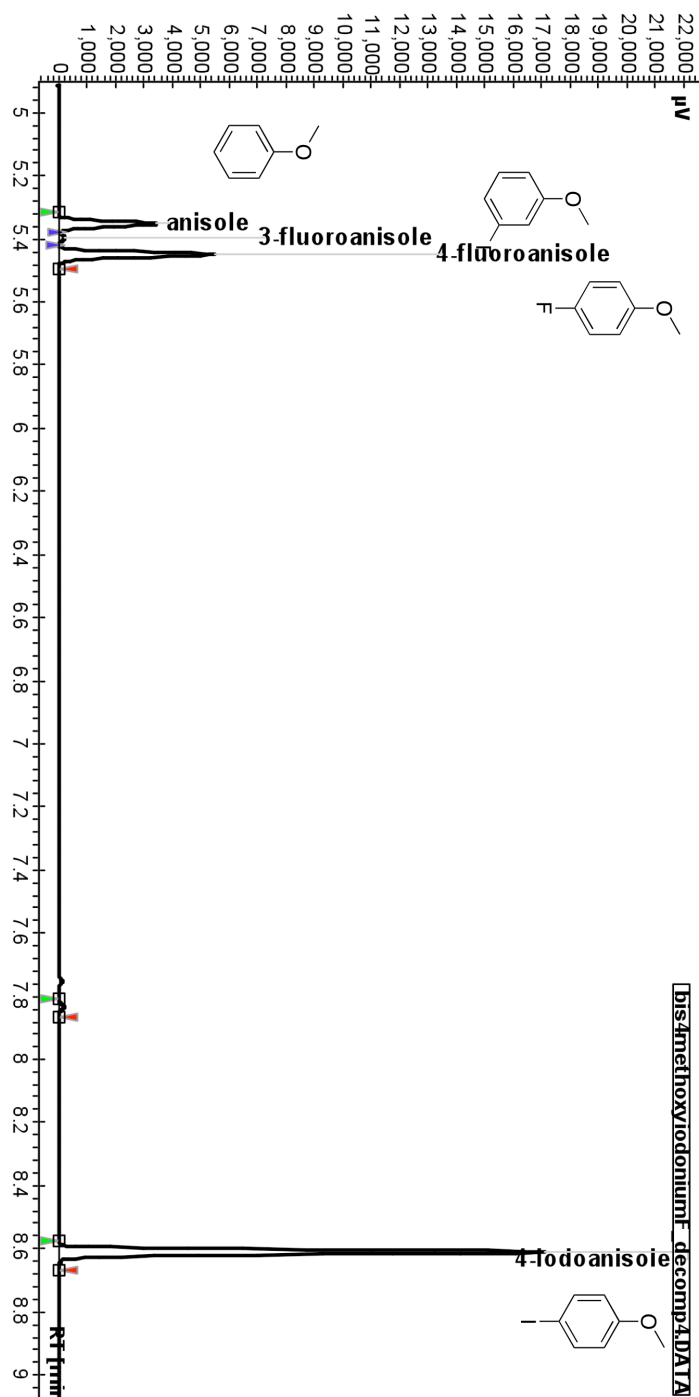
**Chromatogram 10 GC chromatogram of (3-(trifluoromethyl)phenyl)(4'-methoxyphenyl)-fluoro- $\lambda^3$ -iodane decomposition mixture (acetonitrile)**



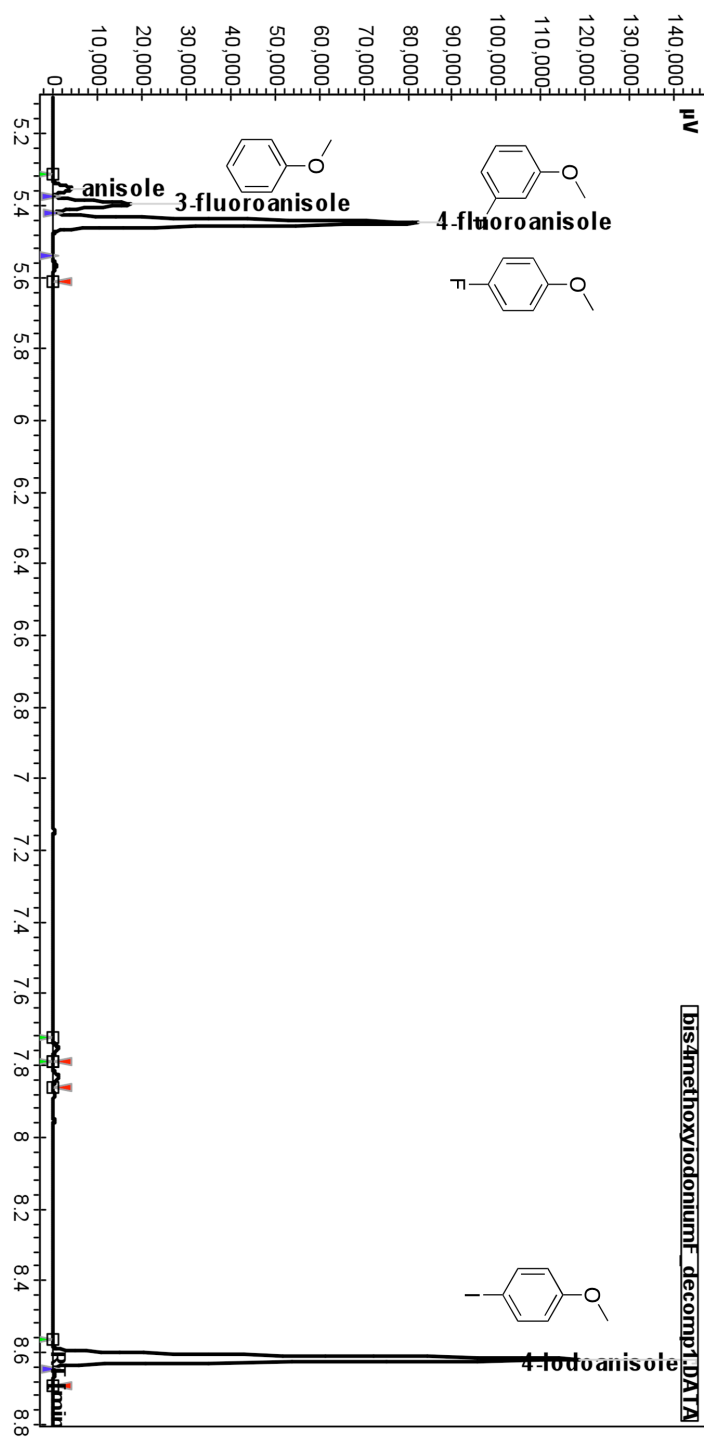
**Chromatogram 11** GC chromatogram of bis(4-methoxyphenyl)-fluoro- $\lambda^3$ -iodane decomposition mixture (benzene)



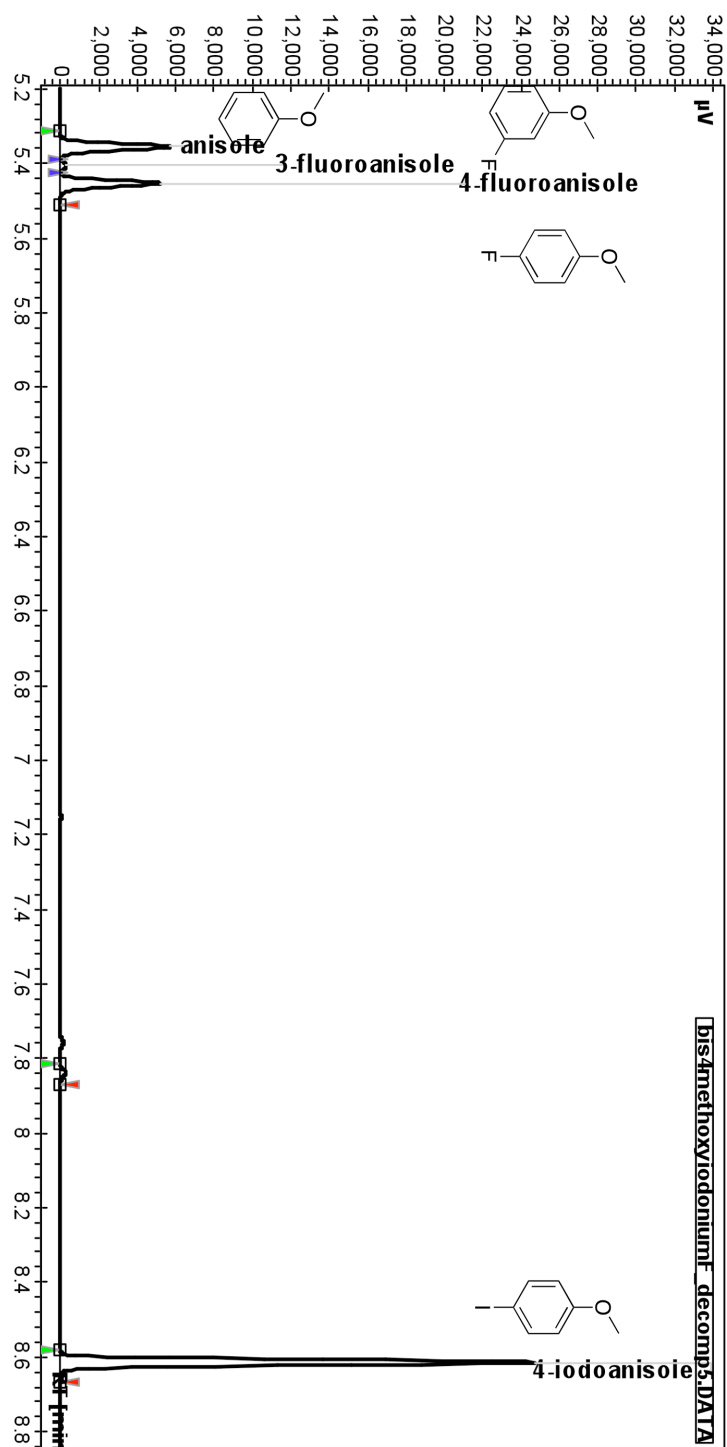
**Chromatogram 12** GC chromatogram of bis(4-methoxyphenyl)-fluoro- $\lambda^3$ -iodane decomposition mixture (acetonitrile)



**Chromatogram 13** GC chromatogram of bis(4-methoxyphenyl)-fluoro- $\lambda^3$ -iodane decomposition mixture (wet benzene)

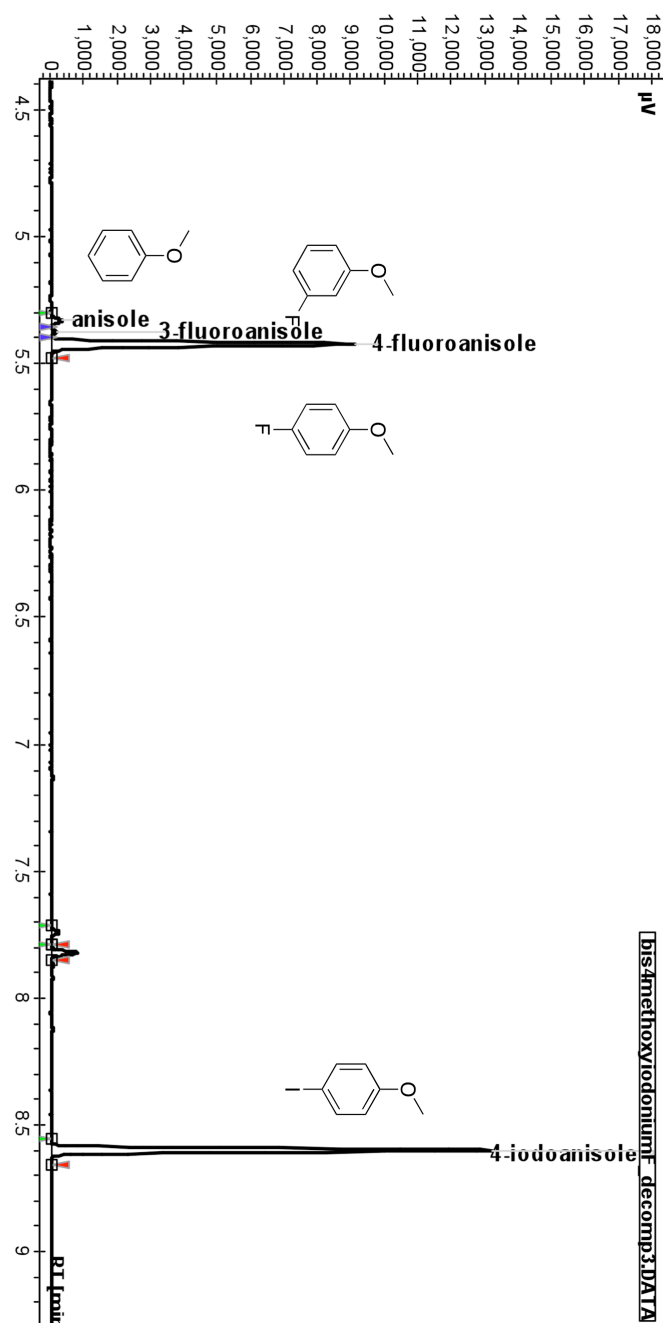


**Chromatogram 14** GC chromatogram of bis(4-methoxyphenyl)-fluoro- $\lambda^3$ -iodane decomposition mixture (acetonitrile)





**Chromatogram 15** GC chromatogram of bis(4-methoxyphenyl)-fluoro- $\lambda^3$ -iodane decomposition mixture (benzene, with added salt)



## REFERENCES

1. Henne, A. L., Preparation of aliphatic F compounds. **1944**, Pp 49-93.
2. Lal, G. S.; Pez, G. P.; Syvret, R. G., Electrophilic NF Fluorinating Agents. *Chemical Reviews (Washington, D. C.)* **1996**, 96 (5), 1737-1755.
3. Vilela, A. F. A.; Gargano, R.; Barreto, P. R. P., Quasi-classical dynamical properties and reaction rate of the Na + HF system on two different potential energy surfaces. *International Journal of Quantum Chemistry* **2005**, 103 (5), 695-702.
4. Ventura, O. N.; Kieninger, M.; Cachau, R. E., Density Functional Theory Is More Accurate Than Coupled-Cluster Theory in the Study of the Thermochemistry of Species Containing the F-O Bond. *Journal of Physical Chemistry A* **1999**, 103 (1), 147-151.
5. Hodson, H. F.; Madge, D. J.; Slawin, A. N. Z.; Widdowson, D. A.; Williams, D. J., Electrophilic fluorination in the synthesis of new fluorindoles. *Tetrahedron* **1994**, 50 (6), 1899-98.
6. Hodson, H. F.; Madge, D. J.; Widdowson, D. A., Regioselective electrophilic fluorination of alkenyl and related stannanes using cesium fluoroxysulfate. *Synlett* **1992**, (10), 831-2.
7. Snieckus, V.; Baulieu, F.; Mohri, K.; Han, W.; Murphy, C. K.; Davis, F. A., Directed ortho metalation-mediated F<sup>+</sup> introduction. Regiospecific synthesis of fluorinated aromatics. *Tetrahedron Lett.* **1994**, 35 (21), 3465-8.
8. Poss, A. J., Fluorination of organolithium reagents. *Speciality Chemicals Magazine* **2003**, 23 (3), 36-38, 40.

9. Ghosh, A. K.; Lagisetty, P.; Zajc, B., Direct Synthesis of 8-Fluoro Purine Nucleosides via Metalation-Fluorination. *J. Org. Chem.* **2007**, *72* (22), 8222-8226.
10. Hull, K. L.; Anani, W. Q.; Sanford, M. S., Palladium-Catalyzed Fluorination of Carbon-Hydrogen Bonds. *Journal of the American Chemical Society* **2006**, *128* (22), 7134-7135.
11. Kimura, Y.; Suzuki, H., Freeze-dried potassium fluoride: Synthetic utility as a fluorinating agent. *Tetrahedron Letters* **1989**, *30* (10), 1271-1272.
12. Liotta, C. L.; Harris, H. P., Chemistry of naked anions. I. Reactions of the 18-crown-6 complex of potassium fluoride with organic substrates in aprotic organic solvents. *Journal of the American Chemical Society* **1974**, *96* (7), 2250-2252.
13. Yoshida, Y.; Kimura, Y., An improved and practical synthesis of 4-fluorobenzaldehyde by halogen-exchange fluorination reaction. *Journal of Fluorine Chemistry* **1989**, *44* (2), 291-298.
14. Zhan, C.-G.; Dixon, D. A., Hydration of the Fluoride Anion: Structures and Absolute Hydration Free Energy from First-Principles Electronic Structure Calculations. *Journal of Physical Chemistry A* **2004**, *108* (11), 2020-2029.
15. Cox, D. P.; Terpinski, J.; Lawrynowicz, W., "Anhydrous" tetrabutylammonium fluoride: a mild but highly efficient source of nucleophilic fluoride ion. *J. Org. Chem.* **1984**, *49* (17), 3216-19.
16. Sharma, R. K.; Fry, J. L., Instability of anhydrous tetra-n-alkylammonium fluorides. *The Journal of Organic Chemistry* **1983**, *48* (12), 2112-2114.

17. Bredt, J.; Thouet, H.; Schmitz, J., Steric hindrance in the bridge ring (Bredt's rule) and the meso-trans-position in condensed ring systems of the hexamethylenes. *Justus Liebigs Annalen der Chemie* **1924**, 437, 1-13.
18. Sun, H.; DiMagno, S. G., Anhydrous Tetrabutylammonium Fluoride. *Journal of the American Chemical Society* **2005**, 127 (7), 2050-2051.
19. Cox, D. P.; Terpinski, J.; Lawrynowicz, W., "Anhydrous" tetrabutylammonium fluoride: a mild but highly efficient source of nucleophilic fluoride ion. *The Journal of Organic Chemistry* **1984**, 49 (17), 3216-3219.
20. Bennett, B. K.; Harrison, R. G.; Richmond, T. G., Cobaltocenium Fluoride: A Novel Source of "Naked" Fluoride Formed by Carbon-Fluorine Bond Activation in a Saturated Perfluorocarbon. *Journal of the American Chemical Society* **1994**, 116 (24), 11165-11166.
21. Pilcher, A. S.; Ammon, H. L.; DeShong, P., Utilization of Tetrabutylammonium Triphenylsilyldifluoride as a Fluoride Source for Nucleophilic Fluorination. *Journal of the American Chemical Society* **1995**, 117 (18), 5166-5167.
22. Sun, H.; DiMagno, S. G., Room-temperature nucleophilic aromatic fluorination: experimental and theoretical studies. *Angew. Chem., Int. Ed.* **2006**, 45 (17), 2720-2725.
23. Fernandez, I.; Martinez-Viviente, E.; Pregosin, P. S., Multinuclear PGSE Diffusion and Overhauser NMR Studies on a Variety of Salts in THF Solution. *Inorganic Chemistry* **2005**, 44 (15), 5509-5513.

24. Streitwieser, A.; Xie, L.; Wang, P.; Bachrach, S. M., Carbon acidity. 77. Ion pair carbon acidities of some silanes in tetrahydrofuran. *The Journal of Organic Chemistry* **1993**, *58* (7), 1778-1784.
25. Sun, H.; DiMagno, S. G., Competitive demethylation and substitution in N,N,N-trimethylanilinium fluorides. *Journal of Fluorine Chemistry* **2007**, *128* (7), 806-812.
26. Ford, W. T., Synthesis of trineopentylamine. *J. Org. Chem.* **1973**, *38* (20), 3614-15.
27. Frisch, M. J. T., G. W.; Schlegel, H. B.; Scuseria, G. E.; Robb, M. A.; Cheeseman, J. R.; Montgomery, Jr., J. A.; Vreven, T.; Kudin, K. N.; Burant, J. C.; Millam, J. M.; Iyengar, S. S.; Tomasi, J.; Barone, V.; Mennucci, B.; Cossi, M.; Scalmani, G.; Rega, N.; Petersson, G. A.; Nakatsuji, H.; Hada, M.; Ehara, M.; Toyota, K.; Fukuda, R.; Hasegawa, J.; Ishida, M.; Nakajima, T.; Honda, Y.; Kitao, O.; Nakai, H.; Klene, M.; Li, X.; Knox, J. E.; Hratchian, H. P.; Cross, J. B.; Bakken, V.; Adamo, C.; Jaramillo, J.; Gomperts, R.; Stratmann, R. E.; Yazyev, O.; Austin, A. J.; Cammi, R.; Pomelli, C.; Ochterski, J. W.; Ayala, P. Y.; Morokuma, K.; Voth, G. A.; Salvador, P.; Dannenberg, J. J.; Zakrzewski, V. G.; Dapprich, S.; Daniels, A. D.; Strain, M. C.; Farkas, O.; Malick, D. K.; Rabuck, A. D.; Raghavachari, K.; Foresman, J. B.; Ortiz, J. V.; Cui, Q.; Baboul, A. G.; Clifford, S.; Cioslowski, J.; Stefanov, B. B.; Liu, G.; Liashenko, A.; Piskorz, P.; Komaromi, I.; Martin, R. L.; Fox, D. J.; Keith, T.; Al-Laham, M. A.; Peng, C. Y.; Nanayakkara, A.; Challacombe, M.; Gill, P. M. W.; Johnson, B.; Chen, W.; Wong, M. W.; Gonzalez, C.; and Pople, J. A.; Gaussian, Inc., Wallingford CT, 2004., Gaussian 03, Revision C.02.,

28. Mosher, H.; Blanz, J. E., Notes - Reduction of o-Bromoanisole by Lithium Dineopentylamide. *The Journal of Organic Chemistry* **1957**, 22 (4), 445-446.
29. Zhdankin, V. V., Product subclass 1: hypervalent iodoarenes and arylodonium salts. *Sci. Synth. FIELD Full Journal Title: Science of Synthesis* **2007**, 31a, 161-233.
30. Matveeva, E. D.; Proskurnina, M. V.; Zefirov, N. S., Polyvalent iodine in organic chemistry: recent developments, 2002-2005. *Heteroatom Chemistry* **2006**, 17 (6), 595-617.
31. Stang, P. J.; Zhdankin, V. V., Organic Polyvalent Iodine Compounds. *Chemical Reviews (Washington, D. C.)* **1996**, 96 (3), 1123-78.
32. Sawaguchi, M.; Ayuba, S.; Hara, S., A practical synthetic method of iodoarene difluorides without fluorine gas and mercury salts. *Synthesis* **2002**, (13), 1802-1803.
33. Naumann, D.; Ruether, G., Synthesis of aryl iodine difluorides by direct fluorination of aryl iodides. *Journal of Fluorine Chemistry* **1980**, 15 (3), 213-22.
34. Ruppert, I., Fluorinated non-metalloorganics: oxidative liquid-phase direct oxidation. 8. *Journal of Fluorine Chemistry* **1980**, 15 (2), 173-8.
35. Sket, B.; Zupan, M.; Zupet, P., Role of the polymer backbone on the reactivity of polymer-supported (dichloriodo)benzene. *Tetrahedron* **1984**, 40 (9), 1603-6.
36. Gregorcic, A.; Zupan, M., Fluorination of norbornadiene and 1,4-dihydro-1,4-methanonaphthalene with substituted (difluoriodo)benzenes. *Journal of the Chemical Society, Perkin Transactions 1: Organic and Bio-Organic Chemistry (1972-1999)* **1977**, (12), 1446-9.

37. Gregorcic, A.; Zupan, M., Fluorination with substituted (difluoriodo)arenes. *Bull. Chem. Soc. Jpn.* **1977**, *50* (2), 517-20.
38. Zupan, M.; Pollak, A., Fluorination with xenon difluoride. Preparation of aryl iodine(III) difluoride. *Journal of Fluorine Chemistry* **1976**, *7* (4), 445-7.
39. Zupan, M.; Pollak, A., Iodofluorination of phenyl-substituted olefins with methyl iodine(III) difluoride. *J. Org. Chem.* **1976**, *41* (12), 2179-2182.
40. Zupan, M.; Pollak, A., Stereochemistry of iodofluorination of phenyl-substituted olefins with (difluoriodo)methane. *Journal of the Chemical Society, Perkin Transactions 1: Organic and Bio-Organic Chemistry (1972-1999)* **1976**, (16), 1745-8.
41. Zupan, M., Polymer-supported reagents in organic synthesis. I. Polymer-supported aryl iodine(III) difluoride. *Collection of Czechoslovak Chemical Communications* **1977**, *42* (1), 266-74.
42. F. Bailly, P. B. W. B. H. J. F. M. G. J. H. G. H. A. P., Pentafluorophenyl iodine(III)-Verbindungen. 3 Pentafluorophenyl iodine difluoride: alternative Darstellungsmethoden, Molekülstruktur und Eigenschaften. *Zeitschrift für anorganische und allgemeine Chemie* **2000**, *626* (6), 1406-1413.
43. Ye, C.; Twamley, B.; Shreeve, J. n. M., Straightforward Syntheses of Hypervalent Iodine(III) Reagents Mediated by Selectfluor. *Organic Letters* **2005**, *7* (18), 3961-3964.
44. Lyalin, V. V.; Orda, V. V.; Alekseeva, L. A.; Yagupol'skii, L. M., Difluoriodine derivatives of organic compounds. *Zhurnal Organicheskoi Khimii* **1970**, *6* (2), 329-32.
45. Sun, H.; Wang, B.; DiMaggio, S. G., A method for detecting water in organic solvents. *Org. Lett.* **2008**, *10* (20), 4413-4416.

46. Nussbaum, R.; Lischke, D.; Paxmann, H.; Wolf, B., Quantitative GC determination of water in small samples. *Chromatographia* **2000**, *51* (1/2), 119-121.
47. Hogan, J. M.; Engel, R. A.; Stevenson, H. F., Versatile internal standard technique for the gas chromatographic determination of water in liquids. *Analytical Chemistry* **1970**, *42* (2), 249-52.
48. Pasika, W. M.; West, A. C., III, Quantitative determination of water in a hydrophilic macromolecular sample (dextran) bby gas chromatography. *Analytical Chemistry* **1971**, *43* (2), 275-6.
49. Knight, H. S.; Weiss, F. T., Determination of traces of water in hydrocarbons. A calcium carbide gas-liquid chromatography method. *Anal. Chem.* **1962**, *34*, 749-51.
50. van de Voort, F. R.; Sedman, J.; Cocciardi, R.; Juneau, S., An automated FTIR method for the routine quantitative determination of moisture in lubricants: An alternative to Karl Fischer titration. *Talanta* **2007**, *72* (1), 289-295.
51. Li, M.; Pacey, G. E., Spectrophotometric determination of trace water in organic solvents with a near infrared absorbing dye. *Talanta* **1997**, *44* (11), 1949-1958.
52. Garrigues, S.; Gallignani, M.; de la Guardia, M., Flow-injection determination of water in organic solvents by near-infrared spectrometry. *Analytica Chimica Acta* **1993**, *281* (2), 259-64.
53. Meeker, R. L.; Critchfield, F. E.; Bishop, E. T., Water Determination by Near Infrared Spectrophotometry. *Anal. Chem.* **1962**, *34* (11), 1510-1511.
54. Streim, H. G.; Boyce, E. A.; Smith, J. R., Determination of Water in 1, 1-Dimethylhydrazine, Diethylenetriamine, and Mixtures. *Anal. Chem.* **1961**, *33* (1), 85-89.



55. Scholz, E., *Karl Fischer Titration*. 1984; p 138 pp.
56. Mitchell, J., Jr.; Smith, D. M., *Chemical Analysis: A Series of Monographs on Analytical Chemistry and Its Applications, Vol. 5: Aquametry: A Treatise on Methods for the Determination of Water, Pt. 1. 2nd Ed.* 1977; p 624 pp.
57. Langsteiger, W.; Heinisch, M.; Fogelman, I., The role of fluorodeoxyglucose, 18F-dihydroxyphenylalanine, 18F-choline, and 18F-fluoride in bone imaging with emphasis on prostate and breast. *Seminars in nuclear medicine* **2006**, 36 (1), 73-92.
58. Dolle, F., Fluorine-18-Labelled Fluoropyridines: Advances in Radiopharmaceutical Design. *Current Pharmaceutical Design* **2005**, 11 (25), 3221-3235.
59. Snyder, S. E.; Kilbourn, M. R., Chemistry of fluorine-18 radiopharmaceuticals. *Handb. Radiopharm.* **2003**, 195-227.
60. Stocklin, G.; Qaim, S. M.; Roesch, F., The impact of radioactivity on medicine. *Radiochim. Acta* **1995**, 70/71, 249-72.
61. Wester, H. J., 18F: labeling chemistry and labeled compounds. *Handbook of Nuclear Chemistry* **2003**, 4, 167-209.
62. Cai, L.; Lu, S.; Pike, V. W., Chemistry with [18F]fluoride ion. *Eur. J. Org. Chem.* **2008**, (17), 2853-2873.
63. Bergman, J.; Solin, O., Fluorine-18-labeled fluorine gas for synthesis of tracer molecules. *Nucl Med Biol* **1997**, 24 (7), 677-83.
64. Ding, Y. S.; Shiue, C. Y.; Fowler, J. S.; Wolf, A. P.; Plenevaux, A., No-carrier-added (NCA) aryl [18F]fluorides via the nucleophilic aromatic substitution of electron-rich aromatic rings. *Journal of Fluorine Chemistry* **1990**, 48 (2), 189-206.

65. Reddy, G. N.; Haeberli, M.; Berr, H. F.; Hasler, P.; Schubiger, A. P., Quality assurance and quality control methods for animal and human applications of no-carrier-added 6-[<sup>18</sup>F]fluorodopa for PET investigations of dopaminergic systems. *Applied Radiation and Isotopes* **1993**, *44* (7), 993-8.
66. Lemaire, C.; Damhaut, P.; Plenevaux, A.; Comar, D., Enantioselective synthesis of 6-[fluorine-18]-fluoro-L-dopa from no-carrier-added fluorine-18-fluoride. *Journal of Nuclear Medicine* **1994**, *35* (12), 1996-2002.
67. Lemaire, C., Production of L-[<sup>18</sup>F]fluoro amino acids for protein synthesis: overview and recent developments in nucleophilic syntheses. *Developments in Nuclear Medicine* **1993**, *23* (PET Studies on Amino Acid Metabolism and Protein Synthesis), 89-108.
68. Grushin, V. V.; Marshall, W. J., Ar-F Reductive Elimination from Palladium(II) Revisited. *Organometallics* **2007**, *26* (20), 4997-5002.
69. Watson, D. A.; Su, M.; Teverovskiy, G.; Zhang, Y.; Garcia-Fortanet, J.; Kinzel, T.; Buchwald, S. L., Formation of ArF from LPdAr(F): Catalytic Conversion of Aryl Triflates to Aryl Fluorides. *Science (Washington, DC, United States)* **2009**, *325* (5948), 1661-1664.
70. Grushin, V. V., The Organometallic Fluorine Chemistry of Palladium and Rhodium: Studies toward Aromatic Fluorination. *Acc. Chem. Res.* **2010**, *43* (1), 160-171.
71. Pike, V. W.; Aigbirhio, F. I., Reactions of cyclotron-produced [<sup>18</sup>F]fluoride with diaryliodonium salts - a novel single-step route to no-carrier-added [<sup>18</sup>]fluoroarenes. *J. Chem. Soc., Chem. Commun.* **1995**, (21), 2215-6.

72. Ermert, J.; Hocke, C.; Ludwig, T.; Gail, R.; Coenen, H. H., Comparison of pathways to the versatile synthon of no-carrier-added 1-bromo-4-[18F]fluorobenzene. *J. Labelled Compd. Radiopharm.* **2004**, *47* (7), 429-441.
73. Grushin, V. V.; Tolstaya, T. P.; Lisichkina, I. N., Phenyl-2-p-carboranyliodonium fluoroborate. *Izv. Akad. Nauk SSSR, Ser. Khim.* **1983**, (9), 2165-8.
74. Van der Puy, M., Conversion of diaryliodonium salts to aryl fluorides. *Journal of Fluorine Chemistry* **1982**, *21* (3), 385-92.
75. Grushin, V. V.; Kantor, M. M.; Tolstaya, T. P.; Shcherbina, T. M., Arylation of anions by diarylhalonium tetrafluoroborates under phase transfer catalysis conditions. *Izv. Akad. Nauk SSSR, Ser. Khim.* **1984**, (10), 2332-8.
76. Yamada, Y.; Kashima, K.; Okawara, M., Substituent effect in the nucleophilic attack by the bromide ion on the p-tolyl-substituted phenyliodonium ions. *Bull. Chem. Soc. Jpn.* **1974**, *47* (12), 3179-80.
77. Ross, T. L.; Ermert, J.; Hocke, C.; Coenen, H. H., Nucleophilic 18F-Fluorination of Heteroaromatic Iodonium Salts with No-Carrier-Added [18F]Fluoride. *Journal of the American Chemical Society* **2007**, *129* (25), 8018-8025.
78. Yamada, Y.; Okawara, M., Steric effect in the nucleophilic attack of bromide anion on diaryl- and aryl-2-thienyliodonium ions. *Bull. Chem. Soc. Jap.* **1972**, *45* (6), 1860-3.
79. Lancer, K. M.; Wiegand, G. H., The ortho effect in the pyrolysis of iodonium halides. A case for a sterically controlled nucleophilic aromatic (SN) substitution reaction. *J. Org. Chem.* **1976**, *41* (21), 3360-4.

80. Carroll, M. A.; Martin-Santamaria, S.; Pike, V. W.; Rzepa, H. S.; Widdowson, D. A., An ab initio and MNDO-d SCF-MO computational study of stereoelectronic control in extrusion reactions of R<sub>2</sub>I-F iodine(III) intermediates. *Journal of the Chemical Society, Perkin Transactions 2: Physical Organic Chemistry* **1999**, (12), 2707-2714.
81. Martin-Santamaria, S.; Carroll, M. A.; Carroll, C. M.; Carter, C. D.; Rzepa, H. S.; Widdowson, D. A.; Pike, V. W., Fluoridation of heteroaromatic iodonium salts: experimental evidence supporting theoretical prediction of the selectivity of the process. *Chemical Communications (Cambridge)* **2000**, (8), 649-650.
82. Carroll, M. A.; Jones, C.; Tang, S.-L., Fluoridation of 2-thienyliodonium salts. *J. Labelled Compd. Radiopharm.* **2007**, 50 (5-6), 450-451.
83. Zhang, M.-R.; Kumata, K.; Suzuki, K., A practical route for synthesizing a PET ligand containing [18F]fluorobenzene using reaction of diphenyliodonium salt with [18F]F. *Tetrahedron Letters* **2007**, 48 (49), 8632-8635.
84. Carroll, M. A.; Nairne, J.; Smith, G.; Widdowson, D. A., Radical scavengers: A practical solution to the reproducibility issue in the fluoridation of diaryliodonium salts. *Journal of Fluorine Chemistry* **2007**, 128 (2), 127-132.
85. Sun, H.; DiMagno, S. G., Fluoride relay: a new concept for the rapid preparation of anhydrous nucleophilic fluoride salts from KF. *Chem. Commun. (Cambridge, U. K.)* **2007**, (5), 528-529.
86. Ding, Y. S.; Fowler, J. S.; Gatley, S. J.; Dewey, S. L.; Wolf, A. P.; Schlyer, D. J., Synthesis of high specific activity 6-[18F]fluorodopamine for positron emission tomography studies of sympathetic nervous tissue. *J Med Chem* **1991**, 34 (2), 861-3.

87. Hostetler, E. D.; Jonson, S. D.; Welch, M. J.; Katzenellenbogen, J. A., Synthesis of 2-[18F]Fluoroestradiol, a Potential Diagnostic Imaging Agent for Breast Cancer: Strategies to Achieve Nucleophilic Substitution of an Electron-Rich Aromatic Ring with [18F]F. *J. Org. Chem. FIELD Full Journal Title:Journal of Organic Chemistry* **1999**, *64* (1), 178-185.
88. Stang, P. J.; Tykwinski, R.; Zhdankin, V., Preparation of bis(heteroaryl)iodonium salts via an iodonium transfer reaction between di(cyano)iodonium triflate and organostannanes. *J. Heterocycl. Chem.* **1992**, *29* (4), 815-18.
89. Kitamura, T.; Matsuyuki, J.; Nagata, K.; Furuki, R.; Taniguchi, H., A convenient preparation of diaryliodonium triflates. *Synthesis* **1992**, (10), 945-6.
90. Koser, G. F.; Wettach, R. H.; Smith, C. S., New methodology in iodonium salt synthesis. Reactions of [hydroxy(tosyloxy)iido]arenes with aryltrimethylsilanes. *J. Org. Chem.* **1980**, *45* (8), 1543-4.
91. Christe, K. O.; Wilson, W. W.; Wilson, R. D.; Bau, R.; Feng, J. A., Syntheses, properties, and structures of anhydrous tetramethylammonium fluoride and its 1:1 adduct with trans-3-amino-2-butenenitrile. *Journal of the American Chemical Society* **1990**, *112* (21), 7619-25.
92. Grushin, V. V.; Marshall, W. J., Fluorination of Nonactivated Haloarenes via Arynes under Mild Conditions, Resulting from Further Studies toward Ar,àF Reductive Elimination from Palladium(II). *Organometallics* **2008**, *27* (19), 4825-4828.

93. Reich, H. J.; Cooperman, C. S., Structure and stereolability of triaryliodine (III) compounds. Degenerate isomerization of 5-phenyl-5H-dibenziodole. *J. Am. Chem. Soc.* **1973**, *95* (15), 5077-8.
94. Stang, P. J.; Zhdankin, V. V.; Tykwinski, R.; Zefirov, N. S., (Dicyano)iodonium triflate- novel iodonium species and a versatile reagent for the preparation of iodonium salts via an iodonium transfer reaction with organostannanes. *Tetrahedron Letters* **1992**, *33* (11), 1419-1422.
95. Ochiai, M.; Kitagawa, Y.; Takayama, N.; Takaoka, Y.; Shiro, M., Synthesis of Chiral Diaryliodonium Salts, 1,1'-Binaphthyl-2-yl(phenyl)iodonium Tetrafluoroborates: Asymmetric  $\alpha$ -Phenylation of  $\alpha$ -Keto Ester Enolates. *Journal of the American Chemical Society* **1999**, *121* (39), 9233-9234.
96. Ochiai, M.; Toyonari, M.; Sueda, T.; Kitagawa, Y., Boron-iodine(III) exchange reaction: direct synthesis of diaryliodonium tetraarylborates from (diacetoxyiodo)arenes by the reaction with alkali metal tetraarylborates in acetic acid. *Tetrahedron Lett.* **1996**, *37* (46), 8421-8424.
97. Carroll, M. A.; Pike, V. W.; Widdowson, D. A., New synthesis of diaryliodonium sulfonates from arylboronic acids. *Tetrahedron Letters* **2000**, *41* (28), 5393-5396.
98. Margida, A. J.; Koser, G. F., Exchange of carbon ligands at iodine in iodonium salts. A direct synthesis of aryl(2-furyl)iodonium tosylates from aryl(tert-butylethynyl)iodonium tosylates. *J. Org. Chem.* **1984**, *49* (24), 4703-6.

99. Kitamura, T.; Kotani, M.; Fujiwara, Y., An efficient ligand exchange reaction of  $\text{C} \equiv \text{C}-(\text{triflyloxy})\text{vinylidonium}$  triflates with aryllithium reagents leading to diaryliodonium triflates. *Tetrahedron Lett.* **1996**, 37 (21), 3721-3722.
100. Beringer, F. M.; Forgione, P. S.; Yudis, M. D., Diaryliodonium salts. XII. Phenylation of dimedon, dibenzoylmethane, and tribenzoylmethane. *Tetrahedron* **1960**, 8, 49-63.
101. Beringer, F. M.; Galton, S. A., Diaryliodonium salts. XX. Steric effects in radical coupling. Arylation of 1,3-indandiones with dimesityliodonium chloride. *J. Org. Chem.* **1963**, 28 (12), 3417-21.
102. Ryan, J. H.; Stang, P. J., Direct  $\text{C}^{\pm}$ -arylation of ketones: the reaction of cyclic ketone enolates with diphenyliodonium triflate. *Tetrahedron Lett.* **1997**, 38 (28), 5061-5064.
103. Oh, C. H.; Kim, J. S.; Jung, H. H., Highly Efficient Arylation of Malonates with Diaryliodonium Salts. *J. Org. Chem.* **1999**, 64 (4), 1338-1340.
104. Carroll, M. A.; Wood, R. A., Arylation of anilines: formation of diarylamines using diaryliodonium salts. *Tetrahedron* **2007**, 63 (46), 11349-11354.
105. Beringer, F. M.; Brierley, A.; Drexler, M.; Gindler, E. M.; Lumpkin, C. C., Diaryliodonium Salts. II. The Phenylation of Organic and Inorganic Bases<sup>1,2</sup>. *Journal of the American Chemical Society* **1953**, 75 (11), 2708-2712.
106. Beringer, F. M.; Falk, R. A., Diaryliodonium salts. XXIII. Competitive arylation of nucleophiles and reductants by substituted diphenyliodonium cations. *J. Chem. Soc.* **1964**, (Nov.), 4442-51.

107. Uchiyama, M.; Suzuki, T.; Yamazaki, Y., Transition metal catalyzed reactions of diaryliodonium salts. II. The reductive coupling reaction of diaryliodonium salts catalyzed by the palladium-zinc system. *Chemistry Letters* **1983**, (8), 1165-6.
108. Kang, S.-K.; Jung, K.-Y.; Park, C.-H.; Jang, S.-B., Palladium-catalyzed coupling of allylic cyclic carbonates with iodobenzene and hypervalent iodonium salts. *Tetrahedron Lett.* **1995**, 36 (44), 8047-50.
109. Kang, S.-K.; Lee, H.-W.; Choi, W.-K.; Hong, R.-K.; Kim, J.-S., Palladium-catalyzed synthesis of arylamines from diphenyliodonium tetrafluoroborate and secondary amine. *Synth. Commun.* **1996**, 26 (22), 4219-4224.
110. Kang, S.-K.; Lee, H.-W.; Jang, S.-B.; Ho, P.-S., Palladium-Catalyzed Cross-Coupling of Organoboron Compounds with Iodonium Salts and Iodanes. *J. Org. Chem.* **1996**, 61 (14), 4720-4724.
111. Aggarwal, V. K.; Olofsson, B., Enantioselective  $\text{C}\pm$ -arylation of cyclohexanones with diaryl iodonium salts: Application to the synthesis of (-)-epibatidine. *Angew. Chem., Int. Ed.* **2005**, 44 (34), 5516-5519.
112. Krief, A.; Dumont, W.; Robert, M., Arylation of n-hexylthiol and n-hexyl phenyl sulfide using diphenyliodonium triflate: Synthetic and mechanistic aspects - application to the transformation of n-hexylthiol to n-hexyl selenide. *Synlett* **2006**, (3), 484-486.
113. Aydin, J.; Larsson, J. M.; Selander, N.; Szabo, K. J., Pincer Complex-Catalyzed Redox Coupling of Alkenes with Iodonium Salts via Presumed Palladium(IV) Intermediates. *Org. Lett.* **2009**, 11 (13), 2852-2854.



114. Deprez, N. R.; Sanford, M. S., Synthetic and Mechanistic Studies of Pd-Catalyzed C-H Arylation with Diaryliodonium Salts: Evidence for a Bimetallic High Oxidation State Pd Intermediate. *Journal of the American Chemical Society* **2009**, *131* (31), 11234-11241.
115. Reutov, O. A.; Ertel, G. A.; Ptitsina, O. A., Reaction of isotope exchange between diaryliodonium fluoborates and aryl iodides labeled with I-131. *Dokl. Akad. Nauk SSSR* **1960**, *133*, 1108-10.
116. Kitamura, T.; Matsuyuki, J.; Taniguchi, H., Improved preparation of diaryliodonium triflates. *Synthesis* **1994**, (2), 147-8.
117. Pike, V. W.; Butt, F.; Shah, A.; Widdowson, D. A., Facile synthesis of substituted diaryliodonium tosylates by treatment of aryltributylstannanes with Koser's reagent. *J. Chem. Soc., Perkin Trans. I* **1999**, (3), 245-248.
118. Caserio, M. C.; Glusker, D. L.; Roberts, J. D., Hydrolysis of diaryliodonium salts. *Journal of the American Chemical Society* **1959**, *81*, 336-42.
119. Grushin, V. V., Carboranylhalonium ions: from striking reactivity to a unified mechanistic analysis of polar reactions of diarylhalonium compounds. *Acc. Chem. Res.* **1992**, *25* (11), 529-36.
120. Grushin, V. V.; Demkina, I. I.; Tolstaya, T. P., Unified mechanistic analysis of polar reactions of diaryliodonium salts. *Journal of the Chemical Society, Perkin Transactions 2: Physical Organic Chemistry* **1992**, (4), 505-11.
121. Martin-Santamaria, S.; Carroll, M. A.; Pike, V. W.; Rzepa, H. S.; Widdowson, D. A., An ab initio and MNDO-d SCF-MO computational study of the extrusion reactions of

R2I-F iodine(III) via dimeric, trimeric and tetrameric transition states. *Perkin 2* **2000**, (10), 2158-2161.

122. Creveling, C. R.; Kirk, K. L., The effect of ring-fluorination on the rate of O-methylation of dihydroxyphenylalanine (DOPA) by catechol-O-methyltransferase: significance in the development of <sup>18</sup>F-PETT scanning agents. *Biochemical and Biophysical Research Communications* **1985**, 130 (3), 1123-31.

123. Brooks, D. J., PET studies and motor complications in Parkinson's disease. *Trends in Neurosciences* **2000**, 23 (10, Suppl.), S101-S108.

124. Brooks, D. J., Monitoring neuroprotection and restorative therapies in Parkinson's disease with PET. *Advances in Research on Neurodegeneration* **2000**, 8, 125-137.

125. Elsinga, P. H.; Hatano, K.; Ishiwata, K., PET tracers for imaging of the dopaminergic system. *Curr. Med. Chem.* **2006**, 13 (18), 2139-2153.

126. Fischman Alan, J., Role of [<sup>18</sup>F]-dopa-PET imaging in assessing movement disorders. *Radiologic clinics of North America* **2005**, 43 (1), 93-106.

127. Ishiwata, K.; Ido, T.; Takahashi, T.; Iwata, R.; Brady, F.; Hatazawa, J.; Itoh, M., Feasibility study of fluorine-18 labeled dopa for melanoma imaging. *Nuclear Medicine and Biology* **1989**, 16 (4), 371-4.

128. Ishiwata, K.; Kubota, K.; Kubota, R.; Iwata, R.; Takahashi, T.; Ido, T., Selective 2-[<sup>18</sup>F]fluorodopa uptake for melanogenesis in murine metastatic melanomas. *Journal of Nuclear Medicine* **1991**, 32 (1), 95-101.

129. Mishima, Y.; Imahori, Y.; Honda, C.; Hiratsuka, J.; Ueda, S.; Ido, T., In vivo diagnosis of human malignant melanoma with positron emission tomography using

specific melanoma-seeking  $^{18}\text{F}$ -DOPA analogue. *Journal of neuro-oncology* **1997**, *33* (1-2), 163-9.

130. Dimitrakopoulou-Strauss, A.; Strauss, L. G.; Burger, C., Quantitative PET studies in pretreated melanoma patients: A comparison of 6- $^{18}\text{F}$ fluoro-L-dopa with  $^{18}\text{F}$ -FDG and  $^{15}\text{O}$ -water using compartment and noncompartment analysis. *Journal of Nuclear Medicine* **2001**, *42* (2), 248-256.

131. Jager, P. L.; Chirakal, R.; Marriott, C. J.; Brouwers, A. H.; Koopmans, K. P.; Gulenchyn, K. Y., 6-L- $^{18}\text{F}$ -fluorodihydroxyphenylalanine PET in neuroendocrine tumors: basic aspects and emerging clinical applications. *Journal of Nuclear Medicine* **2008**, *49* (4), 573-586.

132. Pestourie, C.; Theze, B.; Kuhnast, B.; Helleix, S.; Gombert, K.; Dolle, F.; Tavitian, B.; Duconge, F., PET imaging of medullary thyroid carcinoma in MEN2A transgenic mice using 6- $^{18}\text{F}$ F-L-DOPA. *European Journal of Nuclear Medicine and Molecular Imaging* **2010**, *37* (1), 58-66.

133. Lange-Nolde, A.; Zajic, T.; Slawik, M.; Brink, I.; Reincke, M.; Moser, E.; Hoegerle, S., PET with  $^{18}\text{F}$ -DOPA in the imaging of parathyroid adenoma in patients with primary hyperparathyroidism: a pilot study. *Nuklearmedizin* **2006**, *45* (5), 193-196.

134. Nanni, C.; Rubello, D.; Fanti, S.,  $^{18}\text{F}$ -DOPA PET/CT and neuroendocrine tumours. *Eur J Nucl Med Mol Imaging* **2006**, *33* (5), 509-13.

135. Kauhanen, S.; Seppanen, M.; Minn, H.; Gullichsen, R.; Salonen, A.; Alanen, K.; Parkkola, R.; Solin, O.; Bergman, J.; Sane, T.; Salmi, J.; Valimaki, M.; Nuutila, P., Fluorine-18-L-dihydroxyphenylalanine ( $^{18}\text{F}$ -DOPA) positron emission tomography as a

tool to localize an insulinoma or  $\alpha$ -cell hyperplasia in adult patients. *Journal of Clinical Endocrinology and Metabolism* **2007**, 92 (4), 1237-1244.

136. Ambrosini, V.; Tomassetti, P.; Castellucci, P.; Campana, D.; Montini, G.; Rubello, D.; Nanni, C.; Rizzello, A.; Franchi, R.; Fanti, S., Comparison between  $^{68}\text{Ga}$ -DOTA-NOC and  $^{18}\text{F}$ -DOPA PET for the detection of gastro-entero-pancreatic and lung neuroendocrine tumors. *European Journal of Nuclear Medicine and Molecular Imaging* **2008**, 35 (8), 1431-1438.

137. Haug, A.; Auernhammer, C. J.; Waengler, B.; Tiling, R.; Schmidt, G.; Goeke, B.; Bartenstein, P.; Poepperl, G., Intraindividual comparison of  $^{68}\text{Ga}$ -DOTA-TATE and  $^{18}\text{F}$ -DOPA PET in patients with well-differentiated metastatic neuroendocrine tumours. *European Journal of Nuclear Medicine and Molecular Imaging* **2009**, 36 (5), 765-770.

138. Kauhanen, S.; Seppanen, M.; Ovaska, J.; Minn, H.; Bergman, J.; Korsoff, P.; Salmela, P.; Saltevo, J.; Sane, T.; Valimaki, M.; Nuutila, P., The clinical value of [ $^{18}\text{F}$ ]fluoro-dihydroxyphenylalanine positron emission tomography in primary diagnosis, staging, and restaging of neuroendocrine tumors. *Endocrine-Related Cancer* **2009**, 16 (1), 255-265.

139. Minn, H.; Kauhanen, S.; Seppanen, M.; Nuutila, P.,  $^{18}\text{F}$ -FDOPA: a multiple-target molecule. *Journal of Nuclear Medicine* **2009**, 50 (12), 1915-1918.

140. Dolle, F.; Demphel, S.; Hinnen, F.; Fournier, D.; Vaufrey, F.; Crouzel, C., 6-[ $^{18}\text{F}$ ]Fluoro-L-DOPA by radiofluorodestannylation: a short and simple synthesis of a new labeling precursor. *J. Labelled Compd. Radiopharm.* **1998**, 41 (2), 105-114.

141. De Vries, E. F. J.; Luurtsema, G.; Brussermann, M.; Elsinga, P. H.; Vaalburg, W., Fully automated synthesis module for the high yield one-pot preparation of 6-[18F]fluoro-L-DOPA. *Applied Radiation and Isotopes* **1999**, *51* (4), 389-394.
142. Forsback, S.; Eskola, O.; Haaparanta, M.; Bergman, J.; Solin, O., Electrophilic synthesis of 6-[18F]fluoro-L-DOPA using post-target produced [18F]F<sub>2</sub>. *Radiochim. Acta* **2008**, *96* (12), 845-848.
143. Fuechtner, F.; Zessin, J.; Maeding, P.; Wuest, F., Aspects of 6-[18F]fluoro-L-DOPA preparation: deuteriochloroform as a substitute solvent for Freon 11. *Nuklearmedizin* **2008**, *47* (1), 62-64.
144. Zhang, L.; Tang, G.; Yin, D.; Tang, X.; Wang, Y., Enantioselective synthesis of no-carrier-added (NCA) 6-[18F]fluoro-L-DOPA. *Applied Radiation and Isotopes* **2002**, *57* (2), 145-151.
145. Katritzky, A. R.; Gallos, J. K.; Durst, H. D., Structure of and electronic interactions in aromatic polyvalent iodine compounds: a carbon-13 NMR study. *Magn. Reson. Chem. FIELD Full Journal Title:Magnetic Resonance in Chemistry* **1989**, *27* (9), 815-22.
146. Cerioni, G.; Uccheddu, G., Solution structure of bis(acetoxy)iodoarenes as observed by 17O NMR spectroscopy. *Tetrahedron Lett. FIELD Full Journal Title:Tetrahedron Letters* **2004**, *45* (3), 505-507.
147. Hossain, M. D.; Kitamura, T., Unexpected, Drastic Effect of Triflic Acid on Oxidative Diacetoxylation of Iodoarenes by Sodium Perborate. A Facile and Efficient

One-Pot Synthesis of (Diacetoxyiodo)arenes. *J. Org. Chem. FIELD Full Journal Title:Journal of Organic Chemistry* **2005**, 70 (17), 6984-6986.

148. Kazmierczak, P.; Skulski, L., A simple, two-step conversion of various iodo arenes to (diacetoxyiodo) arenes with chromium(VI) oxide as the oxidant. *Synthesis FIELD Full Journal Title:Synthesis* **1998**, (12), 1721-1723.

149. Kozyrod, R. P.; Morgan, J.; Pinhey, J. T., Reaction of aryltrialkylstannanes with lead tetraacetate: a convenient route to aryllead triacetates. *Aust. J. Chem. FIELD Full Journal Title:Australian Journal of Chemistry* **1985**, 38 (8), 1147-53.

150. Ma, H. M.; Liu, Z. Z.; Chen, S. Z., Regioselective bromination of 3,4-dimethoxytoluene with N-bromosuccinimide. *Chin. Chem. Lett. FIELD Full Journal Title:Chinese Chemical Letters* **2003**, 14 (4), 371-374.

151. Tomaszewski, M. J.; Warkentin, J.; Werstiuk, N. H., Free-radical chemistry of imines. *Aust. J. Chem. FIELD Full Journal Title:Australian Journal of Chemistry* **1995**, 48 (2), 291-321.

152. Vitale, A. A.; Stahl, A. E.; Cecilia dos Santos Claro, P.; Alejandra Floridia Addato, M.; Pis Diez, R.; Jubert, A. H., Experimental and theoretical study of the proton methoxy chemical shifts of substituted 3,4-dimethoxyphenethylamines and maleimide/phthalimide derivatives. *J. Mol. Struct.* **2008**, 881 (1-3), 167-174.

153. Biel, J. H., Reduction of estrone and estrogen esters. *J. Am. Chem. Soc. FIELD Full Journal Title:Journal of the American Chemical Society* **1951**, 73, 847-8.

154. Edsall, A. B.; Mohanakrishnan, A. K.; Yang, D.; Fanwick, P. E.; Hamel, E.; Hanson, A. D.; Agoston, G. E.; Cushman, M., Effects of Altering the Electronics of 2-

Methoxyestradiol on Cell Proliferation, on Cytotoxicity in Human Cancer Cell Cultures, and on Tubulin Polymerization. *J. Med. Chem. FIELD Full Journal Title:Journal of Medicinal Chemistry* **2004**, 47 (21), 5126-5139.

155. Edsall, A. B.; Mohanakrishnan, A. K.; Yang, D.; Fanwick, P. E.; Hamel, E.; Hanson, A. D.; Agoston, G. E.; Cushman, M., Effects of Altering the Electronics of 2-Methoxyestradiol on Cell Proliferation, on Cytotoxicity in Human Cancer Cell Cultures, and on Tubulin Polymerization. *J. Med. Chem.* **2004**, 47 (21), 5126-5139.

156. Carreno, M. C.; Garcia Ruano, J. L.; Sanz, G.; Toledo, M. A.; Urbano, A., N-Bromosuccinimide in Acetonitrile: A Mild and Regiospecific Nuclear Brominating Reagent for Methoxybenzenes and Naphthalenes. *J. Org. Chem.* **1995**, 60 (16), 5328-31.

157. Kozyrod, R. P.; Morgan, J.; Pinhey, J. T., Reaction of aryltrialkylstannanes with lead tetraacetate: a convenient route to aryllead triacetates. *Aust. J. Chem.* **1985**, 38 (8), 1147-53.

158. Reimann, E.; Ettmayr, C., An Improved Stereocontrolled Route to cis-Erythrinanes by Combined Intramolecular Strecker and Bruylants Reaction. *Monatsh. Chem.* **2004**, 135 (9), 1143-1155.

159. Merritt, E. A.; Malmgren, J.; Klinke, F. J.; Olofsson, B., Synthesis of diaryliodonium triflates using environmentally benign oxidizing agents. *Synlett* **2009**, (14), 2277-2280.

160. Zhdankin, V. V.; Stang, P. J., Recent Developments in the Chemistry of Polyvalent Iodine Compounds. *Chemical Reviews (Washington, DC, United States)* **2002**, 102 (7), 2523-2584.

161. Stang, P. J., Polyvalent Iodine in Organic Chemistry. *J. Org. Chem.* **2003**, 68 (8), 2997-3008.
162. Zhdankin, V. V.; Stang, P. J., Chemistry of Polyvalent Iodine. *Chemical Reviews (Washington, DC, United States)* **2008**, 108 (12), 5299-5358.
163. Koser, G. F., Halonium ions. *Chem. Halides, Pseudo-Halides Azides* **1995**, (Pt.2), 1173-1274.
164. Koser, G. F., Heteroatom-heteroatom-bond forming reactions. *Top. Curr. Chem.* **2003**, 224 (Hypervalent Iodine Chemistry), 173-183.
165. Ochiai, M., Reactivities, properties and structures. *Top. Curr. Chem.* **2003**, 224 (Hypervalent Iodine Chemistry), 5-68.
166. Wirth, T., Hypervalent iodine chemistry in synthesis: Scope and new directions. *Angewandte Chemie, International Edition* **2005**, 44 (24), 3656-3665.
167. Beringer, F. M.; Daniel, W. J.; Galton, S. A.; Rubin, G., Phenylation of monoketones with diphenyliodonium chloride. *J. Org. Chem.* **1966**, 31 (12), 4315-18.
168. Kornblum, N.; Taylor, H. J., Aliphatic and alicyclic nitro compounds. XX. Phenylation of nitroparaffins. *J. Org. Chem.* **1963**, 28, 1424-5.
169. Park, K. P.; Clapp, L. B., Phenylation of dinitroalkanes. *J. Org. Chem.* **1964**, 29 (7), 2108.
170. Chen, Z.; Jin, Y.; Stang, P. J., Polyvalent iodine in synthesis. 1. An efficient route to isopropylidene arylmalonates (5-aryl-substituted Meldrum's acid). *J. Org. Chem.* **1987**, 52 (18), 4115-17.



171. Rossi, R. A.; Bunnett, J. F., Sense of cleavage of substituted benzenes on reaction with solvated electrons, as determined by a product criterion. *Journal of the American Chemical Society* **1974**, *96* (1), 112-17.
172. Barton, D. H. R.; Finet, J. P.; Khamisi, J., Copper salt catalysis of N-phenylation of amines by trivalent organobismuth compounds. *Tetrahedron Lett.* **1987**, *28* (8), 887-90.
173. Nesmeyanov, A. N.; Makarova, L. G.; Tolstaya, T. P., Heterolytic decomposition of onium compounds (diphenyl halogenonium and triphenyloxonium salts). *Tetrahedron* **1957**, *1* (1-2), 145-157.
174. Lubinkowski, J. J.; McEwen, W. E., Reactions of diarylbromonium salts with sodium alkoxides. *Tetrahedron Letters* **1972**, *13* (47), 4817-4820.
175. Lubinkowski, J. J.; Knapczyk, J. W.; Calderon, J. L.; Petit, L. R.; McEwen, W. E., Reactions of diaryliodonium salts with sodium alkoxides. *J. Org. Chem.* **1975**, *40* (21), 3010-15.
176. Lubinkowski, J. J.; Gomez, M.; Calderon, J. L.; McEwen, W. E., Reactions of diaryliodonium fluoroborates with inorganic anions. *The Journal of Organic Chemistry* **1978**, *43* (12), 2432-2435.
177. Varvoglis, A., Diaryl Iodonium Salts. In *Hypervalent Iodine in Organic Synthesis*, Academic Press: London, 1997; pp 133-153.
178. Deprez, N. R.; Kalyani, D.; Krause, A.; Sanford, M. S., Room Temperature Palladium-Catalyzed 2-Arylation of Indoles. *Journal of the American Chemical Society* **2006**, *128* (15), 4972-4973.

179. Beringer, F. M.; Galton, S. A.; Huang, S. J., Diaryliodonium salts. XVII. The phenylation of 1,3-indandiones. *J. Am. Chem. Soc.* **1962**, *84*, 2819-23.
180. Beringer, F. M.; Forgione, P. S., Diaryliodonium salts. XVIII. The phenylation of esters in tert-butyl alcohol. *J. Org. Chem.* **1963**, *28*, 714-17.
181. Gronowitz, S.; Holm, B., Inverted reactivity of aryllithium derivatives. II. Influence of copper ions on the product distribution in the reaction of di(3-thienyl)iodonium chloride with nucleophiles. *Chemica Scripta* **1974**, *6* (3), 133-6.
182. Gronowitz, S.; Holm, B., Inverted reactivity of aryllithium derivatives. V. On the syntheses of thiocyano, phenylsulfinyl, and phenoxy derivatives of thiophenes and furans. *J. Heterocycl. Chem.* **1977**, *14* (2), 281-8.
183. Gronowitz, S.; Holm, B., Inverted reactivity of aryllithium derivatives. IV. The reaction of thienyl-aryliodonium chlorides with nucleophiles. *Tetrahedron* **1977**, *33* (5), 557-61.
184. Haydock, D. B.; Mulholland, T. P. C.; Telford, B.; Thorp, J. M.; Wain, J. S., Analogs of clofibrate and clobuzarit containing fluorine in the side chains. *European Journal of Medicinal Chemistry* **1984**, *19* (3), 205-14.
185. Kang, S.-K.; Lee, S.-H.; Lee, D., Copper-catalyzed N-arylation of amines with hypervalent iodonium salts. *Synlett* **2000**, (7), 1022-1024.
186. Zhou, T.; Chen, Z.-C., Hypervalent iodine in synthesis. 52. Palladium-catalyzed arylation of O,O-dialkyl phosphites with diaryliodonium salts: a convenient method for synthesis of arylphosphonates. *Synth. Commun.* **2001**, *31* (21), 3289-3294.

187. Liu, Z.; Zeng, H.; Chen, Z., Hypervalent iodine in synthesis. XV: A convenient new method for the preparation of unsymmetric diaryl selenides. *Synth. Commun.* **1994**, *24* (4), 475-9.
188. Chen, D.-J.; Chen, Z.-C., Hypervalent iodine in synthesis 58: synthesis of aryl esters of dithiocarbamic acids using polymeric diaryliodonium salts. *J. Chem. Res., Synop.* **2000**, (7), 352-353.
189. You, J.; Chen, Z., Hypervalent iodine in synthesis. 5. The reaction between diaryliodonium salts and thiocarboxylic acid salts: a convenient method for the synthesis of S-aryl thiocarboxylates. *Synthesis* **1992**, (6), 521-2.
190. Chen, Z.; Jin, Y.; Stang, P. J., Polyvalent iodine in synthesis. 2. A new method for the preparation of aryl esters of dithiocarbamic acids. *J. Org. Chem.* **1987**, *52* (18), 4117-18.
191. Neilands, O. Y.; Sudmale, I.; Schnell, B.; Georgieva, K.; Kappe, T., Synthesis of 5-dialkylaminothiocarbonylthiobarbituric acids and 5-diethylaminothiocarbonylthio-6-aminouracil. *J. Heterocycl. Chem.* **1998**, *35* (1), 157-160.
192. Makarova, L. G.; Nesmeyanov, A. N., The decomposition and formation of onium salts and the synthesis of organoelemental compounds through onium compounds. I. Two types of decomposition of diphenyliodonium salts. *Izv. Akad. Nauk SSSR, Ser. Khim.* **1945**, 617-25; English, 626.
193. Abramovitch, R. A.; Alvernhe, G.; Bartnik, R.; Dassanayake, N. L.; Inbasekaran, M. N.; Kato, S., Aryloxenium ions. Generation from N-(aryloxy)pyridinium

tetrafluoroborates and reaction with anisole and benzonitrile. *Journal of the American Chemical Society* **1981**, *103* (15), 4558-65.

194. Canty, A. J.; Rodemann, T.; Ryan, J. H., Transition metal organometallic synthesis utilising diorganoiodine(III) reagents. *Advances in Organometallic Chemistry* **2008**, *55*, 279-313.

195. Okuyama, T.; Takino, T.; Sueda, T.; Ochiai, M., Solvolysis of Cyclohexenylodonium Salt, a New Precursor for the Vinyl Cation: Remarkable Nucleofugality of the Phenylodonio Group and Evidence for Internal Return from an Intimate Ion-Molecule Pair. *Journal of the American Chemical Society* **1995**, *117* (12), 3360-7.

196. Beringer, F. M.; Mausner, M., Diaryliodonium Salts. VIII. Decomposition of Substituted Diphenyliodonium Halides in Inert Solvents<sup>1,2</sup>. *Journal of the American Chemical Society* **1958**, *80* (17), 4535-4536.

197. Beringer, F. M.; Gindler, E. M., Diaryliodonium salts. III. Kinetics of the reaction of diphenyliodonium and phenoxide ions. *Journal of the American Chemical Society* **1955**, *77*, 3203-7.

198. Cadogan, J. I. G.; Rowley, A. G.; Sharp, J. T.; Sledzinski, B.; Wilson, N. H., Three routes to benzyne. Decomposition of diphenyliodonium acetate, nitrosation of N-phenylphosphylamidates, and deoxygenation of benzenediazotoluene-p-sulfonate N'-oxide (cupferron p-toluenesulfonate) by phosphorus trichloride. *J. Chem. Soc., Perkin Trans. I* **1975**, (11), 1072-4.

199. Crivello, J. V.; Lam, J. H. W., A new preparation of triarylsulfonium and -selenonium salts via the copper(II)-catalyzed arylation of sulfides and selenides with diaryliodonium salts. *J. Org. Chem.* **1978**, *43* (15), 3055-8.
200. Xia, M.; Chen, Z.-C., Hypervalent iodine in synthesis. XXII. A novel way for the preparation of unsymmetric S-aryl thiosulfonates by the reaction of potassium thiosulfonates with diaryliodonium salts. *Synth. Commun.* **1997**, *27* (8), 1309-1313.
201. Ley, S. V.; Thomas, A. W., Modern synthetic methods for copper-mediated C(aryl)-O, C(aryl)-N, and C(aryl)-S bond formation. *Angew. Chem., Int. Ed.* **2003**, *42* (44), 5400-5449.
202. Nishizono, N.; Baba, R.; Nakamura, C.; Oda, K.; Machida, M., A novel method for the synthesis of 4'-thiopyrimidine nucleosides using hypervalent iodine compounds. *Org. Biomol. Chem.* **2003**, *1* (21), 3692-3697.
203. Moore, H. W.; Goldish, D. M., Vinyl, aryl and acyl azides. *Chem. Halides, Pseudo-Halides Azides FIELD Full Journal Title:* **1983**, *1*, 321-68.
204. Scriven, E. F. V.; Turnbull, K., Azides: their preparation and synthetic uses. *Chem. Rev. FIELD Full Journal Title:Chemical Reviews (Washington, DC, United States)* **1988**, *88* (2), 297-368.
205. Braese, S.; Gil, C.; Knepper, K.; Zimmermann, V., Organic azides. An exploding diversity of a unique class of compounds. *Angew. Chem., Int. Ed. FIELD Full Journal Title:Angewandte Chemie, International Edition* **2005**, *44* (33), 5188-5240.
206. Braese, S.; Keck, D., Aryl azides. *Sci. Synth. FIELD Full Journal Title:Science of Synthesis* **2007**, *31b*, 1827-1843.

207. Breinbauer, R.; Koehn, M., Azide-alkyne coupling: A powerful reaction for bioconjugate chemistry. *ChemBioChem* **2003**, *4* (11), 1147-1149.
208. Speers, A. E.; Adam, G. C.; Cravatt, B. F., Activity-based protein profiling in vivo using a copper(I)-catalyzed azide-alkyne [3 + 2] cycloaddition. *Journal of the American Chemical Society* **2003**, *125* (16), 4686-4687.
209. Wang, Q.; Chan, T. R.; Hilgraf, R.; Fokin, V. V.; Sharpless, K. B.; Finn, M. G., Bioconjugation by copper(I)-catalyzed azide-alkyne [3 + 2] cycloaddition. *Journal of the American Chemical Society* **2003**, *125* (11), 3192-3193.
210. Li, Y.; Ju, Y.; Zhao, Y.-F., Applications of azoles synthesis in bioconjugate chemistry. *Youji Huaxue* **2006**, *26* (12), 1640-1646.
211. Beatty, K. E.; Xie, F.; Wang, Q.; Tirrell, D. A., Selective Dye-Labeling of Newly Synthesized Proteins in Bacterial Cells. *Journal of the American Chemical Society* **2005**, *127* (41), 14150-14151.
212. Deiters, A.; Schultz, P. G., In vivo incorporation of an alkyne into proteins in *Escherichia coli*. *Bioorganic & Medicinal Chemistry Letters* **2005**, *15* (5), 1521-1524.
213. van Steenis, D. J. V. C.; David, O. R. P.; van Strijdonck, G. P. F.; van Maarseveen, J. H.; Reek, J. N. H., Click-chemistry as an efficient synthetic tool for the preparation of novel conjugated polymers. *Chem. Commun. (Cambridge, U. K.)* **2005**, (34), 4333-4335.
214. Golas, P. L.; Tsarevsky, N. V.; Sumerlin, B. S.; Matyjaszewski, K., Catalyst Performance in "Click" Coupling Reactions of Polymers Prepared by ATRP: Ligand and Metal Effects. *Macromolecules* **2006**, *39* (19), 6451-6457.

215. Liu, Y.; Diaz, D. D.; Accurso, A. A.; Sharpless, K. B.; Fokin, V. V.; Finn, M. G., Click chemistry in materials synthesis. III. Metal-adhesive polymers from Cu(I)-catalyzed azide-alkyne cycloaddition. *Journal of Polymer Science, Part A: Polymer Chemistry* **2007**, *45* (22), 5182-5189.
216. Kauer, J. C.; Carboni, R. A., Aromatic azapentalenes. III. 1,3a,6,6a-Tetraazapentalenes. *Journal of the American Chemical Society* **1967**, *89* (11), 2633-7.
217. Biffin, M. E. C.; Miller, J.; Paul, D. B., Directing and activating effects of the azido group. **1971**, 203-20.
218. Takahashi, M.; Suga, D., Synthesis of 2-aryl-3-(arylsulfonyl)indoles and 2-anilino-3-(arylsulfonyl)indoles from 2-[(arylsulfonyl)methyl]anilines using the aza-Wittig reaction of iminophosphoranes. *Synthesis* **1998**, (7), 986-990.
219. Stadlbauer, W.; Fiala, W.; Fischer, M.; Hojas, G., Organic azides in heterocyclic synthesis. 26. Thermal cyclization of 4-azido-3-nitropyridines to furoxanes. *J. Heterocycl. Chem.* **2000**, *37* (5), 1253-1256.
220. Chehade, K. A. H.; Spielmann, H. P., Facile and Efficient Synthesis of 4-Azidotetrafluoroaniline: A New Photoaffinity Reagent. *J. Org. Chem.* **2000**, *65* (16), 4949-4953.
221. Miller, D. R.; Swenson, D. C.; Gillan, E. G., Synthesis and Structure of 2,5,8-Triazido-s-Heptazine: An Energetic and Luminescent Precursor to Nitrogen-Rich Carbon Nitrides. *Journal of the American Chemical Society* **2004**, *126* (17), 5372-5373.

222. Zhu, W.; Ma, D., Synthesis of aryl azides and vinyl azides via proline-promoted CuI-catalyzed coupling reactions. *Chem. Commun. (Cambridge, U. K.)* **2004**, (7), 888-889.
223. Liu, Q.; Tor, Y., Simple Conversion of Aromatic Amines into Azides. *Organic Letters* **2003**, 5 (14), 2571-2572.
224. Zhdankin, V. V.; Kuehl, C. J.; Krasutsky, A. P.; Fromanek, M. S.; Bolz, J. T., Preparation and chemistry of stable azidoiodinanes: 1-azido-3,3-bis(trifluoromethyl)-3-(1H)-1,2-benziodoxole and 1-azido-1,2-benziodoxol-3-(1H)-one. *Tetrahedron Lett. FIELD Full Journal Title:Tetrahedron Letters* **1994**, 35 (52), 9677-80.
225. Zhdankin, V. V.; Krasutsky, A. P.; Kuehl, C. J.; Simonsen, A. J.; Woodward, J. K.; Mismash, B.; Bolz, J. T., Preparation, X-ray Crystal Structure, and Chemistry of Stable Azidoiodinanes - Derivatives of Benziodoxole. *J. Am. Chem. Soc. FIELD Full Journal Title:Journal of the American Chemical Society* **1996**, 118 (22), 5192-5197.
226. Kita, Y.; Tohma, H.; Inagaki, M.; Hatanaka, K.; Yakura, T., A novel oxidative azidation of aromatic compounds with hypervalent iodine reagent, phenyliodine(III) bis(trifluoroacetate) (PIFA) and trimethylsilyl azide. *Tetrahedron Letters* **1991**, 32 (34), 4321-4324.
227. Magnus, P.; Lacour, J.; Weber, W., Direct N-alkyl azidonation of N,N-dialkylarylamines with the iodosylbenzene/trimethylsilyl azide reagent combination. *Journal of the American Chemical Society* **1993**, 115 (20), 9347-9348.



228. Magnus, P.; Hulme, C., Oxidation of L-Proline methyl ester derivatives with the iodosylbenzene/trimethylsilylazide reagent combination. *Tetrahedron Letters* **1994**, 35 (44), 8097-8100.
229. Magnus, P.; Lacour, J.; Evans, P. A.; Roe, M. B.; Hulme, C., Hypervalent Iodine Chemistry: New Oxidation Reactions Using the Iodosylbenzene&#x2212;Trimethylsilyl Azide Reagent Combination. Direct &#x03B1;- and &#x03B2;-Azido Functionalization of Triisopropylsilyl Enol Ethers. *Journal of the American Chemical Society* **1996**, 118 (14), 3406-3418.
230. Carroll, M. A.; Nairne, J.; Woodcraft, J. L., Diaryliodonium salts: a solution to 3-[18F]fluoropyridine. *J. Labelled Compd. Radiopharm.* **2007**, 50 (5-6), 452-454.
231. Shah, A.; Pike, V. W.; Widdowson, D. A., Synthesis of [18F]fluoroarenes from the reaction of cyclotron-produced [18F]fluoride ion with diaryliodonium salts. *J. Chem. Soc., Perkin Trans. I* **1998**, (13), 2043-2046.
232. Fujita, M.; Mishima, E.; Okuyama, T., Solvolysis of methoxy-substituted diaryliodonium tetrafluoroborates: attempted generation of a stabilized aryl cation. *Journal of Physical Organic Chemistry* **2007**, 20 (4), 241-244.
233. Wang, B. G., Joseph W.; Qin, Linlin; DiMagno, Stephen G. , Regiospecific reductive elimination from diaryliodonium salts. *Angew Chem Int Ed Engl FIELD Full Journal Title:Angewandte Chemie (International ed. in English)* **2010**, (Accepted).
234. Cram, D. J.; Steinberg, H., Macro rings. I. Preparation and spectra of the paracyclophanes. *Journal of the American Chemical Society* **1951**, 73, 5691-5704.

235. Brown, C. J.; Farthing, A. C., Preparation and structure of di-p-xylylene. *Nature (London, United Kingdom)* **1949**, *164*, 915-16.
236. Reich, H. J.; Cram, D. J., Macro rings. XXXVII. Multiple electrophilic substitution reactions of [2.2]paracyclophanes and interconversions of polysubstituted derivatives. *Journal of the American Chemical Society* **1969**, *91* (13), 3527-33.
237. Gibson, S. E.; Knight, J. D., [2.2]paracyclophane derivatives in asymmetric catalysis. *Org. Biomol. Chem.* **2003**, *1* (8), 1256-1269.
238. Reich, H. J.; Cram, D. J., Transannular directive influences in electrophilic substitution of 2.2-paracyclophane. *Journal of the American Chemical Society* **1968**, *90* (5), 1365-7.
239. Beringer, F. M.; Nathan, R. A., Iodonium salts from organolithium reagents with transchlorovinylidioso dichloride. *J. Org. Chem.* **1970**, *35* (6), 2095-6.
240. Beringer, F. M.; Chang, L. L., Exchange of aryl ligands to polyvalent iodine. *The Journal of Organic Chemistry* **1972**, *37* (10), 1516-1519.
241. Cram, D. J.; Day, A. C., Macro rings. XXXI. Quinone derived from [2.2]paracyclophane, an intramolecular-molecular complex. *J. Org. Chem.* **1966**, *31* (4), 1227-32.
242. Krohn, K.; Rieger, H.; Hopf, H.; Barrett, D.; Jones, P. G.; Doering, D., Transition metal-catalyzed oxidations. 3. Reaction of 4-hydroxy[2.2]paracyclophane with the mimon molybdenum oxodiperoxo complex  $[\text{Mo}(\text{O}_2)_2\text{O}]\text{--}\Sigma\text{Py--}\Sigma\text{HMPT}$ . *Chem. Ber.* **1990**, *123* (8), 1729-32.

243. Rozenberg, V.; Zhuravsky, R.; Sergeeva, E., Design, classification, and strategies of synthesis of modular bidentate ligands based on aryl[2.2]paracyclophane backbone. *Chirality* **2006**, *18* (2), 95-102.